University of Ghana http://ugspace.ug.edu.gh

UNIVERSITY OF GHANA

DEPARTMENT OF CHEMISTRY



DESIGN, SYNTHESIS, AND MEDICINAL CHEMISTRY PROFILING OF ANALOGUES OF MMV676444 AND MMV1794959, FOR THEIR BIOLOGICAL ACTIVITIES.

BY

CRYSTAL FUNMILAO ADE

(10599443)

Thesis submitted to the Department of Chemistry of the College of Basic and Applied Science, University of Ghana, in partial fulfilment of the requirements for the award of Doctor of Philosophy Degree in Chemistry

OCTOBER 2025

University of Ghana http://ugspace.ug.edu.gh

DECLARATION

I, **CRYSTAL FUNMILAYO ADE**, the author of this thesis hereby declare that the work presented was solely done by me, under supervision, in the Department of Chemistry, University of Ghana, Legon.

Candidate's Signature: Date: 09-10-2025

Crystal Funmilayo Ade

Principal Supervisor's Signature: Date: 09-10-2025

Prof. Richard K. Amewu

Co-Supervisor's Signature: *MaryChama* Date: 09-10-2025

Prof. Mary Anti Chama

INTEGRI PROCEDAMUS

University of Ghana http://ugspace.ug.edu.gh

DEDICATION

This thesis is dedicated to my father, Mr. Lawani Bakari Ade, whose lifelong hope has been to witness the successful end of this journey. His constant encouragement and earnest prayers have been a great source of inspiration, especially at critical junctions of my studies. May this achievement bring joy and blessings to his old age.



University of Ghana http://ugspace.ug.edu.gh

ACKNOWLEDGEMENT

My sincere appreciations go to my supervisor, Professor Richard Amewu, for his guidance throughout this research. Starting as a novice, the opportunity to explore and gain invaluable experience in his laboratory, as well as participate in training opportunities through his professional affiliations, has equipped me with the skills and confidence for independent research. I also appreciate the support of my co-supervisor Professor, Mary Chama, whose kind words and encouragement have been a source of inspiration and comfort.

The Bill and Melinda Gates Foundation, Science for Africa foundation, African Academy of Sciences, Medicines for Malaria Ventures, Holistic Drug Discovery and Development (H3D) centre and foundation of the University of CapeTown, South Africa, Wellcome Center for Anti-Infectives Research (WCAIR) of the university of Dundee, Scotland, have all played various roles in providing funding, training and technical support throughout the research. I am also thankful to Prof. Fabrice F. Boyom's laboratory, of the University of Yaounde, Dr. Arnold Forkuo Donkor's laboratory of the Kwame Nkrumah University of Science and Technology (KNUST), as well as the Immunology Department of the Noguchi Memorial Institute for Medical Research, for biological and solubility screening.

I am grateful to the Department of Chemistry of the University of Ghana where this research was principally conducted, for providing the necessary facilities including access to their NMR instrument. The immense support from technicians, Mr. Samuel Kwadwo Owusu (General), Thomas Mensah and Mr. Eric Coffie, was of great help. The invaluable counsel and encouragement from Professor Donkor (of blessed memory), especially at the early stages of the research, was a source of stability during very challenging times. I am deeply grateful to Mr. Ernest Kwasi Ntiamoah (of blessed memory) whose unwavering support extended beyond the laboratory throughout this research. I thank Dr. Michael Ainooson, who offered

University of Ghana http://ugspace.ug.edu.gh

valuable suggestions, during challenging times with my reactions in the laboratory. To all the lecturers in the department, whose classes imparted knowledge valuable to my research, I am grateful.

I acknowledge my mentor Professor Marian Asantewah Nkansah (Director of student affairs (KNUST) and the founder and convenor of the Women in Chemistry Network) for continually checking on my progress and offering encouragement throughout my studies. Her shared experiences and the exposure I obtained through her professional affiliations have been very impactful to my personal development as a feminine African scientist.

I appreciate the role of my colleagues at the Drug Innovation research Group throughout this journey. The meal and fun times we shared, was helpful in easing the stress and frustrations associated with graduate school. Especially to Dr. Patrick Sakyi and Dr. Gideon Atinga Akolgo whose doors I often knocked when I encountered challenges, I am much grateful. I also appreciate the efforts of Richard Opoku, Edward Odoi and Jones Annan as well as Fritz Plange, Shaban Mohammed and Deborah Annor who provided essential support in analysing my data. Not forgetting my comrade Stanley Dugbatey (Great Tseko) who silently taught me perseverance in the face of adversity. The collective contribution of every member of the team has been valuable to this research and is much appreciated.

I am highly indebted to my supportive parents, whose unwavering love and guidance taught me to embrace life's challenges with courage, faith and hope, and whose support and prayers enabled me to successfully balance academic work and family life.

Very importantly, I am thankful to my immediate family. To Mr. Richard Kabutey who doubles as my husband and 'psychologist', and consistently goes above and beyond to ensure my comfort and happiness, I am deeply grateful. My heartfelt gratitude also goes to my daughter,

University of Ghana http://ugspace.ug.edu.gh

Keren Kabutey, whose birth within the research period, fuelled my motivation and resilience to deliver my best.



University of Ghana http://ugspace.ug.edu.gh

ABSTRACT

The impact of the global disease burden leaves a lasting toll of mortality and disability, particularly on the most affected regions, impeding development and economic advancement. A prevalent disease with devastating public health challenges particularly in sub-Saharan Africa is malaria. Despite some positive impact of global efforts on its prevalence, morbidity, and mortality, the emergence and spread of drug-resistant strains of malaria's causative agent, raises concerns about the long-term therapeutic efficacy of the most potent drugs for its treatment. In view of this, the discovery of more potent, user-friendly drugs, remains crucial for addressing drug resistance in malaria. Drug discovery employs phenotypic screening to identify new chemical entities for medicinal chemistry explorations, potentially leading to first-in-class medicines. These drugs have the potential to serve as candidates for multiple diseases, often exhibiting novel mechanisms of action, highlighting their critical role in combating drug resistance. In this project, two scaffolds, **MMV676444** and **MMV1794959,** identified in phenotypic screens were explored for their therapeutic potential, primarily against malaria.

A total of **36** analogues of the **MMV676444** scaffold were synthesised and characterized using spectroscopic and spectrometric techniques, including Nuclear Magnetic Resonance (NMR) spectroscopy, Mass spectroscopy (MS) and Fourier-Transform Infrared (FTIR). The prepared analogues were tested *in vitro* against the sensitive strain NF54 of the malaria parasite and H37rv of *Mycobacterium tuberculosis* (MTB). While poor antitubercular activities (**MIC 33.3 µM – > 62.5 µM**) were generally observed, some of the analogues showed promising antimalarial activity, with the most active analogue, CFA/092, yielding an IC_{50} value of **12 nM**. Further studies conducted on CFA/092 indicated favourable metabolic stability, confirming its suitability for further optimization as a lead scaffold. Furthermore, preliminary

University of Ghana http://ugspace.ug.edu.gh

investigations on selected analogues also showed encouraging activity (**IC_{50} = 1.16 µM – 3.71 µM)** against *L. donovani* promastigotes.

On the other hand, **2** analogues of **MMV1794959** were successfully synthesised and characterised with ^{1}H and ^{13}C NMR, LC-MS, and FTIR. Though the analogues (CFA/P3021 and CFA/P3076) exhibited reduced lipophilicity and improved solubility in comparison to the hit scaffold, they were poorly active against malaria (*P. falciparum* (3D7)).



University of Ghana http://ugspace.ug.edu.gh

TABLE OF CONTENTS

DECLARATION.....**ii**

DEDICATION..... **iii**

ACKNOWLEDGEMENT.....**iv**

ABSTRACT.....**vii**

TABLE OF CONTENTS .....**ix**

LIST OF FIGURES .....**xxxi**

LIST OF TABLES .....**xxxv**

LIST OF SCHEMES .....**xxxvii**

LIST OF ABBREVIATIONS .....**xxxix**

CHAPTER ONE **1**

1.0 Introduction.....**1**

1.1 The global disease burden.....**1**

1.2 Malaria Overview. **2**

1.2.1 Introduction to malaria.....2

1.2.2 Global prevalence and distribution. 3

1.2.2.1 Malaria in Ghana.....5

1.2.3 Social and Economic Impact. 6

1.3 Malaria Research and Development **8**

University of Ghana http://ugspace.ug.edu.gh

1.3.1 Funding 8

Funding is one of the critical and often fragile pillars sustaining malaria research and development. Global investments over the last two decades have significantly accelerated progress in malaria control and elimination with major contributions coming from governments, multilateral organizations, philanthropic foundations and product development partnerships. 8

1.3.1.1 Bill &Melinda Gates Foundation (BM&GF) Global Health programme 9

1.3.2 Malaria Vaccine Development 9

1.3.2.1 RTS,S/AS01 9

1.3.2.2 R21/Matrix-M 11

1.3.3 Vector Control 12

1.3.3.1 Insecticide Treated Nets (ITNs) 12

1.3.3.2 Indoor Residual Spraying (IRS) 14

1.3.3.3 Larval Source Management (LSM) 15

1.3.3.4 Additional Vector Control Tools 16

1.3.4 Antimalarial Drugs 17

1.3.4.1 Artemisinin and ACTs 18

1.4 Drug Discovery 21

1.4.1 MMV and the Malaria Boxes 23

1.4.1.1 Selected Lead Scaffolds from the MMV Pathogen Box 24

1.5 Problem Statement 26

1.6 Justification 27

1.7 Hypothesis 28

1.8 Research Aim and Objectives 28

References ..... Error! Bookmark not defined.

University of Ghana http://ugspace.ug.edu.gh

CHAPTER TWO **29**

2.0 Literature Review **29**

2.1 Introduction **29**

2.2 Global Initiatives and Progress **29**

2.2.1 Roll Back Malaria Partnership 30

2.2.2 The Global Fund to fight AIDS, TB and malaria 30

2.2.3 The President's Malaria Initiative 31

2.2.4 Global Malaria Programme 31

2.2.5 'Malaria no more'. 32

2.2.6 African Leaders Malaria Alliance 32

2.2.7 End Malaria Council (EMC) 32

2.2.8 E-2025 Initiative 33

2.3 Etiological Agent of Malaria **34**

2.3.1 Life cycle of the *Plasmodium* parasite. 34

2.3.2 Plasmodium Parasites Responsible for Human Malaria. 37

2.3.2.1 *Plasmodium falciparum* 37

2.3.2.2 *Plasmodium Vivax* 38

2.3.2.3 *Plasmodium Ovale* 39

2.3.2.4 *Plasmodium malariae* 40

2.3.2.5 *Plasmodium Knowlesi* 41

2.4 Existing antimalarial drug classes **41**

2.4.1 Antifolates 43

2.4.2 Aminoalcohols 45

2.4.3 4-Aminoquinolines 47

2.4.4 Hydroxynapthoquinones 49

University of Ghana http://ugspace.ug.edu.gh

2.4.5 Endoperoxides.....51

2.4.5.1 Artemisinin 52

2.4.5.1.1 ACTs.....53

2.4.5.1.2 Artemisinin Resistance 56

2.4.5.1.3 Triple ACTs (TACTs).....58

2.5 The role of small molecules in malaria drug discovery 59

2.5.1 Target Based Screening (TBS) 60

2.5.2 Phenotypic Screening (PS). 61

2.5.3: Comparative advances in Phenotypic and Target-Based Screening in the development of antimalarial small molecules.....62

2.5.4 Artificial Intelligence/Machine Learning (AI/ML) for antimalarial Drug Discovery. 65

2.6 Next-Generation Antimalarials 66

2.6.1 Endoperoxides.....67

2.6.1.1 Arterolane (OZ277) 67

2.6.1.2 Artefenomel 69

2.6.1.2.1 RLA-3107 71

2.6.2 MMV390048.....72

2.6.3 Cipargamin (KAE609).....75

2.6.4 Ganaplacide (KAF156).....78

2.6.5 DSM265.....80

2.6.6 SJ733 ((+)-SJ000557733).....82

2.6.7 Ferroquine (SSR97913) 85

2.7 Hit scaffolds MMV676444 and MMV1794959.....89

2.7.1 MMV676444.....90

University of Ghana http://ugspace.ug.edu.gh

2.7.2 MMV1794959.....92

References.....Error! Bookmark not defined.

CHAPTER THREE.....**94**

3.0 Experimental.....**94**

3.1.1 Reagents and solvents......**94**

3.1.2 Thin Layer Chromatography (TLC)......**94**

3.1.3 Column chromatography......**94**

3.2 Instrumentation.....**94**

3.2.1 Fourier-Transform Infrared (FT-IR) Spectroscopy.....**94**

3.2.2 Nuclear Magnetic Resonance Spectra (NMR)......**94**

3.2.3 LC-MS.....**95**

3.2.4 Melting Point......**95**

3.3 Synthesis and Characterisation......**96**

3.3.1 General Procedures......**96**

3.3.1.1 General procedures for MMV676444 analogues.....96

3.3.1.1.1 General procedure for preparation of Boc-protected urea.....97

3.3.1.1.1.1 Preparation of *tert*-butyl 4-((4-methoxyphenyl)carbamoyl)piperazine-1-carboxylate, 3.2.....97

3.3.1.1.1.2 Preparation of *tert*-butyl 4-((4-(trifluoromethyl)phenyl)carbamoyl)piperazine-1-carboxylate, 3.3.....97

3.3.1.1.1.3 Preparation of *tert*-butyl 4-((3,5-bis(trifluoromethyl)phenyl)carbamoyl)piperazine-1-carboxylate, 3.4.....98

3.3.1.1.1.4 Preparation of *tert*-butyl 4-((2,6-dichloropyridin-4-yl)carbamoyl)piperazine-1-carboxylate, 3.5.....99

University of Ghana http://ugspace.ug.edu.gh

3.3.1.1.1.5 Preparation of *tert*-butyl 4-((3,5-difluorophenyl)carbamoyl)piperazine-1-carboxylate, 3.6. 99

3.3.1.1.1.6 Preparation of *tert*-butyl 4-(phenylcarbamoyl)piperazine-1-carboxylate, 3.7. 100

3.3.1.1.1.7 Preparation of *tert*-butyl 4-((4-chloro-3-nitrophenyl)carbamoyl)piperazine-1-carboxylate, 3.8.....100

3.3.1.1.1.8 Preparation of *tert*-butyl 4-((perfluorophenyl)carbamoyl)piperazine-1-carboxylate, 3.9.....101

3.3.1.1.1.9 Preparation of *tert*-butyl 4-((4-fluorobenzyl)carbamoyl)piperazine-1-carboxylate, 3.10. 101

3.3.1.1.1.10 Preparation of *tert*-butyl 4-((3,5-dimethoxyphenyl)carbamoyl)piperazine-1-carboxylate, 3.11. 102

3.3.1.1.1.11 Preparation of *tert*-butyl 4-((3,5-dimethylphenyl)carbamoyl)piperazine-1-carboxylate, 3.12. 102

3.3.1.1.1.12 Preparation of *tert*-butyl 4-(cyclopropylcarbamoyl)piperazine-1-carboxylate, 3.13. 103

3.3.1.1.1.13 Preparation of *tert*-butyl 4-((4-fluorophenyl)carbamoyl)piperazine-1-carboxylate, 3.14.....103

3.3.1.1.1.14 Preparation of *tert*-butyl 4-((2,4-difluorophenyl)carbamoyl)piperazine-1-carboxylate, 3.15. 104

3.3.1.1.1.15 Preparation of *tert*-butyl 4-(p-tolylcarbamoyl)piperazine-1-carboxylate, 3.16. 104

3.3.1.1.1.16 Preparation of *tert*-butyl 4-(benzo[d][1,3]dioxol-5-ylcarbamoyl)piperazine-1-carboxylate, 3.17. 105

University of Ghana http://ugspace.ug.edu.gh

3.3.1.1.1.17 Preparation of *tert*-butyl 4-((4-bromophenyl)carbamoyl)piperazine-1-carboxylate, 3.18.....105

3.3.1.1.2 General procedure for deprotection of the Boc-protected urea. 106

3.3.1.1.2.1 Preparation of *N*-(4-methoxyphenyl)piperazine-1-carboxamide, 3.19. 106

3.3.1.1.2.2 Preparation of *N*-(2,6-dichloropyridin-4-yl)piperazine-1-carboxamide, 3.20.....106

3.3.1.1.2.3 Preparation of *N*-(perfluorophenyl)piperazine-1-carboxamide, 3.21. 107

3.3.1.1.2.4 Preparation of *N*-(4-(trifluoromethyl)phenyl)piperazine-1-carboxamide, 3.22. 107

3.3.1.1.2.5 Preparation of *N*-(3,5-bis(trifluoromethyl)phenyl)piperazine-1-carboxamide, 3.23. 108

3.3.1.1.2.6 Preparation of *N*-(3-chloro-4-nitrophenyl)piperazine-1-carboxamide, 3.24.....108

3.3.1.1.2.7 Preparation of *N*-phenylpiperazine-1-carboxamide, 3.25. 109

3.3.1.1.2.8 Preparation of *N*-(3,5-difluorophenyl)piperazine-1-carboxamide, 3.26. 109

3.3.1.1.2.9 Preparation of *N*-(3,5-dimethoxyphenyl)piperazine-1-carboxamide, 3.27.....110

3.3.1.1.2.10 Preparation of *N*-(3,5-dimethylphenyl)piperazine-1-carboxamide, 3.28.....110

3.3.1.1.2.11 Preparation of *N*-(4-fluorophenyl)piperazine-1-carboxamide, 3.29. 111

University of Ghana http://ugspace.ug.edu.gh

3.3.1.1.2.12 Preparation of *N*-(4-cyclopropylphenyl)piperazine-1-carboxamide, 3.30.....111

3.3.1.1.2.13 Preparation of *N*-(2,4-difluorophenyl)piperazine-1-carboxamide, 3.31.....111

3.3.1.1.2.14 Preparation of *N*-(p-tolyl)piperazine-1-carboxamide, 3.32. 112

3.3.1.1.2.15 Preparation of *N*-(benzo[d][1,3]dioxol-5-yl)piperazine-1-carboxamide, 3.33.....112

3.3.1.1.2.16 Preparation of *N*-(4-fluorobenzyl)piperazine-1-carboxamide, 3.34. 113

3.3.1.1.2.17 Preparation of *N*-(4-bromophenyl)piperazine-1-carboxamide, 3.35. 113

3.3.1.1.3 General procedure for reductive amination. 114

3.3.1.1.3.1 Preparation of 4-(benzo[*d*][1,3]dioxol-5-ylmethyl)-*N*-(4-(trifluoromethyl)phenyl)piperazine-1-carboxamide, 3.36. 114

3.3.1.1.3.2 Preparation of 4-(4-(trifluoromethyl)benzyl)-*N*-(4-(trifluoromethyl)phenyl)piperazine-1-carboxamide, 3.37. 115

3.3.1.1.3.3 Preparation of 4-((6-bromobenzo[d][1,3]dioxol-5-yl)methyl)-N-(4-bromophenyl)piperazine-1-carboxamide, 3.38.....115

3.3.1.1.3.4 Preparation of 4-((2,2-difluorobenzo[*d*][1,3]dioxol-5-yl)methyl)-*N*-(3,5-dimethoxyphenyl)piperazine-1-carboxamide, 3.39.....116

3.3.1.1.3.5 Preparation of 4-(benzo[*d*][1,3]dioxol-5-ylmethyl)-*N*-(3,5-dimethoxyphenyl)piperazine-1-carboxamide, 3.40. 117

3.3.1.1.3.6 Preparation of 4-((6-bromobenzo[*d*][1,3]dioxol-5-yl)methyl)-*N*-(3,5-dimethoxyphenyl)piperazine-1-carboxamide, 3.41. 118

University of Ghana http://ugspace.ug.edu.gh

3.3.1.1.3.7 Preparation of *N*-(benzo[*d*][1,3]dioxol-5-yl)-4-benzylpiperazine-1-carboxamide, 3.42. 119

3.3.1.1.3.8 Preparation of *N*-(benzo[*d*][1,3]dioxol-5-yl)-4-((2,2-difluorobenzo[d][1,3]dioxol-5-yl)methyl)piperazine-1-carboxamide, 3.43. 119

3.3.1.1.3.9 Preparation of *N*-(benzo[*d*][1,3]dioxol-5-yl)-4-((6-bromobenzo[d][1,3]dioxol-5-yl)methyl)piperazine-1-carboxamide, 3.44. 120

3.3.1.1.3.10 Preparation of *N*-(benzo[*d*][1,3]dioxol-5-yl)-4-(benzo[*d*][1,3]dioxol-5-ylmethyl)piperazine-1-carboxamide, 3.45. 121

3.3.1.1.3.11 Preparation of 4-((6-bromobenzo[*d*][1,3]dioxol-5-yl)methyl)-*N*-(4-methoxyphenyl)piperazine-1-carboxamide, 3.46. 122

3.3.1.1.3.12 Preparation of 4-(benzo[d][1,3]dioxol-5-ylmethyl)-N-(4-methoxyphenyl)piperazine-1-carboxamide, 3.47. 123

3.3.1.1.3.13 Preparation of *N*-(3,5-bis(trifluoromethyl)phenyl)-4-((6-bromobenzo[*d*][1,3]dioxol-5-yl)methyl)piperazine-1-carboxamide, 3.48. 123

3.3.1.1.3.14 Preparation of 4-((6-bromobenzo[*d*][1,3]dioxol-5-yl)methyl)-*N*-(perfluorophenyl)piperazine-1-carboxamide, 3.49. 124

3.3.1.1.3.15 Preparation of 4-(benzo[*d*][1,3]dioxol-5-ylmethyl)-*N*-cyclopropylpiperazine-1-carboxamide, 3.50. 125

3.3.1.1.3.16 Preparation of N-cyclopropyl-4-((2,2-difluorobenzo[d][1,3]dioxol-5-yl)methyl)piperazine-1-carboxamide, 3.51. 126

3.3.1.1.3.17 Preparation of 4-(benzo[*d*][1,3]dioxol-5-ylmethyl)-*N*-phenylpiperazine-1-carboxamide, 3.52. 126

3.3.1.1.3.18 Preparation of 4-((6-bromobenzo[*d*][1,3]dioxol-5-yl)methyl)-*N*-phenylpiperazine-1-carboxamide, 3.53. 127

University of Ghana http://ugspace.ug.edu.gh

3.3.1.1.3.19 Preparation of 4-((2,2-difluorobenzo[*d*][1,3]dioxol-5-yl)methyl)-*N*-phenylpiperazine-1-carboxamide, 3.54.....128

3.3.1.1.3.20 Preparation of 4-(benzo[*d*][1,3]dioxol-5-ylmethyl)-*N*-(p-tolyl)piperazine-1-carboxamide, 3.55.....129

3.3.1.1.3.21 Preparation of 4-((6-bromobenzo[*d*][1,3]dioxol-5-yl)methyl)-*N*-(p-tolyl)piperazine-1-carboxamide, 3.56.....129

3.3.1.1.3.22 Preparation of 4-((6-bromobenzo[*d*][1,3]dioxol-5-yl)methyl)-*N*-(3,5-dimethylphenyl)piperazine-1-carboxamide, 3.57.....130

3.3.1.1.3.23 Preparation of 4-(3,4-bis(difluoromethoxy)benzyl)-N-(3,5-dimethylphenyl)piperazine-1-carboxamide, 3.58.....131

3.3.1.1.3.24 Preparation of *N*-(2,6-dichloropyridin-4-yl)-4-((2,2-difluorobenzo[*d*][1,3]dioxol-5-yl)methyl)piperazine-1-carboxamide, 3.59.....132

3.3.1.1.3.25 Preparation of 4-(benzo[*d*][1,3]dioxol-5-ylmethyl)-*N*-(2,6-dichloropyridin-4-yl)piperazine-1-carboxamide, 3.60.....132

3.3.1.1.3.26 Preparation of 4-(benzo[*d*][1,3]dioxol-5-ylmethyl)-*N*-(4-fluorophenyl)piperazine-1-carboxamide, 3.61.....133

3.3.1.1.3.27 Preparation of *N*-(4-fluorophenyl)-4-(4-(trifluoromethyl)benzyl)piperazine-1-carboxamide, 3.62. 134

3.3.1.1.3.28 Preparation of 4-((2,2-difluorobenzo[*d*][1,3]dioxol-5-yl)methyl)-*N*-(4-fluorophenyl)piperazine-1-carboxamide, 3.63.....135

3.3.1.1.3.29 Preparation of 4-(benzo[d][1,3]dioxol-5-ylmethyl)-N-(4-fluorobenzyl)piperazine-1-carboxamide, 3.64.....135

3.3.1.1.3.30 Preparation of 4-((2,2-difluorobenzo[*d*][1,3]dioxol-5-yl)methyl)-*N*-(4-fluorobenzyl)piperazine-1-carboxamide, 3.65.....136

University of Ghana http://ugspace.ug.edu.gh

3.3.1.1.3.31 Preparation of 4-((6-bromobenzo[d][1,3]dioxol-5-yl)methyl)-N-(4-fluorobenzyl)piperazine-1-carboxamide, 3.66. 137

3.3.1.1.3.32 Preparation of 4-((6-bromobenzo[*d*][1,3]dioxol-5-yl)methyl)-*N*-(2,4-difluorophenyl)piperazine-1-carboxamide, 3.67. 138

3.3.1.1.3.33 Preparation of 4-((6-bromobenzo[*d*][1,3]dioxol-5-yl)methyl)-*N*-(2,4-difluorophenyl)piperazine-1-carboxamide, 3.68. 138

3.3.1.1.3.34 Preparation of 4-((2,2-difluorobenzo[d][1,3]dioxol-5-yl)methyl)-N-(2,4-difluorophenyl)piperazine-1-carboxamide, 3.69. 139

3.3.1.1.3.35 Preparation of 4-(benzo[d][1,3]dioxol-5-ylmethyl)-N-(3,5-difluorophenyl)piperazine-1-carboxamide, 3.70. 140

3.3.1.1.3.36 Preparation of 4-((2,2-difluorobenzo[*d*][1,3]dioxol-5-yl)methyl)-*N*-(3,5-difluorophenyl)piperazine-1-carboxamide, 3.71. 141

3.3.1.2 General procedures for MMV1794959 analogues. 141

3.3.1.2.1 General procedure for preparation of (*Z*)-*N*-(piperidin-2-ylidene)cyanamide, 3.73. 142

3.3.1.2.2 General procedure for preparation of ethyl (*Z*)-2-(2-(cyanoimino)piperidin-1-yl)acetate, 3.74. 143

3.3.1.2.3 General procedure for cyclisation of ethyl 2-amino-5,6,7,8-tetrahydroimidazo[1,2-a]pyridine-5-carboxylate, 3.75. 143

3.3.1.2.4 General procedure for amide coupling. 144

3.3.1.2.4.1 Preparation of ethyl 2-(3-(trifluoromethyl)benzamido)-5,6,7,8-tetrahydroimidazo[1,2-*a*]pyridine-5-carboxylate, 3.76. 145

3.3.1.2.4.2 Preparation of ethyl 2-(2-(trifluoromethyl)benzamido)-5,6,7,8-tetrahydroimidazo[1,2-a]pyridine-5-carboxylate, 3.77. 145

3.3.1.2.5 General procedure for ester hydrolysis. 146

University of Ghana http://ugspace.ug.edu.gh

3.3.1.2.5.1 Preparation of 2-(3-(trifluoromethyl)benzamido)-5,6,7,8-tetrahydroimidazo[1,2-*a*]pyridine-5-carboxylic acid, 3.78.....146

3.3.1.2.5.2 Preparation of 2-(2-(trifluoromethyl)benzamido)-5,6,7,8-tetrahydroimidazo[1,2-*a*]pyridine-5-carboxylic acid, 3.79.....147

3.3.1.2.6 General procedure for amide coupling of carboxylic acids. 147

3.3.1.2.6.1 Preparation of *N*-cyclopentyl-2-(3-(trifluoromethyl)benzamido)-5,6,7,8-tetrahydroimidazo[1,2-*a*]pyridine-5-carboxamide, 3.80. 148

3.3.1.2.6.2 Preparation of *N*-cyclopentyl-2-(2-(trifluoromethyl)benzamido)-5,6,7,8-tetrahydroimidazo[1,2-*a*]pyridine-3-carboxamide, 3.81. 148

3.4 Physicochemical properties 149

3.5 Anti-tubercular Activity.....149

3.6 Antimalarial Activity of MMV676444.....150

3.6.1 Antimalarial Activity of MMV676444.....150

3.6.2 Antimalarial Activities of MMV1794959 analogues. 150

3.7 Solubility.....151

3.8 Leishmanicidal activity.....151

References.....Error! Bookmark not defined.

CHAPTER FOUR.....**153**

4.0 Design, Synthesis, and Medicinal Chemistry Progression of MMV676444 Analogues for their Biological Activities.....**153**

4.1 Introduction.....**153**

4.1.1 Objectives 153

4.1.2 Medicinal chemistry plan.....153

4.2 Results and Discussion.....**154**

University of Ghana http://ugspace.ug.edu.gh

4.2.1 Chemistry 154

4.2.1.2 Synthesised Analogues 157

4.2.2 Spectral Analysis 160

4.2.2.1 NMR Spectroscopy 161

4.2.2.1.1 NMR spectrum of *tert*-butyl 4-((4-methoxyphenyl)carbamoyl)piperazine-1-carboxylate (CFA005), 3.2. 161

4.2.2.1.2 NMR spectrum of *N*-(4-methoxyphenyl)piperazine-1-carboxamide (CFA008), 3.19. 165

4.2.2.1.3 NMR spectrum of 4-((6-bromobenzo[*d*][1,3]dioxol-5-yl)methyl)-*N*-(4-methoxyphenyl)piperazine-1-carboxamide, (CFA026), 3.46. 166

4.2.2.2 LC-Mass Spectrometry. 168

4.2.2.3 Fourier-Transform Infrared (FT-IR) Spectroscopy 171

4.2.3 Physicochemical properties 172

4.2.4 Assessment of Biological Activities and Solubility of Synthesised Analogues. 175

4.2.4.1 Anti-tubercular Activity 175

4.2.4.2 Antimalarial Activity 176

4.2.4.3 Solubility 181

4.2.4.4 Metabolic Stability Studies 181

4.2.4.5 Leishmanicidal activity. 182

4.2.4.5.1 Selectivity studies on mammalian cell lines. 185

4.3 Conclusion 186

References 219

CHAPTER FIVE 188

University of Ghana http://ugspace.ug.edu.gh

5.0 Design, Synthesis and Antimalarial Activities of analogues of MMV1794959. ...188

5.1 Introduction.....188

5.1.1 Objectives 188

5.1.2 Medicinal Chemistry Plan.....188

With a substantial aromatic presence in the scaffold, likely contributing to its low solubility and consequent toxicity [1], the synthetic strategy involved the replacement of the aromatic rings with 188

5.2 Results and Discussion.....190

5.2.1 Chemistry.....190

5.2.1.1 Re-synthesis of MMV9794959.....190

5.2.1.2 Formation of piperidinylidene cyanamide. 191

5.2.1.3 *N*-alkylation piperidinylidene cyanamide. 192

5.2.1.4 Base mediated cyclisation.....193

5.2.1.5 Amide coupling with trifluorophenyl carboxylic acids. 194

5.2.1.6 Base Hydrolysis of amide ester.....196

5.2.2 Spectral Analysis 198

5.2.2.1 NMR Spectroscopy.....199

5.2.2.1.1 NMR Spectrum of (*Z*)-*N*-(piperidin-2-ylidene)cyanamide, 3.73.....199

5.2.2.1.2 NMR Spectrum of ethyl (*Z*)-2-(2-(cyanoimino)piperidin-1-yl)acetate, 3.74.....200

5.2.2.1.3 NMR Spectrum of ethyl 2-amino-5,6,7,8-tetrahydroimidazo[1,2-a]pyridine-5-carboxylate, 3.75.....203

5.2.2.1.4 NMR Spectrum of ethyl ethyl 2-(3-(trifluoromethyl)benzamido)-5,6,7,8-tetrahydroimidazo[1,2-*a*]pyridine-5-carboxylate, 3.76. 204

University of Ghana http://ugspace.ug.edu.gh

5.2.2.1.5 NMR Spectrum of *N*-cyclopentyl-2-(2-(trifluoromethyl)benzamido)-5,6,7,8-tetrahydroimidazo[1,2-*a*]pyridine-3-carboxamide 3.81 (CFA/P3/076) and 3.80(CFA/P3/021). 209

5.2.2.2 LC-MS Spectroscopy. 211

5.2.2.3 Fourier-Transform Infrared (FT-IR) Spectroscopy. 212

5.2.3 Physicochemical properties, solubility and biological activities of 3.80 and 3.81. 214

5.3 Conclusion 216

References ..... Error! Bookmark not defined.

CHAPTER SIX 217

6.0 Conclusions and Recommendations. 217

6.1 Conclusions 217

6.2 Recommendations 218

6.2.1 MMV676444 218

6.2.2 MMV1794959 218

APPENDICES 257

Appendix 1: ^{1}H and ^{13}C NMR Spectra. 257

Appendix 1.1: 257

Appendix 1.2: 258

Appendix 1.3: 258

Appendix 1.4: 259

Appendix 1.5: 259

Appendix 1.6: 260

Appendix 1.7: 260

University of Ghana http://ugspace.ug.edu.gh

Appendix 1.8: **261**

Appendix 1.9: **261**

Appendix 1.10: **262**

Appendix 1.11: **262**

Appendix 1.12: **263**

Appendix 1.14: **264**

Appendix 1.15: **264**

Appendix 1.16: **265**

Appendix 1.17: **265**

Appendix 1.18: **266**

Appendix 1.19: **266**

Appendix 1.20: **267**

Appendix 1.21: **267**

Appendix 1.22: **268**

Appendix 1.23: **268**

Appendix 1.24 ..... **269**

Appendix 1.25: **269**

Appendix 1.26: **270**

Appendix 1.27: **270**

Appendix 1.29: **271**

Appendix 1.30: **272**

Appendix 1.31: **272**

Appendix 1.32 ..... **273**

Appendix 1.33 ..... **273**

Appendix 1.34 ..... **274**

University of Ghana http://ugspace.ug.edu.gh

Appendix 1.35 ..... **274**

Appendix 1.36 ..... **275**

Appendix 1.37 ..... **275**

Appendix 1.38 ..... **276**

Appendix 1.39 ..... **276**

Appendix 1.40: **277**

Appendix 1.41 ..... **277**

Appendix 1.42 ..... **278**

Appendix 1.43 ..... **278**

Appendix 1.44 ..... **279**

Appendix 1.45 ..... **279**

Appendix 1.46 ..... **280**

Appendix 1.47 ..... **280**

Appendix 1.48 ..... **281**

Appendix 1.49: **281**

Appendix 1.51 ..... **282**

Appendix 1.52 ..... **283**

Appendix 1.54 ..... **284**

Appendix 1.55 ..... **284**

Appendix 1.56: **285**

Appendix 1.57 ..... **285**

Appendix 1.58 ..... **286**

Appendix 1.59 ..... **286**

Appendix 1.60: **287**

Appendix 1.61 ..... **287**

University of Ghana http://ugspace.ug.edu.gh

Appendix 1.62 ..... **288**

Appendix 1.63 ..... **288**

Appendix 1.64: **289**

Appendix 1.65 ..... **289**

Appendix 1.66: **290**

Appendix 1.67: **290**

Appendix 1.68 ..... **291**

Appendix 1.69 ..... **291**

Appendix 1.70 ..... **292**

Appendix 1.71: **292**

Appendix 1.72 ..... **293**

Appendix 1.73 ..... **293**

Appendix 1.74 ..... **294**

Appendix 1.75 ..... **294**

Appendix 1.76 ..... **295**

Appendix 1.77 ..... **295**

Appendix 1.78 ..... **296**

Appendix 1.79 ..... **296**

Appendix 1.80 ..... **297**

Appendix 1.81 ..... **297**

Appendix 1.82 ..... **298**

Appendix 1.83 ..... **298**

Appendix 1.84 ..... **299**

Appendix 1.85 ..... **299**

Appendix 1.86 ..... **300**

University of Ghana http://ugspace.ug.edu.gh

Appendix 1.87 ..... **300**

Appendix 1.88 ..... **301**

Appendix 1.89 ..... **301**

Appendix 1.90 ..... **302**

Appendix 1.91 ..... **302**

Appendix 1.92: **303**

Appendix 1.93 ..... **303**

Appendix 1.94 ..... **304**

Appendix 1.95 ..... **304**

Appendix 1.96 ..... **305**

Appendix 1.97 ..... **305**

Appendix 1.98 ..... **306**

Appendix 1.99 ..... **306**

Appendix 1.100: **307**

Appendix 1.101 ..... **307**

Appendix 1.102 ..... **308**

Appendix 1.103 ..... **308**

Appendix 1.104 ..... **309**

Appendix 1.105 ..... **309**

Appendix 1.106 ..... **310**

Appendix 1.107 ..... **310**

Appendix 1.108 ..... **311**

Appendix 1.109 ..... **311**

Appendix 2: LC-MS Data **312**

Appendix 2.6 ..... **315**

University of Ghana http://ugspace.ug.edu.gh

Appendix 2.7 ..... **316**

Appendix 2.8 ..... **317**

Appendix 2.9 ..... **318**

Appendix 2.10 ..... **319**

Appendix 2.11: **320**

Appendix 2.12 ..... **321**

Appendix 2.14 ..... **323**

Appendix 2.15 ..... **324**

Appendix 2.16 ..... **325**

Appendix 2.17 ..... **326**

Appendix 2.18 ..... **327**

Appendix 2.19 ..... **328**

Appendix 2.20 ..... **329**

Appendix 2.21 ..... **330**

Appendix 2.22: **331**

Appendix 2.24 ..... **333**

Appendix 2.25 ..... **334**

Appendix 2.26 ..... **335**

Appendix 2.27 ..... **336**

Appendix 2.28 ..... **337**

Appendix 2.29 ..... **338**

Appendix 2.30 ..... **339**

Appendix 2.31 ..... **340**

Appendix 2.32 ..... **341**

Appendix 2.33 ..... **342**

University of Ghana http://ugspace.ug.edu.gh

Appendix 2.34.....343

Appendix 2.35.....344

Appendix 2.37.....345

Appendix 2.39:.....346

Appendix 2.40:.....347

Appendix 2.41:.....348

Appendix 2.42.....349

Appendix 2.43.....350

Appendix 2.44:.....351

Appendix 2.45.....352

Appendix 2.46.....353

Appendix 2.46.....354

Appendix 2.48.....355

Appendix 3: FTIR Spectra.....356

Appendix 3.1.....356

Appendix 3.2.....356

Appendix 3.3.....357

Appendix 3.4.....357

Appendix 3.5.....358

Appendix 3.6.....358

Appendix 3.7.....359

Appendix 3.8.....359

Appendix 3.9.....360

Appendix 3.10:.....360

Appendix 3.11:.....361

University of Ghana http://ugspace.ug.edu.gh

Appendix 3.13:.....**362**

Appendix 3.14.....**363**

Appendix 3.15.....**363**

Appendix 3.16.....**364**

Appendix 3.17.....**364**

Appendix 3.18.....**365**

Appendix 3.19.....**365**

Appendix 3.20.....**366**

Appendix 3.21.....**366**

Appendix 3.22.....**367**

Appendix 3.23.....**367**

Appendix 3.24.....**368**

Appendix 3.25.....**368**

Appendix 3.27.....**369**

Appendix 3.28.....**370**

Appendix 3.29.....**370**

Appendix 3.32.....**372**

Appendix 3.33.....**372**

Appendix 3.34.....**373**

Appendix 3.35.....**373**

Appendix 3.36.....**374**

Appendix 3.38.....**375**

Appendix 4: Antitubercular activities of screened analogues.....**376**

University of Ghana http://ugspace.ug.edu.gh

LIST OF FIGURES

Figure 1.1: Current estimates and forecasted trend of malaria incidence and deaths according to the 2024 World Malaria and Global Technical Strategy for Malaria reports [42]. 4

Figure1.2: Administration and interaction of RTS,S/AS01 with Plasmodium sporozoites 11

Figure 1.3: Insecticides used for ITNs and IRS. 13

Figure 1.4: Chemical structure of insecticides used for IRS. 15

Figure 1. 5: Artemisinin and other potent antimalarial drugs for malaria chemotherapy. 18

Figure 1. 6: Partner drugs used in ACTs. 20

Figure 1.7: A prediction study by Watson et al. on the spread of Kelch-13 mutations of *P. falciparum* across the African continent up to April 2040 21

Figure 1.8: A graphical comparison between phenotypic (B) and target-based (A) drug discovery 22

Figure 1.9: Examples of clinically used drugs identified through PS and their therapeutic functions. 23

Figure 1.10: Chemical Structures of MMV676444 and MMV1794959. 25

Figure 1.11: Chemical structures of early and contemporary potent antimalarials. 27

University of Ghana http://ugspace.ug.edu.gh

Figure 2.1: Life cycle of the Plasmodium parasite [7]. 35

Figure 2.2: Chemical structures of antibiotics 2.3, 2.4 and 2.5, and 8-aminoquinoline antimalarial agents 2.1 and 2.2. 43

Figure 2.3: Antifolates employed in antimalarial chemotherapy. 45

Figure 2.4: Aminoalcohols used in malaria chemotherapy. 46

Figure 2.5: 4-aminoquinolines used for malaria treatment. 48

Figure 2.6: Structures of Atovaquone and other hydroxynaphthoquinone derivatives investigated for their antimalarial potential. 50

Figure 2.7: Artemisinin drugs employed in ACTs. 53

Figure 2.8: Structural relationship among Pyronaridine and 4-aminoquinolines. 55

Figure 2.9: Structures of select antimalarial candidates identified through target-based screening. 61

Figure 2.10: Examples of clinically used drugs identified through PS and their therapeutic functions. 62

Figure 2.11: Various scaffolds from the MMV Pathogen Box that have demonstrated multi-stage antimalarial activities. 64

Figure 2.12: Structural modification of MMV390048 towards the development of UCT943. 75

Figure 2.13: Structural evolution from initial hit to Ganaplacide. 78

University of Ghana http://ugspace.ug.edu.gh

Figure 2.14: Crystal structure of *P. falciparum* DHODH in complex with DSM265 (shown in green) [289]. 82

Figure 2.15: Structural modifications on hit compound, 2.98 that led to SJ733. 83

Figure 2.16: Molecular hybridisation towards ferroquine. 85

Figure 2.17: Other candidates in the antimalarial discovery pipeline. 89

Figure 2.18: Chemical Structures of Hit Scaffolds MMV676444 and MMV1794959. 90

Figure 2.19: Structurally related analogues of MMV676444 with promising antimalarial activities. 91

Figure 2.20: Molecular structures of MMV1183932 and MMV1794959. 92

Figure 4.1: Chemical Structure of MMV676444. 153

Figure 4.2: Medicinal chemistry plan for MMV676444 optimisation for the present study. 154

Figure 4.7: ^{1}H NMR of 4-((6-bromobenzo[*d*][1,3]dioxol-5-yl)methyl)-*N*-(4-methoxyphenyl)piperazine-1-carboxamide, CFA026. 167

Figure 4.8: ^{13}C NMR of 4-((6-bromobenzo[*d*][1,3]dioxol-5-yl)methyl)-*N*-(4-methoxyphenyl)piperazine-1-carboxamide, CFA026. 168

Figure 4.10: Mass spectrum of CFA026, confirming the molecular ion at m/z 448.0 $[M+H]^{+}$, consistent with the calculated exact molecular mass 448.08 Da. 170

Figure 4.11: HR-MS of analogue, CFA067, showing expected isotopic distribution of Br. 171

University of Ghana http://ugspace.ug.edu.gh

Figure 4.12: IR spectrum of 3.46 (CFA026). 172

Figure 4.13: Comparison of biological activities of reported and resynthesized MMV676444. 176

Figure 4.14: Synthesised analogues of MMV676444 with promising antimalarial activity. 178

Figure 4.15: Analogues of MMV676444 exhibiting the most potent antileishmanial activity. 184

Figure 5.1: Molecular structure of MMV1794959. 188

Figure 5.2: Medicinal chemistry plan for MMV9794959 optimisation. 190

Figure 5.3: Structures of attempted analogues. 198

Figure 5.4: ^{1}H NMR (500 MHz, $CDCl_3$) of (*Z*)-*N*-(piperidin-2-ylidene) cyanamide, 3.73 (CFA/P3/001). 199

Figure 5.5: ^{13}C NMR (126 MHz, $CDCl_3$) of (*Z*)-*N*-(piperidin-2-ylidene) cyanamide, 3.73 (CFA/P3/001). 200

Figure 5.6: Comparison of ^{1}H NMR (500 MHz, $CDCl_3$) of CFA/P3001 and CFA/P3002. 201

Figure 5.7: ^{13}C NMR (126 MHz, $CDCl_3$) of CFA/P3002. 202

Figure 5.8: Comparison of ^{1}H NMR (500 MHz, $CDCl_3$) of 3.74 and 3.75. 203

Figure 5.9: ^{13}C NMR (126 MHz, $CDCl_3$) of CFA/P3003. 204

University of Ghana http://ugspace.ug.edu.gh

Figure 5.10: Comparison of ^{1}H NMR (500 MHz, $CDCl_3$) of 3.75 and 3.76. 206

Figure 5.12: ^{13}C NMR (126 MHz, $CDCl_3$) of 3.76 (CFA/P3016).....208

Figure 5.13: ^{1}H NMR (500 MHz, $CDCl_3$) of 3.81. 209

Figure 5.14: ^{13}C NMR (126 MHz, $CDCl_3$) of 3.81. 210

Figure 5.15: ^{1}H NMR (500 MHz, $CDCl_3$) of 3.80. 211

Figure 5.16: Liquid chromatography (LC) of 3.80 and 3.81.....212

Figure 5.17: Mass Spectrum of 3.80 and 3.81.....212

Figure 5.18: IR spectrum of 3.81 213

Figure 5.19: IR spectrum of 3.80. 214

Figure 5.20: Summary of physochochemical properties, solubility profiles and antimalarial activities of synthesised analogues.....215

LIST OF TABLES

Table 2.1: Overview of employed ACTs in malaria chemoprevention 54

Table 2.2: Summary the Biological and physicochemical 90

Table 2.3: Scaffold Profile of MMV1794959. 92

Table 4.1: Synthesised Analogues with Phenyl and Piperonyl Substituents. 158

Table 4.2: Synthesised Analogues with non-phenyl or non-piperonyl substituents. 159

University of Ghana http://ugspace.ug.edu.gh

Table 4.3: Physicochemical parameters of synthesised analogues. 172

Table 4.4: Antimalarial Activities and Solubility of Tested Analogues. 176

Table 4.5: Results of metabolic stability studies on CFA092 (3.41). 182

Table 4.6: Leishmanial Activity of screened analogues.....182

Table 4.7: Selectivity data for most active analogues on mammalian cell lines.....186



University of Ghana http://ugspace.ug.edu.gh

LIST OF SCHEMES

Scheme 2.1: Synthesis of 1,2,4-trioxolanes through Griesbaum co-ozonolysis 68

Scheme 2.2: Synthesis of Arterolane from dispiro 1,2,4-trioxolane 69

Scheme 2.3: Structural modification on arterolone towards the synthesis of artefenomel 70

Scheme 2.4: Structural optimization of artefenomel, leading to the development of RLA-3107.....72

Scheme 2.5: Synthetic route for MMV390048 73

Scheme 2.6: Paymode et al's proposed synthetic route for MMV390048 74

Scheme 2.7: Synthetic route for the preparation of Cipargamin (KAE609).....77

Scheme 2.9: Synthetic route to DSM265.....81

Scheme 2.10: Synthetic route to SJ733 84

Scheme 2.11: Synthetic route to Ferroquine 86

Scheme 3.1: Synthetic route for the synthesis of MMV676444 analogues.....96

Scheme 3.2: Synthetic route for MMV1794959 analogues.....142

Scheme 4.1: Synthetic route to target analogues of MMV676444.....155

Scheme 4.2: Proposed mechanism towards Boc-protected urea formation. 155

Scheme 4.3: Proposed mechanism for Boc deprotection.....156

University of Ghana http://ugspace.ug.edu.gh

Scheme 5.1: a) Proposed Synthetic route to MMV9794959. 191

Scheme 5.3 Plausible mechanism for the formation of 3.73.....192

Scheme 5.4: Mechanism for *N*-alkylation of 3.74.....193

Scheme 5.5: Plausible mechanism for base mediated cyclisation of 3.75. 194

Scheme 5.6: Reaction mechanism for the formation of a) acyl chlorides 195



University of Ghana http://ugspace.ug.edu.gh

LIST OF ABBREVIATIONS

^{13}C NMR	Carbon -13 Nuclear Magnetic Resonance Spectra
^{1}H NMR	Proton Nuclear Magnetic Resonance Spectra
ADC	Albumin-Dextrose-Catalase
AIDS	Acquired Immunodeficiency Syndrome
ALMA	African Leaders Malaria Alliance
AS-AQ	Artesunate-piperaquine
AS-MQ	Artesunate-mefloquine
AS-SP	Artesunate-sulfadoxine-pyrimethamine
AS-SP	Artesunate-sulfadoxine-pyrimethamine
ATBS	Attractive Toxic Sugar Baits
ATP	Adenosine Triphosphate
B&MGF	Bill and Melinda Gates Foundation
CFP	Chlorfenapyr
COVID	Corona Virus Disease
CSP	circumsporozoite protein
CYP	cytochrome P450
DAD	Diode-Array Detection
DCM	Dichlormethane
DHF	Dihydrofolate
DHFR	Dihydrofolate Reductase
DHODH	Dihydroorotate dehydrogenase
DHPS	Dihydropteroate synthase
DMF	Dimethylformamide
DMPK	Drug Metabolism and Pharmacokinetics
DMSO	Dimethyl Sulfoxide
EDC.HCl	1-Ethyl-3-(3-dimethylaminopropyl)carbodiimide hydrochloride
EMC	End Malaria Council
ETC	Electron Transport Chain
EWD	Electron Withdrawing Group
FTIR	Fourier-Transform Infrared
GAST	Glutamate-Asparagine Salts-Tween
GMP	Global Malaria Programme
GNF	Genomics Institute of the Novartis Research Foundation
HATU	Hexafluorophosphate Azabenzotriazole Tetramethyl Uronium)
HIV	Human Immunodeficiency Virus
HLM	Human Liver Microsomes
HMBC	Heteronuclear Multiple Bond Correlation
HPA	Homophthalic Anhydride
HPLC	High-Performance Liquid Chromatography
HRMS	High-Resolution Mass Spectrometry
HSQC	Heteronuclear Single Quantum Coherence

University of Ghana http://ugspace.ug.edu.gh

HTS	High Throughput Screening
IRS	Indoor Residual spraying
ITN	Insecticide Treated Nets
KOH	Potassium Hydroxide
LC-MS	Liquid Chromatography Mass Spectrometry
LSM	Larval Source Management
LSM	Larval Source Management
MABA	Microplate Alama Blue Assay
MAIP	MAalria Inhibitor Prediction
MIC	Minimum Inhibitory Concentration
ML-QSAR	Machine Learning Quantitative Structure-Activity Relationship
MMV	Medicines for Malaria Ventures
MPL	Monophosphoryl Lipid
MSD	Mass Spectroscopy Detector
MTB	*Mycobacterium tuberculosis*
MVI	Malaria Vaccine Initiative
NADPH	Nicotinamide Adenine Dinucleotide Phosphate
NPV	Net Present Value
PASS	Prediction of Activity Spectra for Substances
PATH	Program for Appropriate Technology in Health
PBO	Piperonyl Butoxide
PfATP4	*P. falciparum* ATPase
PfCLK	*P. falciparum* Cyclin-dependent kinase-like kinases
PfCRT	*P. falciparum* Chloroquine Transporter
PfNDH2	*P. falciparum* II NADPH dehydrogenase
PfNMT	*P. falciparum N*-myristoyltransferase
PfMDR	*P. falciparum* Multidrug Resistance
PfPI4K	Phosphatidylinositol-4-OH kinase
PMI	President's Malaria Initiative
POP	Persistent Organic Pollutants
PPF	Pyriproxyfen
PS	Phenotypic Screening
RDT	Rapid Diagnostic Test
RNA	Ribonucleic Acid
ROS	Reactive Oxygen Species
SAR	Structure Activity relationship
SMILES	Simplified Molecular Input Line Entry System
STAB	Sodium triacetoxyborohydride
TBS	Target Based Screening
TCP	Target Candidate Profile
TMS	Tetramethylsilane
TPP	Target Product Profiles
TPSA	Topological Polar Surface Area

University of Ghana http://ugspace.ug.edu.gh

WHO World Health Organization



University of Ghana http://ugspace.ug.edu.gh

CHAPTER ONE

1.0 Introduction

1.1 The global disease burden

Infectious diseases leave a lasting toll of mortality and morbidity globally, particularly in the most affected regions, impeding development and economic advancement [1-3]. Historical records vividly depict humanity's unending struggling against various infectious diseases. From the ruinous' Plague of Justinian' (541-549 AD) [4] through the perils of the 'Black Death' (1347-1351) [5], to the recent catastrophic 'COVID-19' (2019-2023) [6], the cascading repercussions of pandemics caused by infectious diseases extended beyond endemic zones. They resulted in millions of deaths, disrupted trade and economic instability, crippled military strength and weakened empires, as well as increased global unemployment and mental health crises [7-9]. Fortunately, lessons learnt from these pandemics have offered long-term advantages in preventing and tackling infectious diseases [10]. For instance, the realisation of the need for public health measures led to a more formalised system of quarantine, sanitation, and disease tracking after the 'black death'. Increased global collaboration in medical research, focusing on infectious diseases, led to greater healthcare investments, infrastructure, and telemedicine innovation, strengthening international health organizations and frameworks [11, 12]. Additionally, the Spanish Flu (1918-1920) [13]; considered to be one of the most deadly pandemics in history, as well as epidemics like malaria, tuberculosis and cholera, strongly influenced the establishment of the World Health organization (WHO) [14] which has since been a key global authority in protecting public health and reducing the global disease burden. More so, COVID 19 spurred rapid advancements in medical research and technology, accel-

University of Ghana http://ugspace.ug.edu.gh

erating the development and distribution of mRNA vaccines [15, 16]. These left indelible prints toward global preparedness for future pandemics.

Despite the lessons learnt and actions taken to prevent and tackle pandemic phases and epidemic surges, the impact of the global disease burden is obviously unevenly distributed. Africa accounts for ~18.3% of the world's population, yet shoulders a disproportionate share of the worldwide disease burden, accounting for a substantial percentage of top killer diseases like HIV, tuberculosis (TB), and malaria. Being a continent already contending with myriad obstacles to its development, its weak healthcare systems lack the capacity to manage both new and existing health crises [17-19].

Particularly in sub-Saharan Africa, where warm and humid conditions favour the spread of vector-borne diseases like malaria, factors such as poor sanitation and water quality, high poverty levels and overcrowding, political instability and conflict, lifestyle and traditions strongly influence the high prevalence of diseases that are more easily controlled or treated in other parts of the world [20-23]. Malaria is the most prevalent and one of the deadliest infectious diseases in Africa, accounting for ~95% of the global morbidity and mortality [18]. Though a significant challenge in Africa, it has profound global implications. The repercussions of imported cases into non-endemic regions, a rise in drug-resistant pathogens, and inadequate local and international funding are issues the international community is contending with, calling for concerted efforts to reduce and eliminate them [21, 23-25].

1.2 Malaria Overview.

1.2.1 Introduction to malaria

Malaria is a life-threatening disease with catastrophic consequences. The disease has plagued generations for several decades. Despite substantial advancements in mitigating its overall

University of Ghana http://ugspace.ug.edu.gh

burden, the morbidity and mortality due to malaria remain a pressing global issue. Of greater concern is the disproportionate burden placed on disadvantaged populations, who have limited resources to combat the disease [18, 26, 27].

Malaria is caused by *Plasmodium* parasites transmitted primarily through the bites of an infected female *Anopheles* mosquito. Symptoms of infection range from fever, chills, headaches, fatigue and muscle aches, to severe anaemia, cerebral complications, organ failure and death [28, 29]. These clinical indicators may display subtle variations depending on the *Plasmodium* species causing the infection. Five (5) *Plasmodium* species are recognised to be responsible for human malaria. They are, *Plasmodium falciparum, P. vivax, P. ovale, P. malariae and P. knowlesi* [30, 31]. Each species is characterised by unique features that distinguish its biology, pathology and clinical presentation. Though some may linger for an extended period before exhibiting symptoms, others can rapidly escalate into complicated infections. While *P. falciparum* infections are the most lethal and cause of morbidity in many endemic areas, *P. ovale* infections are the most widely distributed [32-34]. Given the emphasis in the literature on host deterioration associated with malaria progression [32, 35, 36], it is imperative that all malaria cases, regardless of the *Plasmodium* species involved, be addressed promptly to mitigate the risks [26].

1.2.2 Global prevalence and distribution.

Prior to the COVID-19 pandemic, global efforts yielded a steady reduction in malaria incidence and death. Malaria infections decreased from 262 million in 2000 to 233 million in 2019, while fatalities decreased from 864,000 to 576,000 over the same period, representing 27% and 51% declines in malaria morbidity and mortality, respectively [37, 38]. Unfortunately, a cascade of challenges presented by the pandemic, disrupted malaria treatment, ac-

University of Ghana http://ugspace.ug.edu.gh

cess to healthcare and control efforts. These contributed to a rise in the global malaria burden, undermining the efficacy of prior control measures [39]. Despite renewed efforts after the pandemic to combat the disease, global malaria incidence has increased consistently over the past 3 years [38, 40]. Available global reports indicate that malaria infections reached 263 million in 2023, returning the incidence to levels before the decline. On the other hand, malaria deaths have gradually decreased since the 2020 spike, from 631,000 to 597,000 in 2023 (**Figure 1.1**) [18]. Despite this being an improvement over the past few years, the current death toll surpasses that recorded preceding the pandemic, amplifying the urgency for groundbreaking interventions to curb this growing menace.

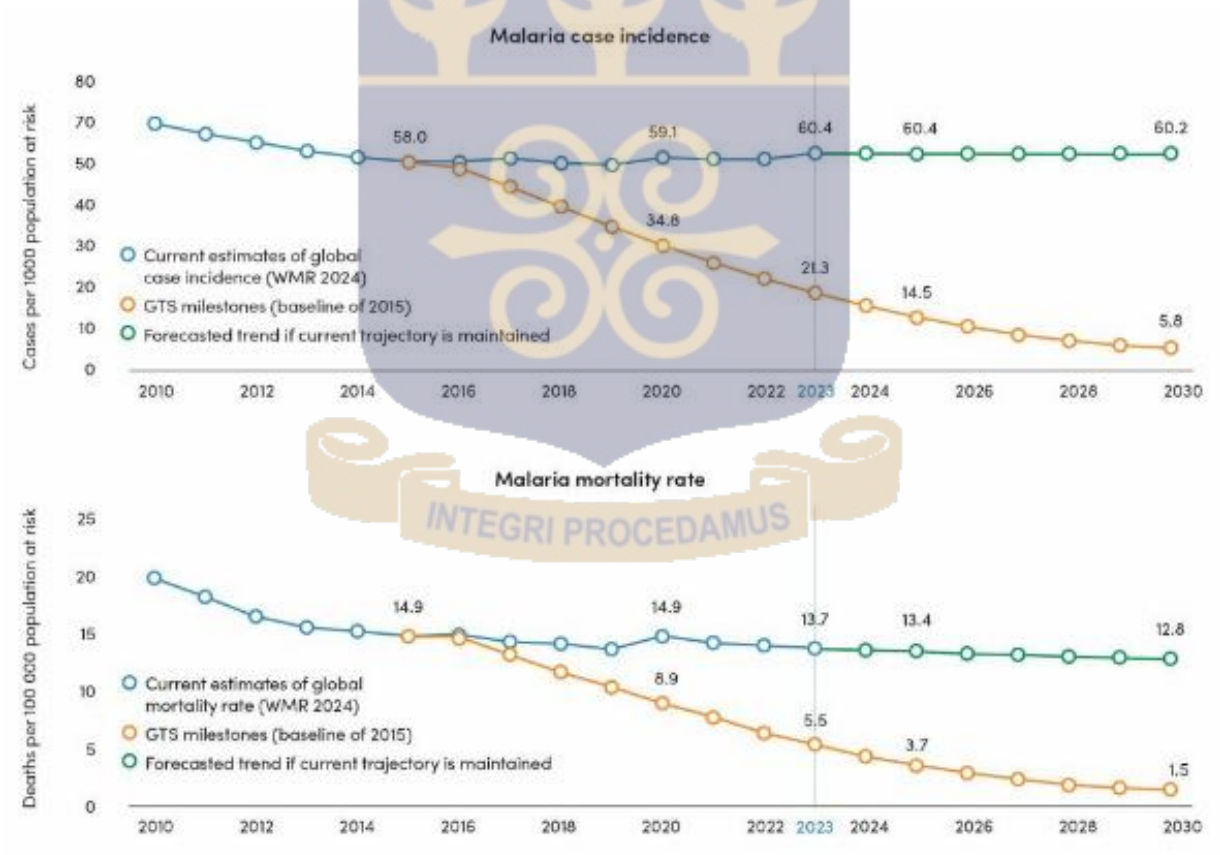


Figure 1.1: Current estimates and forecasted trend of malaria incidence and deaths according to the 2024 World Malaria and Global Technical Strategy for Malaria reports [42].

University of Ghana http://ugspace.ug.edu.gh

Malaria transmission is linked to climatic conditions (temperature, rainfall, humidity) that provide suitable breeding grounds for its vectors [41]. It is widely distributed across the globe with high transmission in tropical and subtropical regions, particularly, sub-Saharan Africa, Southeast Asia, South Asia, Latin America, West Pacific and some parts of the Middle East [42-44]. The WHO African region remains the most afflicted region, accounting for 94% of the global malaria incidence and 95% deaths. The top 5 countries bearing the heaviest malaria burden are Nigeria, the Democratic Republic of Congo, Uganda and Ethiopia and Mozambique. Non-endemic regions include Europe, North America, Australia, and parts of the Middle East[18].

Vulnerable populations that require targeted measures for prevention, early detection and treatment are mainly children under the age of 5, pregnant women, immunocompromised individuals, travellers to endemic regions and inhabitants of economically disadvantaged or remote areas [45, 46].

1.2.2.1 Malaria in Ghana

Within the sub-Saharan African Region, Ghana is one of the countries where malaria contributes substantially to regional morbidity and mortality. Malaria is a leading cause of hospital admissions, outpatient attendance and preventable deaths particularly among the vulnerable population in the country [47]. Ghana is amongst the top 15 highest-burden malaria countries globally, accounting for 5.3% of cases in West Africa. Its stable year-round transmission (with seasonal intensification during the rainy season) and significant public health impact provides a relevant endemic context for evaluating the persistent challenges for malaria elimination and control, as well as antimalarial drug discovery [48, 49].

University of Ghana http://ugspace.ug.edu.gh

1.2.3 Social and Economic Impact.

The repercussions of malaria are not limited to deteriorating health and loss of life. Its ripple effect extends beyond affected regions, with significant financial implications on a global scale [50].

The inability of infected individuals to work and earn a living collectively contributes to workforce disruption, reducing overall productivity, thereby affecting revenue generation [51]. For instance, a mining company in Mozambique realized a US$ 2.7 million loss owing to malaria among employees [52].

In children, malaria infections lead to school absenteeism and poor academic performance, resulting in a skills gap in the labour force. Complications like cerebral malaria may induce neurological damage and cognitive impairments in children. This may increase the dropout rate, thereby harming long-term economic growth [53-55].

Additionally, expenses on malaria treatment and prophylaxis could drive poor households into debt, exacerbating the living conditions of already economically struggling communities. Death or incapacitation of a family member could deprive an entire family of their bread-winner, causing a disruption in the family structure and support system [55-58].

Moreover, malaria incurs a risk of gender inequality and social discrimination against women. Forming a significant component of the vulnerable population, the repercussions of miscarriages, low birth weight and maternal death influences their social standing [59-62]. Again, the responsibility of caregiving to children and spouses afflicted by malaria lies heavily on women. This restricts their social mobility, economic and academic participation [63, 64].

University of Ghana http://ugspace.ug.edu.gh

In endemic countries, about 30%-50% of in-patient admissions and out-patient visits are malaria-related [65]. This burden causes overcrowding in health facilities during peak endemic seasons, leading to shortages of supplies and a diversion of resources and attention from critical matters such as maternal and child health [66, 67]. The situation exerts considerable pressure on limited resources, consequently affecting the quality of care.

Approximately 40% of public health funds in such regions are allocated to tackling malaria [65, 68, 69] due to the high treatment costs for severe cases, and investments required for prevention and control programmes [70]. For example, in 2023, global malaria funding reached US$ 4 billion, across 90 countries with 75% of this funding allocated to the WHO African region. International sources contributed 67% of the total, while domestic sources accounted for 33% [18]. This reliance on external funding limits the autonomy of endemic countries in addressing public health measures.

Furthermore, studies conducted in some African countries indicate that malaria can significantly reduce Gross Domestic Product (GDP) growth [50, 51, 71, 72]. This compounds over time, leading to a substantial economic prosperity gap between endemic and non-endemic countries [73]. In Uganda, a loss of US $577 million was estimated due to a diminished productivity, resulting from malaria-related absenteeism and mortality [74]. A study by Snyman *et al.*, found that, a 10% decrease in malaria incidence, led to a 0.11% increase in per capita per annual incidence. The same study reported a *ceteris paribus* 70% lower per capita income in endemic countries compared to non-endemic countries [75]. Another study estimated a $208.6 billion economic benefit in NPV (Net Present Value) terms from malaria reduction and eradication [76].

University of Ghana http://ugspace.ug.edu.gh

These substantial findings highlight the significant impact of a malaria-free world on global socioeconomic development, emphasizing the critical need for malaria elimination.

1.3 Malaria Research and Development

Having attained the status of a global, persistent, and deadly infectious disease, malaria research and development (R&D) encompasses a broad range of scientific and technological efforts to develop new drugs, more effective and accessible diagnostic tools, innovative vector control strategies, and vaccines.

1.3.1 Funding

Funding is one of the critical and often fragile pillars sustaining malaria research and development. Global investments over the last two decades have significantly accelerated progress in malaria control and elimination with major contributions coming from governments, multilateral organizations, philanthropic foundations and product development partnerships.

In 2023, funding for malaria research and development reached US$690 million, a 9% increase from 2022. According to the WHO, this signals an encouraging shift in malaria R&D funding after 4 years of decline. While the United States National Institutes of Health is the largest donor (US$201 million), the Bill & Melinda Gates Foundation is the single philanthropic foundation to have contributed the largest share of funds (US$181 million) to malaria R&D [18]. Over the last two decades, the B&M Gates Foundation has been the most influential philanthropic organisation, widely involved in global efforts to control and eliminate malaria. It has been particularly impactful through its Global Health Programme [77-79].

University of Ghana http://ugspace.ug.edu.gh

1.3.1.1 Bill &Melinda Gates Foundation (BM&GF) Global Health programme

As a core division of the B&MGF, the Global Health Programme aims to improve health outcomes, especially in low- and middle-income countries. As part of its operations, the programme provides direct grants to research institutions in high-burden settings. Malaria has been one of its key disease areas, with substantial support for the development of new vaccines, antimalarial drugs, and innovative vector control tools and surveillance systems [78].

These key focus areas: vaccine development, vector control, and novel antimalarial drug innovations are central in malaria R&D with several groundbreaking achievements that have advanced malaria treatment and powered on a global scale.

1.3.2 Malaria Vaccine Development

Malaria vaccine development has been a long-standing global health priority. In the face of challenges, particularly related to the parasite's complex life cycle, genetic variability, and ability to evade the immune system, numerous biologically derived vaccines have been developed, with modest successes recorded [80]. Notwithstanding, two vaccines have made headway in clinical development and deployment especially among vulnerable populations (children) in endemic regions. In 2021, the first vaccine to be approved for a human parasitic disease, RTS, S/AS01, was recommended by the WHO [81, 82].

1.3.2.1 RTS,S/AS01

RTS, S/AS01 (Mosquirix) was developed by GlaxoSmithKline in partnership with the PATH Malaria Vaccine Initiative (MVI) with significant funding and technical support from BM&GF. It was approved for public use in children living in areas endemic for *P. falciparum*.

University of Ghana http://ugspace.ug.edu.gh

The development of the vaccine spanned across 3 decades, with clinical trials conducted across several African countries [83].

RTS, S is a recombinant protein-based antigen composed of the central repeat region (R) and immunodominant segregated epitopes of T lymphocytes (T) derived from the circumsporozoite protein (CSP) of *P. falciparum*. This combined RT peptide is genetically fused to hepatitis B surface antigen (HBsAg) (S) to enhance the immune response. An excess amount of HBsAg is added to co-assemble with the RTS fusion protein to form virus-like particles (VLPs), thereby boosting its immunogenicity. With a structured, repetitive nature, the RTS, S antigen is efficiently recognised by the immune system, driving the potent anti-CSP antibody and T-cell responses observed in vaccinated individuals. Its adjuvant system, AS01, comprising lyposomes, monophosphoryl lipid A (MPL), and a natural saponin from the bark of *Quillaja saponaria* tree, provides improved antibody and T-cell immune responses. The production of antibodies and cellular immune responses induced by RTS, S/AS01 impairs the ability of *P. falciparum* sporozoites to invade the liver (**Figure 1.2**), thereby halting the parasite's development before it reaches the symptomatic blood stage [84-86].

Though RTS, S/AS01 offers moderate efficacy (~36% against clinical malaria and ~31% against severe malaria) [87], it represents a significant public health breakthrough. However, its modest protection is insufficient in highly endemic areas. Additionally, the high efficacy shortly after vaccination wanes over time, requiring booster doses to maintain moderate protection. Moreover, RTS, S/AS01 specifically targets the pre-erythrocyte stage of *P. falciparum*. It does not offer protection against other phases of the parasite's life cycle nor target other *Plasmodium* species. It is therefore insufficient as a stand-alone intervention, under-

University of Ghana http://ugspace.ug.edu.gh

scoring the need for more efficacious vaccines, which led to the development of the R21/Matrix-M vaccine [87-90].

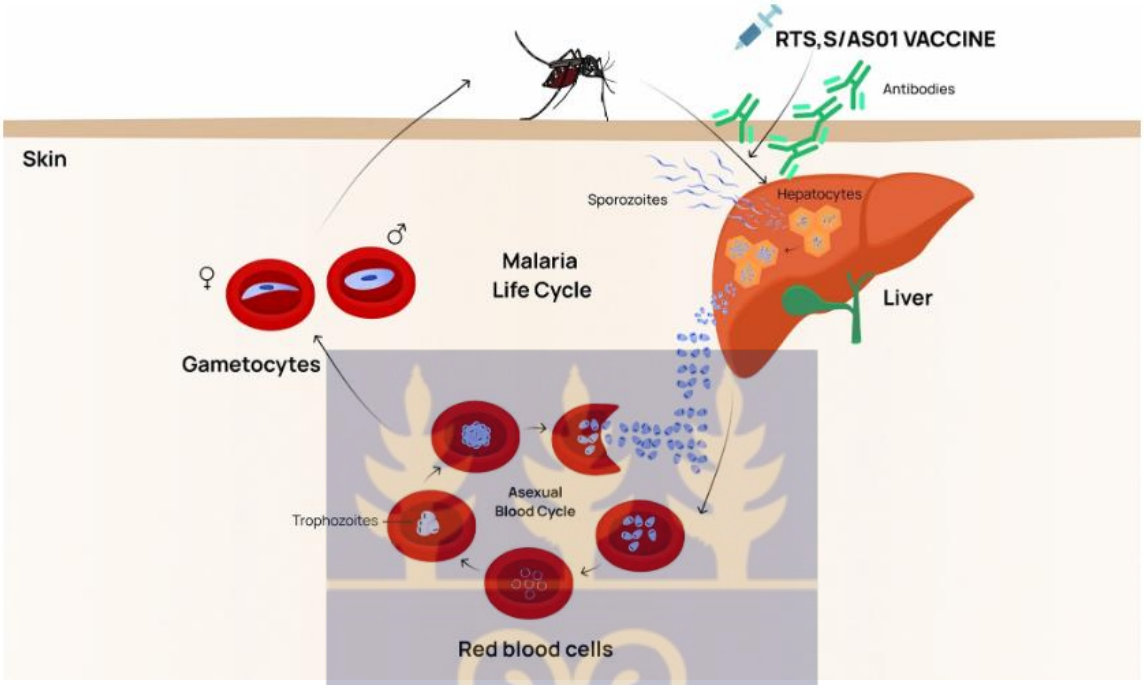


Figure1.2: Administration and interaction of RTS,S/AS01 with Plasmodium sporozoites [110].

1.3.2.2 R21/Matrix-M

R21/Matrix-M is an improved version of RTS, S/AS01 developed by the University of Oxford's Jenner Institute in collaboration with the Serum Institute of India and Novavax. The WHO recommended it in 2023 for use in children in malaria-endemic regions alongside RTS, S/AS01 [91].

The R21/Matrix-M addresses several limitations of its antecedent vaccine. It is enhanced with a higher circumsporozoite (CSP) antigen density. This stimulates a stronger immune response while inducing higher levels of anti-CSP antibodies, which are crucial for neutralizing *Plasmodium* sporozoites before they infect the liver [80, 86, 92]. It is also equipped with the more

University of Ghana http://ugspace.ug.edu.gh

potent saponin-based adjuvant, Matrix-M. R21/Matrix-M offers superior efficacy (~77 %) over 12 months, surpassing the WHO's malaria vaccine roadmap target of 75 % efficacy. Its lower production costs and higher manufacturing capacity make it more affordable and adaptable to large-scale production [93-95]. However, like RTS,S/AS01, it only targets the pre-erythrocytic stage of *P. falciparum*.

Ensuring sustained and efficient malaria control and elimination will require the development of vaccines with higher efficacies, capable of targeting additional species and diverse stages of the parasite's life cycle [96]. Alongside vaccination, interrupting malaria transmission through vector control is a vital complementary strategy for effective malaria control and elimination.

1.3.3 Vector Control

Interventions designed to reduce mosquito populations and prevent human contact with mosquitoes are critical to interrupting the malaria transmission cycle, thereby reducing malaria incidence and mortality. Conventional strategies towards malaria vector control are centred on Insecticide Treated Nets (ITNs), Indoor Residual Spraying (IRS), and Larval Source Management (LSM). Additional tools such as spatial repellents, attractive toxic sugar baits, mosquito sterilization, and genetic control techniques are being explored to complement the interventions mentioned above [97-99].

1.3.3.1 Insecticide Treated Nets (ITNs)

Since the early 2000s, ITNs have been a cornerstone of malaria vector control, significantly contributing to global declines in malaria morbidity and mortality. They are designed to pro-

University of Ghana http://ugspace.ug.edu.gh

tect against mosquito bites through a physical barrier, as well as to kill or repel mosquitoes attempting to cross the barrier through insecticide action [100].

ITNs are usually made from polyester, polyethylene, or polypropylene mesh fabric, coated or impregnated with an insecticide. Pyrethroids like Deltamethrin (**1.1)** and Permethrin (**1.2)** (**Figure 1.3**) are usually used as insecticides due to their low toxicity to humans and high efficacy against mosquitoes. While conventional ITNs require periodic re-treatment (usually 6-12 months), Long-Lasting Insecticide Nets (LLINs) are impregnated with insecticides during manufacture and designed to retain insecticide activity for at least 3 years or withstand 20 standard washes [101, 102].

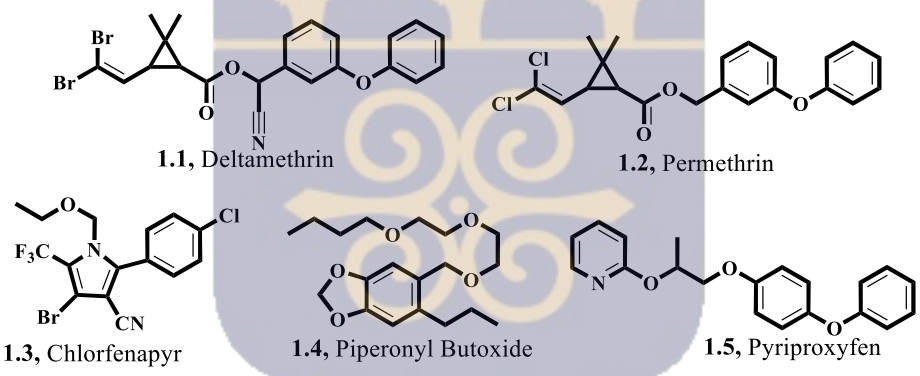


Figure 1.3: Insecticides used for ITNs and IRS.

Though simple, cost-effective, and highly effective, ITNs' protective effectiveness depends on their appropriate and continuous use by at-risk populations. Additionally, the propensity of nets to degrade over time and the growing resistance of mosquitoes to pyrethroids threaten their long-term efficacy [97, 103, 104]. Next-generation ITNs are therefore being explicitly explored to tackle pyrethroid resistance. In the production of these ITNs, a secondary chemical is combined with pyrethroid to improve the net's overall efficacy. More recently, the WHO has recommended three classes of next-generation ITNs: pyrethroid combined with

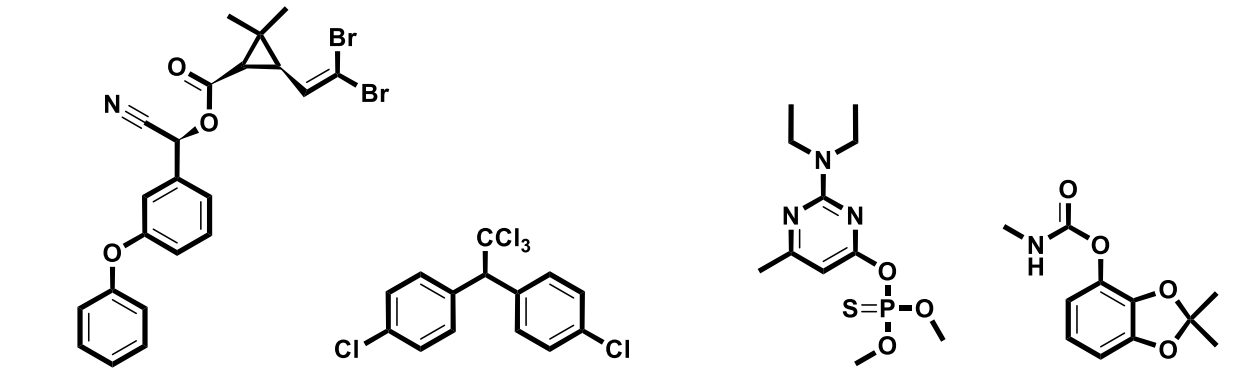
University of Ghana http://ugspace.ug.edu.gh

chlorfenapyr (CFP), 1.**3**; piperonyl butoxide (PBO), **1.4;** and Pyriproxyfen (PPF), **1.5 (Figure 1.3)**. These compounds are known to address pyrethroid resistance by inhibiting its metabolic degradation in malaria vectors [105].

1.3.3.2 Indoor Residual Spraying (IRS)

IRS targets a critical stage in the mosquito's life cycle: its resting period after feeding. Thus, likely places such as interior walls, ceilings, and other surfaces of homes and buildings where mosquitoes are likely to rest are sprayed with long-acting insecticides [106]. Mosquitoes that come into contact with these treated surfaces absorb a lethal dose of the insecticide which eventually kills them, disrupting their ability to transmit the *Plasmodium* parasite to the next victim. Factors such as the vector species involved, residual efficacy, cost, resistance patterns and environmental safety influence the choice of insecticides. Typical insecticides used for IRS include pyrethroids (deltamethrin, **1.6**), organophosphates (pyrimiphos-methyl, **1.8**), carbamates, (bendiocarb, **1.9**) and organochlorines (dichlorodiphenyltrichloroethane, **1.7**) (**Figure 1.4**) [107, 108].. Unfortunately, the sustained effectiveness of the of the insecticides mentioned above has been mainly undermined by the development of insecticide resistance, alongside environmental concerns such as persistent organic pollutants (POPs), bioaccumulation, and biomagnification within ecological food chains [109, 110]. To combat insecticide resistance, minimize toxicity, and alleviate the high operational costs associated with IRS, alternative insecticides and vector control strategies are being explored [106, 111].

University of Ghana http://ugspace.ug.edu.gh



1.6, Deltamethrin **1.7**, Dichlorodiphenyltrichloroethane **1.8**, Pyrimiphos-methyl **1.9**, Bendiocarb

Figure 1.4: Chemical structure of insecticides used for IRS.

1.3.3.3 Larval Source Management (LSM)

Larval Source Management is an intervention that targets habitats (mostly aquatic) where the mosquito larvae develop. By disrupting the mosquito maturation, its population density is significantly reduced, impeding the transmission cycle. This method is effective in urban and comparable settings where breeding sites are few and locatable [112].

The primary strategies by the WHO under LSM include;

- **Habitat Modification**: Permanent environmental changes such as draining, leveling or filling breeding sites [112].
- **Habitat Manipulation**: Temporary changes such as irrigation or water-level regulation to reduce larval habitats [113].
- **Larviciding**: Introducing chemicals (eg., Temephos, an organophosphate) or biological agents (eg., Baccillus sphaericus) to water bodies, to kill mosquito larvae [114].
- **Biological Control**: Releasing natural predators or microbial agents that feed on mosquito larvae [115].

University of Ghana http://ugspace.ug.edu.gh

Unlike other vector control methods, LSM affects both indoor and outdoor vector transmission, however, its requirement for regular cite identification and treatment makes it labour-intensive and logistically demanding. Additionally, its preference for urban-like areas and demand for trained personel, limit its application in endemic areas [116, 117].

1.3.3.4 Additional Vector Control Tools

Given limitations of ITNs, IRS, and LSM, more effective, complementary vector control methods must be developed and implemented to strengthen malaria control. The WHO Vector Control Advisory Group is considering **spatial repellents** as a public tool for malaria control. These interfere with the mosquito's host-finding continuously releasing volatile active ingredients *via* spatial emanators [118-120].

Attractive Toxic Sugar Baits (ATSB) also represent another promising tool for malaria vector control. Through a combination of sugar solution, alluring scents, and oral toxins, ATSB exploits mosquitoes' sugar-feeding behaviour to ingest a lethal substance, thereby reducing mosquito populations [121, 122]. This control method is suitable in areas where ITNs and IRS are less effective [122].

The Sterile Insect Technique (SIT) is also another new control tool being exploited to suppress mosquito populations [123]. In this approach, various strategies are employed to sterilize male mosquitoes [124, 125]. The sterilized mosquitoes are subsequently released into the environment where they mate with wild females resulting in no viable offspring [126]. This method offers a sustainable solution for long-term vector control. SIT falls within a broader spectrum of genetic innovations in malaria vector control [127]. Genetic control techniques rely on targeted genetic engineering to introduce heritable genetic changes in mosquitoes to reduce their populations or suppress their ability to transmit malaria. Genetic approaches in

University of Ghana http://ugspace.ug.edu.gh

vector control presents eco-friendly alternatives through their species-specific approaches, minimizing harm to non-target organisms [128-131].

While malaria vaccines and vector control interventions have substantially contributed to reductions in malaria incidence, their impact on malaria prevalence remains insufficient, particularly in high transmission zones. Where preventive measures are inadequate, effective case management and access to antimalarial drugs are crucial in reducing malaria morbidity and mortality. Against this backdrop, the importance of continued research and development in malaria therapeutics becomes increasingly evident [132, 133].

1.3.4 Antimalarial Drugs

Since the discovery of the malaria parasite in human blood in 1880 by French Physician Alphonse Laveran [134], and subsequent understanding of its transmission and life cycles in later years [135], research and development of malaria therapeutics have undergone transformative progress. From the traditional use of the cinchona bark and Qinghao in treating fevers, modern medicine derived two of the most effective antimalarial agents: Quinine (**1.10; Figure 1.5**), the first standard treatment [136], and artemisinin, **1.11**, the current backbone for malaria chemotherapy [137]. Between the use of quinine and artemisinin, knowledge of the synthetic and mechanism pathways of these and other existing drugs, led to the development and clinical use of 5 classes of potent antimalarials for first-line treatment. These are, 4-aminoquinolines, aminoalcohols, antifolates, hydronaphthoquinone and endoperoxides [138]. Unfortunately, efficacy of four of these classes has been compromised the emergence of drug-resistant *Plasmodium* strains. In the era of succumbing therapeutic agents to drug resistance, artemisinin has remained resilient and is currently the front-line drug with reliable therapeutic activity [139].

University of Ghana http://ugspace.ug.edu.gh

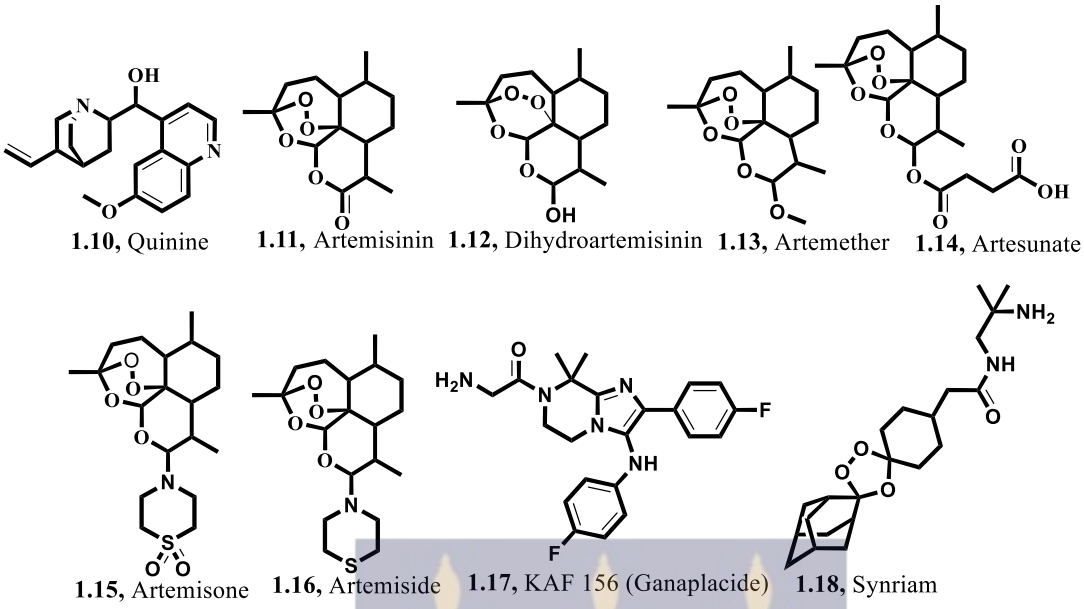


Figure 1. 5: Artemisinin and other potent antimalarial drugs for malaria chemotherapy.

1.3.4.1 Artemisinin and ACTs

Artemisinin is a colourless, crystalline sesquiterpene lactone that contains an endoperoxide bridge, which is responsible for its unique antimalarial action. It is a naturally derived compound, extracted from the Chinese sweet wormwood, *Artemisia annua* (Qinghaosu) [140, 141]. Due to seasoned agricultural production and inconsistencies in harvest, the supply and price of Artemisinin has been unsteady for the past decade. To meet the growing global demand, especially since it became a front-line therapeutic agent, researchers have successfully developed semi-synthetic Artemisinin for commercial production [142]. As the purity of natural artemisinin may vary based on the plant source and extraction process, semi-synthetic artemisinin offers a higher purity due to standardized control and processing [143]. However, both natural and semi-synthetic forms of artemisinin are poorly soluble in water and oil. This limits its solubility and bioavailability [144]. To address this and other associated problems, derivatives of artemisinin were synthesised. Artemisinin derivatives have improved solubilities, extended half-lives, and faster parasite clearance than artemisinin [145, 146]. Moreover,

University of Ghana http://ugspace.ug.edu.gh

the various artemisinin derivatives offer flexible routes of clinical administration. While di-hydroartemisinin, **1.12**, is preferred for oral formulations, artemether, **1.13,** and artesunate, **1.14**, are used for intravenous infusions and intramuscular injections, respectively [147-149].

Artemisinins are fast-acting antimalarial agents that target the asexual blood stages of the *Plasmodium* parasite (typically *P.falciparum*). They can rapidly reduce parasite biomass, within a short time, alleviating symptoms within 24 to 48 hours of initiation. For this reason, the efficacy of present-day antimalarial chemotherapy largely depends on Artemisinins. Due to their short half-lives however, their inability to completely eliminate all parasites poses a risk for treatment failure and drug resistance. Artemisinins are therefore used in combination with other drugs for the treatment of malaria in Artemisinin Combination Therapies (ACTs). Partner drugs (**Figure 1.6)** in these combination therapies eliminate any residual parasites that may persist following the rapid parasite clearance by Artemisinins. ACT combinations include Artemeter-lumefantrine (AL; popular in Africa), Artesunate-mefloquine (AS-MQ), Artesunate-amodiaquine (AS-AQ), Artesunate-piperaquine (DHA-PPQ), and Artesunate-sulfadoxine-pyrimethamine (AS-SP; used for prophylaxis in some regions). Since 2001, ACTs have been used as first-line treatment for uncomplicated *P. falciparum* infections as recommended by the WHO, and have been pivotal in reducing malaria infections and deaths [150-152].

University of Ghana http://ugspace.ug.edu.gh

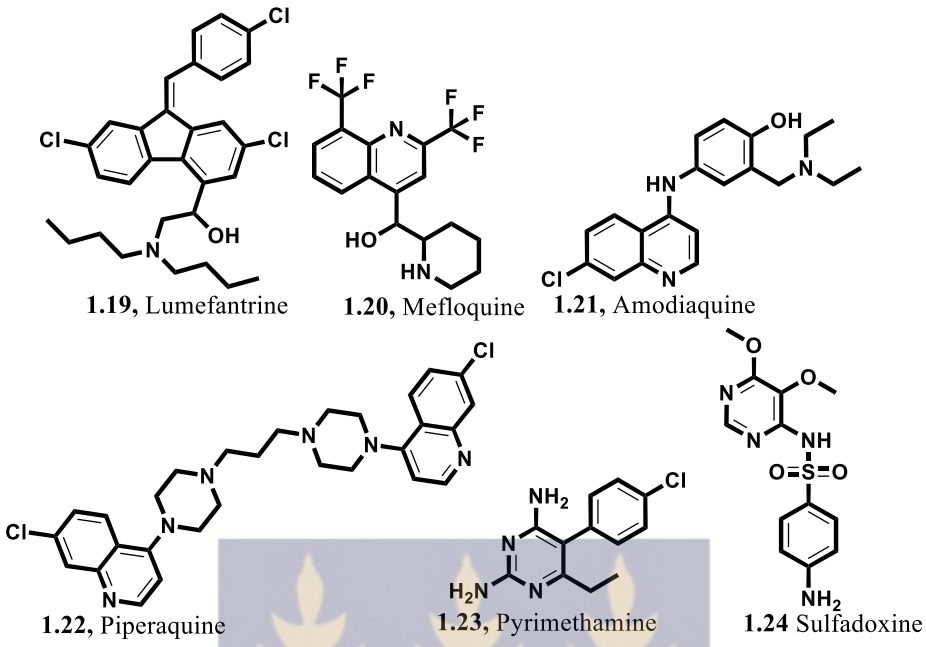


Figure 1. 6: Partner drugs used in ACTs.

Nonetheless, reports of growing resistance commencing from the Greater Mekong sub-region (South East Asia) and now emerging in parts of Africa pose a threat to the clinical efficacy of the current mainstay for malaria treatment [153-155]. Artemisinin drug resistance is reportedly linked to mutations in the kelch-13 propeller protein of *P. falciparum* and other pathways [156]. Prediction studies indicate an alarming speed of the spread of artemisinin resistance across Africa (the most endemic malaria zone) (**Figure 1.7**) if the situation is left unchecked [157-159]. There is therefore a need for continued research into alternative antimalarials to stay ahead of the evolving parasite.

University of Ghana http://ugspace.ug.edu.gh

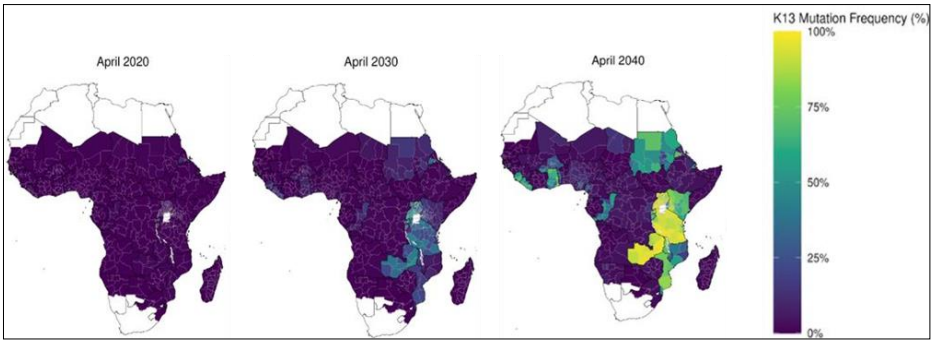


Figure 1.7: A prediction study by Watson et al. on the spread of Kelch-13 mutations of *P. falciparum* across the African continent up to April 2040 [185].

1.4 Drug Discovery

In the on-going race against drug resistance, drug discovery has been very critical in global malaria control and elimination. Knowledge from modern medicinal chemistry, pharmacology, and genomics contributes to strategies to tackle drug resistance.

Two complementary approaches at the front line of drug discovery are Phenotypic Screening (PS) and Target-Based Screening (TBS) [160]. While PS involves the screening of compound libraries directly on whole organisms, parasites, and cells for a desired biological effect, TBS identifies compounds based on their ability to bind or inhibit a biologically validated molecular target (**Figure 1.8**). The advantages and disadvantages of these approaches are further discussed in section **2.5** of **Chapter 2** of this thesis. Among the two, PS holds a greater potential for identifying molecules with novel mechanisms of action. This is particularly significant to tackling drug resistance since resistant pathogens will not be familiar with these novel modes of action, hence succumb to their therapeutic influence.

University of Ghana http://ugspace.ug.edu.gh

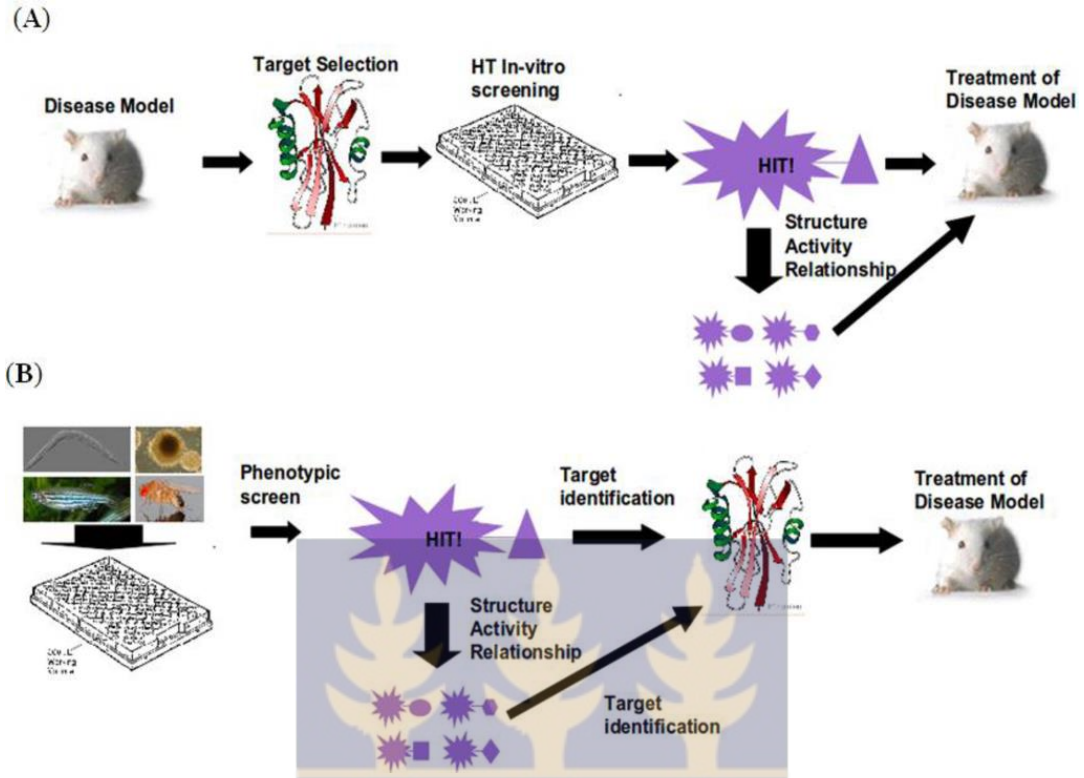


Figure 1.8: A graphical comparison between phenotypic (B) and target-based (A) drug discovery [195].

The historical therapeutic successes of quinine, chloroquine and artemisinin, discovered through PS [161] have influenced the reliance of modern malaria research on PS as a first line of discovery for identifying hits with strong parasite killing activity. Target validation studies (target deconvolution) then follow to rationally refine these compounds [162, 163]. Examples of clinically used drugs identified through PS are showed in **Figure 1.9**, with their respective therapeutic activities.

University of Ghana http://ugspace.ug.edu.gh

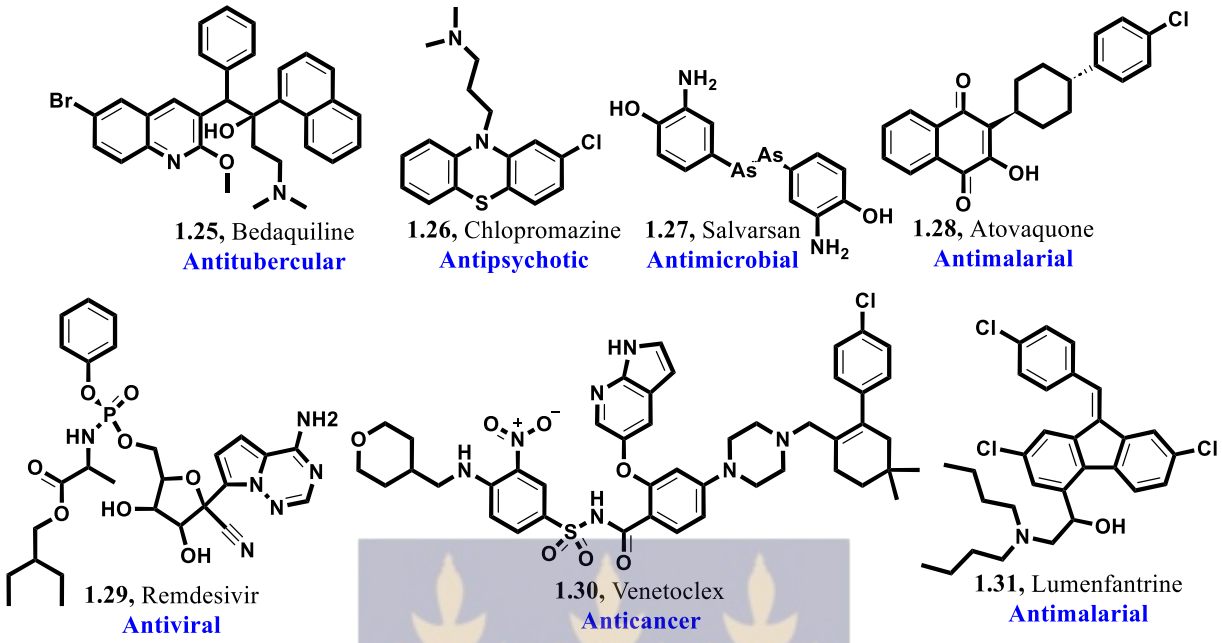


Figure 1.9: Examples of clinically used drugs identified through PS and their therapeutic functions.

With empirical healers and herbalists at the forefront of early PS, contemporary PS is dependent on the joint efforts of several scientists including biologists, pharmacologists, medicinal chemists, biochemists, High Throughput specialists and data scientists. Organisations such as the Medicines for Malaria Ventures (MMV) have formed strong collaborations with these scientists in advancing phenotypic hits into viable drug candidates [164, 165].

1.4.1 MMV and the Malaria Boxes

MMV is a public-private partnership dedicated to the discovery, development, and delivery of new and innovative antimalarial drugs and treatment [166]. The organization has been instrumental in the advancing ACTs and potent antimalarial candidates including piperaquine, **1.22**, Lumefantrine **1.19** (**Figure 1.6**), Ganaplacide, **1.17** and Synriam, **1.18** (**Figure 1.5**). Bridging the gap between early-stage drug discovery and clinical application, MMV works

University of Ghana http://ugspace.ug.edu.gh

jointly with academic institutions, pharmaceutical companies and non-profit organizations, to accelerate malaria drug discovery [167, 168]. With a core mission to combat antimalarial drug resistance, MMV utilizes phenotypic screening, leveraging its diverse boxes, to identify novel compounds with potentially diverse mechanisms, aimed at overcoming resistant pathogens [169].

Among the MMV boxes, the pathogen box was strategically curated to accelerate drug discovery for neglected tropical diseases including malaria. Built on the success of the malaria box, the pathogen box broadened its scope to a range of neglected tropical diseases, while retaining its relevance in identifying novel leads against *Plasmodium.* It is a library of 400 drug-like compounds pre-screened against a range of pathogens responsible for malaria and most of the world's Neglected Tropical Diseases (NTDs). Compounds in the Pathogen Box are derived from natural products, synthetic molecules, and previously failed drug candidates. This provides a diversity of mechanisms, essential for overcoming the resistance mechanisms of the involved pathogens. The Pathogen Box is a valuable tool to the scientific community, accelerating drug discovery and fostering an efficient drug discovery ecosystem facilitating of partnerships with research, clinical, and manufacturing institutions [170]. MMV presently maintains its support for drug discovery research through its Pandemic Response and Global Health Priority Boxes [171, 172].

1.4.1.1 Selected Lead Scaffolds from the MMV Pathogen Box

Two chemical scaffolds from the MMV pathogen box; MMV676444 and MMV1794959 (**Figure 1.10**), are the core focus of this study. While both scaffolds offer significant antimalarial potency, their distinct structural motifs and respective profiles offer opportunities for further optimization through a systematic SAR (Structure Activity Relationship) study to ac-

University of Ghana http://ugspace.ug.edu.gh

cess a lead compound with improved potency and more desirable drug-like properties. In addition to its reported potency against malaria, records for MMV676444 indicated some promising antitubercular potential [173]. Analagues of this scaffold could therefore have improved potency against TB.

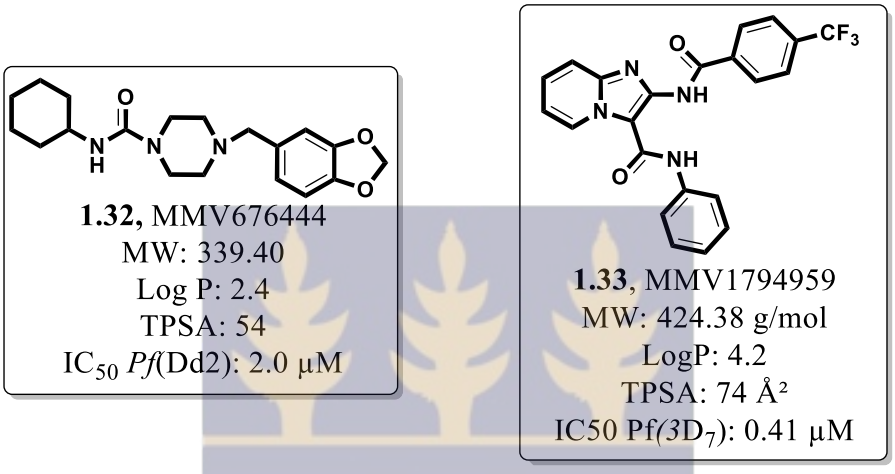


Figure 1.10: Chemical Structures of MMV676444 and MMV1794959.

The causative agent of TB; *Mycobacterium tuberculosis* (*Mtb*) have the ability to live and replicate inside alveola macrophages [174]. Macrophages act as a first line of defence for the immune system, engulfing and digesting foreign substances and pathogens through a process known as phagosome maturation. Here, the engulfed pathogen is trapped into a bubble (phagosome) which increasingly becomes acidic and eventually fuses with digestive acid and enzymes located in the lysosomes of the pathogen. The combined bubble (phagolysome) eventually destroys the pathogen through a multi-pronged strategy involving acidification, oxidative stress and enzymatic degradation [175]. However *Mtb* strategically prevents the fusion of its lysosomes with phagosome, preventing acidification and creating a more neutral environment for its growth and replication. This explains why *Mtb* can persist in the host for a long time (it is trapped inside phagosmes, away from circulating antibodies in the blood-

University of Ghana http://ugspace.ug.edu.gh

stream) [174, 176]. Similar to *Mtb*, other pathogens like *Leishmania* have also evolved to survive inside macrophages. It is therefore likely that a scaffold with efficacy against Mtb could cross the macrophage membrane to reach these pathogens [177]. Additionally, coming from a phenotypic screen with an added advantage of interacting with multiple targets, making it a potential multi-disease candidate, MMV676444 and its analogues, could possess additional leishmanicidal properties. This therefore provides a compelling rationale to extend the therapeutic evaluation of MMV676444 to Leishmania.

A detailed discussion of MMV676444 and MMV1794959 is provided in **2.7** of **Chapter 2** of this thesis.

1.5 Problem Statement

Malaria remains a major global health challenge despite several advances in the development of tools and strategies for its control and eradication. Prominent among the obstacles hindering progress in malaria elimination is drug resistance [178]. Of the five drug classes that have been consistently used as frontline therapeutic agents against malaria for several years, only the Artemisinins remain the most potent antimalarials, especially against *P.falciparum* infections (the most prevalent malaria infection in endemic zones). Due to drug resistance, the clinical efficacy of other drug classes has been compromised [179]. With the onset of artemisinin resistance in South East Asia, and its spread to some African countries, studies predict a faster rate of spread, with associated treatment failures across endemic zones over time [157, 180, 181]. It is therefore imperative that immediate action be taken to disrupt the parasite's resistance mechanisms. One such way is the introduction of new drugs with novel mechanisms of action unfamiliar to these pathogens.

University of Ghana http://ugspace.ug.edu.gh

1.6 Justification

Phenotypic screening is an essential tool in drug discovery that can of yield first-in-class drugs (drugs with novel mechanisms of action) [182]. From the early discoveries of quinine, chloroquine, **1.34** (**Figure 1.11**), and artemisinin to the current discoveries of OZ439, **1.35,** KAE 609, **1.36**, and MMV390048, **1.37**, PS has consistently yielded potent antiplasmodial drug candidates whose mechanisms of action were unknown at the time of discovery [161].

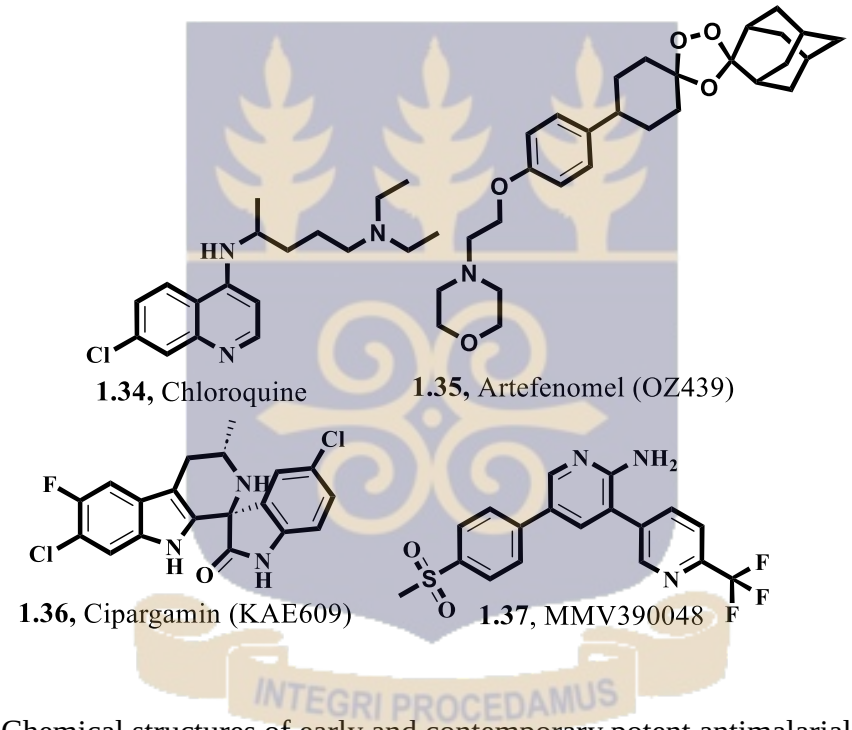


Figure 1.11: Chemical structures of early and contemporary potent antimalarials.

With drug resistance as a significant challenge confronting global progress towards malaria control and elimination, the indispensable role of phenotypic screening in identifying chemo-types with novel mechanisms of action cannot be overemphasized [183].

Synthesis and optimization of small molecules from phenotypic screens is therefore, a critical avenue for advancing malaria drug discovery research in addressing the urgent need for new

University of Ghana http://ugspace.ug.edu.gh

drugs with novel mechanisms of action to offset the resistance mechanisms of the involved pathogens.

1.7 Hypothesis

The optimization and further development of scaffolds from phenotypic screens such as the MMV pathogen box could potentially yield analogues with improved antimalarial activity, enhanced selectivities, favourable drug-like properties and most importantly novel mechanisms of action, making them suitable for further pre-clinical development into drug candidates to combat malaria drug resistance.

1.8 Research Aim and Objectives

This research aims to design, synthesize, and characterize analogues of two scaffolds from phenotypic screens: MMV676444, **1.32** and MMV1794959, **1.33** (**Figure 1.10**). Analogues from the scaffolds would be optimized, screened, and evaluated for their antimalarial properties.

Objectives of the study are to:

- Re-synthesise and re-evaluate the scaffolds for their antimalarial blood-stage activity
- Optimize the scaffolds through the design and synthesis of chemical derivatives,
- Evaluate MMV676444 as a multi-pathogen hit against TB and leishmaniasis.
- Profile the synthesized analogues of MMV1794959 for their antimalarial blood stage activities.
- Profile lead candidates for their *in vitro* DMPK properties.

University of Ghana http://ugspace.ug.edu.gh

CHAPTER TWO

2.0 Literature Review

2.1 Introduction

Having established the necessity for renewed efforts towards malaria elimination, the discovery and development of new therapeutic agents with novel mechanisms of action is critical in addressing the growing resistance of the Plasmodium parasite. It is worthy noting that a broader comprehension of the complex mechanisms underlying the parasite's activity and its evolving resistance to existing drugs is crucial to the development of more potent antimalarials, capable of circumventing known resistance pathways.

This chapter provides an overview of major collaborative global initiatives that have played, and continue to play, an important role in advancing the long-term goal of malaria elimination. Also, the life cycle of the malaria parasite, highlighting critical stages most amendable to antimalarial drug action is discussed. Additionally, modes of action of existing antimalarials are reviewed, shedding light on how they disrupt parasite development and survival, as well as the mechanisms by which the parasite has acquired resistance. Finally, advances in Phenotypic Screening (PS) and Target-Base (TBS) in advancing small molecules to next-generation antimalarials are explored, highlighting prominent examples that have shown promise and are in advanced stages of the drug discovery pipeline.

2.2 Global Initiatives and Progress

For over two decades, consistent coordinated efforts, funding and policy implementation, have averted over 1.5 billion malaria cases, saving 7.6 million lives [184]. These initiatives,

University of Ghana http://ugspace.ug.edu.gh

including 'Roll Back Malaria', the 'President's Malaria Initiative', 'Malaria No More', etc., were carried out through joint efforts by national governments and international organizations.

2.2.1 Roll Back Malaria Partnership

The Roll Back Malaria partnership (RBM) is among the early campaigns to eliminate malaria. Established in 1998 through joint efforts among the WHO, UNICEF, UNDP and the World Bank, it provided guidance and support, partnering with governments, the private sector, civil society and NGOs to halve malaria deaths by 2010. RBM played a critical role in prioritizing malaria in global and national agendas, improved access to interventions such as Rapid Diagnostic Test (RDT) kits, Artemisinin-based Combination Therapies (ACT) and Insecticide Treated Nets (ITN), as well as increased international funding for control and prevention programmes [185-187]. However, amid an escalating malaria burden, the RBM campaign appeared to achieve only limited success [188]. Further interventions were therefore required to achieve sustainable disease control and prevention.

2.2.2 The Global Fund to fight AIDS, TB and malaria

In 2002, in response to a global health crisis caused by these diseases, the Global Fund to fight AIDS, TB, and malaria was established by various organisations, including the WHO, the World Bank, and the Bill & Melinda Gates Foundation. It operates independently, issuing grants to nations to improve healthcare quality and reduce disparities in the respective disease areas. Contributions toward the fund primarily come from the US, UK, and France. The fund has been immensely beneficial in supporting and distributing ITNs, ACTs, and malaria RDT kits, and has saved over 65 million lives through its campaigns [189, 190].

University of Ghana http://ugspace.ug.edu.gh

2.2.3 The President's Malaria Initiative

Established in 2005 by the US government, the President's Malaria Initiative (PMI) aimed to reduce malaria morbidity and mortality, especially in endemic regions. Partnering with other initiatives such as RBM and the Global Fund to fight AIDS, TB, and Malaria, PMI has expanded its reach beyond a handful of high-burden countries to over 27 endemic nations. Benefits bestowed by this initiative include increased access to similar interventions provided by the RBM, strengthened communities and health systems through education and training on malaria prevention tools, and enhanced surveillance systems for tracking malaria incidence [191-193].

2.2.4 Global Malaria Programme

The Global Malaria Programme (GMP) is the WHO's principal coordinating body for malaria control and elimination. It is primarily focused on global malaria prevention and elimination, with a strong interest in endemic regions, on maintaining sustainable control measures. A unique feature of this initiative is its evidence-based blueprint, which highlights long-term frameworks such as the Global Technical Strategy for Malaria 2016-2030 [194].

Objectives of the Global Technical Strategy for Malaria 2016-2030 focus on: worldwide access to treatment and prevention tools, refinement of malaria surveillance, optimization of elimination strategies, and acceleration of innovation in malaria research. By 2030, this initiative targets to reduce morbidity and mortality by 90%, eradicate malaria in more than 35 countries, prevent a resurgence of malaria cases in malaria-free states, and drastically mitigate malaria burden in endemic regions. To achieve these targets, the GMP channels show keen interest in research and innovation to discover new preventive tools and alternatives for malaria treatment [195, 196].

University of Ghana http://ugspace.ug.edu.gh

2.2.5 'Malaria no more'.

The 'malaria no more' initiative has been instrumental in fostering political engagement, funding, and innovation towards malaria eradication. The core strategies of this initiative focus on advocacy and political engagement, innovative financing, and advanced technology to improve malaria surveillance and response systems. Through this initiative, political leaders raised a historic $4.1 billion in 2018 to combat malaria. Also in Nigeria, the leading contributor among the four African countries responsible for half of global malaria mortality, the Malaria No More initiative has been pivotal in promoting innovative methods for malaria diagnosis and treatment [197-199].

2.2.6 African Leaders Malaria Alliance

In 2009, a coalition of African leaders established the African Leaders Malaria Alliance (ALMA) to foster coordinated action and unified accountability in the fight against malaria. Similar to earlier discussed initiatives, ALMA was inaugurated to accelerate high-level political will and fund mobilisation towards data-driven decision making in addressing malaria and has been crucial in the establishment of 'End malaria councils' [200-202] across various African countries.

2.2.7 End Malaria Council (EMC)

Initially launched globally in 2017 and spearheaded by notable global health advocates, the EMC was established to mobilize domestic resources and political will for malaria elimination through national councils in malaria-endemic countries [203]. With support from ALMA, endemic countries such as Zambia, Kenya, Eswatini, Mozambique, Uganda and more recently, Nigeria have established the council to address specific challenges to their progress to-

University of Ghana http://ugspace.ug.edu.gh

ward malaria eradication. Fortunately, this initiative has significantly accelerated progress in these countries' efforts to tackle the disease [202, 204].

2.2.8 E-2025 Initiative

A strategic plan by the WHO to eliminate malaria in 25 countries by the year 2025, led to the E-2025 initiative. This is a continuation of an earlier initiative; E-2020, which targeted malaria elimination in 21 countries between 2017-2020 [205, 206]. The beneficiary countries under the initiative were selected based on low malaria transmission and strong political commitment, placing them in a better position to achieve zero indigenous cases by the end of the period. However, progress in some countries stalled, especially as health systems were overwhelmed by the demands of the COVID-19 pandemic [207]. In 2021, the list was revised based on a country's malaria burden, elimination readiness and progress achieved during the E-2020 phase, leading to the new E-2025 initiative. The core objectives of the E-2025 initiative are to provide technical support, strengthen malaria surveillance, promote cross-border collaboration, and mobilize political, financial, and community commitment towards malaria elimination. Of the 36 unique countries benefiting from both initiatives, only 8 are from Africa: Algeria (certified malaria-free in 2019), Botswana, South Africa, Cape Verde (certified malaria-free in 2024), Eswatini, Comoros, the Republic of Congo, and Namibia. The combined initiatives have resulted in at least eight countries attaining malaria-free certifications, with the most recent being Egypt (October 2024), Cape Verde (January 2024), Belize (June 2023) [18] and Georgia (January 2025) [208]. This raises the WHO's global tally of officially certified malaria-free states to 44 [209].

The global fight against malaria, driven by collective efforts from organisations, initiatives, governments, etc., has undoubtedly spurred significant progress toward elimination, with

University of Ghana http://ugspace.ug.edu.gh

documented evidence of substantial economic and socioeconomic growth in countries that have succeeded in reducing or eliminating malaria incidence [68]. However, achieving long-term, sustainable control ultimately relies on continued investment in research and development (R&D). Scientific innovation in malaria diagnostics, therapeutics, and vaccine development is essential to address emerging challenges, such as drug and insecticide resistance.

2.3 Etiological Agent of Malaria

The causative organism responsible for malaria is a protozoan parasite of the genus *Plasmodium* within the phylum Apicomplexa [210, 211]. It was first recognised as the etiological agent of malaria in 1880 by Charles Louis Alphonse Laveran [134] and has since been the subject of extensive investigations, especially to understand its pathogenesis. Malaria is transmitted to humans by the bites of infected female *Anopheles* mosquitoes. The life cycle of *Plasmodium* (**Figure 2.1**) requires a vertebrate host, where asexual replication occurs after sexual reproduction in the mosquito vector [212].

2.3.1 Life cycle of the *Plasmodium* parasite.

When the *Anopheles* mosquito bites a human, **sporozoites** are injected into the bloodstream. Within an hour of injection, the sporozoites migrate into the liver, invade hepatocytes and undergo an asexual **exoerythrocytic schizogonic cycle** (liver stage) [213, 214]. Here, a multinucleated **schizont** forms, ruptures, and releases a host of **merozoites** into liver sinuzoids. The exoerythrocytic schizogonic cycle, though clinically silent, is essential for establishing infection [211].

University of Ghana http://ugspace.ug.edu.gh

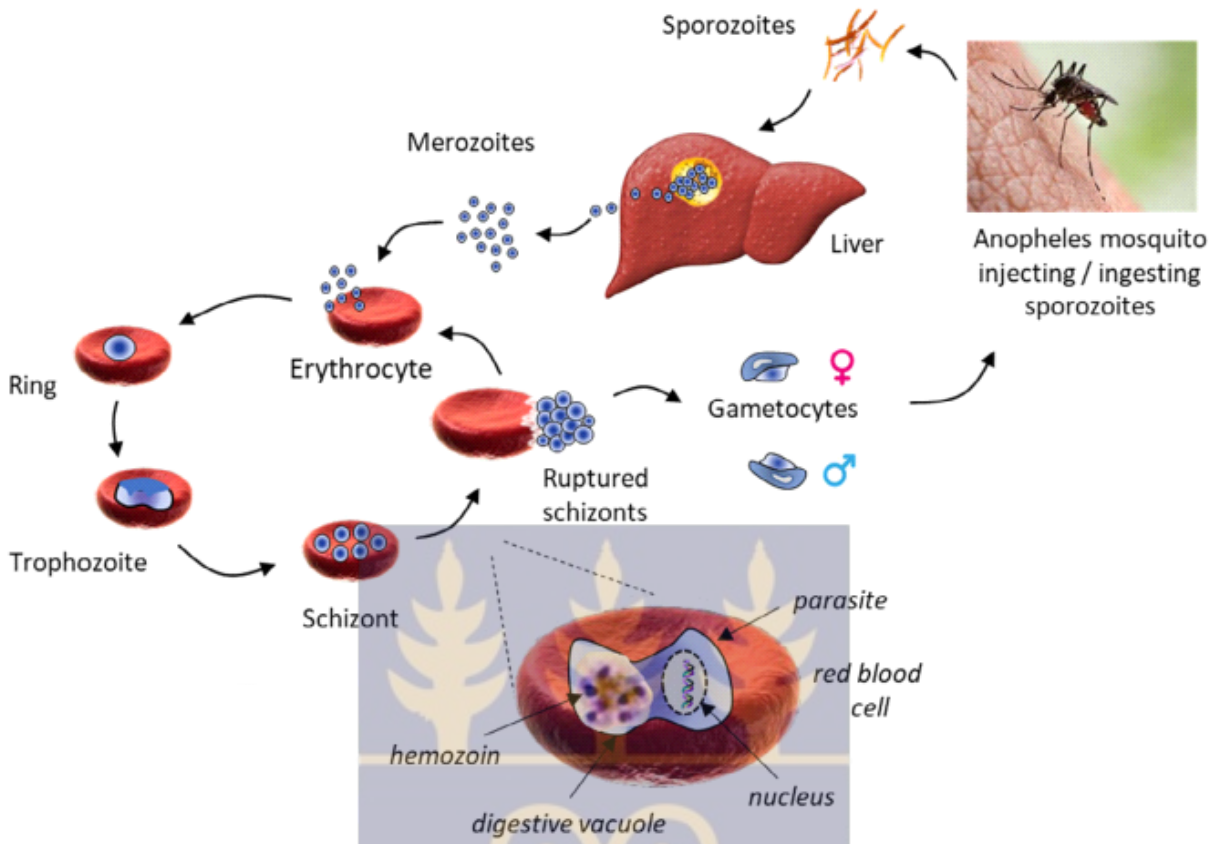


Figure 2.1: Life cycle of the Plasmodium parasite [7].

The liver stage is followed by the **erythrocytic schizony cycle** (blood stage), during which the released merozoites swiftly invade an erythrocyte and transform into a ring form (commonly seen in blood smears for malaria diagnosis). During the **ring stage**, the parasite is relatively inactive as it prepares for growth. It then undergoes a series of developments in the **trophozoite stage** shortly thereafter, actively feeding on haemoglobin, and losing its ring-like shape [215]. As the parasite digests haemoglobin, it releases amino acids, (essential for its growth) and free heme (ferriprotoporphyrin IX). Free heme is a lipophilic and redox-active by-product of haemoglobin digestion, which intercalates into lipid membranes, forms reactive oxygen species (ROS), and disrupts parasite organelles, leading to oxidative stress and membrane destabilization, ultimately compromising cell viability. The build-up of free heme in

University of Ghana http://ugspace.ug.edu.gh

the malaria parasite is therefore consequently fatal to its survival. To counter the toxic effects of free heme, the plasmodium parasite bio-crystallizes free heme into an inert **hemozoin**, also known as malaria pigment [216]. This heme detoxification pathway is a vulnerable aspect of the parasite's metabolism, and many classic and modern antimalarial drugs exploit it [217]. Its absence in humans makes it an ideal selective drug target. Additionally, hemozoin can be detected in blood smears as a dark brown or black granular pigment. Its presence provides additional evidence of infection, and is currently being evaluated as a diagnostic biomarker for malaria [218].

The trophozoite stage is the most metabolically active and destructive stage of the parasite. The parasite becomes more visible and motile, often occupying a larger portion of the erythrocyte. Development and nuclear divisions continue until a desired number of merozoites is achieved, (depending on the species involved), ending the schizogonic cycle [219, 220]. The **schizont stage** follows, typically characterised by the rupture of red blood cells, releasing merozoites and toxic debris (free heme, parasite waste, and proteins) into the blood stream. New erythrocytes are consequently invaded, and the cycle is repeated until an effective therapeutic intervention or sufficient immune response is achieved [214, 221]. The release of merozoites and toxic debris into the bloodstream triggers a strong host immune response, leading to the hallmark clinical symptoms of malaria (fever, chills, headache, etc.) [222].

A fraction of merozoites mature into **gametocytes**: the sexual forms of the *Plasmodium* parasite responsible for malaria transmission. These exist in male (microgametocytes) and female (macrogametocytes) forms and are ingested alongside the blood when another mosquito feeds on an infected individual.

University of Ghana http://ugspace.ug.edu.gh

Inside the mosquito's gut, the microgametocyte and macrogametocyte mature into gametes (sperm and egg cells) and fuse to form a **diploid zygote**. The zygote matures into a motile **ookinete,** which penetrates the mosquito's gut wall and develops into **oocysts**. Oocysts birth thousands of sporozoites which travel to the mosquito's salivary glands to initiate a new cycle [221, 223, 224].

The above-described cycle is conserved across the *Plasmodium* genus [225]. However, each species exhibits notable variations which are elaborated on in the subsequent paragraphs.

2.3.2 Plasmodium Parasites Responsible for Human Malaria.

More than 150 species of the Plasmodium genus are known; however, human malaria is caused by five species: *P. falciparum, P. vivax, P. knowlesi, P. oval* and *P. malariae*. Each of the five species responsible for human malaria possesses distinct characteristics that influence the severity and progression of the disease [226]. For example, the length of the schizogonic cycle in the liver varies for each species. Similarly, the quantity of merozoites released at the end of each cycle also differs across the species [211, 214].

2.3.2.1 *Plasmodium falciparum*

Among the species responsible for human malaria, *P. falciparum* is the most lethal. Its infections are pre-dominant in sub-Saharan Africa, Southeast Asia and other parts of South America, and are responsible for over 90 % of the global malaria mortality [33, 34, 223, 226].

The life cycle of *P. falciparum* differs from other species in its liver and erythrocyte stages, as well as gametocyte development. Despite having the shortest exoerythrocytic schizogonic cycle (5.5 days), *P. falciparum* produces as many as 30,000 merozoites (the highest number among the species) per cycle. The erythrocyte stage lasts approximately 48 hours and occurs

University of Ghana http://ugspace.ug.edu.gh

in red blood cells of all ages, characterized by aggressive replication that results in very high parasitic loads, thereby, increasing the risk of anaemia and blood clot formation. There is also a high risk of cerebral malaria with these infections due to the sequestration of mature infected Red Blood Cells (RBCs) in small blood vessels [227-229]. Symptoms of the disease usually manifest 9-14 days after infection and can quickly escalate to complications with delayed treatment [34]. Unlike the other four species which possess a round morphological structure, and take longer (7-15 days) to mature. Additionally, the formation of gametocytes is initiated only after multiple cycles of asexual reproduction, unlike in other species where gametocytes are produced continuously [223].

The global dominance of *P. falciparum* infections, its aggressive replication in red blood cells, and its tendency to escalate rapidly demand strategic interventions to combat malaria.

2.3.2.2 *Plasmodium Vivax*

P. vivax is the most ubiquitous among the species. Although less endemic in sub-Saharan Africa, it is a significant contributor to the malaria burden in tropical and sub-tropical regions, including South-East Asia, South Asia, Central and South America. It contributes 30-40 % of the global malaria infections [34, 230, 231].

P. vivax presents an intricate life cycle, owing to its multiple stages with unique characteristics in both vector and host, and its famous hypnozoite stage, which is primarily responsible for triggering relapses. Liver schizogony usually lasts for eight (8) days and yields nearly 10,000 merozoites at the end of the cycle [229, 230, 232]. Inside the hepatocytes, not all sporozoites mature into schizonts. Some persist as dormant hypnozoites, which resume development when activated. While the mechanism of reactivation remains anunresolved controversy, discussions oscillate between parasite biology and host-related factors [230, 233, 234].

University of Ghana http://ugspace.ug.edu.gh

Similar to *P. falciparum*, the erythrocyte stage lasts 48 hours, producing fewer merozoites (24) than the former (36) [214]. *P. vivax* prefers reticulocytes (immature red blood cells), which are less abundant and therefore characterized by low parasitaemia. Milder clinical symptoms are consequently observed (12 to 17 days) with minimised opportunities for disease progression. In addition to its hypnozoite reservoir, the ability of *P.* vivax's ability to rapidly produce gametocytes (as early as 2 days post-infection) enhances its potential for broader distribution, as the disease is transmitted long before any symptomatic manifestations [233].

P. vivax infections may present a façade of mildness in compared to *P. falciparum* infections. However, the attributes mentioned above highlight a range of factors that complicate the control and elimination of malaria. This is evidenced in its reputation as the most geographically widespread human malaria parasite, with reports of significant morbidity, including respiratory distress and splenomegaly. Furthermore, reports of its asymptomatic nature in endemic regions warrant the same level of attention as that given to more clinically severe species [235-237].

2.3.2.3 *Plasmodium Ovale*

P. ovale shares some similarities with *P. vivax*, though it is less prevalent and less studied. Its predominance overlaps with endemic regions of *P. falciparum* with records documented across sub-Saharan Africa, the Western Pacific Islands, and Southeast Asia [238-240].

Like *P. vivax*, *P. ovale* prefers reticulocytes, forms hypnozoites, and exhibits mild to moderate symptoms. However, it has a more extended latency period and fewer relapses of less frequent relapses [241-243]. Both species also exhibit a comparable durations of the liver schizogony cycle, and similar amounts numbers of merozoites at the end of the cycle. They are

University of Ghana http://ugspace.ug.edu.gh

also characterised by tertian fever, a 48-hour fever pattern associated with the erythrocytic schizogony cycle [244, 245].

The persistence of *P. ovale* in highly endemic regions, coupled with its ability to cause relapses, makes it a clinically significant contributor to the global malaria burden, and therefore requires strategic treatment and continued surveillance efforts [246].

2.3.2.4 *Plasmodium malariae*

P. malariae is also referred to as the quartan malaria parasite of humans. It is comparatively less prevalent and has a more restricted geographical distribution than the previously discussed species, with infections primarily in sub-Saharan Africa, Southeast Asia and South America. Its infections are characterised by immune invasion, relapse-like persistence, and low-grade inflammation [247, 248].

P. malariae has the slowest erythrocytic cycle (~72 hours). The extended cycle duration results in a reduced rate of merozoite production, consequently leading to low parasitaemia. Although it does not form hypnozoites, *P. malariae* can persist in low-level parasitaemia without triggering a profound immune response for a very long period (years to decades) [247, 249, 250]. This also impedes timely diagnosis, contributing to subclinical or cryptic transmission because the parasite persists in the host [245, 246].

Long-term organ damage, prolonged illness, and immune exhaustion from extended exposure of *P. malariae* to the host are substantial concerns that necessitate prudence in its detection and eradication.

University of Ghana http://ugspace.ug.edu.gh

2.3.2.5 *Plasmodium Knowlesi*

Until early 2004, *Plasmodium Knowlesi* was only known to infect non-human primates**,** particularly long-tailed macaques. A rise in urbanization and deforestation, however, caused an increase in human-primate interactions, immensely contributing to its recognition as the 5th *Plasmodium* species responsible for human malaria. *P. knowlesi* is currently recognised as a zoonotic malaria parasite prevalent in Southeast Asia, notably in the rural and forested regions of Thailand, Indonesia, Myanmar and Malaysia [30, 251-253].

P. knowlesi has the fastest erythrocytic cycle among human *Plasmodia*. The 24-hour cycle occurs in red blood cells of all ages, increasing the number of cells available for parasite replication. This consequently affects the number of merozoites produced per cell (8-12), leading to high parasitaemia. *P. knowlesi* malaria typically presents quotidian fever in addition to the common symptoms of malaria and can swiftly escalate into severe malaria [33, 252].

With the ongoing overlap of human and primate habitats, there are growing concerns about the possible adaptation of *P. knowlesi* towards humans. Its rapid erythrocyte cycle potentially leading to clinical deterioration characterised by multi-organ failure as evidenced in endemic regions [254], endangers the effectiveness of malaria control initiatives.

Advances in the understanding the *Plasmodium* parasite's life cycle have influenced and guided the discovery and use of various antimalarial drugs. Existing drugs target different species of *Plasmodium* and multiple stages of its cycle.

2.4 Existing antimalarial drug classes

Between the early use of quinine and chloroquine and the widespread adoption of Artemisinin Combination Therapy (ACTs), several drugs have saved lives and shaped malaria treat-

University of Ghana http://ugspace.ug.edu.gh

ment protocols [255]. Five core antimalarial drug classes have historically served as front-line antimalarial therapies. These are: Antifolates, Aminoalcohols, 4-Aminoquinolines, Hydroxynapthoquones, and Endoperoxides [138]. Each of these drug classes targets various forms of malaria and serves a range of clinical applications. Beyond these principal classes, however, other agents, notably, 8-aminoquinolines and selected antibiotics have played supporting roles [256, 257]. 8-Aminoquinolines represented by primaquine, **2.1 (Figure 2.2)** and tafenoquine, **2.2** are indispensable for eliminating dormant hypnozoites of *P. vivax* and *P. ovale*, as well as exerting potent gametocytocidal effects on *P. falciparum* to block transmission [258]. On the other hand, antibiotics, Doxycycline, **2.3,** Clindamycin, **2.4** and Azithromycin, **2.5** are employed as adjunctive and context-specific agents. These are used in combination with antimalarials, such as quinine, for malaria treatment, particularly in regions with limited drug options [259]. Additionally, **2.3** and **2.4** are recommended for treatment in vulnerable populations and for prophylaxis in travellers to endemic areas respectively [260, 261]. With these complementary agents acknowledged, the discussion now turns to the principal drug classes that have historically formed the cornerstone of malaria therapeutic strategies.

INTEGRI PROCEDAMUS

University of Ghana http://ugspace.ug.edu.gh

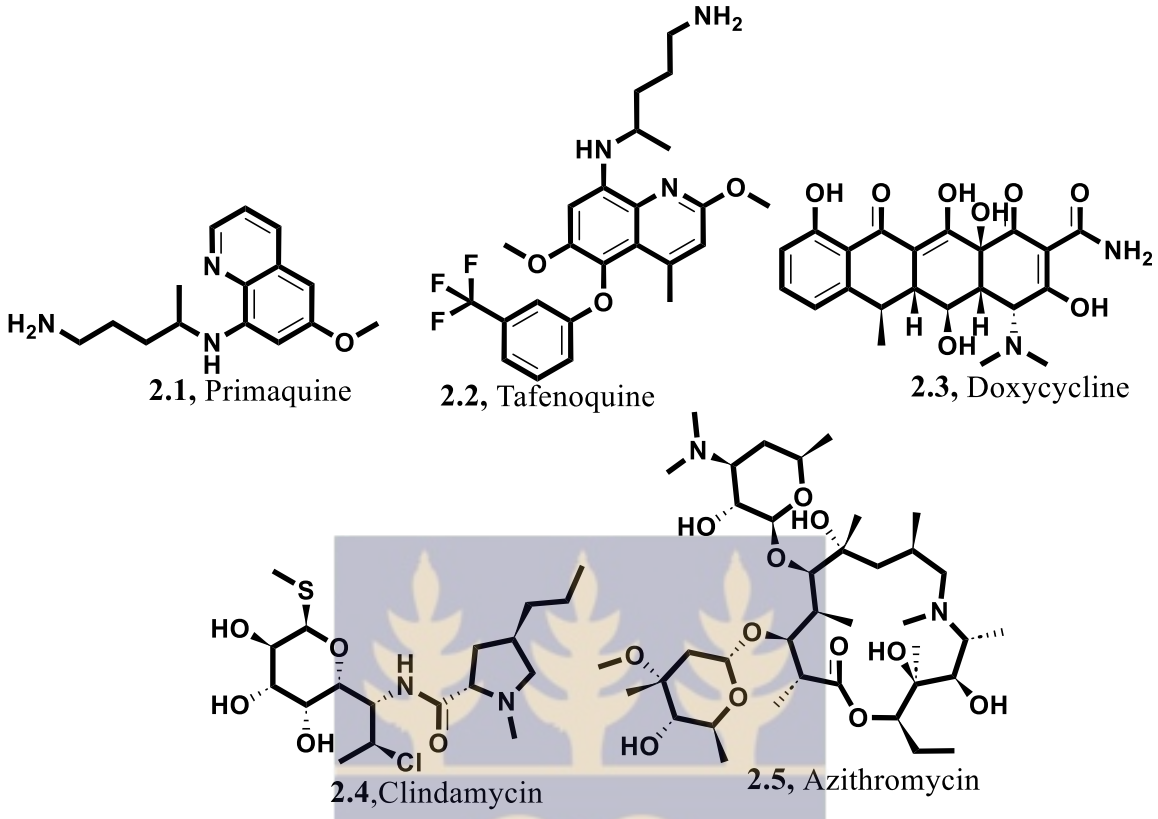


Figure 2.2: Chemical structures of antibiotics **2.3**, **2.4** and **2.5**, and 8-aminoquinoline antimalarial agents **2.1** and **2.2**.

2.4.1 Antifolates

Antifolates primarily target the asexual blood stage of the *Plasmodium* parasite, when it is actively time the parasite is actively replicating inside red blood cells. They inhibit the folate biosynthetic pathway in *Plasmodium* parasites. This is an essential metabolic route for producing the cofactor necessary for DNA replication and cell division: Tetrahydrofolate (THF). THF is a one-carbon carrier created by the reduction of Dihydrofolate (DHF), a reaction catalysed by Dihydrofolate Reductase (DHFR). It donates a carbon unit for the synthesis of biomolecular precursors: purines, pyrimidines and amino acids, which are essential building blocks for the genetic replication and transcription of the *Plasmodium* parasite. Inhibiting THF, therefore, disrupts the parasite's growth and ultimately results in its death [262, 263].

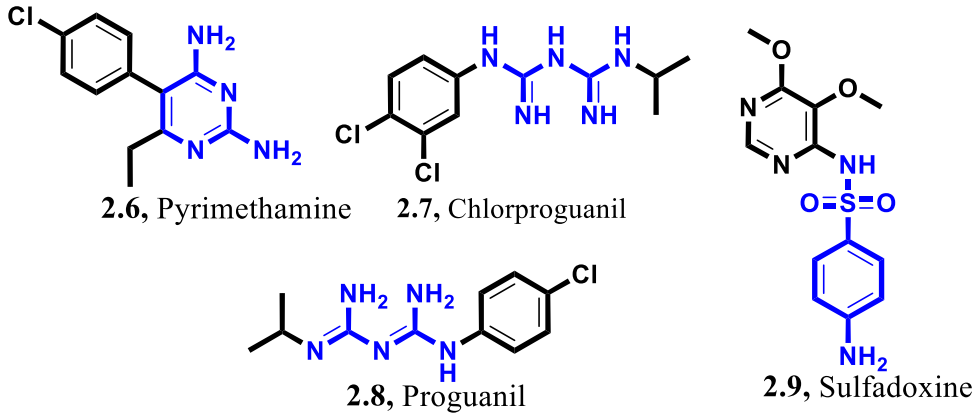
University of Ghana http://ugspace.ug.edu.gh

Antifolates such as Pyremethamine, **2.6** and Proguanil, **2.8** (**Figure 2.3)** mimic the structure of DHFR. They therefore bind tightly to the active site of DHFR, inhibiting the enzyme's ability to catalyse the reduction of DHF to THF. Selective targeting of the DHFR active site is possible due to structural differences between human and *Plasmodium* DHFR [263].

Antifolates such as Sulfadoxine, **2.9,** also competitively bind to the active site of Dihydropteroate synthase (DHPS), another enzyme that catalyses the formation of a precursor of DHF, disrupting the *de novo* folate synthesis pathway of *Plasmodium*, and ultimately impeding DNA synthesis and cell division. DHPS is absent in humans, making it a suitable for antimalarial drug target [264].

Antifolates are used in combination therapies, primarily to prevent malaria. Sulfadoxine-Pyremethamine (SP) is the most extensively used antifolate combination therapy, particularly as Intermittent Preventive Treatment in Pregnancy and Infants (IPTp & IPTi). It is also combined with amodiaquine for seasonal malaria chemoprevention in children under 5 years of age [265, 266]. Proguanil, a significant antimalarial antifolate, is commonly formulated with Atovaquone in a fixed-dose combination (Malarone), which is used for chemoprophylaxis in travellers to endemic regions [267]. Antifolates were widely used for the treatment of uncomplicated *P. falciparum* malaria. However, due to drug resistance, their use malaria treatment is currently restricted, especially in areas with wide-spread chloroquine resistance [268].

University of Ghana http://ugspace.ug.edu.gh



2.6, Pyrimethamine **2.7,** Chlorproguanil **2.9,** Sulfadoxine

2.8, Proguanil

Figure 2.3: Antifolates employed in antimalarial chemotherapy.

Plasmodium evades antifolates primarily through target- resistance. Point mutations in the genes encoding DHFR and DHPS, alter the structural conformations of their active sites, thereby impairing the interactions and binding affinities of antifolates [269].

2.4.2 Aminoalcohols

Aminoalcohols are primarily active against the blood stage of *P. falciparum* and have been effective, especially against chloroquine-resistant strains. The most validated and well-characterised mechanism of action of Aminoalcohols, is their interference with heme detoxification in the parasite, disrupting cellular integrity, and eventually leading to cell death [270].

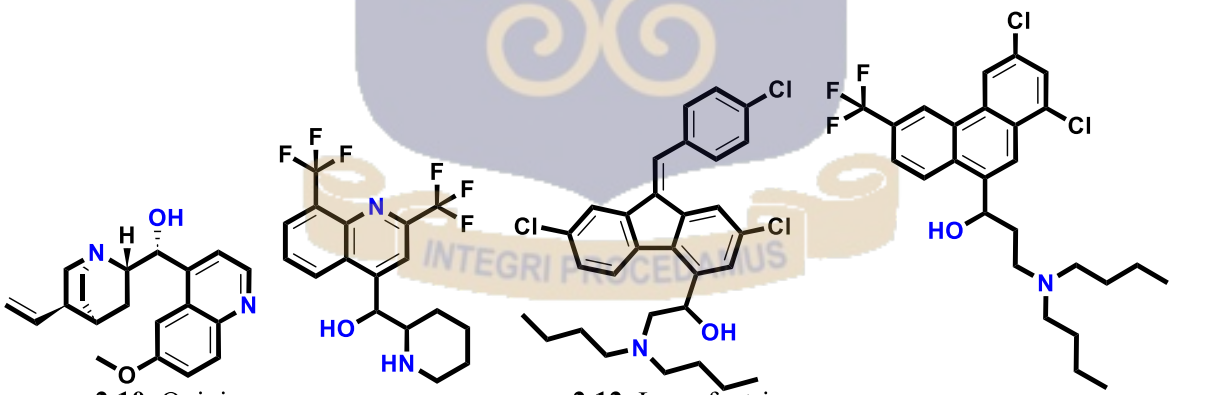
Aminoalcohols like quinine, **2.10** (**Figure 2.4**), and mefloquine **2.11**, are known to accumulate in the digestive vacuoles of the parasite and bind to free heme or growing hemozoin, preventing its conversion into its non-toxic form. This leads to the accumulation of toxic heme which disrupts the parasite's membrane and promotes oxidative damage, eventually leading to its death [271]. Aside from the accumulation of poisonous heme, the stable complexes formed when quinine or mefloquine binds to free heme, are also considered cytotoxic. Both toxic heme and drug-heme complexes can permeate vacuolar and cellular membranes, further compromising the parasite's survival and enhancing the antimalarial effect [272, 273]. Fur-

University of Ghana http://ugspace.ug.edu.gh

thermore, **2.11** is reported to disrupt the parasite's food vacuole, depriving it of nutrients, essential to its survival [273].

Some studies have also reported extravascuolar mechanisms of action of aminoalcohols against the *Plasmodium* parasite. They include: polyamine metabolism inhibition [274], DNA binding [275], and repression of DNA biosynthesis [276]. Though experimental data support these mechanisms, they are not as robustly validated as those in the parasite's food vacuole, and are therefore considered supplementary mechanisms of action [277].

Aminoalcohols are useful in malaria prophylaxis (mefloquine) [278] as well as in treating severe and uncomplicated forms of the disease (quinine) [279]. Lumefantrine, **2.12**, represents aminoalcohols as an integral component of ACTs. It is co-formulated exclusively with artemether in the combination known commercially as Coartem, a highly efficacious treatment for uncomplicated *P. falciparum* malaria [280].



2.10, Quinine **2.11,** Mefloquine **2.12,** Lumefantrine **2.13,** Halofantrine

Figure 2.4: Aminoalcohols used in malaria chemotherapy.

As a useful antimalarial class in front-line malaria treatment, the widespread reliance on aminoalcohol-based combinations like Coartem intensifies selective pressure on them. This sets the stage for the emergence of drug resistance, threatening the long-term efficacy of aminoal-

University of Ghana http://ugspace.ug.edu.gh

cohols [281]. Moreover, reports of adverse neurological effects associated with aminoalcohols like mefloquine limit its clinical potential [282]

Plasmodium resistance to aminoalcohols, particularly mefloquine is majorly linked to amplification in the *P. falciparum* multidrug resistance gene 1 (*pfmdr1* gene), a gene that encodes an ATP-binding cassette (ABC) transporter located on the membrane of the parasite's digestive vacuole [271, 283]. The PfMDR1 protein is believed to transport solutes such as amino acids (from haemoglobin digestion), and to play a homeostatic role in regulating the vacuolar environment. Its activity, therefore, influences the influx or export of drugs at its site of action [284, 285]. Amplification of the PfMDR1 protein thus sequesters aminoalcohols away from their target sites, decreasing their intracellular concentration and enabling the parasite to survive therapeutic drug levels [286, 287].

2.4.3 4-Aminoquinolines

4-Aminoquinolines are among the most studied antimalarial drug classes owing to chloroquine's (**2.14, Figure 2.5**) long-standing importance in global malaria therapy, and their efficacy against all five human *Plasmodia* [288-290]. The development of chloroquine resistance, therefore, increased curiosity in elucidating its mode of action, aiming to uncover the underlying mechanisms of the parasite's resistance [271]. As with aminoalcohols, 4-aminoquinolines interfere with heme detoxification in the parasite's digestive vacuoles [291, 292].

As weak bases, they selectively accumulate in the acidic region of the parasite's food vacuole, bind to free heme, and prevent its polymerization into hemozoin. The repercussions of this action are similar to those described for aminoalcohols [273]. Chloroquine is a prominent 4-aminoquinoline that served as a highly potent first-line treatment for malaria (particularly

University of Ghana http://ugspace.ug.edu.gh

P.vivax) for several decades before the onset of widespread resistance [292] in the mid-20th century. Though its clinical utility has vastly diminished, it remains a potent antimalarial in regions where *P. falciparum* is sensitive prevails, and is still highly effective against other *Plasmodium* strains [293, 294]. On the other hand, amodiaquine, **2.15**, has retained efficacy in several endemic areas and is incorporated into ACTs in combination with artesunate, a derivative of artemisinin [295].

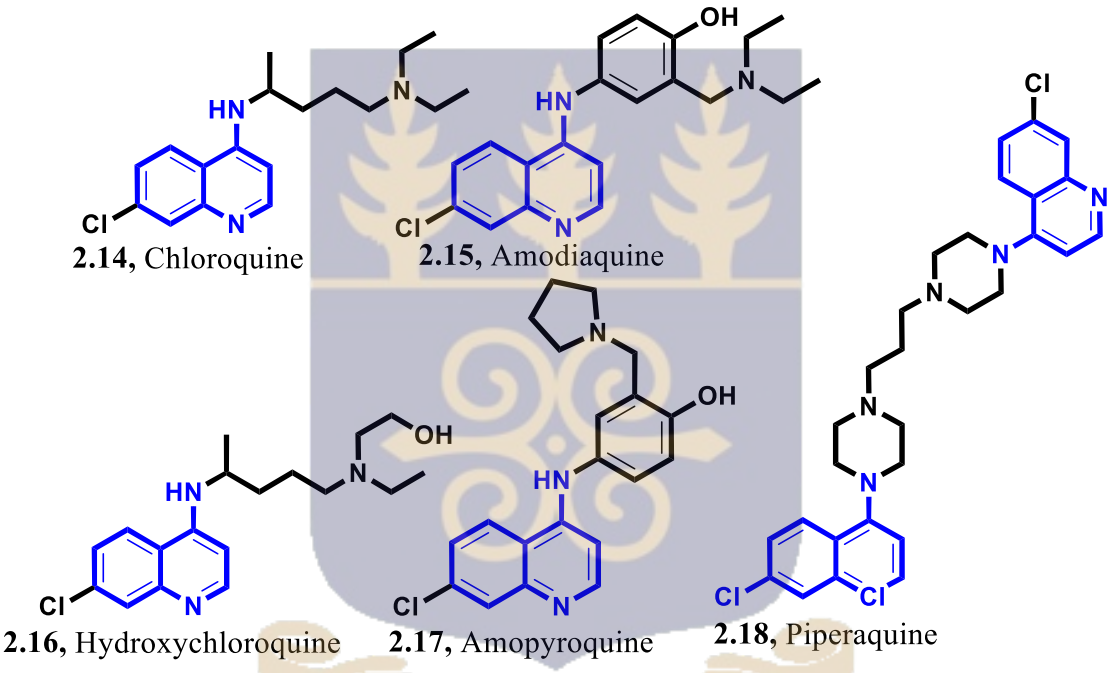


Figure 2.5: 4-aminoquinolines used for malaria treatment.

The onset and global spread of resistance to 4-aminoquinolines were among the earliest substantial setbacks in malaria chemotherapy. Resistance to 4-aminoquinolines, notably, chloroquine and amodiaquine, is primarily driven by mutations in the *P. falciparum* chloroquine transporter (*pfcrt*) gene; a gene that encodes a vacuolar membrane transporter, located on the membrane of the parasite's food vacuole [271]. Similar to PfMDR1, the original role of the PfCRT protein in the parasite is to transport metabolic by-products and small solutes across the parasite's digestive vacuole to maintain osmotic balance and vacuolar homeostasis [296].

University of Ghana http://ugspace.ug.edu.gh

Though not fully defined, evidence suggests that PfCRT is also involved in modulating vacuolar pH, maintaining ionic balance and transporting toxic metabolites or degradation products from haemoglobin digestion [297, 298]. Under selective pressure from prolonged chloroquine use, mutations in the *pfcrt* gene altered the structure of the PfCRT protein, thereby influencing its efflux of chloroquine from the vacuole. This action reduces the intravacuolar concentration of chloroquine below therapeutic levels, allowing the continued detoxification of heme to hemozoin and enabling the parasite to survive despite sufficient drug exposure [299-301].

Additionally, PfMDR1 plays a modulatory and secondary role in 4-aminoquinoline resistance. Due to reduced chloroquine concentrations in the food vacuole caused by *Pfcrt* gene mutations, specific PfMDR1 mutations further, reduce chloroquine sensitivity [302, 303]. Amplification of the *Pfmdr1* gene, also leads to overexpression (increased protein synthesis and RNA levels), resulting in additional drug elimination from the vacuole [287]. In drugs such as Amodiaquine, **2.15**, and Piperaquine, **2.18**, combined mutations in both *Pfmdr1* and *Pfcrt* genes leads to higher levels of resistance [304].

2.4.4 Hydroxynapthoquinones

Hydroxynapthoquinones are a subclass of naphthoquinones, characterized by a redox core that enables them to act as electron carriers, interfering with biological redox processes and disrupting electron transport chains, particularly in mitochondria [305]. Though several analogues and derivatives of hydroxynapthoquinones (**2.19**-**2.24**; **Figure 2.6)** have been investigated in pre-clinical and early clinical studies as potential antimalarials, Atovaquone (**2.19**) remains the only approved hydroxynapthoquinone, used for clinical malaria treatment [306-309].

University of Ghana http://ugspace.ug.edu.gh

Atovaquone is active against the asexual blood and liver stages of all five human-infecting *Plasmodium* species, although it cannot eliminate hypnozoites. It binds selectively to a strategic site of the cytochrome Bc_1 complex located in the inner membrane of the mitochondria. This complex plays critical role in part of the Electron Transport Chain (ETC) of *Plasmodium.* Electron flow is therefore inhibited, halting proton pumping across the mitochondrial membrane. Because proton pumping is essential for generating the electrochemical potential required for Adenosine Triphosphate (ATP) synthesis, the action of Atovaquone deprives the parasite of the energy needed for metabolic functions vital to its survival, replication, and invasion. Aside from blocking electron flow, Atovaquone also halts the recycling of ubiquinone, an electron pair acceptor for the enzyme, Dihydroorotate dehydrogenase (DHODH). DHODH is required for the *de novo* synthesis of pyrimidines, which serve as critical precursers for DNA and RNA synthesis. The mechanism of Atovaquone therefore halts the synthesis of DNA and RNA, leading to parasite death [272, 310, 311].

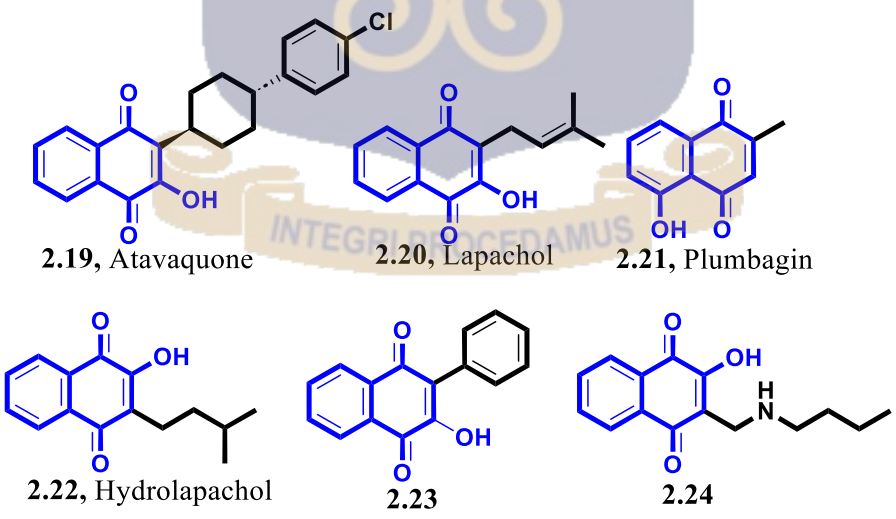


Figure 2.6: Structures of Atovaquone and other hydroxynaphthoquinone derivatives investigated for their antimalarial potential.

As previously indicated, Atovaquone constitutes a significant component of the combination therapy, Malarone, used for the prophylaxis and treatment of uncomplicated *P. falciparum*

University of Ghana http://ugspace.ug.edu.gh

malaria [312-314]. Beyond its use in the fixed-dose combination, Atovaquone has been evaluated in combination with other novel or existing antimalarials in drug development and clinical studies [272, 315, 316]. However, its primary and clinically approved use remains within the Malarone combination.

Atovaquone has a high propensity for resistance development as a stand-alone drug. Its primary mode of resistance is linked to mutations in the cytochrome b (*cytb*) gene of the parasite's mitochondrial genome [317]. Point mutations in the gene alter the amino acid sequence in the region of the binding site of atovaquone on the parasite's protein. This affects hydrophobic/hydrophilic interactions at the binding site, thereby reducing the binding affinity and the subsequent efficacy of atovaquone. With electron transport inhibited, the parasite's mitochondria maintain their function, ensuring its survival [318, 319].

2.4.5 Endoperoxides

The incorporation of peroxides into a cyclic framework endows them with unique chemical properties, making them valuable therapeutic agents, especially in antimalarial chemotherapy [320]. Endoperoxides possess greater stability than linear peroxides, thereby enhancing their pharmacological performance and reducing their susceptibility to premature degradation [321, 322]. The inherently weak O-O bonds characteristic of peroxides, however, do not entirely make endoperoxides resistant to decomposition. In the presence of stimuli such as redox-active metals, they undergo homolytic cleavage, generating reactive oxygen species (ROS) and free radicals. This is attributed to their pronounced biological efficacy especially against malaria [323, 324]. Endoperoxides are an exceptional class of antimalarials that demonstrate a radical divergence from conventional drug design [325]. Their unstable and reactive nature, make them a rare chemical moiety in natural products. The discovery of the first potent anti-

University of Ghana http://ugspace.ug.edu.gh

malarial endoperoxide, artemisinin, has therefore been significant an interesting and ground-breaking advance in medicinal chemistry and drug discovery [323, 326].

2.4.5.1 Artemisinin

Artemisinin, (**2.25**; **Figure 2.7**), contains a 1,2,4-trioxane ring embedded with a peroxide linkage. Though it shows some activity against other human *Plasmodium* parasites, its clinical use and robust efficacy are primarily focused on *P. falciparum* [327].

Artemisinin is a pro-drug that requires activation within the parasite to exert its antimalarial action [328]. They target the early ring and trophozoite stages, which are usually less susceptible to other antimalarials. During the erythrocyte stage, the *Plasmodium* parasite exists in a highly redox-active environment, owing to the abundance of ROS generated by heme and metabolic by-products. Its adaptation to survive this hostile oxidative environment (apart from hemozoin formation) relies on its own oxidant mechanisms, such as glutathione, thioredoxin and NADPH-dependent reductases. These systems can directly or indirectly reduce ferric iron (Fe^{3+}) (predominant form released from haemoglobin) to the more reactive ferrous iron (Fe^{2+}). Fe^{2+} is exploited by drugs like artemisinin and its derivatives for their lethal effect. It cleaves the endoperoxide bridge of artemisinin, producing highly reactive free radicals and ROS [217, 255, 329]. These unselective free radicals and ROS attack multiple essential parasite structures and biomolecules, including proteins, lipids, and membranes. Also, free radicals overwhelm the parasite's reducing systems, driving it into oxidative stress-induced cell death [328].

Artemisinins have a rapid parasite clearance, often reducing the parasite biomass by approximately 10,000-fold per asexual cycle. This swift reduction in parasite load usually leads to a faster relief, a lowere risk of complications and decreased transmission potential [149, 330]. Moreover, the rapid metabolism of Artemisinins reduces drug pressure, potentially limiting

University of Ghana http://ugspace.ug.edu.gh

the long-term development of resistance, while minimizing the side-effects usually associated with prolonged drug exposure [331]. However, artemisinin's short half-life limits its effectiveness when used in monotherapy. As a result, they are used in combination with longer lasting partner drugs to ensure complete parasite clearance and prevent malaria recrudescence [332].

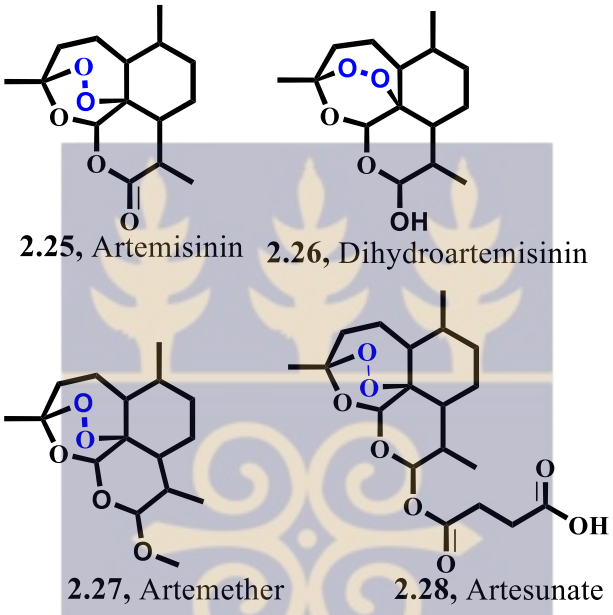


Figure 2.7: Artemisinin drugs employed in ACTs.

2.4.5.1.1 ACTs

For almost 2 decades, ACTs have been widely recognised as the most potent antimalarial agents for the treatment of uncomplicated *P. falciparum* malaria. The choice of ACTs depends on local resistance patterns, drug availability and cost. They are widely used in highly endemic malaria regions, such as sub-Saharan Africa and Southeast Asia [151, 333, 334]. There are 6 WHO recommended ACTs for the treatment of uncomplicated *P. falciparum* infections [335]. **Table 2.1** gives a summary of the various ACTs, their regional deployment and specific areas of application.

University of Ghana http://ugspace.ug.edu.gh

Table 2.1: Overview of employed ACTs in malaria chemoprevention

ACT Combination	Predominant Region	Specific Area of Application
Artemether-Lumefantrine (AL)	Sub-Saharan Africa	First-line treatment of uncomplicated *P.falciparum* malaria [336].
Artesunate-Amodiaquine (AS-AQ)	Sub-Saharan Africa	First-line treatment of uncomplicated *P.falciparum* malaria, seasonal malarial chemoprevention (SMC) [337].
Artesunate-Mefloquine (AS-MQ)	South-East Asia, South America	First-line treatment of uncomplicated *P.falciparum* malaria [338].
Dihydroartemisinin-Piperaquine (DHA-PPQ)	South-East Asia	First-line (or second-line in specific contexts) treatment of uncomplicated *P.falciparum* malaria [339].
Artesunate-Sulfadoxine-Pyremethamine (AS-SP)	South-East Asia, East Africa	First-line treatment of uncomplicated *P.falciparum* malaria [340].
Artesunate-Pyronaridine (AS-PYR)	Sub-Saharan Africa, South-East Asia	First-line treatment of uncomplicated *P.falciparum/P.vivax* malaria [341].

The most recent addition to ACTs is AS-PYR (Pyrimax) [342, 343]. Pyronaridine, **2.30** (**Figure 2.8**) is a benzonaphthyridine derivative whose discovery can be traced to the search for potent alternatives for chloroquine. Pyronaridine was synthesised based on the mepacrine scaffold, **2.29** (a potent antimalarial drug that was later replaced by chloroquine), with an in-

University of Ghana http://ugspace.ug.edu.gh

corporated amodiaquine side chain [344]. It has been a potent antimalarial against *P. falciparum* in China for over 5 decades, and has recently gained attention as a potent candidate against drug-resistant strains of *P. falciparum* and *P. Vivax* [345-347]. Studies on Pyronaridine indicate that it is an efficacious agent in reducing sporozoites and oocyst formation when combined with other antimalarial drugs [348-350].

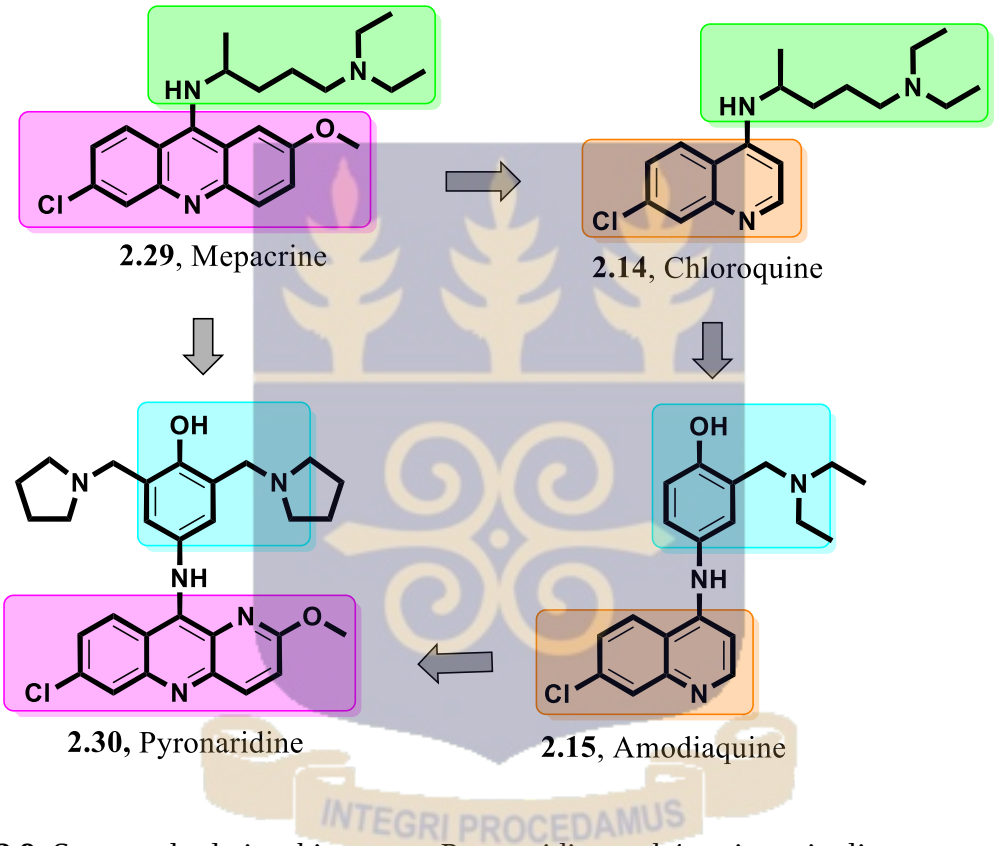


Figure 2.8: Structural relationship among Pyronaridine and 4-aminoquinolines.

Pyronaridine is described as a schizonticide with a multifaceted mechanism of action, primarily targeting *plasmodium* hemozoin formation and DNA metabolism [351]. The mannich base-like structure of pyronaridine, similar to 4-aminoquinolines such as amodiaquine, is believed to enhance its ability to inhibit hemozoin formation, leading to the accumulation of free heme in the parasite's digestive vacuoles of the [352]. It is also reported to bind to the parasite's DNA, disrupting its structure and causing DNA damage, subsequently leading to

University of Ghana http://ugspace.ug.edu.gh

cell death [353, 354]. Bailey (2021) further suggests that, pyronaridine may exert immuno-modulatory effects and engage mitochondrial oxidative pathways [348].

Although a few studies have observed reduced susceptibility of *P. falciparum* to Pyronaridine, in specific regions [355-357], there is no evidence of widespread clinical resistance to the drug [348, 354]. Its limited use outside China also associates it with reduced selective drug pressure, potentially limiting the emergence and spread of resistance [351]. These make its inclusion in ACT regimens, therefore, a strategic action in curbing the propagation of drug resistance.

In most clinical settings, ACTs have demonstrated >95% recovery rates against uncomplicated *P. falciparum* infections within 28-days after treatment, as well as very low recrudescence rates (with adequate patient compliance) [358-360]. However, the revolving resistance of *Plasmodium* to artemisinins, the backbone of ACT chemotherapy, poses a critical threat to their sustained efficacy [361].

2.4.5.1.2 Artemisinin Resistance

Mutations in the *kelch13* gene encoding the kelch13 (K13) protein, within the parasite, are the key driver for artemisinin resistance and are used as a biomarker in tracking studies [362]. Though the primary site of action of artemisinin is yet to be discovered, studies suggest that alterations within the propeller domain of the K13 protein as a result of the gene mutations enable the protein to engage stress tolerance mechanisms, allowing the parasite to survive the oxidative outburst at the early ring stage [155, 363]. Artemisinin-induced damaged proteins are degraded through the proteasome pathway (cellular recycling system), where they are broken down into peptides, allowing the cell to maintain control, rather than undergo apoptosis (programmed cell death) or necrosis (uncontrolled cell death) [364]. K13 mutations also impair endocytosis in the parasite, reducing heme levels, and consequently, limiting artemis-

University of Ghana http://ugspace.ug.edu.gh

inin activation (fewer radicals) [365]. Again, the development of the parasite at the ring stage slows down (a dormant-like state), thereby circumventing the cytotoxic effects of fast-acting artemisinins by delaying its exposure to free heme [156].

The mechanisms described above qualify artemisinin resistance as delayed parasite clearance (>10% of parasites remaining after 72 hours) rather than outright resistance [366]. This may offer a nuance of hope for its continued use. However, it signals an early warning of the potential progression of ACTs toward complete resistance or treatment failures. From the earliest confirmed evidence of artemisinin resistance in the late 2000s [367], surveillance and mapping studies to track its geographical spread have been extensively documented in literature. Dondorp *et al*. reported decreased *in vivo* sensitivity to artesunate in western Cambodia in 2009, establishing the onset of artemisinin resistance [368]. A few years later, Ashley *et al*. confirmed its spread to other countries within the Greater Mekong Sub-region, linking delayed parasite clearance with *kelch13* mutations [369]. In 2016, Menard *et al*., covered a wider geographical region, confirming artemisinin resistance in South-East Asia as reported by earlier studies. Although K13 mutations (A578S) were identified in some African countries in the study, subsequent investigations showed that these mutations were not associated with delayed artemisinin clearance [370]. In 2018, however, the WHO confirmed the presence of mutations associated with artemisinin prolonged clearance (C580Y) in Africa [371]. This finding was especially concerning, considering Africa's status as a central endemic region. Subsequent studies validated WHO's earlier report, emphasizing the spread of delayed parasitic clearance-associated mutations (R561H) from Rwanda [372] to Tanzania [373] and Uganda [374]. Furthermore, other mutations with evidence of clinical artemisinin resistance were also detected in different African countries [375-377]. Fortunately, therapeutic efficacy studies across the continent show high cure rates (>90%) for most ACTs [378-380], despite

University of Ghana http://ugspace.ug.edu.gh

the presence of significant artemisinin resistance biomarkers. Nonetheless, projections from studies investigating the spread of K13 mutations linked to artemisinin resistance question the long-term efficacy of ACTs as front-line antimalarials [157, 381, 382]. Moreover, the rapid spread of artemisinin resistance across Southeast Asia, has translated into adverse treatment outcomes, suggesting a high probability of a comparable effect in Africa [383, 384]. With already established parasite resistance mechanisms to parasite to antimalarial drug classes that serve as ACT partner components, residual parasites that survive artemisinin exposure may not be cleared, further compromising the efficacy of ACTs by developing more resistant phenotypes.

2.4.5.1.3 Triple ACTs (TACTs)

In mitigating the spread of artemisinin and consequently ACT resistance, the concept of ACT was extended into a new combination therapy by adding an extra drug. Hence, TACTs contain an artemisinin derivative, a first partner drug, and another partner drug with a different mechanism of action and half-life [385]. TACTs are designed to provide broader protection against resistance to one or two components, enhancing parasite clearance and prolonging the lifespan of existing antimalarials [386]. Three combinations are currently recognised under TACTs: Dihydroartemisinin-Piperaquine-Mefloquin (DHA-PPQ-MQ) [387], Artemether-Lumefantrine-Amodiaquine (AL-AQ) and Artesunate-mefloquine-piperaquine (AS-MQ-PPQ) [388]. These have shown promise as safe, equally potent replacements for ACTS. Nguyen *et al*. and *Dini et al.*, used mathematical modelling to predict that replacing ACTs with TACTs could significantly delay the development and evolution of artemisinin resistance [388, 389]. Other studies have also emphasised the safety and efficiency of TACTs, particularly in regions with emerging ACT resistance [385, 388]. Preliminary deductions from a major clinical trial comparing TACTs to ACTs (DeTACT trial) further confirm that TACTs are well toler-

University of Ghana http://ugspace.ug.edu.gh

ated and safe [390-392]. The DeTACT (Development of Triple Artemisinin-Based Combination Therapy) trial was conducted across 14 sites in 8 African countries (including Nigeria, DR Congo and Tanzania) and 5 Asian countries (including Cambodia and Vietnam), focusing on two TACT regimens: AL-AQ to their corresponding ACTs; AL and AS-MQ [393, 394]. There are, however, concerns about tolerability (increased side reactions), drug-drug interactions, in terms of cost and access, especially for African countries, as well as policy and regulations regarding the implementation of TACTs [395-400]. As the global health community awaits the pending publication of the DeTACT trial, it is not unwarranted to regard TACTs as a promising interim strategy for sustaining the therapeutic efficacy of Artemisinins in the face of escalating parasite resistance. The follow-up trial, FD-TACT (Fixed-Dose Triple Artemisinin-Based Combination Therapy) aimed at developing a single-pill formulation for TACTs [401, 402] would address some projected challenges integrating TACTs.

Until a more potent antimalarial is developed, it is imperative to safeguard the efficacy of artemisinin and its derivatives by all available means to ensure that previous and on-going therapeutic efforts in malaria eradication are not undermined or rendered futile.

2.5 The role of small molecules in malaria drug discovery

Despite concerted efforts to safeguard the efficacy of ACTs, it is imminent that prolonged reliance on partner drugs with well-characterized resistance mechanisms, particularly in regions with reduced susceptibility to Artemisinin, may ultimately compromise malaria control efforts. It is therefore necessary that alternative antimalarial agents and novel drug combinations are critical for a sustained advancement in malaria eradication. At the core of developing next-generation antimalarials lies the strategic use of small molecules [403-405].

Defined as molecules with molecular weights less than 900 Da, small molecules constitute over 90% of FDA-approved drugs [406, 407]. Their unique functional properties and versatil-

University of Ghana http://ugspace.ug.edu.gh

ity enable modifications and optimizations through Structure-Activity Relationship (SAR) studies to interact with specific biological targets while modulating the required physiological processes in treating a disease [408]. This allows medicinal chemists to improve the potency, selectivity and the overall pharmacokinetic profile of small molecules through hit-to-lead and lead optimisation, permitting their administration in convenient forms (capsule or tablet) that enhance patient compliance [406]. Additionally, the small molecular weights and lipophilicity (in most cases) of small molecules enable their penetration into biological membranes, reaching intracellular targets and enabling their ability to addressing a wide range of therapeutic situations [409-411]. Owing to established synthetic routes and scalable production processes, small molecules are cost effective-tools in validating biological targets, elucidating mechanisms of action, identifying off-target and refining or re-defining hypotheses in early-stage drug discovery [412-414]. In malaria therapeutic research, phenotypic and target-based screening, contribute uniquely to the discovery of novel small molecules with therapeutic potential [404, 415, 416].

2.5.1 Target Based Screening (TBS)

Since molecules are identified through TBS based on their ability to interact with a biological target, binding affinity and selectivity optimization through structure-based drug design, is easily established, offering a more rational and hypothesis-driven approach to drug discovery. Additionally, the known mode of action of a given molecule at the onset of discovery facilitates an efficient hit-to-lead Structure-Activity-Relationship (SAR) evaluation, as well as downstream development and safety profiling [417, 418]. Some compounds identified through TBS (**2.31** – **2.35**) that have advanced to pre-clinical/clinical stages or remained valuable leads for further optimization and development are shown in **Figure 2.9** [418-422].

University of Ghana http://ugspace.ug.edu.gh

Despite the discussed strengths of TBS, several limitations make it a less favourable option compared to PS, especially in addressing diseases like malaria. TBS usually occurs in targets (proteins or enzymes) outside its native context (reductionist system). This may not accurately reflect the complexity of the disease in a whole cell or organism. Again, if the selected target turns out to be redundant or non-essential *in vivo*, progressing with the molecule will not be necessary.

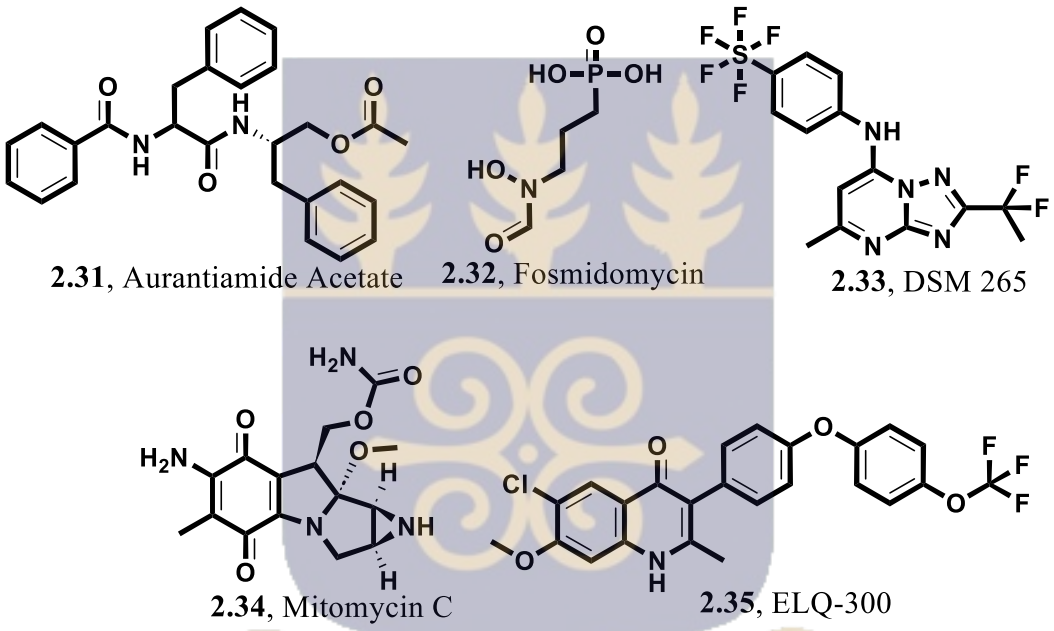


Figure 2.9: Structures of select antimalarial candidates identified through target-based screening.

2.5.2 Phenotypic Screening (PS).

PS on the other hand selects a compound based on its ability to create a desired effect in a live cell (or organism), and is not dependent on target validation. Biological activity, cellular permeability and some extent of metabolic stability are therefore inherently addressed from the onset, expediting advancement into *in vivo* studies. PS enables the identification of drug candidates without requiring prior knowledge of their specific molecular targets at the initial

University of Ghana http://ugspace.ug.edu.gh

stages of discovery. Moreover, identified compounds through PS may have mechanisms of action addressing multiple targets making them potential multi disease candidates [163, 423]. This is of greater significance in mitigating drug resistance, which TBS may miss [160, 424]. Examples of clinically used drugs identified through PS (**2.36-2.42**) are showed in **Figure 2.10**, with their respective therapeutic activities.

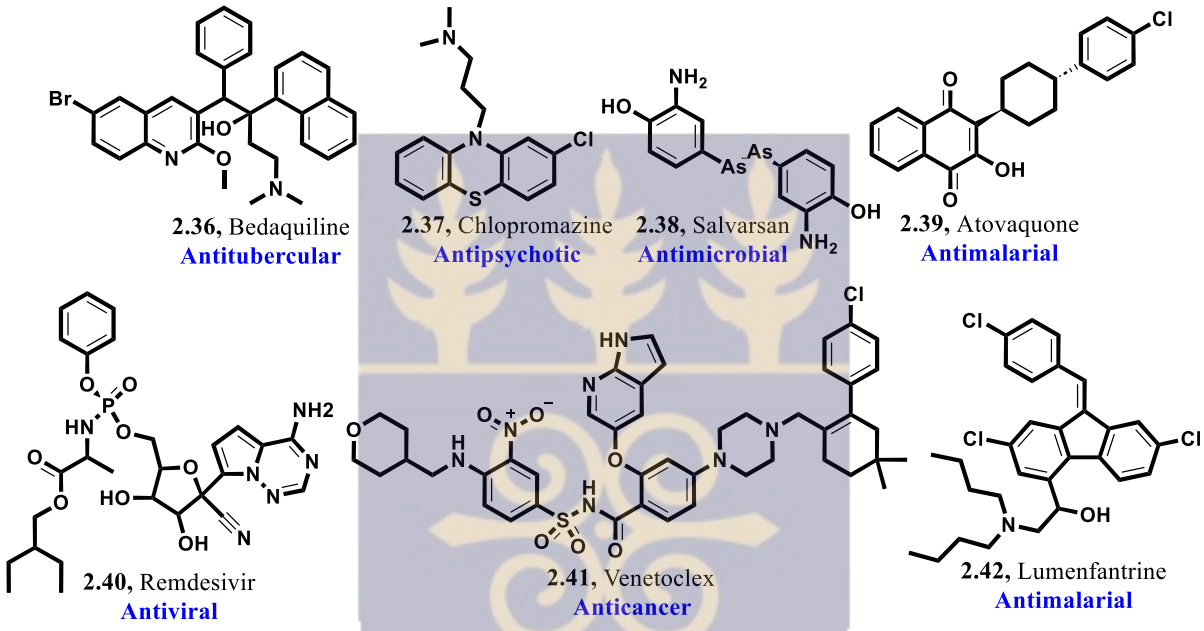


Figure 2.10: Examples of clinically used drugs identified through PS and their therapeutic functions.

2.5.3: Comparative advances in Phenotypic and Target-Based Screening in the development of antimalarial small molecules.

The historical success of Phenotypic Screening (PS) in discovering first-in-class drugs has motivated modern drug discovery, particularly in malaria chemotherapy, where the pursuit for drugs with novel mechanisms of action is on high demand [425-427]. PS has led to the discovery of relevant hit and lead compounds, resulting in several PS-derived drug candidates that have progressed to pre-clinical or phase 1 stages of development [428]. Recent literature

University of Ghana http://ugspace.ug.edu.gh

outlines advancements that have significantly enhanced the resolution and interpretation of phenotypic assays while addressing limitations associated with hit validation and target deconvolution [429-431]. In a study to identify schizont inhibitors from the MMV pathogen box, Patra *et al*. integrated high-resolution PS with an advanced assay design (a calcium-triggered egress assay) to precisely quantify parasite development and merozoite release [432]. Similarly, Kato *et al*. developed a single assay to simultaneously assess compound activities across the asexual development, sexual commitment, and sexual development of the *Plasmodium* parasite [433]. Comparable studies have also been evaluated by Luo *et al* [434]. Findings from these studies emphasize how refined PS platforms can enhance hit discovery and provide early mechanistic insights, influencing rational lead optimization. Given the narrow spectrum of antimalarial drugs such as chloroquine, which contributes to resistance, the identification of small molecules with multi-stage activities offers prospects for the development of emerging antimalarials. As previously established, the unique therapeutic properties of Artemisinins spurred the exploration of endoperoxides as new antimalarial agents [326, 435].

Endoperoxides such as 1,2-dioxolanes, 1,2-dioxanes, 1,2,4-trioxanes, 1,2,4-trioxolanes, and 1,2,4,5-tetraoxanes have been explored for their antimalarial properties [436]. Other small molecules with multi-stage antimalarial activities include imidazolepiperazines [437], spiroindolones [438], quinolone diarylethers [439], etc. Further analysis of emerging antimalarials derived from these scaffolds will be discussed in subsequent sections of this review. Some scaffolds from the MMV pathogen box (**2.43-2.50**; **Figure 2.11**) have also shown significant potential, advancing them as potent antimalarial agents. Kumari *et al*. demonstrated that pyrazole-pyrimidine scaffolds **2.47-2.49** were multi-stage inhibitors of *P. falciparum* (IC_{50} = 0.15 µM-11.0 µM) [440].

University of Ghana http://ugspace.ug.edu.gh

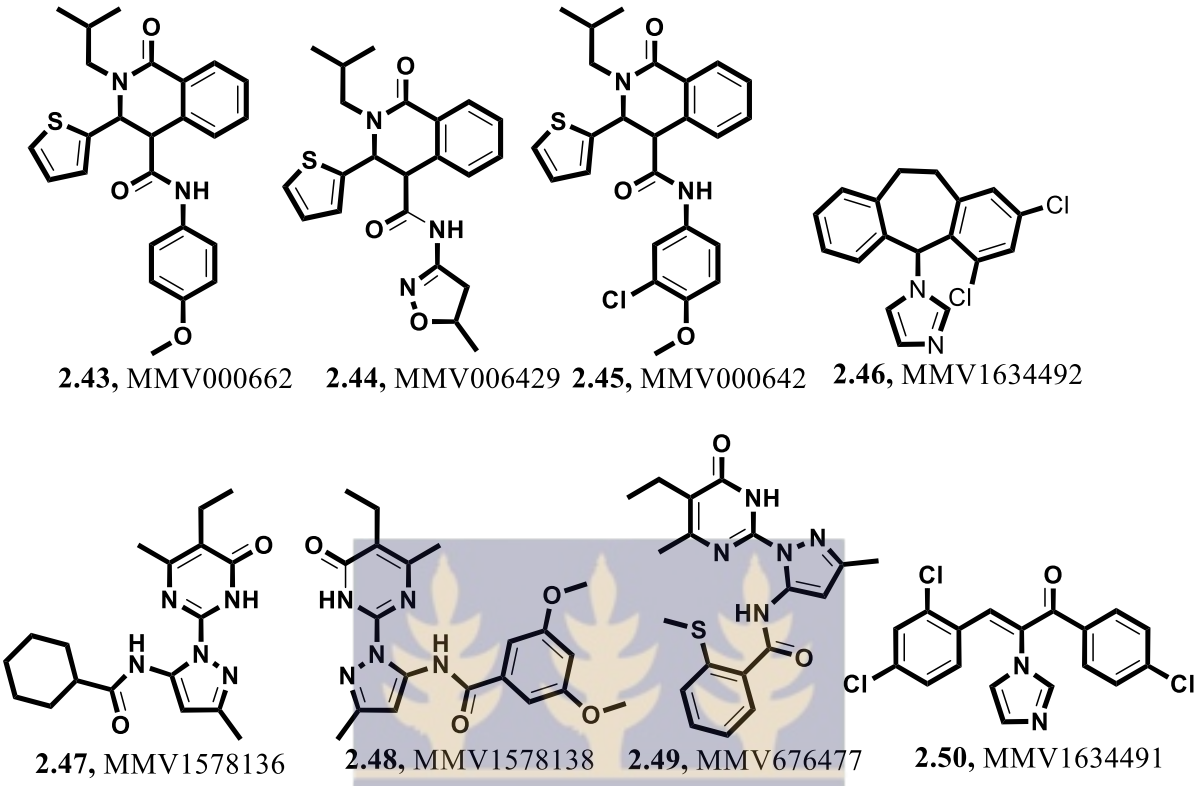


Figure 2.11: Various scaffolds from the MMV Pathogen Box that have demonstrated multi-stage antimalarial activities.

Furthermore, Malebo *et al.* reported the asexual blood-stage and gametocyte-stage activities (IC_{50} = 0.07 µM - 0.13 µM) of 1,2,3,4 –tetrahydroisoquinoline-4-carboxamide scaffolds **2.43-2.45**. The molecules also displayed moderate potential against early sporogonic development [441]. Fascinating insights into imidazole scaffolds **2.46** and **2.50** have also been highlighted by Reader *et al* (*P.falciparum* late stage gametocytes (IC_{50} = 0.21 µM – 0.23 µM), suggesting a possible unveiling of an unexplored mode of action [442].

Despite promising conclusions from literature, PS however remains resource-intensive and prone to false positives, necessitating careful downstream validation [183]. The integration of advanced screening technologies into its conceptual and methodological frame-work, therefore contributes to addressing this challenge while blurring its traditional boundaries with TBS [443, 444]. High-resolution PS is currently being merged with reliable molecular tools

University of Ghana http://ugspace.ug.edu.gh

such as chemo proteomics, genomics, and omics profiling to detect bioactive leads, confirm their activity across the various stages of the parasite's cycle, elucidate their mechanisms of action, and suggest rational lead optimization routes down to the molecular level [434, 445, 446]. The inverse relationship between PS and TBS, supported by cheminformatics and bio-informatics in the hit-to-target elucidation process, has facilitated the identification, validation, and prioritisation of several molecular targets of *P. falciparum* [447]. These include Cyclin-dependent kinase-like kinases (PfCLKs) [448], Phosphatidylinositol-4-OH kinase (PfPI4K) [449], ATPase 4 (PfATP4) [450], *N*-myristoyltransferase (PfNMT) [451], Dihydroorotate dehydrogenase (PfDHODH) [452], and type II NADPH dehydrogenase (PfNDH2) [453].

2.5.4 Artificial Intelligence/Machine Learning (AI/ML) for antimalarial Drug Discovery.

The emergence of Artificial Intelligence (AI) and Deep Learning (DL) in recent years and its inclusion in drug discovery has accelerated various stages through its ability to improve the speed and efficiency of compound identification and optimization. Also by analyzing patterns in chemical structures and biological activity data, AI models are capable of predicting the likelihood of a compound exhibiting desirable pharmacological properties, drastically reducing the number of compounds that will need experimental testing [454-456]. With the proliferation of tools from Artificial Intelligence/Machine Learning (AI/ML), the prioritization of novel hits through reverse-engineering approaches (tracing from ligand to data and vice-versa) further refines antimalarial drug discovery into a more comprehensive and holistic paradigm [454, 457-459]. Commencing from the Prediction of Activity Spectra for Substances (PASS), which predicts over 300 types of biological activities [460], several AI drug discovery tools such as DeepChem [461], Chemprop [462], and MolMapNet [463] have emerged based on its fundamental assumptions. More specifically, for malaria drug discovery, the MAalria Inhibi-

University of Ghana http://ugspace.ug.edu.gh

tor Prediction (MAIP) web platform [464] and the Machine Learning Quantitative Structure-Activity Relationship (ML-QSAR) [465] models have been developed to predict predictive blood-stage, and multi-stage activities, respectively, of small molecules against *Plasmodium* parasites. Similarly, DeepMalaria, developed by Keshavarzi *et al*., predicts the antiplasmodial inhibitory properties of small molecules based on their SMILES [466]. More recently, Lamptey *et al*. optimized and deployed models into a web application, PLASMOpred, equipping researchers with an accessible tool for the efficient prediction of small-molecule inhibitors of two parasite proteins relevant to erythrocyte invasion [467].

Clearly, innovative advancements bridging the empirical power and mechanistic insights of PS and TBS, respectively, into hybrid workflows have enabled the exploration of previously inaccessible chemical and biological spaces. The identification and development of potent small molecules into the next-generation of antimalarials, therefore, hold the promise of transcending the limitations of existing drugs [416, 468].

2.6 Next-Generation Antimalarials

Next-generation antimalarials are deliberately designed to anticipate and outpace the malaria parasite's adaptability. The concepts underlying their development extend beyond potency and selectivity to embrace a therapeutic agenda. They are envisioned to address complex challenges such as multi-stage efficacy, transmission-blocking, resistance evasion and hypnozoite clearance, while achieving radical cure [404]. Next-generation antimalarials are expected to possess favourable pharmacokinetic and pharmacodynamic properties, novel mechanisms of action (to circumvent resistance), minimal toxicity, and alignment with Target Candidate Profile (TCP) and Target Product Profiles (TPP) defined by global health priorities [469]. The list of antimalarial drugs in clinical trials is extensive. A limited number of candi-

University of Ghana http://ugspace.ug.edu.gh

dates that have provided valuable lessons and currently serve as pharmacological blueprints for future antimalarials, as well as a select group of candidates in advanced clinical (patient exploratory) stages, are examined in the subsequent paragraphs [404, 469].

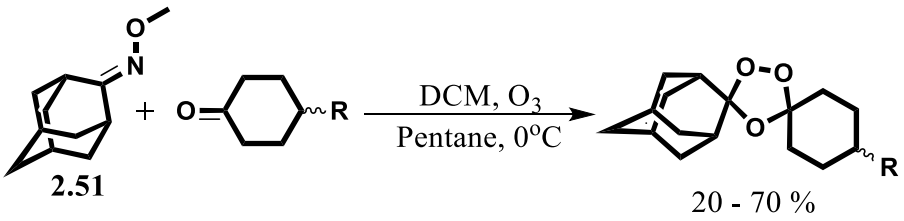
2.6.1 Endoperoxides

The distinctive chemical structure and ability to engage multiple parasite targets, coupled with rapid parasite clearance and the short half-life of Artemisinins, distinguish them both pharmacologically and therapeutically from other antimalarials [470]. These unique qualities spurred investigations into endoperoxides, solidifying their role as key scaffolds in the development of next-generation antimalarials [471]. Artefenomel and Arterolane are fully synthetic endoperoxides that have made significant headway in clinical development [472].

2.6.1.1 Arterolane (OZ277)

Arterolane (**2.54**; **Scheme 2.2**) is a first-generation 1,2,4-trioxolane, discovered through multidimensional lead optimization of dispiro 1,2,4-trioxolanes as part of a collaborative drug discovery programme (involving MMV and Ranbaxy) to identify improved alternatives to artemisinin [473]. 1,2,4-trioxolanes can be synthesised through the Griesbaum co-ozonolysis of methyl oximes and ketones (**Scheme 2.1)** [474]. The incorporation of an adamantanone moiety into ozonide antimalarials imparts lipophilic functionality, enabling flexible modifications at the opposite end of the molecule, with various polar functional groups [475].

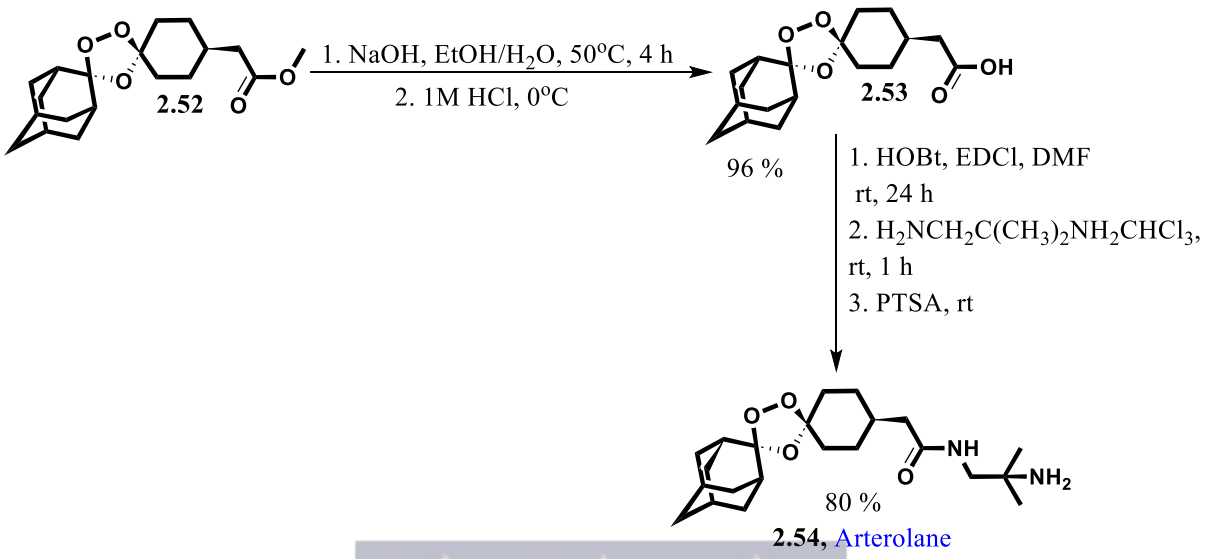
University of Ghana http://ugspace.ug.edu.gh



Scheme 2.1: Synthesis of 1,2,4-trioxolanes through Griesbaum co-ozonolysis [474].

Having established decreasing antimalarial activity with an overly exposed or sterically hindered peroxide bond, Vennerstrom *et al.*, went ahead to synthesise analogues bearing asymmetrical bulky substituents (Adamantanone) on one side of the ring. This ensured stereoelectronic stability while controlling Fe^{2+}-mediated cleavage of the peroxide bond, thereby initiating radical formation that leads to oxidative damage in the parasite. The physicochemical and biopharmaceutical properties of the analogues were improved to achieve an intermediate **2.53**, which led to the synthesis of Arterolane (**Scheme 2.2**) [476]. Arterolane is reported to have rapid parasite clearance, comparable to that of Artemisinin, with high efficacy against all erythrocyte stages of *P. falciparum* and *P. vivax* [477]. However, its half-life (~3-4 h), though longer than artemisinin (~1 h), requires combination with a longer half-life partner drug. Phase III clinical studies of the fixed-dose Artemisinin-piperaquine combination (Synriam) indicate cure rates comparable to those of standard ACTs [478, 479], and have been approved for use in India and some African countries [480]. Aterolane's partner dependence on piperaquine, which itself is vulnerable to *Plasmodium* resistance and other concerns, made it less patronised [481]. The search for an ozonide with a comparatively longer half-life led to the discovery of Artefenomel (OZ439) [475].

University of Ghana http://ugspace.ug.edu.gh



Scheme 2.2: Synthesis of Arterolane from dispiro 1,2,4-trioxolane [476].

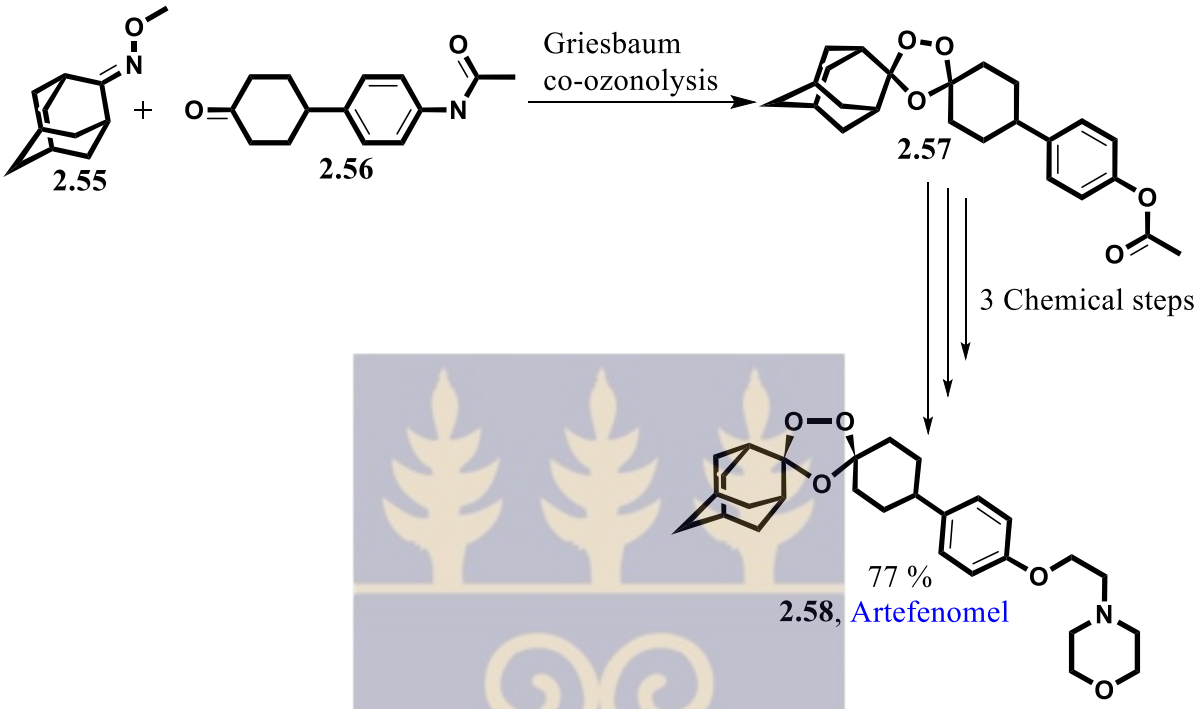
2.6.1.2 Artefenomel

Artefenomel (OZ439) (**2.58**; **Scheme 2.3**) is a 1,2,4-trioxolane second-generation synthetic ozonide discovered through extensive SAR studies on first-generation 1,2,4-trioxolanes. It has a longer half-life (~46-60 h), higher exposure, and excellent metabolic stability in compared to arterolane, making it a more suitable candidate for a single-dose cure [482]. The key medicinal chemistry strategy in the synthesis of artefenomel was focused on improving the metabolic stability and half-life of arterolane without compromising its antimalarial activity [483].

The metabolic breakdown of arterolane both in the blood and in the liver, reportedly eliminates the active peroxide responsible for its antimalarial activity [484]. Dong *et al*. therefore reduced metabolism by placing the cyclohexyl linker into an axial position, thereby making it less accessible to metabolic enzymes. This was achieved by introducing an aryl cyclohexyl

University of Ghana http://ugspace.ug.edu.gh

linker (**2.56**), consequently increasing its half-life while retaining its strong antimalarial activity. Further optimization of the aryl analogues led to Artefenomel [485].



Scheme 2.3: Structural modification on arterolone towards the synthesis of artefenomel [485].

In addition to its long half-life, Artefenomel, it was also effective against resistant strains of *Plasmodium* [486]. However, though structurally different from artemisinin, its peroxide-based mechanism could be undermined by *de novo* or cross-resistance if used as a stand-alone drug [487]. To slow down the emergence of resistance, it was combined with piperaquine in a randomised, double-blind, phase II clinical trial. Unfortunately, the combination showed suboptimal performance in terms of parasite clearance and recrudescence prevention [488, 489]. Promising early-stage results in combination with other drugs (DSM265 and ferroquine) were also dampened by limitations in its therapeutic window and overall efficacy [490-492]. Ultimately, the clinical development of Artefenomel was halted due to additional challenges associated with solubility and lipophilicity [493], as well as insufficient single-

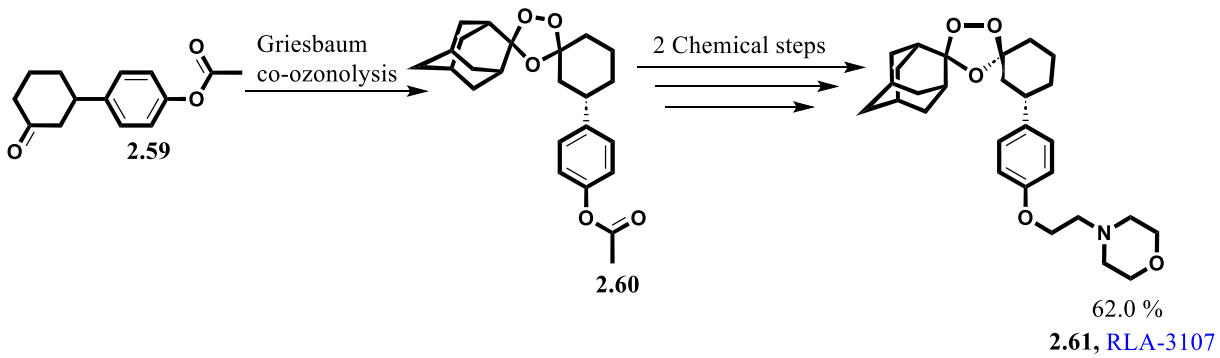
University of Ghana http://ugspace.ug.edu.gh

dose efficacy (in combination and monotherapy) beneath the WHO's target of ≥95% [489]. Though Artefenomel no longer plays an active role in malaria treatment, its development has heavily influenced the design and expectations for next-generation endoperoxide antimalarials such as RLA-3107 [493].

2.6.1.2.1 RLA-3107

Following limited clinical outcomes with Artefenomel in late-stage clinical studies, it was redesigned to improve its solubility and metabolic stability. Artefenomel's regioisomeric analogue RLA-3107 (**2.61**; **Scheme 2.4**), which contains a desymmetrized trioxolane core, preserves its therapeutic potency while displaying enhanced solubility and stability in human liver microsomes [493, 494].

It has been established earlier that the Griesbaum co-ozonolysis reaction is diastereoselective, predominantly yielding a *trans* diastereoisomer when C-3 substituted cyclohexanones are used. Blank *et al.* therefore inferred that an enantiomerically pure cyclohexanone was not necessarily required to influence the 3D structure of the resulting trioxolane. Consequently, they initiated a Griesbaum co-ozonolysis with a racemic cyclohexanone, to afford the *trans* diastereoisomer of Artefenomel, RLA-3107 [493] (**Scheme 2.4**). This was a cost -ffective and successful reaction.



University of Ghana http://ugspace.ug.edu.gh

Scheme 2.4: Structural optimization of artefenomel, leading to the development of RLA-3107 [493].

RLA-3107 is still in preclinical studies and may enter clinical trials if subsequent studies are successful. Hopefully this compound will emerge as the most successful fully synthetic endoperoxide to gain approval for antimalarial treatment [493].

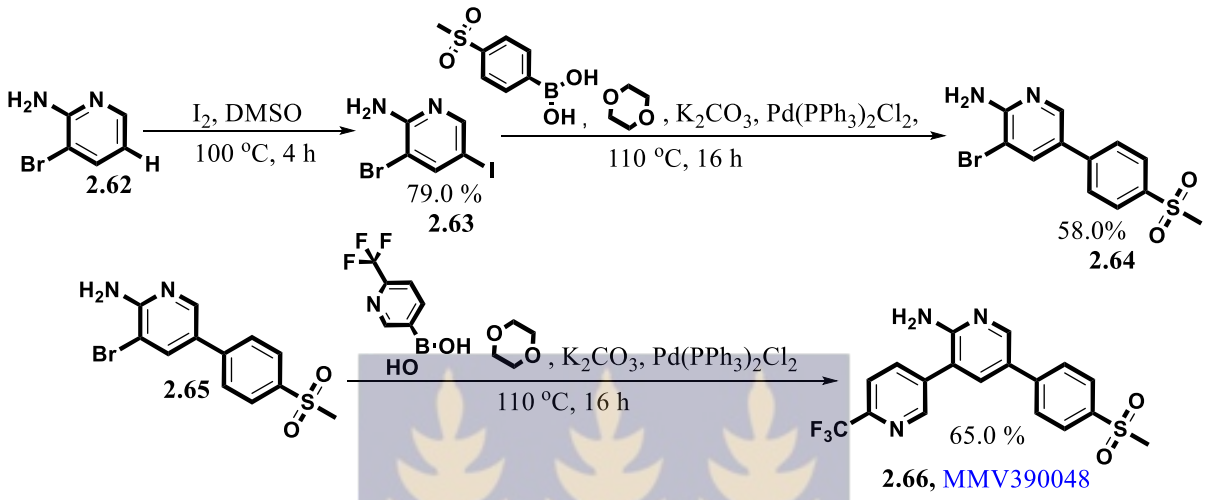
2.6.2 MMV390048

MMV390048 (**2.66**; **Scheme 2.5**); 2-aminopyridine, discovered through phenotypic screening (within MMV's portfolio), is a molecule that marked Africa's entry into world-class antimalarial drug discovery. It was the first antimalarial compound discovered and developed entirely on African soil (H3D center, University of Cape Town, South Africa) to enter clinical trials, showcasing the research and innovation capacity of drug discovery scientists on the continent. With malaria being a leading cause of death in Africa, its clinical trials held on the continent allowed for the assessment of efficacy, safety, and pharmacokinetics under real-world transmission conditions, enhancing the relevance and reliability of clinical data, and supporting the development of solutions tailored to the continent's unique health challenges. It also affirmed Africa's capability to host sophisticated clinical studies [495].

As a first-in-class drug, MMV390048, was anticipated to evade cross-resistance mechanisms, positioning it as an ideal candidate to address drug-resistant malaria. Further screening of the scaffold confirmed its activity against drug-resistant strains and multiple stages of the parasite, as well as evidence of transmission-blocking efficacy [496]. With its 2-aminopyridine core being responsible for its antimalarial activity, the synthesis of MMV390048 followed a 3-step synthetic route, commencing with an iodination on a 3-bromopyridin-2-amine, **2.62**, and sub-

University of Ghana http://ugspace.ug.edu.gh

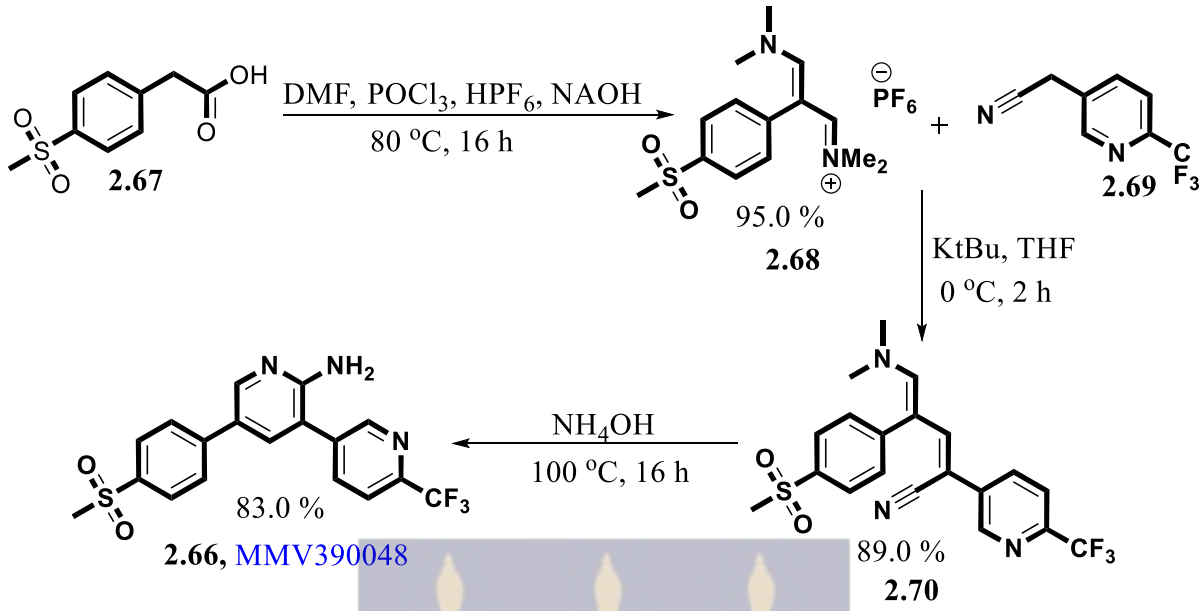
sequent Suzuki-Miyaura cross-coupling reactions to attach the aryl moieties (**Scheme 2.5**) [497].



Scheme 2.5: Synthetic route for MMV390048 [497].

Owing to the success of MMV390048 which attracted global interest, Paymode *et al.* proposed an alternative synthetic route. The synthetic route, described as more efficient and cost-effective, involved an initial preparation of a Vinamidinium salt, **2.68**, from sulfonylphenyl acetic acid, **2.67**, which was coupled with pyridyl acetonitrile, **2.69,** using potassium tert-butoxide as a base, to yield a key intermediate, **2.70**. A subsequent reaction with ammonium hydroxide afforded the desired analogue (**Scheme 2.6**) [498].

University of Ghana http://ugspace.ug.edu.gh



Scheme 2.6: Paymode et al's proposed synthetic route for MMV390048 [498].

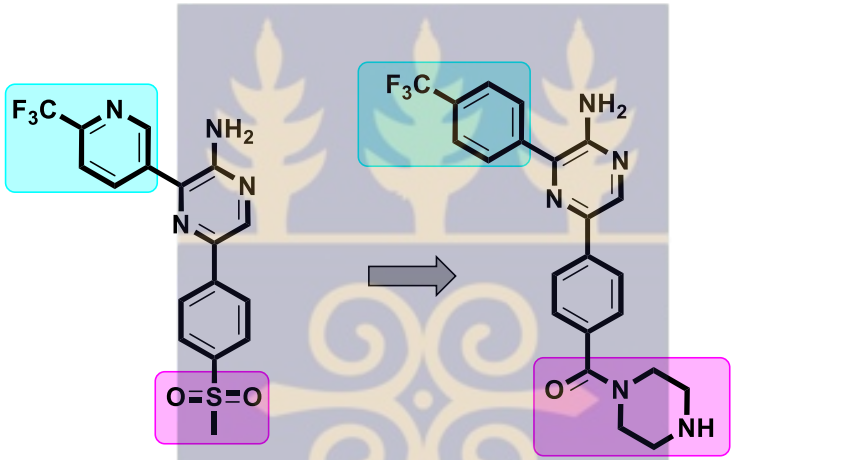
Further studies through genomics and chemoproteomics identified PI4K of *P. falciparum* as the target of MMV390048. As an essential kinase, PI4K plays a central role in the parasite's membrane and vesicular systems. Its role in the parasite spans multiple life-cycle stages. Its inhibition therefore disrupts the parasite's intracellular membrane transport systems, which are critical for its survival and replication [496, 499].

Clinical studies also indicated that MMV390048's favourable pharmacokinetic and pharmacodynamic properties support its feasibility for a single-dose cure. Its activity across multiple stages of the parasite's cycle qualifies it as a triple-action antimalarial (prophylactic, treatment, and transmission-blocking), a key objective in MMV's TPPs [499-501]. Additionally, MMV390048's success at validating Plasmodium PI4K as a druggable antimalarial target opened a new mechanistic class of targets, distinct from known and exploited ones [496]. Further development of MMV390048 was discontinued following its deprioritization, primarily due to safety concerns arising from toxicology studies in animal models [502]. Attempts

University of Ghana http://ugspace.ug.edu.gh

to address the challenges associated with MMV'048 led to the development of its second-generation PI4K inhibitor; UCT943 (**2.71**; **Figure 2.12**).

To enhance its solubility, the methyl sulfonyl group was substituted with a piperazinyl carboxamide. Additionally, replacing the 2-aminopyridine ring with 2-aminopyrazine increased its asexual blood and liver stage potencies, 5- to 6-fold higher than MMV390048, while maintaining equal activity against other stages. UCT943 has been approved for pre-clinical studies [503, 504].



2.66, MMV390048
IC_{50}(NF54) = 28 nM
IC_{50}(K1*Pf*) = 25 nM
Solubility (pH 7.4) = 4 µg/mL

2.71, UCT943
IC_{50}(NF54) = 5.4 nM
IC_{50}(K1*Pf*) = 4.7 nM
Solubility (pH 8) = 31 µg/mL

Figure 2.12: Structural modification of MMV390048 towards the development of UCT943.

2.6.3 Cipargamin (KAE609)

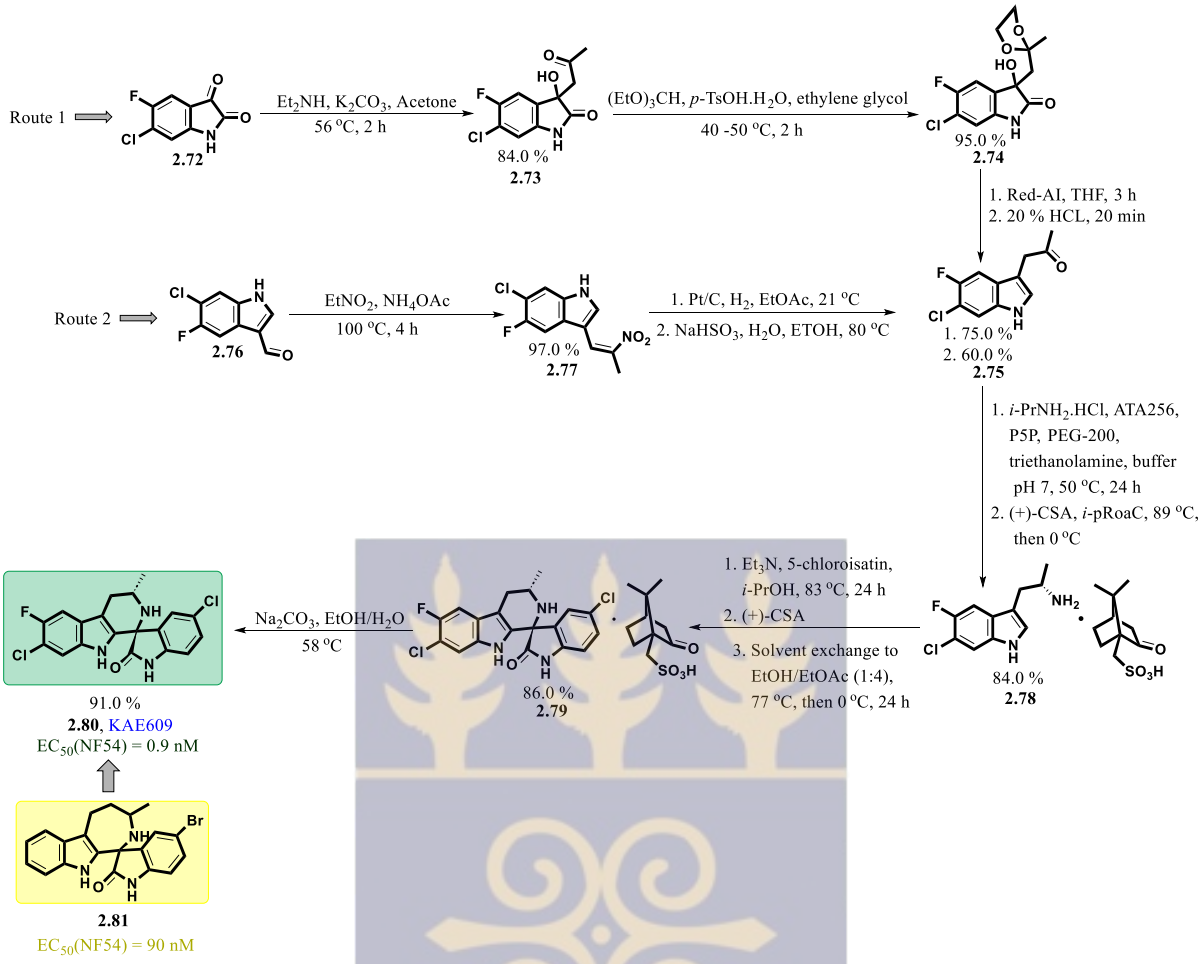
Cipargamin (**2.80**; **Scheme 2.7**) is a spiroindolone identified through phenotypic screening of an extensive library of small molecules against *P. falciparum*. It has exhibited greater potency in rodent models than artesunate and artemether [505].

University of Ghana http://ugspace.ug.edu.gh

The discovery of Cipargamin originated from the identification of spiroazepineindole scaffold, **2.81**, as the most promising hit. However, its synthesis resulted in four possible enantiomers. Further investigations identified that the *1R*, *3S* configuration is essential for activity. Subsequently, detailed SAR studies on the indole motif to address metabolic stability led to Cipargamin. The synthesis of the key intermediate towards Cipargamin was approached *via* two complementary routes: the first commenced from an Isatin, **2.72**, and the other from an aldehyde, **2.76**. The resulting indole ketone, **2.75**, was converted to a chiral tryptamine, **2.78,** which was isolated as an enantiopure compound. **2.78** was then processed through a Pictet-Spengler reaction (which is diastereoselective and favours the formation of the active enantiomer of KAE609), to form a spiroindoline salt, **2.79**, and subsequently neutralised to afford Cipargamin (**Scheme 2.7)** [497, 506, 507].

The mechanism of action of KAE609 was unravelled through docking and functional analysis studies, revealing it as an inhibitor of *PfATP4, a* protein responsible for Na^+ efflux from the parasite's cytoplasm to maintain ionic balance. The disruption of sodium efflux leads to a build of Na^+ in the parasite, causing osmotic swelling of the RBCs. Their normal morphology is therefore distorted, making them easily recognised and cleared by the spleen, which routinely filters out abnormal or rigid cells. In parallel, the parasite's internal pH, membrane potential, and nutrient transport systems are severely disrupted, leading to metabolic collapse and ultimately death [508-510].

University of Ghana http://ugspace.ug.edu.gh



Scheme 2.7: Synthetic route for the preparation of Cipargamin (KAE609) [497].

Cipargamin is a potential candidate for single-dose therapy, with fast-acting multi-stage potency against *P. falciparum* (and some level of efficacy against *P. vivax*), as well as rapid *in vitro* and *in vivo* clearance. It is also reported to also exhibit acceptable tolerability and safety profiles, demonstrating efficacy, consistent with its novel mechanism of action (as a first-in-class molecule). Reports on its combination with piperaquine indicate that it is well tolerated, with no adverse effects. With on-going Phase II clinical trials on its combination with other antimalarials, KAE609 offers potential as a promising next-generation antimalarial, capable of overcoming drug resistance in both complicated and severe malaria [511-514].

University of Ghana http://ugspace.ug.edu.gh

2.6.4 Ganaplacide (KAF156)

Ganaplacide (KAF156) (**2.84**; **Figure 2.13**) is one of the few antimalarial candidates that have advanced to Phase III clinical trials. Obtained from a phenotypic screen, it is a leading second-generation imidazolopiperazine with multiple life stage activities against *P. falciparum* and *P. vivax*, as well as a novel class of antimalarials with a unique mechanism of action [515, 516].

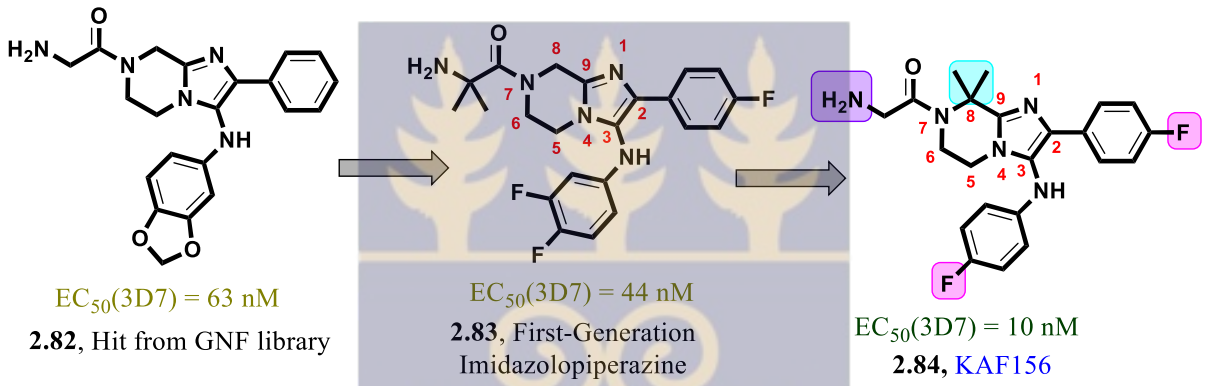
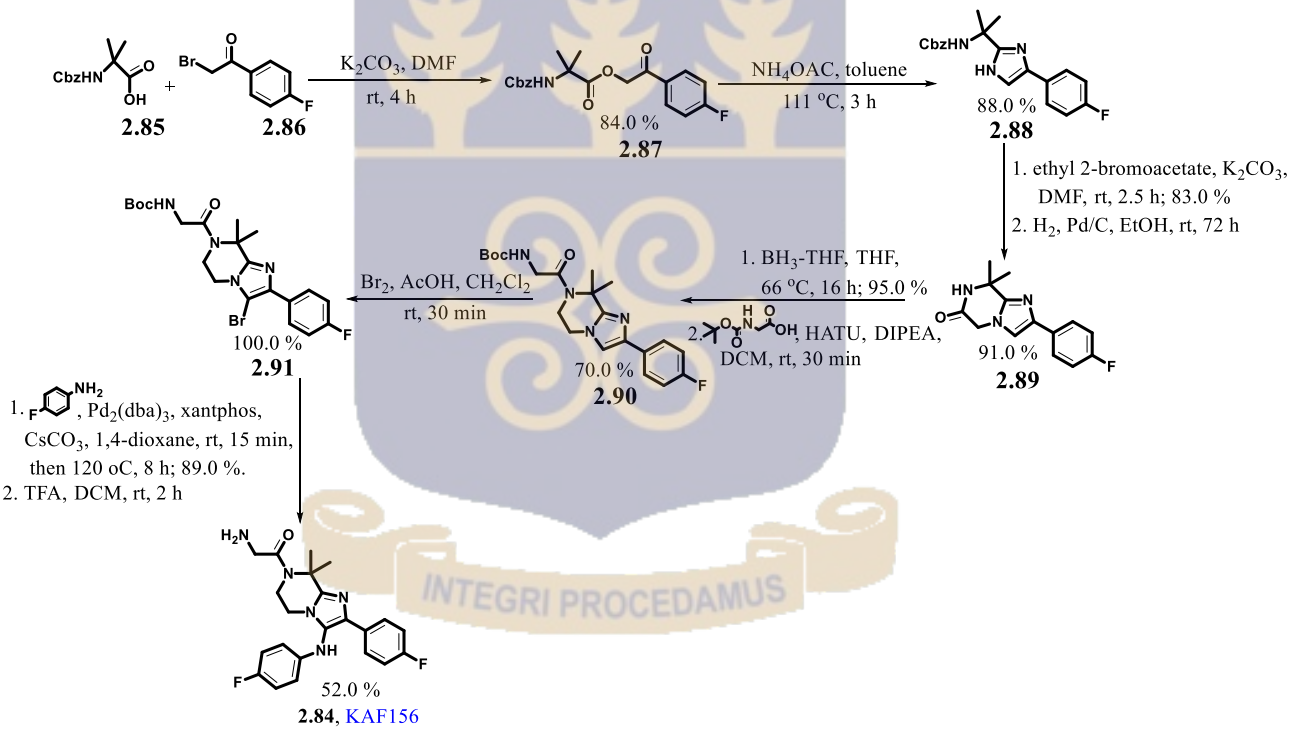


Figure 2.13: Structural evolution from initial hit to Ganaplacide.

Ganaplacide was discovered following a high-throughput screening of 1.7 million compounds from the Genomics Institute of the Novartis Research Foundation (GNF) library in a *P. falciparum* cell-based proliferation assay. The hit compound, **2.82,** was subsequently progressed through hit-to-lead refinement and iterative optimization to yield KAF156 [469, 497]. Benzodioxole and phenyl moieties of the compound were substituted with fluoro groups (to yield first-generation imidazolopiperazine, **2.83)** by Wu *et al.*, to address metabolic susceptibility [517]. However, it was later observed that although the removal of the glycine side chain from the piperazine ring increased *in vitro* potency, it reduced in reduced parasitaemia, highlighting its critical role in maintaining *in vivo* efficacy [469]. Further substitution of alkyl groups at the 8-position of the piperazine core by Nagle *et al*. led to the more potent

University of Ghana http://ugspace.ug.edu.gh

ganaplacide [437]. The synthesis of KAF156 began with an ester formation from a protected 2-amino-2-methylpropionic acid, **2.85**, and 4-fluorophenacyl bromide, **2.86**. Condensation of the ester (**2.87**) furnished the imidazole core, which was subsequently alkylated under basic conditions. The resulting benzyl carbamate, **2.89**, was subjected to hydrogenolysis to yield the corresponding lactam, **2.90**, which was reduced and Boc-protected, allowing substitution of a bromide on the imidazole ring (**2.91**). This created a favourable condition for a Buchwald-Hartwig amination with 4-fluoroaniline. Deprotection of the glycine sidechain then led to the final compound, Ganaplacide (**Scheme 2.8**).



Scheme 2.8: Synthetic route to ganaplacide (KAF156) [437, 497].

The exact mechanism of action of Ganaplacide is still under investigation; however, recent studies indicate that it disrupts the parasite's protein trafficking and secretory pathways [469, 518]. In preclinical and clinical trials, Ganaplacide has demonstrated consistent *multi-stage in vitro* and *in vivo* efficacy against drug-sensitive and drug-resistant strains. It's safety and favourable pharmacokinetic properties in healthy human volunteers is compatible with once-

University of Ghana http://ugspace.ug.edu.gh

daily oral dosing, making it more suited for use as a therapeutic, prophylactic and transmission-blocking agent [469, 519, 520]. To improve the therapeutic efficacy, prevent the emergence of resistance, and extend prophylactic duration, Ganaplacide is currently under investigation in combination with other antimalarial agents [520, 521]. Its fast-acting, multistage activity complements the longer half-life and blood-stage potency of antimalarial agents such as lumefantrine. Studies from Phase II and Phase III clinical trials confirm its compatibility with lumefantrine, with both compounds exhibiting strong potential in treating and preventing malaria [522-524]. With its multistage activity, favourable pharmacokinetics, and compatibility in combination therapies, Ganaplacide represents a compelling next-generation antimalarial for future global malaria control efforts.

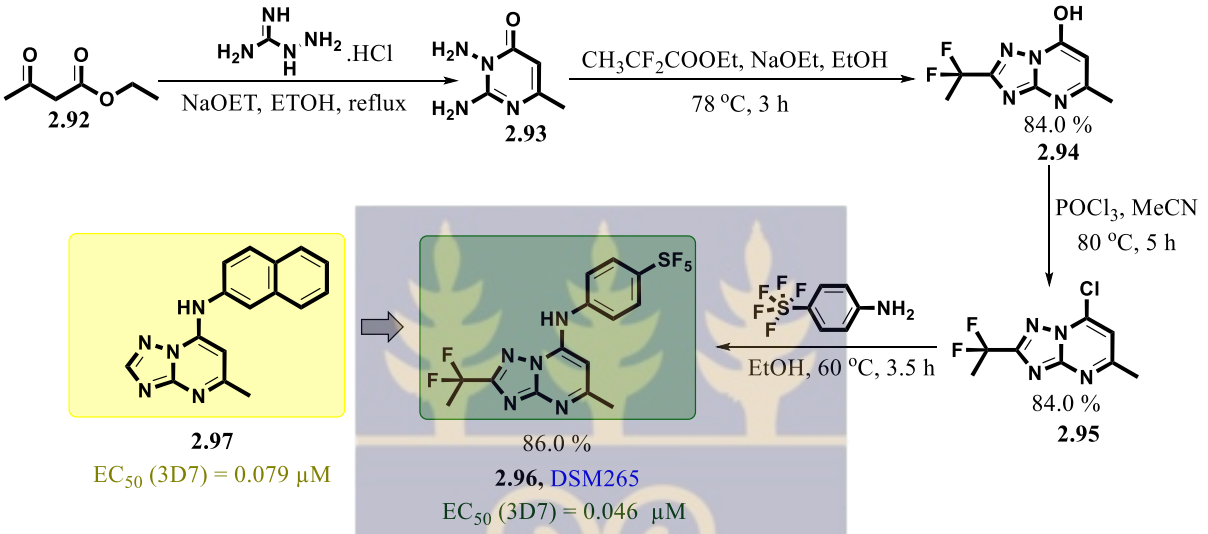
2.6.5 DSM265

DSM265 (**2.81**; **Scheme 2.9**) is a triazolopyrimidine rationally designed and optimised to target a flavin mononucleotide-dependent enzyme; dihydroorotate dehydrogenase (DHODH) [525]. Its discovery through TBS and as the first clinical inhibitor of *P. falciparum* DHODH, marks a clear departure from phenotypic screening, which has dominated antimalarial drug discovery for decades. It is considered one of the most advanced candidates in the global antimalarial drug development pipe-line [526].

A high-throughput screen against the parasite's DHODH led to the identification of **2.82** as the most promising inhibitor of DHODH. However, **2.82** demonstrated poor *in vivo* efficacy. With the bulky naphthyl group identified as a key contributor to the observed poor pharmacokinetic performance, its replacement with various substituted phenyl groups and other structural modifications *via* a comprehensive SAR study led to DSM265, with improved potency, solubility and metabolic stability [497, 527]. The synthesis of DSM proceeded *via* the

University of Ghana http://ugspace.ug.edu.gh

cyclo-condensation of ethyl acetoacetate, **2.92,** with aminoguanidine hydrochloride, yielding pyrimidinone, **2.93**, which was converted into a hydroxyl pyrazolopyrimidine, **2.94**. A chlorination with phosphoryl chloride subsequently followed this. Further substitution of chloride **2.95**, with pentafluorosulfonyl aniline, afforded DSM265 (**Scheme 2.9**) [497, 525].



Scheme 2.9: Synthetic route to DSM265.

DSM265 is designed to selectively bind to the ubiquinone binding site (Q-site/ quinine tunnel) of the DHODH enzyme of *P. falciparum* (**Figure 2.14**). Studies demonstrate that it forms strong hydrophobic interactions, π-π stacking and direct or water-mediated hydrogen bonds with several amino acids of the *P. falciparum* DHODH [528-530]. DHODH catalyzes the conversion of dihydroorotate to orotate, an acid that plays a crucial role in the *de novo* pyrimidine (building blocks of DNA/RNA) biosynthesis pathway. The action of DSM265 therefore blocks DHODH activity, preventing the synthesis of DNA/RNA and ultimately killing the parasite [527, 531].

University of Ghana http://ugspace.ug.edu.gh

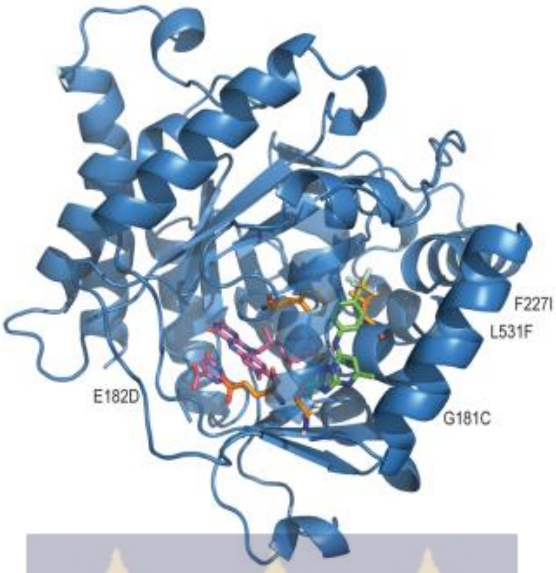


Figure 2.14: Crystal structure of *P. falciparum* DHODH in complex with DSM265 (shown in green) [289].

DSM265 stands out as a first-in-class DHODH inhibitor, making it a strong candidate to address drug resistance. Its dual-stage activity (asexual and liver stages), long half-life, low clearance rate, good safety profile, selectivity, and transmission-blocking abilities, highlighted by pre-clinical, Phase I, and II reports, offer therapeutic potential beyond existing treatment options [420, 532, 533]. Like any other antimalarial, its combination with other antimalarials particularly artefenomel is under study to reduce resistance risk [534, 535].

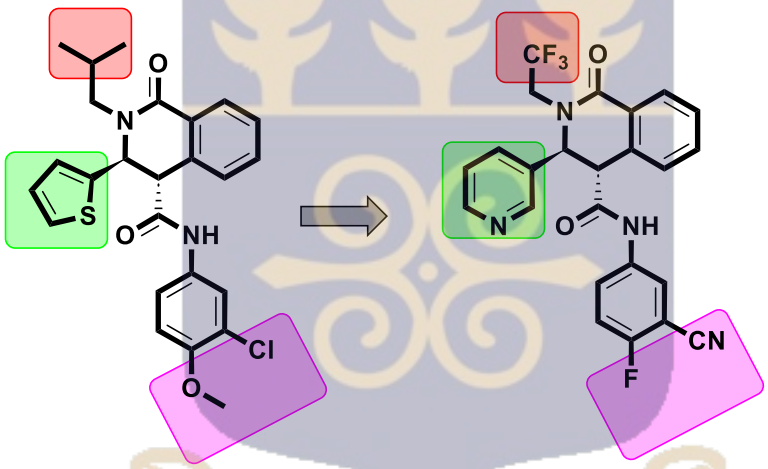
2.6.6 SJ733 ((+)-SJ000557733)

Another promising next-generation antimalarial in the drug discovery pipeline is SJ733 (**2.99**; **Figure 2.13**). The tetrahydroisoquinolone carboxanilide, discovered through PS is reported to inhibit gametocytogenesis and the maturation of blood-stage schizonts in the parasite. It is potent against drug-sensitive and drug-resistant strains of *P. falciparum* and *P. vivax,* and has

University of Ghana http://ugspace.ug.edu.gh

been recommended as a promising candidate for further investigation as both a treatment and a transmission-blocking agent [536-538].

Following a high-throughput screening, compound **2.98** was identified as an inhibitor of the asexual blood stage of *P. falciparum*. Metabolic studies on **2.98**, identified susceptibilities to the methoxy, thiophene, and isobutyl functional groups. To address these, substituting aniline with fluoro and cyano groups led to a 2-fold increase in potency. Further replacement of the thiophene and isobutyl groups with pyridyl and trifluoromethyl moieties, respectively, led to SJ733, which showed improved solubility (**Figure 2.15**) [527].



2.98
EC_{50} (3D7) = 53 nM
Solubility (pH 6.5) = 1.8 µM

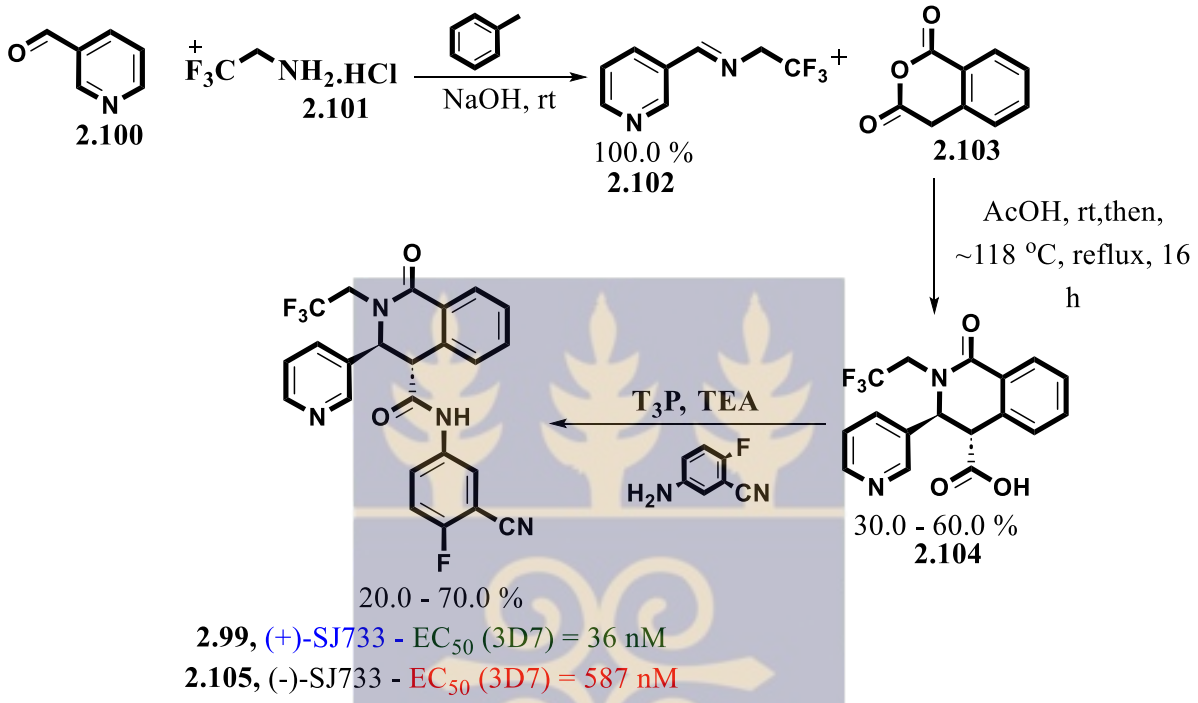
2.99, SJ733
EC_{50} (3D7) = 36 nM
Solubility (pH 6.5) = 63.8 µM

Figure 2.15: Structural modifications on hit compound, **2.98** that led to SJ733.

Hit-to-lead optimization for SJ733 was carried out according to the synthetic route outlined in **Scheme 2.10**. 2,2,2-trifluoroethylamine, **2.102**, was first prepared from its equivalent amine hydrochloride salt, **2.101**, and nicotinaldehyde in toluene. The aldimine was then condensed with homophthalic anhydride (HPA) to yield *trans*-carboxylic acid, **2.104**, which was coupled with cyano-4-fluoroaniline to yield the desired compound. SJ733 was obtained as a ra-

University of Ghana http://ugspace.ug.edu.gh

cemic mixture. To establish if there is any enantiomeric preference, separation of the individual enantiomers and biological evaluation confirmed the (+)- enantiomer as the most potent [539].



Scheme 2.10: Synthetic route to SJ733 [539].

Similar to KAE609, SJ733 exerts its antimalarial activity by blocking the PfATP4-mediated export of sodium ions from the parasite [536, 540].

SJ733 has demonstrated good oral bioavailability, low toxicity and moderate half-life [538]. In Phase I clinical trials, no serious adverse effects were recorded in healthy human volunteers [540]. Further studies have documented its efficacy against uncomplicated *P. falciparum* and *P. vivax* infections and its potential as a candidate for an effective combination regimen. [469, 537, 541].

University of Ghana http://ugspace.ug.edu.gh

2.6.7 Ferroquine (SSR97913)

Ferroquine (**2.106**; **Figure 2.16**) is an organometallic antimalarial designed to overcome resistance-associated challenges with chloroquine. It is a hybrid molecule, derived from the incorporation of a ferrocene moiety (**2.107**) into the side chain of chloroquine (**Figure 2.16**). Ferroquine has demonstrated potent activity against chloroquine-resistant and multidrug-resistant strains of *P. falciparum*, targeting the asexual blood stage, and is the most advanced organometallic drug candidate [535, 542, 543].

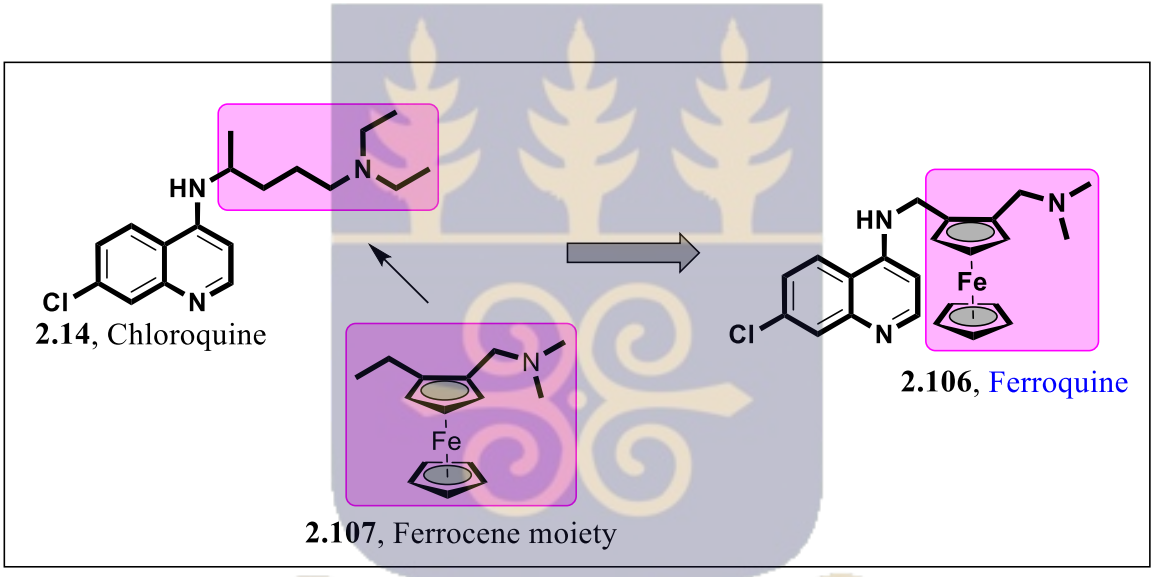
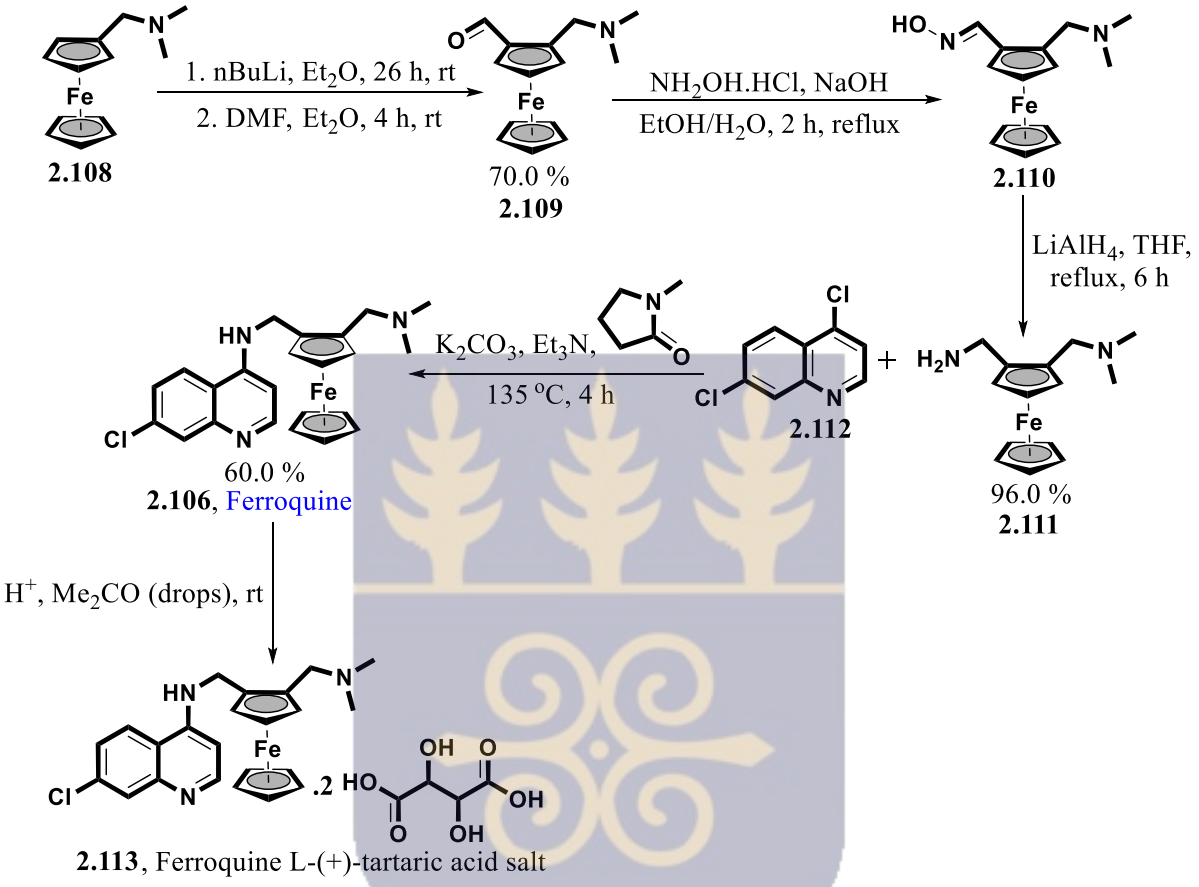


Figure 2.16: Molecular hybridisation towards ferroquine.

The rapidly expanding interest in transition-metal complexes in medicinal chemistry, coupled with the pursuit of novel chloroquine analogues with enhanced potency, motivated Biot *et al.* to develop ferrocenyl compounds. As described in their published report, the 6-step synthesis was initiated with a metalation and subsequent conversion of ((dimethylamino)methyl)ferrocene, **2.108**, to an aldehyde, **2.109,** which was then converted to an oxime, **2.110**, and to its corresponding amine, **2.111**. Regioselective amination between **2.96** and 4,7-

University of Ghana http://ugspace.ug.edu.gh

dichloroquinoline, **2.112**, led to the free base, ferroquine. Ferroquine was further treated with L-(+)-tartaric acid to yield the ammonium salt, **2.113** (**Scheme 2.11)** [543, 544].



Scheme 2.11: Synthetic route to Ferroquine [544].

Though ferroquine is biologically active as a free base, its salt form is the biological version used in studies and development. This is because it offers improved solubility, crucial for oral bioavailability and absorption, enhanced stability, and easy formulation (especially in aqueous media). Studies also show that the dissociation of the salt under physiological conditions (pH (~7.4)) releases the active free base, thus, the full antimalarial activity is still retained nonetheless [542, 545, 546].

University of Ghana http://ugspace.ug.edu.gh

The medicinal chemistry strategy underlying the synthesis of ferroquine opens another chapter in drug discovery.

Molecular hybridization involves the strategic combination of two bioactive pharmacophores into a single molecule to exhibit the biological properties of their original compounds. It is a synthetic strategy employed to usually overcome resistance, enhance biological activity, or improve pharmacokinetics [547-549]. Ferrocene is a stable organometallic compound with unique redox properties. It is a moiety that can be easily functionalized and stably incorporated into a drug-like molecule without disrupting its overall pharmacophore. Its sandwich structure offers planarity and conformational flexibility, favourable for interacting with biological targets [550, 551]. Moreover, ferrocenyl derivatives with other therapeutic properties have demonstrated biocompatibility in organometallic scaffolds [550, 552]. Its incorporation into the chloroquine scaffold, therefore, offers synthetic tractability and improved pharmacological properties, with an additional advantage of a novel redox-based mechanism of action [553].

The ferrocene-chloroquine hybrid exerts its antimalarial activity through a multi-faceted mechanism of action. It combines the heme detoxification inhibition properties of chloroquine with the redox potential of ferrrocene. Reversible redox cycling of the ferrocene unit produces ROS in the parasite's vacuole, leading to oxidative stress and cytotoxicity [543, 553, 554]. Furthermore, ferroquine’s increased lipophilicity and molecular bulk (due to ferrocene) enable its evasion of PfCRT-mediated efflux mechanisms, facilitating its accumulation within the parasite’s digestive vacuole. This further contributes to its efficacy against chloroquine-resistant *P. falciparum* strains [555, 556].

University of Ghana http://ugspace.ug.edu.gh

Ferroquine demonstrated equipotent activity with chloroquine-sensitive strains, and superior activitiy, against semi-resistant, and highly resistant strains of chloroquine [544]. With SAR studies linking this improvement in potency to the presence of ferrocene, ferroquine has successfully advanced through Phase I and II trials, demonstrating a favourable safety profile and potent efficacy (especially in combination therapies) [552]. While recent single-dose regimen trials have yielded mixed results, ongoing combination studies could meet the effectiveness and regulatory benchmarks required for its approval to full participation in combating drug-resistant malaria [535, 542].

Numerous other candidates continue to emerge within this expanding pipeline [161, 527]. While many molecules including M5717 (cabamiquine), **2.114** [557], MMV688533, **2.119** [558], Zy19489 (Sutidiazine), **2.118** [457], ACT-451840, **2.115** [559], P218, **2.116** [560] and AN13762, **2.117** [561] (**Figure 2.17**) are still in early phases of clinical development, their unique pharmacological profiles and mechanisms of action represent a foundational step toward more effective, durable, and globally relevant malaria interventions [562, 563].

As resistance to current front-line therapies continues to rise, the timely integration of these and newer next-generation molecules into combination treatment regimens may prove pivotal in sustaining the gains made in malaria control and eradication [564].

University of Ghana http://ugspace.ug.edu.gh

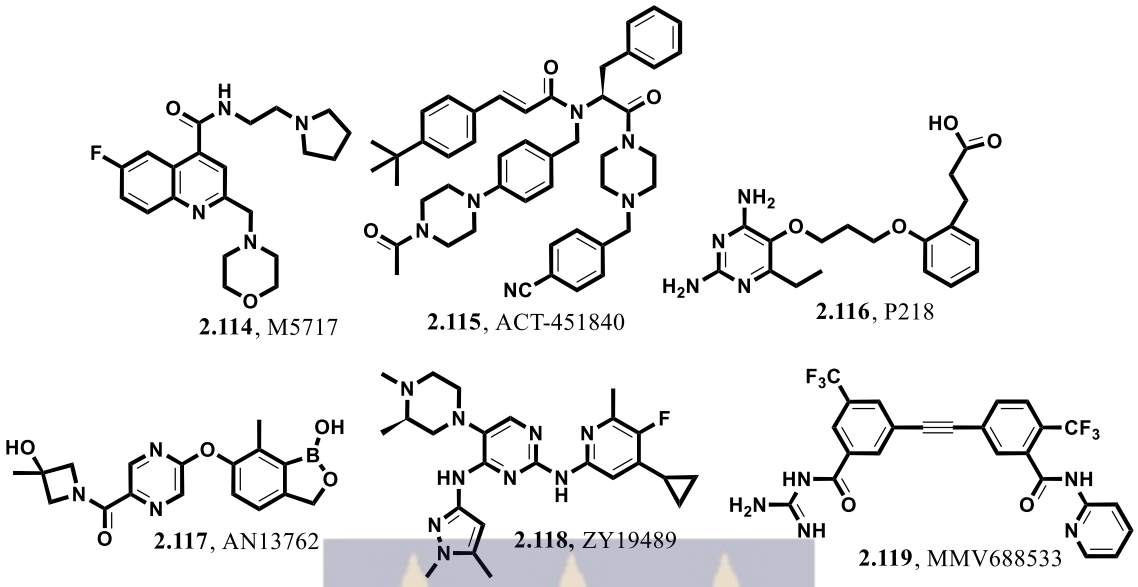


Figure 2.17: Other candidates in the antimalarial discovery pipeline.

Obviously, the pivotal role of phenotypic screening in identifying next-generation antimalarial candidates in contemporary drug discovery cannot be overstated. While it has led to the discovery of novel molecules, its strategic combination with TBS has unveiled unique mechanisms of action that are highly efficacious against drug-resistant strains [563, 565]. The continued complementary use and integration of these key approaches will be critical for sustaining a robust and diverse antimalarial drug discovery pipeline, capable of meeting global eradication goals.

INTEGRI PROCEDAMUS

2.7 Hit scaffolds MMV676444 and MMV1794959.

To contribute to the current pipeline of phenotypically derived antimalarials that would potentially tackle drug resistance, this study focuses on two scaffolds (MMV676444 and MMV1794959) from the MMV pathogen Box (**Figure 2.18**). They represent chemically diverse starting points that have demonstrated significant antimalarial activities in phenotypic assays, but require further structural modifications to optimise their therapeutic potential.

University of Ghana http://ugspace.ug.edu.gh

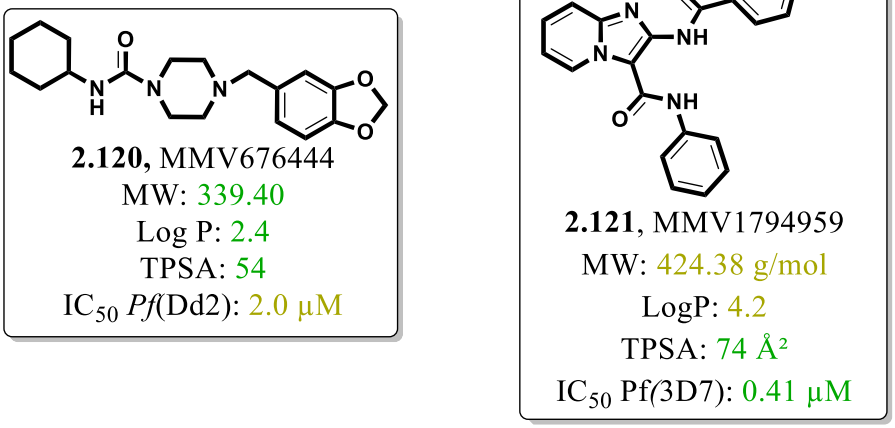


Figure 2.18: Chemical Structures of Hit Scaffolds MMV676444 and MMV1794959.

2.7.1 MMV676444

MMV676444 is one of the 400 analogues in the MMV pathogen box with good antitubercular activity. Although discovered through antitubercular screening, it was also reported to exhibit significant antimalarial activity (IC_{50} *pf*(Dd2 = 2.0 µM)).

Table 2.2: Summary the Biological and physicochemical profile of MMV676444.

Scaffold Profile	
Dd2 Sybr green (µM)	**2.0**
2-week GAST/Fe MIC (µM)	**1.2**
Log P CYP2C9 inhibition µM	**20.0**
Hepatocyte stability (Clint (µL/min/10^6 cells))	**1.31**
Hepatocyte stability ($t_{1/2}$ (min))	**250**
Microsomal stability (Clint (µL/min/mg protein))	**1.15**
Microsomal stability ($t_{1/2}$ (min))	**464.0**

With physicochemical parameters within acceptable limits for drug-likeness [566, 567], MMV676444 exhibited a microsomal half-life of 464 min (Clint = 1.15 µL/min/mg protein)

University of Ghana http://ugspace.ug.edu.gh

(**Table 2.2**), indicating high metabolic stability and suggesting minimal susceptibility to CYP450-mediated metabolism [568, 569]. Hepatocyte stability studies also confirmed its resistance to hepatic metabolism (half-life: 250 min (Clint 1.31 µL/min/10^6 cells)), validating minimal susceptibility to Phase I as well as Phase II metabolism, therefore implying low intrinsic clearance [570, 571]. Furthermore, MMV676444 displayed acceptable CYP2C9 inhibition (IC_{50} = 20 µM) for an early lead, suggesting a manageable risk of drug-drug interactions at this stage of development [572]. Collectively, these properties contribute to the compound's favourable pharmacokinetic potential, supporting its suitability as a drug-like lead.

In a related development, preliminary analogues of the scaffold previously synthesized, have also been reported to exhibit promising antimalarial activity (**2.122-2.127**; **Figure 2.19**), suggesting that MMV676444 may have additional potential against malaria [173].

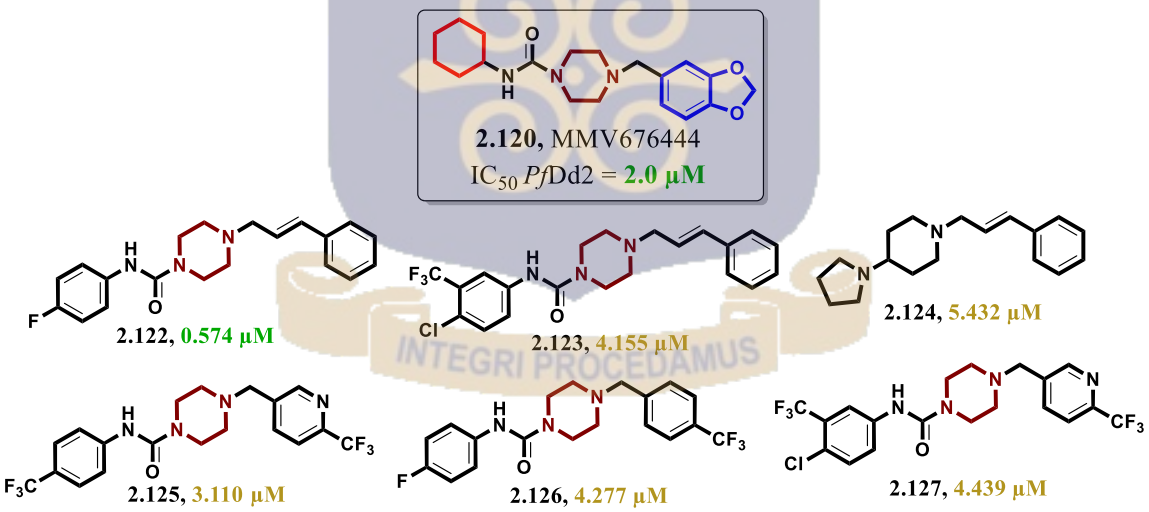


Figure 2.19: Structurally related analogues of MMV676444 with promising antimalarial activities.

University of Ghana http://ugspace.ug.edu.gh

2.7.2 MMV1794959

MMV1794959 is a promising molecule identified through a hit expansion Structure Activity Relationship (SAR) study on a scaffold from the MMV pathogen box; MMV1183932 (**5.1**) (**Figure 2.20**).

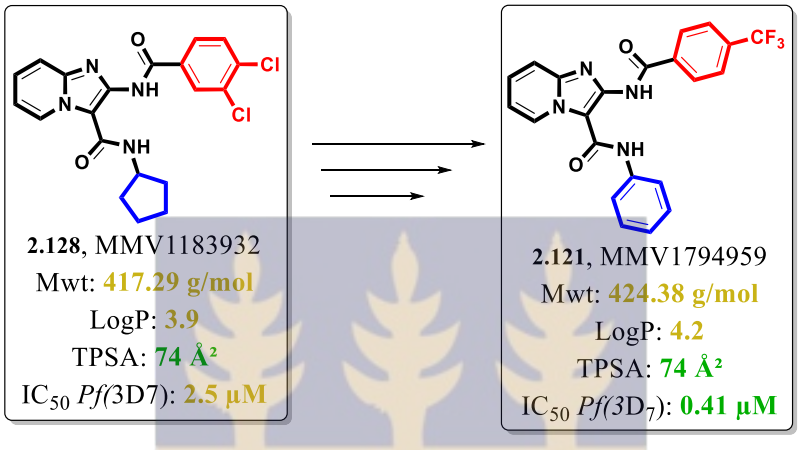


Figure 2.20: Molecular structures of MMV1183932 and MMV1794959.

Table 2.3: Scaffold Profile of MMV1794959.

Scaffold Profile of MMV1794959	
HepG2 (µM)	**8.5**
Selectivity Index (SI)	**21.0**
LogD	**3.3**
HLM (Clint (µL/min/mg))	**0.6**
Solubility (µM)	**3.4**
CYP Inhibition (µM)	**>30**

As indicated in **Table 2.3**, the compound's profile displays its antimalarial activity (IC_{50} = 0.41 µM), alongside a good safety margin (SI = 21.0), balanced hydrophilicity/lipophilicity (Log D = 3.3 µM), excellent metabolic stability (HLM (Clint = 0.6 µL/min/mg), and low risk of metabolic liability (CYP inhibition >30 µM). These favourable properties collectively support the scaffolds prioritization for hit-to-lead optimization [568, 569, 573]. Though the

University of Ghana http://ugspace.ug.edu.gh

scaffold exhibits high toxicity against human liver cells and sub-optimal solubility requires improvement, these parameters are highly amendable to Structure-Activity SAR optimization [574]. Standard medicinal chemistry manoeuvres could therefore transform this potent hit into a safe, viable and deliverable antimalarial drug.



University of Ghana http://ugspace.ug.edu.gh

CHAPTER THREE

3.0 Experimental

3.1 Materials/Reagents.

3.1.1 Reagents and solvents.

All reagents and solvents were of analytical grade, procured from commercial suppliers and utilized without further purification, unless specified.

3.1.2 Thin Layer Chromatography (TLC).

Reactions were monitored with thin-layer chromatography (TLC) on pre-coated silica gel (0.25 mm layer of silica gel F254) aluminium sheets and visualised under UV light (254 nm).

3.1.3 Column chromatography.

Chromatographic separations were carried out using Merck 938S Kieselgel 60 silica gel as the stationary phase, under flash conditions.

3.2 Instrumentation.

3.2.1 Fourier-Transform Infrared (FT-IR) Spectroscopy.

FTIR spectra were recorded using a Perkin-Elmer 100 FTIR spectrometer on neat compounds. Samples placed directly on the spectrometer diamond plate were compressed and processed. Observed absorptions of analytical relevance were then reported in wave numbers (cm^{-1}), with band intensities recorded as strong (s), medium (m), weak (w), and broad (b).

3.2.2 Nuclear Magnetic Resonance Spectra (NMR).

^{1}H NMR and ^{13}C NMR spectra were acquired using a Bruker Avance III 400 Hz and 500 MHz instrument, where proton NMR (^{1}H NMR) and Carbon NMR (^{13}C NMR) were acquired at the indicated 400, 101, 500 and 126 MHz respectively, as dilute solutions in either deuter-

University of Ghana http://ugspace.ug.edu.gh

ated dimethyl sulfoxide, (DMSO-d_6), methanol (MeOD- d_4) or chloroform ($CDCl_3$), obtained from sigma Aldrich, with TMS as internal standard. Chemical shifts (δ) were expressed in parts per million (ppm), relative to the residual protonated solvent peak (δ_H: DMSO-d_6 = 2.50, MeOD- d_4, = 3.31, $CHCl_3$ = 7.26 ppm or δ_C: DMSO-d_6 = 39.52, MeOD- d_4, = 49.0, $CHCl_3$ = 77.16 ppm), and coupling constants (J), measured in hertz (Hz). Multiplicities were designated as follows: s: singlet, d: doublet, t: triplet, q: quartert, dd: doublet of doublets, and m: multiplet. Chemical shifts are listed from highest to lowest in the format: chemical shift (multiplicity, coupling constant, integration).

3.2.3 LC-MS.

Mass spectra for most analogues were obtained using the Agilent HPLC system, fitted with an Agilent Jet Stream Electrospray (AJS-E) machine, located at the H3D Center, University of Cape Town (South Africa). Ionization was performed in positive mode with a mobile phase of 10 nM NH_4OAc in 90 % CH_3OH in H_2O, and a stationary phase of Kinetex Cores C18, 2.6 µM, 3 × 50 nm, 100 Å , maintained at 40 ^oC.

MS spectra for other analogues were recorded at the Department of Chemistry, University of Ghana, with a Waters Acquity Ultra (WAU) performance LC system coupled to a Quadrupole LC/MS/MS mass spectrometer (AB SCIEX instruments), fitted with an electrospray interface of SCIEX Triple Quad 3500 with ionization in both positive and negative modes. Mobile phase was 100% CH_3OH containing 0.1% Formic acid, and 100% H_2O containing 0.1% Formic acid, with ACQUITY Premier CSH C18, 1.7 µm VanGuard FIT 2.1 × 50 mm, maintained at 30 ^oC, being the stationary phase.

3.2.4 Melting Point.

Melting points were determined using a Gallenkamp melting apparatus and reported in degrees Celsius (^oC).

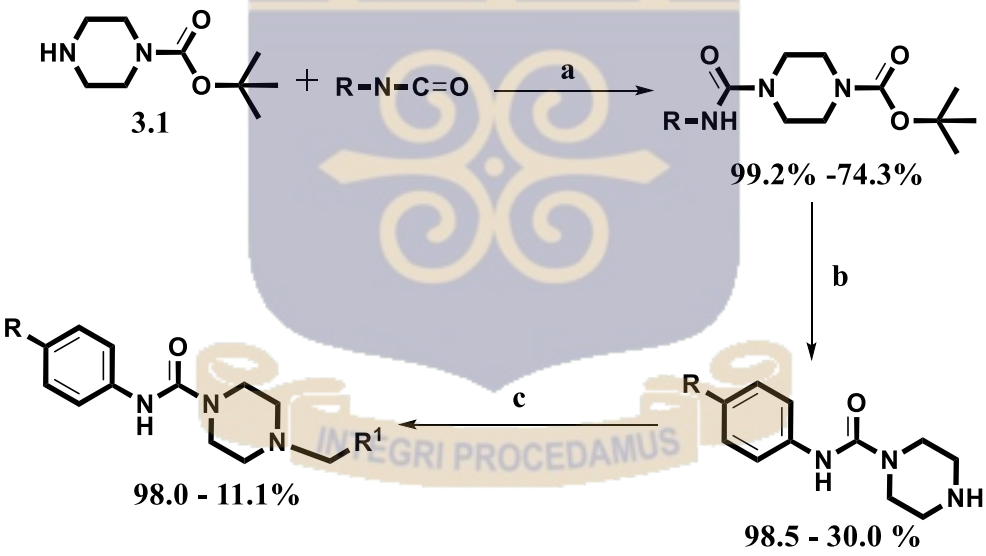
University of Ghana http://ugspace.ug.edu.gh

3.3 Synthesis and Characterisation.

3.3.1 General Procedures.

3.3.1.1 General procedures for MMV676444 analogues.

The target analogues were synthesised in three (3) chemical steps (**Scheme 3.1**), commencing with the formation of a Boc-protected urea, *via* the reaction of *tert*-butyl piperidin-4-ylcarbamate (**3.1**) with commercially available isocyanates. This was followed by a removal of the *Boc*-protection to furnish the key amine intermediate which was subsequently converted to the desired analogues, *via* reductive amination with a variety of aldehydes.



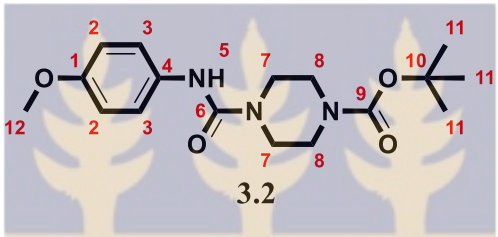
Scheme 3.1: Synthetic route for the synthesis of MMV676444 analogues. a) DCM, 0 ^{o}C, 1 h, then rt, 16 h, b) MeOH, acetyl chloride, 0 ^{o}C, 1 h, then rt, 16 h, c) DCM, 0 ^{o}C, R^{1}CHO, 1 h, $Na(OAc)_3BH$, then rt, 16 h.

University of Ghana http://ugspace.ug.edu.gh

3.3.1.1.1 General procedure for preparation of Boc-protected urea.

A solution of *N*-(*tert*-butoxycarbonyl) piperazine (1.0 g, 5.4 mmol, 1.1 eqv) in DCM (10 mL) was treated with various isocyanates (1.0 eqv.) in ice and stirred for 1 hour. Then subsequently stirred at room temperature for 16 hours. The resulting solution was then filtered, and the white solid obtained was washed with DCM (3 × 10 mL), giving the desired compound.

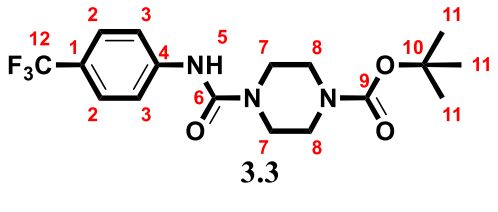
3.3.1.1.1.1 Preparation of *tert*-butyl 4-((4-methoxyphenyl)carbamoyl)piperazine-1-carboxylate, 3.2.



3.2

Compound **3.2** was synthesised following the general procedure for the preparation of Boc-protected urea with 4-methoxyphenyl isocyanate (0.6 mL, 4.9 mmol, 1.0 eqv.) and was obtained in 93.8 % yield as a white solid. **^{1}H NMR** (500 MHz, $CDCl_3$) δ_H 7.26 (dd, 2H, *J* = 9.0, 5.0 Hz **H3**), 6.83 (dd, 2H, *J* = 9.0, 5.0 Hz **H2**), 6.46 (s, 1H, **H5**), 3.77 (s, 3H, **H12**), 3.49 – 3.46 (m, 4H, **H7**), 3.46 – 3.42 (m, 4H, **H8**), 1.47 (s, 9H, **H11**). **^{13}C NMR** (126 MHz, $CDCl_3$) δ_C 156.27 (**C1**), 155.66 (**C6**), 154.76 (**C9**), 131.75 (**C4**), 122.76 (**C3**), 114.29 (**C2**), 80.43 (**C10**), 55.63 (**C12**), 44.01 (**C7, C8**), 28.52 (**C11**).

3.3.1.1.1.2 Preparation of ***tert*-butyl 4-((4-(trifluoromethyl)phenyl)carbamoyl)piperazine-1-carboxylate, 3.3.**

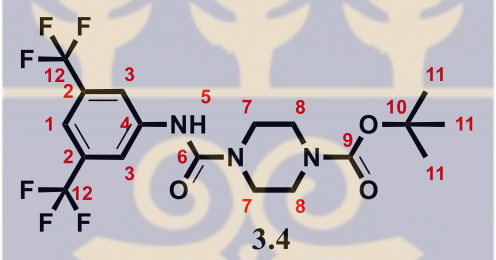


3.3

University of Ghana http://ugspace.ug.edu.gh

Compound **3.3** was synthesised following the general procedure for the preparation of Boc-protected urea with 4-(trifluoromethyl)phenyl isocyanate (0.6 mL, 4.9 mmol, 1.0 eqv.) and obtained in 74.3 % yield as a white solid. **^{1}H NMR** (500 MHz, $CDCl_3$) δ_H 7.53 (d, *J* = 8.4 Hz, 2H, **H3**), 7.47 (d, *J* = 8.6 Hz, 2H, **H2**), 6.66 (s, 1H, **H5**), 3.50 (s, 8H, **H7, H8**), 1.48 (s, 9H, **H11**). **^{13}C NMR** (126 MHz, $CDCl_3$) δ_C 154.74 (**C6**), 154.48 (**C9**), 142.15 (**C4**), 126.37, 126.34, 126.31, 126.28 (**C2**), 125.44, 127.60, 125.26, 125.00 (**C12**), 124.74, 123.28, 121.12 (**C1**), 119.34 (**C3**), 80.65 (**C10**), 44.02 (**C8, C7**), 28.52 (**C11**).

3.3.1.1.1.3 Preparation of *tert*-butyl 4-((3,5-bis(trifluoromethyl)phenyl)carbamoyl)piperazine-1-carboxylate, 3.4.



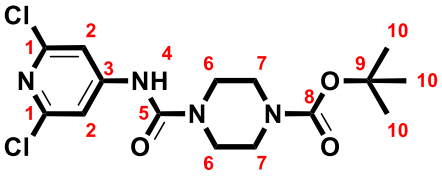
3.4

Compound **3.4** was synthesised following the general procedure for the preparation of Boc-protected urea with bis(trifluoromethyl)phenyl isocyanate (1.5g, 5.9 mmol, 1.0 eqv.) and obtained in 87.8 % yield as a white solid. **^{1}H NMR** (500 MHz, $CDCl_3$) δ_H 7.88 (d, *J* = 1.5 Hz, 2H, **H3**), 7.50 (s, 1H, **H1**), 7.15 (s, 1H, **H5**), 3.53-3.37 (m, 8H, **H7, H8**), 1.47 (s, 9H, **H11**). **^{13}C NMR** (126 MHz, $CDCl_3$) δ_C 154.77 (**C6**), 154.36 (**C9**), 140.72 (**C4**), 132.61, 132.35, 132.08, 131.81 (**C2**), 126.57, 124.40, 122.23, 120.06 (**C12**), 119.56 (**C3**), 116.37(**C1**), 80.79 (**C10**), 48.62 (**C8**), 46.15 (**C7**), 28.49 (**C11**).

INTEGRI PROCEDAMUS

University of Ghana http://ugspace.ug.edu.gh

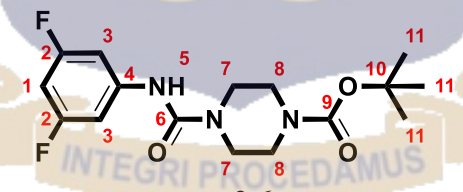
3.3.1.1.1.4 Preparation of *tert*-butyl 4-((2,6-dichloropyridin-4-yl)carbamoyl)piperazine-1-carboxylate, 3.5.



3.5

Compound **3.5** was synthesised following the general procedure for the preparation of Boc-protected urea with 2,6-dichloropyridine-4-isocyanate (0.6 mL, 4.9 mmol, 1.0 eqv.) and obtained in 98.0 % yield as an amber oil. **^{1}H NMR** (500 MHz, $CDCl_3$) δ_H 7.89 (s, 1H, **H4**), 7.41 (s, 2H, **H2**), 3.48 (ddd, *J* = 27.3, 7.5, 4.3 Hz, 8H, **H6, H7**), 1.45 (d, *J* = 6.2 Hz, 9H, **H10**). **^{13}C NMR** (126 MHz, $CDCl_3$) δ_C 154.65 (**C5**), 154.49 (**C8**), 153.25 (**C3**), 150.55 (**C1**), 111.72 (**C2**), 80.62 (**C9**), 45.30 (**C6, C7**), 28.23 (**C10**).

3.3.1.1.1.5 Preparation of *tert*-butyl 4-((3,5-difluorophenyl)carbamoyl)piperazine-1-carboxylate, 3.6.

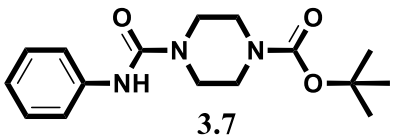


3.6

Compound **3.6** was synthesised following the general procedure for the preparation of Boc-protected urea with 3,5-difluorophenyl isocyanate (0.6 mL, 4.9 mmol, 1.0 eqv), and obtained in 98.0 % yield as an amber oil. ^{1}H NMR (500 MHz, $CDCl_3$) δ_H 6.99 (d, *J* = 8.6 Hz, 1H, **H3**), 6.84 (s, 1H, **H5**), 6.46 (td, *J* = 8.9, 2.2 Hz, 1H, **H1**), 3.48 (s, 8H, **H7, H8**), 1.47 (d, *J* = 1.7 Hz, 9H, **H11**). ^{13}C NMR (126 MHz, $CDCl_3$) δ_C 164.09, 162.02 (**C2**), 154.51 (**C6**), 154.17 (**C9**), 141.38 (**C4**), 102.58 (**C3**), 98.09 (**C1**), 80.39 (**C10**), 44.45 (**C7, C8**), 28.26 (**C11**).

University of Ghana http://ugspace.ug.edu.gh

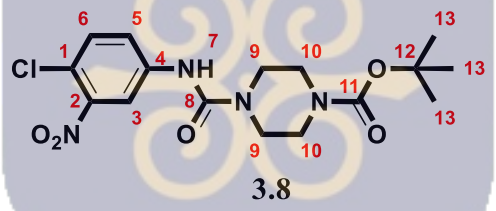
3.3.1.1.1.6 Preparation of *tert*-butyl 4-(phenylcarbamoyl)piperazine-1-carboxylate, 3.7.



3.7

Compound **3.7** was synthesised following the general procedure for the preparation of Boc-protected urea with phenyl isocyanate (0.5 mL, 5.0 mmol, 1.0 eqv.) and obtained in 98.0 % yield as an oil. This intermediate was used directly in the subsequent reaction step without further characterization. Its formation was inferred from the successful synthesis and spectroscopic characterization of the product obtained in the following step.

3.3.1.1.1.7 Preparation of *tert*-butyl 4-((4-chloro-3-nitrophenyl)carbamoyl)piperazine-1-carboxylate, 3.8.

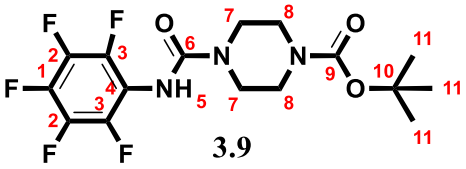


3.8

Compound **3.8** was synthesised following the general procedure for the preparation of Boc-protected urea with 4-chloro-3-nitrophenyl isocyanate (0.5 mL, 5.0 mmol, 1.0 eqv.) and obtained in 98.0 % yield as a white solid. **^{1}H NMR** (500 MHz, $CDCl_3$) δ_H 7.94 (d, *J* = 2.6 Hz, 1H, **H3**), 7.61 (dd, *J* = 8.8, 2.6 Hz, 1H, **H5**), 7.42 (s, 1H, **H7**), 7.37 (d, *J* = 8.8 Hz, 1H, **H6**), 3.52 – 3.49 (m, 4H, **H9**), 3.48 – 3.46 (m, 4H, **H10**), 1.46 (s, 9H, **H13**). **^{13}C NMR** (126 MHz, $CDCl_3$) δ_C 154.79 (**C8**), 154.49 (**C11**), 147.67 (**C2**), 139.20 (**C4**), 131.96 (**C6**), 124.40 (**C5**), 120.10 (**C1**), 116.48 (**C3**), 80.74 (**C12**), 45.31 (**C9, C10**), 28.49 (**C13**).

University of Ghana http://ugspace.ug.edu.gh

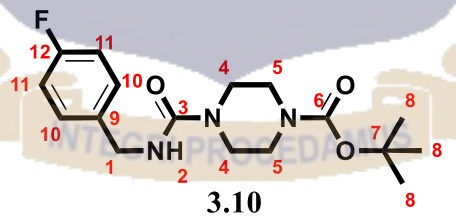
3.3.1.1.1.8 Preparation of *tert*-butyl 4-((perfluorophenyl)carbamoyl)piperazine-1-carboxylate, 3.9**.**



3.9

Compound **3.9** was synthesised following the general procedure for the preparation of Boc-protected urea with pentafluorophenyl isocyanate (0.6 mL, 5.0 mmol, 1.0 eqv.) and was obtained in 80.7 % yield as a white solid. ^{1}H NMR (500 MHz, $CDCl_3$) δ_H 6.76 (s, 1H, **H5**), 3.59 (s, 8H, **H7, H8**), 1.72 (d, *J* = 1.7 Hz, 9H, **H11**). ^{13}C NMR (101 MHz, $CDCl_3$) δ 154.4 (**C6**), 153.7 (**C9**)143.6 (**C3**), 139.6 (**C1**), 135.6 (**C2**), , 113.82 (**C4**), 80.9 (**C10**), 51.8 (**C8**), 43.7 (**C7**), 27.9 (**C11**). **LC-MS:** retention time: 5.0980 min; **WAU-ESI** *(m/z)*: for $[C_{16}H_{18}F_5N_3O_3]^+$ $[M+H]^+$: exact mass calcd.: 395.13; found: 395.90; [M+Na]: 418.18.

3.3.1.1.1.9 Preparation of *tert*-butyl 4-((4-fluorobenzyl)carbamoyl)piperazine-1-carboxylate, 3.10.



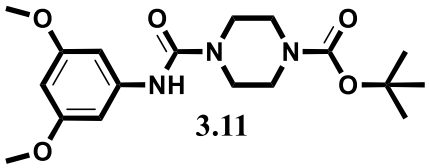
3.10

Compound **3.10** was synthesised following the general procedure for the preparation of Boc-protected urea with 4-fluorobenzyl isocyanate (0.8 mL, 6.6 mmol, 1.0 eqv.) and was obtained in 99.2 % yield as a white solid. **^{1}H NMR** (500 MHz, $CDCl_3$) δ_H 7.35 – 7.19 (m, 2H, **H10**), 7.06 – 6.94 (m, 2H, **H11**), 4.75 (d, *J* = 6.4 Hz, 1H, **H2**), 4.38 (d, *J* = 5.5 Hz, 2H, **H1**), 3.43 (t, *J* = 4.9 Hz, 4H, **H4**), 3.36 (t, *J* = 5.1 Hz, 4H, **H5**), 1.46 (d, *J* = 1.4 Hz, 9H, **H8**). **^{13}C NMR**

University of Ghana http://ugspace.ug.edu.gh

(126 MHz, $CDCl_3$) δ_C 163.01, 161.06 (**C12**), 157.25 (**C3**), 154.53 (**C6**), 134.92 (**C9**), 129.35, 129.29 (**C10**), 115.44, 115.27 (**C11**), 80.12 (**C7**), 45.36 (**C1**), 44.21 (**C4, C5**), 28.27 (**C8**).

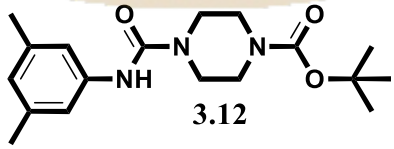
3.3.1.1.1.10 Preparation of *tert*-butyl 4-((3,5-dimethoxyphenyl)carbamoyl)piperazine-1-carboxylate, 3.11.



3.11

Compound **3.11** was synthesised following the general procedure for the preparation of Boc-protected urea with 3,5-dimethoxyphenyl isocyanate (0.9 g, 4.9 mmol, 1.0 eqv.) and obtained in 97.3 % yield as a white solid. **LC-MS:** retention time: 4.883 min; **WAU-ESI** *(m/z)*: for $[C_{18}H_{27}N_3O_5]^+$ $[M+H]^+$: exact mass calcd.: 366.20; found: 366.05; [M+Na]: 388.43; [M+K]: 404.01. This intermediate was used directly in the subsequent reaction step without further characterization. Its formation was inferred from the successful synthesis and spectroscopic characterization of the product obtained in the following step.

3.3.1.1.1.11 Preparation of *tert*-butyl 4-((3,5-dimethylphenyl)carbamoyl)piperazine-1-carboxylate, 3.12.



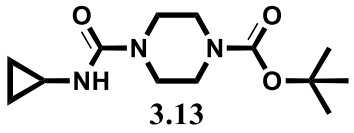
3.12

Compound **3.12** was synthesised following the general procedure for the preparation of Boc-protected urea with 3,5-dimethylphenyl isocyanate (0.7 mL, 4.9 mmol, 1.0 eqv.) and obtained in 83.3 % yield as a white solid. **LC-MS:** retention time: 5.2754 min; **WAU-ESI** *(m/z)*: for $[C_{18}H_{27}N_3O_3]^+$ $[M+H]^+$: exact mass calcd.: 334.21; found: 334.03; [M+Na]: 355.96; [M+K]: 372.11. This intermediate was used directly in the subsequent reaction step without further

University of Ghana http://ugspace.ug.edu.gh

characterization. Its formation was inferred from the successful synthesis and spectroscopic characterization of the product obtained in the following step.

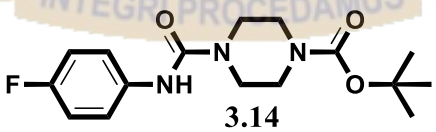
3.3.1.1.1.12 Preparation of *tert*-butyl 4-(cyclopropylcarbamoyl)piperazine-1-carboxylate, 3.13.



3.13

Compound **3.13** was synthesised following the general procedure for the preparation of Boc-protected urea with cyclopropyl isocyanate (0.3 mL, 4.9 mmol, 1.0 eqv.) and obtained in 98.0 % yield as a white solid. **LC-MS:** retention time: 4.248 min; **WAU-ESI** *(m/z)*: for $[C_{13}H_{23}N_3O_3]^+$ $[M+H]^+$: exact mass calcd.: 270.174; found: 270.02; [M+Na]: 292.08. This intermediate was used directly in the subsequent reaction step without further characterization. Its formation was inferred from the successful synthesis and spectroscopic characterization of the product obtained in the following step.

3.3.1.1.1.13 Preparation of *tert*-butyl 4-((4-fluorophenyl)carbamoyl)piperazine-1-carboxylate, 3.14.

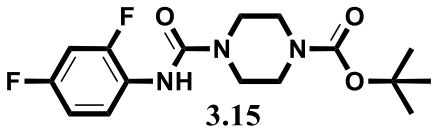


3.14

Compound **3.14** was synthesised following the general procedure for the preparation of Boc-protected urea with 4-fluorophenyl isocyanate (0.6 mL, 4.9 mmol, 1.0 eqv.) and obtained in 79.0 % yield as a white solid. This intermediate was used directly in the subsequent reaction step without further characterization. Its formation was inferred from the successful synthesis and spectroscopic characterization of the product obtained in the following step.

University of Ghana http://ugspace.ug.edu.gh

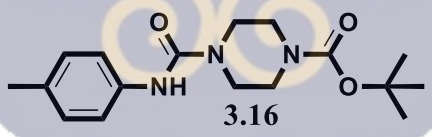
3.3.1.1.1.14 Preparation of *tert*-butyl 4-((2,4-difluorophenyl)carbamoyl)piperazine-1-carboxylate, 3.15.



3.15

Compound **3.15** was synthesised following the general procedure for the preparation of Boc-protected urea with 2,4-difluorophenyl isocyanate (0.6 mL, 4.9 mmol, 1.0 eqv.) and obtained in 93.9 % yield as a white solid. **LC-MS:** retention time: 4.7290 min; **WAU-ESI** *(m/z)*: for $[C_{16}H_{21}F_2N_3O_3]^+$ $[M+H]^+$: exact mass calcd.: 342.16; found: 341.97; [M+Na]: 364.10. This intermediate was used directly in the subsequent reaction step without further characterization. Its formation was inferred from the successful synthesis and spectroscopic characterization of the product obtained in the following step.

3.3.1.1.1.15 Preparation of *tert*-butyl 4-(p-tolylcarbamoyl)piperazine-1-carboxylate, 3.16.

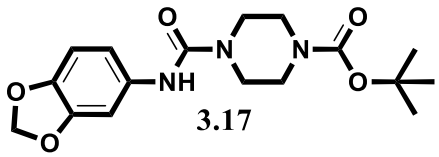


3.16

Compound **3.16** was synthesised following the general procedure for the preparation of Boc-protected urea with *ρ*-tolyl isocyanate (0.6 mL, 4.9 mmol, 1.0 eqv.) and obtained in 98.9 % yield as a white solid. **LC-MS:** retention time: 4.9868 min; **WAU-ESI** *(m/z)*: for $[C_{17}H_{25}N_3O_3]^+$ $[M+H]^+$: exact mass calcd.: 320.19; found: 320.00; [M+Na]: 342.13. This intermediate was used directly in the subsequent reaction step without further characterization. Its formation was inferred from the successful synthesis and spectroscopic characterization of the product obtained in the following step.

University of Ghana http://ugspace.ug.edu.gh

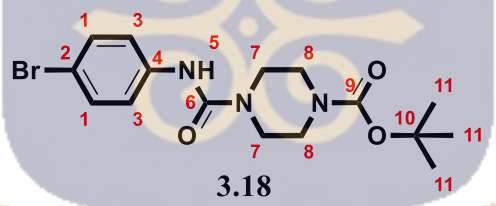
3.3.1.1.1.16 Preparation of *tert*-butyl 4-(benzo[d][1,3]dioxol-5-ylcarbamoyl)piperazine-1-carboxylate, 3.17.



3.17

Compound **3.17** was synthesised following the general procedure for the preparation of Boc-protected urea with 1,3-benzodioxol-5-yl isocyanate (0.6 mL, 4.9 mmol, 1.0 eqv.) and obtained in 98.0 % yield as a white solid. This intermediate was used directly in the subsequent reaction step without further characterization. Its formation was inferred from the successful synthesis and spectroscopic characterization of the product obtained in the following step.

3.3.1.1.1.17 Preparation of *tert*-butyl 4-((4-bromophenyl)carbamoyl)piperazine-1-carboxylate, 3.18.



3.18

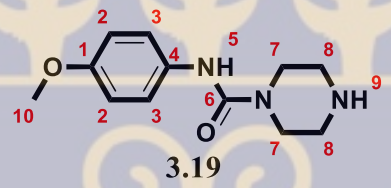
Compound **3.18** was synthesised following the general procedure for the preparation of Boc-protected urea with 4-bromophenyl isocyanate (1 g, 5.1 mmol, 1.0 eqv.) and obtained in 98.0 % yield as a white solid. **^{1}H NMR** (500 MHz, DMSO) δ_H 8.60 (s, 1H, **H5**), 7.51 – 7.37 (m, 2H, **H3**), 7.08 – 7.03 (m, 2H, **H1**), 3.20 – 3.22 (m, 4H, **H7**), 2.61 – 2.62 (m, 4H, **H8**), 1.38 (s, 9H, **H11**). **^{13}C NMR** (126 MHz, DMSO) δ_C 156.49 (**C6**), 155.03 (**C9**), 153.98 (**C4**), 136.70 (**C2**), 121.45 (**C1**), 114.88 (**C3**), 78.58 (**C10**), 45.29 (**C8**), 43.50 (**C7**), 28.09 (**C11**).

University of Ghana http://ugspace.ug.edu.gh

3.3.1.1.2 General procedure for deprotection of the Boc-protected urea.

To a solution of the Boc-protected urea (1 eqv.) intermediate in MeOH (30 mL) was added acetyl chloride (10 eqv.), and the mixture was stirred for 20 minutes at 0 ℃. The reaction was subsequently stirred for 16 hours at room temperature, and the resulting suspension was filtered. The residue was then washed with diethyl ether (3 x 20 mL) to yield a hydrochloride salt of the amine, then partitioned between DCM and 10% aqueous KOH. The aqueous layer was extracted with DCM (3 × 10 mL), and the combined organic extracts were dried over $MgSO_4$ and concentrated to yield the title compound as a white solid or oil.

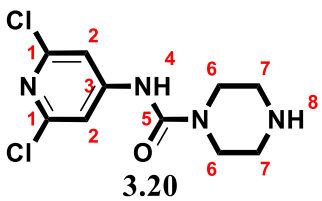
3.3.1.1.2.1 Preparation of *N*-(4-methoxyphenyl)piperazine-1-carboxamide, 3.19.



3.19

Compound **3.19** was synthesised following the general procedure for deprotection of the Boc-protected urea (**3.2**; 1.70 g, 5.07 mmol), yielding 86.0 % of white solid. **^{1}H NMR** (500 MHz, $CDCl_3$) δ_H 7.21 (dd, 2H, *J* = 9.0, 7.2 Hz, **H3**), 6.80 (dd, 2H, *J* = 9.0, 7.0 Hz **H2**), 6.45 (s, 1H, **H5**), 3.75 (s, 3H, **H10**), 3.44 – 3.37 (m, 4H, **H7**), 2.90 – 2.81 (m, 4H, **H8**), 2.50 (s, 1H, **H9**). **^{13}C NMR** (126 MHz, $CDCl_3$) δ_C 155.99 (**C1**), 155.87(**C6**), 132.10 (**C4**), 122.66 (**C3**), 114.17 (**C2**), 55.60 (**C10**), 45.88 (**C7**), 45.16 (**C8**).

3.3.1.1.2.2 Preparation of *N*-(2,6-dichloropyridin-4-yl)piperazine-1-carboxamide, 3.20.

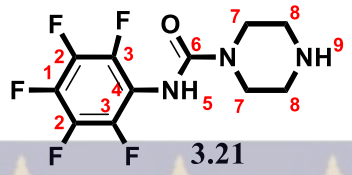


3.20

University of Ghana http://ugspace.ug.edu.gh

Compound **3.20** was synthesised following the general procedure for deprotection of the Boc-protected urea (**3.5**; 2.30 g, 6.75 mmol) and obtained in 64.6 % yield as a white solid. **^{1}H NMR** (500 MHz, DMSO) δ 9.29 (s, 1H, **H4**), 7.54 (s, 2H, **H2**), 2.73 – 2.57 (m, 8H, **H6, H7**), 1.30 – 1.13 (m, 1H, **H8**).

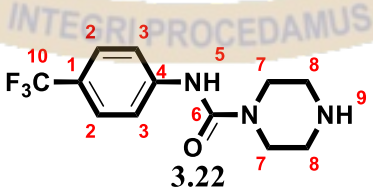
3.3.1.1.2.3 Preparation of *N*-(perfluorophenyl)piperazine-1-carboxamide, 3.21.



3.21

Compound **3.21** was synthesised following the general procedure for deprotection of the Boc-protected urea (**3.9;** 1.50 g, 3.80 mmol), and obtained 39.4 % yield as an oil. ^{1}H NMR (500 MHz, $CDCl_3$) δ_H 6.0 (s, 1H, **H5**), 3.50-3.42 (m, 4H, **H7**), 2.47-2.40 (m, 4H, **H8**), 1.58 (d, *J* = 1.7 Hz, 1H, **H9**). ^{13}C NMR (101 MHz, $CDCl_3$) δ 152.5 (**C6**), 153.0 (**C9**)142.9 (**C3**), 138.2 (**C1**), 135.0 (**C2**), 112.9 (**C4**), 51.2 (**C8**), 42.9 (**C7**).

3.3.1.1.2.4 Preparation of *N*-(4-(trifluoromethyl)phenyl)piperazine-1-carboxamide, 3.22.



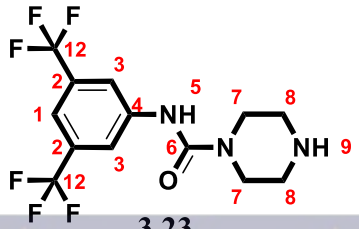
3.22

Compound **3.22** was synthesised following the general procedure for deprotection of the Boc-protected urea (**3.3**; 1.5 g, 4.02 mmol), and obtained in 87.8 % yield as a white solid. **^{1}H NMR** (500 MHz, $CDCl_3$) δ_H 7.51 (d, *J* = 8.8 Hz, 2H, **H3**), 7.46 (d, *J* = 8.6 Hz, 2H, **H2**), 6.64 (s, 1H, **H5**), 3.55 – 3.37 (m, 4H, **H7**), 2.96 – 2.84 (m, 4H, **H8**), 1.74 (s, 1H, **H9**). **^{13}C NMR** (126 MHz, $CDCl_3$) δ_C 154.61 (**C6**), 142.41 (**C4**), 126.28, 126.25, 126.22, 126.19 (**C2**),

University of Ghana http://ugspace.ug.edu.gh

125.48, 125.22, 124.96, 124.70 (**C1**), 127.63, 124.44, 123.32, 121.16 (**C10**), 119.24 (**C3**), 45.94 (**C7**), 45.32 (**C8**).

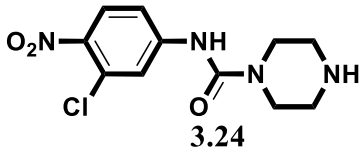
3.3.1.1.2.5 Preparation of *N*-(3,5-bis(trifluoromethyl)phenyl)piperazine-1-carboxamide, 3.23.



3.23

Compound **3.23** was synthesised following the general procedure for deprotection of the Boc-protected urea (**3.4**; 2.10 g, 4.80 mmol), and obtained in 73.3 % yield as a white solid. **^{1}H NMR** (500 MHz, $CDCl_3$) δ_H 7.88 (d, *J* = 1.5 Hz, 2H, **H3**), 7.48 (s, 1H, **H1**), 7.14 (s, 1H, **H5**), 3.51 3.56 – 3.38 (m, 4H, **H7**), 3.31 – 2.53 (m, 4H, **H8**), 1.63 (d, *J* = 4.3 Hz, 9H, **H9**). **^{13}C NMR** (126 MHz, $CDCl_3$) δ_C 152.7 (**C6**), 128.2 (**C4**), 129.8, 129.5, 128.9, 128.7 (**C2**), 124.9, 122.5, 120.3, 118.3 (**C12**), 117.7 (**C3**), 115.5(**C1**), 77.8 (**C10**), 45.3 (**C8**), 45.9 (**C7**), 26.9 (**C11**). **LC-MS:** retention time: 3.8184 min; **WAU-ESI** *(m/z)*: for $[C_{13}H_{13}F_6NO_3]^+$ $[M+H]^+$: exact mass calcd.: 342.10; found: 342.03; [M+Na]:363.97.

3.3.1.1.2.6 Preparation of *N*-(3-chloro-4-nitrophenyl)piperazine-1-carboxamide, 3.24.



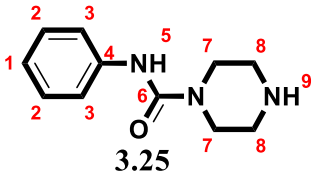
3.24

Compound **3.24** was synthesised following the general procedure for deprotection of the Boc-protected urea (**3.8**; 2.70 g, 7.02 mmol), and obtained in 67.3 % yield as a white solid. This intermediate was used directly in the subsequent reaction step without further characteriza-

University of Ghana http://ugspace.ug.edu.gh

tion. Its formation was inferred from the successful synthesis and spectroscopic characterization of the product obtained in the following step.

3.3.1.1.2.7 Preparation of *N*-phenylpiperazine-1-carboxamide, 3.25.

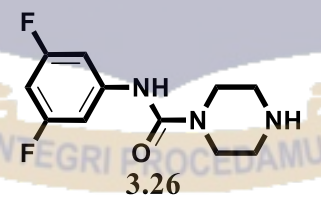


3.25

Compound **3.25** was synthesised following the general procedure for deprotection of the Boc-protected urea (**3.7**;1.70 g, 5.50 mmol), and obtained in 87.4 % yield as a white solid.

^{1}H NMR (500 MHz, $CDCl_3$) δ 7.25 – 7.21(m, 2H, **H3**), 7.12 – 7.09 (m, 2H, **H2**), 6.85 – 6.80 (m, 1H, **H1**), 6.20 (s, 1H, **H5**), 3.45 – 3.42 (m, 4H, **H7**), 2.44 – 2.41 (m, 4H, **H8**) 1.37 (s, 1H, **H9**).**^{13}C NMR** (126 MHz, $CDCl_3$) δ 154.0 (**C6**), 137.2 (**C4**), 128.1 (**C2**), 122.3 (**C1**), 119.0(**C3**), 51.9 (**C8**), 48. 6 (**C7**).

3.3.1.1.2.8 Preparation of *N*-(3,5-difluorophenyl)piperazine-1-carboxamide, 3.26.

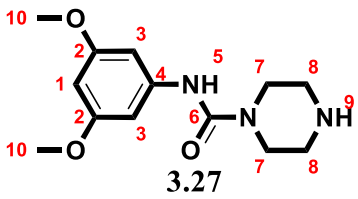


3.26

Compound **3.26** was synthesised following the general procedure for deprotection of the Boc-protected urea (**3.6**; 1.87 g, 5.50 mmol), and obtained in 77.6 % yield as a white solid. This intermediate was used directly in the subsequent reaction step without further characterization. Its formation was inferred from the successful synthesis and spectroscopic characterization of the product obtained in the following step.

University of Ghana http://ugspace.ug.edu.gh

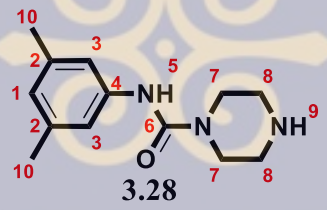
3.3.1.1.2.9 Preparation of *N*-(3,5-dimethoxyphenyl)piperazine-1-carboxamide, 3.27.



3.27

Compound **3.27** was synthesised following the general procedure for deprotection of the Boc-protected urea (**3.11**; 1.92 g, 5.25 mmol), and obtained in 86.2 % as a white solid. **^{1}H NMR** (500 MHz, DMSO) δ 8.34 (s, 1H, **H5**), 6.74 (d, *J* = 2.2 Hz, 2H, **H3**), 6.08 (dd, *J* = 14.0, 2.3 Hz, 1H, **H1**), 3.67 (d, *J* = 6.2 Hz, 6H, **H10**), 3.46 (t, *J* = 5.0 Hz, 5H, **H7**), 2.66 (t, *J* = 5.0 Hz, 4H, **H8**). **^{13}C NMR** (126 MHz, DMSO) δ 160.25 (**C2**), 154.87 (**C6**), 142.40 (**C4**), 97.56 (**C3**) 93.87 (**C1**), 54.96 (**C10**), 45.55 (**C7**), 44.89 (**C8**).

3.3.1.1.2.10 Preparation of *N*-(3,5-dimethylphenyl)piperazine-1-carboxamide, 3.28.

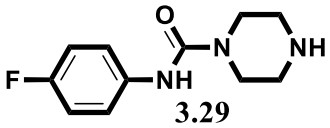


3.28

Compound **3.28** was synthesised following the general procedure for deprotection of the Boc-protected urea (**3.12**; 1.50 g, 6.40 mmol), and obtained in 62.6 % yield as an oil. ^{1}H NMR (400 MHz, $CDCl_3$) δ 7.03 (d, *J* = 2.1 Hz, 2H, **H3**) 6.55 – 6.54 (m, 1H, **H1**), 5.92 (s, 1H, **H5**), 3.47 – 3.45 (m, 4H, **H7**), 2.05 – 2.02 (m, 4H, **H8**), 1.40 (s, 1H, **H9**). ^{13}C NMR (101 MHz, $CDCl_3$) δ 154.0 (**C6**), 137.7 (**C4**), 137.5 (**C2**), 124.12 (**C1**), 116.92 (**C3**), 52.0 (**C8**), 38.97 (**C7**). **LC-MS:** retention time: 2.6873 min; **WAU-ESI** *(m/z)*: for $[C_{13}H_{19}N_3O]^+$ $[M+H]^+$: exact mass calcd.: 234.15; found: 234.05; [M+Na]: 256.06.

University of Ghana http://ugspace.ug.edu.gh

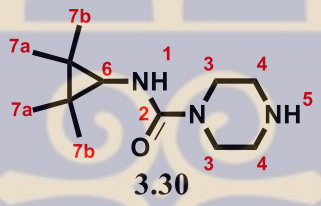
3.3.1.1.2.11 Preparation of *N*-(4-fluorophenyl)piperazine-1-carboxamide, 3.29.



3.29

Compound **3.29** was synthesised following the general procedure for deprotection of the Boc-protected urea (**3.14**; 1.40 g, 4.15 mmol), and obtained in 98.0 % yield as a white solid. This intermediate was used directly in the subsequent reaction step without further characterization. Its formation was inferred from the successful synthesis and spectroscopic characterization of the product obtained in the following step.

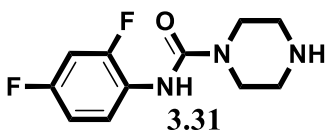
3.3.1.1.2.12 Preparation of *N*-(4-cyclopropylphenyl)piperazine-1-carboxamide, 3.30.



3.30

Compound **3.30** was synthesised following the general procedure for deprotection of the Boc-protected urea (**3.13**; 1.50 g, 5.70 mmol),and obtained in 67.0 % yield as a white solid. ^{1}H NMR (400 MHz, $CDCl_3$) δ 4.55 (s, 1H, **H1**), 3.32 – 3.28 (m, 4H, **H3**), 2.64 (m, 1.8 Hz, 1H, **H6**), 2.45 – 2.32 (m, 4H, **H4**), 1.37 (s, 1H, **H5**), 0.76 – 0.62 (m, 2H, **H7b**), 0.51 – 0.40 (m, 2H, **H7a**). ^{13}C NMR (101 MHz, $CDCl_3$) δ 158.2 (**C2**), 52.5 (**C4**), 43.6 (**C3**), 23.5 (**C6**), 6.7(**C7**).

3.3.1.1.2.13 Preparation of *N*-(2,4-difluorophenyl)piperazine-1-carboxamide, 3.31.

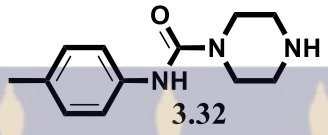


3.31

University of Ghana http://ugspace.ug.edu.gh

Compound **3.31** was synthesised following the general procedure for deprotection of the Boc-protected urea (**3.15**;1.73 g, 4.90 mmol),and obtained in 98.5 % yield as an oil. This intermediate was used directly in the subsequent reaction step without further characterization. Its formation was inferred from the successful synthesis and spectroscopic characterization of the product obtained in the following step.

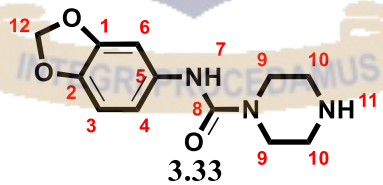
3.3.1.1.2.14 Preparation of *N*-(p-tolyl)piperazine-1-carboxamide, 3.32.



3.32

Compound **3.32** was synthesised following the general procedure for deprotection of the Boc-protected urea (**3.16**; 2.1 g, 6.57 mmol), and obtained in 97.2 % yield as an oil. This intermediate was used directly in the subsequent reaction step without further characterization. Its formation was inferred from the successful synthesis and spectroscopic characterization of the product obtained in the following step.

3.3.1.1.2.15 Preparation of *N*-(benzo[d][1,3]dioxol-5-yl)piperazine-1-carboxamide, 3.33.



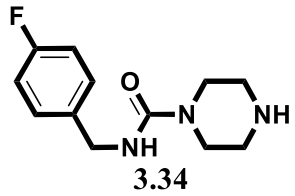
3.33

Compound **3.33** was synthesised following the general procedure for deprotection of the Boc-protected urea (**3.17**; 2.5 g, 7.20 mmol), and obtained in 55.7 % yield as a white solid. **^{1}H NMR** (500 MHz, $CDCl_3$) δ_H 7.00 (t, *J* = 2.7 Hz, 1H, **H4**), 6.68 (d, *J* = 8.3 Hz, 1H, **H6**), 6.61 (dd, *J* = 8.3, 2.1 Hz, 1H, **H3**), 6.41 (s, 1H, **H7**), 5.90 (s, 2H, **H12**), 3.45 – 3.28 (m, 4H, **H9**), 2.95 – 2.84 (m, 4H, **H10**), 1.83 (s, 1H, **H11**). **^{13}C NMR** (126 MHz, $CDCl_3$) δ_C 155.69 (**C8**),

University of Ghana http://ugspace.ug.edu.gh

147.87 (**C1**), 143.85 (**C2**), 133.31 (**C5**), 113.79 (**C4**), 107.98 (**C3**), 103.90 (**C6**), 101.23 (**C12**), 45.87 (**C9**), 45.19 (**C10**).

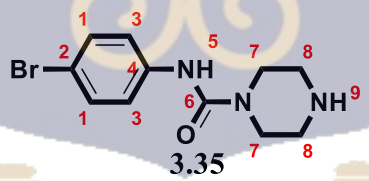
3.3.1.1.2.16 Preparation of *N*-(4-fluorobenzyl)piperazine-1-carboxamide, 3.34.



3.34

Compound **3.34** was synthesised following the general procedure for deprotection of the Boc-protected urea (**3.10**; 2.10 g, 6.22 mmol), and obtained in 31.2 % yield as an oil. This intermediate was used directly in the subsequent reaction step without further characterization. Its formation was inferred from the successful synthesis and spectroscopic characterization of the product obtained in the following step.

3.3.1.1.2.17 Preparation of *N*-(4-bromophenyl)piperazine-1-carboxamide, 3.35.



3.35

Compound **3.35** was synthesised following the general procedure for deprotection of the Boc-protected urea (**3.18**; 2.5 g, 6.50 mmol) and obtained in 51.39 % yield as an oil. **^{1}H NMR** (500 MHz, $CDCl_3$) δ_H 7.46 – 7.32 (m, 2H, **H1**), 7.25 (dd, *J* = 9.0, 2.2 Hz, 2H, **H3**), 6.40 (s, 1H, **H5**), 3.53 – 3.41 (m, 4H, **H7**), 2.98 – 2.82 (m, 4H, **H8**), 1.71 (s, 1H, **H9**). **^{13}C NMR** (126 MHz, $CDCl_3$) δ_C 154.90 (**C6**), 138.28 (**C4**), 131.92 (**C1**), 121.63 (**C3**), 115.72 (**C2**), 45.95 (**C7**), 45.28 (**C8**).

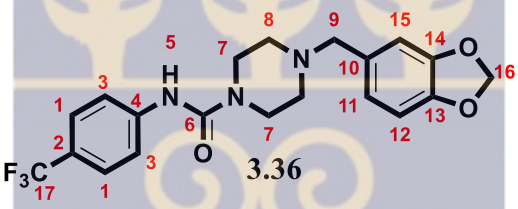
INTEGRI PROCEDAMUS

University of Ghana http://ugspace.ug.edu.gh

3.3.1.1.3 General procedure for reductive amination.

To a solution of the deprotected urea (1 eqv.) in DCM (15 mL) was added various aldehydes (2 eqv.), and the resulting mixture was stirred at room temperature for 30 minutes. $NaBH(OAc)_3$ or in a few cases, $NaCNBH_3$ (1.5 eqv.) was then added and stirred for a further 16 hours. The reaction was then quenched with $NaHCO_3$, extracted with DCM (3 × 20 mL), and the combined organic extracts were washed with brine, dried over $MgSO_4$ and filtered. Purification by flash column chromatography afforded the required products.

3.3.1.1.3.1 Preparation of 4-(benzo[*d*][1,3]dioxol-5-ylmethyl)-*N*-(4-(trifluoromethyl)phenyl)piperazine-1-carboxamide, 3.36.

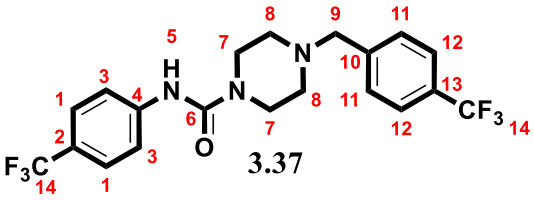


3.36

Compound **3.36** was synthesised following the general procedure for reductive amination, using previously prepared amine, **3.22** (0.35 g, 1.28 mmol), $NaB(OAc)_3H$ (0.41 g, 1.92 mmol), and piperonal (0.38 g, 2.56 mmol), and was obtained in 28.0 % yield as a white solid. **^{1}H NMR** (500 MHz, $CDCl_3$) δ_H 7.51 (d, *J* = 8.6 Hz, 2H, **H3**), 7.45 (d, *J* = 8.6 Hz, 2H, **H1**), 6.85 (d, *J* = 1.4 Hz, 1H, **H15**), 6.78 – 6.72 (m, 2H, **H11, H12**), 6.69 (s, 1H, **H5**), 5.95 (s, 2H, **H16**), 3.56 – 3.49 (m, 4H, **H7**), 3.48 (s, 2H, **H9**), 2.52 – 2.46 (m, 4H, **H8**). **^{13}C NMR** (126 MHz, $CDCl_3$) δ_C 154.3 (**C6**), 147.7 (**C13**), 146.8 (**C14**), 142.1 (**C4**), 130.6 (**C10**), 126.0 (**C7**), 125.2, 125.0, 124.7 (**C2**), 124.5, 124.2 (**C17**), 123.1 (**C3**), 109.4 (**C11**), 107.9 (**C12**), 100.9 (**C14**), 62.3 (**C16**), 52.2 (**C9**), 50.7 (**C8**), 43.8 (**C7**). **LC-MS:** retention time: 0.961 min; **AJS-ESI** *(m/z)*: for $[C_{20}H_{19}F_6N_3O]^+$ $[M+H]^+$: exact mass calcd.: 432.14; found: 432.1. **FTIR** (cm^{-1}): υ(N–H s) 3341, υ(C-H s) 2939, 2890, υ(C=O s) 1646, δ(N–H s), υ(C-Ns) 1541, υ(C-N m) 1314, υ(C-O s) 1238, υ(C-F s) 1110, γ(C-H m) 839. mp 146-149 ^oC.

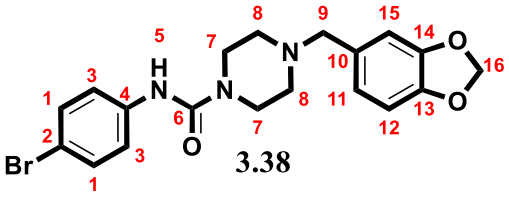
University of Ghana http://ugspace.ug.edu.gh

3.3.1.1.3.2 Preparation of 4-(4-(trifluoromethyl)benzyl)-*N*-(4-(trifluoromethyl)phenyl)piperazine-1-carboxamide, 3.37.



Compound **3.37** was synthesised following the general procedure for reductive amination, using previously prepared amine, **3.22** (0.30 g, 1.34 mmol), $NaB(OAc)_3H$ (0.43 g, 2.02 mmol), and 4-(trifluoromethyl) benzaldehyde (0.38 g, 2.56 mmol), and obtained in 46.7 % yield as a white solid. **^{1}H NMR** (500 MHz, $CDCl_3$) δ_H 7.60 (d, *J* = 8.0 Hz, 2H, **H11**), 7.47 (q, *J* = 8.6 Hz, 4H, **H12**, **H1**), 7.27 (d, *J* = 10.2 Hz, 2H, **H3**), 5.53 (s, 1H, **H5**), 2.50 (t, *J* = 5.1 Hz, 6H, **H9**, **H7**), 2.05 (s, 4H, **H8**). **^{13}C NMR** (126 MHz, $CDCl_3$) δ_C 154.7 (**C6**), 142.2 (**C4**), 140.6 (**C10**), 129.8, 129.6 (**C13**), 129.4 (**C11**), 125.8 (**C12**), 125.2 (**C1**), 124.6, 124.4 (**C2**), 123.0, 122.9 (**C14**), 119.8 (**C3**), 61.8 (**C9**), 52.2 (**C8**), 43.6 (**C7**). **LC-MS:** retention time: 1.128 min; **AJS-ESI** *(m/z)*: for $[C_{20}H_{19}F_6N_3O]^+$ $[M+H]^+$: exact mass calcd.: 432.14; found: 432.1. **FTIR** (cm^{-1}): υ(N–H s) 3389, υ(C-H s) 2930, 2880, υ(C=O s) 1666, δ(N–H s), υ(C-N s) 1533, 1320, υ(C-F s) 1244, 1113, 1118, γ(C-H m) 841. mp 126-129 ^oC.

3.3.1.1.3.3 Preparation of 4-((6-bromobenzo[d][1,3]dioxol-5-yl)methyl)-N-(4-bromophenyl)piperazine-1-carboxamide, 3.38.

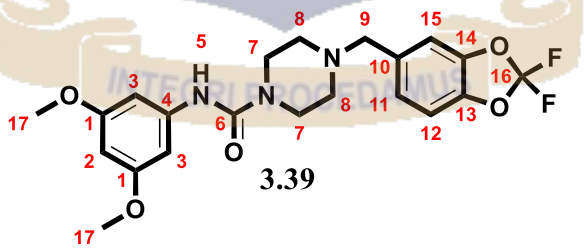


Compound **3.38** was synthesised following the general procedure for reductive amination, using previously prepared amine, **3.35** (0.23 g, 0.81 mmol), $NaB(OAc)_3H$ (0.26 g, 1.22

University of Ghana http://ugspace.ug.edu.gh

mmol), and 6-bromo-benzo[1,3]dioxole-5-carbaldehyde (0.37 g, 1.62 mmol), and obtained in 27.1 % yield as a white solid. **^{1}H NMR** (500 MHz, DMSO) δ_H 8.64 (s, 1H, **H5**), 7.44 – 7.41 (m, 2H, **H3**), 7.38 – 7.35 (m, 2H, **H1**), 7.16 (s, 1H, **H12**), 7.03 (s, 1H, **H15**), 6.04 (s, 2H, **H16**), 3.47 (d, *J* = 2.7 Hz, 2H, **H9**), 3.42 (t, *J* = 5.0 Hz, 4H, **H7**), 2.40 (t, *J* = 4.9 Hz, 4H, **H8**). **^{13}C NMR** (126 MHz, DMSO) δ_C 154.8 (**C6**), 147.4 (**C13**), 147.3 (**C14**), 140.2 (**C4**), 131.2 (**C3**), 130.4 (**C10**), 121.5 (**C1**), 114.3 (**C2**), 113.3 (**C11**), 112.4 (**C12**), 110.5 (**C15**), 102.1 (**C16**), 60.9 (**C9**), 52.6 (**C8**), 44.0 (**C7**). **LC-MS:** retention time: 2.5245 min; **WAU-ESI** *(m/z)*: for $[C_{19}H_{19}Br_2N_3O_3]^+$ $[M+H]^+$: exact mass calcd.: 495.98 (^{79}Br, ^{79}Br); found: 495.77; exact mass calcd.: 497.979 (^{79}Br, ^{81}Br); found: 497.83; exact mass calcd.: 499.979 (^{81}Br, ^{81}Br); found: 499.72; [M+Na]: 517.81(^{79}Br, ^{79}Br); [M+Na]: 519.73(^{79}Br, ^{81}Br); [M+Na]: 521.78(^{81}Br, ^{81}Br). **FTIR** (cm^{-1}): υ(N–H s) 3351, υ(C-H s) 2941, 2860, υ(C=O s) 1639, δ(C-H s) 1423, υ((Aryl) C-O s) 1233, υ(C-O s) 1000, γ(C-H m) 827, υ(C-Br m) 502. mp 179-181 ^{o}C.

3.3.1.1.3.4 Preparation of 4-((2,2-difluorobenzo[*d*][1,3]dioxol-5-yl)methyl)-*N*-(3,5-dimethoxyphenyl)piperazine-1-carboxamide, 3.39.

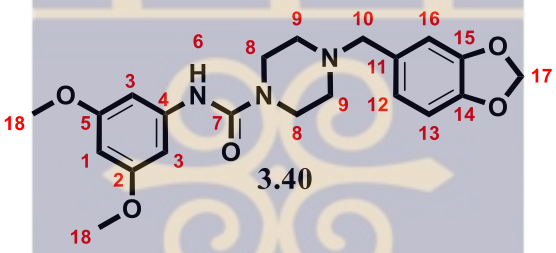


Compound **3.39** was synthesised following the general procedure for reductive amination, using previously prepared amine, **3.27** (0.24 g, 0.90 mmol), $NaB(OAc)_3H$ (0.30 g, 1.35 mmol), and 2,2-difuorobenzo[*d*][1,3]dioxole-5-carbaldehyde (0.24 mL, 1.80 mmol), and obtained in 71.5 % yield as a white solid. **^{1}H NMR** (500 MHz, $CDCl_3$) δ_H 7.12 (d, *J* = 3.7 Hz, 1H, **H15**), 7.05 – 6.92 (m, 2H, **H12, H11**), 6.60 (t, *J* = 2.1 Hz, 2H, **H3**), 6.49 (s, 1H, **H5**),

University of Ghana http://ugspace.ug.edu.gh

6.16 (q, *J* = 2.2 Hz, 1H, **H2**), 3.75 (d, *J* = 3.5 Hz, 7H, **H17**), 3.59 – 3.41 (m, 7H, **H9, H7**), 2.51 – 2.41 (m, 5H, **H8**). **^{13}C NMR** (126 MHz, $CDCl_3$) δ_C 161.2 (**C1**), 154.9 (**C6**), 144.1 (**C14**), 143.2 (**C4**), 141.0 (**C13**), 133.8 (**C10**), 131.8, 129.8 (**C16**), 124.2 (**C11**), 110.3 (**C15**), 109.2 (**C12**), 98.1 (**C3**), 95.8 (**C2**), 62.4 (**C9**), 55.5 (**C17**), 52.6 (**C8**), 44.1 (**C7**). **LC-MS:** retention time: 2.506 min; **AJS-ESI** *(m/z)*: for $[C_{21}H_{23}F_2N_3O_5]^+$ $[M+H]^+$: exact mass calcd.: 436.16; found: 436.2. **FTIR** (cm^{-1}): υ(N–H s) 3347, υ(C-H s) 2970, 2856, υ(C=O s) 1641, υ(C=C s) 1606, δ(C-H s) 1452, υ((Aryl) C-O s) 1232, υ(C-O s) 1001, γ(C-H m) 832. mp 137-139 ^oC.

3.3.1.1.3.5 Preparation of 4-(benzo[*d*][1,3]dioxol-5-ylmethyl)-*N*-(3,5-dimethoxyphenyl)piperazine-1-carboxamide, 3.40.



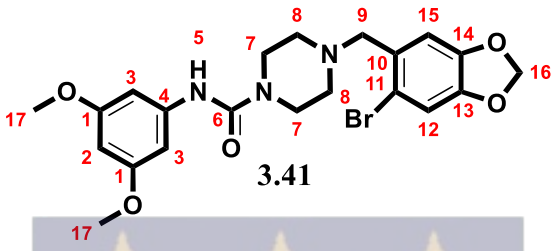
3.40

Compound **3.40** was synthesised following the general procedure for reductive amination, using previously prepared amine, **3.27** (0.20 g, 0.75 mmol), $NaB(OAc)_3H$ (0.24 g, 1.13 mmol), and piperonal (0.23 g, 1.50 mmol), and obtained in 44.5 % yield as an oil. **^{1}H NMR** (400 MHz, $CDCl_3$) δ_H 6.89 – 6.84 (m, 1H, **H16**), 6.75 (t, *J* = 1.2 Hz, 2H, **H12, H13**), 6.61 (d, *J* = 2.3 Hz, 2H, **H3**), 6.29 (s, 1H, **H6**), 6.17 (t, *J* = 2.2 Hz, 1H, **H1**), 5.95 (s, 2H, **H17**), 3.77 (s, 6H, **H18**), 3.54 – 3.47 (m, 4H, **H8**), 3.45 (s, 2H, **H10**), 2.50 – 2.44 (m, 4H, **H9**).**^{13}C NMR** (101 MHz, $CDCl_3$) δ_C 160.0 (**C2, C5**), 153.9 (**C7**), 146.7 (**C14**), 145.8 (**C15**), 139.8 (**C4**), 130.5 (**C11**), 121.1 (**C12**), 108.4 (**C16**), 106.9 (**C13**), 99.9 (**C3**), 96.7 (**C17**), 94.7 (**C1**), 61.6 (**C10**), 54.3 (**C18**), 51.5 (**C9**), 43.1 (**C8**). **LC-MS:** retention time: 0.863 min; **AJS-ESI** *(m/z)*: for $[C_{21}H_{25}N_3O_5]^+$ $[M+H]^+$: exact mass calcd.: 400.18; found: 400.2. **FTIR** (cm^{-1}): υ(N–H s)

University of Ghana http://ugspace.ug.edu.gh

3348, υ(C-H s) 2936, 2856, υ(C=O s) 1640, υ(C=C s) 1606, υ(C-N s), δ(N-H s) 1542, υ((Aryl) C-O s) 1236, υ(C-O s) 1143, γ(C-H m) 831.

3.3.1.1.3.6 Preparation of 4-((6-bromobenzo[*d*][1,3]dioxol-5-yl)methyl)-*N*-(3,5-dimethoxyphenyl)piperazine-1-carboxamide, 3.41.

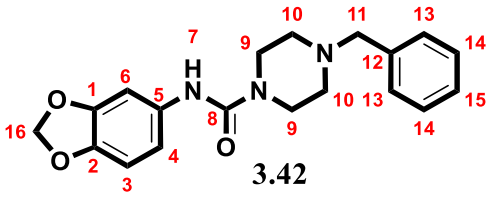


3.41

Compound **3.41** was synthesised following the general procedure for reductive amination, using previously prepared amine, **3.27** (0.20 g, 0.75 mmol), $NaB(OAc)_3H$ (0.24 g, 1.13 mmol), and 6-bromo-benzo[1,3]dioxole-5-carbaldehyde (0.35 g, 1.50 mmol), and obtained in 33.3 % yield as a white solid. **^{1}H NMR** (500 MHz, $CDCl_3$) δ_H 6.99 (d, *J* = 7.2 Hz, 2H, **H12, H15**), 6.61 (d, *J* = 2.2 Hz, 2H, **H3**), 6.31 (s, 1H, **H5**), 6.17 (d, *J* = 2.4 Hz, 1H, **H1**), 5.97 (s, 2H, **H16**), 3.77 (s, 6H, **H17**), 3.55 (s, 2H, **H9**), 3.49 (t, *J* = 5.0 Hz, 4H, **H7**), 2.54 (t, *J* = 5.0 Hz, 4H, **H8**). **^{13}C NMR** (126 MHz, $CDCl_3$) δ_C 160.95 (**C2**), 154.63 (**C6**), 147.34 (**C13, C14**), 140.75 (**C4**), 130.15 (**C16**), 114.70 (**C11**), 112.55 (**C12**), 110.20 (**C15**), 101.59 (**C16**), 97.73 (**C3**), 95.61 (**C1**), 61.31 (**C9**), 55.26 (**C17**), 52.45 (**C8**), 44.12 (**C7**). **LC-MS:** retention time: 0.937 min; **AJS-ESI** *(m/z)*: for $[C_{21}H_{24}BrN_3O_5]^+$ $[M+H]^+$: exact mass calcd.: 478.09 (^{79}Br); found: 478.1. **FTIR** (cm^{-1}): υ(N–H s) 3299, υ(C-H s) 2808, υ(C=O s) 1635, υ((Aryl) C-O s) 1235, υ(C-O s) 1147, γ(C-H m) 755, υ(C-Br m) 507. mp 166-168 ^oC.

University of Ghana http://ugspace.ug.edu.gh

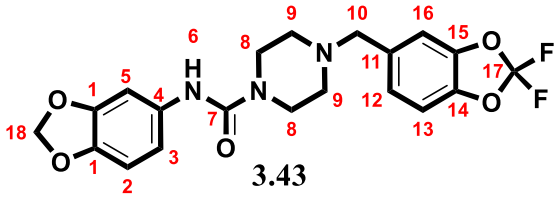
3.3.1.1.3.7 Preparation of *N*-(benzo[*d*][1,3]dioxol-5-yl)-4-benzylpiperazine-1-carboxamide, 3.42.



3.42

Compound **3.42** was synthesised following the general procedure for reductive amination, using previously prepared amine, **3.33** (0.20 g, 0.8 mmol), $NaB(OAc)_3H$ (0.25 g, 1.20 mmol), and benzaldehyde (0.16 mL, 1.60 mmol), and obtained in 50.5 % yield as white solid. **^{1}H NMR** (400 MHz, $CDCl_3$) δ_H 7.27 (d, *J* = 0.8 Hz, 2H, **H14**), 7.23 – 7.19 (m, 3H, **H13, H15**), 6.97 (d, *J* = 2.1 Hz, 1H, **H6**), 6.64 (d, *J* = 8.3 Hz, 1H, **H4**), 6.54 (dd, *J* = 8.3, 2.1 Hz, 1H, **H3**), 6.14 (s, 1H, **H7**), 5.86 (s, 2H, **H16**), 3.48 (s, 2H, **H11**), 3.45 – 3.36 (m, 4H, **H9**), 2.51 – 2.34 (m, 4H, **H10**). **^{13}C NMR** (101 MHz, $CDCl_3$) δ_C 155.1 (**C8**), 147.7 (**C1**), 143.6 (**C2**), 137.5 (**C12**), 133.0 (**C5**), 129.0 (**C14**), 128.2 (**C13**), 127.1 (**C15**), 113.2 (**C4**), 107.7 (**C3**), 103.5 (**C6**), 101.0 (**C24**), 63.0 (**C11**), 52.5 (**C10**), 43.9 (**C9**). **LC-MS:** retention time: 0.980 min; **AJS-ESI** *(m/z)*: for $[C_{19}H_{21}N_3O_3]^+$ $[M+H]^+$: exact mass calcd.: 340.158; found: 340.2. **FTIR** (cm^{-1}): υ(N–H s) 3328, υ(C-H m) 2898, 2797, υ(C=O s) 1627, υ(C-N s) 1537, υ(C=C m) 1487, υ((Aryl) C-O s) 1233, γ(C-H m) 733. mp 187-189 ^oC.

3.3.1.1.3.8 Preparation of *N*-(benzo[*d*][1,3]dioxol-5-yl)-4-((2,2-difluorobenzo[d][1,3]dioxol-5-yl)methyl)piperazine-1-carboxamide, 3.43.

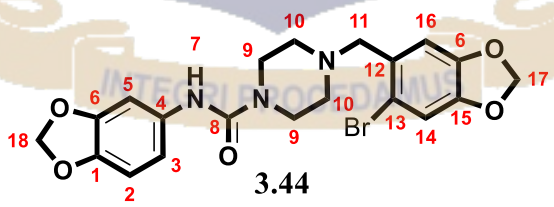


3.43

University of Ghana http://ugspace.ug.edu.gh

Compound **3.43** was synthesised following the general procedure for reductive amination, using previously prepared **3.33** (0.22 g, 0.89 mmol), $NaB(OAc)_3H$ (0.28 g, 1.34 mmol), and 2,2-difuorobenzo[*d*][1,3]dioxole-5-carbaldehyde (0.23 mL, 1.80 mmol), and obtained in 51.5 % yield as an oil. **^{1}H NMR** (400 MHz, $CDCl_3$) δ_H 7.13 – 7.11 (m, 1H, **H3**), 7.03 (d, *J* = 2.1 Hz, 1H, **H5**), 7.00 (dd, *J* = 1.7, 1.0 Hz, 2H, **H16, H13**), 6.70 (d, *J* = 8.2 Hz, 1H, **H12**), 6.61 (dd, *J* = 8.3, 2.2 Hz, 1H, **H2**), 6.20 (s, 1H, **H6**), 5.92 (s, 2H, **18**), 3.50 (s, 2H, **H10**), 3.49 – 3.43 (m, 4H, **H8**), 2.50 – 2.41 (m, 4H, **H9**). **^{13}C NMR** (101 MHz, $CDCl_3$) δ_C 155.1 (**C7**), 147.7 (**C1**), 143.8 (**C15**), 143.6 (**C5**), 142.8 (**C14**), 134.0 (**C11**), 132.90 (**C17**), 123.7 (**C12**), 113.3 (**C3**), 109.9 (**C16**), 108.8 (**C13**), 107.7 (**C2**), 103.5 (**C18**), 101.0 (**C5**), 62.2 (**C10**), 52.4 (**C9**), 43.9 (**C8**). **LC-MS:** retention time: 0.754 min; **AJS-ESI** *(m/z)*: for $[C_{20}H_{19}F_2N_3O_5]^+$ $[M+H]^+$: exact mass calcd.: 420.13; found: 420.1. **FTIR** (cm^{-1}): υ(N–H s) 3324, υ(C-H m) 2970, 2811, υ(C=O s) 1622, δ(N–H m), υ(C-N m) 1529, υ(C=C s) 1490, υ((Aryl) C-O s) 1226, υ(C-F m) 1197, γ(C-H m) 801.

3.3.1.1.3.9 Preparation of *N*-(benzo[*d*][1,3]dioxol-5-yl)-4-((6-bromobenzo[d][1,3]dioxol-5-yl)methyl)piperazine-1-carboxamide, 3.44.



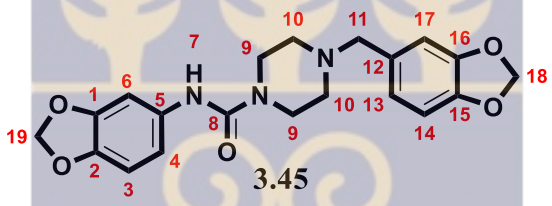
3.44

Compound **3.44** was synthesised following the general procedure for reductive amination, using previously prepared amine, **3.33** (0.20 g, 0.80 mmol), $NaB(OAc)_3H$ (0.25 g, 1.20 mmol), and 6-bromobenzo[1,3]dioxole-5-carbaldehyde (0.37 g, 1.60 mmol), and obtained in 32.5 % yield as a white solid. **^{1}H NMR** (500 MHz, MeOD) δ_H 7.03 (d, *J* = 3.8 Hz, 2H, **H14, H5**), 6.96 – 6.90 (m, 1H, **H16**), 6.75 – 6.65 (m, 2H, **H3, H2**), 5.98 (s, 1H, **H18**), 5.89 (s, 1H, **H17**), 3.58 (s, 2H, **H11**), 3.56 – 3.48 (m, 4H, **H9**), 2.58 – 2.48 (m, 4H, **H10**). **^{13}C NMR** (126

University of Ghana http://ugspace.ug.edu.gh

MHz, MeOD) δ_C 158.1 (**C8**), 148.9 (**C6**), 145.0 (**C15**), 134.5 (**C1**), 131.2 (**C4**), 115.8 (**C12**), 115.6 (**C13**), 113.3 (**C3**), 111.5 (**C14**), 108.5 (**C16**), 105.1 (**C2**), 103.1 (**C5**), 102.2 (**C17, C18**), 62.3(**C11**), 53.7 (**C10**), 44.9 (**C9**). **LC-MS:** retention time: 2.418 min; **AJS-ESI** *(m/z)*: for $[C_{20}H_{20}BrN_3O_5]^+$ $[M+H]^+$: exact mass calcd.: 462.06 (^{79}Br); found: 462.10; exact mass calcd.: 464.06 (^{81}Br); found: 464.10. **FTIR** (cm^{-1}): υ(N–H s) 3350, υ(C-H s) 2910, υ(C=O s) 1629, υ(C-N m), δ(N-H m) 1506, δ(C-H s) 1446, υ((Aryl) C-O s) 1240, υ(C-O s) 1036, γ(C-H m) 812, υ(C-Br m) 544. mp 173-175 ^oC.

3.3.1.1.3.10 Preparation of *N*-(benzo[*d*][1,3]dioxol-5-yl)-4-(benzo[*d*][1,3]dioxol-5-ylmethyl)piperazine-1-carboxamide, 3.45.



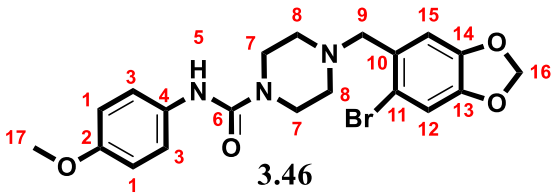
3.45

Compound **3.45** was synthesised following the general procedure for reductive amination, using previously prepared amine (**3.33**; 0.20 g, 0.80 mmol), $NaB(OAc)_3H$ (0.25 g, 1.20 mmol), and piperonal (0.24 g, 1.60 mmol), and obtained in 45.6 % yield as an oil. **^{1}H NMR** (400 MHz, $CDCl_3$) δ_H 7.03 (d, *J* = 2.2 Hz, 1H, **H4**), 6.86 (d, *J* = 1.2 Hz, 1H, **H6**), 6.75 (d, *J* = 1.6 Hz, 2H, **H3, H13**), 6.70 (d, *J* = 8.3 Hz, 1H, **H7**), 6.61 (dd, *J* = 8.3, 2.2 Hz, 1H, **H14**), 6.21 (s, 1H, **H7**), 5.95 (s, 2H, **H19**), 5.92 (s, 2H, **H18**), 3.49 – 3.44 (m, 5H, **H9**), 3.44 (s, 2H, **H11**), 2.55 – 2.40 (m, 4H, **H10**). **^{13}C NMR** (101 MHz, $CDCl_3$) δ_C 155.41 (**C8**), 147.96 (**C16**), 147.88 (**C15**), 146.91 (**C1**), 143.87 (**C2**), 133.30 (**C5**), 131.70 (**C12**), 122.35 (**C13**), 113.56 (**C4**), 109.53 (**C3**), 108.08 (**C14**), 108.04 (**C17**), 103.77 (**C6**), 101.28 (**C19**), 101.10 (**C18**), 62.78 (**C11**), 52.69 (**C10**), 44.24 (**C9**). **LC-MS:** retention time: 0.902 min; **AJS-ESI** *(m/z)*: for $[C_{20}H_{21}N_3O_5]^+$ $[M+H]^+$: exact mass calcd.: 384.15; found: 384.1. **FTIR** (cm^{-1}): υ(N–H s)

University of Ghana http://ugspace.ug.edu.gh

3282, υ(C-H s) 2970, υ(C=O s) 1627, δ(C-O m) 1488, υ((Aryl) C-O s) 1229, υ(C-O m) 1036, γ(C-H m) 806.

3.3.1.1.3.11 Preparation of 4-((6-bromobenzo[*d*][1,3]dioxol-5-yl)methyl)-*N*-(4-methoxyphenyl)piperazine-1-carboxamide, 3.46.

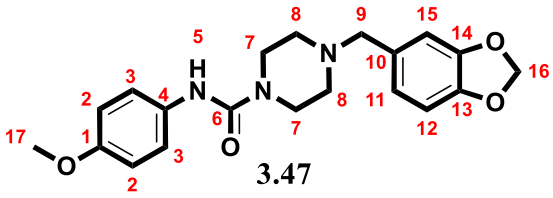


3.46

Compound **3.46** was synthesised following the general procedure for reductive amination, using previously prepared amine, **3.19** (0.20 g, 0.90 mmol), $NaB(OAc)_3H$ (0.30 g, 1.35 mmol), and 6-bromo-benzo[1,3]dioxole-5-carbaldehyde (0.4 g, 1.70 mmol), and obtained in 37.2 % yield as an oil. **^{1}H NMR** (500 MHz, $CDCl_3$) δ_H 7.23 (dd, 2H, *J* = 9.0, 4.6 Hz **H3**), 7.0 (s, 1H, **H15**), 6.99 (s, 1H, **H12**), 6.83 (dd, 2H, *J* = 9.0, 4.6 Hz **H1**), 6.28 (s, 1H, **H5**), 5.97 (s, 2H, **H16**), 3.77 (s, 3H, **H17**), 3.55 (s, 2H, **H9**), 3.50 – 3.44 (m, 4H, **H7**), 2.59 – 2.48 (m, 4H, **H8**). **^{13}C NMR** (126 MHz, $CDCl_3$) δ_C 156.1 (**C2**), 155.7 (**C6**), 147.6 (**C14, C13**), 132.1 (**C4**), 130.4 (**C10**), 122.6 (**C3**), 114.9 (**C11**), 114.3 (**C2**), 112.8 (**C12**), 110.5 (**C15**), 101.8 (**C16**), 61.6 (**C9**), 55.7 (**C17**), 52.7 (**C8**), 44.3(**C7**). **LC-MS:** retention time: 0.894 min; **AJS-ESI** *(m/z)*: for $[C_{20}H_{22}BrN_3O_4]^+$ $[M+H]^+$: exact mass calcd.: 448.079 (^{79}Br); found: 448.0. **FTIR** (cm^{-1}): υ(N–H s) 3368, υ(C-H s) 2910, 2827, υ(C=O s) 1638, δ(C-H m) 1475, υ((Aryl) C-O s) 1241, υ(C-O s) 1003, γ(C-H m) 82, υ(C-Br m) 499.

University of Ghana http://ugspace.ug.edu.gh

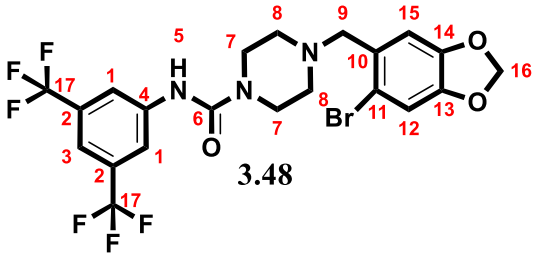
3.3.1.1.3.12 Preparation of 4-(benzo[d][1,3]dioxol-5-ylmethyl)-N-(4-methoxyphenyl)piperazine-1-carboxamide, 3.47.



3.47

Compound **3.47** was synthesised following the general procedure for reductive amination, using previously prepared amine, **3.19** (0.25 g, 1.1 mmol), $NaCNBH_3$ (0.14 g, 2.2 mmol), and piperonal (0.33 g, 2.2 mmol), and obtained in 25.5 % yield as a white solid. **^{1}H NMR** (500 MHz, $CDCl_3$) δ_H 7.25 – 7.20 (m, 2H, **H3**), 6.86 (s, 1H, **H15**), 6.84 – 6.80 (m, 2H, **H2**), 6.74 (d, *J* = 2.0 Hz, 2H, **H11, H12**), 6.29 (s, 0H, **H5**), 5.94 (s, 1H, **H16**), 3.77 (s, 3H, **H17**), 3.46 (t, *J* = 5.1 Hz, 4H, **H8**), 3.43 (s, 2H, **H9**), 2.44 (t, *J* = 5.1 Hz, 4H, **H7**). **^{13}C NMR** (126 MHz, $CDCl_3$) δ_C 155.82 (**C1**), 155.38 (**C6**), 147.65 (**C14**), 146.67 (**C13**), 131.90 (**C4**), 131.49 (**C10**), 122.29 (**C11**), 122.16, 122.09 (**C3**), 114.05, 114.02 (**C2**), 109.31 (**C15**), 107.81 (**C12**), 100.83 (**C116**), 62.54 (**C9**), 55.40 (**C17**), 52.46 (**C8**), 43.96 (**C7**). **LC-MS:** retention time: 0.615 min; **AJS-ESI** *(m/z)*: for $[C_{20}H_{23}N_3O_4]^+$ $[M+H]^+$: exact mass calcd.: 370.169; found: 370.2. **FTIR** (cm^{-1}): υ(N–H s) 3326, υ(C-H s) 2971, 2869, υ(C=O s) 1662, δ(N–H) m, υ(C-N m) 1515, υ((Aryl) C-O s) 1230, υ(C-O m) 1028, γ(C-H m) 820. mp 136-138 ^oC.

3.3.1.1.3.13 Preparation of *N*-(3,5-bis(trifluoromethyl)phenyl)-4-((6-bromobenzo[*d*][1,3]dioxol-5-yl)methyl)piperazine-1-carboxamide, 3.48.

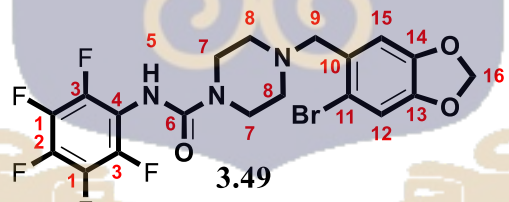


3.48

University of Ghana http://ugspace.ug.edu.gh

Compound **3.48** was synthesised following the general procedure for reductive amination, using previously prepared amine, **3.23** (0.23 g, 0.60 mmol), $NaB(OAc)_3H$ (0.20 g, 0.90 mmol), and 6-bromo-benzo[1,3]dioxole-5-carbaldehyde (0.30 g, 1.2 mmol), and obtained in 35.2 % yield as an oil. **^{1}H NMR** (500 MHz, $CDCl_3$) δ_H 7.90 (s, 2H, **H1**), 7.50 (s, 1H, **H3**), 7.05 (s, 1H, **H5**), 7.01 (s, 1H, **H12, H15**), 5.98 (s, 2H, **H16**), 3.65 (s, 2H, **H9**), 3.63 – 3.58 (m, 4H, **H7**), 2.76 – 2.52 (m, 4H, **H8**). **^{13}C NMR** (126 MHz, $CDCl_3$) δ_C 154.2(**C6**), 147.7 (**C13, C14**), 140.8 (**C4**), 132.6, 132.3, 132.1, 131.8 (**C2**), 124.4 (**C17**), 122.3 (**C10**), 119.5 (**C1**), 116.3 (**C3**), 115.3 (**C11**), 112.8 (**C12**), 110.7 (**C15**), 102.0 (**C16**), 61.3 (**C9**), 52.4 (**C8**), 44.0 (**C7**). **LC-MS:** retention time: 0.978; **AJS-ESI** *(m/z)*: for $[C_{21}H_{18}BrF_6N_3O_3]^+$ $[M+H]^+$: exact mass calcd.: 556.04 (^{81}Br); found: 556.0. **FTIR** (cm^{-1}): υ(N–H s) 3320, υ(C-H m) 2880, 2800, υ(C=O s) 1638, υ(C-N s) 1372, υ((Aryl s) C-O) 1277, υ(C-F m) 1173, υ(C-O m) 1100.

3.3.1.1.3.14 Preparation of 4-((6-bromobenzo[*d*][1,3]dioxol-5-yl)methyl)-*N*-(perfluorophenyl)piperazine-1-carboxamide, 3.49.



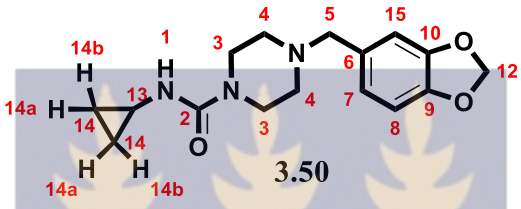
3.49

Compound **3.49** was synthesised following the general procedure for reductive amination, using previously prepared amine, **3.21** (0.22 g, 0.75 mmol), $NaB(OAc)_3H$ (0.24 g, 1.12 mmol), and 6-bromo-benzo[1,3]dioxole-5-carbaldehyde (0.34 g, 1.50 mmol), and obtained in 18.7 % yield as an oil. **^{1}H NMR** (400 MHz, $CDCl_3$) δ_H 7.00 (s, 1H, **H12**), 6.98 (s, 1H, **H15**), 5.98 (s, 2H, **H16**), 5.95 (s, 1H, **H5**), 3.56 (s, 2H, **H9**), 3.55 – 3.52 (m, 4H, **H7**), 2.62 – 2.50 (m, 4H, **H8**). **^{13}C NMR** (101 MHz, $CDCl_3$) δ_C 153.51 (**C6**), 147.31 (**C13**), 147.28 (**C14**), 143.63 (**C3**), 141.17 (**C1**), 136.33 (**C2**), 129.98 (**C10**), 114.65 (**C11**), 113.82 (**C4**), 112.50 (**C12**), 110.10 (**C15**), 101.54 (**C16**), 61.22 (**C9**), 52.19 (**C8**), 44.36 (**C7**). **LC-MS:** retention

University of Ghana http://ugspace.ug.edu.gh

time: 0.981 min; **AJS-ESI** *(m/z)*: for $[C_{19}H_{15}BrF_5N_3O_3]^+$ $[M+H]^+$: exact mass calcd.: 510.02 (^{81}Br); found: 510.0. **FTIR** (cm^{-1}): υ(N–H s) 3336, υ(C-H s) 2935, 2906, υ(C=O s) 1639, δ(C-H m) 1447, υ((Aryl) C-O s) 1248, υ(C-F m) 1124, υ(C-O m) 1000, γ(C-H s) 754, υ(C-Br m) 509.

3.3.1.1.3.15 Preparation of 4-(benzo[*d*][1,3]dioxol-5-ylmethyl)-*N*-cyclopropylpiperazine-1-carboxamide, 3.50.

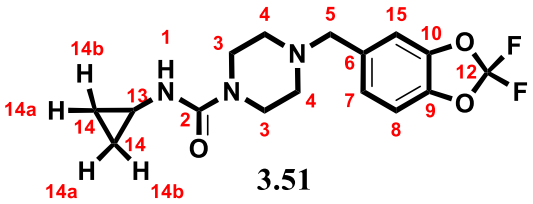


3.50

Compound **3.50** was synthesised following the general procedure for reductive amination, using previously prepared amine, **3.30** (0.22 g, 1.30 mmol), $NaB(OAc)_3H$ (0.41 g, 1.95 mmol), and piperonal (0.39 g, 2.60 mmol), and obtained in 35.5 % yield as a white solid. **^{1}H NMR** (500 MHz, $CDCl_3$) δ_H 6.84 (s, 1H, **H11**), 6.80 – 6.65 (m, 2H, **H7, H8**), 5.93 (s, 2H, **H12**), 4.65 (s, 1H, **H1**), 3.40 (s, 2H, **H5**), 3.32 (t, *J* = 5.0 Hz, 5H, **H3**), 2.64 (dq, *J* = 7.9, 3.6 Hz, 1H, **H13**), 2.38 (t, *J* = 5.0 Hz, 4H, **H4**), 0.71 (q, *J* = 6.1 Hz, 2H, **H14b**), 0.45 (q, *J* = 4.9 Hz, 2H, **H14a**).**^{13}C NMR** (126 MHz, $CDCl_3$) δ_C 158.69 (**C2**), 147.84 (**C10**), 146.86 (**C9**), 131.80 (**C6**), 122.32 (**C7**), 109.53 (**C8**), 108.03 (**C9**), 101.06 (**C12**), 62.82 (**C5**), 52.69 (**C4**), 43.88 (**C3**), 23.67 (**C13**), 6.93 (**C14**). **LC-MS:** retention time: 0.417 min; **AJS-ESI** *(m/z)*: for $[C_{16}H_{21}N_3O_3]^+$ $[M+H]^+$: exact mass calcd.: 304.16; found: 304.1. **FTIR** (cm^{-1}): υ(N–H s) 3330, υ(C-H s) 2901, 2818, υ(C=O s) 1628, δ(N–H s), υ(C-N s) 1534, δ(C-O m) 1255, υ(C-O m) 1039, γ(C-H s) 811. mp 128-129 ^oC.

University of Ghana http://ugspace.ug.edu.gh

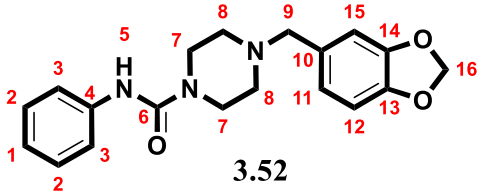
3.3.1.1.3.16 Preparation of N-cyclopropyl-4-((2,2-difluorobenzo[d][1,3]dioxol-5-yl)methyl)piperazine-1-carboxamide, 3.51.



3.51

Compound **3.51** was synthesised following the general procedure for reductive amination, using previously prepared amine, **3.30** (0.19 g, 1.12 mmol), $NaB(OAc)_3H$ (0.36 g, 1.68 mmol), and 2,2-difuorobenzo[*d*][1,3]dioxole-5-carbaldehyde (0.29 mL, 2.24 mmol), and obtained in 46.0 % yield as a white solid. **^{1}H NMR** (400 MHz, $CDCl_3$) δ_H 7.10 (s, 1H, **H11**), 6.98 (d, *J* = 1.4 Hz, 2H, **H7, 8**), 4.65 (s, 1H, **H1**), 3.47 (s, 2H, **H5**), 3.38 – 3.30 (m, 4H, **H3**), 2.64 (ddq, *J* = 5.3, 3.6, 1.8 Hz, 1H, **H13**), 2.47 – 2.35 (m, 4H, **H14**), 0.78 – 0.66 (m, 2H, **H14b**), 0.54 – 0.42 (m, 2H, **H14a**). **^{13}C NMR** (101 MHz, $CDCl_3$) δ_C 158.6 (**C2**), 144.1 (**C10**), 143.0 (**C9**), 134.4 (**C6**), 131.8 (**C12**), 124.0 (**C7**), 110.2 (**C11**), 109.1 (**C8**), 62.5 (**C5**), 52.7 (**C4**), 43.9 (**C3**), 23.7 (**C13**), 6.9 (**C14**). **LC-MS:** retention time: 0.582 min; **AJS-ESI** *(m/z)*: for $[C_{16}H_{19}F_2N_3O_3]^+$ $[M+H]^+$: exact mass calcd.: 340.14; found: 340.1. **FTIR** (cm^{-1}): υ(N–H s) 3259, υ(C-H s) 2889, υ(C=O s) 1645, δ(C–H s) 1436, δ(C-O s) 1240, υ(C-F s) 1112, γ(C-H m) 845. mp 137-139 ^oC.

3.3.1.1.3.17 Preparation of 4-(benzo[*d*][1,3]dioxol-5-ylmethyl)-*N*-phenylpiperazine-1-carboxamide, 3.52.

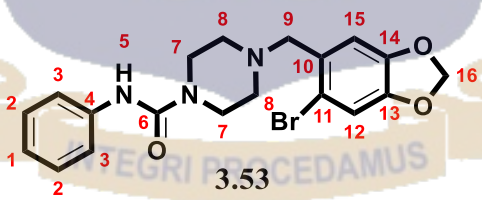


3.52

University of Ghana http://ugspace.ug.edu.gh

Compound **3.52** was synthesised following the general procedure for reductive amination, using previously prepared amine, **3.25** (0.25 g, 1.22 mmol), $NaB(OAc)_3H$ (0.39 g, 1.83 mmol), and piperonal (0.37 g, 2.44 mmol), and obtained in 94.2 % yield as a white solid. **^{1}H NMR** (500 MHz, $CDCl_3$) δ_H 7.34 (dt, *J* = 8.5, 1.4 Hz, 2H, **H3**), 7.30 – 7.22 (m, 2H, **H2**), 7.02 (t, *J* = 7.3 Hz, 1H, **H1**), 6.85 (d, *J* = 1.4 Hz, 1H, **H15**), 6.78 – 6.71 (m, 2H, **H11, H12**), 6.45 (s, 1H, **H5**), 5.94 (s, 2H, **H16**), 3.48 (t, *J* = 5.1 Hz, 4H, **H7**), 3.44 (s, 2H, **H9**), 2.44 (t, *J* = 5.1 Hz, 4H, **H8**).**^{13}C NMR** (126 MHz, $CDCl_3$) δ_C 154.86 (**C6**), 147.6 (**C13**), 146.7 (**C14**), 138.9 (**C4**), 131.4 (**C10**), 128.8 (**C2**), 123.0 (**C1**), 122.1 (**C11**), 119.8 (**C3**), 109.3 (**C15**), 107.8 (**C12**), 100.8 (**C16**), 62.5 (**C9**), 52.4 (**C8**), 44.0 (**C7**). **LC-MS:** retention time: 0.590 min; **AJS-ESI** *(m/z)*: for $[C_{19}H_{21}N_3O_3]^+$ $[M+H]^+$: exact mass calcd.: 340.16; found: 340.2. **FTIR** (cm^{-1}): υ(N–H s) 3223, υ(C-H s) 2928, υ(C=O s) 1635, δ(N–H m), υ(C-N m) 1533, δ(C-H s) 1447, δ(C-O s) 1235, υ(C-O s) 1000, γ(C-H s) 755. mp 224-227 ^oC.

3.3.1.1.3.18 Preparation of 4-((6-bromobenzo[*d*][1,3]dioxol-5-yl)methyl)-*N*-phenylpiperazine-1-carboxamide, 3.53.



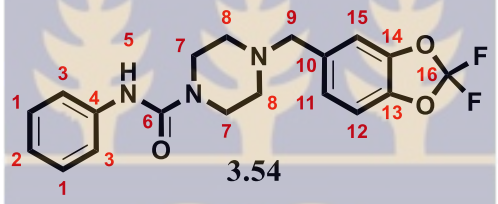
3.53

Compound **3.53** was synthesised following the general procedure for reductive amination, using previously prepared amine, **3.25 (**0.25 g, 1.22 mmol), $NaB(OAc)_3H$ (0.39 g, 1.83 mmol), and 6-bromobenzo[1,3]dioxole-5-carbaldehyde (0.56 g, 2.44 mmol), and obtained in 77.7 % yield as a white solid. **^{1}H NMR** (500 MHz, $CDCl_3$) δ_H 7.35 (d, *J* = 8.0 Hz, 1H, **H3**), 7.28 (d, *J* = 7.8 Hz, 1H, **H1**), 7.04 (d, *J* = 7.4 Hz, 0H, **H2**), 7.01 (d, *J* = 1.5 Hz, 1H, **H12, 15**), 6.49 (s, 1H, **H5**), 5.98 (s, 1H, **H16**), 3.56 (s, 1H, **H9**), 3.50 (t, *J* = 5.2 Hz, 2H, **H7**), 2.53 (t, *J* = 5.1 Hz, 2H, **H8**). **^{13}C NMR** (126 MHz, $CDCl_3$) δ_C 155.0 (**C6**), 147.5 (**C13**), 147.5 (**C14**),

University of Ghana http://ugspace.ug.edu.gh

139.0 (**C4**), 128.9 (**C10**), 123.1 (**C1**), 120.0 (**C2**), 114.8 (**C3**), 112.7 (**C11**), 110.4 (**C12**), 101.7 (**C15**), 61.4 (**C9**), 52.6 (**C8**), 44.2 (**C7**). **LC-MS:** retention time: 2.427 min; **AJS-ESI** *(m/z)*: for $[C_{19}H_{20}BrN_3O_3]^+$ $[M+H]^+$: exact mass calcd.: 418.07 (^{79}Br); found: 418.10; exact mass calcd.: 420.07 (^{81}Br); found: 420.10. **FTIR** (cm^{-1}): υ(N–H s) 3299, υ(C-H s) 2899, 2826, υ(C=O s) 1636, δ(N–H), υ(C-N s) 1527, δ(C-H s) 1455, υ(C-O s) 1235, υ(C-O s) 1001, γ(C-H s) 760. mp 161-163 ^oC.

3.3.1.1.3.19 Preparation of 4-((2,2-difluorobenzo[*d*][1,3]dioxol-5-yl)methyl)-*N*-phenylpiperazine-1-carboxamide, 3.54.

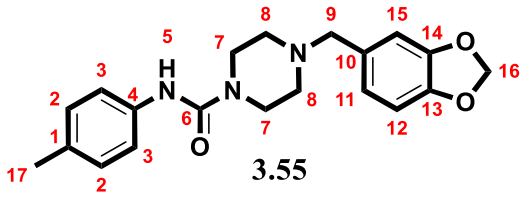


3.54

Compound **3.54** was synthesised following the general procedure for reductive amination, using previously prepared amine, **3.25** (0.25 g, 1.22 mmol), $NaB(OAc)_3H$ (0.39 g, 1.83 mmol), and 2,2-difuorobenzo[*d*][1,3]dioxole-5-carbaldehyde (0.32 mL, 2.44 mmol), and obtained in 56.8 % yield as a white solid. **^{1}H NMR** (500 MHz, $CDCl_3$) δ_H 7.34 (d, *J* = 8.0 Hz, 2H, **H1**), 7.30 – 7.24 (m, 2H, **H3**), 7.12 (s, 1H, **H15**), 7.03 (t, *J* = 7.3 Hz, 1H, **H2**), 7.00 (d, *J* = 2.6 Hz, 2H, **H12, 11**), 6.40 (s, 1H, **H5**), 3.60 – 3.44 (m, 6H, **H9, 7**), 2.46 (t, *J* = 5.0 Hz, 4H, **H8**). **^{13}C NMR** (126 MHz, $CDCl_3$) δ_C 155.02 (**C6**), 144.00 (**C14**), 142.95 (**C13**), 138.92 (**C4**), 134.11 (**C10**), 131.66 (**C16**), 128.90 (**C1**), 123.90 (**C2**), 123.20 (**C11**), 120.02 (**C3**), 110.06 (**C15**), 109.00 (**C12**), 62.34 (**C9**), 52.59 (**C8**), 44.11 (**C7**). **LC-MS:** retention time: 2.432 min; **AJS-ESI** *(m/z)*: for $[C_{19}H_{19}F_2N_3O_3]^+$ $[M+H]^+$: exact mass calcd.: 376.14; found: 376.20. **FTIR** (cm^{-1}): υ(N–H s) 3301, υ(C-H s) 2811, υ(C=O s) 1635, δ(C-H s) 1448, υ(C-O s) 1236, υ(C-F s) 1145, υ(C-Os) 1006, γ(C-H s) 755. mp 128-130 ^oC.

University of Ghana http://ugspace.ug.edu.gh

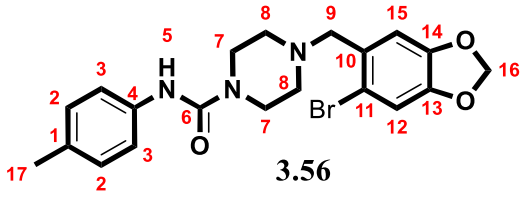
3.3.1.1.3.20 Preparation of 4-(benzo[*d*][1,3]dioxol-5-ylmethyl)-*N*-(p-tolyl)piperazine-1-carboxamide, 3.55.



3.55

Compound **3.55** was synthesised following the general procedure for reductive amination, using previously prepared amine, **3.32 (**0.25 g, 1.14 mmol), $NaB(OAc)_3H$ (0.36 g, 1.70 mmol), and piperonal (0.34 mL, 2.28 mmol), and obtained in 32.3 % yield as an oil. **^{1}H NMR** (400 MHz, $CDCl_3$) δ_H 7.27 – 7.18 (m, 2H, **H3**), 7.16 – 7.03 (m, 2H, **H2**), 6.86 (d, *J* = 1.1 Hz, 1H, **H15**), 6.75 (t, *J* = 0.9 Hz, 2H, **H11, H12**), 6.24 (s, 1H, **H5**), 5.95 (s, 2H, **H16**), 3.52 – 3.47 (m, 4H, **H8**), 3.45 (s, 2H, **H9**), 2.50 – 2.43 (m, 4H, **H7**), 2.29 (s, 3H, **H17**). **^{13}C NMR** (101 MHz, $CDCl_3$) δ_C 154.96 (**C6**), 147.57 (**C14**), 146.60 (**C13**), 136.13 (**C4**), 132.53 (**C1**), 131.37 (**C10**), 129.23 (**C2**), 122.05 (**C11**), 119.95 (**C3**), 109.23 (**C12**), 107.76 (**C15**), 100.78 (**C16**), 62.47 (**C9**), 52.39 (**C8**), 43.94 (**C7**), 20.57 (**C17**). **LC-MS:** retention time: 0.705 min; **AJS-ESI** *(m/z)*: for $[C_{20}H_{23}N_3O_3]^+$ $[M+H]^+$: exact mass calcd.: 354.17; found: 354.1. **FTIR** (cm^{-1}): υ(N–Hs) 3289, υ(C-H s) 2852, 2772, υ(C=O s) 1635, δ(N-H s), υ(C-N s) 1513, υ(C-O s) 1232, υ(C-O m) 994, γ(C-H m) 807.

3.3.1.1.3.21 Preparation of 4-((6-bromobenzo[*d*][1,3]dioxol-5-yl)methyl)-*N*-(p-tolyl)piperazine-1-carboxamide, 3.56.

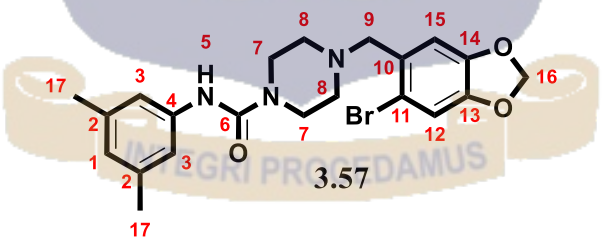


3.56

University of Ghana http://ugspace.ug.edu.gh

Compound **3.56** was synthesised following the general procedure for reductive amination, using previously prepared amine, **3.32** (0.25 g, 1.14 mmol), $NaB(OAc)_3H$ (0.36 g, 1.70 mmol), and 6-bromo-benzo[1,3]dioxole-5-carbaldehyde (0.52 g, 2.28 mmol), and obtained in 11.6 % yield as an oil. **^{1}H NMR** (400 MHz, $CDCl_3$) δ_H 6.98 (d, *J* = 1.5 Hz, 2H, **H3**), 6.86 (d, *J* = 1.3 Hz, 1H, **H15**), 6.75 (d, *J* = 1.6 Hz, 2H, **H1**), 6.68 (s, 1H, **H12**), 6.21 (s, 1H, **H5**), 5.95 (s, 2H, **H16**), 3.49 – 3.46 (m, 4H, **H7**), 3.44 (s, 2H, **H9**), 2.53 – 2.42 (m, 4H, **H8**), 2.27 (s, 3H, **H17**). **^{13}C NMR** (101 MHz, $CDCl_3$) δ_C 154.85 (**C6**), 147.56 (**C13**), 146.59 (**C14**), 138.58 (**C4**), 138.38 (**C2**), 131.40 (**C10**), 124.71 (**C1**), 122.04 (**C3**), 117.47 (**C11**), 109.23 (**C12**), 107.76 (**C15**), 100.77 (**C16**), 62.48 (**C19**), 52.39 (**C8**), 43.97 (**C7**), 21.19 (**C17**). **LC-MS:** retention time: 0.784 min; **AJS-ESI** *(m/z)*: for $[C_{20}H_{22}BrN_3O_3]^+$ $[M+H]^+$: exact mass calcd.: 434.09 (^{81}Br); found: 434.0. **FTIR** (cm^{-1}): υ(N–H s) 3349, υ(C-H s) 2902, 2818, υ(C=O s) 1623, δ(N-H s), υ(C-Ns) 1531, υ(C-O s) 1255, υ(C-O s) 1039, γ(C-H s) 811.

3.3.1.1.3.22 Preparation of 4-((6-bromobenzo[*d*][1,3]dioxol-5-yl)methyl)-*N*-(3,5-dimethylphenyl)piperazine-1-carboxamide, 3.57.

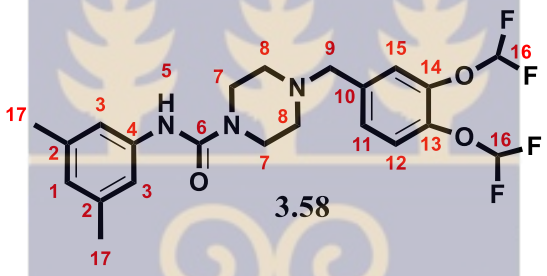


Compound **3.57** was synthesised following the general procedure for reductive amination, using previously prepared amine, **3.28 (**0.22 g, 0.94 mmol), $NaB(OAc)_3H$ (0.30 g, 1.41 mmol), and 6-bromo-benzo[1,3]dioxole-5-carbaldehyde (0.43 g, 1.89 mmol), and obtained in 15.0 % yield as an oil**. ^{1}H NMR** (400 MHz, $CDCl_3$) δ_H 7.06 – 6.93 (m, 4H, **H3, H12, H15**), 6.68 (dq, *J* = 1.6, 0.9 Hz, 1H, **H2**), 6.23 (s, 1H, **H5**), 5.97 (s, 2H, **H16**), 3.55 (s, 2H, **H9**), 3.52 – 3.43 (m, 4H, **H7**), 2.60 – 2.46 (m, 4H, **H8**), 2.27 (d, *J* = 0.7 Hz, 6H, **H17**). **^{13}C NMR** (101

University of Ghana http://ugspace.ug.edu.gh

MHz, $CDCl_3$) δ_C 154.85 (**C6**), 147.3 (**C14**), 147.2 (**C13**), 138.6 (**C4**), 138.4 (**C1**), 130.1 (**C10**), 124.7 (**C2**), 117.5 (**C3**), 114.6 (**C11**), 112.5 (**C12**), 110.1 (**C15**), 101.5 (**C16**), 61.3 (**C9**), 52.4 (**C8**), 44.0 (**C7**), 21.2 (**C17**). **LC-MS:** retention time: 0.705 min; **AJS-ESI** *(m/z)*: for $[C_{21}H_{24}BrN_3O_3]^+$ $[M+H]^+$: exact mass calcd.: 448.10 (^{81}Br); found: 448.1. **FTIR** (cm^{-1}): υ(N–H s) 3359, υ(C-H s) 2850, 2809, υ(C=O s) 1629, δ(N-H s), υ(C-N s) 1523, δ(C-H m) 1471, υ(C-O s) 1228, υ(C-O m) 998.

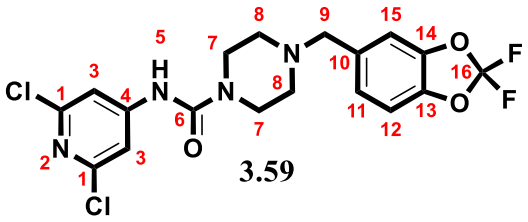
3.3.1.1.3.23 Preparation of 4-(3,4-bis(difluoromethoxy)benzyl)-N-(3,5-dimethylphenyl)piperazine-1-carboxamide, 3.58.



Compound **3.58** was synthesised following the general procedure for reductive amination, using previously prepared amine, **3.28** (0.20 g, 0.86 mmol), $NaB(OAc)_3H$ (0.11 g, 1.70 mmol), and 3,4-bis(difluoromethoxy) benzaldehyde (0.4 g, 1.70 mmol), and obtained in 22.0 % yield as an oil. **^{1}H NMR** (500 MHz, $CDCl_3$) δ_H 7.28 (s, 1H, **H5**), 7.21 (s, 2H, **H3**), 6.98 (s, 2H, **H16**), 6.68 (s, 1H, **H1**), 6.53 (dd, *J* = 12.9, 2.8 Hz, 1H, **H11**), 6.39 (dd, *J* = 13.0, 2.7 Hz, 1H, **H12**), 6.24 (s, 1H **H15**), 3.53 (s, 2H, **H9**), 3.50 (s, 4H, **H7**), 2.49 (s, 4H **H8**), 2.27 (s, 6H **H17**). **^{13}C NMR** (126 MHz, $CDCl_3$) δ_C 155.0 (**C6**), 141.3 (**C14**), 138.7 (**C13**), 138.5 (**C4**), 126.8 (**C2**), 124.9 (**C10**), 122.6 (**C1**), 122.2 (**C11**), 117.8 (**C12**), 117.7 (**C3**), 115.8 (**C15**), 113.7 (**C16**), 61.6 (**C9**), 52.6 (**C7**), 44.0 (**C8**), 21.2 (**C17**). **LC-MS:** retention time: 0.848 min; **AJS-ESI** *(m/z)*: for $[C_{22}H_{25}F_4N_3O_3]^+$ $[M+H]^+$: exact mass calcd.: 356.18; found: 356.2. **FTIR** (cm^{-1}): υ(N–H s) 3311, υ(C-H s) 2814, υ(C=O s) 1636, δ(C-H s) 1448, υ(C-O s) 1236, 1006, υ(C-F m) 1145, γ(C-H m) 825.

University of Ghana http://ugspace.ug.edu.gh

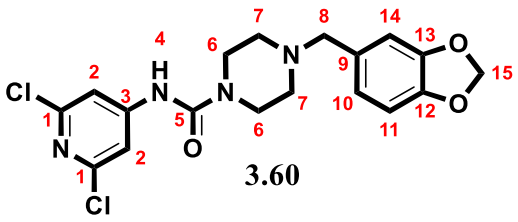
3.3.1.1.3.24 Preparation of *N*-(2,6-dichloropyridin-4-yl)-4-((2,2-difluorobenzo[*d*][1,3]dioxol-5-yl)methyl)piperazine-1-carboxamide, 3.59.



3.59

Compound **3.59** was synthesised following the general procedure for reductive amination, using previously prepared amine, **3.20 (**0.20 g, 0.73 mmol), $NaB(OAc)_3H$ (0.09 g, 1.50 mmol), and 2,2-difuorobenzo[*d*][1,3]dioxole-5-carbaldehyde (0.20 mL, 1.50 mmol), and obtained in 22.5 % yield as a white solid. **^{1}H NMR** (500 MHz, $CDCl_3$) δ_H 7.38 (s, 2H, **H3**), 7.19 – 7.09 (m, 2H, **H15, H12**), 7.06 – 6.91 (m, 2H, **H11, H5**), 3.61 – 3.50 (m, 6H, **H9, H7**), 2.58 – 2.43 (m, 4H, **H8**). **^{13}C NMR** (126 MHz, $CDCl_3$) δ_C 153.3 (**C6**), 151.3 (**C1**), 150.7 (**C4**), 144.5 (**C14**), 143.6 (**C13**), 132.1 (**C10**), 134.1, 130.0 (**C16**), 124.5 (**C11**), 112.2 (**C3**), 110.6 (**C15**), 109.6 (**C12**), 62.5 (**C9**), 52.8 (**C8**), 44.5 (**C7**). **LC-MS:** retention time: 0.834 min; **AJS-ESI** *(m/z)*: for $[C_{18}H_{16}Cl_2F_2N_4O_3]^+$ $[M+H]^+$: exact mass calcd.: 445.057 (^{35}Cl, ^{35}Cl); found: 445.0; exact mass calcd.: 447.057 (^{35}Cl, ^{37}Cl); found: 447.0; exact mass calcd.: 449.06 (^{37}Cl, ^{37}Cl); found: 449.0. υ(N–H s) 3460, υ(C-H s) 2905, υ(C=C s) 1660, υ(C=O s) 1579, υ(C-N s), δ(N-H s) 1501, δ(C–H m) 1414, υ(Aryl C-O s) 1236, υ(C-F s) 1159, γ(C-H s) 804, υ(C-Cl s) 615. mp 108-110 ^{o}C.

3.3.1.1.3.25 Preparation of 4-(benzo[*d*][1,3]dioxol-5-ylmethyl)-*N*-(2,6-dichloropyridin-4-yl)piperazine-1-carboxamide, 3.60.

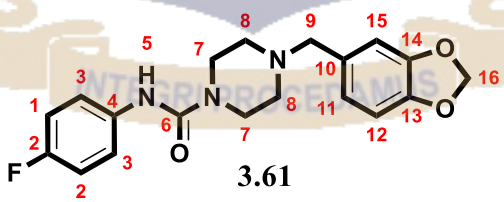


3.60

University of Ghana http://ugspace.ug.edu.gh

Compound **3.60** was synthesised following the general procedure for reductive amination, using previously prepared amine, **3.20 (**0.20 g, 0.73 mmol), $NaB(OAc)_3H$ (0.09 g, 1.50 mmol), and piperonal (0.23 g, 1.50 mmol), and obtained in 77.0 % yield as a white solid. **^{1}H NMR** (500 MHz, $CDCl_3$) δ_H 7.41 (s, 2H, **H2**), 7.37 (s, 1H, **H4**), 6.88 (d, *J* = 5.3 Hz, 1H, **H10**), 6.76 (d, *J* = 5.7 Hz, 2H, **H11, H14**), 5.95 (s, 2H, **H15**), 3.62 – 3.56 (m, 4H, **H6**), 3.54 (s, 2H, **H8**), 2.59 – 2.52 (m, 4H, **H7**) . **^{13}C NMR** (126 MHz, $CDCl_3$) δ_C 152.9 (**C5**), 150.8 (**C1**), 150.3 (**C3**), 147.9 (**C13**), 147.2 (**C12**), 122.6 (**C9**), 111.7 (**C2**), 111.6 (**C10**), 109.5 (**C14**), 108.0 (**C11**), 101.0 (**C15**), 62.2 (**C8**), 52.1 (**C7**), 43.9(**C6**). **LC-MS:** retention time: 0.707 min; **AJS-ESI** *(m/z)*: for $[C_{18}H_{18}Cl_2N_4O_3]^+$ $[M+H]^+$: exact mass calcd.: 409.08 (^{35}Cl, ^{35}Cl); found: 409.1; exact mass calcd.: 411.076 (^{35}Cl, ^{37}Cl); found: 411.0; exact mass calcd.: 413.076 (^{37}Cl, ^{37}Cl); found: 413.1. **FTIR** (cm^{-1}): υ(N–H s) 3349, υ(C-H s) 2946, 2828, υ(C=C s) 1658, υ(C=O s) 1576, δ(C–H s) 1413, υ(Aryl C-O s) 1256, υ(C-O m) 1096, γ(C-H m) 795. mp 189-191 ^oC.

3.3.1.1.3.26 Preparation of 4-(benzo[*d*][1,3]dioxol-5-ylmethyl)-*N*-(4-fluorophenyl)piperazine-1-carboxamide, 3.61.



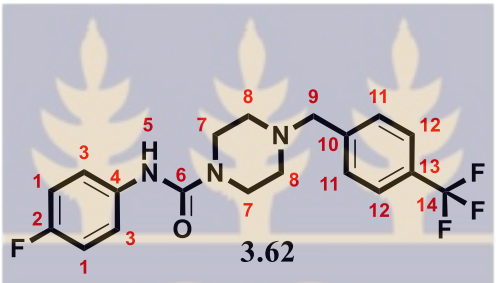
3.61

Compound **3.61** was synthesised following the general procedure for reductive amination, using previously prepared amine, **3.29** (0.35 g, 1.56 mmol), $NaB(OAc)_3H$ (0.50 g, 2.34 mmol), and piperonal (0.47 g, 3.13 mmol), and obtained in 37.3 % yield as a white solid. **^{1}H NMR** (500 MHz, $CDCl_3$) δ_H 7.34 – 7.22 (m, 2H, **H3**), 7.00 – 6.92 (m, 2H, **H2**), 6.85 (s, 1H, **H15**), 6.80 – 6.66 (m, 2H, **H12, H11**), 6.44 (s, 1H, **H5**), 5.94 (s, 2H, **H16**), 3.44 (s, 2H, **H9**), 2.45 (t, *J* = 5.1 Hz, 4H, **H7**), 1.72 (t, *J* = 5.1 Hz, 4H, **H8**). **^{13}C NMR** (126 MHz, $CDCl_3$) δ_C

University of Ghana http://ugspace.ug.edu.gh

159.8, 157.9 (**C2**), 155.1 (**C6**), 147.6 (**C14**), 146.7 (**C13**), 134.7 (**C4**), 131.3 (**C10**), 122.1 (**C11**), 122.0, 121.9 (**C3**), 115.4, 115.2 (**C1**), 109.3 (**C12**), 107.8 (**C15**), 100.8 (**C16**), 62.5 (**C9**), 52.4 (**C8**), 43.9 (**C7**). **LC-MS:** retention time: 0.636 min; **AJS-ESI** *(m/z)*: for $[C_{19}H_{20}FN_3O_3]^+$ $[M+H]^+$: exact mass calcd.: 358.15; found: 358.1. **FTIR** (cm^{-1}): υ(N–H s) 3340, υ(C-H s) 2932, 2875, υ(C=O s) 1638, δ(N–H s), υ(C-N s) 1510, υ(C-O s) 1206, 1040, γ(C-H s) 829. mp 97-98 ^oC.

3.3.1.1.3.27 Preparation of *N*-(4-fluorophenyl)-4-(4-(trifluoromethyl)benzyl)piperazine-1-carboxamide, 3.62.

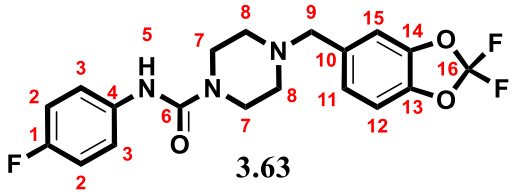


3.62

Compound **3.62** was synthesised following the general procedure for reductive amination, using previously prepared amine, **3.29** (0.35 g, 1.56 mmol), $NaB(OAc)_3H$ (0.50 g, 2.34 mmol), and 4-trifuoromethyl benzaldehyde (0.55 g, 3.14 mmol), and obtained in 33.5 % yield as an oil. **^{1}H NMR** (500 MHz, $CDCl_3$) δ_H 7.58 (d, *J* = 7.9 Hz, 2H, **H3**), 7.45 (d, *J* = 7.9 Hz, 2H, **H1**), 7.29 – 7.27 (m, 2H, **H12**), 6.96 (m, 2H, **H11**), 6.46 (s, 1H, **H5**), 3.58 (s, 2H, **H9**), 3.52 – 3.47 (m, 4H, **H7**), 2.50 – 2.44 (m, 4H, **H8**). **^{13}C NMR** (126 MHz, $CDCl_3$) δ_C 160.1, 158.1 (**C2**), 155.6 (**C6**), 141.9 (**C10**), 135.0 (**C4**), 129.4 (**C11**), 125.5 (**C13**), 125.4, 125.4 (**C12**), 125.4 (**C14**), 122., 122.4 (**C3**), 115.6, 115.4 (**C1**), 52.8 (**C9**), 50.7 (**C8**), 44.1 (**C7**). **LC-MS:** retention time: 0.953 min; **AJS-ESI** *(m/z)*: for $[C_{19}H_{19}F_4N_3O]^+$ $[M+H]^+$: exact mass calcd.: 381.15; found: 382.1. **FTIR** (cm^{-1}): υ(N–H s) 3343, υ(C-H m) 2961, 2815, υ(C=Os) 1634, δ(N–H s), υ(C-N s) 1537, δ(C-H s) 1423, υ(C-O m) 1235, υ(C-F s) 1130, 1005, γ(C-H m) 834.

University of Ghana http://ugspace.ug.edu.gh

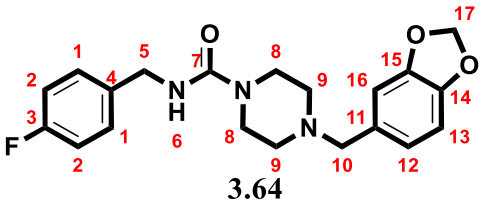
3.3.1.1.3.28 Preparation of 4-((2,2-difluorobenzo[*d*][1,3]dioxol-5-yl)methyl)-*N*-(4-fluorophenyl)piperazine-1-carboxamide, 3.63.



3.63

Compound **3.63** was synthesised following the general procedure for reductive amination, using previously prepared amine, **3.29** (0.23 g, 1.03 mmol), $NaB(OAc)_3H$ (0.13 g, 2.1 mmol), and 2,2-difuorobenzo[*d*][1,3]dioxole-5-carbaldehyde (0.27 mL, 2.10 mmol), and obtained in 71.6 % yield as an oil. **^{1}H NMR** (400 MHz, $CDCl_3$) δ_H 7.30 – 7.18 (m, 2H, **H3**), 7.08 (d, *J* = 1.2 Hz, 1H, **H15**), 7.01 – 6.88 (m, 4H, **H2, H12, H11**), 6.30 (s, 1H, **H5**), 3.46 (s, 2H, **H9**), 3.46 – 3.43 (m, 4H, **H7**), 2.48 – 2.37 (m, 4H, **H8**). **^{13}C NMR** (101 MHz, $CDCl_3$) δ_C 157.9 (**C1**), 155.2 (**C6**), 144.1 (**C14**), 143.1 (**C13**), 135.0 (**C4**), 134.3 (**C16**), 124.0 (**C10**), 122.1 (**C11**), 115.7 (**C3**), 115.5 (**C2**), 110.2 (**C15**), 109.1 (**C12**), 62.5 (**C9**), 52.7 (**C8**), 44.2 (**C7**). **LC-MS:** retention time: 0.767 min; **AJS-ESI** *(m/z)*: for $[C_{19}H_{18}F_3N_3O_3]^+$ $[M+H]^+$: exact mass calcd.: 394.13; found: 394.1. **FTIR** (cm^{-1}): υ(N–H m) 3287, υ(C-H m) 2942, 2799, υ(C=O s) 1633, δ(N–H s), υ(C-N s) 1509, υ(C-O s) 1208, 1002, υ(C-F m) 1143, γ(C-H s) 822.

3.3.1.1.3.29 Preparation of 4-(benzo[d][1,3]dioxol-5-ylmethyl)-N-(4-fluorobenzyl)piperazine-1-carboxamide, 3.64.



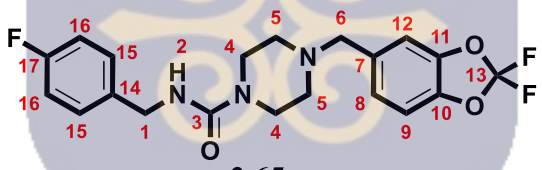
3.64

Compound **3.64** was synthesised following the general procedure for reductive amination, using previously prepared amine, **3.34** (0.15 g, 0.63 mmol), $NaB(OAc)_3H$ (0.2 g, 0.95 mmol),

University of Ghana http://ugspace.ug.edu.gh

and piperonal (0.19 g, 1.26 mmol), and obtained in 95.8 % yield as a white solid. **^{1}H NMR** (500 MHz, DMSO) δ_H 7.22 – 7.11 (m, 2H, **H1**), 7.03 (s, 3H, **H6, H2**), 7.02 – 6.99 (m, 1H, **H12**), 6.81 – 6.71 (m, 1H, **H13**), 6.65 (dd, *J* = 8.0, 1.6 Hz, 1H, **H16**), 5.89 (s, 2H, **H17**), 4.10 (d, *J* = 5.8 Hz, 2H, **H5**), 3.28 (s, 2H, **H10**), 3.21 (t, *J* = 5.0 Hz, 4H, **H8**), 2.19 (t, *J* = 5.0 Hz, 4H, **H9**). **^{13}C NMR** (126 MHz, DMSO) δ_C 162.0, 160.0 (**C3**), 157.4 (**C7**), 147.2 (**C15**), 146.2 (**C14**), 137.2 (**C4**), 131.8 (**C11**), 128.9 (**C1**), 122.1 (**C12**), 114.8 (**C2**), 109.1 (**C13**), 107.9 (**C16**), 100.8 (**C17**), 61.7 (**C10**), 52.3 (**C9**), 43.5 (**C8**), 42.8 (**C5**). retention time: 2.0171 min; **WAU-ESI** *(m/z)*: for $[C_{20}H_{22}FN_3O_3]^+$ $[M+H]^+$: exact mass calcd.: 372.17; found: 371.90. $[M+Na]^+$: 371.90. **FTIR** (cm^{-1}): υ(N–H m) 3344, υ(C-H m) 2936, 2869, υ(C=C m) 1614, δ(N–H m), υ(C-N m) 1500, υ(C-O m) 1246, 1000, γ(C-H m) 825. mp 176-179 ^{o}C.

3.3.1.1.3.30 Preparation of 4-((2,2-difluorobenzo[*d*][1,3]dioxol-5-yl)methyl)-*N*-(4-fluorobenzyl)piperazine-1-carboxamide, 3.65.



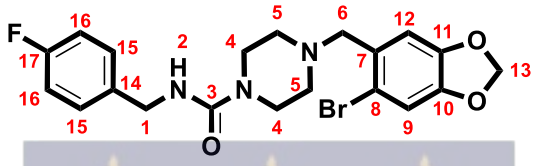
3.65

Compound **3.65** was synthesised following the general procedure for reductive amination, using previously prepared amine **3.34** (0.15 g, 0.63 mmol), $NaB(OAc)_3H$ (0.2 g, 0.95 mmol), and 2,2-difuorobenzo[*d*][1,3]dioxole-5-carbaldehyde (0.16 mL, 1.26 mmol), and obtained in 81.8 % yield as a white solid. **^{1}H NMR** (500 MHz, $CDCl_3$) δ_H 7.26 (dd, *J* = 8.3, 5.6 Hz, 2H, **H15**), 7.11 (s, 1H, **H12**), 7.00 (d, *J* = 8.7 Hz, 2H, **H16**), 6.99 – 6.96 (m, 2H, **H9, H8**), 4.80 (s, 1H, **H2**), 4.37 (d, *J* = 5.5 Hz, 2H, **H1**), 3.50 (s, 2H, **H6**), 3.40 (t, *J* = 5.1 Hz, 4H, **H4**), 2.43 (t, *J* = 5.1 Hz, 4H, **H5**). **^{13}C NMR** (126 MHz, $CDCl_3$) δ_C 163.2, 161.3 (**C17**), 157.6 (**C3**), 144.2 (**C11**), 143.2 (**C10**), 135.4 (**C14**), 133.8 (**C7**), 131.8, 129.8 (**C13**), 129.5 (**C15**), 124.1 (**C8**), 115.5 (**C16**), 110.3 (**C9**), 109.2 (**C12**), 62.4 (**C6**), 52.7 (**C5**), 44.4 (**C4**), 43.9 (**C1**). **LC-MS:**

University of Ghana http://ugspace.ug.edu.gh

retention time: 2.463 min; **AJS-ESI** *(m/z)*: for $[C_{20}H_{20}F_3N_3O_3]^+$ $[M+H]^+$: exact mass calcd.: 408.15; found: 408.2. **FTIR** (cm^{-1}): υ(N–H s) 3326, υ(C-H s) 2811, υ(C=O s) 1625, υ(C=C s) 1547, υ(C-F m) 1144, γ(C-H m) 789. mp 116-119 ^oC.

3.3.1.1.3.31 Preparation of 4-((6-bromobenzo[d][1,3]dioxol-5-yl)methyl)-N-(4-fluorobenzyl)piperazine-1-carboxamide, 3.66.

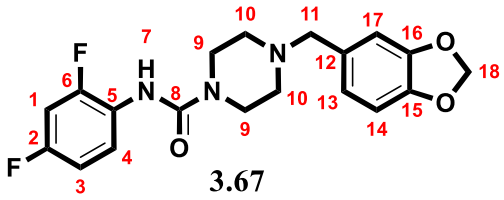


3.66

Compound **3.66** was synthesised following the general procedure for reductive amination, using previously prepared amine, **3.34** (0.15 g, 0.63 mmol), $NaB(OAc)_3H$ (0.2 g, 0.95 mmol), and 6-bromo-benzo[1,3]dioxole-5-carbaldehyde (0.3 g, 1.26 mmol), and obtained in 60.0 % yield as a white solid. **^{1}H NMR** (400 MHz, $CDCl_3$) δ_H 7.28 – 7.25 (m, 2H, **H15**), 7.04 – 6.97 (m, 4H, **H16, 9, 12**), 5.96 (s, 2H, **H13**), 4.39 (d, *J* = 5.5 Hz, 2H, **H1**), 3.52 (s, 2H, **H6**), 3.45 – 3.33 (m, 4H, **H4**), 2.58 – 2.39 (m, 4H, **H5**). **^{13}C NMR** (101 MHz, $CDCl_3$) δ_C 163.5, 161.0 (**C17**), 157.6 (**C3**), 147.6, 147.5 (**C11, C10**), 135.4, 135.4 (**C14**), 130.5 (**C7**), 129.6, 129.5 (**C15**), 115.7, 115.5 (**C16**), 114.9 (**C8**), 112.8 (**C9**), 110.4 (**C12**), 101.8 (**C13**), 61.6 (**C6**), 52.7 (**C5**), 44.4 (**C4**), 44.1(**C1**). **LC-MS:** retention time: 2.2741 min; **LC-MS:** retention time: 2.2741 min; **WAU-ESI** *(m/z)*: for $[C_{20}H_{21}BrFN_3O_3]^+$ $[M+H]^+$: exact mass calcd.: 450.08 (^{79}Br); found: 449.75; exact mass calcd.: 452.08 (^{81}Br); found: 451.12, [M+Na]: 471.88(^{79}Br); [M+Na]: 473.82(^{81}Br). **FTIR** (cm^{-1}): υ(N–H m) 3341, υ(C-H m) 2971, υ(C=C s) 1607, υ(C=O s) 1645, δ(C-H m) 1435, υ(C-O s) 1238, 982, υ(C-F s) 1110, γ(C-H s) 837. mp 142-145 ^oC.

University of Ghana http://ugspace.ug.edu.gh

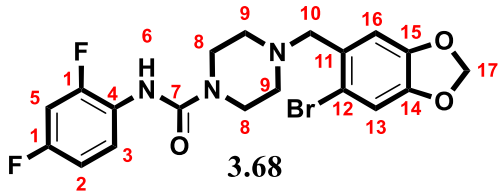
3.3.1.1.3.32 Preparation of 4-((6-bromobenzo[*d*][1,3]dioxol-5-yl)methyl)-*N*-(2,4-difluorophenyl)piperazine-1-carboxamide, 3.67.



3.67

Compound **3.67** was synthesised following the general procedure for reductive amination, using previously prepared amine, **3.31** (0.25 g, 1.04 mmol), $NaB(OAc)_3H$ (0.35 g, 1.7 mmol), and piperonal (0.31 g, 2.1 mmol), and obtained in 15.4 % yield as a white solid. **^{1}H NMR** (500 MHz, MeOD) δ_H 7.42 (td, *J* = 8.9, 6.0 Hz, 1H, **H4**), 7.01 (ddd, *J* = 10.5, 8.8, 2.9 Hz, 1H, **H1**), 6.97 – 6.91 (m, 2H, **H3, H17**), 6.85 – 6.79 (m, 2H, **H13, H14**), 5.97 (s, 2H, **H18**), 3.58 (t, *J* = 5.1 Hz, 4H, **H9**), 3.52 (s, 2H, **H11**), 2.52 (t, *J* = 5.1 Hz, 4H, **H10**). ^{13}C NMR (126 MHz, $CDCl_3$) δ_C 154.51 (**C1**), 147.62 (**C7**), 130.34 (**C15**), 122.93 (**C14**), 114.99 (**C4**), 112.82 (**C2**), 111.36 (**C11**), 111.18 (**C3**), 110.47 (**C16**), 103.60 (**C12**), 103.41 (**C13**), 103.20 (**C17**), 101.85 (**C5**), 61.53 (**C10**), 52.61 (**C9**), 44.32 (**C8**). **LC-MS:** retention time: 2.470 min; **AJS-ESI** *(m/z)*: for $[C_{19}H_{19}F_2N_3O_3]^+$ $[M+H]^+$: exact mass calcd.: 376.14; found: 376.10. **FTIR** (cm^{-1}): υ(N–H m) 3230, υ(C-H m) 2918, υ(C=O s) 1634, δ(N–H s), υ(C-N s) 1508, δ(C–H s) 1431, υ(C-O s) 1242, 996, υ(C-F m) 1189. mp 117-120 ^{o}C.

3.3.1.1.3.33 Preparation of 4-((6-bromobenzo[*d*][1,3]dioxol-5-yl)methyl)-*N*-(2,4-difluorophenyl)piperazine-1-carboxamide, 3.68.

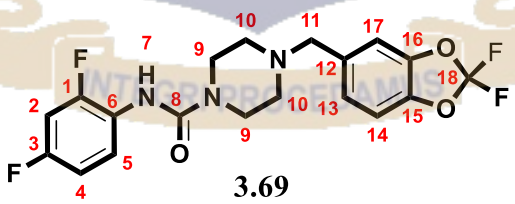


3.68

University of Ghana http://ugspace.ug.edu.gh

Compound **3.68** was synthesised following the general procedure for reductive amination, using previously prepared amine **3.31** (0.25 g, 1.04 mmol), $NaB(OAc)_3H$ (0.33 g, 1.56 mmol), and 6-bromo-benzo[1,3]dioxole-5-carbaldehyde (0.47 g, 2.08 mmol), and obtained in 29.6 % yield as a white solid. **^{1}H NMR** (500 MHz, $CDCl_3$) δ_H (td, *J* = 9.4, 9.0, 5.9 Hz, 1H, **H3**), 7.00 (s, 1H, **H6**), 6.98 (s, 1H, **H13**), 6.91 – 6.77 (m, 2H, **H5, H2**), 6.44 (d, *J* = 3.5 Hz, 1H, **H16**), 5.97 (s, 2H, **H17**), 3.56 (s, 2H, **H10**), 3.51 (t, *J* = 5.3 Hz, 4H, **H8**), 2.55 (t, *J* = 5.0 Hz, 4H, **H9**). **^{13}C NMR** (126 MHz, $CDCl_3$) δ_C 159.1, 157.1, 153.8, 151.7, (**C1**), 154.5 (**C7**), 147.6 (**C14, C15**), 130.3 (**C11**), 123.9 (**C4**), 122.9 (**C3**), 115.0 (**C12**), 112.8 (**C13**), 111.4, 111.2 (**C2**), 110.5 (**C21**), 103.6, 103.4, 103.2 (**C5**), 101.9 (**C17**), 61.5 (**C10**), 52.6 (**C9**), 44.3 (**C8**). **LC-MS:** retention time: 2.470 min; **AJS-ESI** *(m/z)*: for $[C_{19}H_{18}BrF_2N_3O_3]^+$ $[M+H]^+$: exact mass calcd.: 454.05 (^{79}Br); found: 454.00; exact mass calcd.: 456.05 (^{81}Br); found: 456.10. **FTIR** (cm^{-1}): υ(N–H s) 3278, υ(C-H s) 2971, υ(C=O s) 1633, υ(C=C s) 1567, δ(N-H m), υ(C-N m) 1498, υ(C-O s) 1228, 965, υ(C-F s) 1108, γ(C-H m) 852. mp 115-116 ^oC.

3.3.1.1.3.34 Preparation of 4-((2,2-difluorobenzo[d][1,3]dioxol-5-yl)methyl)-N-(2,4-difluorophenyl)piperazine-1-carboxamide, 3.69.



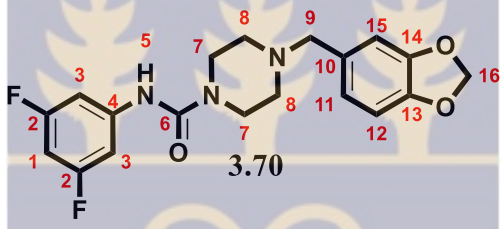
3.69

Compound **3.69** was synthesised following the general procedure for reductive amination, using previously prepared amine, **3.31** (0.23 g, 0.95 mmol), $NaB(OAc)_3H$ (0.12 g, 1.9 mmol), and 2,2-difuorobenzo[*d*][1,3]dioxole-5-carbaldehyde (0.24 mL, 1.9 mmol), and obtained in 38.2 % yield as a white solid. **^{1}H NMR** (500 MHz, MeOD) δ_H 7.41 (td, *J* = 8.9, 6.0 Hz, 1H, **H5**), 7.31 (s, 1H , **H7**), 7.19 (s, 2H, **H2, H4**), 7.00 (m, 2H, **H17, H14**), 6.97 – 6.91 (m, 1H, **H13**), 3.68 (s, 2H, **H11**), 3.60 (t, *J* = 5.1 Hz, 4H, **H9**), 2.60 (t, *J* = 5.5 Hz, 4H, **H10**). **^{13}C**

University of Ghana http://ugspace.ug.edu.gh

NMR (126 MHz, MeOD) δ_C 162.4, 160.4 (**C3**), 158.9, 156.9 (**C1**), 157.9 (**C8**), 145.1 (**C16**), 144.3 (**C15**), 135.1 (**C12**), 133.0 (**C18**), 131.0 (**C6**), 129.2 (**C5**), 126.3 (**C13**), 111.9 (**C4**), 111.7 (**C14**), 110.3 (**C17**), 105.1 (**C2**), 62.9 (**C11**), 53.6 (**C10**), 44.9 (**C9**). **LC-MS:** retention time: 0.750 min; **AJS-ESI** *(m/z)*: for $[C_{19}H_{17}F_4N_3O_3]^+$ $[M+H]^+$: exact mass calcd.: 412.12; found: 412.1. **FTIR** (cm^{-1}): υ(N–H s) 3385, υ(C-H s) 2929, υ(C=O s) 1665, δ(N-H s), υ(C-N s) 1532, υ(C-O s) 1321, 1246, υ(C-F m) 1115, γ(C-H m) 841. mp 145-148 ^oC.

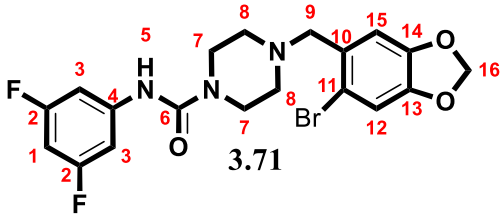
3.3.1.1.3.35 Preparation of 4-(benzo[d][1,3]dioxol-5-ylmethyl)-N-(3,5-difluorophenyl)piperazine-1-carboxamide, 3.70.



Compound **3.70** was synthesised following the general procedure for reductive amination, using previously prepared amine, **3.26** (0.23 g, 0.95 mmol), $NaCNBH_3$ (0.12 g, 1.9 mmol), and piperonal (0.29 g, 1.9 mmol), and obtained in 48.9 % yield as a white solid. **^{1}H NMR** (500 MHz, $CDCl_3$) δ_H 7.02 – 6.94 (m, 2H, **H3**), 6.86 (s, 1H, **H15**), 6.74 (t, *J* = 5.5 Hz, 2H, **H11, H12**), 6.52 (s, 1H, **H5**), 6.45 (t, *J* = 9.2 Hz, 1H, **H1**), 5.95 (s, 2H, **H16**), 3.49 (t, *J* = 5.1 Hz, 4H, **H7**), 3.45 (s, 2H), 2.47 (t, *J* = 5.0 Hz, 4H, **H8**). **^{13}C NMR** (126 MHz, $CDCl_3$) δ_C 164.16, 164.04, 162.21, 162.09 (**C2**), 153.93 (**C6**), 147.70 (**C14**), 146.79 (**C13**), 141.36 (**C4**), 131.17 (**C10**), 122.16 (**C11**), 109.28 (**C12**), 107.87 (**C15**), 102.40, 102.34, 102.22, 102.16 (**C3**), 100.87 (**C16**), 98.16, 97.96, 97.75 (**C1**), 62.46 (**C9**), 52.34 (**C8**), 44.04 (**C7**). **LC-MS:** retention time: 0.695 min; **AJS-ESI** *(m/z)*: for $[C_{19}H_{19}F_2N_3O_3]^+$ $[M+H]^+$: exact mass calcd.: 376.14; found: 376.1. **FTIR** (cm^{-1}): υ(N–H s) 3424, υ(C-H s) 2959, 2899, υ(C=O s) 1663, δ(N–H s), υ(C-N s) 1513, υ(C-O s) 1030, γ(C-H m) 820. mp 136-139 ^oC.

University of Ghana http://ugspace.ug.edu.gh

3.3.1.1.3.36 Preparation of 4-((2,2-difluorobenzo[*d*][1,3]dioxol-5-yl)methyl)-*N*-(3,5-difluorophenyl)piperazine-1-carboxamide, 3.71.



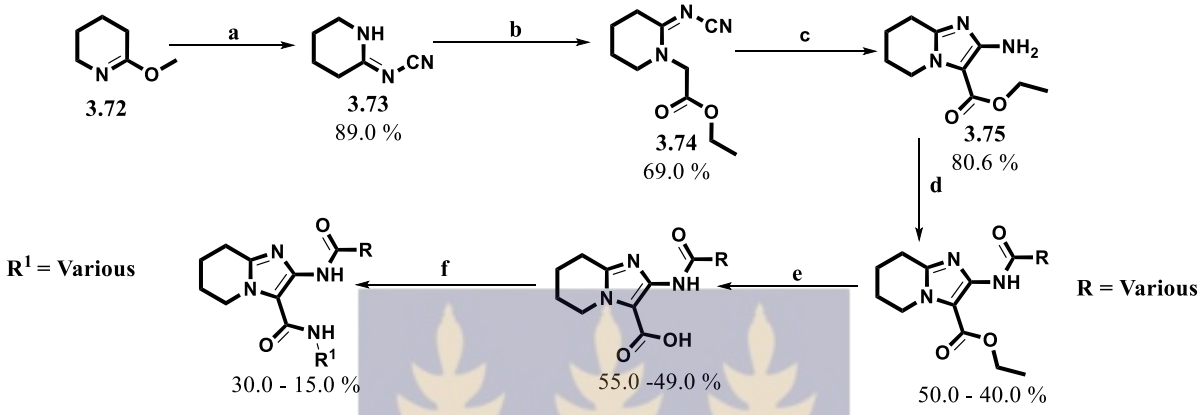
Compound **3.71** was synthesised following the general procedure for reductive amination, using previously prepared amine, **3.26** (0.19 g, 0.79 mmol), $NaB(OAc)_3H$ (0.25 g, 1.18 mmol), and 6-bromo-benzo[1,3]dioxole-5-carbaldehyde (0.36 g, 1.58 mmol), and obtained in 72.7 % yield as a white solid. **^{1}H NMR** (500 MHz, $CDCl_3$) δ_H 6.98 (d, *J* = 2.9 Hz, 1H, **H12**), 6.96 (d, *J* = 2.4 Hz, 2H, **H3**), 6.53 (s, 1H, **H5**), 6.46 (tt, *J* = 9.0, 2.3 Hz, 1H, **H1**), 5.97 (s, 2H, **H16**), 3.55 (s, 2H, **H9**), 3.50 (t, *J* = 5.1 Hz, 4H, **H7**), 2.54 (t, *J* = 5.0 Hz, 4H, **H8**). **^{13}C NMR** (126 MHz, $CDCl_3$) δ_C 164.38, 164.26, 162.43, 162.31 (**C2**), 154.19 (**C6**), 147.65 (**C13**), 147.61 (**C14**), 141.58 (**C4**), 130.22 (**C10**), 114.99 (**C11**), 112.82 (**C12**), 110.46 (**C15**), 102.66, 102.60, 102.48, 102.42 (**C3**), 101.87 (**C16**), 98.42, 98.22, 98.01 (**C1**), 61.51 (**C9**), 52.59 (**C8**), 44.34 (**C7**). **LC-MS:** retention time: 0.978 min; **AJS-ESI** *(m/z)*: for $[C_{19}H_{18}BrF_2N_3O_3]^+$ $[M+H]^+$: exact mass calcd.: 456.05 (^{81}Br); found: 456.0. **FTIR** (cm^{-1}): υ(N–H m) 3329, υ(C-H m) 2821, υ(C=C s) 1606, υ(C=O s) 1644, δ(N–H s), υ(C-N s) 1479, δ(C-H s) 1432, δ(C-O s) 1236, υ(C-F s) 1110, γ(C-H m) 843. mp 113-115 ^oC.

3.3.1.2 General procedures for MMV1794959 analogues.

Target analogues for this scaffold were synthesised *via* a six-step chemical route **(Scheme 3.2)**. The synthesis commenced with the formation of a piperidinylidene cyanamide, **3.73**, from *O*-methyl valerolactim, **3.72**, and cyanamide. **3.73** was then *N*-alkylated with ethyl chloroacetate in the presence of potassium carbonate, to afford its corresponding ethyl ester**.** Cyclisation of the ethyl ester yielded an amino tetrahydroindolizine ester, which was subse-

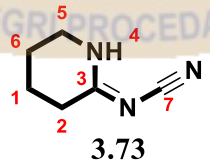
University of Ghana http://ugspace.ug.edu.gh

quently coupled with various trifluoromethyl benzoic acids to form amide esters. The amide esters were then hydrolysed to produce their corresponding carboxylic acids, and further coupled with diverse amines to give the desired analogues.



Scheme 3.2: Synthetic route for MMV1794959 analogues. **a**) MeOH, cyanamide, rt, 72 h **b**) CH_3CN, K_2CO_3, ethyl chloroacetate, 85 ^oC, then, reflux 22 h. **c**) EtOH, Na ethoxide, 85 ^oC, then, reflux 30 min. **d**) i) DCM, $SOCl_2$, trifluoromethyl benzoic acid ii) Et_3N, rt, 16 h. **e**) THF/H_2O, LiOH, 16 h. **f**) DMF, HATU, Et_3N, 16 hr.

3.3.1.2.1 General procedure for preparation of (*Z*)-*N*-(piperidin-2-ylidene)cyanamide, 3.73.



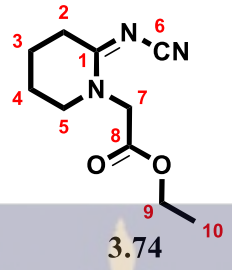
3.73

O-methyl valerolactim (5 g, 44.18 mmol, 1 eqv.) **3.72,** was dissolved in MeOH (50 mL), followed by the gradual addition of cyanamide (1.5 mL, 44.18 mmol, 1eqv.). The resulting suspension was stirred at room temperature for 72 hours, then filtered to produce a white solid in 89.0 % yield. **^{1}H NMR** (500 MHz, $CDCl_3$) δ_H 7.76 (s, 1H**, H4**), 3.40 (s, 2H**, H5**), 2.68 (s, 2H**,**

University of Ghana http://ugspace.ug.edu.gh

H2), 1.81 (q, *J* = 3.1 Hz, 4H**, H1, H6**). ^{13}C NMR (126 MHz, $CDCl_3$) δ_C 173.40 (**C3**), 116.97 (**C7**), 42.25 (**C5**), 28.50 (**C2**), 21.17 (**C6**), 19.01 (**C1**).

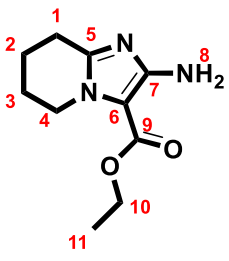
3.3.1.2.2 General procedure for preparation of ethyl (*Z*)-2-(2-(cyanoimino)piperidin-1-yl)acetate, 3.74.



3.74

To a solution of **3.73** (4.9 g, 39.79 mmol, 1 eqv.) in acetonitrile (50 mL) under low heat was added potassium carbonate (6.6 g, 47.8 mmol, 1.2 eqv.) and ethyl chloroacetate (8.52 ml, 79.58 mmol, 2.0 eqv). The resulting suspension was refluxed at 85 ^{o}C for 24 hours. The cooled suspension was then filtered, and the solid residue was washed with DCM. The filtrate was subsequently purified by flash column chromatography to give an oil in 69.0 % yield. **^{1}H NMR** (500 MHz, $CDCl_3$) δ_H 4.27 – 4.03 (m, 4H**, H7, H9**), 3.38 (t, *J* = 5.7 Hz, 2H**, H5**), 2.77 (d, *J* = 6.1 Hz, 2H**, H2**), 1.91 – 1.75 (m, 4H**, H3, H4**), 1.22 (td, *J* = 7.2, 2.5 Hz, 3H**, H10**). **^{13}C NMR** (126 MHz, $CDCl_3$) δ_C 172.11 (**C8**), 167.21 (**C9**), 116.55 (**C6**), 61.29 (**C9**), 50.91 (**C7**), 49.90 (**C5**), 28.95 (**C2**), 22.01 (**C4**), 19.19 (**C3**), 13.77 (**C12**).

3.3.1.2.3 General procedure for cyclisation of ethyl 2-amino-5,6,7,8-tetrahydroimidazo[1,2-a]pyridine-5-carboxylate, 3.75.

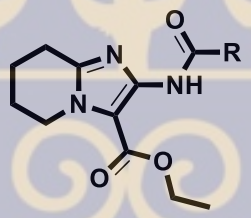


3.75

University of Ghana http://ugspace.ug.edu.gh

3.74 (3.6 g, 17.2 mmol, 1 eqv.) was added to a solution of sodium ethoxide (1.17 g, 17.2 mmol, 1eqv.) in ethanol (50 mL). The resulting mixture was refluxed at 85 ^{o}C for 30 minutes, then evaporated and purified by flash column chromatography to yield 80.6 % of the desired product as a white solid. **^{1}H NMR** (500 MHz, $CDCl_3$) δ_H 4.93 (s, 2H**, H8**), 4.39 – 4.24 (m, 2H**, H10**), 4.14 (t, *J* = 6.0 Hz, 2H**, H4**), 2.77 (t, *J* = 6.4 Hz, 2H **, H1**), 1.94 (q, *J* = 6.1 Hz, 2H**, H3**), 1.86 (dp, *J* = 9.7, 6.1, 4.0 Hz, 2H**, H2**), 1.34 (dd, *J* = 7.8, 6.3 Hz, 3H**, H11**). **^{13}C NMR** (126 MHz, $CDCl_3$) δ_C 160.97 (**C9**), 146.65 (**C7, C5**), 101.30 (**C6**), 59.35 (**C10**), 45.05 (**C4**), 24.43 (**C1**), 22.49 (**C3**), 19.52 (**C2**), 14.53 (**C11**).

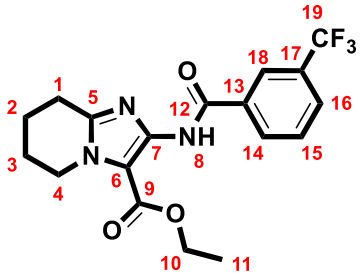
3.3.1.2.4 General procedure for amide coupling.



A mixture of thionyl chloride (10 eqv.) 3 drops of DMF, and trifluoromethylbenzoic acid (1.5 eqv.) in THF was stirred at room temperature for 4 hours. THF and excess thionyl chloride were removed by vacuum, and the resulting acid chloride was dissolved in DCM. Triethyl amine (4 eqv.) was then added, followed by the slow addition of the required amine (1 eqv.). The resulting mixture was stirred at room temperature for 16 hours and purified by flash column chromatography to afford the expected amides in 50.0 % to 40.0 % yields.

University of Ghana http://ugspace.ug.edu.gh

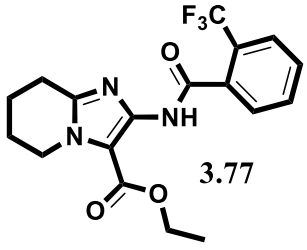
3.3.1.2.4.1 Preparation of ethyl 2-(3-(trifluoromethyl)benzamido)-5,6,7,8-tetrahydroimidazo[1,2-*a*]pyridine-5-carboxylate, 3.76.



3.76

Compound **3.76** was synthesised according to the general procedure for amide coupling (**3.3.1.2.4**), using 3-(trifluoromethyl)benzoic acid (0.45 g, 2.37 mmol) and **3.75** (0.30 g, 1.43 mmol). The product was obtained in 50.0 % yield as an oil. **^{1}H NMR** (500 MHz, $CDCl_3$) δ_H 9.69 (s, 1H**, H8**), 7.86 (s, 1H**, H18**), 7.78 (d, *J* = 7.8 Hz, 1H**, H14**), 7.44 (d, *J* = 7.8 Hz, 1H**, H16**), 7.28 (t, *J* = 7.8 Hz, 1H**, H15**), 4.02 (q, *J* = 7.1 Hz, 2H**, H10**), 3.86 (t, *J* = 6.1 Hz, 2H**, H4**), 2.62 (t, *J* = 6.4 Hz, 2H**, H1**), 1.65 (q, *J* = 6.0 Hz, 2H**, H3**), 1.56 (q, *J* = 5.8 Hz, 2H**, H2**), 1.02 (t, *J* = 7.1 Hz, 3H**, H11**). **^{13}C NMR** (126 MHz, $CDCl_3$) δ_C 162.09 (**C9**), 160.72 (**C12**), 147.83 (**C7**), 145.67 (**C5**), 135.16 (**C13**), 131.41, 131.15, 130.89, 130.63 (**C17**), 130.23 (**C14**), 129.16 (**C15**), 128.23 (**C16**), 124.18 (**C18**), 126.70, 124.53, 122.36, 120.20 (**C19**), 107.14 (**C6**), 60.49 (**C10**), 45.46 (**C4**), 24.85 (**C1**), 22.29 (**C3**), 19.37 (**C2**), 14.12 (**C11**).

3.3.1.2.4.2 **Preparation of** ethyl 2-(2-(trifluoromethyl)benzamido)-5,6,7,8-tetrahydroimidazo[1,2-a]pyridine-5-carboxylate, 3.77**.**



3.77

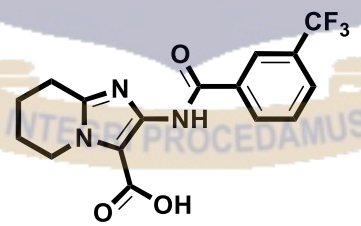
University of Ghana http://ugspace.ug.edu.gh

Compound **3.77** was synthesised according to the general procedure for amide coupling of (**3.3.1.2.4**), using 2-(trifluoromethyl)benzoic acid (0.45 g, 2.37 mmol) and **3.75** (0.30 g, 1.43 mmol). The product was obtained in 40.0 % yield as an oil. This intermediate was used directly in the subsequent reaction step without further characterization. Its formation was inferred from the successful synthesis and spectroscopic characterization of the product obtained in the following step.

3.3.1.2.5 General procedure for ester hydrolysis.

To a solution of the required ester (1 eqv.) in THF (15.0 mL)/H_2O (5.0 mL) was added 2M LiOH (10.0 mL). The mixture was stirred for 16 hours at room temperature, acidified to pH 4 with 1 M HCl, and extracted with chloroform (3 × 20 mL). The organic layer was washed with brine, dried over $MgSO_4$ and evaporated to afford the carboxylic acid in 55.0 % - 49.0 % yield.

3.3.1.2.5.1 Preparation of 2-(3-(trifluoromethyl)benzamido)-5,6,7,8-tetrahydroimidazo[1,2-*a*]pyridine-5-carboxylic acid, 3.78.

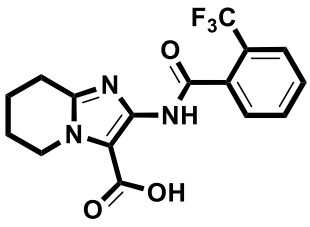


3.78

Compound **3.78** was synthesised according to the general procedure for ester hydrolysis (**3.3.1.2.5**) with **3.76** (0.15 g, 0.39 mmol), and obtained as a white solid in 49.0 % yield. This intermediate was used directly in the subsequent reaction step without further characterization. Its formation was inferred from the successful synthesis and spectroscopic characterization of the product obtained in the following step.

University of Ghana http://ugspace.ug.edu.gh

3.3.1.2.5.2 Preparation of 2-(2-(trifluoromethyl)benzamido)-5,6,7,8-tetrahydroimidazo[1,2-*a*]pyridine-5-carboxylic acid, 3.79.



3.79

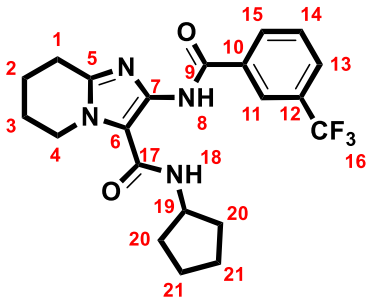
Compound **3.79** was synthesised according to the general procedure for ester hydrolysis with **3.77** (0.12 g, 0.32 mmol), and was obtained as a white solid in 55.0 % yield. This intermediate was used directly in the subsequent reaction step without further characterization. Its formation was inferred from the successful synthesis and spectroscopic characterization of the product obtained in the following step.

3.3.1.2.6 General procedure for amide coupling of carboxylic acids.

Et_3N (4 eqv.) and HATU (1.5 eqv.) were added to a solution of the carboxylic acid (1 eqv.) in DMF (5 mL). The mixture was stirred for 2 hours at room temperature, and the required amine (1.3 eqv.) was added. The reaction was stirred for 16 hours at room temperature, quenched with water, extracted with ethyl acetate, washed with brine, dried over $MgSO_4$ and purified with flash column chromatography. The desired analogues were obtained in 30-15 % yields.

University of Ghana http://ugspace.ug.edu.gh

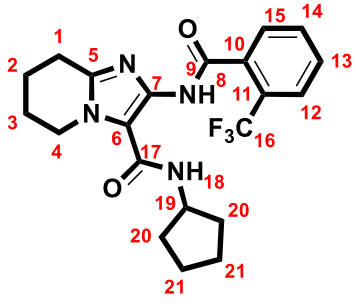
3.3.1.2.6.1 Preparation of *N*-cyclopentyl-2-(3-(trifluoromethyl)benzamido)-5,6,7,8-tetrahydroimidazo[1,2-*a*]pyridine-5-carboxamide, 3.80.



3.80

Compound **3.80** was synthesised according to the general procedure for amide coupling of carboxylic acids using **3.78** (0.06 g, 0.17 mmol, 1.0 eqv)), Et_3N (0.10 mL, 0.68 mmol, 4 eqv.), HATU (0.10 g, 0.26 mmol, 1.5 eqv.), and cyclopentylamine (0.02 mL, 0.20 mmol, 1.3 eqv.). It was obtained as a white solid in 15.0 % yield. **^{1}H NMR** (400 MHz, $CDCl_3$) δ_H 8.29 (s, 1H**, H11**), 8.24 (d, *J* = 7.9 Hz, 1H**, H15**), 7.99 (s, 1H**, H18**), 7.83 (d, *J* = 7.8 Hz, 1H**, H14**), 7.63 (t, *J* = 7.9 Hz, 1H**, H13**), 4.27 (t, *J* = 5.8 Hz, 2H**, H4**), 3.13 (dd, *J* = 7.4, 4.6 Hz, 1H**, H19**), 2.85 (t, *J* = 6.3 Hz, 2H**, H1**), 2.05 – 1.85 (m, 4H**, H3, H2**), 1.71 – 1.35 (m, 8H**, H20, H21**). . **LC-MS:** retention time: 2.301 min; **AJS-ESI** *(m/z)*: for $[C_{21}H_{23}F_3N_4O_2]^+$ $[M+H]^+$: exact mass calcd.: 421.18; found: 421.4. **FTIR** (cm^{-1}): υ(**N–H**) 3262, υ(**C-H**) 2956, 2864 υ(**C=O**) 1657, υ(**C=C**) 1627, δ(**N–H**), υ(**C-N**) 1538, υ(**C-N**), υ(**C-F**) 1271, 1121, γ(**C-H**) 702.

3.3.1.2.6.2 Preparation of *N*-cyclopentyl-2-(2-(trifluoromethyl)benzamido)-5,6,7,8-tetrahydroimidazo[1,2-*a*]pyridine-3-carboxamide, 3.81.



3.81

University of Ghana http://ugspace.ug.edu.gh

Compound **3.81** was synthesised according to the general procedure for amide coupling of carboxylic acids using **3.79** (0.07 g, 0.18 mmol, 1.0 eqv)), Et_3N (0.10 mL, 0.73 mmol, 4 eqv.) HATU (0.19 g, 0.51 mmol, 1.5 eqv.), and cyclopentylamine (0.02 mL, 0.73 mmol, 1.3 eqv.). It was obtained as a white solid in 30.0 % yield. **^{1}H NMR** (400 MHz, $CDCl_3$) δ_H 10.21 (s, 1H**, H8**), 8.10 (d, *J* = 7.0 Hz, 1H**, H15**), 7.75 (d, *J* = 7.5 Hz, 1H**, H12**), 7.64 (dt, *J* = 16.9, 8.0 Hz, 3H**, H13, H14, H18**), 4.25 (q, *J* = 6.9 Hz, 1H**, H19**), 4.19 (t, *J* = 6.0 Hz, 2H**, H4**), 2.53 (t, *J* = 6.4 Hz, 2H**, H1**), 2.06 – 1.86 (m, 4H**, H3, H2**), 1.86 – 1.41 (m, 8H**, H20, H21**). **^{13}C NMR** (101 MHz, $CDCl_3$) δ_C 169.25 (**C9**), 159.43 (**C17**), 144.83 (**C5**), 134.67 (**C7**), 132.21 (**C10**), 130.64 (**C13**), 128.79 (**C14**), 127.93, 127.61, 126.91 (**C11**), 126.86 (**C15**), 126.81, 125.01, 122.29 (**C16**), 119.72 (**C12**), 119.57 (**C6**), 51.53 (**C19**), 45.62 (**C4**), 32.78 (**C20**), 31.06 (**C1**), 24.09 (**C21**), 22.62 (**C3**), 19.72 (**C2**). **LC-MS:** retention time: 0.971 min; **AJS-ESI** *(m/z)*: for $[C_{21}H_{23}F_3N_4O_2]^+$ $[M+H]^+$: exact mass calcd.: 421.177; found: 421.2. **FTIR** (cm^{-1}): υ(**N–H**) 3330, 3253 υ(**C-H**) 2957, 2881 υ(**C=O**) 1652, δ(**N–H**), υ(**C-N**) 1547, υ(**C-N**) 1320, υ(**C-F**) 1174, 1130, γ(**C-H**) 771.

3.4 Physicochemical properties

The molecular weight (MW), partition coefficient between *n*-octanol and water (Log P), and Topological Polar Surface Area (TPSA), were calculated using Chemdraw Professional version 22.0.0.22 (PerkinElmer).

3.5 Anti-tubercular Activity

Anti-TB activities of the analogues were evaluated at the Holistic Drug Discovery and Development Laboratory in Cape Town, South Africa, using their validated in-house protocols. Compounds were incubated with *Mycobacterium Tuberculosis* (*Mtb*) in Middlebrook 7H9 media (Difco), supplemented with glucose, albumin-dextrose-catalase (ADC) or Casitone (Gibco Bacto), and either Tween 80 or Tyloxapol under the specified conditions. Test com-

University of Ghana http://ugspace.ug.edu.gh

pounds were prepared in 2-fold serial dilutions and incubated with bacterial cultures with Isoniazid and Moxifloxacin as reference drugs. Growth inhibition was assessed using the Microplate Alamar Blue Assay (MABA), and MIC values were calculated from fluorescence measurements, which served as an indicator of bacterial growth.

3.6 Antimalarial Activity of MMV676444.

3.6.1 Antimalarial Activity of MMV676444.

Antimalarial activities were evaluated in the same laboratory as anti-TB activities against the wild-type drug-sensitive strain, NF54 of *Plasmodium falciparum*. Parasites were cultured in human erythrocytes following the method described by Trager and Jensen (1976) [575]. The starting concentration of the test compounds was 10 µM, and they were then serially diluted 2-fold in the growth medium to generate a concentration range for IC_{50} determination. *In vitro* antiplasmodial activity was determined using the parasite lactate dehydrogenase assay, as described by Makler and Hinrichs (1993) [576], in which parasite growth was measured colourimetrically *via* the breakdown of a dye by the metabolic enzymes of the glycolytic pathway. Standard antimalarial drugs chloroquine and artesunate were included as controls. Survival was plotted against concentration, and the IC_{50} values were obtained using a non-linear dose-response curve fitting analysis. Compounds that did not achieve 50 % inhibition at the highest concentration tested (6 µM) are reported ashaving an $IC_{50} > 6$ µM.

3.6.2 Antimalarial Activities of MMV1794959 analogues.

Solubility assays were conducted at the department of Pharmacology, KNUST, using their defined standard procedures. Antimalarial screening on the other hand was carried out against drug-sensitive reference strain, 3D7 of *Plasmodium falciparum* at the Immunology Department of the Noguchi Memorial Institute for Medical Research. The compounds were pre-

University of Ghana http://ugspace.ug.edu.gh

pared in stock solutions of 10 µM in DMSO, then serially diluted (1:3) in the growth medium to generate 12 working concentrations (10 µM – 0.56 nm) for IC_{50} determination. *In vitro* antiplasmodial activity was determined *via* the SYBR Green 1 Assay, where parasite growth was determined through fluorescent intensities measured at a wavelength of 497 nm excitation and 530 nm emission. Standard antimalarial drug artesunate was used as control.

3.7 Solubility

Aqueous solubility of the synthesised analogues was determined at the H3D laboratory. Adapting the miniaturised shake-flask method described in Zhou et al., 2007 and Kerns & Di 2008 [577, 578], 4 µL of the compounds in 10 mM stock in DMSO was evaporated and incubated in Phosphate buffer, pH 7.4, at 25 ℃ for 24 hours, with continuous shaking until equilibrium was attained. Following a separation of undissolved solids, the concentrations of dissolved compounds were quantified using HPLC-DAD, and their Solubility determined from the corresponding calibration curve.

3.8 Leishmanicidal activity.

Leishmanicidal activity data for the analogues were obtained by the kind courtesy of Boyom's laboratory, situated at the Department of Biochemistry at the University of Yaounde, Cameroon. The assay was conducted against *Leishmania donovani* promastigotes, according to the method described in Siqueira-Neto et al., (2010) [579]. Compounds were incubated with parasites from an exponential-phase culture in complete medium, under standard conditions. Culture plates were read on a Magellan Infinite M200 fluorescence multi-well plate reader (Tecan) at an excitation and emission wavelength of 530 nm and 590 nm, respectively. Relative growth percentages were calculated in Microsoft Excel, and dose–response curves were constructed in GraphPad Prism-version 5.0 software, to determine IC_{50} values. IC_{50} values

University of Ghana http://ugspace.ug.edu.gh

were determined in duplicates, and the results are presented as mean ± standard deviation (**Table 4.7**). Standard antileishmanial drug Amphotericin B, was used as the control in the assay.



University of Ghana http://ugspace.ug.edu.gh

CHAPTER FOUR

4.0 Design, Synthesis, and Medicinal Chemistry Progression of MMV676444 Analogues for their Biological Activities.

4.1 Introduction

This chapter presents the outcomes of the synthetic work and biological evaluations of the scaffold MMV676444 (**Figure 4.1**; **4.1**) undertaken in this study.

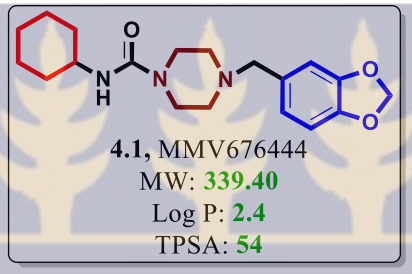


Figure 4.1: Chemical Structure of MMV676444.

4.1.1 Objectives.

The primary objective of this study was therefore to conduct a structure-activity relationship (SAR) study of the scaffold to identify an optimized lead. This was proposed to be achieved through:

- Re-synthesis of the hit compound
- Optimization through the design and synthesis of derivatives
- Profiling the compounds for their antimalarial, anti-TB and leishmanicidal activities.
- Evaluating promising analogues for *in vitro* DMPK properties.

4.1.2 Medicinal chemistry plan

The strategy for designing analogues of MMV676444 involved chemical modifications on the left and right portions of the scaffold, as indicated in **Figure 4.2**.

University of Ghana http://ugspace.ug.edu.gh

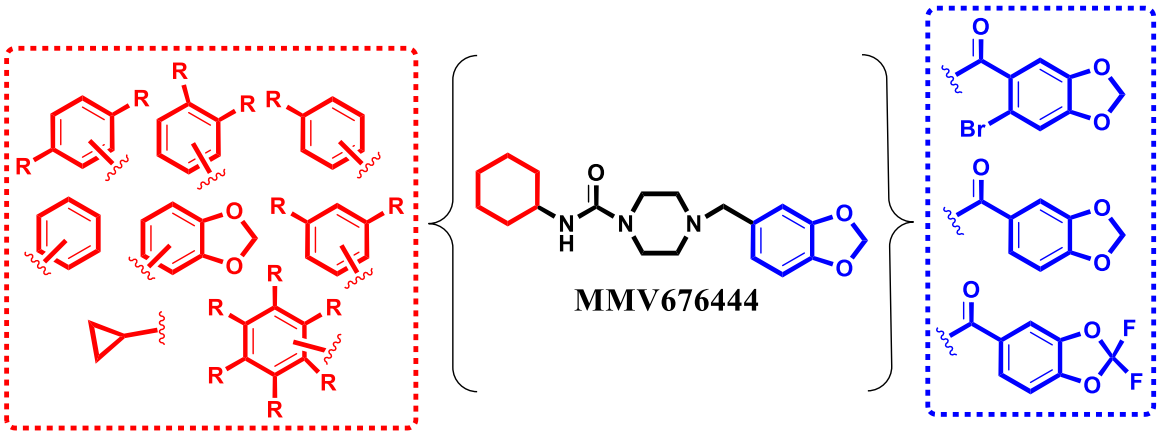


Figure 4.2: Medicinal chemistry plan for MMV676444 optimisation for the present study.

As demonstrated in earlier synthesised molecules (**Figure 4.1**), various phenyl groups with electron-donating (EDG) or electron-withdrawing groups (EWG) were substituted on the left-hand side of the molecule to investigate their contribution to biological activity. Additionally, an alternative cycloalkane was introduced to probe its functional significance for activity. Conversely, the benzo dioxole moiety on the right-hand side of the scaffold was maintained using piperonal, and alternating with two other commercially available conjugates of its derivative (**Figure 4.2**).

While the Bromo-substituted moiety was to ascertain if a substitution on the benzo dioxole had any effect on activity, a diflouro substitution on the methylene bridging the two oxygen atoms, alongside expanding the library for SAR evaluation, was introduced to block metabolic liability of the methylenedioxy group (prone to Phase 1 metabolism by cytochrome P450 enzymes leading to toxicity) [580-582].

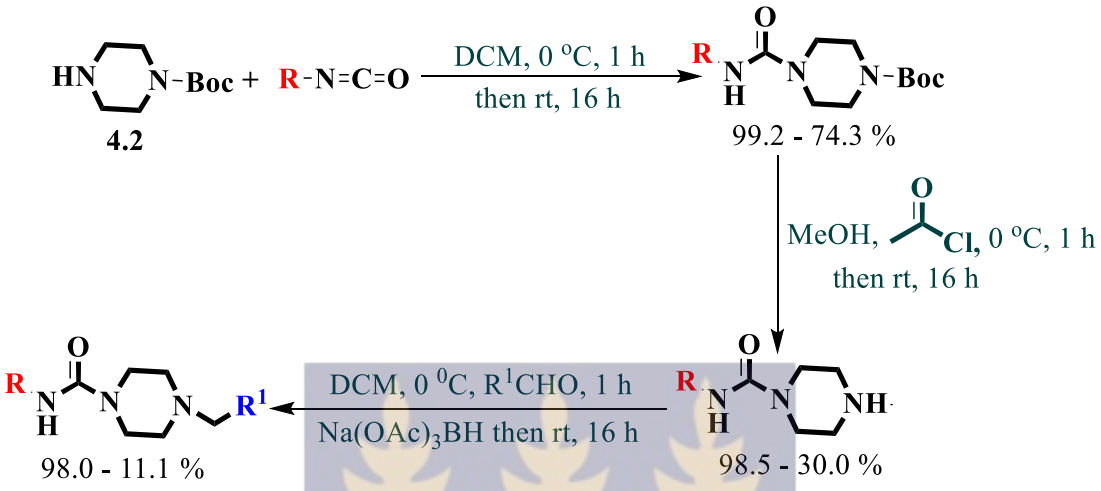
4.2 Results and Discussion

4.2.1 Chemistry

The target analogues were synthesised in 3 chemical steps (**Scheme 4.1**). First, a Boc-protected urea was formed from piperazine (**4.2**) and various commercially available isocya-

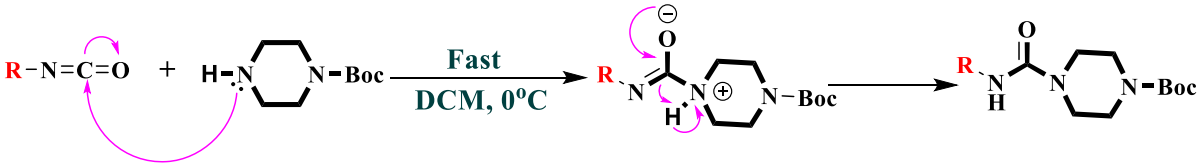
University of Ghana http://ugspace.ug.edu.gh

nates. The initiation of this reaction was driven by the nucleophilicity of the piperazine amine and the electrophilicity of the isocyanate carbon drove the initiation of this reaction.



Scheme 4.1: Synthetic route to target analogues of MMV676444.

An electrophilic attack on the isocyanate carbon by the free nitrogen of the Boc-protected urea, shifts the π electrons of the C=O bond towards oxygen, forming a carboxylate ion. The C=O bond then reforms, pushing the electrons back toward nitrogen. The electron-rich N, then deprotonates a nitronium ion from the piperazine ring, leading to the formation of urea (**Scheme 4.2**) [583]. Due to the very reactive nature of isocyanates [584], this step was conducted at low temperatures to avoid side reactions and possible decomposition of the inherently labile Boc protecting group.

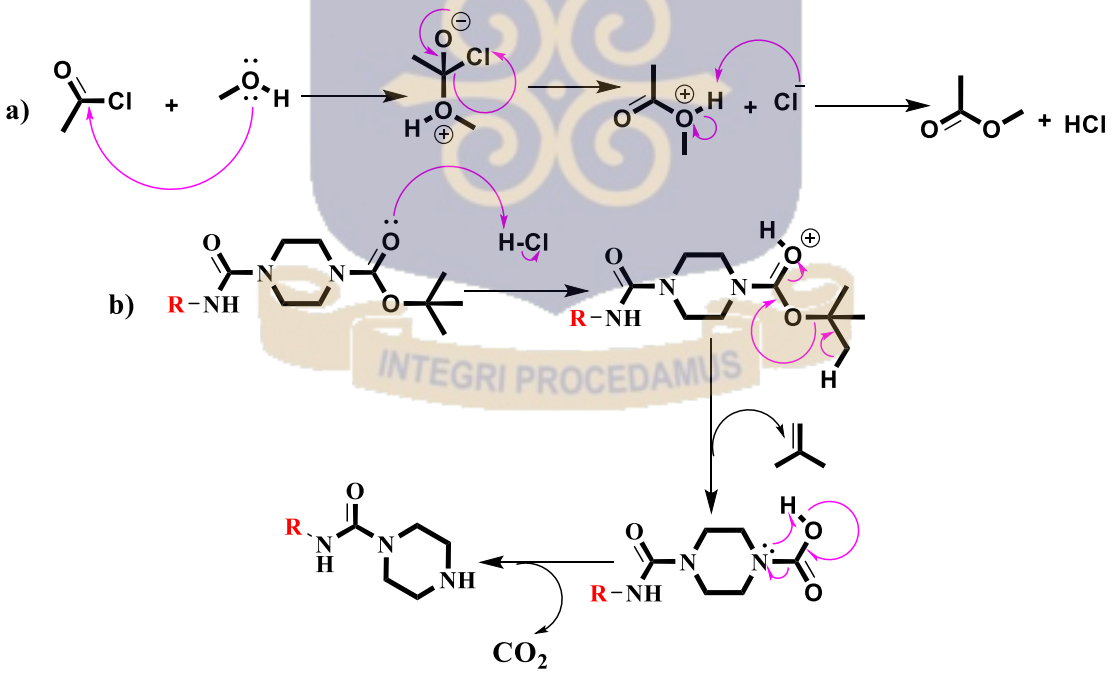


Scheme 4.2: Proposed mechanism towards Boc-protected urea formation.

Boc protection on the urea moiety was subsequently removed by an acidolytic cleavage, promoted by *in situ*-generated HCl from the reaction of methanol with acetyl chloride

University of Ghana http://ugspace.ug.edu.gh

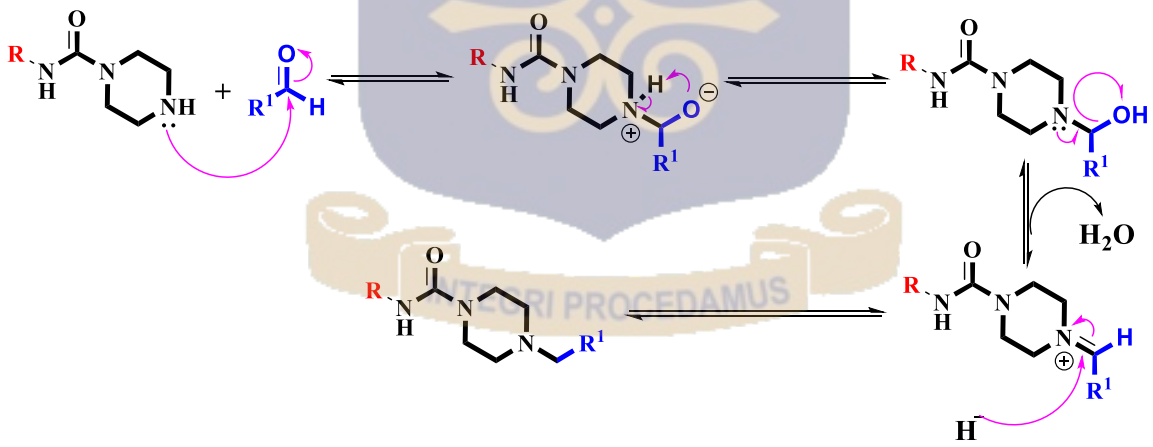
(**Scheme 4.3a**) [585, 586]. A protonation of the carbonyl oxygen of the Boc group by HCl makes the carbonyl carbon more electrophilic and susceptible to cleavage. This causes the tert-butyl group to break off as a carbocation (often accompanied by the release of volatile isobutene), forming a carbamic acid intermediate. A spontaneous decarboxylation subsequently leads to the free amine (**Scheme 4.3b**). However, the amine is rapidly converted to a salt as a result of protonation by HCl still present in the reaction mixture. To obtain the neutral amine, the reaction mixture is basified with sodium bicarbonate to neutralise the acid, then extracted and dried. It must be noted that the reaction between methanol and acetyl chloride is highly exothermic. The reaction was therefore conducted at low temperatures to control its rate, avoid decomposition of sensitive groups, and improve the overall yield of the products.



Scheme 4.3: Proposed mechanism for Boc deprotection. **a)** *In situ* generation of HCl from MeOH and AcCl. **b)** Formation of the de-protected piperazine moiety.

University of Ghana http://ugspace.ug.edu.gh

Following Boc deprotection, the piperazine moiety undergoes reductive amination with piperonal and its derivatives. The intrinsic nucleophilicity of the piperazine of the amine, in addition to the partial positive charge on the aldehyde carbon (due to the electronegativity of oxygen), drives the initiation of this step. A carbinolamine intermediate is first formed because of a nucleophilic attack on the carbonyl carbon of the aldehyde by the amine nitrogen, after which proton transfer facilitates the elimination of water, leading to the formation of an imine (**Scheme 4.4**). The addition of sodium triacetoxy borohydride (STAB) to the reaction mixture delivers a hydride to the electrophilic iminium C atom, converting the C=N bond to C-N, and forming a tertiary amine. Because imine formation is exothermic, the reaction was cooled in ice to control the rate (preventing over-reduction of the aldehyde to an alcohol), and ensure selective reduction of the iminium intermediate. Sodium triacetoxyborohydride (STAB) was preferred due to its mild reactivity and stability at low temperatures [587-589].



Scheme 4.4: Proposed mechanism for Reductive Amination.

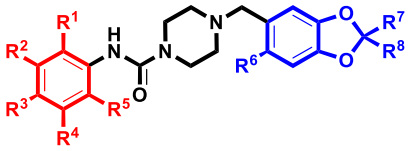
4.2.1.2 Synthesised Analogues

A total of thirty-six (36) analogues were synthesised (in 98.0-11.1 % yields) and characterised with ^{1}H and ^{13}C NMR spectrometry, LC-MS, and IR spectroscopy. For clarity of comparison, the analogues have been organized by their structural features. Compounds bearing phenyl and piperonyl moieties are presented in **Table 4.1**, while those lacking any of these

University of Ghana http://ugspace.ug.edu.gh

substituents are summarised in **Table 4.2**. The compound numbering used in the experimental section (**Chapter 3**) is maintained to facilitate easy comparison with the corresponding spectroscopic interpretation data.

Table 4.1: Synthesised Analogues with Phenyl and Piperonyl Substituents.



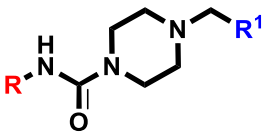
No.	Cmpd ID	R^1	R^2	R^3	R^4	R^5	R^6	R^7	R^8	Yield (%)
3.36	CFA015	H	H	CF_3	H	H	H	H	H	28.0
3.38	CFA208	H	H	Br	H	H	Br	H	H	27
3.39	CFA214	H	OCH_3	H	OCH_3	H	H	F	F	72
3.40	CFA099	H	OCH_3	H	OCH_3	H	H	H	H	45
3.41	CFA092	H	OCH_3	H	OCH_3	H	Br	H	H	33
3.43	CFA147	H	OCH_2	H	OCH_2	H	H	F	F	52
3.44	CFA189	H	OCH_2	H	OCH_2	H	Br	H	H	33
3.45	CFA140	H	OCH_2	H	OCH_2	H	H	H	H	46
3.46	CFA026	H	H	OCH_3	H	H	Br	H	H	37
3.47	CFA170	H	H	OCH_3	H	H	H	H	H	26
3.48	CFA196	H	CF_3	H	CF_3	H	Br	H	H	35
3.49	CFA117	F	F	F	F	F	Br	H	H	19

INTEGRI PROCEDAMUS

University of Ghana http://ugspace.ug.edu.gh

3.52	**CFA066**	**H**	**H**	**H**	**H**	**H**	**H**	**H**	**H**	94
3.53	**CFA067**	**H**	**H**	**H**	**H**	**H**	**Br**	**H**	**H**	78
3.54	**CFA068**	**H**	**H**	**H**	**H**	**H**	**H**	**F**	**F**	57
3.55	**CFA130**	**H**	**H**	**CH_3**	**H**	**H**	**H**	**H**	**H**	32
3.56	**CFA131**	**H**	**H**	**CH_3**	**H**	**H**	**Br**	**H**	**H**	12
3.57	**CFA134**	**H**	**CH_3**	**H**	**CH_3**	**H**	**Br**	**H**	**H**	15
3.61	**CFA014**	**H**	**F**	**H**	**H**	**H**	**H**	**H**	**H**	37
3.63	**CFA146**	**H**	**H**	**H**	**H**	**H**	**H**	**F**	**F**	72
3.67	**CFA127**	**F**	**H**	**F**	**H**	**H**	**H**	**H**	**H**	15
3.68	**CFA198**	**F**	**H**	**F**	**H**	**H**	**Br**	**H**	**H**	30
3.69	**CFA163**	**F**	**H**	**F**	**H**	**H**	**H**	**F**	**F**	38
3.70	**CFA176**	**H**	**F**	**H**	**F**	**H**	**H**	**H**	**H**	49
3.71	**CFA070**	**H**	**F**	**H**	**F**	**H**	**Br**	**H**	**H**	73

Table 4.2: Synthesised Analogues with non-phenyl or non-piperonyl substituents.



No.	**Compd. ID**	**R**	**R^1**	**Yield (%)**

University of Ghana http://ugspace.ug.edu.gh

3.60	**CFA016**	**4-fluorophenyl**	**4-(trifluoromethyl) phenyl**	34
3.37	**CFA017**	**4-(trifluoromethyl) phenyl**	**4-(trifluoromethyl) phenyl**	47
3.50	**CFA119**	**cyclopropyl**	**benzo[d][1,3]dioxol-5-yl**	36
3.51	**CFA121**	**cyclopropyl**	**2,2-difluoro-5-methylbenzo[d][1,3]dioxol-5-yl**	46
3.59	**CFA160**	**2,6-dichloro-4-methylpyridin-3-yl**	**2,2-difluoro-5-methylbenzo[d][1,3]dioxol-5-yl**	23
3.60	**CFA161**	**2,6-dichloro-4-methylpyridin-3-yl**	**benzo[d][1,3]dioxol-5-yl**	77
3.58	**CFA187**	**3,5-dimethyl phenyl**	**1,2-bis(difluoromethoxy)-4-methylphenyl**	22
3.64	**CFA209**	**1-ethyl-4-fluorobenzyl-**	**benzo[d][1,3]dioxol-5-yl**	96
3.66	**CFA210**	**1-ethyl-4-fluorobenzyl-**	**5-bromo-6-methylbenzo[d][1,3]dioxol-3-yl**	72
3.65	**CFA211**	**1-ethyl-4-fluorobenzyl-**	**2,2-difluoro-5-methylbenzo[d][1,3]dioxol-5-yl**	82
3.42	**CFA222**	**benzo[d][1,3]dioxol-5-yl**	**Phenyl**	51

4.2.2 Spectral Analysis

In the course of the synthetic work, not all intermediates were subjected to complete spectroscopic characterization. Some were directly advanced to the next synthetic step. Nevertheless, representative intermediates and all final analogues outlined in the experimental section (**Chapter 3.0**), were carefully analysed, thereby confirming key structural features and validating the overall synthetic route. For clarity, this discussion is centred on a representative analogue and its corresponding intermediate. Complete spectral data for all other synthesised analogues are included in Chapter 3.0.

University of Ghana http://ugspace.ug.edu.gh

4.2.2.1 NMR Spectroscopy

To illustrate the spectral features of the synthesised synthetic pathway, the NMR discussion begins with representative intermediate CFA005 (**3.2**), as its structure embodies key transformations common to other intermediates. A detailed discussion of its NMR data, as well as its subsequent intermediate leading to its final analogue, therefore, provides insight into the characteristic signals expected across the series. Signal assignments were rationalised based on electronic and steric influences of adjacent substituents, as well as documented observations from literature.

4.2.2.1.1 NMR spectrum of *tert*-butyl 4-((4-methoxyphenyl)carbamoyl)piperazine-1-carboxylate (CFA005), 3.2.

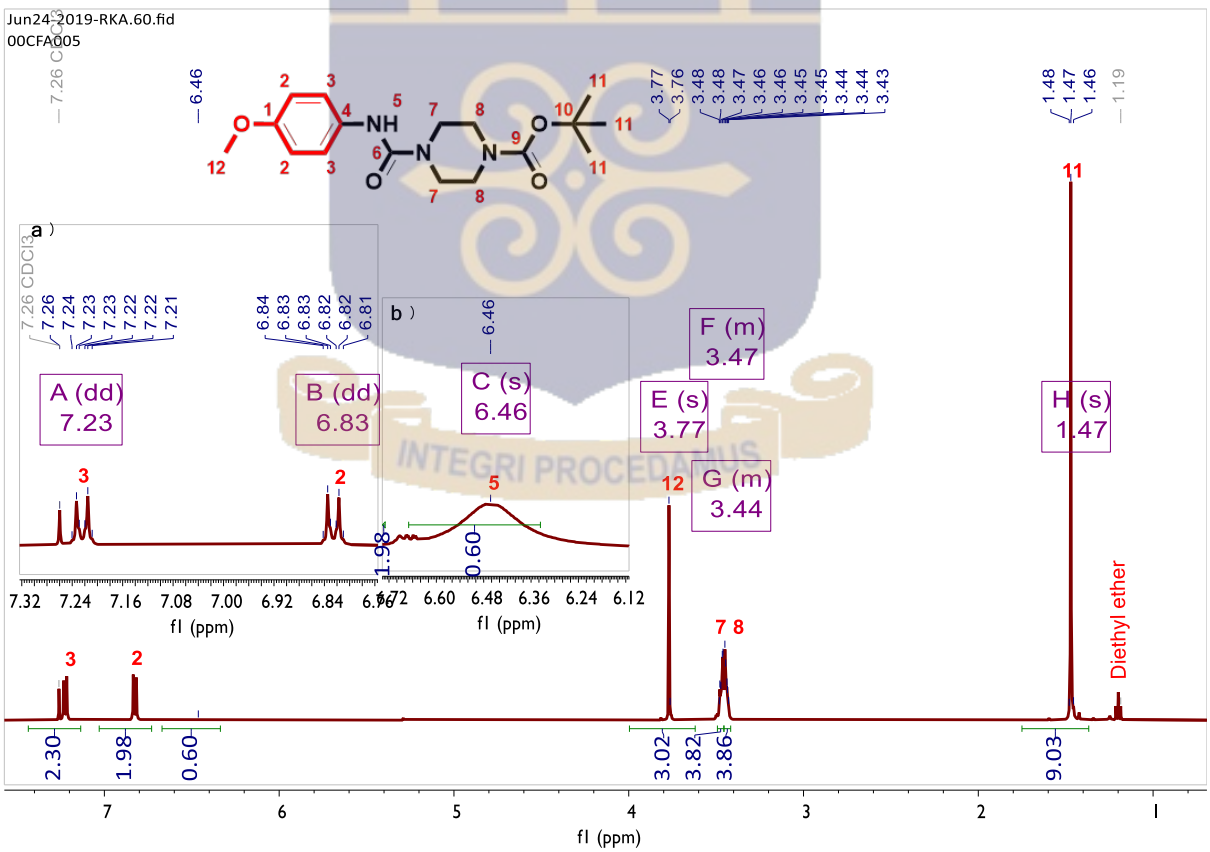


Figure 4.3: 1H NMR (500 MHz, CDCl3) of tert-butyl 4-((4-methoxyphenyl)carbamoyl)piperazine-1-carboxylate, **3.2**, showing an expansion of the aro-

University of Ghana http://ugspace.ug.edu.gh

matic region a) and an increase in spectral intensity to highlight the broadened peak of the amide proton b).

The ^{1}H NMR spectrum of CFA005 displayed characteristic signals consistent with the proposed structure. The aromatic region showed two sets of doublets of doublets (dd) at δ ~7.23 and δ ~6.83 ppm, corresponding to the phenyl protons (**Figure 4.3a**).

The phenyl methoxy moiety was confirmed in the aliphatic region as a singlet at δ ~3.77 ppm. Most importantly, all piperazine-1-carboxylate (Boc-protected piperazine) intermediates, exhibited a characteristic singlet around δ 1.47 ppm (integrating for 9 protons), confirming the presence of the tert-butyl moiety of the Boc protecting group. Additionally, methylene protons of the piperazine ring typically appeared around δ 3.50-2.68 ppm, integrating for 8 protons. These were observed as two closely spaced sets of triplets or multiplets (integrating for 4H each). This splitting behaviour arises from unsymmetric substituents on the nitrogen atoms of the ring (amide and carboxyl groups), disrupting the electronic environment of the ring protons and thus rendering the ethylene protons magnetically non-equivalent. In the spectra of other intermediates, these signals were observed as overlapping, appearing as a single broad resonance (integrating for 8 protons). The differences in how the signals appear could be attributed to the various substitutions at the amide moiety attached to the left-hand side of the substituted piperazine ring. These substitutions may exert subtle electronic influences on the magnetic environment of the piperazine protons [590, 591]. The signal corresponding to the amide proton ranged from δ 8.50 to 6.20 ppm across the intermediate spectra. This shiftin of observations can be attributed to rapid proton exchange with residual water and trace acids/bases in the deuterated solvent. The exchange also causes the amide peak to broaden or disappear as observed in some spectra (**Figure 4.3b**) [592, 593]. The unassigned

University of Ghana http://ugspace.ug.edu.gh

peak at δ 1.19 ppm was attributed to trace residual diethyl ether [594] which was used in the washing of the product to obtain a white solid.

^{13}C NMR spectrum further confirmed the structure with characteristic signals at δ 80.4 and 28.5 ppm, corresponding to the tert-butyl carbons of the Boc protecting group. The highly deshielded carbonyl carbons of the carboxylate and aromatic amide appeared at δ 154.8 and 155.7 ppm, respectively. Additional signals were recorded at δ 55.6 ppm, for the methoxy carbon as well as δ 156.3 and 131.8 ppm for the phenyl quatenary carbons, respectively. Other carbons of the aromatic moiety (ortho/meta carbons) showed signals at δ 122.8 and 114.3 ppm (**Figure 4.4**). While electronic differences between the amide-substituted and Boc-protected side of the ring were enough to separate protons, they may not have been strong enough to split the carbons into distinct peaks. Moreover, since both substitutions contain carbonyls, the resulting resonance donations could nearly equalize electron density across the piperazine carbons [595, 596]. Additionally, rapid chair-boat conformational exchange of piperazine rings may cause carbons in similar positions to appear equivalent (even with magnetically distinct protons) [591]. These could be possible reasons why the piperazine ring appears as a single peak at δ 44.0 ppm.

INTEGRI PROCEDAMUS

University of Ghana http://ugspace.ug.edu.gh

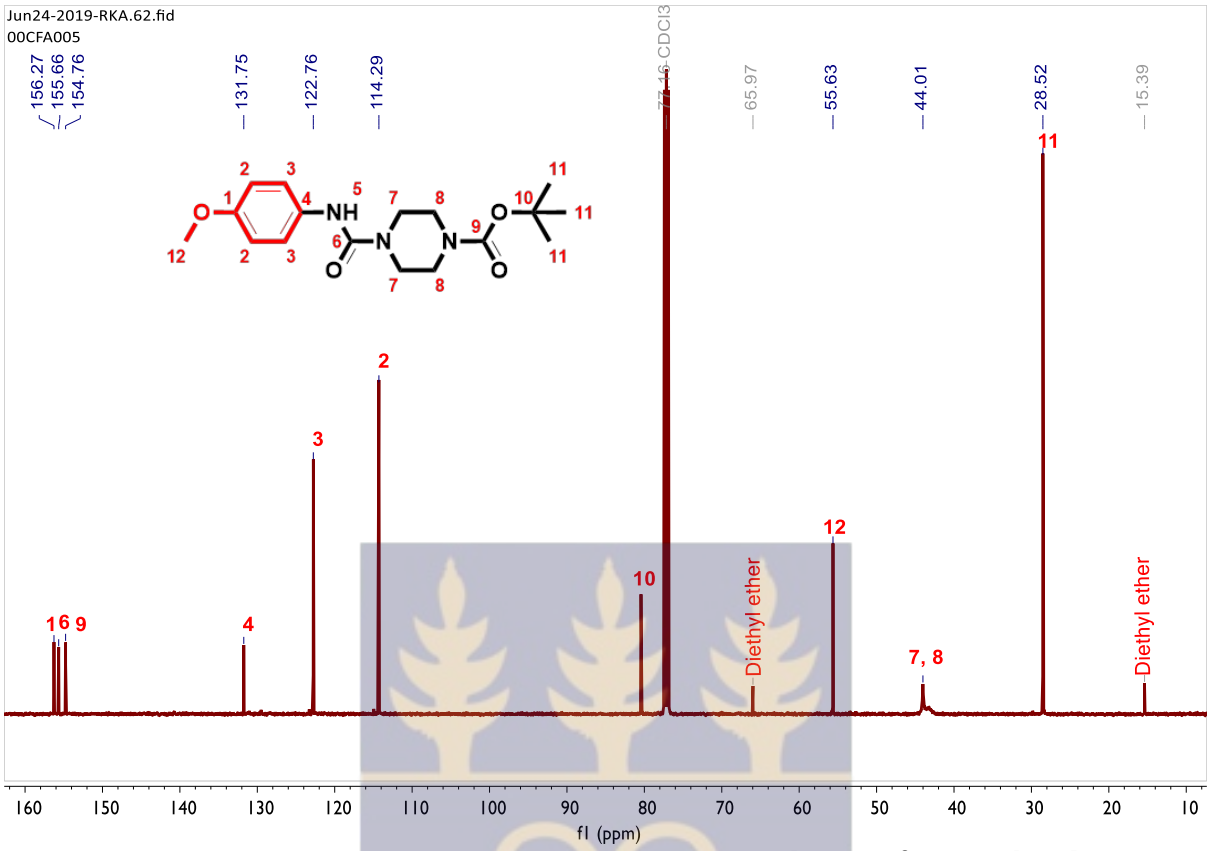


Figure 4.4: 13C NMR (126 MHz, CDCl3) of tert-butyl 4-((4-methoxyphenyl)carbamoyl)piperazine-1-carboxylate, **3.2**.

INTEGRI PROCEDAMUS

University of Ghana http://ugspace.ug.edu.gh

4.2.2.1.2 NMR spectrum of *N*-(4-methoxyphenyl)piperazine-1-carboxamide (CFA008), 3.19.

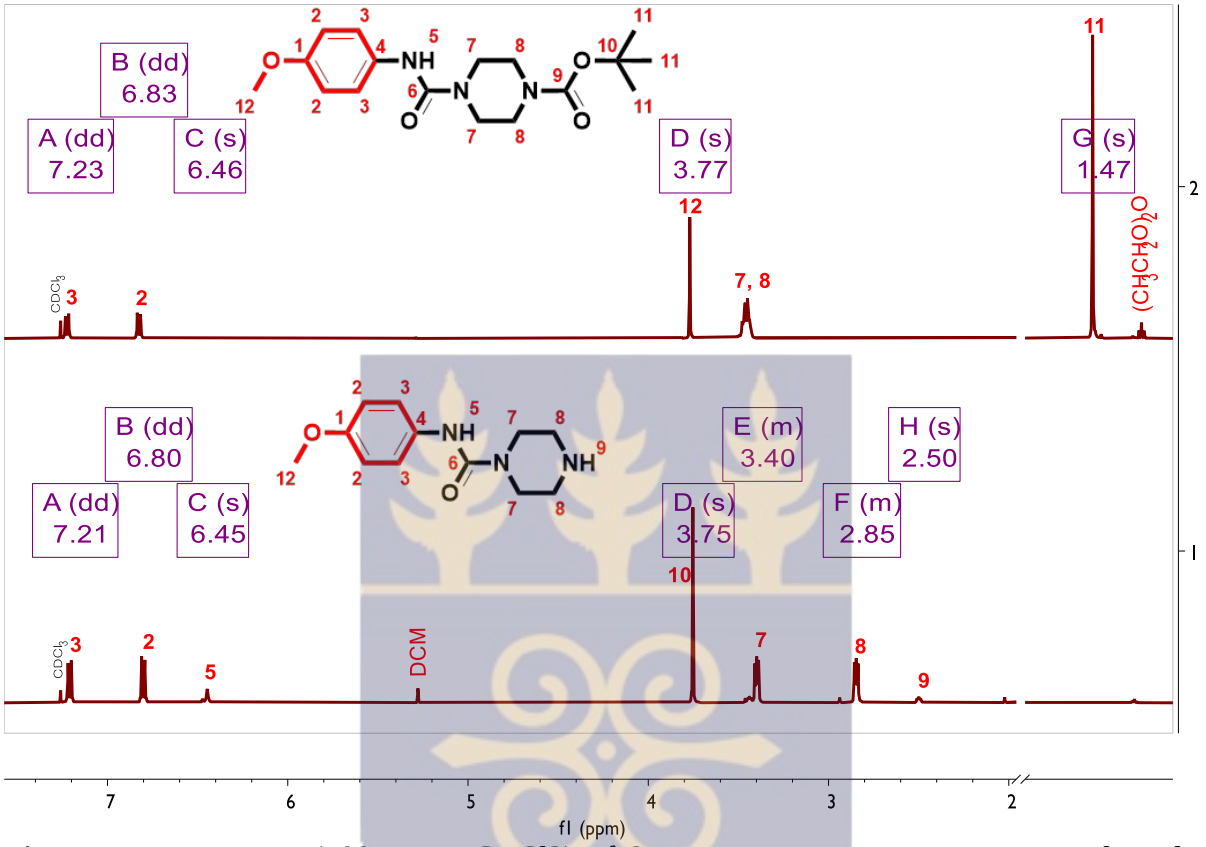


Figure 4.5: 1H NMR (500 MHz, CDCl3) of 3.1 in comparison to its corresponding de-protected analogue, **3.19**.

The disappearance of the carboxylate signal and the appearance of a triplet at δ ~2.50 ppm, corresponding to the piperazine amine, confirmed the formation of a urea intermediate from **3.2**. Due to the lesser deshielding effect of an amine (compared to a carboxylate) on the piperazine protons, more apparent distinction between the signals of the two sets of methylene protons (δ ~3.40 and ~2.85 ppm) is observed in this spectrum (**Figure 4.5**). ^{13}C NMR of **3.19** further validated the presence of a urea moiety with the absence of the tert-butyl and carbonyl carbons of the Boc-group (**Figure 4.6**). Trace residual Dichloromethane (DCM) used to purify the intermediate through column chromatography was observed at δ 5.3 ppm in the spec-

University of Ghana http://ugspace.ug.edu.gh

trum [594]. All final analogues were, however, thoroughly dried to remove residual solvents before biological testing.

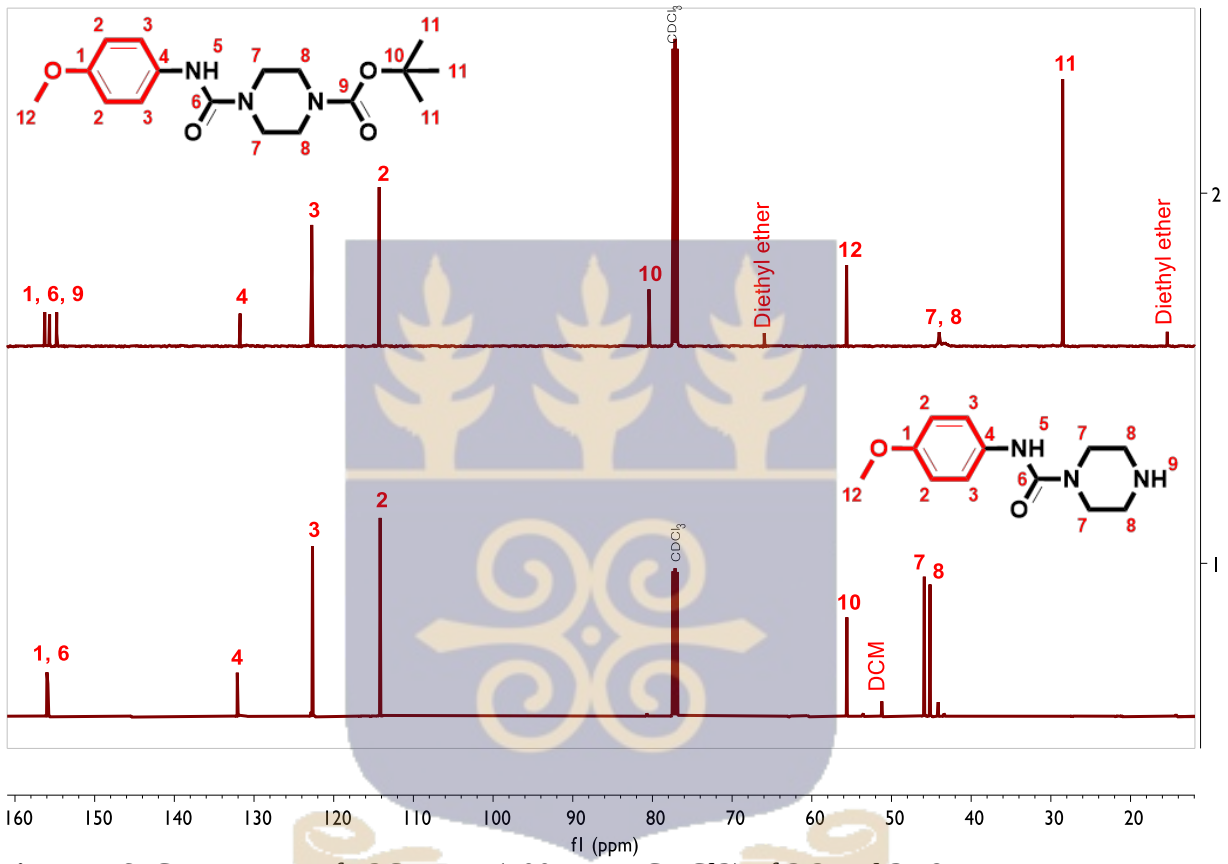


Figure 4.6: Comparison of 13C NMR (500 MHz, CDCl3) of **3.2** and **3.19**.

INTEGRI PROCEDAMUS

4.2.2.1.3 NMR spectrum of 4-((6-bromobenzo[*d*][1,3]dioxol-5-yl)methyl)-*N*-(4-methoxyphenyl)piperazine-1-carboxamide, (CFA026), 3.46.

Following the discussion of the NMR spectra on representative intermediate analogues, attention is now directed to the corresponding final analogue. Additional signals in the aromatic region (δ 6.83, 6.99, and 5.97 ppm) of the ^{1}H NMR spectrum (**Figure 4.7**) confirmed the presence of a benzodioxole moiety. The substitution of an additional aromatic group on the right-hand side of the molecule was anticipated to influence the local electronic environment of its adjacent piperazine methylene groups. Such substitution is known to induce anisotropic

University of Ghana http://ugspace.ug.edu.gh

and inductive effects, thereby demonstrating an interplay between inductive deshielding and resonance shielding, which could yield trends in ^{13}C NMR spectra, opposite to those observed in their respective ^{1}H NMR spectra [597, 598]. Heteronuclear correlation experiments are thus accurate for resonance assignment. The chemical shift patterns for the piperazine protons and carbons in this study were observed to align with well-established substituent effects reported in literature, where 2D techniques (HSQC and HMBC) were employed to confirm the CH_2 resonances unambiguously [599-601].

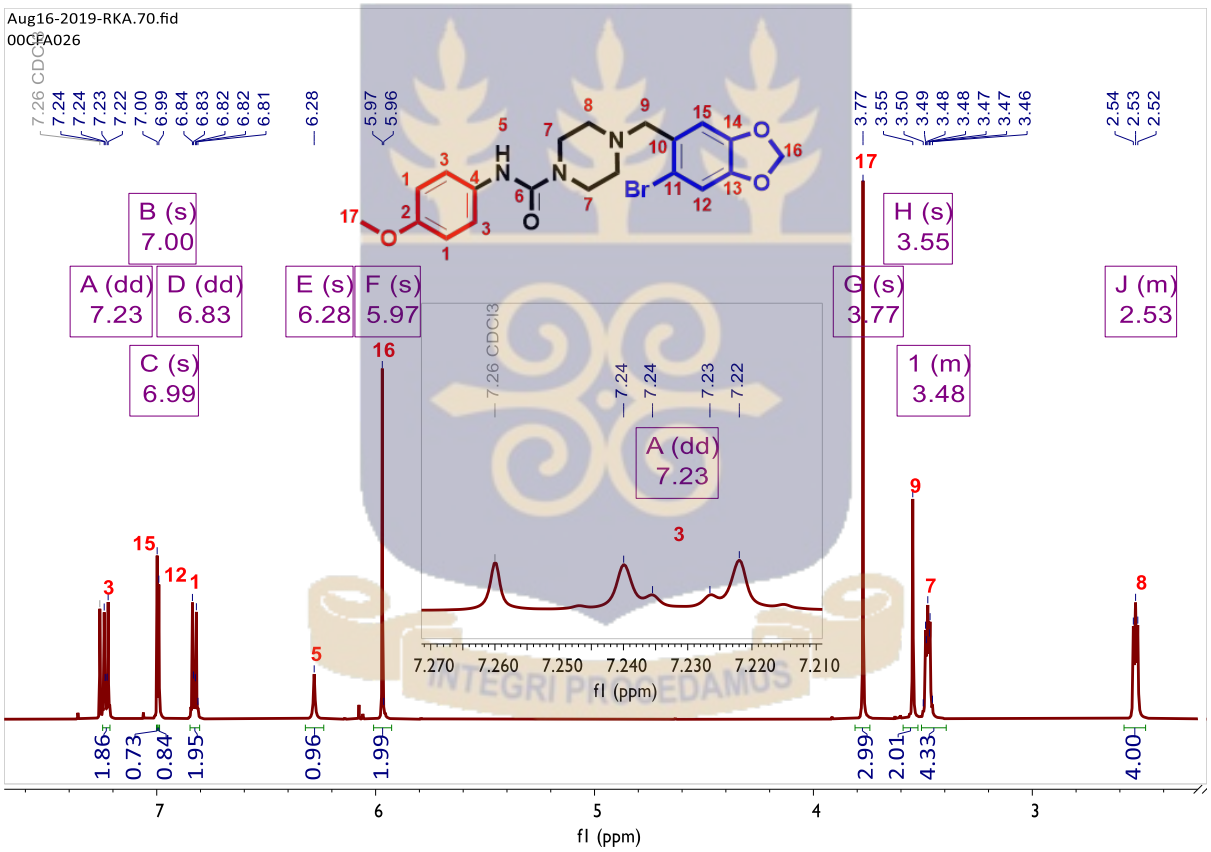


Figure 4.7: ^{1}H NMR of 4-((6-bromobenzo[*d*][1,3]dioxol-5-yl)methyl)-*N*-(4-methoxyphenyl)piperazine-1-carboxamide, CFA026.

The characteristic ^{13}C resonance at δ 101.8 ppm, corresponding to the methylene bridge of the benzodioxole moiety, alongside aromatic resonances at δ 112.8 and 110.5 ppm, further confirmed a successful reductive amination with 6-bromobenzo[1,3]dioxole-5-carbaldehyde (**Figure 4.8**).

University of Ghana http://ugspace.ug.edu.gh

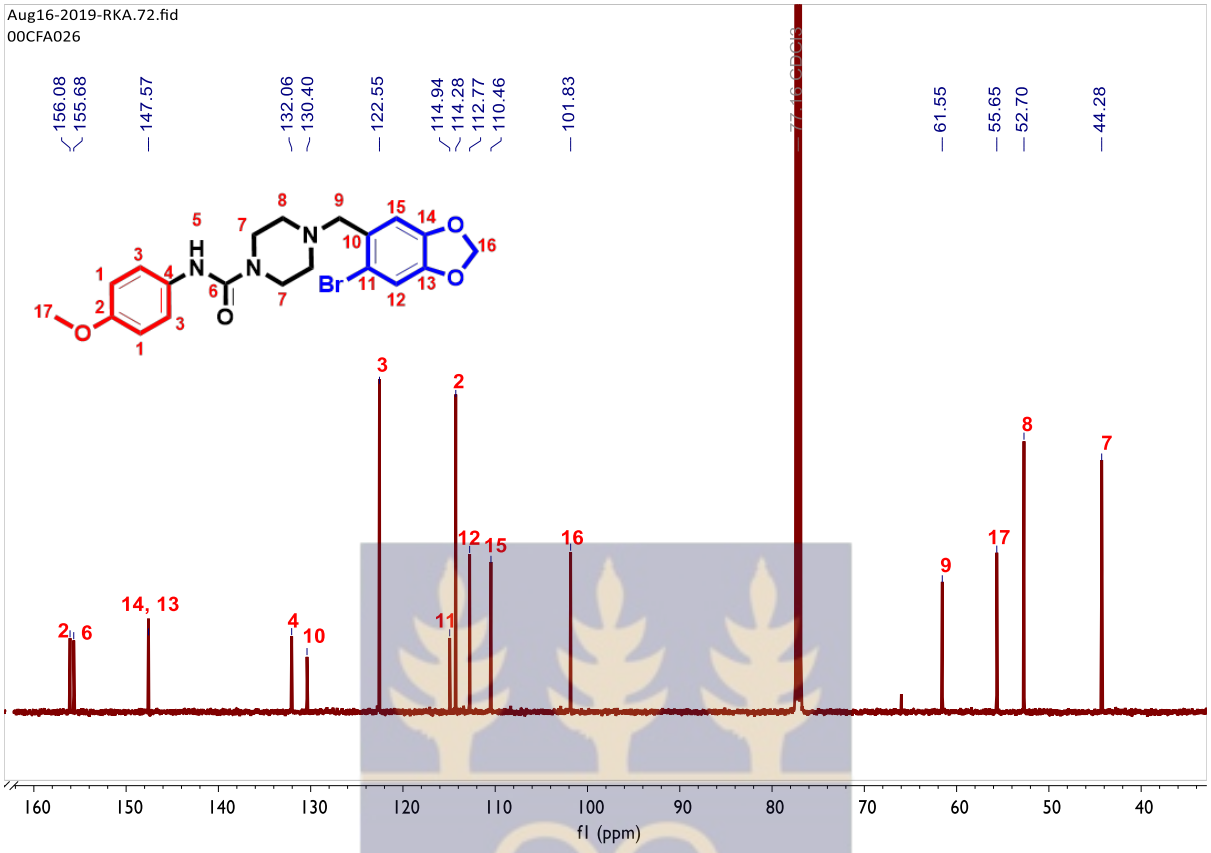


Figure 4.8: ^{13}C NMR of 4-((6-bromobenzo[*d*][1,3]dioxol-5-yl)methyl)-*N*-(4-methoxyphenyl)piperazine-1-carboxamide, CFA026.

4.2.2.2 LC-Mass Spectrometry.

LC-MS analysis of CFA026, showed a single, well-resolved peak across all four detectors (DAD1 A, DAD1 B, DAD1 C, MSD), with no evidence of additional or co-eluting compounds (**Figure 4.9**). This consistent observation confirmed the compound's purity. Furthermore, the mass spectrum of the analogue (**Figure 4.10**) exhibited a prominent molecular ion peak at *m/z* 448.0 $[M+H]^+$, in agreement with the calculated exact mass (448.08 Da). The characteristic M+H and M+2H isotope pair ($^{79}Br/^{81}Br$ with intensity ratio ~1:1), typical of Br-containing compounds, was, however, not observed. This could be attributed to data-processing/de-isotoping settings under the LC-MS acquisition parameters. However, High-

University of Ghana http://ugspace.ug.edu.gh

resolution MS (HRMS) performed for some of the analogues (e.g., in **Figure 4.11**) confirmed the brominated composition and the expected isotope distribution.

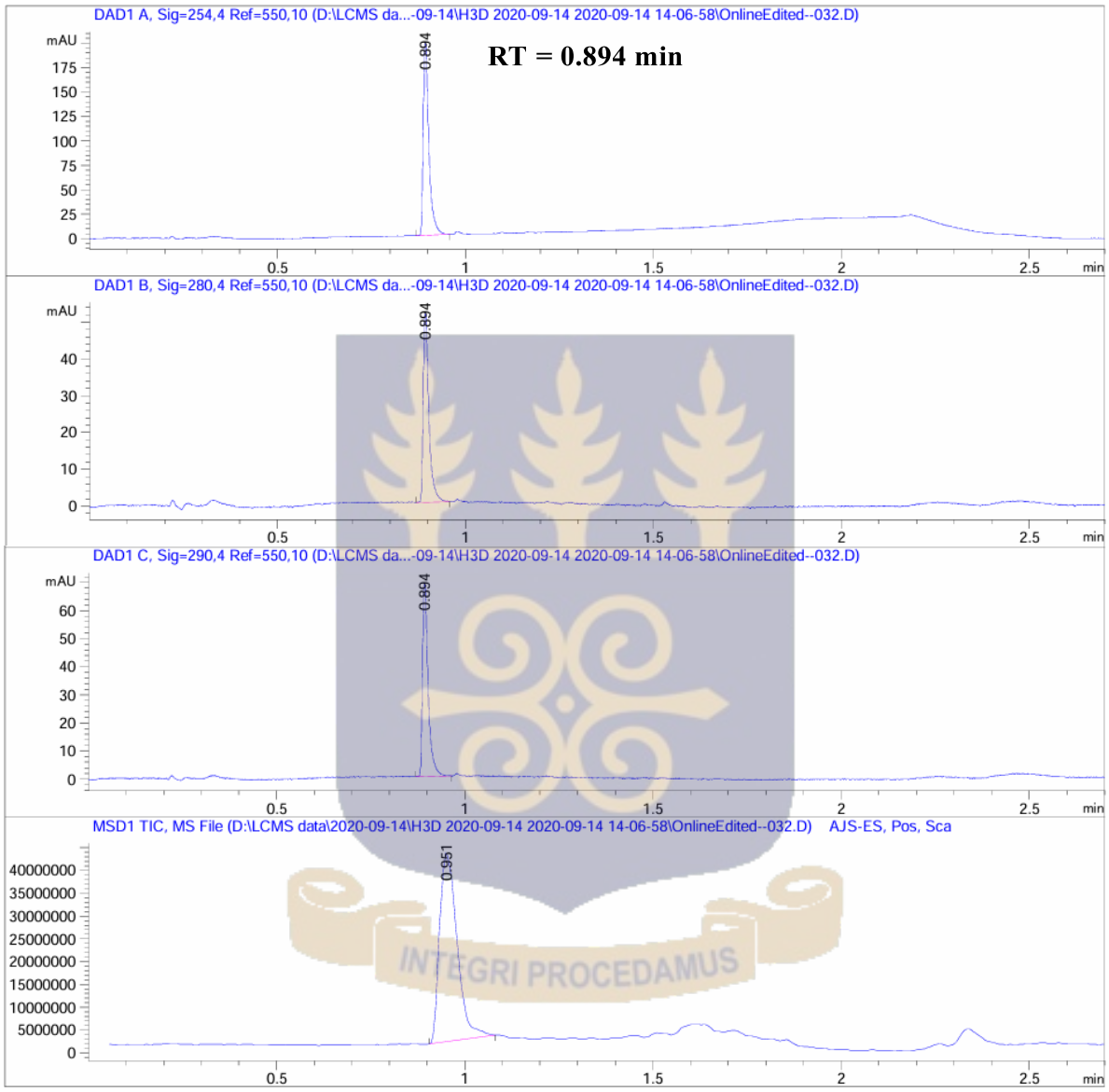


Figure 4.9: Liquid chromatography (LC) of CFA026, showing a single peak at retention time 0.894 min.

University of Ghana http://ugspace.ug.edu.gh

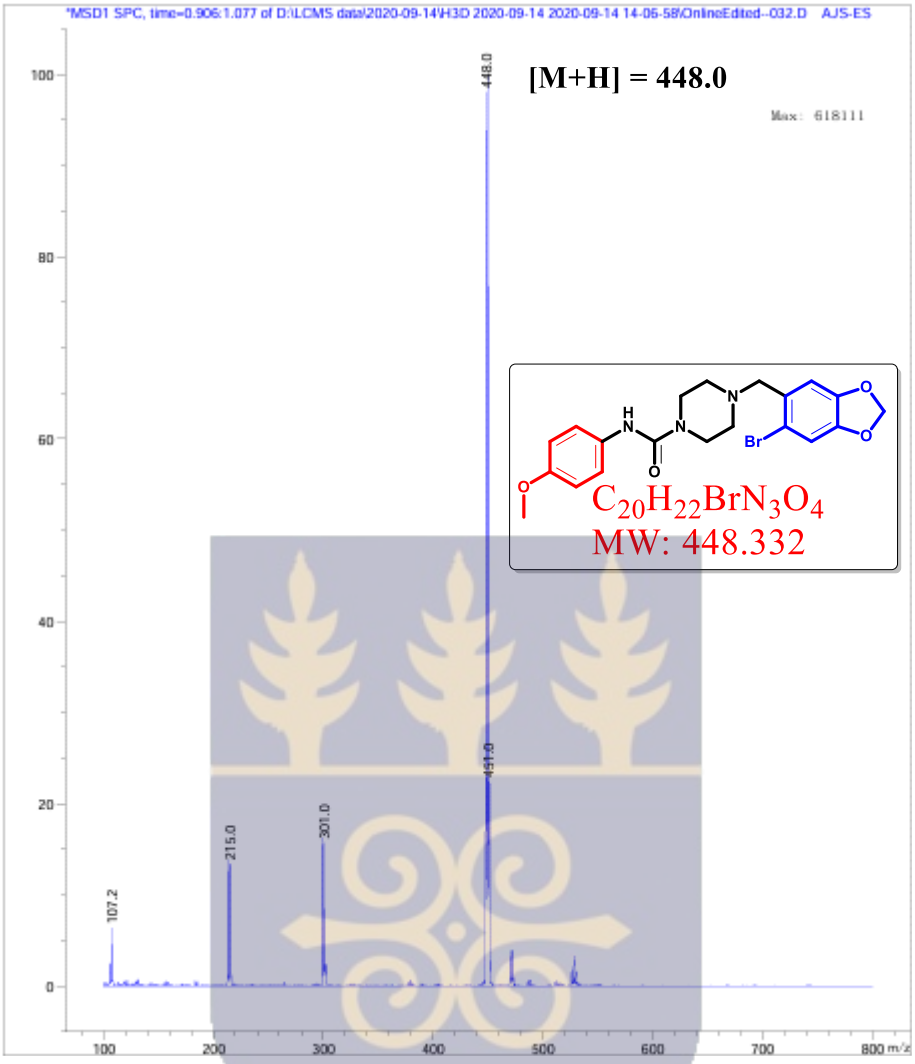


Figure 4.10: Mass spectrum of CFA026, confirming the molecular ion at m/z 448.0 $[M+H]^+$, consistent with the calculated exact molecular mass 448.08 Da.

University of Ghana http://ugspace.ug.edu.gh

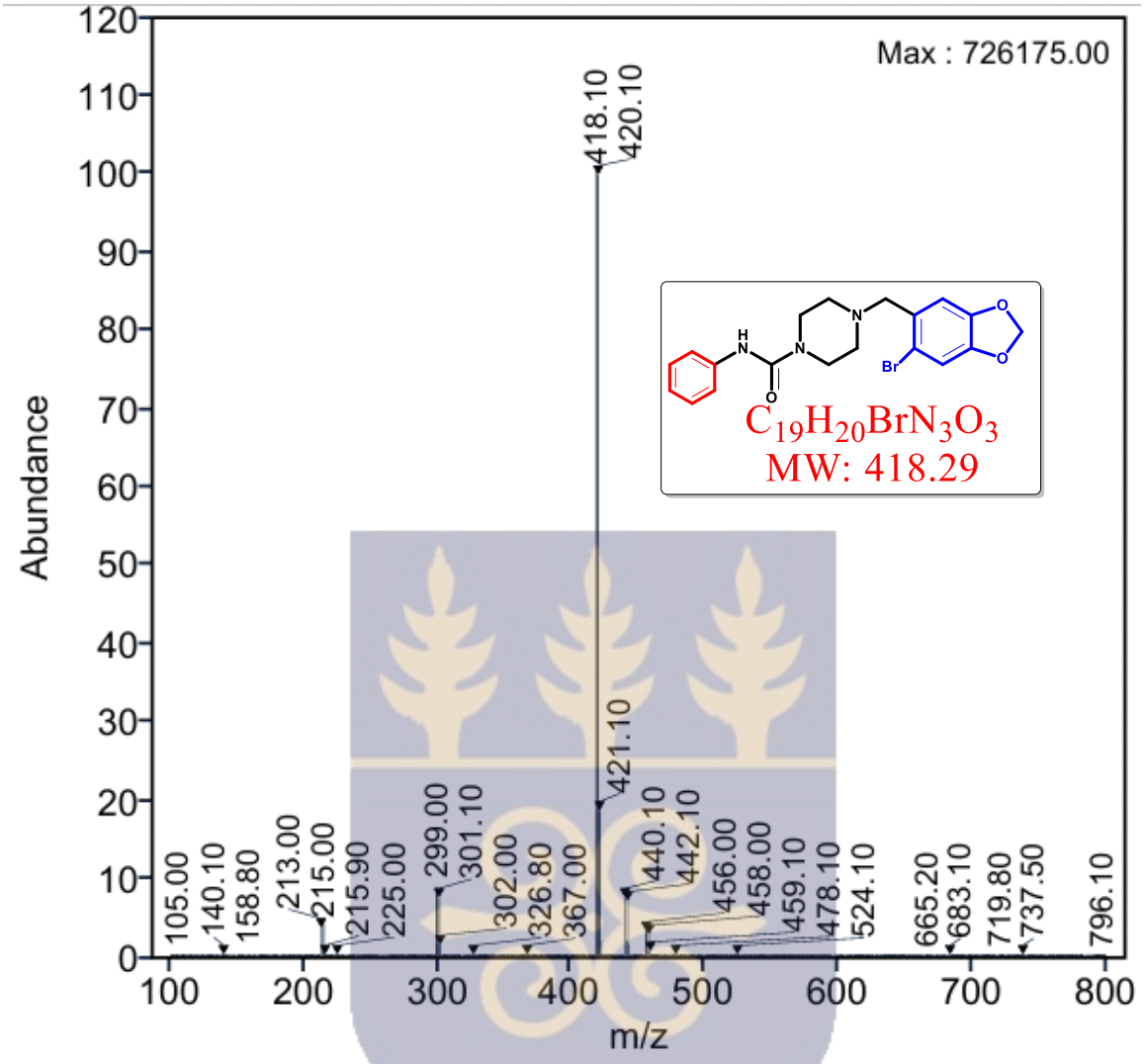


Figure 4.11: HR-MS of analogue, CFA067, showing expected isotopic distribution of Br.

4.2.2.3 Fourier-Transform Infrared (FT-IR) Spectroscopy

The IR spectrum of compound CFA026 (**Figure 4.12**) displayed a strong absorption at 3368 cm^{-1} and 1638 cm^{-1}, corresponding to the amide N-H and C=O stretches, respectively. Aliphatic C-H stretches were represented at 2910 cm^{-1} and 2827 cm^{-1}, while C-H bend absorbance was observed at 1475 cm^{-1}. Peaks at 1585 cm^{-1} and 1476 cm^{-1} correspond to aromatic C-H stretches, while the aromatic C-H out-of-plane band is represented by the absorption at 827 cm^{-1}. Other fingerprint peaks, 1241 cm^{-1} and 1003 cm^{-1}, were assigned to ether (=C-O and –C-O) stretches, confirming the presence of the benzodioxole group [602-604].

University of Ghana http://ugspace.ug.edu.gh

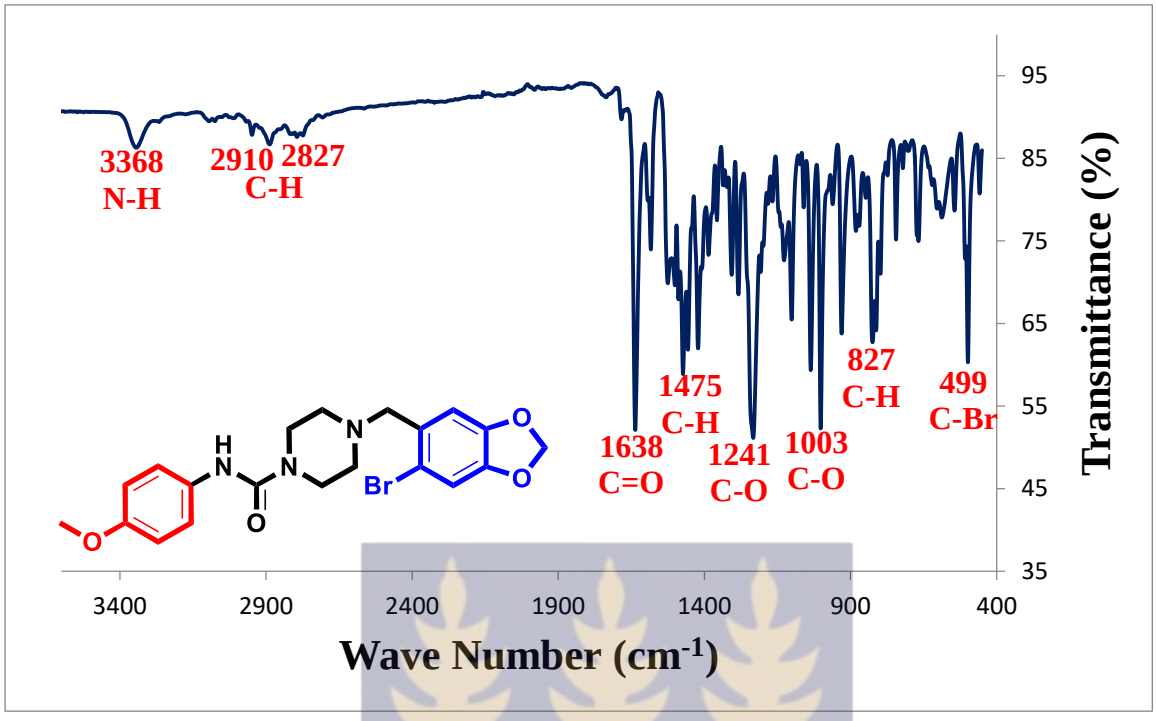


Figure 4.12: IR spectrum of **3.46** (CFA026).

Following structural confirmation, the physicochemical properties, solubility and biological activities of the analogues were assessed.

4.2.3 Physicochemical properties

Table 4.3: Physicochemical parameters of synthesised analogues.

No.	Cmpd ID	MW (Da)	Log P	TPSA (Å ²)
3.36	CFA015	407.39	3.3	54
3.38	CFA208	494.98	4.0	54
3.39	CFA214	435.43	3.5	73
3.40	CFA099	399.18	2.1	73

University of Ghana http://ugspace.ug.edu.gh

3.41	CFA092	435.43	3.5	73
3.43	CFA147	419.38	3.5	73
3.44	CFA189	461.08	3.0	73
3.45	CFA140	383.40	2.1	73
3.46	CFA026	448.32	3.1	63
3.47	CFA170	369.42	2.2	63
3.48	CFA196	554.29	5.0	54
3.49	CFA117	508.24	4.0	54
3.52	CFA066	339.40	2.4	54
3.53	CFA067	417.07	3.2	54
3.54	CFA068	375.38	3.8	54
3.55	CFA130	353.42	2.8	54
3.56	CFA131	432.32	3.7	54
3.57	CFA134	446.35	4.6	54
3.61	CFA014	357.39	2.5	54
3.63	CFA146	393.37	3.9	54
3.67	CFA127	375.14	2.7	54
3.68	CFA198	454.27	3.5	54

University of Ghana http://ugspace.ug.edu.gh

3.69	**CFA163**	**411.36**	**4.1**	**54**
3.70	**CFA176**	**435.28**	**3.3**	**54**
3.71	**CFA070**	**454.27**	**3.5**	**54**
3.60	**CFA016**	**381.37**	**3.7**	**36**
3.37	**CFA017**	**431.38**	**4.4**	**36**
3.50	**CFA119**	**303.36**	**1.0**	**54**
3.51	**CFA121**	**339.34**	**2.4**	**54**
3.59	**CFA160**	**445.25**	**4.2**	**66**
3.60	**CFA161**	**409.27**	**2.8**	**66**
3.58	**CFA187**	**455.45**	**4.71**	**54**
3.64	**CFA209**	**371.41**	**2.6**	**54**
3.66	**CFA210**	**450.31**	**3.4**	**54**
3.65	**CFA211**	**407.39**	**4.0**	**54**
3.42	**CFA222**	**339.40**	**2.4**	**54**

The synthesised analogues exhibit a range of physicochemical properties relevant to drug-likeness and biological evaluation (**Table 4.3**). While MW ranged from 303.36 to 554.29 Da, log P and TPSA values were within the ranges of 1.0 - 5.0 and 73 - 36 Å ², respectively. Though the two analogues that possess MW above 500.0 Da (**3.48** and **3.49**) may be challenged by reduced permeability (with further addition of functional groups as the chemistry progresses), their larger size could favour interactions with biological targets, potentially en-

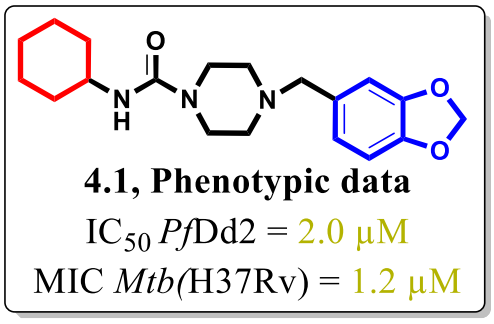
University of Ghana http://ugspace.ug.edu.gh

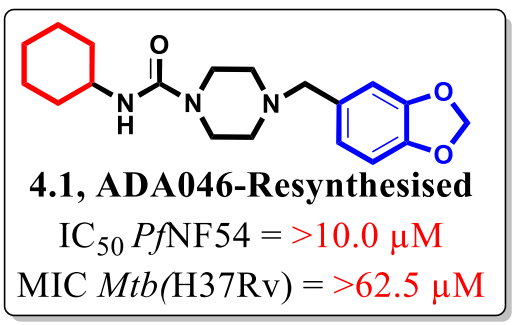
hancing activity [605]. Compounds with lower lipophilicities are likely to have higher aqueous solubility while those with higher LogP values, though potentially limited by solubility, may benefit from better membrane permeability [606, 607]. Despite a few analogues exceeding typical thresholds, TPSA values for all the analogues suggest moderate polarity and excellent absorption and permeability [608]. Overall, the values fall within acceptable ranges for drug-like molecules (MW ≤ 500.0 Da; logP ≤ 5.0; TPSA ≤ 140 Å ²), indicating that the analogues possess balanced lipophilicity, polarity, and size, suitable for biological evaluation and Structure-Activity-Relationship (SAR) studies [609].

4.2.4 Assessment of Biological Activities and Solubility of Synthesised Analogues.

4.2.4.1 Anti-tubercular Activity

Despite the reported promising anti-TB potential of the lead compound, all the analogues tested showed poor Anti-TB activities (**Appendix 4.1**). This suggests that structural modifications did not preserve or enhance activity. Evaluation of the resynthesised lead also showed minimal inhibition across all the media conditions (**Figure 4.13**). The discrepancy between the reported and observed activities of the lead scaffold may be attributed to several factors. These include variations in assay conditions, potential degradation that may produce active fragments not present in the resynthesised molecule, and the possibility that the phenotypic hit was a false positive [610, 611]. Therefore based on the results obtained, the scaffold does not possess promising potential against TB.





University of Ghana http://ugspace.ug.edu.gh

Figure 4.13: Comparison of biological activities of reported and resynthesized MMV676444.

4.2.4.2 Antimalarial Activity

Table 4.4: Antimalarial Activities and Solubility of Tested Analogues.

No.	Cmpd ID	IC_{50} *Pf*NF54 (µM)	Solubility, pH 7.4 (µM)
3.36	CFA015	>6.0	115
3.40	CFA099	>6.0	140
3.41	CFA092	0.01	20
3.43	CFA147	5.2	70
3.45	CFA140	>6.0	15
3.46	CFA026	>6.0	60
3.47	CFA170	>6.0	-
3.49	CFA117	>6.0	35
3.53	CFA067	>6.0	100
3.54	CFA068	>6.0	165
3.55	CFA130	>6.0	150
3.56	CFA131	5.8	20
3.57	CFA134	>6.0	25
3.61	CFA014	>6.0	-

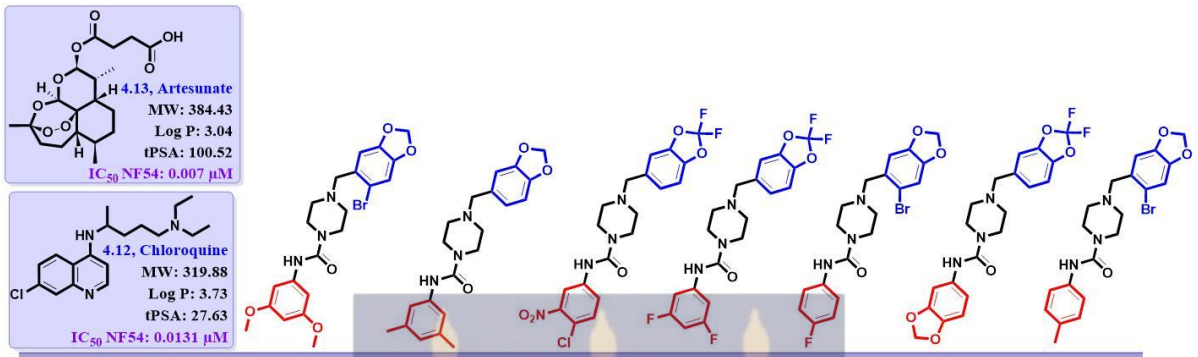
INTEGRI PROCEDAMUS

University of Ghana http://ugspace.ug.edu.gh

3.63	CFA146	>6.0	150
3.69	CFA163	>6.0	50
3.71	CFA070	>6.0	15
3.60	CFA016	>6.0	20
3.37	CFA017	>6.0	<5
3.50	CFA119	>6.0	175
3.51	CFA121	>6.0	180
3.59	CFA160	>6.0	10
3.60	CFA161	>6.0	35
3.58	CFA187	>6.0	5
4.3	CFA077	3.6	<5
4.4	CFA126	4.8	70
4.5	CFA133	1.2	45
4.6	CFA093	1.74	35
4.1	ADA046	>6.0	95.0
4.7	Chloroquine	0.01	-
4.8	Artesunate	0.01	-

University of Ghana http://ugspace.ug.edu.gh

Most of the synthesised analogues exhibited poor antimalarial activity (IC_{50} > 6 µM) (**Table 4.4**). 7 analogues demonstrated measurable inhibition below the 6 µM threshold, with compound (CFA092) being the most active (**Figure 4.14**).



Compound ID	CFA092	CFA133	CFA077	CFA093	CFA126	CFA147	CFA131
No.	3.41	4.5	4.3	4.6	4.4	3.43	3.56
MW (g/mol)	478.34	367.19	454.81	411.36	436.28	419.38	432.32
Log P	2.9	3.3	2.7	4.1	3.3	3.5	3.7
TPSA	73	54	106	54	54	73	54
Solubility (µM)	20	45	<5	35	70	70	20
IC_{50} NF54 (µM)	0.0118	1.2	3.6	4.8	4.8	5.2	5.8

Figure 4.14: Synthesised analogues of MMV676444 with promising antimalarial activity.

Focusing on the left-hand side of the molecule, while replacing the aliphatic cyclohexyl of the lead scaffold with a phenyl ring yielded no significant impact on activity, various substitutions on the aromatic ring resulted in measurable activity. This suggests that the unsubstituted phenyl moiety may not provide sufficient molecular features to achieve effective target interactions under the assay conditions. Substitutions on the ring may therefore have influenced the electronic distribution and conformation of the molecule to probably improve cellular exposure and stability [612, 613]. Notably, substitutions at the *meta* and *para* positions of the phenyl ring resulted in significant antimalarial activity. The absence of any *ortho*-substituted phenyl moiety amongst the most active analogues suggests that steric or electronic effects associated with *ortho* substitutions may be detrimental to activity. Since *ortho* substi-

University of Ghana http://ugspace.ug.edu.gh

tutions are proximal to the point of attachment, steric interference or conformational distortion could be responsible for this observation. On the other hand, *meta* and *para* substitutions most likely preserve planarity, causing less steric interference [614]. It was also observed that di-substituted analogues were generally more impactful on activity than mono-substitutions. The presence of two substituents likely enhances the electronic environment of the scaffold towards the activity threshold, while also restricting the rotation of the phenyl ring towards a favourable conformation for activity [615].

Generally, more analogues with Electron Withdrawing Groups (EWGs) appeared in the active subset. The analogue with nitro-substitution (CFA077), being the most active amongst them. 3,5-difluoro (CFA093) and 4-fluoro (CFA126) analogues displayed equal activity, while 2,4-difluoro analogues were poorly active, further highlighting the inverse relationship between ortho substitutions on the phenyl ring and antimalarial activity. It is established in literature that phenyl rings with EWGs have enhanced binding affinity in biological systems due to π-stacking interactions with electron-rich aromatic amino acids (eg. tryptophan, tyrosine), in the protein binding site [616, 617]. Given that the molecular target in this situation is unknown, the observation could be rationalised in terms of physicochemical effects particularly relating to lipophilicity. By pulling electron density away from adjacent polar groups, EWGs can weaken their ability to form hydrogen bonds with water, reducing their hydrophilicity. In this case, membrane permeability is enhanced, consequently increasing intracellular exposure and therefor influencing potency [618].

The most active antimalarial analogues CFA092 (0.012 µM) and CFA 133 (1.2 µM) however contained Electron Donating Group (EDG) substitutions on the phenyl ring. In this case, the EDGs may have enhanced hydrogen bonding beneficial for biological activity or increased polarity without compromising permeability [619]. Particularly at the 3,5- positions of the

University of Ghana http://ugspace.ug.edu.gh

phenyl ring, EDG substitutions were observed to markedly enhance potency. This provides some evidence that electron donating groups at the *meta* position could play a critical role in the activity of the molecule.

With analogues bearing similar substitutions displaying poor antimalarial activities, the role of the benzodioxo- substitutions on the right hand side of the molecule cannot be ignored. Though no clear pattern was observed, analogues with un-substituted benzodioxo- moieties generally showed no measurable activity in comparison to the other two moieties. As expected the Log P values of analogues bearing substitued benzodioxo- moieties were generally higher than unsubstituted benzodioxo- moieties. While the influence of Br substitution slightly increased lipophilicity, the presence of strongly electron withdrawing F atoms further increased the Log P values of the analogues. A significant presence of Br- and F- substituted benzodioxo- moieties in the active subset therefore further emphasizes the influence of EWGs on the overall lipophilicity of the compound, thereby impacting biological activity [619]. Interestingly analogue CFA133, though bearing an unsubstituted benzodioxo moiety displayed good activity (1.2 µM). Despite the absence of EWG substitutions on this analogue, its moderate lipophilicity (Log P = 3.3), could have influenced the observed activity. Additionally, as opposed the observation with substituted positions on the left-hand side of the molecule, CFA092 (containing an *ortho*-benzodioxo substitution) emerged the most active analogue with an impressive IC_{50} value of 12 nM. Undoubtedly, balanced contributions from both sides of the molecule influenced antimalarial activities of the analogues, with moderate lipophilicity identified as a pivotal factor necessary for superior potency.

It is also important to note that while the initial reported activity of the lead scaffold was against the drug-resistant strain Dd2, the re-synthesised hit and its analogues were tested against the drug-sensitive strain NF54 (**Figure 4.13**). This conforms to standard workflow

University of Ghana http://ugspace.ug.edu.gh

(baseline susceptibility), in biological screening assays. However, although it is uncommon for a compound to be active against resistant strains but less active against sensitive strains, testing the lead and analogues across various strains of *P. falciparum* could clarify if the observed activities are strain-specific or an actual scaffold property [620-622]. This will also enhance the scaffold's antimalarial potential and improve the reproducibility of the resulting data.

4.2.4.3 Solubility

Solubility at pH values corresponding to physiological plasma conditions which is crucial for assessing drug-likeness [623]. Though records of the solubility of synthesised analogues ranged from 180.0 µM to > 5.5 µM (**Table 4.5**), the solubility of analogues with measurable activity was generally poor. Of particular interest, the most active analogue to CFA092 exhibited low solubility (20.0 µM). This inverse correlation between activity, and solubility, therefore warrants that future work could modify lipophilic regions of the analogue to improve solubility without losing activity, as well as include solubility profiling across a range of physiologically relevant pH values to predict oral absorption better.

4.2.4.4 Metabolic Stability Studies

Given the promising activity of CFA092, preliminary metabolic stability studies in human, rat, and mouse liver microsomes were carried out to evaluate its profile as a lead compound and assess its potential for further optimization. As shown in **Table 4.5**, over 70 % of the compound remained across the tested species after the designated incubation periods, demonstrating favourable metabolic properties, stability and suitability for further optimization as a lead scaffold.

University of Ghana http://ugspace.ug.edu.gh

Table 4.5: Results of metabolic stability studies on CFA092 (**3.41**).

Species	% Remaining	Time (min)
Rat	**81.0**	98
Human	**76.0**	74
Mouse	**80.0**	91

4.2.4.5 Leishmanicidal activity.

To access the possibility of the scaffold's potential against another disease besides malaria and TB, a selected number of analogues were screened for leishmanicidal activity and returned interesting results (**Table 4.6**). Considering the inherent polypharmacological potential of scaffolds of phenotypic origin, this finding, while introducing an intriguing dimension to the study, was not unexpected.

Table 4.6: Leishmanial Activity of screened analogues.

No.	Cmpd ID	Mean IC_{50} ± SD (µM)
3.36	**CFA015**	**2.89 ± 1.17**
3.40	**CFA099**	**>10.0**
3.41	**CFA092**	**>10.0**
3.43	**CFA147**	**>10.0**
3.45	**CFA140**	**>10.0**
3.46	**CFA026**	**2.30 ± 0.01**

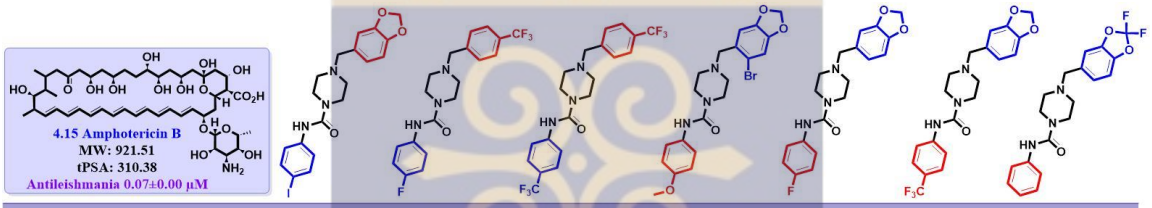
University of Ghana http://ugspace.ug.edu.gh

3.49	**CFA117**	**>10.0**
3.52	**CFA066**	**5.51 ± 1.00**
3.53	**CFA067**	**7.15 ± 0.06**
3.54	**CFA068**	**2.99 ± 1.11**
3.61	**CFA014**	**2.80 ± 0.88**
3.63	**CFA146**	**8.38 ± 0.47**
3.60	**CFA016**	**2.09 ± 0.22**
3.37	**CFA017**	**2.25 ± 0.18**
3.59	**CFA160**	**>10.0**
3.57	**CFA134**	**>10.0**
4.9	**CFA024**	**1.32 ± 0.22**
4.5	**CFA133**	**>10.0**
4.10	**Amphotericin B**	**0.07 ± 00**

The results provide preliminary cues about which structural motifs influence antileishmanial activity. Seven analogues within the active subset demonstrated low-micromolar potencies, with IC_{50} values ≤ 3 µM, and analogue CFA024 being the most active (**Figure 4.15**). A general trend observed among the active compounds suggest that, mono-substitution, specifically on the para position of the phenyl ring, on the left hand side of the molecule, was favourable for activity. Notably, EWG substitutions were favourable for activity with the three most potent analogues (CFA024, CFA016, CFA017) followed an increasing trend in electron-

University of Ghana http://ugspace.ug.edu.gh

withdrawing strength. Some studies have established a direct relationship between EWG aromatic substitutions and efficacy against *Leishmania* promastigotes [624, 625]. EWGs pull electron density away from the scaffold, making the molecule more electrophilic. Consequently, the electron-deficient centers of the molecule become susceptible to attack by nucleophilic groups (thiol groups in cysteine or amine groups in lysine) in the parasite's essential enzymes and proteins. This leads to irreversible binding and inhibition of the enzymes. Alternatively, electrophilic molecules drain the parasite's pool of protective nucleophiles (which are major components of a unique antioxidant defense system the parasite relies on for survival), making the promastigotes vulnerable to oxidative stress, subsequently leading to its death [626, 627].



Compound ID	CFA024	CFA016	CFA017	CFA026	CFA014	CFA015	CFA068
No.	4.9	3.60	3.37	3.46	3.61	3.36	3.54
MW (g/mol)	465.29	381.37	431.38	448.32	357.39	407.39	375.38
Log P	3.7	3.7	4.4	3.1	2.5	3.3	3.8
TPSA	54	35	35	63	54	54	54
Solubility (µM)	5	20	<5	60	-	115	165
Antileishmania Mean IC_{50} ± SD (µM)	1.32±0.22	2.09±0.22	2.25±0.18	2.30±0.01	2.80±0.88	2.89±1.17	2.99±1.11
IC_{50} NF54 (µM)	>6	>6	>6	>6	>6	>6	>6

Figure 4.15: Analogues of MMV676444 exhibiting the most potent antileishmanial activity.

On the right portion of the molecule, contributions of the substitutions remain unclear. Interestingly, analogues CFA016 and CFA017, lacking benzodioxo substitutions, displayed superior activity. A critical observation of both analogues, point out a significant presence of EWG substitutions on both sides of the molecule. With more F group substitutions on CFA017 than CFA016, the slight difference in IC_{50} values may have been influenced by the

University of Ghana http://ugspace.ug.edu.gh

difference in their lipophilicities. Again, comparing CFA016 to the most active analogue, CFA024, the modest (1.6-fold) increase in activity despite having same Log P values points back to the influence of EWG substitutions on antileishmanial activity. Factors such as off-target toxicity, reduced lipophilicity, and metabolic instability which affect potency are usually associated with the presence of an excessive number of EWGs [628, 629]. Given the limited number of analogues tested, these observations should be regarded as prelimnary and warrant further investigation through systematic screening of the entire series and rational optimization of the scaffold.

4.2.4.5.1 Selectivity studies on mammalian cell lines.

To assess the safety profile of the most active analogues, selectivity studies were conducted using 2 mammalian cell lines: macrophages (Raw 246.7) and African green monkey kidney epithelial cells (Vero). The compounds were evaluated for cytotoxicity, and the concentration required to reduce cell viability by 50 % (CC_{50}) was determined. The selectivity index (SI), calculated as the ratio of CC_{50} to the IC_{50} values of the analogues, returned encouraging results (>30) for both cell lines (**Table 4.7**). This implies that the active analogues are selective for *L. donovani*, have low mammalian toxicity, and are therefore generally safe. Considering the modest Log P values of the analogues are selective there is a clear positive correlation between lipophilicity and cytotoxicity.

University of Ghana http://ugspace.ug.edu.gh

Table 4.7: Selectivity data for most active analogues on mammalian cell lines.

No.	Compd. ID	CC_{50} (Raw 264.7)(µM)	CC_{50} (Vero cells)(µM)	Mean IC_{50} ± SD (µM)	SI (Raw 264.7)	SI (Vero cells)
4.14	CFA024	> 100	> 100	1.32 ± 0.22	>75.98	>75.98
3.60	CFA016	> 100	> 100	2.09 ± 0.22	>47.76	>47.76
3.37	CFA017	> 100	> 100	2.25 ± 0.18	>41.36	>41.36
3.46	CFA026	> 100	> 100	2.30 ± 0.01	>43.55	>43.55
3.61	CFA014	> 100	> 100	2.80 ± 0.88	>35.70	>35.70
3.36	CFA015	> 100	> 100	2.89 ± 1.17	>34.62	>34.62

4.3 Conclusion

In summary, a total of 36 analogues of MMV676444 were synthesised and charactized using ^{1}H and ^{13}C NMR, LC-MS and FTIR. The hit analogue was successfully re-synthesised but was poorly active against TB and malaria as opposed earlier reports. The analogues generally displayed minimal antitubercular activities against the H37rv strain of *Mtb*, while a few exhibited promising antimalarial potentials against NF54 of *P. falciparum*. The observed trend amongst the most active antimalarial analogues was that they possessed meta/para disubstituted phenyl rings on the left hand-side of the scaffold. The most potent analogues also exhibited low solubility (pH 7.4). CFA092 (**3.41**) emerged as the most active antimalarial analogue, displaying an IC_{50} value of 12 nM. Further studies on this analogue also proved that it was metabolically stable.

Some of the analogues were screened against *L. donovani*. Preliminary results suggest that the scaffold possesses inhibitory effects on *Leishmania* Promastigotes, thereby expanding its therapeutic relevance beyond malaria and tuberculosis.

Furthermore, none of the synthesised analogues exhibited dual activity, signifying selective potency. While this may limit immediate broad-spectrum applicability, the likelihood of off-

University of Ghana http://ugspace.ug.edu.gh

target effects and toxicity is largely minimized. This provides mechanistic clarity for further optimization and SAR studies, with a focus on improving potency and selectivity against the primary pathogen of interest.



University of Ghana http://ugspace.ug.edu.gh

CHAPTER FIVE

5.0 Design, Synthesis and Antimalarial Activities of analogues of MMV1794959.

5.1 Introduction

In this chapter, an account of the synthetic strategies and key transformations leading to analogues of MMV1794959 (**5.1**, **Figure 5.1**) and their biological data is provided.

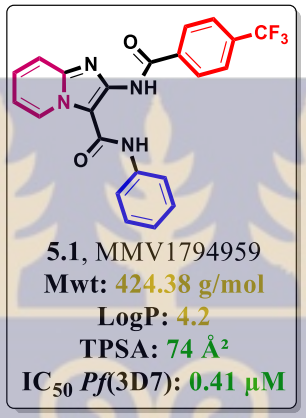


Figure 5.1: Molecular structure of MMV1794959.

5.1.1 Objectives.

The aim of this study was therefore to establish the minimal pharmacophore necessary for antimalarial activity. This was to be achieved through;

- Re-synthesis of the hit compound
- Optimization through the design and synthesis of derivatives
- Profiling the analogues for their antimalarial activities.

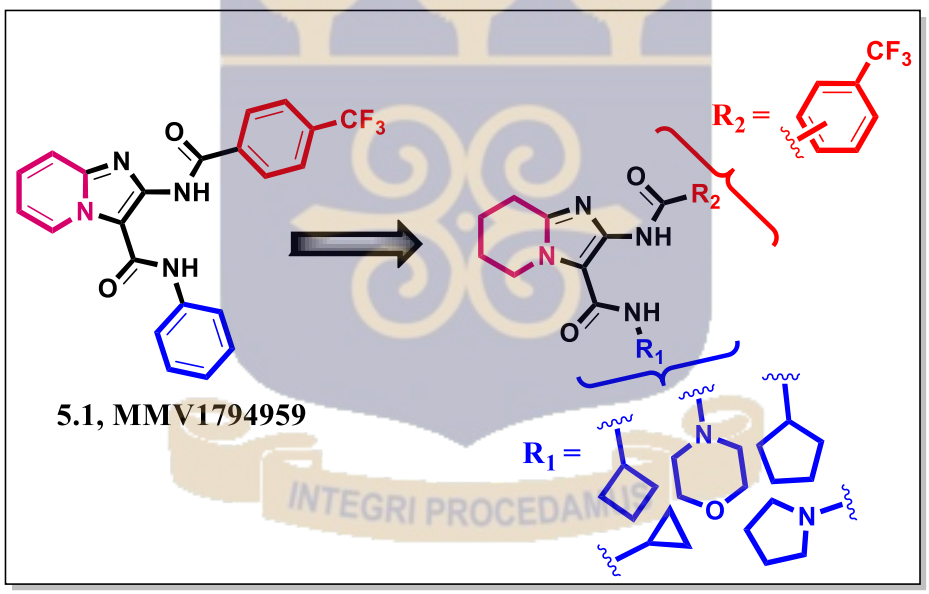
5.1.2 Medicinal Chemistry Plan.

With a substantial aromatic presence in the scaffold, likely contributing to its low solubility and consequent toxicity [630], the synthetic strategy involved the replacement of the aromatic rings with less rigid, non-planar moieties to reduce molecular flatness. Furthermore, to ascertain the essentiality of the pyridine core for activity, it was also necessary to maintain or in-

University of Ghana http://ugspace.ug.edu.gh

troduce substituted variants. Additionally polar/hydrophilic groups were rationally incorporated into the scaffold. These modifications were ultimately expected to increase the SI (Selectivity Index) window of the molecule, while providing optimal lipophilicity, and improving solubility [631].

With the trifluoromethylphenyl ring established to be critical for activity during hit validation, ortho, meta and para variations, with additional substitutions were made at the indicated positions of the scaffold in **Figure 5.2**. Furthermore, the aniline moiety of the molecule was targeted for substitution with various substituted and un-substituted aromatic and non-aromatic moieties, to build a library of analogues for a comprehensive SAR study.



University of Ghana http://ugspace.ug.edu.gh

Figure 5.2: Medicinal chemistry plan for MMV9794959 optimisation.

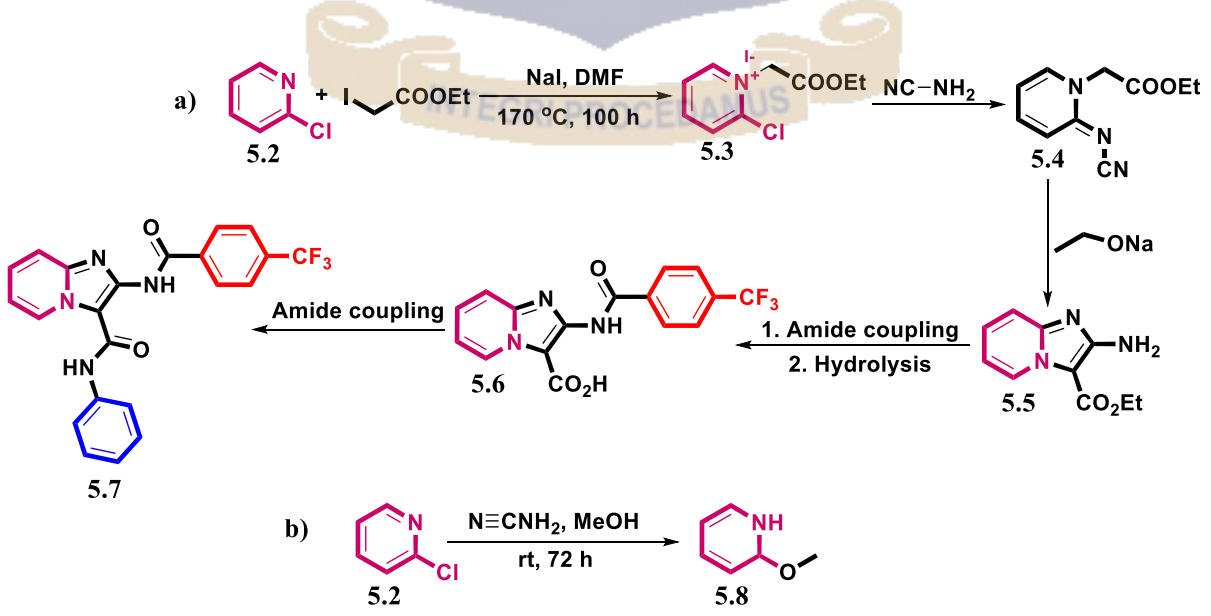
5.2 Results and Discussion

5.2.1 Chemistry

5.2.1.1 Re-synthesis of MMV9794959.

To validate initial screening results and reported biological activity, attempts were made to re-synthesise the hit compound. The route was through a previously reported procedure, outlined in **Scheme 5.1a.**

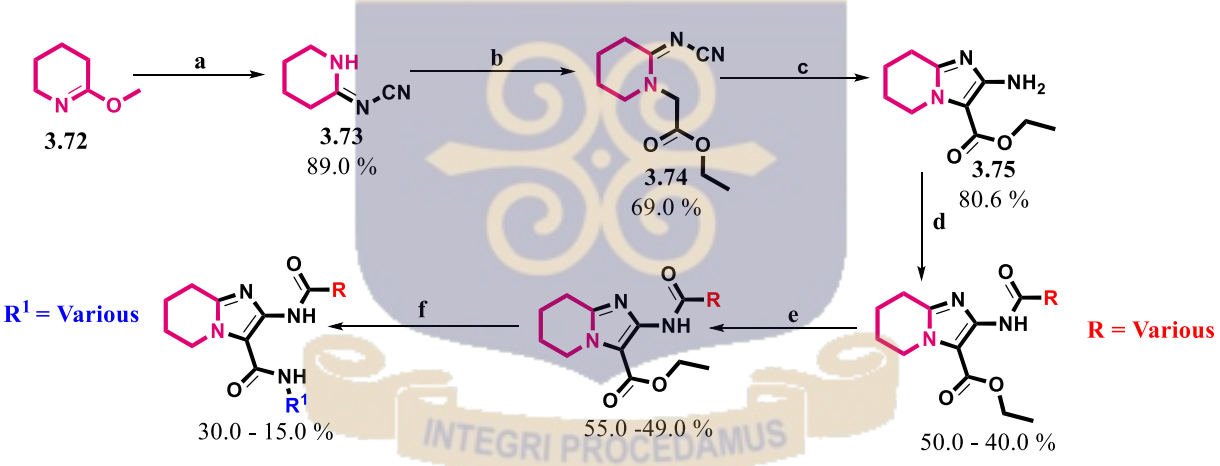
Considering the experimental conditions (170 ^{o}C for 100 h), for the first step, specialised settings (stainless-steel autoclave, sealed tube, microwave reactor tube, etc.) is required, but our laboratory is not equipped with those, hence an alternative procedure was adapted but it failed (a charred product was obtained). A second attempt at obtaining an aromatic core through a different route (**Scheme 5.1b**) did not yield any product. The re-synthesis of the hit molecule was therefore discontinued.



University of Ghana http://ugspace.ug.edu.gh

Scheme 5.1: **a**) Proposed Synthetic route to MMV9794959. **b**) Alternative synthetic approach to an aromatic core.

Attention was then shifted to the preparation of the intended analogues. The synthesis leading to analogues with a non-aromatic core was carried out in 7 chemical steps. First, the tetrahydroimidazo[1,2-a]pyridine core, **3.75**, was obtained from an initial formation of a piperidinylidene cyanamide, **3.73**, then, *N*-alkylation of **3.73** with ethyl chloroacetate, and a subsequent cyclisation under basic conditions (**Scheme 5.2**). This was followed by the installation of the trifluoromethylphenyl moiety through an amide coupling, from its corresponding acid chloride. Hydrolysis of the resulting amide ester, **3.75**, led to its conversion to a carboxylic acid which was coupled with various amines to afford the final analogues.



Scheme 5.2: Synthetic route leading to analogues of MMV1794959. **a**) MeOH, cyanamide, rt, 72 h **b**) CH_3CN, K_2CO_3, ethyl chloroacetate, 85 ^oC, then, reflux 22 h. **c**) EtOH, Na ethoxide, 85 ^oC, then, reflux 30 min. **d**) i) DCM, $SOCl_2$, trifluoromethyl benzoic acid ii) Et_3N, rt, 16 h. **e**) THF/H_2O, LiOH, 16 h. **f**) DMF, HATU, Et_3N, 16 hr.

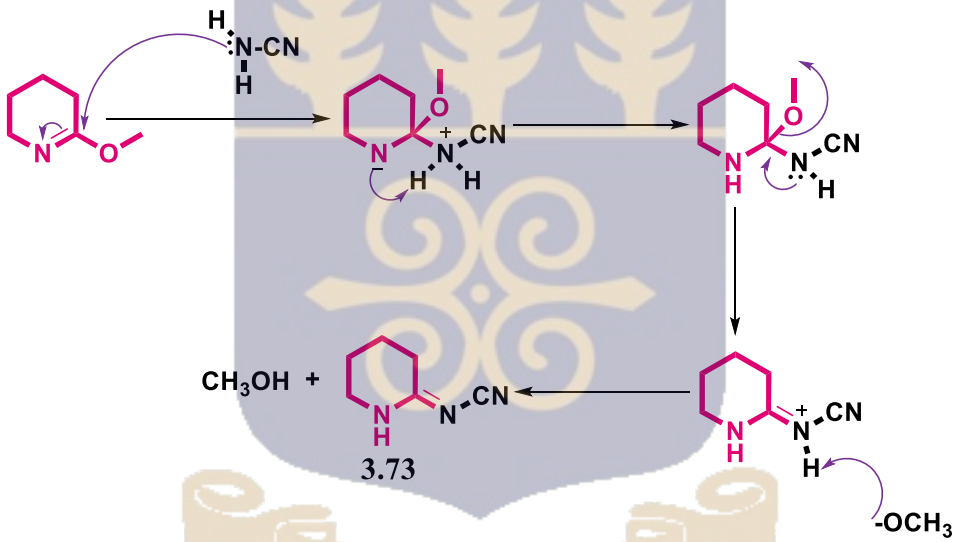
5.2.1.2 Formation of piperidinylidene cyanamide.

The piperidinylidene cyanamide, **3.73** was formed through an addition-elimination mechanism [632]. The reaction was initiated *via* the inherent electrophilicity of the carbon bearing the methoxy substituent, which is susceptible to a nucleophilic attack by the nucleophilic ni-

University of Ghana http://ugspace.ug.edu.gh

trogen of cyanamide. This led to the formation of a tetrahedral intermediate, followed by an intramolecular proton transfer, and consequent C=N bond formation, resulting in the loss of the methoxy group as methonol, yielding the desired product (**Scheme 5.3)**.

Cynamide was added slowly to allow for an optimal concentration in the reaction mixture, providing enough time for the intermediate to eliminate methanol and form the desired product. After a few minutes of its addition, a white precipitate (indicating the formation of the product) was observed. Notwithstanding, the reaction mixture was allowed to stir for an extended period (72 h), to ensure full conversion at the electrophilic cite.

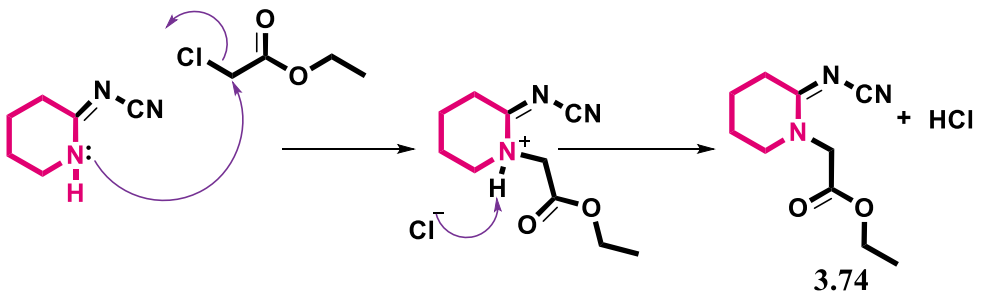


Scheme 5.3 Plausible mechanism for the formation of **3.73**.

5.2.1.3 *N*-alkylation piperidinylidene cyanamide.

Following the piperidinylidene cyanamide formation, *N*-alkylation of its amine was achieved through an S_N2 mechanism as shown in scheme (**Scheme 5.4**) [633]. The presence of potassium carbonate, enhanced the nucleophilicty of the amine by maintaining a basic environment. Additionally, its primary role was to neutralise the acid (HCl) generated, preventing a possible protonation of the amine, thus driving the reaction towards product formation.

University of Ghana http://ugspace.ug.edu.gh



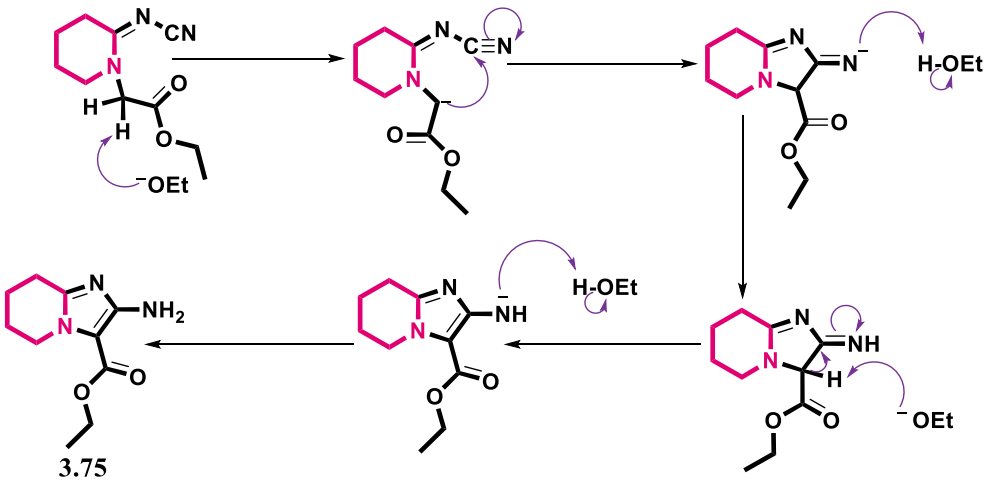
Scheme 5.4: Mechanism for *N*-alkylation of **3.74**.

5.2.1.4 Base mediated cyclisation.

The mechanism for the formation of the key intermediate ester, **3.75**, followed a base mediated cyclisation [634]. In the presence of a strong base, sodium ethoxide (NaOEt), an acidic proton of the α-carbon of the ester was abstracted to form a nucleophilic center. The nucleophile then attacks the electrophilic cyano carbon, creating a ring. Consequently, the nucleophilic nitrogen created from breaking a bond of the nitrile group, abstracts a proton from ethanol (reaction solvent). Following this, the loss of the second acidic proton of the α-carbon of the ester, leads to a rearrangement of the molecule to yield the desired product (**Scheme 5.5**). Heating the reaction facilitates the nucleophilic attack on the cyano carbon leading to cyclisation.

INTEGRI PROCEDAMUS

University of Ghana http://ugspace.ug.edu.gh



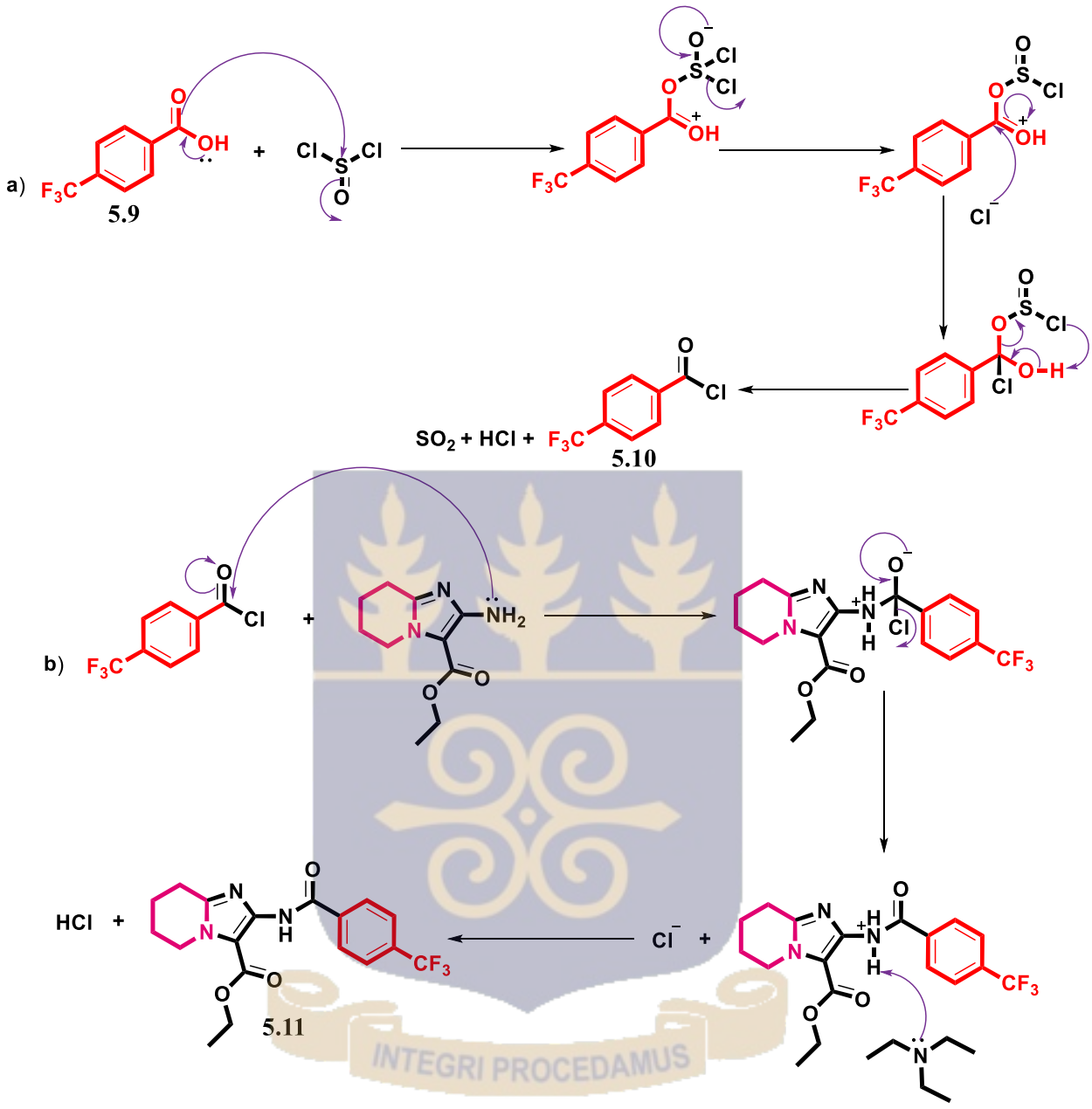
Scheme 5.5: Plausible mechanism for base mediated cyclisation of **3.75**.

While the initial 3 steps of the synthesis afforded the desired intermediates in excellent yields without significant difficulties, the latter stages were less efficient, giving lower yields.

5.2.1.5 Amide coupling with trifluorophenyl carboxylic acids.

Attempts at installing the trifluoromethylphenyl moiety using amide coupling agents HATU/ EDC.HCl, were largely unsuccessful, yielding either no detectable products or highly impure mixtures. This could be due to a compromise on the nucleophilicity of the amine of **3.75**, owing to steric effects imposed by the attached bicyclic moiety [635]. On the other hand, aromatic carboxylic acids are less electrophilic due to conjugation with lone pairs [636]. Even with the attached electron-withdrawing substituent (CF_3), efficient amide formation with trifluoromethylphenyl carboxylic acid was only achieved after converting the acid to an acyl chloride.

University of Ghana http://ugspace.ug.edu.gh



Scheme 5.6: Reaction mechanism for the formation of **a**) acyl chlorides and **b**) subsequent amidation, leading to compound **5.11**.

Due to the high reactivity and moisture sensitivity of the acid chlorides as well as the exothermic nature of the reaction, complicating reaction control and purification [637], the reaction was conducted on a small scale and in batches. This also ensured a controlled release of HCl which otherwise necessitated careful handling and efficient quenching. Nonetheless, de-

University of Ghana http://ugspace.ug.edu.gh

spite these measures, reaction yields were generally below 50 %. Thin Layer Chromatography (TLC) showed a bulk of unreacted amine, despite earlier TLC results confirming a complete conversion of the carboxylic acid to its corresponding acid chloride. To rule out the possibility of the generated HCl reacting with the amine (to form ammonium salt) which drastically reduces its nucleopilicity [638], excess triethyl amine was added to the reaction mixture to neutralise the acid formed (**Scheme 5.6**). The bulky nature of the amine could also make it liable to a very slow nuleophilic attack [635]. Hence, the reaction was left to run for a longer time, but with precaution (since products and excess reagents could also undergo side reactions). Unfortunately, very little improvements were observed despite the described interventions.

Among the successful amidation reactions, ortho- and meta-substituted derivatives were more efficient than para-substituted derivatives. The para position allows electron withdrawal effect of CF_3 to be inductively transmitted through the aromatic ring's resonance system. This increases the polarization of the C=O bond, making the carbonyl more electrophilic and therefore more prone to a nucleophilic attack than ortho and meta substituents. With a reverse trend being observed, it is likely the high electrophilicity of the carbonyl made the molecule more susceptible to self-decompostition or more prone to hydrolysis by trace water that might have been present in the reaction mixture. It is also likely to generate HCl more rapidly to protonate or deactivate the amine, making it unavailable for a nucleophilic attack [639, 640].

5.2.1.6 Base Hydrolysis of amide ester.

As a result of the low yields from the amidation reactions, the available starting material for subsequent steps, were significantly reduced. Though base hydrolysis is known to be an un-

University of Ghana http://ugspace.ug.edu.gh

complicated and highly efficient reaction [641], practical limitations during workup further diminished the recovered yields.

5.2.1.7 Amide coupling with HATU.

The ultimate step leading to the final analogues was therefore carried out on a smaller scale. HATU mediated amide coupling for these intermediates proceeded smoothly with an initial pre-activation of the carboxylic acids. However, purification was time and labour intensive. The close chromatographic retention of the analogues and co-eluting impurities required multiple rounds of recrystallization, after preliminary column purification. Consequently, the yields of the target molecules were affected.

A total of 12 analogues were synthesised (**Figure 5.3**) and confirmed with LC-MS. However, their very low quantities did not allow for full characterization. Only two analogues were obtained in substantial yields that allowed for additional characterization and biological screening. Data obtained from these analogues are discussed in subsequent paragraphs. The compound numbering used in the experimental section (**Chapter 3**) is maintained to facilitate easy comparison with the corresponding spectroscopic interpretation data.

INTEGRI PROCEDAMUS

University of Ghana http://ugspace.ug.edu.gh

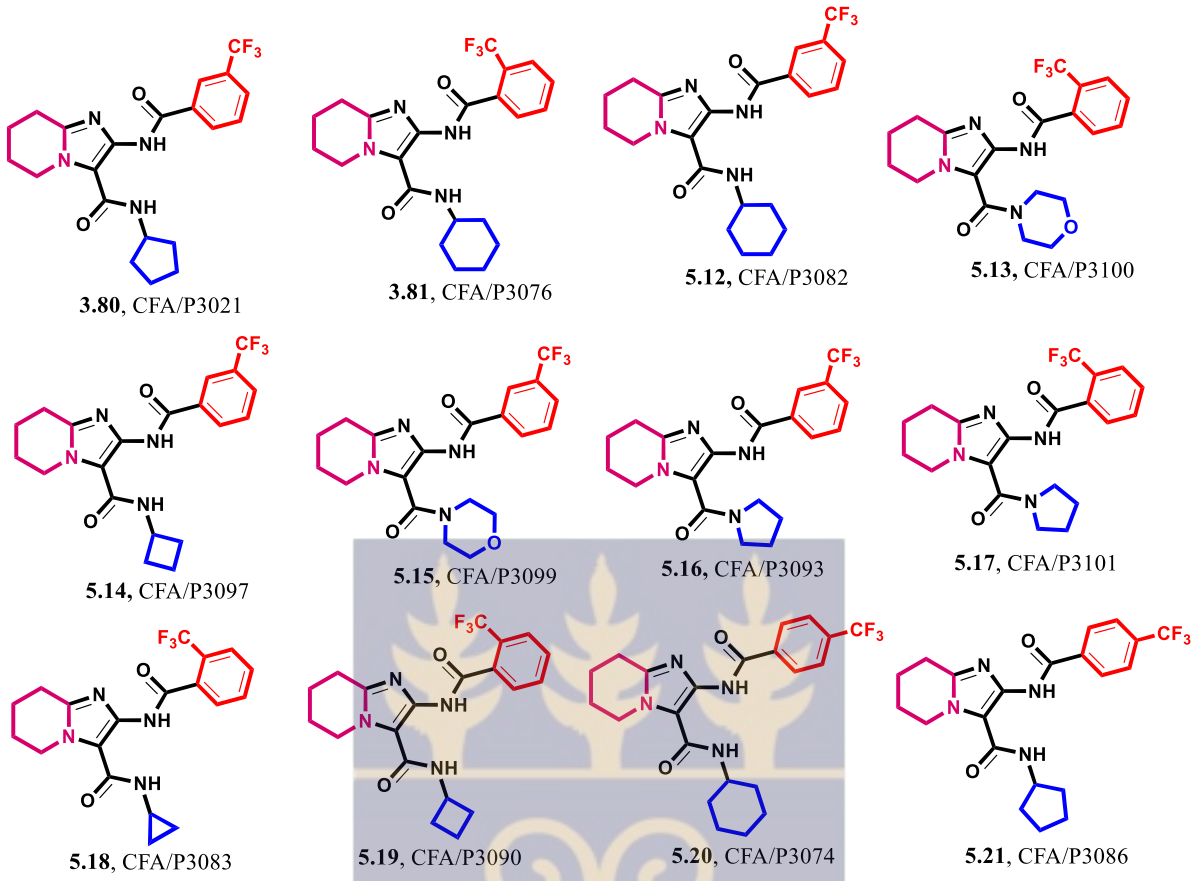


Figure 5.3: Structures of attempted analogues.

5.2.2 Spectral Analysis

Structures of intermediates leading to the final analogues were confirmed with ^{1}H and ^{13}C NMR, while final analogues **3.80** and **3.81** were additionally characterised with LC-MS and FTIR spectroscopy.

INTEGRI PROCEDAMUS

University of Ghana http://ugspace.ug.edu.gh

5.2.2.1 NMR Spectroscopy

5.2.2.1.1 NMR Spectrum of (*Z*)-*N*-(piperidin-2-ylidene)cyanamide, 3.73.

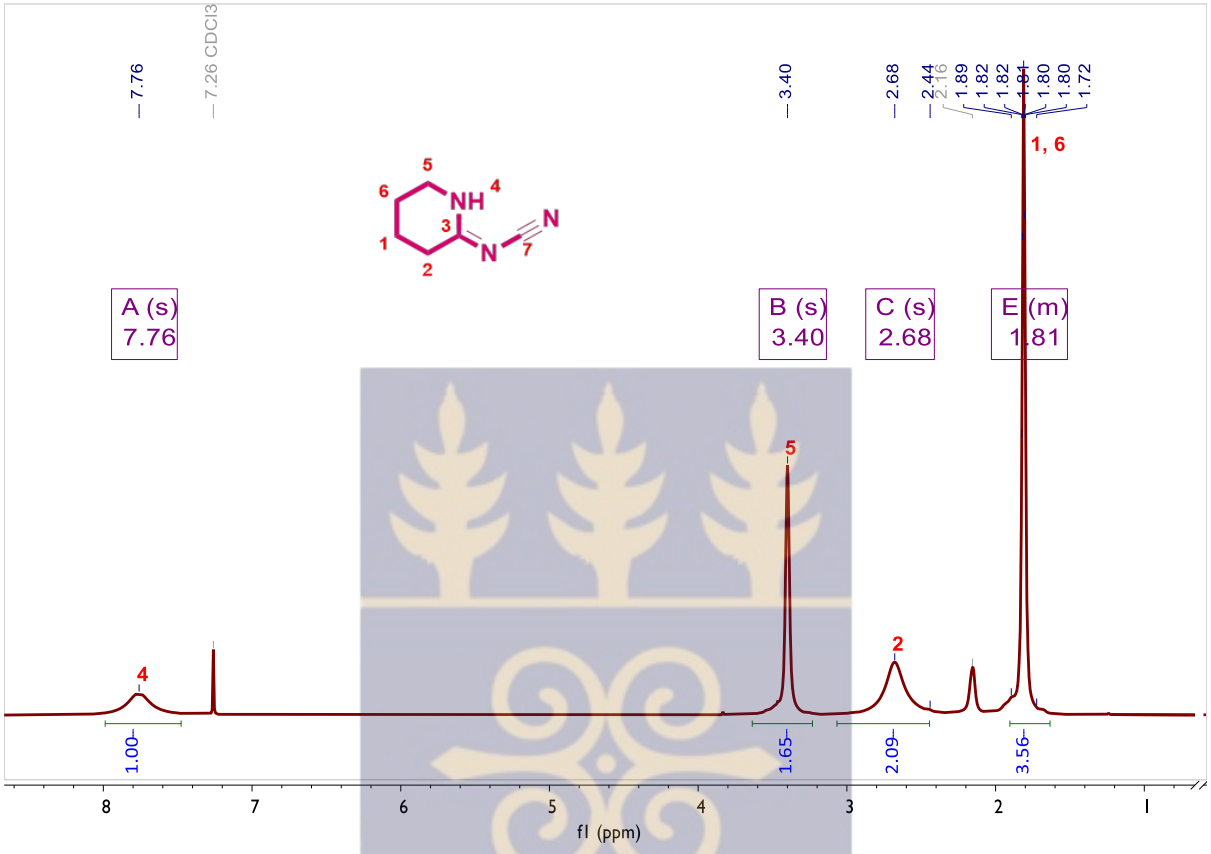


Figure 5.4: ^{1}H NMR (500 MHz, $CDCl_3$) of (*Z*)-*N*-(piperidin-2-ylidene) cyanamide, **3.73** (CFA/P3/001).

Figure 5.4 represents the ^{1}HNMR of **3.73**. Signals for the aliphatic protons were observed with their expected coupling patterns. While protons at position 1 and 6 of the piperidine ring were represented by a multiplet between δ 1.89 ppm and δ 1.72 ppm, the methylene protons adjacent to the amine and imine groups (labelled 5 and 2 respectively) were indicated at δ ~2.68 ppm and δ ~3.40 ppm, respectively. The amine proton (labelled 4) was represented by a singlet at δ ~7.76.

^{13}C NMR showed chemically distinct signals consistent with the unique chemical environments of the 6 carbon atoms in the molecule. Peaks at δ 173.4 and 117.0 ppm corresponded

University of Ghana http://ugspace.ug.edu.gh

to the imine and cyano carbons, labelled as 3 and 7 respectively, while other carbons on the piperidine ring labelled as 5, 2, 1 and 6 were represented at δ 42.3, 28.5, 21.2 and 19.0 ppm respectively (**Figure 5.5**).

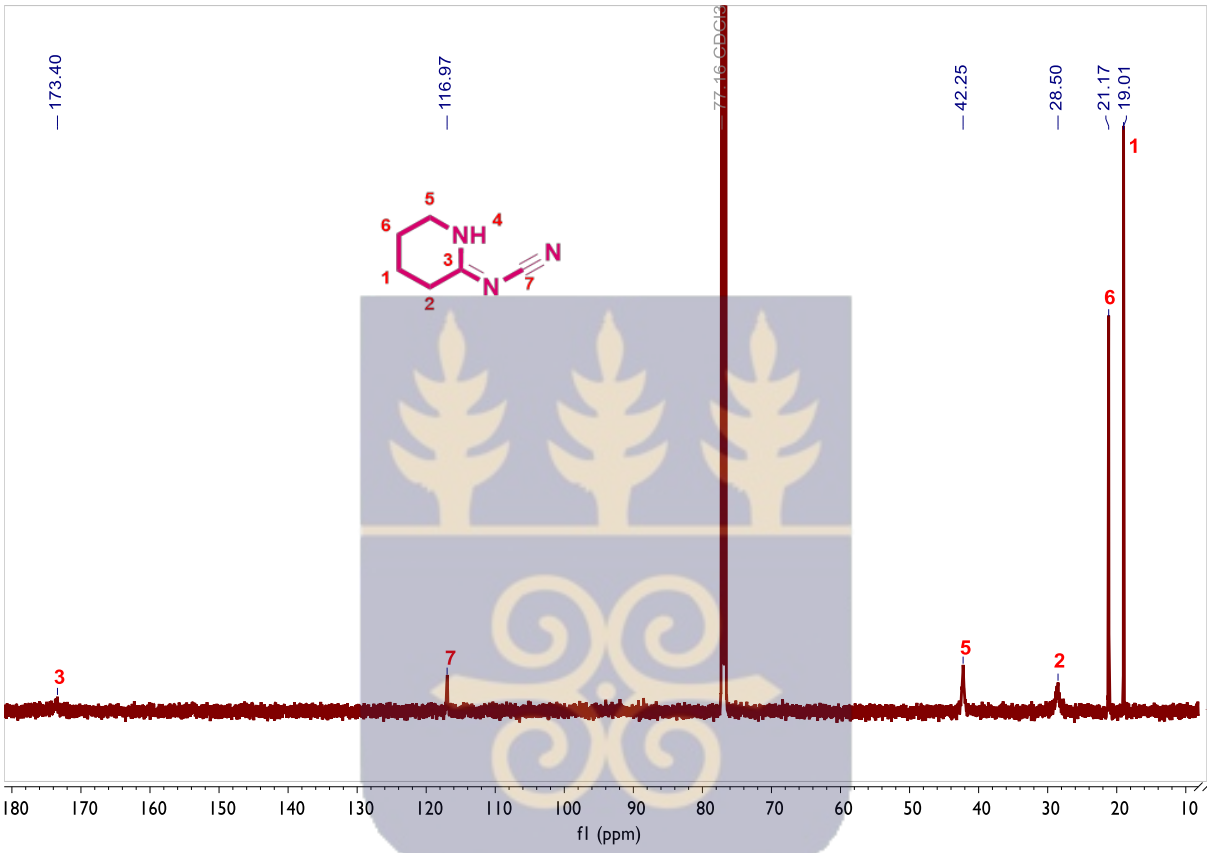


Figure 5.5: ^{13}C NMR (126 MHz, $CDCl_3$) of (*Z*)-*N*-(piperidin-2-ylidene) cyanamide, **3.73** (CFA/P3/001).

5.2.2.1.2 NMR Spectrum of ethyl (*Z*)-2-(2-(cyanoimino)piperidin-1-yl)acetate, 3.74.

Incorporation of the ethyl acetate moiety into the molecular structure was confirmed by the disappearance of the NH signal at δ ~7.76 ppm, and appearance of additional signals in the aliphatic region [642]. Signals characteristic of the oxy-methylene and terminal methyl protons (labelled as 9 and 10 respectively) of the ethyl acetate moiety were observed as a quartet at δ ~ 4.17 – 4.12 ppm and triplet at δ ~1.22 – 1.20 ppm respectively. The singlet correspond-

University of Ghana http://ugspace.ug.edu.gh

ing to the acetyl methylene protons (labelled as 7) was observed further downfield (δ ~4.11) due to the de-shielding influence of the adjacent amine (**Figure 5.6**).

In the ^{13}C NMR, resonances corresponding to acetyl methylene, oxymethylene and terminal methyl carbons (labelled as 7, 9 and 10) of the ethyl acetate moiety were recorded at δ 50.9, 61.3 and 13.8 ppm respectively, while the carbonyl carbon (labelled as 8) was represented at δ 172.1 ppm (**Figure 5.7**).

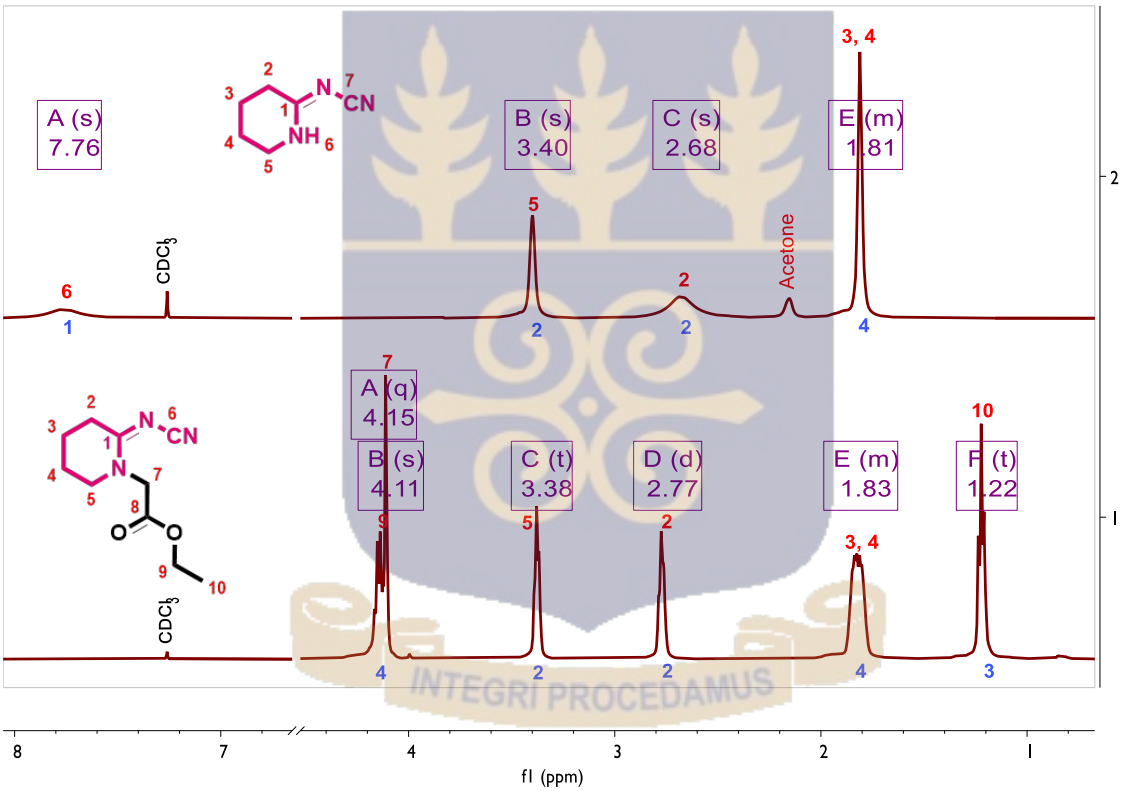


Figure 5.6: Comparison of ^{1}H NMR (500 MHz, $CDCl_3$) of CFA/P3001 and CFA/P3002.

University of Ghana http://ugspace.ug.edu.gh

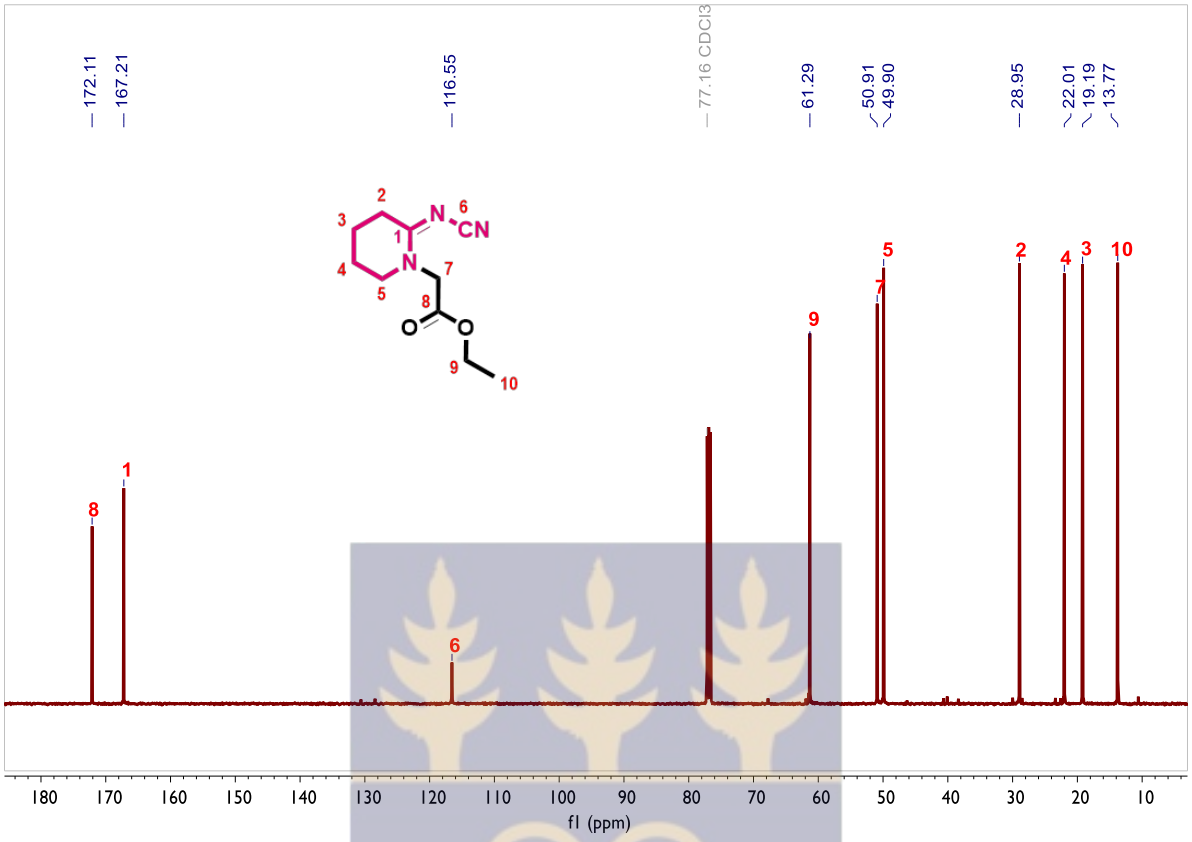


Figure 5.7: ^{13}C NMR (126 MHz, $CDCl_3$) of CFA/P3002.

INTEGRI PROCEDAMUS

University of Ghana http://ugspace.ug.edu.gh

5.2.2.1.3 NMR Spectrum of ethyl 2-amino-5,6,7,8-tetrahydroimidazo[1,2-a]pyridine-5-carboxylate, 3.75.

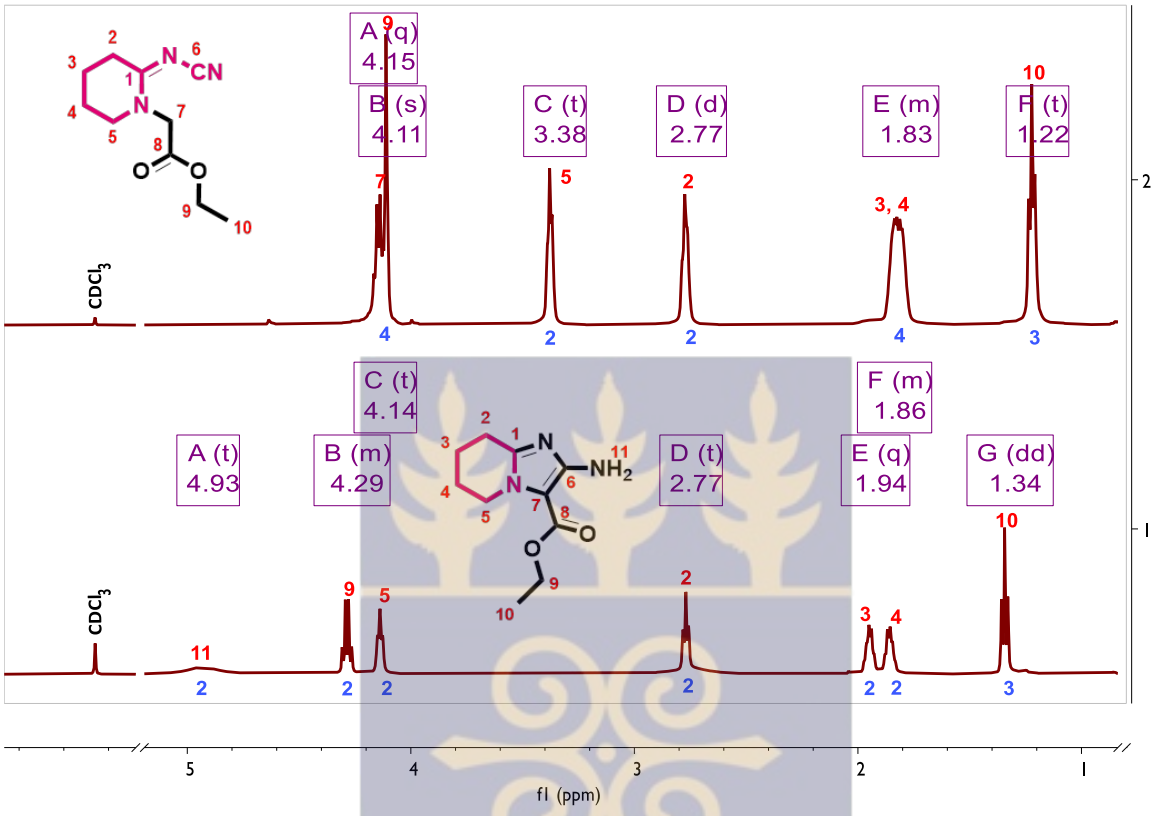


Figure 5.8: Comparison of ^{1}H NMR (500 MHz, $CDCl_3$) of **3.74** and **3.75**.

In the ^{1}H spectrum of **3.75**, the elimination of the acetyl methylene proton signal (δ ~4.13 ppm, multiplet) and presence of a singlet at δ ~4.93 ppm, integrating for two protons of the primary amine (labelled as 11), indicated a successful cyclisation reaction. Moreover, the downfield displacement of the signal of the methylene protons labelled as 5 (from δ ~ 3.38 ppm to δ ~ 4.14 ppm), is indicative of an increased de-shielding effect due to the imidazole formation (**Figure 5.8**). Further evidence from the ^{13}C NMR indicated a general downfield shift in the chemical resonances of carbons proximal to the newly formed ring. Notably, the disappearance of the cyano and acetyl methylene carbons, accompanied by the emergence of a new signal in the aromatic region (δ 146.7 ppm), corresponding to the imidazole carbon

University of Ghana http://ugspace.ug.edu.gh

(labelled as 6) linked to the primary amine, also affirmed a successful cyclisation reaction (**Figure 5.9**).

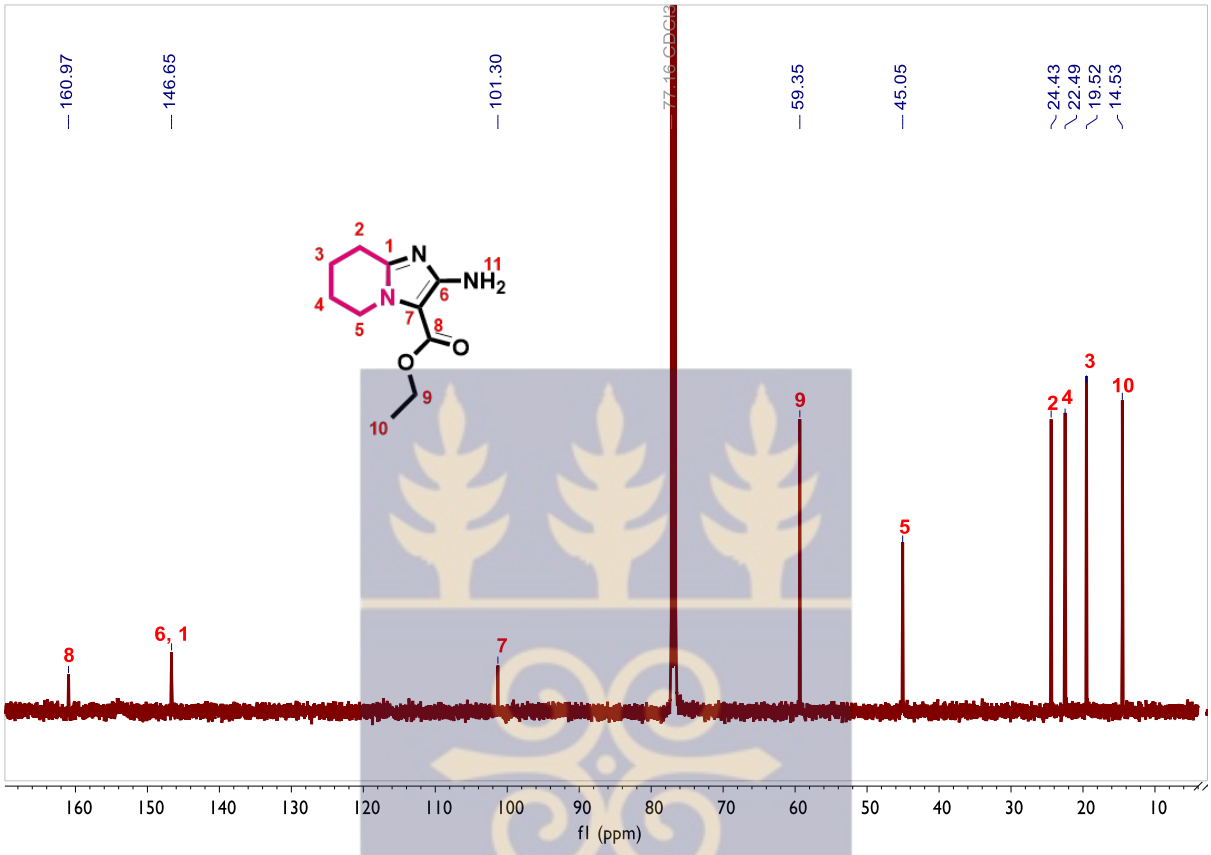


Figure 5.9: ^{13}C NMR (126 MHz, $CDCl_3$) of CFA/P3003.

5.2.2.1.4 NMR Spectrum of ethyl ethyl 2-(3-(trifluoromethyl)benzamido)-5,6,7,8-tetrahydroimidazo[1,2-*a*]pyridine-5-carboxylate, 3.76.

The formation of the amide bond with trifluoromethylphenyl carboxylic acid influenced additional signals in the aromatic region. Typical of amide NH bonds, the singlet at δ ~ 9.69 ppm corresponded to the NH proton [643]. Other signals of the phenyl moiety were also recorded at δ ~ 7.86, 7.78, 7.44 and 7.28 ppm (**Figure 5.10**) for protons labelled 18, 14, 15 and 16 respectively.

Consistently, ^{13}C NMR exhibited aromatic signals between δ ~135.2 - 120.2 ppm, corresponding to the carbons of the phenyl moiety. While the triflouromethyl carbon (labelled 19)

University of Ghana http://ugspace.ug.edu.gh

signal appeared at δ ~ 122.4, additional resonances were observed due to spin-spin C-F coupling, providing further spectroscopic evidence for the presence of the CF_3 substituent (**Figure 5.11**). CF_3 substitutions typically exhibit a distinct quartet with large coupling constants (observed between) that result in peak separation across a broader range on the spectrum. When substituted on a phenyl ring, the ipso aromatic carbons also exhibit a quartet, but with a smaller coupling constant, producing more closely spaced peaks that often appear as a cluster in the spectrum. As observed, the J-couplings follow the order ipso > ortho > meta > para, reflecting the progressive weakening of spin–spin interactions with increasing bond distance, which manifests as a corresponding decrease in the resolution of the observed peaks (**Figure 5.12**) [644, 645].

This observation was consistent with other trifluoromethylphenyl analogues. However, depending on the position of the CF_3 substitution, (ortho, meta, para), the chemical shifts and splitting patterns of the aromatic protons and carbons were varied.

INTEGRI PROCEDAMUS

University of Ghana http://ugspace.ug.edu.gh

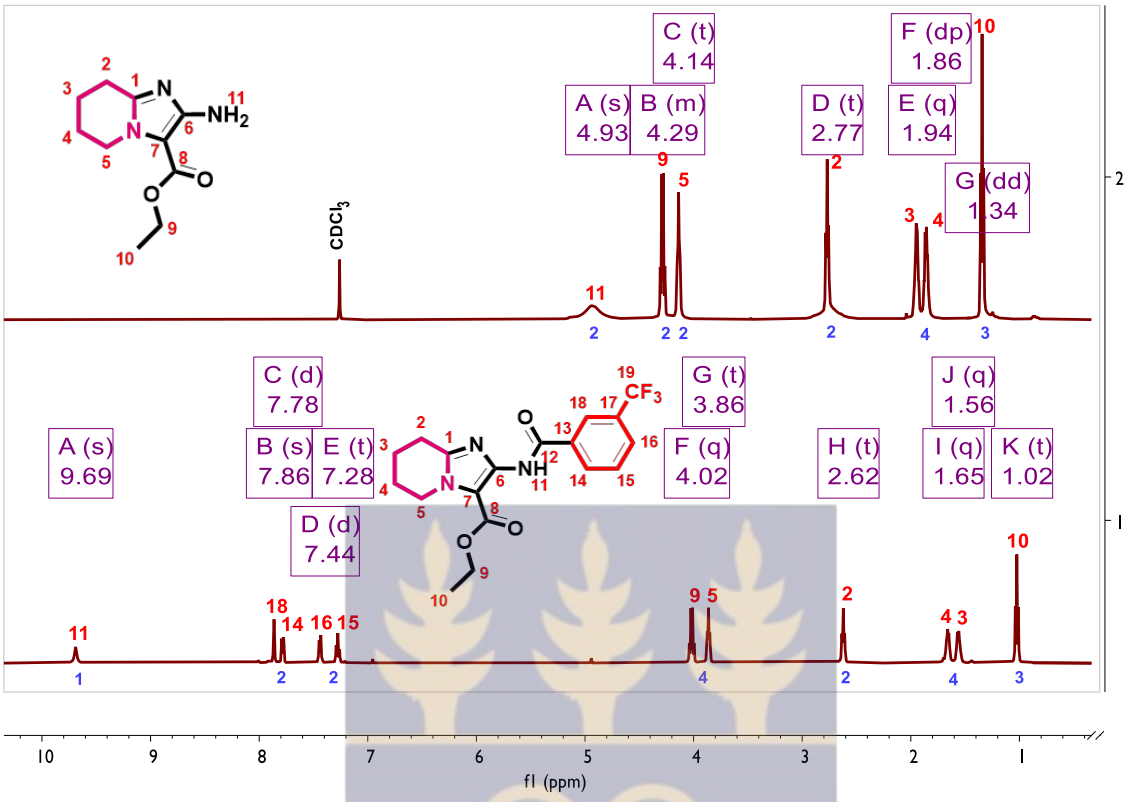


Figure 5.10: Comparison of ^{1}H NMR (500 MHz, $CDCl_3$) of **3.75** and **3.76**.

INTEGRI PROCEDAMUS

University of Ghana http://ugspace.ug.edu.gh

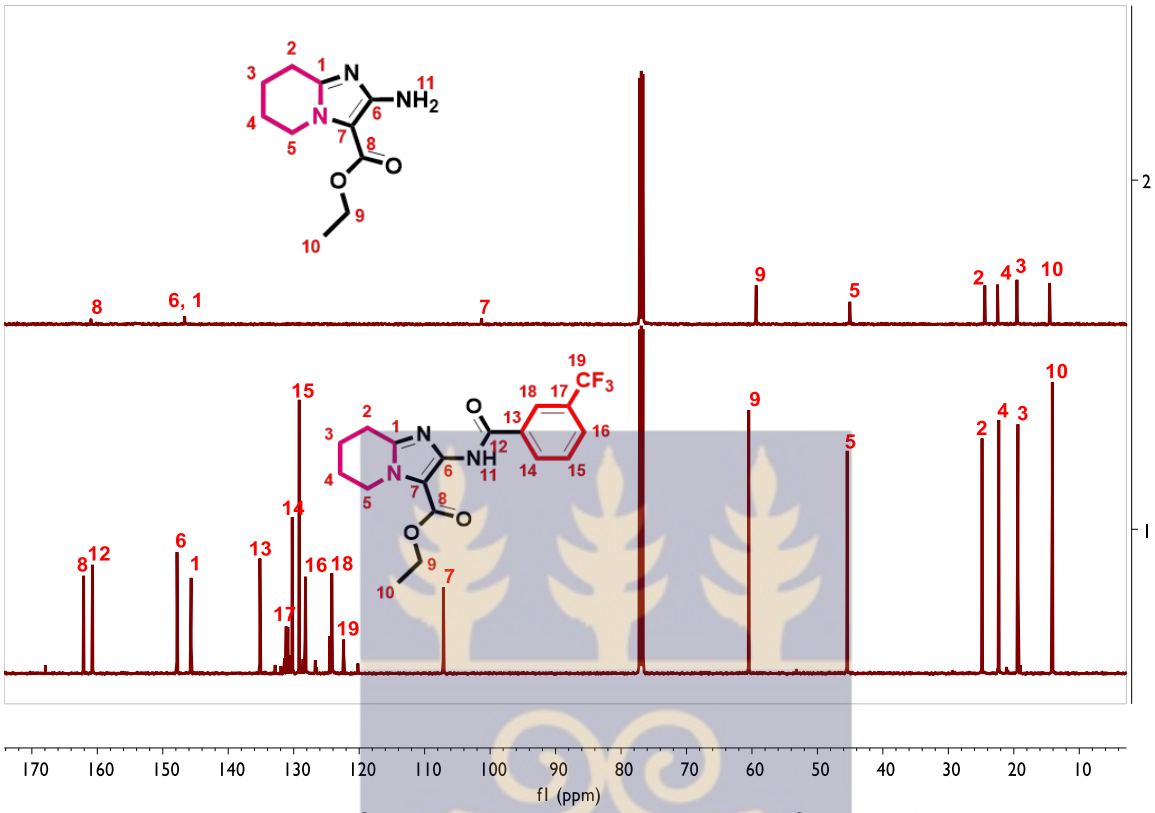


Figure 5.11: Comparison of 13C NMR (126 MHz, CDCl3) of 3.75 and 3.76.

INTEGRI PROCEDAMUS

University of Ghana http://ugspace.ug.edu.gh

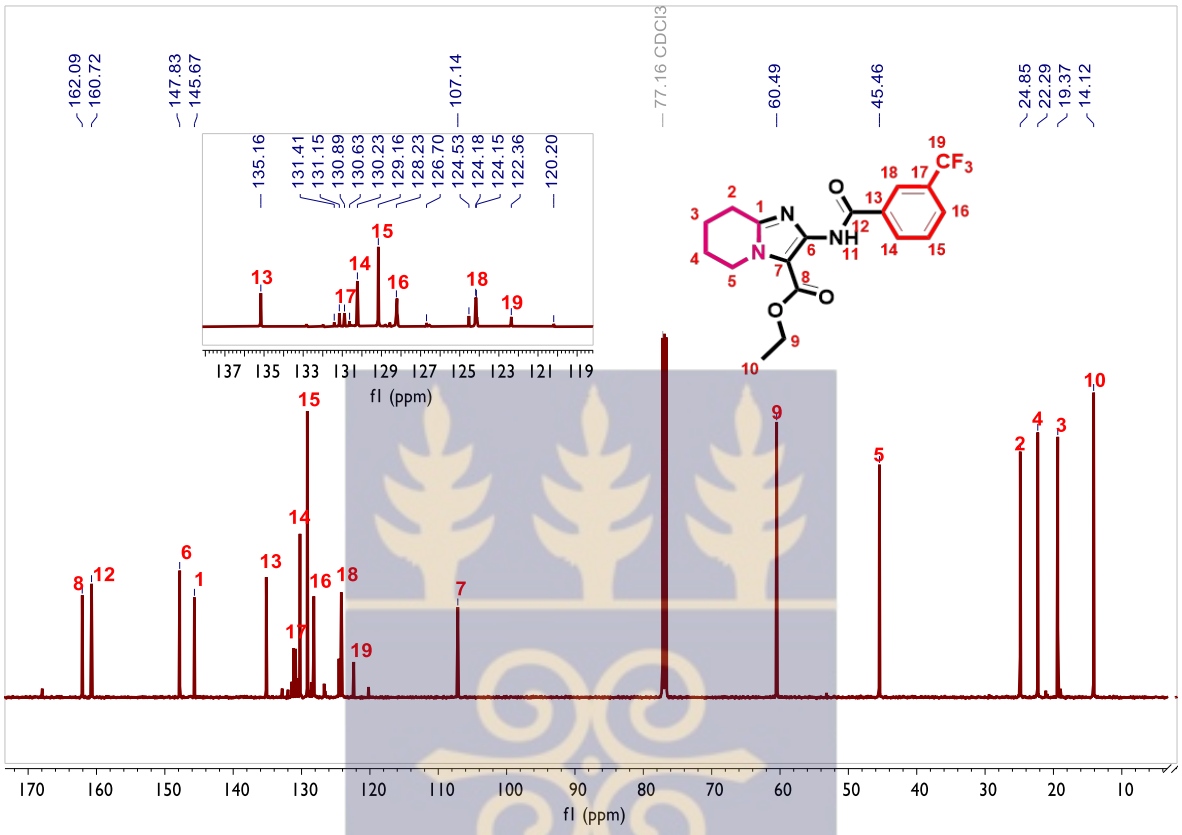


Figure 5.12: ^{13}C NMR (126 MHz, $CDCl_3$) of **3.76 (**CFA/P3016).

Due to very low yields, spectral characterization of the penultimate intermediates was not performed, the success of the hydrolysis reaction was reasonably inferred based on Thin-layer chromatography, and the successful conversion of the obtained intermediates to final analogues which were fully characterised.

University of Ghana http://ugspace.ug.edu.gh

5.2.2.1.5 NMR Spectrum of *N*-cyclopentyl-2-(2-(trifluoromethyl)benzamido)-5,6,7,8-tetrahydroimidazo[1,2-*a*]pyridine-3-carboxamide 3.81 (CFA/P3/076) and 3.80(CFA/P3/021).

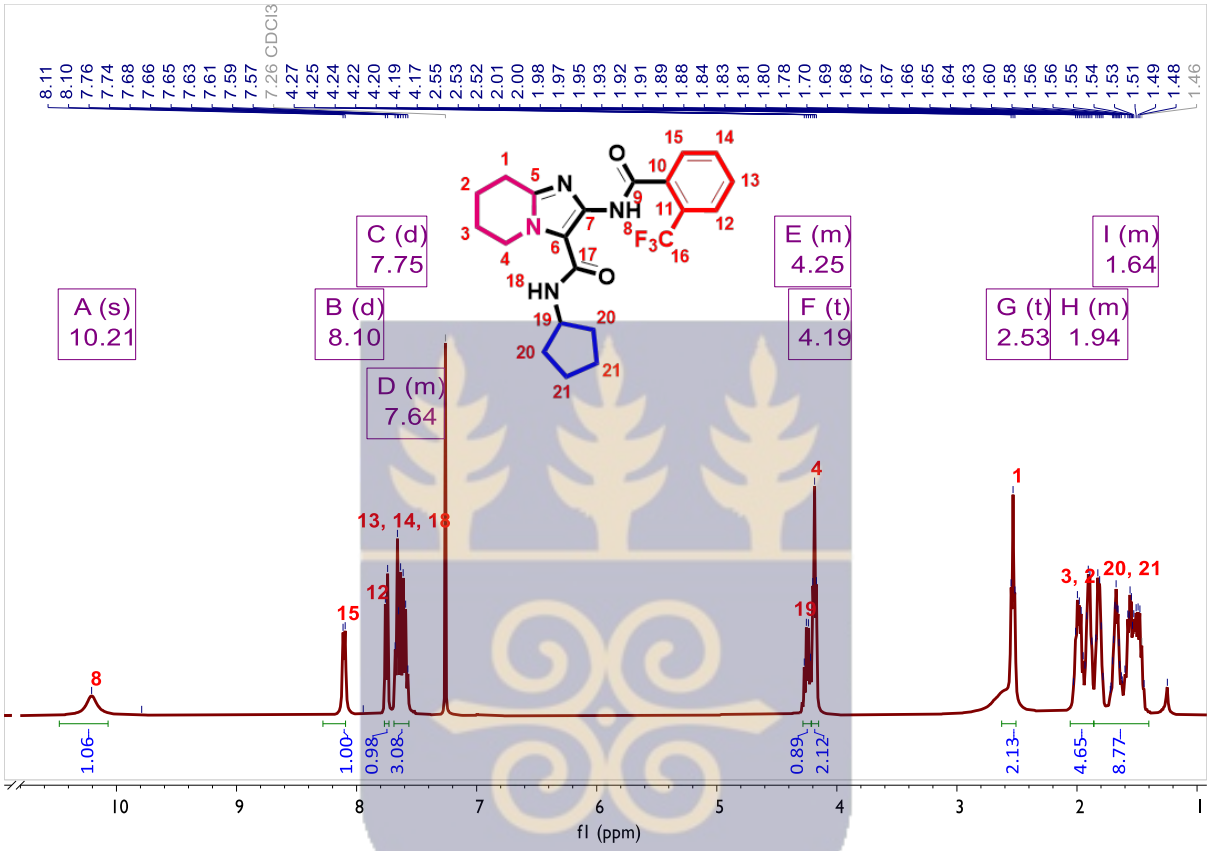


Figure 5.13: ^{1}H NMR (500 MHz, $CDCl_3$) of **3.81.**

The ^{1}H spectra for **3.81** exhibited a crowded aliphatic region, displaying peaks within the range of δ ~2.52 – 1.64 ppm, corresponding to the installed cyclopentyl. Conversely, the signal for the protons of the second amide formed (labelled as 18) was represented at δ ~7.60 ppm. The highly de-shielded cyclopentyl proton linking the NH (labelled as 18) of the amide also showed a multiplet at δ ~4.25 ppm (**Figure 5.13**).

^{13}C NMR for the same structure (**Figure 5.14**) provided further evidence with signals at δ 51.5, 32.8 and 24.1 ppm, for carbons of the cyclopentyl (labelled as 19, 20 and 21 respectively).

University of Ghana http://ugspace.ug.edu.gh

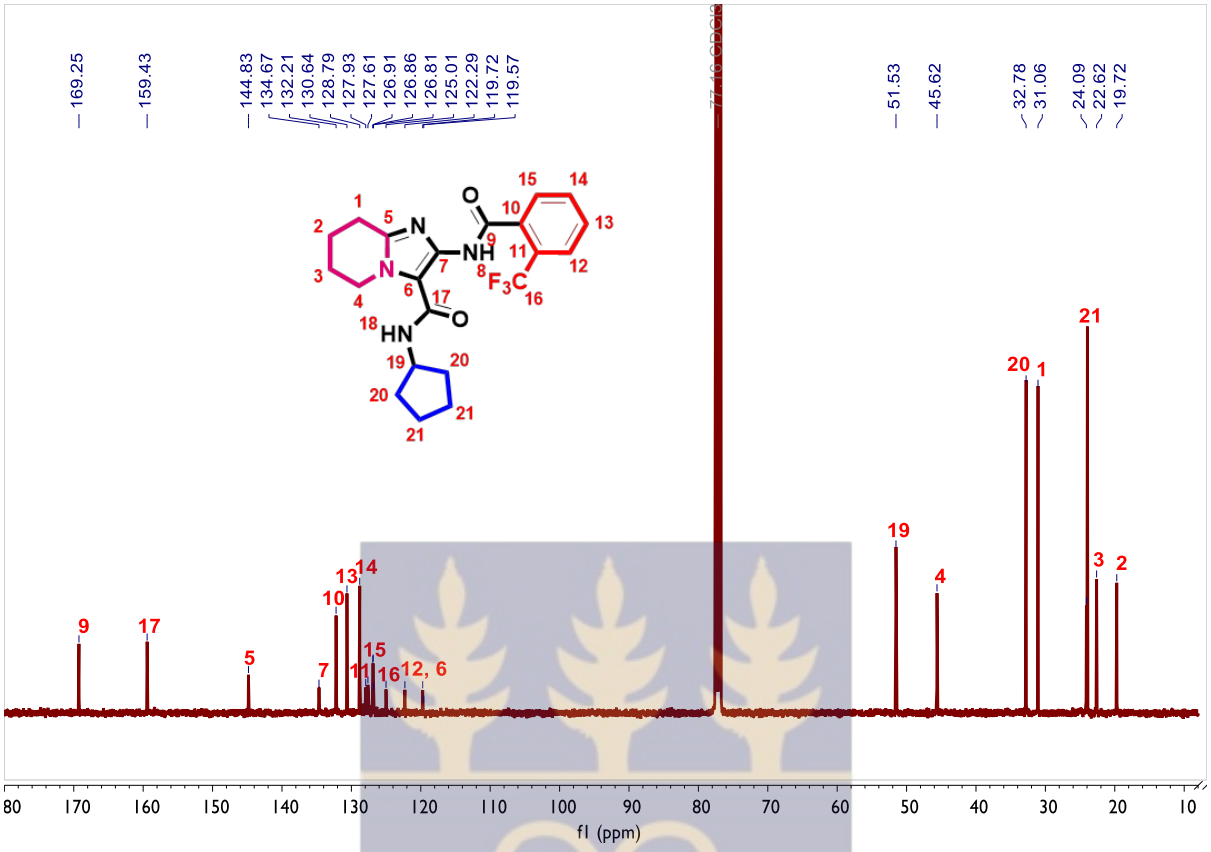


Figure 5.14: ^{13}C NMR (126 MHz, $CDCl_3$) of **3.81.**

The second analogue bearing similar substituents displayed comparable ^{1}H NMR resonances. As expected, the spectral differences were observed in the aromatic region, reflecting the influence of the position of the substituted CF_3 moiety (ortho and meta respectively) (**Figure 5.15**).

INTEGRI PROCEDAMUS

University of Ghana http://ugspace.ug.edu.gh

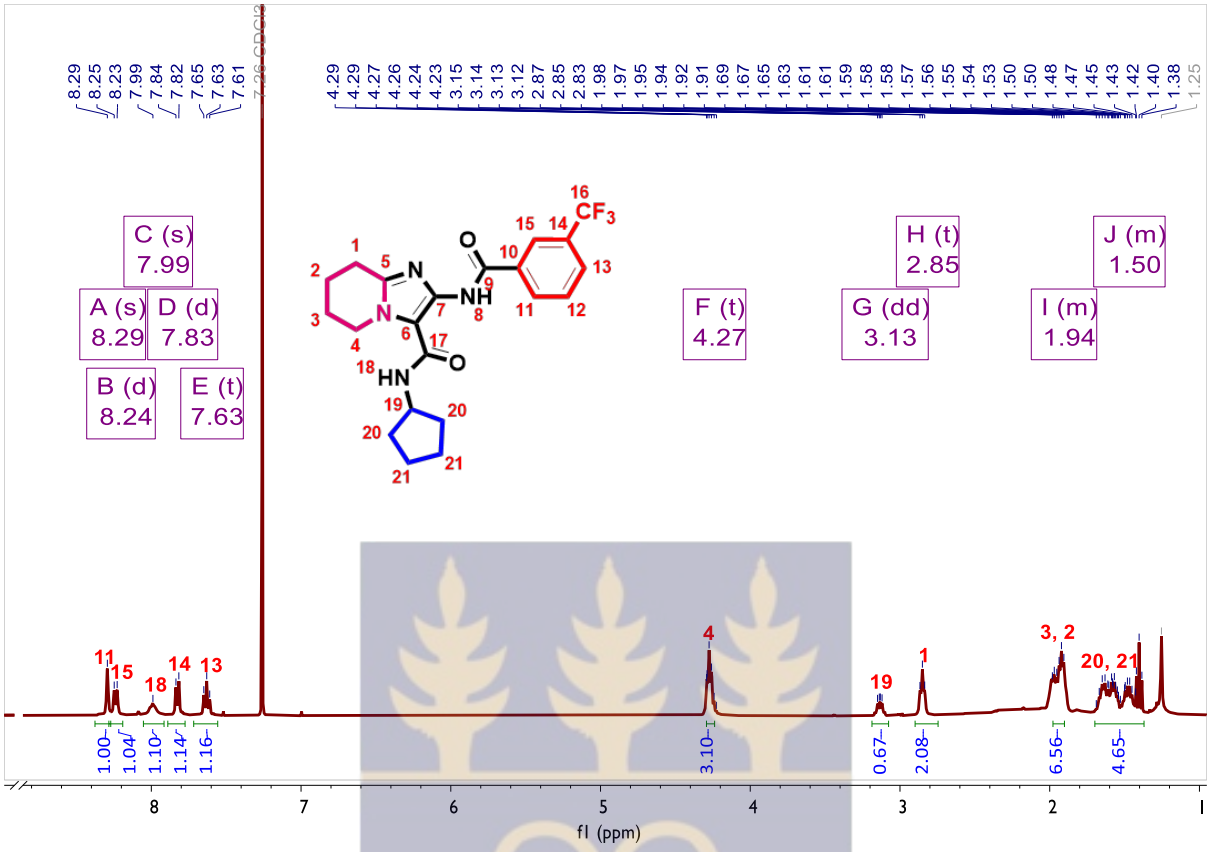


Figure 5.15: ^{1}H NMR (500 MHz, $CDCl_3$) of **3.80.**

5.2.2.2 LC-MS Spectroscopy.

LC-MS analysis for both analogues confirmed the structures with a single, well resolved peak at retention times 2.301 and 0.971 minutes for **3.80** and **3.81** respectively (**Figure 5.16**). Furthermore, the mass spectrum of the analogues (**Figure 5.17**) exhibited a prominent molecular ion peak around *m/z* 421.0 $[M+H]^+$, in agreement with the calculated exact mass (420.18 Da).

University of Ghana http://ugspace.ug.edu.gh

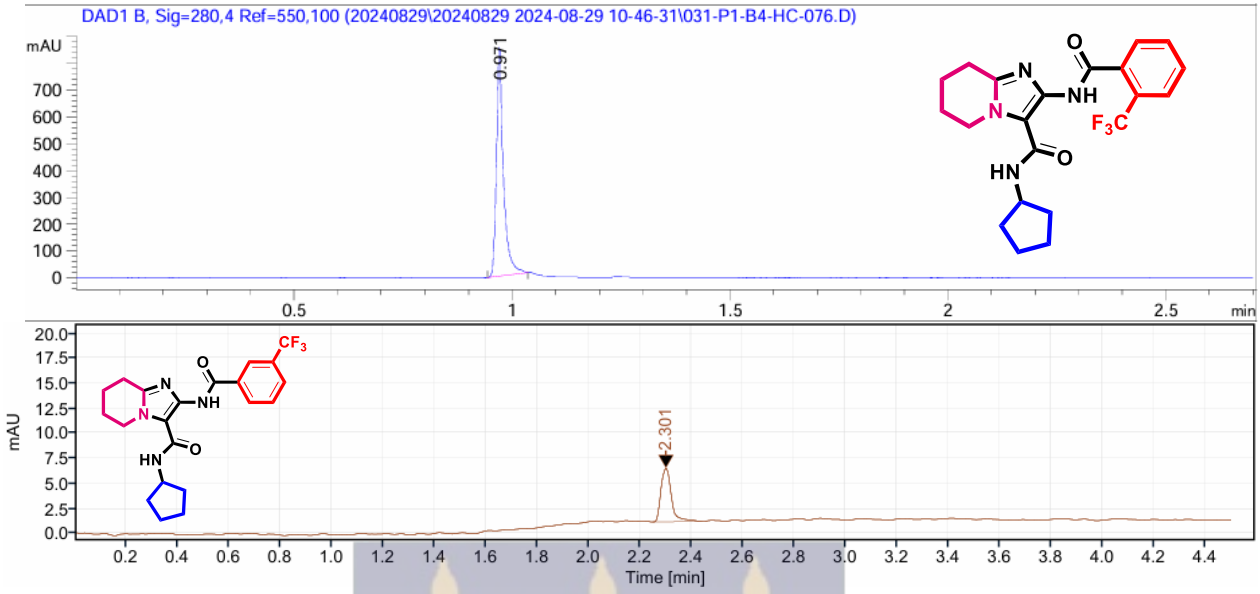


Figure 5.16: Liquid chromatography (LC) of **3.80 and 3.81**.

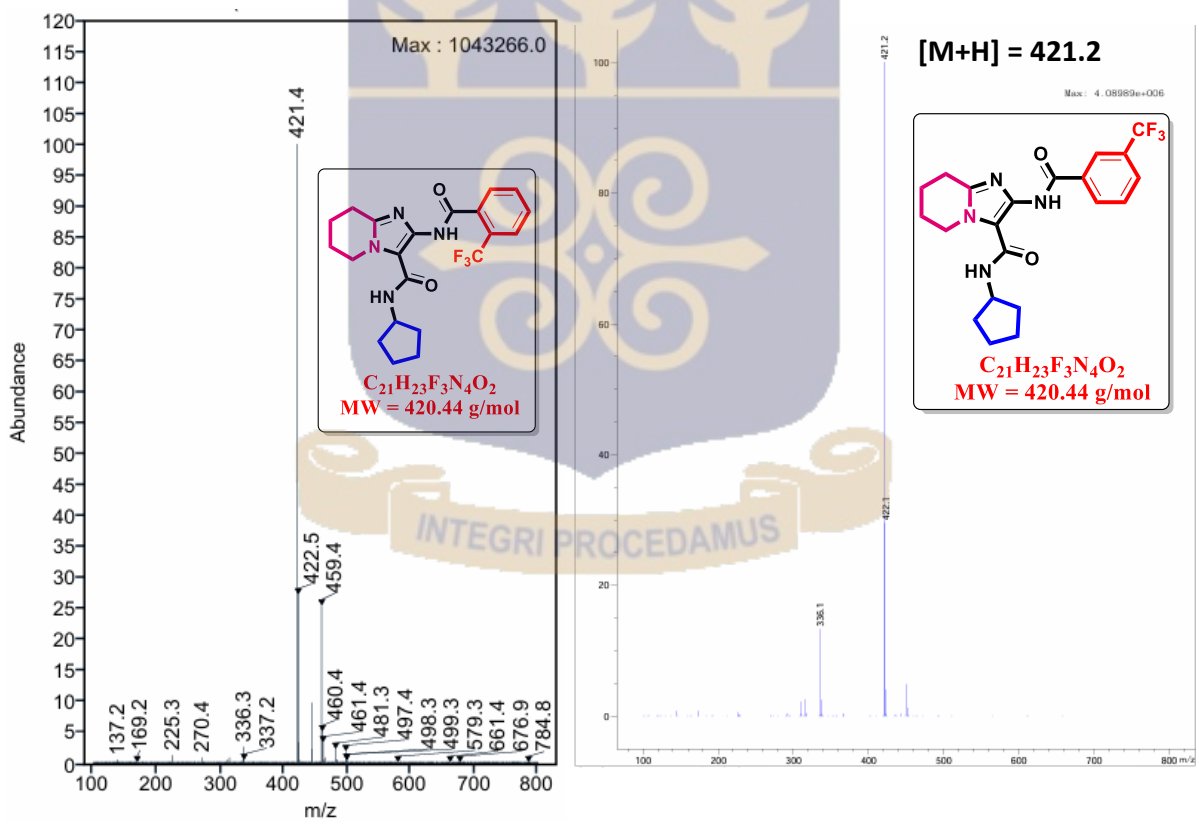


Figure 5.17: Mass Spectrum of 3.80 and 3.81.

5.2.2.3 Fourier-Transform Infrared (FT-IR) Spectroscopy.

Observed IR bands in the FT-IR spectrum of both analogues are consistent with their proposed structures, confirming the presence of expected functional groups (**Figure 5.18** and

University of Ghana http://ugspace.ug.edu.gh

5.19). N-H and C-O stretching vibrations of the amide group were represented at ~3200 cm^{-1}, and ~1650 cm^{-1} respectively. While aliphatic C-H stretches showed strong bands at ~2800 and 2950 cm^{-1}, the aromatic C=C stretch and C-H out of plane band were recorded at ~1627 cm^{-1} and ~700 cm^{-1} respectively. A sharp intense band at ~1100 cm^{-1} also confirmed the substituted C-F group [602-604].

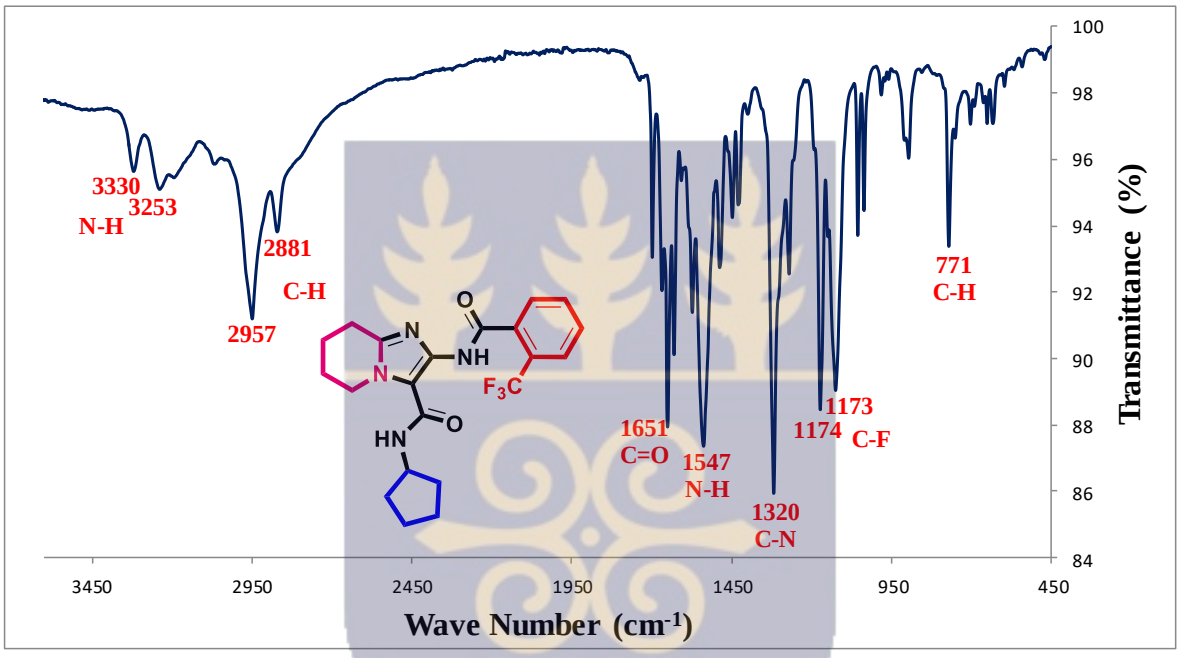


Figure 5.18: IR spectrum of **3.81**

INTEGRI PROCEDAMUS

University of Ghana http://ugspace.ug.edu.gh

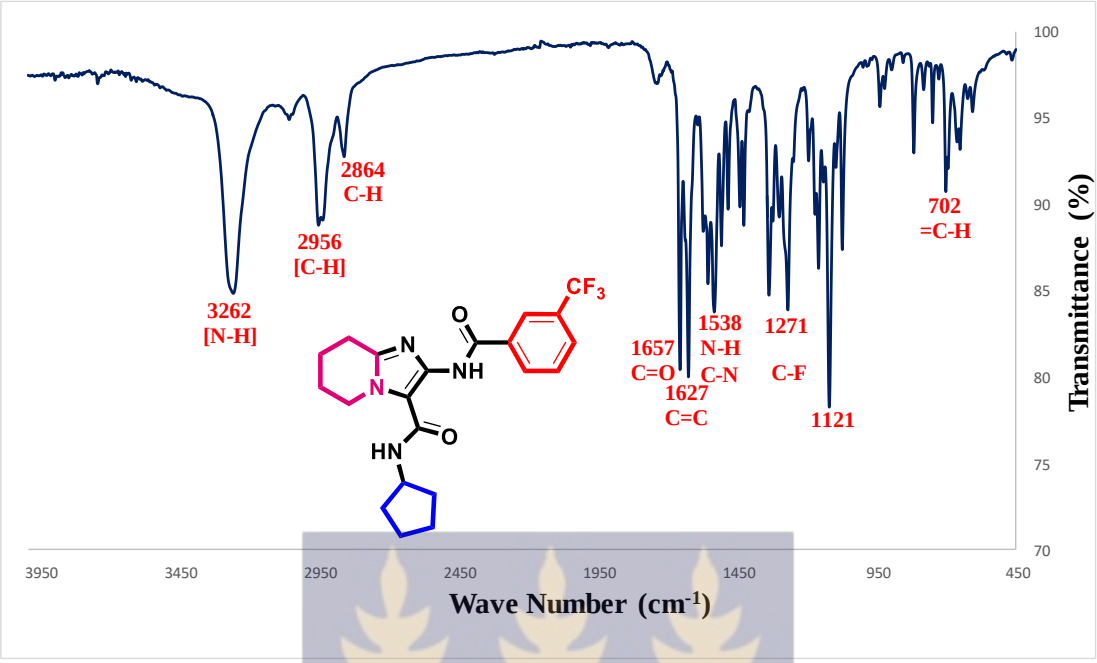


Figure 5.19: IR spectrum of **3.80**.

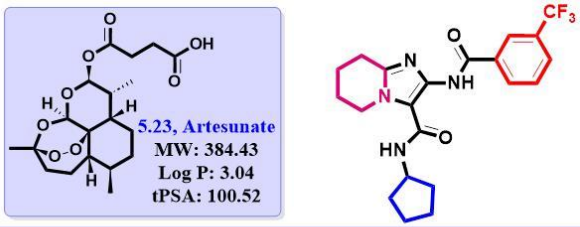
5.2.3 Physicochemical properties, solubility and biological activities of 3.80 and 3.81.

Solubility assays were conducted at the department of Pharmacology, KNUST, using their defined standard procedures. Antimalarial screening on the other hand was carried out against drug-sensitive reference strain, 3D7 of *Plasmodium falciparum* at the Immunology Department of the Noguchi Memorial Institute for Medical Research. The compounds were prepared in stock solutions of 10 µM in DMSO, then serially diluted (1:3) in the growth medium to generate 12 working concentrations (10 µM – 0.56 nm) for IC_{50} determination. *In vitro* antiplasmodial activity was determined *via* the SYBR Green 1 Assay, where parasite growth was determined through fluorescent intensities measured at a wavelength of 497 nm excitation and 530 nm emission. Standard antimalarial drug artesunate was used as control.

Figure 5.20 outlines the physicochemical properties, solubility and antimalarial activities of the two fully characterised analogues. As indicated, the analogues display comparable physi-

University of Ghana http://ugspace.ug.edu.gh

cochemical properties with the hit compound. Clearly, the replacement of the aromatic core and aniline moiety of the hit compound, MMV1794959 with non-aromatic moieties influenced the lipophilicity (Log P) and corresponding solubility of the synthesised analogues.



Compound ID	CFA/P3021	CFA/P3076	MMV1794959
No.	3.80	3.81	5.1
MW (g/mol)	420.44	420.44	424.38
Log P	3.5	3.5	4.2
TPSA	74	74	74
Solubility (µM)	42	165	3.4
IC_{50} Pf(3D7) (µM)	27.84	21.5	0.41

Figure 5.20: Summary of physochochemical properties, solubility profiles and antimalarial activities of synthesised analogues.

Although the analogues **3.80** and **3.81** differ only in the positional orientation of the substituted trifluoromethyl moiety (ortho and meta), they exhibited a pronounced difference in their solubility values (42 µM and 165 µM). This observation emphasizes the impact of steric effects arising from ortho substitution on aromatic rings, disrupting the planarity of the aromatic system and influencing solubility. A disruption of the planarity of the molecule causes a reduction in π–π stacking interactions, consequently decreasing crystal packing and enhancing solubility [646].

Notably, the analogues exhibited a >50-fold decrease in activity in comparison to the hit compound. With a limited number of analogues obtained in sufficient yields for characterisation and biological evaluation, a comprehensive SAR study could not be performed to identi-

University of Ghana http://ugspace.ug.edu.gh

fy functional groups and structural features essential for antimalarial activity. However, the available data offer preliminary insights into the influence of structural variations within this series on solubility and antimalarial activity.

5.3 Conclusion

In conclusion, though the hit compound could not be re-synthesised due to the outlined challenges, structural modifications were attempted on the phenotypic hit to improve upon the biological, physicochemical and pharmacokinetic properties. The synthetic strategy involved the replacement of the aromatic ring(s) with non-aromatic group(s). However, the synthetic route employed presented challenges, preventing the complete achievement of targeted modifications. Despite the challenge, two analogues, **3.80** (CFA/P3021) and **3.81** (CFA/P3076) of MMV1794959 were successfully synthesised and characterised with ^{1}H and ^{13}C NMR, LC-MS and FTIR. With these analogues containing fewer aromatic moieties, results indicate that, replacing the aromatic core and aniline moieties of the hit scaffold with non-aromatic moieties positively impacted the lipophilicity and consequent solubility of the molecule. Unfortunately, the obtained analogues were poorly active against the 3D7 strain of *P. falciparum*. Owing to the limited number of compounds prepared, conclusive deductions cannot be made from the obtained data, particularly with regards to Structure-Activity Relationships. Notwithstanding, the results provide valuable insights for future optimization and analogue design, within this chemical series.

University of Ghana http://ugspace.ug.edu.gh

CHAPTER SIX

6.0 Conclusions and Recommendations.

6.1 Conclusions

In contribution to ongoing efforts toward the discover antimalarial drugs to tackle the increasing threat posed by drug resistance, this study focused on synthesising analogues of two scaffolds; **MMV676444** and **MMV1794959**, derived from phenotypic screens. The analogues were designed and synthesised to achieve enhanced physicochemical and pharmacological profiles, thereby improving overall drug-like behaviour and biological efficacy.

A total of **36** analogues of the **MMV676444** scaffold were synthesised and characterised with NMR, LC-MS, and FTIR. Biological screening indicated good antimalarial potential for some of the analogues, with **CFA092** (**3.41**) emerging as the most active against the NF54 strain of *P. falciparum* (IC_{50} = **12 nM**). Metabolic stability studies on **CFA092** further confirmed its suitability for further optimization as a lead scaffold. Although the lead scaffold exhibited additional antitubercular potential, the analogues screened against the H37rv strain of *Mycobacterium tuberculosis* were poorly active. Furthermore, encouraging results from a preliminary screening of selected analogues against *Leishmania donovani* suggests that, the analogues possess leishmanicidal properties. Notably, the analogues with the best biological activities exhibited low solubility values, underscoring the need to optimize their physicochemical properties further.

On the other hand, two analogues of **MMV1794959** were successfully synthesised and fully characterised. Their physicochemical properties and solubility were significantly improved compared to the lead scaffold. However, both compounds were poorly active against the 3D7 strain of *P. falciparum*. Given the limited dataset owing to challenges encountered during the

University of Ghana http://ugspace.ug.edu.gh

synthesis of the analogues, conclusive deductions could not be made. However, valuable insights can be inferred from the available data, to optimize the scaffolds further.

Taken together, this study contributes to expanding the chemical space available for antimalarial drug discovery and provides a substantial basis for further medicinal chemistry progress towards the development of more potent antimalarial agents to tackle drug resistance, leading to the ultimate eradication of malaria.

6.2 Recommendations

Drawing from the outcomes of this research, the following recommendations are proposed to guide future research efforts.

6.2.1 MMV676444

- The Solubility of most active analogues needs improvement.
- Analogues should be thoroughly screened and optimized for more potent antileishmanial activity.

6.2.2 MMV1794959

- More molecules should be synthesised to establish the minimum pharmacophore through a comprehensive SAR study.
- Synthetic route needs optimisation.
- Advanced chromatographic techniques are required for the isolation and purification of the analogues.

University of Ghana http://ugspace.ug.edu.gh

REFERENCES

1. Shields CL, Bas Z, Laiton A, Silva AMV, Sheikh A, Lally SE, et al. Retinoblastoma: emerging concepts in genetics, global disease burden, chemotherapy outcomes, and psychological impact. Nature Eye. 2023;37(5):815-822.
2. Stein C, Kuchenmüller T, Hendrickx S, Prüss-Űstün A, Wolfson L, Engels D, et al. The global burden of disease assessments—WHO is responsible? PLoS neglected tropical diseases. 2007;1(3):1-8.
3. Rehm J, Shield KD. Global burden of disease and the impact of mental and addictive disorders. Current psychiatry reports. 2019;21(10):1-7.
4. Gardan G-V. "The Justinianic plague": the effects of a pandemic in late antiquity and the early Middle Ages. Romanian Journal of Artistic Creativity. 2020;8(4):3-18.
5. Snowden FM. Epidemics and society: From the black death to the present. 1 ed. United States of America: Yale University Press; 2019. 551 pages.
6. Pokhrel S, Chhetri R. A literature review on impact of COVID-19 pandemic on teaching and learning. Higher education for the future. 2021;8(1):133-141.
7. Tarkar P. Impact of COVID-19 pandemic on education system. International Journal of Advanced Science and Technology. 2020;29(9):3812-3814.
8. Jedwab R, Johnson ND, Koyama M. The economic impact of the Black Death. Journal of Economic Literature. 2022;60(1):132-178.
9. Meier M. The 'Justinianic Plague': The economic consequences of the pandemic in the eastern Roman empire and its cultural and religious effects. Early Medieval Europe. 2016;24(3):267-292.
10. DeWitte SN, Kurth MH, Allen CR, Linkov I. Disease epidemics: lessons for resilience in an increasingly connected world. Journal of Public Health. 2017;39(2):254-257.
11. Cockerell T. The Black Death, and its lessons for to-day. The Scientific Monthly. 1916;3(1):81-86.
12. Herlihy D. The Black Death and the transformation of the West. 1 ed: Harvard University Press; 1997. 111 pages.
13. Berche P. The spanish flu. La Presse Médicale. 2022;51(3):104-127.
14. Charles J. Origins, history, and achievements of the World Health Organization. British Medical Journal. 1968;2(5600):293-296.
15. Hogan MJ, Pardi N. mRNA vaccines in the COVID-19 pandemic and beyond. Annual review of medicine. 2022;73(1):17-39.
16. Sohrabi C, Mathew G, Franchi T, Kerwan A, Griffin M, Del Mundo JSC, et al. Impact of the coronavirus (COVID-19) pandemic on scientific research and implications for clinical academic training–a review. International Journal of Surgery. 2021;86(1):57-63.
17. Madekwe CC, Madekwe CC, Obeagu EI. Inequality of monitoring in human immunodeficiency virus, tuberculosis and malaria: a review. Madonna University journal of Medicine and Health Sciences 2022;2(3):6-15.
18. WHO. World malaria report, 2024

World Health Organization; 2024. Report No.: 924008617X.
19. WHO. State of Inequality. HIV, tuberculosis and malaria. 2021.
20. Baingana FK, Bos ER. Changing patterns of disease and mortality in Sub-Saharan Africa: an overview. Disease and Mortality in Sub-Saharan Africa. 2 ed. Washington DC: The World Bank; 2011.Page; 1-19.

University of Ghana http://ugspace.ug.edu.gh

21. Abdulwahab A, Adebisi Y, Adeniyi A, Olawehinmi T, Olanrewaju O. Climate Change, Vector-Borne Diseases, and Conflict: Intersecting Challenges in Vulnerable States. Infectious Diseases and epidemiology. 2024;10(8):1-5.
22. Funna A. Population Density and Spatial Distribution of Neglected Tropical Diseases in Sierra Leone [PhD]: Walden University; 2020.
23. Zerbo A. Environmental risk factors associated to outbreaks of water and vector-borne diseases in urban areas of Sub-Saharan Africa [PhD]: University of Oviedo; 2022.
24. Whitty CJ, Chiodini PL, Lalloo DG. Investigation and treatment of imported malaria in non-endemic countries. British Medical Journal. 2013;346(f2900):1-7.
25. Zhang S-S, Feng J, Zhang L, Ren X, Geoffroy E, Manguin S, et al. Imported malaria cases in former endemic and non-malaria endemic areas in China: are there differences in case profile and time to response? Infectious diseases of poverty. 2019;8(61):1-10.
26. White NJ. Severe malaria. Malaria Journal. 2022;21(1):1-17.
27. Fikadu M, Ashenafi E. Malaria: an overview. Infection and Drug Resistance. 2023;16(2023):3339-3347.
28. Zambare KK, Thalkari AB, Tour NS. A review on pathophysiology of malaria: A overview of etiology, life cycle of malarial parasite, clinical signs, diagnosis and complications. Asian Journal of Research in Pharmaceutical Science. 2019;9(3):226-230.
29. Warrell DA. Clinical features of malaria. Essential Malariology, 4Ed: CRC Press; 2017.Page; 191-205.
30. Kantele A, Jokiranta TS. Review of cases with the emerging fifth human malaria parasite, Plasmodium knowlesi. Clinical infectious diseases. 2011;52(11):1356-1362.
31. Escalante AA, Cepeda AS, Pacheco MA. Why Plasmodium vivax and Plasmodium falciparum are so different? A tale of two clades and their species diversities. Malaria Journal. 2022;21(139):1-19.
32. Batte A, Berrens Z, Murphy K, Mufumba I, Sarangam ML, Hawkes MT, et al. Malaria-associated acute kidney injury in African children: prevalence, pathophysiology, impact, and management challenges. International Journal of Nephrology and Renovascular Disease. 2021;14(1):235-253.
33. Antinori S, Galimberti L, Milazzo L, Corbellino M. Biology of human malaria plasmodia including Plasmodium knowlesi. Mediterranean journal of hematology and infectious diseases. 2012;4(1):1-10.
34. Tseha ST. Plasmodium species and drug resistance. Plasmodium species and drug resistance: IntechOpen; 2021.Page; 15-19.
35. Gachot B, Ringwald P. Severe malaria. La Revue du praticien. 1998;48(3):273-278.
36. Trampuz A, Jereb M, Muzlovic I, Prabhu RM. Clinical review: Severe malaria. Critical care. 2003;7(315):1-9.
37. Malm KL, Peprah NY, Mohammed W, Adomako B-Y, Oppong S, Boateng P, et al. A retrospective analysis of malaria deaths in the pre-and intra-COVID 19 pandemic era, Ghana, 2016–2021. Plos one. 2024;19(2):1-12.
38. WHO. World malaria report 2023: World Health Organization; 2023.
39. Gao L, Shi Q, Liu Z, Li Z, Dong X. Impact of the COVID-19 pandemic on malaria control in Africa: A preliminary analysis. Tropical Medicine and Infectious Disease. 2023;8(1):1-8.
40. Venkatesan P. The 2023 WHO World malaria report. The Lancet Microbe. 2024;5(3):1.
41. Cella W, Baia-da-Silva DC, Melo GCd, Tadei WP, Sampaio VdS, Pimenta P, et al. Do climate changes alter the distribution and transmission of malaria? Evidence assessment

University of Ghana http://ugspace.ug.edu.gh

and recommendations for future studies. Revista da Sociedade Brasileira de Medicina Tropical. 2019;52(e20190308):1-9.
42. Al-Awadhi M, Ahmad S, Iqbal J. Current status and the epidemiology of malaria in the Middle East Region and beyond. Microorganisms. 2021;9(2):1-20.
43. Sankineni S, Chauhan S, Shegokar R, Pathak Y. Global Health and Malaria: Past and Present. Malarial Drug Delivery Systems: Advances in Treatment of Infectious Diseases: Springer; 2023.Page; 1-16.
44. Kogan F, Kogan F. Remote Sensing for Malaria: Monitoring and Predicting Malaria from Operational Satellites. Malari Burden. 1 ed. Cham, Switzerland: Springer; 2020.Page; 281.
45. Demsash AW, Worku Z, Shibabaw AA, Walle AD, Lemu JC, Jifar WW, et al. Pooled prevalence of malaria and associated factors among vulnerable populations in Ethiopia: a systematic review and meta-analysis. BMC Infectious Diseases. 2024;24(1):09736-09739.
46. Siagian FE. Malaria epidemiology: Specific vulnerable group in the population. International Journal of Research and Reports in Hematology. 2020;3(2):41-52.
47. Asante FA, Asenso-Okyere K. Economic burden of malaria in Ghana. 2003.
48. Oladosu AO, Chanimbe T, Anaduaka US. Effect of public health expenditure on health outcomes in Nigeria and Ghana. Health Policy OPEN. 2022;3(100072):1-7.
49. Kawaguchi K, Donkor E, Lal A, Kelly M, Wangdi K. Distribution and risk factors of malaria in the Greater Accra Region in Ghana. International Journal of Environmental Research and Public Health. 2022;19(12006):1-19.
50. Goodman C, Coleman P, Mills A. Economic analysis of malaria control in sub-Saharan Africa. 1 ed. Geneva: Global Forum for Health Research 2000. 207 pages.
51. Purdy M, Robinson M, Wei K, Rublin D. The economic case for combating malaria. American Journal of Tropical Medicine and Hygiene. 2013;89(5):819-823.
52. McMannis J. Making the Case for Private Sector Engagement in the Fight Against Malaria 2017 [Available from: https://www.theglobalfight.org/making-case-private-sector-engagement/.
53. Vorasan N, Pan-Ngum W, Jittamala P, Maneeboonyang W, Rukmanee P, Lawpoolsri S. Long-term impact of childhood malaria infection on school performance among school children in a malaria endemic area along the Thai–Myanmar border. Malaria Journal. 2015;14(401):1-9.
54. Villamor E, Beer RJ, Seeley AL, López-Arana S, Marín C, Mora-Plazas M. Infectious morbidity and white blood cell count associated with grade repetition and school absenteeism. Acta Paediatrica. 2024;114(5):954-963.
55. Cirera L, Castelló JV, Brew J, Saúte F, Sicuri E. The impact of a malaria elimination initiative on school outcomes: Evidence from Southern Mozambique. Economics & Human Biology. 2022;44(101100):1-10.
56. Alonso S, Chaccour CJ, Elobolobo E, Nacima A, Candrinho B, Saifodine A, et al. The economic burden of malaria on households and the health system in a high transmission district of Mozambique. Malaria Journal. 2019;18(360):1-10.
57. Hailu A, Lindtjørn B, Deressa W, Gari T, Loha E, Robberstad B. Economic burden of malaria and predictors of cost variability to rural households in south-central Ethiopia. Plos one. 2017;12(10):1-16.
58. Snyman K, Pitt C, Aturia A, Aber J, Gonahasa S, Namuganga JF, et al. Who pays to treat malaria and how much? Analysis of the cost of illness, equity and economic burden of malaria in Uganda. Health Policy and Planning. 2024;40(1):52-65.

University of Ghana http://ugspace.ug.edu.gh

59. Wambui Kibibi J. Impact of Malaria on Maternal and Child Health in Uganda: Challenges and Solutions. Research Output Journal of Public Health and Medicine. 2024;3(3):56-59.
60. Omer S, Franco-Jarava C, Noureldien A, Omer M, Abdelrahim M, Molina I, et al. Impact of placental malaria on maternal, placental and fetal cord responses and its role in pregnancy outcomes in women from Blue Nile State, Sudan. Malaria Journal. 2021;20(35):1-8.
61. Romero M, Leiba E, Carrión-Nessi FS, Freitas-De Nobrega DC, Kaid-Bay S, Gamardo Á F, et al. Malaria in pregnancy complications in Southern Venezuela. Malaria Journal. 2021;20(186):1-8.
62. Bakken L, Iversen PO. The impact of malaria during pregnancy on low birth weight in East-Africa: a topical review. Malaria Journal. 2021;20(348):1-9.
63. Onyango E, Maguire R. Gendered exposure, vulnerability, and response: Malaria risk in a changing climate in Western Kenya. Frontiers in Climate. 2022;4(929667):1-14.
64. Quaresima V, Agbenyega T, Oppong B, Awunyo JAD, Adu Adomah P, Enty E, et al. Are malaria risk factors based on gender? a mixed-methods survey in an urban setting in Ghana. Tropical Medicine and Infectious Disease. 2021;6(161):1-14.
65. Rannan-Eliya RP. Financing malaria. PLOS Global Public Health. 2022;2(6):1-11.
66. Tam G. Maximizing the use of human population movement data for malaria control and elimination [PhD]: The University of Hong Kong; 2024.
67. Varo R, Balanza N, Mayor A, Bassat Q. Diagnosis of clinical malaria in endemic settings. Expert Review of Anti-infective Therapy. 2021;19(1):79-92.
68. Paintain L, Kpabitey R, Nyanor-Fosu F, Piccinini Black D, Bertram K, Webster J, et al. Using donor funding to catalyse investment in malaria prevention in Ghana: an analysis of the potential impact on public and private sector expenditure. Malaria Journal. 2022;21(203):1-17.
69. Njau J, Silal SP, Kollipara A, Fox K, Balawanth R, Yuen A, et al. Investment case for malaria elimination in South Africa: a financing model for resource mobilization to accelerate regional malaria elimination. Malaria Journal. 2021;20(344):1-16.
70. Shretta R, Avanceña AL, Hatefi A. The economics of malaria control and elimination: a systematic review. Malaria Journal. 2016;15(593):1-14.
71. Patouillard E, Han S, Lauer J, Barschkett M, Arcand JL. The Macroeconomic Impact of Increasing Investments in Malaria Control in 26 High Malaria Burden Countries: An Application of the Updated EPIC Model. International Journal of Health Policy and Management. 2023;12(e000176):1-8.
72. Elnour Z, Grethe H, Siddig K, Munga S. Malaria control and elimination in Kenya: economy-wide benefits and regional disparities. Malaria Journal. 2023;22(117):1-19.
73. Apeagyei AE, Patel NK, Cogswell I, O'Rourke K, Tsakalos G, Dieleman J. Examining geographical inequalities for malaria outcomes and spending on malaria in 40 malaria-endemic countries, 2010–2020. Malaria Journal. 2024;23(206):1-11.
74. Snyman K, Pitt C, Aturia A, Aber J, Gonahasa S, Namuganga JF, et al. Who pays to treat malaria and how much? Analysis of the cost of illness, equity and economic burden of malaria in Uganda. Health Policy and Planning. 2024;40(1):52-65.
75. Sarma N, Patouillard E, Cibulskis RE, Arcand JL. The Economic Burden of Malaria: Revisiting the Evidence. The American Journal of Tropical Medicine and Hygiene. 2019;101(6):1405-1415.
76. Purdy M, Robinson M, Wei K, Rublin D. The economic case for combating malaria. The American Journal of Tropical Medicine and Hygiene. 2013;89(5):819-823.

University of Ghana http://ugspace.ug.edu.gh

77. Greenwood B, Bhasin A, Targett G. The Gates Malaria Partnership: a consortium approach to malaria research and capacity development. Tropical medicine & international health. 2012;17(5):558-563.
78. McCoy D, Kembhavi G, Patel J, Luintel A. The Bill & Melinda Gates Foundation's grant-making programme for global health. The Lancet. 2009;373(9675):1645-1653.
79. Birn A-E. Philanthrocapitalism, past and present: The Rockefeller Foundation, the Gates Foundation, and the setting (s) of the international/global health agenda. Hypothesis. 2014;12(1):1-27.
80. Molina-Franky J, Cuy-Chaparro L, Camargo A, Reyes C, Gómez M, Salamanca DR, et al. Plasmodium falciparum pre-erythrocytic stage vaccine development. Malaria Journal. 2020;19(56):1-18.
81. Duffy PE, Gorres JP, Healy SA, Fried M. Malaria vaccines: a new era of prevention and control. Nature Reviews Microbiology. 2024;22(12):756-772.
82. Ansar F, Azzam A, Rauf MS, Ajmal Z, Ullah GA, Rauf S, et al. Global Analysis of RTS, S/AS01 Malaria Vaccine Acceptance Rates and Influencing Factors: A Systematic Review. Cureus. 2024;16(5):1-8.
83. Nadeem AY, Shehzad A, Islam SU, Al-Suhaimi EA, Lee YS. Mosquirix™ RTS, S/AS01 vaccine development, immunogenicity, and efficacy. Vaccines. 2022;10(5):1-15.
84. WHO. Full Evidence Report on the RTS,S/AS01

Malaria Vaccine 2021.
85. Laurens MB. RTS,S/AS01 vaccine (Mosquirix™): an overview. Human Vaccines and Immunotherapeutics. 2020;16(3):480-489.
86. Ogieuhi IJ, Ajekiigbe VO, Kolo-Manma K, Akingbola A, Odeniyi TA, Soyemi TS, et al. A narrative review of the RTS S AS01 malaria vaccine and its implementation in Africa to reduce the global malaria burden. Discover Public Health. 2024;21(152):1-13.
87. RTS SCTP. Efficacy and safety of the RTS,S/AS01 malaria vaccine during 18 months after vaccination: a phase 3 randomized, controlled trial in children and young infants at 11 African sites. PLoS Med. 2014;11(7):1-24.
88. Locke E, Flores-Garcia Y, Mayer BT, MacGill RS, Borate B, Salgado-Jimenez B, et al. Establishing RTS, S/AS01 as a benchmark for comparison to next-generation malaria vaccines in a mouse model. npj Vaccines. 2024;9(29):1-14.
89. Yihunie W, Kebede B, Tegegne BA, Getachew M, Abebe D, Aschale Y, et al. Systematic review of safety of RTS, S with AS01 and AS02 adjuvant systems using data from randomized controlled trials in infants, children, and adults. Clinical Pharmacology: Advances and Applications. 2023;15(2023):21-32.
90. Leroux-Roels G, Leroux-Roels I, Clement F, Ofori-Anyinam O, Lievens M, Jongert E, et al. Evaluation of the immune response to RTS, S/AS01 and RTS, S/AS02 adjuvanted vaccines: randomized, double-blind study in malaria-naïve adults. Human vaccines & immunotherapeutics. 2014;10(8):2211-2219.
91. Aderinto N, Olatunji G, Kokori E, Sikirullahi S, Aboje JE, Ojabo RE. A perspective on Oxford's R21/Matrix-M™ malaria vaccine and the future of global eradication efforts. Malaria Journal. 2024;23(16):1-4.
92. Hammershaimb EA, Berry AA. Pre-erythrocytic malaria vaccines: RTS, S, R21, and beyond. Expert Review of Vaccines. 2024;23(1):49-52.
93. Verma A, Anand A, Patel VA, Nazar MW, Mukherjee A, Karim KA, et al. Breaking the malaria barrier: the WHO-approved R21/Matrix-M vaccine and its global impact – an editorial. Annals of Medicine and Surgery. 2024;86(4):1824-1827.

University of Ghana http://ugspace.ug.edu.gh

94. Datoo MS, Natama MH, Somé A, Traoré O, Rouamba T, Bellamy D, et al. Efficacy of a low-dose candidate malaria vaccine, R21 in adjuvant Matrix-M, with seasonal administration to children in Burkina Faso: a randomised controlled trial. The Lancet. 2021;397(10287):1809-1818.
95. Ngou O, Nzoumbou-Boko R, Bakamba P, Boum Y, II. R21/Matrix-M malaria vaccine: a vital tool in the arsenal against malaria, not a silver bullet. The Lancet Infectious Diseases. 2024;24(5):438-439.
96. Dzi KT. Issues related to the approval of the R21/Matrix-M malaria vaccine for use in Nigeria and Ghana. Frontiers in Public Health. 2023;11(1237011):1-3.
97. Raghavendra K, Barik TK, Reddy BPN, Sharma P, Dash AP. Malaria vector control: from past to future. Parasitology research. 2011;108(4):757-779.
98. Takken W, Knols BG. Malaria vector control: current and future strategies. Trends in Parasitology. 2009;25(3):101-104.
99. Kamareddine L. The Biological Control of the Malaria Vector. Toxins. 2012;4(9):748-767.
100. Curtis C, Maxwell C, Magesa S, Rwegoshora R, Wilkes T. Insecticide-treated bed-nets for malaria mosquito control. Journal of the American Mosquito Control Association. 2006;22(3):501-506.
101. Skovmand O, Dang DM, Tran TQ, Bossellman R, Moore SJ. From the factory to the field: considerations of product characteristics for insecticide-treated net (ITN) bioefficacy testing. Malaria Journal. 2021;20(1):1-13.
102. Wheldrake A, Guillemois E, Arouni H, Chetty V, Zappa E, Russell SJ. Physical durability: are bed nets getting any stronger? Malaria Journal. 2024;23(19):1-10.
103. Benelli G, Beier JC. Current vector control challenges in the fight against malaria. Acta Tropica. 2017;174(2017):91-96.
104. Oxborough RM, Chilito KLF, Tokponnon F, Messenger LA. Malaria vector control in sub-Saharan Africa: complex trade-offs to combat the growing threat of insecticide resistance. The Lancet Planetary Health. 2024;8(10):804-812.
105. Böhmert AL, Logan RA, Portwood NM, Hartke J, Ingham VA. A descriptive review of next-generation insecticide-treated bed nets for malaria control. Frontiers in Malaria. 2024;2(1337572):1-8.
106. WHO. Guidelines for malaria vector control. 2019.
107. Grieco JP, Achee NL, Chareonviriyaphap T, Suwonkerd W, Chauhan K, Sardelis MR, et al. A new classification system for the actions of IRS chemicals traditionally used for malaria control. Plos one. 2007;2(8):1-11.
108. Okumu FO, Chipwaza B, Madumla EP, Mbeyela E, Lingamba G, Moore J, et al. Implications of bio-efficacy and persistence of insecticides when indoor residual spraying and long-lasting insecticide nets are combined for malaria prevention. Malaria Journal. 2012;11(378):1-13.
109. Ossè RA, Aïkpon R, Gbédjissi GL, Gnanguenon V, Sèzonlin M, Govoétchan R, et al. A shift from Indoor Residual Spraying (IRS) with bendiocarb to Long-Lasting Insecticidal (mosquito) Nets (LLINs) associated with changes in malaria transmission indicators in pyrethroid resistance areas in Benin. Parasites & Vectors. 2013;6(73):1-12.
110. Haider R, Das GK, Ahmed Z, Zameer S. Current and Future Prospects for Preventing Malaria Transmission via the Use of Insecticides. Clinical Medical Reviews and Reports. 2024;6(9):1-10.
111. Syme T, Fongnikin A, Todjinou D, Govoetchan R, Gbegbo M, Rowland M, et al. Which indoor residual spraying insecticide best complements standard pyrethroid long-

University of Ghana http://ugspace.ug.edu.gh

lasting insecticidal nets for improved control of pyrethroid resistant malaria vectors? Plos one. 2021;16(1):1-16.
112. Fillinger U, Lindsay SW. Larval source management for malaria control in Africa: myths and reality. Malaria Journal. 2011;10(353):1-10.
113. Gowelo S, Meijer P, Tizifa T, Malenga T, Mburu MM, Kabaghe AN, et al. Community Participation in Habitat Management and Larviciding for the Control of Malaria Vectors in Southern Malawi. The American Journal of Tropical Medicine and Hygiene. 2023;108(1):51-60.
114. Newby G, Chaki P, Latham M, Marrenjo D, Ochomo E, Nimmo D, et al. Larviciding for malaria control and elimination in Africa. Malaria Journal. 2025;24(16):1-10.
115. Kendie FA. Potential biological control agents against mosquito vector in the case of larvae stage: A review. World News of Natural Sciences. 2020;28(2020):34-50.
116. Okumu F, Moore SJ, Selvaraj P, Yafin AH, Juma EO, Shirima GG, et al. Elevating larval source management as a key strategy for controlling malaria and other vector-borne diseases in Africa. Parasites & Vectors. 2025;18(45):1-19.
117. Worrall E, Fillinger U. Large-scale use of mosquito larval source management for malaria control in Africa: a cost analysis. Malaria Journal. 2011;10(338):1-21.
118. Swai JK, Moore SJ. Beyond repellents: spatial emanators for the control of malaria in Africa. The Lancet. 2025;405(10473):101-103.
119. Achee NL, Perkins TA, Moore SM, Liu F, Sagara I, Van Hulle S, et al. Spatial repellents: The current roadmap to global recommendation of spatial repellents for public health use. Current Research in Parasitology & Vector-Borne Diseases. 2023;3(100107):1-9.
120. Ogoma SB, Ngonyani H, Simfukwe ET, Mseka A, Moore J, Maia MF, et al. The mode of action of spatial repellents and their impact on vectorial capacity of Anopheles gambiae sensu stricto. Plos one. 2014;9(12):1-21.
121. Beier JC, Müller GC, Gu W, Arheart KL, Schlein Y. Attractive toxic sugar bait (ATSB) methods decimate populations of Anopheles malaria vectors in arid environments regardless of the local availability of favoured sugar-source blossoms. Malaria Journal. 2012;11(31):1-7.
122. Zhang R, Zhao T, Xing D, Zhou X, Yu H, Geng D, et al. Development of Attractive Toxic Sugar Baits (ATSBs) System and Its Effectiveness in Mosquito Control. Insects. 2025;16(3):1-21.
123. Benedict MQ. Sterile Insect Technique: Lessons From the Past. Journal of Medical Entomology. 2021;58(5):1974-1979.
124. Myers A, Fagbohoun J, Houetohossou G, Ndombidje B, Govoetchan R, Todjinou D, et al. Identifying suitable methods for evaluating the sterilizing effects of pyriproxyfen on adult malaria vectors: a comparison of the oviposition and ovary dissection methods. Malaria Journal. 2024;23(164):1-15.
125. Apte RA, Smidler AL, Pai JJ, Chow ML, Chen S, Mondal A, et al. Eliminating malaria vectors with precision-guided sterile males. Proceedings of the National Academy of Sciences. 2024;121(27):1-12.
126. Alphey L, Benedict M, Bellini R, Clark GG, Dame DA, Service MW, et al. Sterile-Insect Methods for Control of Mosquito-Borne Diseases: An Analysis. Vector-Borne and Zoonotic Diseases. 2010;10(3):295-311.
127. Bhandari MK, Paudel M. Genetic, biological and sterile insect techniques: Insect pest management strategies: A review. Agricultural Reviews. 2024;45(3):390-399.
128. James S, Santos M. The Promise and Challenge of Genetic Biocontrol Approaches for Malaria Elimination. Tropical Medicine and Infectious Disease. 2023;8(4):1-16.

University of Ghana http://ugspace.ug.edu.gh

129. Hancock PA, North A, Leach AW, Winskill P, Ghani AC, Godfray HCJ, et al. The potential of gene drives in malaria vector species to control malaria in African environments. Nature Communications. 2024;15(8976):1-13.
130. Kefi M, Cardoso-Jaime V, Saab SA, Dimopoulos G. Curing mosquitoes with genetic approaches for malaria control. Trends in Parasitology. 2024;40(6):487-499.
131. Quinn C. Developing Genome Editing Tools for Functional Genetics in the Major Malaria Vector, Anopheles funestus [PhD]: Liverpool School of Tropical Medicine; 2024.
132. Mulebeke R, Yeka A, van Geertruyden J-P. Enhancing malaria elimination in high-transmission settings: the synergy of concurrent vector control and chemotherapy. Malaria Journal. 2025;24(105):1-6.
133. Alghamdi R. Bridging the gaps: Prioritizing research strategies for enhanced malaria control and elimination. Journal of Vector Borne Diseases. 2025;62(1):24-38.
134. Drouin E, Hautecoeur P, Markus M. Who was the first to visualize the malaria parasite? Parasites & Vectors. 2024;17(184):1-4.
135. Meshnick SR, Dobson MJ. The History of Antimalarial Drugs. In: Rosenthal PJ, editor. Antimalarial Chemotherapy: Mechanisms of Action, Resistance, and New Directions in Drug Discovery. Totowa, NJ: Humana Press; 2001.Page; 15-25.
136. Kayser O. Quinine. In: Kayser O, editor. From the Maluku to Molecules: How Natural Substances Write History. Berlin, Heidelberg: Springer Berlin Heidelberg; 2024.Page; 269-296.
137. Ma N, Zhang Z, Liao F, Jiang T, Tu Y. The birth of artemisinin. Pharmacology & Therapeutics. 2020;216(107658):1-4.
138. Samuel U, Adaeze E, Chinekwu N, Adaeze O, Lydia U, Chinazom A, et al. Combating Antimalarial Drug Resistance: Recent Advances and Future Perspectives. In: Pier Paolo P, editor. Malaria: Recent Advances and Future Perspectives

Rijeka: IntechOpen; 2022.Page; 242-248.
139. Butler A, Khan S, Ferguson E. A brief history of malaria chemotherapy. Journal of the Royal College of Physicians of Edinburgh. 2010;40(2):172-177.
140. Tu Y. Struktur und Eigenschaften von Artemisinin. In: Tu Y, editor. Von Artemisia annua L zu Artemisininen: Die Entdeckung und Entwicklung von Artemisininen und Malariamedikamenten. Berlin, Heidelberg: Springer Berlin Heidelberg; 2024.Page; 231-238.
141. Zheng D, Liu T, Yu S, Liu Z, Wang J, Wang Y. Antimalarial Mechanisms and Resistance Status of Artemisinin and Its Derivatives. Tropical Medicine and Infectious Diseases. 2024;9(9):1-12.
142. Paddon CJ, Keasling JD. Semi-synthetic artemisinin: a model for the use of synthetic biology in pharmaceutical development. Nature Reviews Microbiology. 2014;12(5):355-367.
143. Paddon CJ, Westfall PJ, Pitera DJ, Benjamin K, Fisher K, McPhee D, et al. High-level semi-synthetic production of the potent antimalarial artemisinin. Nature. 2013;496(7446):528-532.
144. Tayyab Ansari M, Saeed Saify Z, Sultana N, Ahmad I, Saeed-Ul-Hassan S, Tariq I, et al. Malaria and artemisinin derivatives: an updated review. Mini reviews in medicinal chemistry. 2013;13(13):1879-1902.
145. Florencia M, Brunella B. Commentary on the Obtention of Semi-Synthetic Derivatives from Natural Products for Medicinal Applications: Advances, Challenges, and Perspectives. Current Medicinal Chemistry. 2024;32(21):4147-4153.
146. Pinheiro L, Feitosa LM, SILVEIRA FF, Boechat N. Current antimalarial therapies and advances in the development of semi-synthetic artemisinin derivatives. Anais da Academia Brasileira de Ciências. 2018;90(Suppl. 2):1251-1271.

University of Ghana http://ugspace.ug.edu.gh

147. Navaratnam V, Mahsufi Mansor S, Sit N-W, Grace J, Li Q, Olliaro P. Pharmacokinetics of artemisinin-type compounds. Clinical pharmacokinetics. 2000;39(2000):255-270.
148. Karunajeewa HA. Artemisinins: Artemisinin, Dihydroartemisinin, Artemether and Artesunate. In: Staines HM, Krishna S, editors. Treatment and Prevention of Malaria: Antimalarial Drug Chemistry, Action and Use. Basel: Springer Basel; 2012.Page; 157-190.
149. Woodrow CJ, Haynes RK, Krishna S. Artemisinins. Postgraduate Medical Journal. 2005;81(952):71-78.
150. Lyu H-N, Ma N, Meng Y, Zhang X, Wong Y-K, Xu C, et al. Study towards improving artemisinin-based combination therapies. Natural product reports. 2021;38(7):1243-1250.
151. Aweeka FT, German PI. Clinical pharmacology of artemisinin-based combination therapies. Clinical pharmacokinetics. 2008;47(2008):91-102.
152. van der Pluijm RW, Amaratunga C, Dhorda M, Dondorp AM. Triple artemisinin-based combination therapies for malaria–a new paradigm? Trends in Parasitology. 2021;37(1):15-24.
153. Björkman A, Gil P, Alifrangis M. Alarming Plasmodium falciparum resistance to artemisinin-based combination therapy in Africa: the critical role of the partner drug. The Lancet Infectious Diseases. 2024;24(9):e540-e541.
154. Balikagala B, Fukuda N, Ikeda M, Katuro OT, Tachibana S-I, Yamauchi M, et al. Evidence of artemisinin-resistant malaria in Africa. New England Journal of Medicine. 2021;385(13):1163-1171.
155. Hanboonkunupakarn B, Tarning J, Pukrittayakamee S, Chotivanich K. Artemisinin resistance and malaria elimination: Where are we now? Frontiers in Pharmacology. 2022;13(876282):1-10.
156. Pandit K, Surolia N, Bhattacharjee S, Karmodiya K. The many paths to artemisinin resistance in Plasmodium falciparum. Trends in Parasitology. 2023;39(12):1060-1073.
157. Watson OJ, Muchiri S, Ward A, Meier-Sherling C, Asua V, Katairo T, et al. Risk of selection and timelines for the continued spread of artemisinin and partner drug resistance in Africa. In: . C-B-NIl, editor. medRxiv2024. p. 1-21.
158. Assefa A, Fola AA, Tasew G. Emergence of Plasmodium falciparum strains with artemisinin partial resistance in East Africa and the Horn of Africa: is there a need to panic? Malaria Journal. 2024;23(34):1-4.
159. Dereje N, Fallah MP, Shaweno T, Duga A, Mazaba ML, Raji T, et al. Resurgence of malaria and artemisinin resistance in Africa requires a concerted response. Nature Medicine. 2025;31(2):362-363.
160. Swinney D. Phenotypic vs. target-based drug discovery for first-in-class medicines. Clinical Pharmacology & Therapeutics. 2013;93(4):299-301.
161. Tisnerat C, Dassonville-Klimpt A, Gosselet F, Sonnet P. Antimalarial drug discovery: from quinine to the most recent promising clinical drug candidates. Current Medicinal Chemistry. 2022;29(19):3326-3365.
162. Hart CP. Finding the target after screening the phenotype. Drug Discovery Today. 2005;10(7):513-519.
163. Zheng W, Thorne N, McKew JC. Phenotypic screens as a renewed approach for drug discovery. Drug Discovery Today. 2013;18(21-22):1067-1073.
164. Lee JA, Uhlik MT, Moxham CM, Tomandl D, Sall DJ. Modern phenotypic drug discovery is a viable, neoclassic pharma strategy. Journal of medicinal chemistry. 2012;55(10):4527-4538.

University of Ghana http://ugspace.ug.edu.gh

165. Gilbert IH. Drug discovery for neglected diseases: molecular target-based and phenotypic approaches: miniperspectives series on phenotypic screening for antiinfective targets. Journal of medicinal chemistry. 2013;56(20):7719-7726.
166. Bathurst I, Hentschel C. Medicines for Malaria Venture: sustaining antimalarial drug development. Trends in Parasitology. 2006;22(7):301-307.
167. Ubben D, Poll EM. MMV in partnership: the Eurartesim® experience. Malaria Journal. 2013;12(211):1-10.
168. Nwaka S, Riopel L, Ubben D, Craft JC. Medicines for Malaria Venture new developments in antimalarials. Travel Medicine and Infectious Disease. 2004;2(3-4):161-170.
169. Rice CA, Troth EV, Russell AC, Kyle DE. Discovery of anti-amoebic inhibitors from screening the MMV pandemic response box on Balamuthia mandrillaris, Naegleria fowleri, and Acanthamoeba castellanii. Pathogens. 2020;9(476):1-17.
170. Samby K, Willis PA, Burrows JN, Laleu B, Webborn PJ. Actives from MMV Open Access Boxes? A suggested way forward. PLoS Pathogens. 2021;17(4):1-11.
171. Samby K, Besson D, Dutta A, Patra B, Doy A, Glossop P, et al. The Pandemic Response Box—Accelerating Drug Discovery Efforts after Disease Outbreaks. ACS Infectious Diseases. 2022;8(4):713-720.
172. Adam A, Besson D, Bryant R, Rees S, Willis PA, Burrows JN, et al. Global Health Priority Box—Proactive Pandemic Preparedness. ACS Infectious Diseases. 2024;10(12):4030-4039.
173. Akwensi J. Synthesis and Evaluation of Piperazine-Carboxamide Derivatives as Potential Antimalarial /Antimycrobial Agents [Mphil]. afribary: University of Ghana; 2018.
174. Xu G, Wang J, Gao GF, Liu CH. Insights into battles between Mycobacterium tuberculosis and macrophages. Protein & cell. 2014;5(10):728-736.
175. McNelis JC, Olefsky JM. Macrophages, immunity, and metabolic disease. Immunity. 2014;41(1):36-48.
176. Rohde K, Yates RM, Purdy GE, Russell DG. Mycobacterium tuberculosis and the environment within the phagosome. Immunological reviews. 2007;219(1):37-54.
177. Ferreira C, Estaquier J, Silvestre R. Immune-metabolic interactions between Leishmania and macrophage host. Current Opinion in Microbiology. 2021;63(1):231-237.
178. Menard D, Dondorp A. Antimalarial drug resistance: a threat to malaria elimination. Cold Spring Harbor perspectives in medicine. 2017;7(a025619):1-25.
179. Uzondu S, Echezona A, Nwagwu C, Onugwu A, Ugorji L, Agbo C, et al. Combating Antimalarial Drug Resistance: Recent Advances and Future Perspectives. Malaria: Recent Advances and Future Perspectives. Infectious diseases: IntechOpen; 2022.Page; 242-248.
180. Stokes BH, Dhingra SK, Rubiano K, Mok S, Straimer J, Gnädig NF, et al. Plasmodium falciparum K13 mutations in Africa and Asia impact artemisinin resistance and parasite fitness. eLife. 2021;10(e66277):1-29.
181. Flegg JA, Kandanaarachchi S, Guerin PJ, Dondorp AM, Nosten FH, Otienoburu SD, et al. Spatio-temporal spread of artemisinin resistance in Southeast Asia. PLOS Computational Biology. 2024;20(4):1-13.
182. Swinney DC. The contribution of mechanistic understanding to phenotypic screening for first-in-class medicines. Journal of biomolecular screening. 2013;18(10):1186-1192.
183. Hovlid ML, Winzeler EA. Phenotypic screens in antimalarial drug discovery. Trends in Parasitology. 2016;32(9):697-707.
184. USAID. Envisioning a Malaria Free World [Available from: https://www.usaid.gov/global-health/health-areas/malaria?utm.

University of Ghana http://ugspace.ug.edu.gh

185. Newby G, Bennett A, Larson E, Cotter C, Shretta R, Phillips AA, et al. The path to eradication: a progress report on the malaria-eliminating countries. The Lancet. 2016;387(10029):1775-1784.
186. Nabarro DN, Tayler EM. The" roll back malaria" campaign. American Association for the Advancement of Science; 1998. p. 2067-2068.
187. Malaria RB. RBM partnership to end malaria. 2019.
188. Yamey G. Roll Back Malaria: a failing global health campaign. British Medical Journal Publishing Group; 2004. p. 1086-1087.
189. Kerouedan D. The Global Fund to fight HIV/AIDS, TB and Malaria 5-y: evaluation policy issues. Bulletin de la Société de pathologie exotique. 2010;103(2):119-122.
190. Fund TG. Framework on private sector engagement. 2019.
191. Jakubowski A, Stearns SC, Kruk ME, Angeles G, Thirumurthy H. The US President's Malaria Initiative and under-5 child mortality in sub-Saharan Africa: A difference-in-differences analysis. PLoS medicine. 2017;14(6):1-20.
192. Plan MO. President's malaria initiative. Mali FY: Malar Oper Plan. 2009.
193. Winskill P, Slater HC, Griffin JT, Ghani AC, Walker PG. The US President's Malaria Initiative, Plasmodium falciparum transmission and mortality: A modelling study. PLoS medicine. 2017;14(11):1-14.
194. WHO. Global Malaria Programme 2025 [Available from: https://www.who.int/teams/global-malaria-programme.
195. Patouillard E, Griffin J, Bhatt S, Ghani A, Cibulskis R. Global investment targets for malaria control and elimination between 2016 and 2030. BMJ global health. 2017;2(e000176):1-11.
196. Organization WH. Global technical strategy for malaria 2016-2030: World Health Organization; 2015.
197. Turner JW, Robinson JD. Malaria no more: Nothing but nets. Health Communication. 2014;29(10):1067-1068.
198. Bhattacharyya B. The role of media campaign in india's quest to eliminate malaria by 2030: A critical analysis. Journal of Scientific Research. 2020;64(1):64-67.
199. More MN. Let's end malaria in our lifetime 2017 [Available from: https://www.malarianomore.org/.
200. Nakweya G. Malaria: African leaders pledge to tackle funding gap amid uncertainty over foreign aid. British Medical Journal Publishing Group; 2025.
201. Sambo LG, Ki-Zerbo G, Kirigia JM, editors. Malaria control in the African Region: perceptions and viewspoints on proceedings of the Africa Leaders Malaria Alliance (ALMA). BMC proceedings; 2011: Springer.
202. Sokunbi TO, Omojuyigbe JO, Bakenne HA, Adebisi YA. Nigeria end malaria council: what to expect. Annals of Medicine and Surgery. 2022;82(104690):1-4.
203. Council Em. End Malaria Council 2020 [cited 2025 15/4/2025]. Available from: https://endmalariacouncil.org/.
204. Mswati IK. An Africa free of malaria. The Lancet. 2019;394(10203):988-989.
205. WHO. WHO Malaria Policy Advisory Group (MPAG) meeting report, 18–20 April 2023: World Health Organization; 2023.
206. Owings L. The 25 countries that could beat malaria by 2025. SciDev net-Health. 2021.
207. Wangmo LD, Belo OMF, Penjor K, Drukpa T, do Rosario de Fatima Mota M, Viegas OdS, et al. Sustaining progress towards malaria elimination by 2025: Lessons from Bhutan & Timor-Leste. The Lancet Regional Health – Western Pacific. 2022;22(100429):1-5.
208. WHO.

University of Ghana http://ugspace.ug.edu.gh

Georgia certified malaria-free by WHO 2025 [cited 2025. Available from: https://www.who.int/news/item/23-01-2025-georgia-certified-malaria-free-by-who.
209. WHO. Global Malaria Programme 2025 [Available from: https://www.who.int/teams/global-malaria-programme/elimination/countries-and-territories-certified-malaria-free-by-who.
210. Baxromovna MS. Malaria disease and its etiology, pathophsiology and treatment. Miasto Przyszłości. 2024;48(1):217-222.
211. Sehrawat N, Sharma A. Malaria: A Concern to Public Health. SHODH PRERAK. 2011;1(3):194-201.
212. Chandley P RR, Kumar S and Rohatgi S Host-parasite interactions during Plasmodium infection: Implications for immunotherapies. Frontiers in Immunology. 2023;13(1):1-27.
213. Tuteja R. Malaria− an overview. The FEBS journal. 2007;274(18):4670-4679.
214. Matteelli A, Castelli F, Caligaris S. Life cycle of malaria parasites. Handbook of Malaria infection in the tropics 1st ed: Bologna: Associazione Italiana" Amici di R. Follereau; 1997.Page; 17-23.
215. Bannister LH, Hopkins JM, Fowler RE, Krishna S, Mitchell GH. A Brief Illustrated Guide to the Ultrastructure of *Plasmodium falciparum* Asexual Blood Stages. Parasitology Today. 2000;16(10):427-433.
216. Sigala PA, Goldberg DE. The peculiarities and paradoxes of Plasmodium heme metabolism. Annual review of microbiology. 2014;68(1):259-278.
217. Klonis N, Creek DJ, Tilley L. Iron and heme metabolism in Plasmodium falciparum and the mechanism of action of artemisinins. Current Opinion in Microbiology. 2013;16(6):722-727.
218. Kloehn J, Harding CR, Soldati-Favre D. Supply and demand—heme synthesis, salvage and utilization by Apicomplexa. The FEBS journal. 2021;288(2):382-404.
219. Fujioka H, Aikawa M. Structure and life cycle. Chemical Immunology. 2002;80(1):1-26.
220. Bakar NA, Klonis N, Hanssen E, Chan C, Tilley L. Digestive-vacuole genesis and endocytic processes in the early intraerythrocytic stages of Plasmodium falciparum. Journal of cell science. 2010;123(3):441-450.
221. Fujioka H, Aikawa M. The malaria parasite and its lifecycle. Malaria: molecular and clinical aspects First edition Amsterdam: Harwood Academic Publishers. 1999:21-36.
222. Meibalan E, Marti M. Biology of malaria transmission. Cold Spring Harbor perspectives in medicine. 2017;7(3):1-16.
223. Alano P. Plasmodium falciparum gametocytes: still many secrets of a hidden life. Molecular microbiology. 2007;66(2):291-302.
224. Gerald N, Mahajan B, Kumar S. Mitosis in the Human Malaria Parasite Plasmodium falciparum. Eukaryotic Cell. 2011;10(4):474-482.
225. Khan SM, Waters AP. Malaria parasite transmission stages: an update. Trends in Parasitology. 2004;20(12):575-580.
226. Maturana CR, De Oliveira AD, Nadal S, Bilalli B, Serrat FZ, Soley ME, et al. Advances and challenges in automated malaria diagnosis using digital microscopy imaging with artificial intelligence tools: A review. Frontiers in microbiology. 2022;13(1006659):1-17.
227. van Dooren GG, Marti M, Tonkin CJ, Stimmler LM, Cowman AF, McFadden GI. Development of the endoplasmic reticulum, mitochondrion and apicoplast during the asexual life cycle of Plasmodium falciparum. Molecular microbiology. 2005;57(2):405-419.
228. Siciliano G, Alano P. Enlightening the malaria parasite life cycle: bioluminescent Plasmodium in fundamental and applied research. Frontiers in microbiology. 2015;6(391):1-8.

University of Ghana http://ugspace.ug.edu.gh

229. Maier AG, Matuschewski K, Zhang M, Rug M. Plasmodium falciparum. Trends in Parasitology. 2019;35(6):481-482.
230. Hulden L, Hulden L. Activation of the hypnozoite: a part of Plasmodium vivax life cycle and survival. Malaria Journal. 2011;10(90):1-6.
231. Galinski MR, Barnwell JW. Plasmodium vivax: who cares? Malaria Journal. 2008;7(S9):1-18.
232. Adams JH, Mueller I. The biology of Plasmodium vivax. Cold Spring Harbor perspectives in medicine. 2017;7(a025585):1-13.
233. Brasil P, de Pina Costa A, Pedro RS, da Silveira Bressan C, da Silva S, Tauil PL, et al. Unexpectedly long incubation period of Plasmodium vivax malaria, in the absence of chemoprophylaxis, in patients diagnosed outside the transmission area in Brazil. Malaria Journal. 2011;10(122):1-5.
234. White NJ. Determinants of relapse periodicity in Plasmodium vivax malaria. Malaria Journal. 2011;10(297):1-36.
235. Surit T, Sripoorote P, Kumpitak C, Suansomjit C, Maneechai N, Cui L, et al. Transmission efficiency of Plasmodium vivax at low parasitaemia. Malaria Journal. 2023;22(22):1-8.
236. Sattabongkot J, Tsuboi T, Zollner GE, Sirichaisinthop J, Cui L. Plasmodium vivax transmission: chances for control? Trends in Parasitology. 2004;20(4):192-198.
237. Tadesse FG, Slater HC, Chali W, Teelen K, Lanke K, Belachew M, et al. The relative contribution of symptomatic and asymptomatic Plasmodium vivax and Plasmodium falciparum infections to the infectious reservoir in a low-endemic setting in Ethiopia. Clinical infectious diseases. 2018;66(12):1883-1891.
238. Oguike MC, Betson M, Burke M, Nolder D, Stothard JR, Kleinschmidt I, et al. Plasmodium ovale curtisi and Plasmodium ovale wallikeri circulate simultaneously in African communities. International journal for parasitology. 2011;41(6):677-683.
239. Alemu A, Fuehrer H-P, Getnet G, Tessema B, Noedl H. Plasmodium ovale curtisi and Plasmodium ovale wallikeri in North-West Ethiopia. Malaria Journal. 2013;12(346):1-7.
240. Lysenko AJ, Beljaev A. An analysis of the geographical distribution of Plasmodium ovale. Bulletin of the World Health Organization. 1969;40(3):383–394.
241. Richter J, Franken G, Mehlhorn H, Labisch A, Häussinger D. What is the evidence for the existence of Plasmodium ovale hypnozoites? Parasitology research. 2010;107(2010):1285-1290.
242. Markus MB. Do hypnozoites cause relapse in malaria? Trends in Parasitology. 2015;31(6):239-245.
243. Kotepui M, Masangkay FR, Kotepui KU, De Jesus Milanez G. Misidentification of Plasmodium ovale as Plasmodium vivax malaria by a microscopic method: a meta-analysis of confirmed P. ovale cases. Scientific reports. 2020;10(21807):1-13.
244. Wångdahl A, Sondén K, Wyss K, Stenström C, Björklund D, Zhang J, et al. Relapse of Plasmodium vivax and Plasmodium ovale Malaria With and Without Primaquine Treatment in a Nonendemic Area. Clinical infectious diseases. 2021;74(7):1199-1207.
245. Collins WE, Jeffery GM. Plasmodium malariae: parasite and disease. Clinical microbiology reviews. 2007;20(4):579-592.
246. Yman V, Wandell G, Mutemi DD, Miglar A, Asghar M, Hammar U, et al. Persistent transmission of Plasmodium malariae and Plasmodium ovale species in an area of declining Plasmodium falciparum transmission in eastern Tanzania. PLoS neglected tropical diseases. 2019;13(5):1-16.

University of Ghana http://ugspace.ug.edu.gh

247. Fuehrer H-P, Campino S, Sutherland CJ. The primate malaria parasites Plasmodium malariae, Plasmodium brasilianum and Plasmodium ovale spp.: genomic insights into distribution, dispersal and host transitions. Malaria Journal. 2022;21(138):1-25.
248. Ansari HR, Templeton TJ, Subudhi AK, Ramaprasad A, Tang J, Lu F, et al. Genome-scale comparison of expanded gene families in Plasmodium ovale wallikeri and Plasmodium ovale curtisi with Plasmodium malariae and with other Plasmodium species. International journal for parasitology. 2016;46(11):685-696.
249. Mackerras M, Ercole Q. Observations on the life-cycle of plasmodium malariae. Australian Journal of Experimental Biology & Medical Science. 1948;26(6):515-521.
250. Bray R, Garnham P. The life-cycle of primate malaria parasites. British medical bulletin. 1982;38(2):117-122.
251. Ahmed M, Cox-Singh J. P lasmodium knowlesi–an emerging pathogen. ISBT science series. 2015;10(S1):134-140.
252. Singh B, Daneshvar C. Human infections and detection of Plasmodium knowlesi. Clinical microbiology reviews. 2013;26(2):165-184.
253. Cox-Singh J, Davis TME, Lee K-S, Shamsul SSG, Matusop A, Ratnam S, et al. Plasmodium knowlesi Malaria in Humans Is Widely Distributed and Potentially Life Threatening. Clinical infectious diseases. 2008;46(2):165-171.
254. Wesolowski R, Wozniak A, Mila-Kierzenkowska C, Szewczyk-Golec K. Plasmodium knowlesi as a threat to global public health. The Korean journal of parasitology. 2015;53(5):575–581.
255. Meshnick SR. Artemisinin: mechanisms of action, resistance and toxicity. International journal for parasitology. 2002;32(13):1655-1660.
256. Pessanha de Carvalho L, Kreidenweiss A, Held J. Drug repurposing: a review of old and new antibiotics for the treatment of malaria: identifying antibiotics with a fast onset of antiplasmodial action. Molecules. 2021;26(2304):1-19.
257. Shanks GD. Historical 8-Aminoquinoline Combinations: Not All Antimalarial Drugs Work Well Together. American Journal of Tropical Medicine and Hygiene 2022;107(5):964-967.
258. Waters NC, Edstein MD. 8-Aminoquinolines: primaquine and tafenoquine. Treatment and prevention of malaria: antimalarial drug chemistry, action and use: Springer; 2011.Page; 69-94.
259. Krishna S, Staines HM. Non-antifolate antibiotics: clindamycin, doxycycline, azithromycin and fosmidomycin. Treatment and prevention of malaria: antimalarial drug chemistry, action and use: Springer; 2011.Page; 141-156.
260. Lell B, Kremsner Peter G. Clindamycin as an Antimalarial Drug: Review of Clinical Trials. Antimicrobial agents and chemotherapy. 2002;46(8):2315-2320.
261. Tan KR, Magill AJ, Parise ME, Arguin PM. Doxycycline for malaria chemoprophylaxis and treatment: report from the CDC expert meeting on malaria chemoprophylaxis. The American Journal of Tropical Medicine and Hygiene. 2011;84(1):1-9.
262. Visentin M, Zhao R, Goldman ID. The antifolates. Hematol Oncol Clin North Am. 2012;26(3):629-648.
263. Pethrak C, Posayapisit N, Pengon J, Suwanakitti N, Saeung A, Shorum M, et al. New Insights into Antimalarial Chemopreventive Activity of Antifolates. Antimicrobial agents and chemotherapy. 2022;66(2):1-13.
264. Oranusi SU, Mameh EO, Oyegbade SA, Balogun DO, Aririguzoh V-GO. Inhibitors of Protein Targets of Plasmodium falciparum. Journal of Pure & Applied Microbiology. 2024;18(4):21-51.

University of Ghana http://ugspace.ug.edu.gh

265. Kayentao K, Garner P, Maria van Eijk A, Naidoo I, Roper C, Mulokozi A, et al. Intermittent Preventive Therapy for Malaria During Pregnancy Using 2 vs 3 or More Doses of Sulfadoxine-Pyrimethamine and Risk of Low Birth Weight in Africa: Systematic Review and Meta-analysis. JAMA. 2013;309(6):594-604.
266. Divala TH, Cohee LM, Laufer MK. The remarkable tenacity of sulfadoxine-pyrimethamine. The Lancet Infectious Diseases. 2019;19(5):460-461.
267. Schnyder JL, Birkhoff DC, Jarings MC, Hermans SM, Grobusch MP, de Jong HK. Travellers' adherence to atovaquone/proguanil malaria chemoprophylaxis after return from endemic areas. Travel Medicine and Infectious Disease. 2025;64(102812):1-7.
268. Gregson A, Plowe CV. Mechanisms of Resistance of Malaria Parasites to Antifolates. Pharmacological Reviews. 2005;57(1):117-145.
269. Basu L, Bhowmik B, Pal A, Roy P, Dey B, Mondal R, et al. Drug resistance and new strategies of prevention against malaria: An ongoing battle. Journal of Vector Borne Diseases. 2025;62(1):9-15.
270. Julianto TS, Rachmawaty FJ, Tamhid HA, Putri BS. The potential antimalarial drug of aryl amino alcohol derivatives from eugenol: synthesis, in-vitro and in-silico analysis of bioactivity. RASAYAN Journal of Chemistry. 2023;16(3):1425-1434.
271. Wicht KJ, Mok S, Fidock DA. Molecular mechanisms of drug resistance in Plasmodium falciparum malaria. Annual review of microbiology. 2020;74(1):431-454.
272. Saifi A. Antimalarial drugs: Mode of action and status of resistance. African Journal of Pharmacy and Pharmacology. 2013;7(5):148-156.
273. Olliaro P. Mode of action and mechanisms of resistance for antimalarial drugs. Pharmacology & Therapeutics. 2001;89(2):207-219.
274. Poulin R, Secrist 3rd J, Pegg A. Effect of 1-amino-oxy-3-aminopropane on polyamine metabolism and growth of L1210 cells. Biochemical Journal. 1989;263(1):215-221.
275. Vaidergorn MM, Carneiro ZA, Lopes CD, de Albuquerque S, Reis FC, Nikolaou S, et al. β-amino alcohols and their respective 2-phenyl-N-alkyl aziridines as potential DNA minor groove binders. European Journal of Medicinal Chemistry. 2018;157(1):657-664.
276. Gevorgyan G, Hakobyan N, Agababyan A, Nersesyan L, Aharonyan A, Danielyan I, et al. Synthesis of Tertiary Piperazine Aminoalcohols and their Dihydrochlorides and their Influence on DNA Methylation Processes In Vitro. Pharmaceutical Chemistry Journal. 2021;55(1):138-141.
277. Egan TJ. Quinoline antimalarials. Expert Opinion on Therapeutic Patents. 2001;11(2):185-209.
278. Palmer KJ, Holliday SM, Brogden RN. Mefloquine. Drugs. 1993;45(3):430-475.
279. Achan J, Talisuna AO, Erhart A, Yeka A, Tibenderana JK, Baliraine FN, et al. Quinine, an old anti-malarial drug in a modern world: role in the treatment of malaria. Malaria Journal. 2011;10(144):1-12.
280. Makanga M, Krudsood S. The clinical efficacy of artemether/lumefantrine (Coartem®). Malaria Journal. 2009;8(S5):1-12.
281. Rojas-Rivero L, Gay F, Bustos MD, Ciceron L, Pichet C, Danis M, et al. Mefloquine-halofantrine cross-resistance in Plasmodium falciparum induced by intermittent mefloquine pressure. The American Journal of Tropical Medicine and Hygiene. 1992;47(3):372-377.
282. Dow GS, Koenig ML, Wolf L, Gerena L, Lopez-Sanchez M, Hudson TH, et al. The antimalarial potential of 4-quinolinecarbinolamines may be limited due to neurotoxicity and cross-resistance in mefloquine-resistant Plasmodium falciparum strains. Antimicrobial agents and chemotherapy. 2004;48(7):2624-2632.
283. Duraisingh MT, Cowman AF. Contribution of the pfmdr1 gene to antimalarial drug-resistance. Acta Tropica. 2005;94(3):181-190.

University of Ghana http://ugspace.ug.edu.gh

284. Reiling SJ, Rohrbach P. Monitoring PfMDR1 transport in Plasmodium falciparum. Malaria Journal. 2015;14(270):1-11.
285. Ferreira PE, Holmgren G, Veiga MI, Uhlén P, Kaneko A, Gil JP. PfMDR1: mechanisms of transport modulation by functional polymorphisms. Plos one. 2011;6(9):1-8.
286. Basco LK, Ringwald P. Molecular epidemiology of malaria in Cameroon. X. Evaluation of PFMDR1 mutations as genetic markers for resistance to amino alcohols and artemisinin derivatives. The American Journal of Tropical Medicine and Hygiene. 2002;66(6):667-671.
287. Ibraheem ZO, Abd Majid R, Noor SM, Sedik HM, Basir R. Role of different Pfcrt and Pfmdr-1 mutations in conferring resistance to Antimalaria drugs in Plasmodium falciparum. Malaria research and treatment. 2014;2014(1):1-17.
288. Siswantoro H, Russell B, Ratcliff A, Prasetyorini B, Chalfein F, Marfurt J, et al. In vivo and in vitro efficacy of chloroquine against Plasmodium malariae and P. ovale in Papua, Indonesia. Antimicrobial agents and chemotherapy. 2011;55(1):197-202.
289. Grigg MJ, William T, Menon J, Dhanaraj P, Barber BE, Wilkes CS, et al. Artesunate-mefloquine versus chloroquine for treatment of uncomplicated Plasmodium knowlesi malaria in Malaysia (ACT KNOW): an open-label, randomised controlled trial. The Lancet Infectious Diseases. 2016;16(2):180-188.
290. Basilico N, Parapini S, Sparatore A, Romeo S, Misiano P, Vivas L, et al. In Vivo and In Vitro Activities and ADME-Tox Profile of a Quinolizidine-Modified 4-Aminoquinoline: A Potent Anti-P. falciparum and Anti-P. vivax Blood-Stage Antimalarial. Molecules. 2017;22(12):1-15.
291. Shreekant D, Bhimanna K. 4-Aminoquinolines: an overview of antimalarial chemotherapy. Medicinal chemistry. 2016;6(1):1-11.
292. O'Neill PM, Barton VE, Ward SA, Chadwick J. 4-Aminoquinolines: Chloroquine, Amodiaquine and Next-Generation Analogues. In: Staines HM, Krishna S, editors. Treatment and Prevention of Malaria: Antimalarial Drug Chemistry, Action and Use. Basel: Springer Basel; 2012.Page; 19-44.
293. Daily JP, Minuti A, Khan N. Diagnosis, Treatment, and Prevention of Malaria in the US: A Review. JAMA. 2022;328(5):460-471.
294. Calderón-Ruiz P, Velez-Tobón G, Bolívar-Hernández S, Murcia-Montaño LM, Tobón-Castaño A. Chloroquine-primaquine therapeutic response and safety in patients with uncomplicated Plasmodium vivax malaria in the Colombian Amazon region. Malaria Journal. 2024;23(348):1-11.
295. Hui Z, Zheng X, Long-can Z, Mao-hua P, Zhao-qing Y. Research progress of amodiaquine as an antimalarial drug. Chinese Journal of Parasitology and Parasitic Diseases. 2022;40(6):786-791.
296. Shafik SH, Cobbold SA, Barkat K, Richards SN, Lancaster NS, Llinás M, et al. The natural function of the malaria parasite's chloroquine resistance transporter. Nature Communications. 2020;11(1):1-16.
297. Berger F, Gomez GM, Sanchez CP, Posch B, Planelles G, Sohraby F, et al. pH-dependence of the Plasmodium falciparum chloroquine resistance transporter is linked to the transport cycle. Nature Communications. 2023;14(1):1-16.
298. Coppée R, Sabbagh A, Clain J. Structural and evolutionary analyses of the Plasmodium falciparum chloroquine resistance transporter. Scientific reports. 2020;10(1):1-15.
299. Johnson DJ, Fidock DA, Mungthin M, Lakshmanan V, Sidhu AB, Bray PG, et al. Evidence for a central role for PfCRT in conferring Plasmodium falciparum resistance to diverse antimalarial agents. Molecular Cell. 2004;15(6):867-877.

University of Ghana http://ugspace.ug.edu.gh

300. Ecker A, Lehane AM, Clain J, Fidock DA. PfCRT and its role in antimalarial drug resistance. Trends in Parasitology. 2012;28(11):504-514.
301. Fidock DA, Nomura T, Talley AK, Cooper RA, Dzekunov SM, Ferdig MT, et al. Mutations in the P. falciparum digestive vacuole transmembrane protein PfCRT and evidence for their role in chloroquine resistance. Molecular Cell. 2000;6(4):861-871.
302. Wurtz N, Fall B, Pascual A, Fall M, Baret E, Camara C, et al. Role of Pfmdr1 in in vitro Plasmodium falciparum susceptibility to chloroquine, quinine, monodesethylamodiaquine, mefloquine, lumefantrine, and dihydroartemisinin. Antimicrobial agents and chemotherapy. 2014;58(12):7032-7040.
303. Shafik SH, Richards SN, Corry B, Martin RE. Mechanistic basis for multidrug resistance and collateral drug sensitivity conferred to the malaria parasite by polymorphisms in PfMDR1 and PfCRT. PLoS biology. 2022;20(5):1-40.
304. Sá JM, Twu O, Hayton K, Reyes S, Fay MP, Ringwald P, et al. Geographic patterns of Plasmodium falciparum drug resistance distinguished by differential responses to amodiaquine and chloroquine. Proceedings of the National Academy of Sciences. 2009;106(45):18883-18889.
305. Lu X, Altharawi A, Gut J, Rosenthal PJ, Long TE. 1,4-Naphthoquinone Cations as Antiplasmodial Agents: Hydroxy-, Acyloxy-, and Alkoxy-Substituted Analogues. ACS Medicinal Chemistry Letters. 2012;3(12):1029-1033.
306. Barton V, Fisher N, Biagini GA, Ward SA, O'Neill PM. Inhibiting Plasmodium cytochrome bc1: a complex issue. Current Opinion in Chemical Biology. 2010;14(4):440-446.
307. Schuck DC, Ferreira SB, Cruz LN, da Rocha DR, Moraes MS, Nakabashi M, et al. Biological evaluation of hydroxynaphthoquinones as anti-malarials. Malaria Journal. 2013;12(234):1-6.
308. Paengsri W, Promsawan N, Baramee A. Synthesis and Evaluation of 2-Hydroxy-1,4-naphthoquinone Derivatives as Potent Antimalarial Agents. Chemical and Pharmaceutical Bulletin. 2021;69(3):253-257.
309. Kapadia GJ, Azuine MA, Balasubramanian V, Sridhar R. Aminonaphthoquinones—a novel class of compounds with potent antimalarial activity against plasmodium falciparum. Pharmacological Research. 2001;43(4):363-367.
310. Nixon GL, Moss DM, Shone AE, Lalloo DG, Fisher N, O'Neill PM, et al. Antimalarial pharmacology and therapeutics of atovaquone. Journal of Antimicrobial Chemotherapy. 2013;68(5):977-985.
311. Luth MR, Gupta P, Ottilie S, Winzeler EA. Using in Vitro Evolution and Whole Genome Analysis To Discover Next Generation Targets for Antimalarial Drug Discovery. ACS Infectious Diseases. 2018;4(3):301-314.
312. Kuemmerle A, Gossen D, Marx MW, Lorch U, Szramowska M, Kumar A, et al. A randomized, open-label two-period crossover pilot study to evaluate the relative bioavailability in the fed state of atovaquone-proguanil (Atoguanil™) versus atovaquone-proguanil hydrochloride (Malarone®) in healthy adult participants. Naunyn-Schmiedeberg's Archives of Pharmacology. 2024;397(12):9823-9832.
313. Sornchai Looareesuwan JDC, Craig J. Canfield, David B. A. Hutsinson. Malarone (Atovaquone and Proguanil Hydrochloride): A Review of its Clinical Development for Treatment of Malaria. American Journal of Tropical Medicine and Hygiene. 1999;60(4):533-541.
314. Blanshard A, Hine P. Atovaquone-proguanil for treating uncomplicated Plasmodium falciparum malaria. Cochrane Database of Systematic Reviews. 2021;1(CD004529):1-133.
315. Stickles AM, Smilkstein MJ, Morrisey JM, Li Y, Forquer IP, Kelly JX, et al. Atovaquone and ELQ-300 combination therapy as a novel dual-site cytochrome bc 1

University of Ghana http://ugspace.ug.edu.gh

inhibition strategy for malaria. Antimicrobial agents and chemotherapy. 2016;60(8):4853-4859.
316. Looareesuwan S, Viravan C, Webster HK, Kyle DE, Hutchinson DB, Canfield CJ. Clinical studies of atovaquone, alone or in combination with other antimalarial drugs, for treatment of acute uncomplicated malaria in Thailand. The American Journal of Tropical Medicine and Hygiene. 1996;54(1):62-66.
317. Vaidya AB, Mather MW. Atovaquone resistance in malaria parasites. Drug Resistance Updates. 2000;3(5):283-287.
318. Akhoon BA, Singh KP, Varshney M, Gupta SK, Shukla Y, Gupta SK. Understanding the mechanism of atovaquone drug resistance in Plasmodium falciparum cytochrome b mutation Y268S using computational methods. Plos one. 2014;9(10):1-12.
319. Korsinczky M, Chen N, Kotecka B, Saul A, Rieckmann K, Cheng Q. Mutations in Plasmodium falciparum Cytochrome That Are Associated with Atovaquone Resistance Are Located at a Putative Drug-Binding Site. Antimicrobial agents and chemotherapy. 2000;44(8):2100-2108.
320. Gautam A, Ahmed T, Batra V, Paliwal J. Pharmacokinetics and pharmacodynamics of endoperoxide antimalarials. Current drug metabolism. 2009;10(3):289-306.
321. Terent'ev AO, Borisov DA, Vil VA, Dembitsky VM. Synthesis of five- and six-membered cyclic organic peroxides: Key transformations into peroxide ring-retaining products. Beilstein Journal of Organic Chemistry. 2014;10(1):34-114.
322. Gomes GDP, Vil V, Terent'ev A, Alabugin IV. Stereoelectronic source of the anomalous stability of bis-peroxides. Chemical Science. 2015;6(12):6783-6791.
323. Meshnick SR, Taylor TE, Kamchonwongpaisan S. Artemisinin and the antimalarial endoperoxides: from herbal remedy to targeted chemotherapy. Microbiology and molecular biology Reviews. 1996;60(2):301-315.
324. Meshnick SR. The mode of action of antimalarial endoperoxides. Transactions of the Royal Society of Tropical Medicine and Hygiene. 1994;88(Supplement_1):31-32.
325. Clennan EL. Aromatic endoperoxides. Photochemistry and Photobiology. 2023;99(2):204-220.
326. O'Neill PM, Posner GH. A Medicinal Chemistry Perspective on Artemisinin and Related Endoperoxides. Journal of medicinal chemistry. 2004;47(12):2945-2964.
327. White NJ. Qinghaosu (artemisinin): the price of success. Science. 2008;320(5874):330-334.
328. O'Neill PM, Barton VE, Ward SA. The Molecular Mechanism of Action of Artemisinin—The Debate Continues. Molecules. 2010;15(3):1705-1721.
329. Cui L, and Su X-z. Discovery, mechanisms of action and combination therapy of artemisinin. Expert Review of Anti-infective Therapy. 2009;7(8):999-1013.
330. Mwaiswelo R, Ngasala B. Evaluation of residual submicroscopic Plasmodium falciparum parasites 3 days after initiation of treatment with artemisinin-based combination therapy. Malaria Journal. 2020;19(162):1-9.
331. Wiesner J, Ortmann R, Jomaa H, Schlitzer M. New antimalarial drugs. Angewandte Chemie International Edition. 2003;42(43):5274-5293.
332. Price RN. Artemisinin drugs: novel antimalarial agents. Expert Opinion on Investigational Drugs. 2000;9(8):1815-1827.
333. Eastman RT, Fidock DA. Artemisinin-based combination therapies: a vital tool in efforts to eliminate malaria. Nature Reviews Microbiology. 2009;7(12):864-874.
334. Duffy PE, Mutabingwa TK. Artemisinin combination therapies. The Lancet. 2006;367(9528):2037-2039.

University of Ghana http://ugspace.ug.edu.gh

335. van der Pluijm RW, Amaratunga C, Dhorda M, Dondorp AM. Triple Artemisinin-Based Combination Therapies for Malaria; A New Paradigm? Trends in Parasitology. 2021;37(1):15-24.
336. Stover KR, King ST, Robinson J. Artemether-lumefantrine: an option for malaria. Annals of Pharmacotherapy. 2012;46(4):567-577.
337. Sirima SB, Gansane A. Artesunate–amodiaquine for the treatment of uncomplicated malaria. Expert Opinion on Investigational Drugs. 2007;16(7):1079-1085.
338. Price R, Nosten F, Luxemburger C, Van Vugt M, Phaipun L, Chongsuphajaisiddhi T, et al. Artesunate/mefloquine treatment of multi-drug resistant falciparum malaria. Transactions of the Royal Society of Tropical Medicine and Hygiene. 1997;91(5):574-577.
339. Keating GM. Dihydroartemisinin/Piperaquine: a review of its use in the treatment of uncomplicated Plasmodium falciparum malaria. Drugs. 2012;72(1):937-961.
340. Priotto G, Kabakyenga J, Pinoges L, Ruiz A, Eriksson T, Coussement F, et al. Artesunate and sulfadoxine-pyrimethamine combinations for the treatment of uncomplicated Plasmodium falciparum malaria in Uganda: a randomized, double-blind, placebo-controlled trial. Transactions of the Royal Society of Tropical Medicine and Hygiene. 2003;97(3):325-330.
341. Karunajeewa H. Pyronaridine–Artesunate. Kucers' The Use of Antibiotics: CRC Press; 2017.Page; 3006-3018.
342. Chu W-Y, Dorlo TPC. Pyronaridine: a review of its clinical pharmacology in the treatment of malaria. Journal of Antimicrobial Chemotherapy. 2023;78(10):2406-2418.
343. Alebachew M, Gelaye W, Abate MA, Sime H, Hailgiorgis H, Gidey B, et al. Therapeutic efficacy of pyronaridine-artesunate (Pyramax. Malaria Journal. 2023;22(186):1-10.
344. Fu S, Xiao SH. Pyronaridine: A new antimalarial drug. Parasitology Today. 1991;7(11):310-313.
345. Manh ND, Thanh NV, Quang HH, Van NTT, San NN, Phong NC, et al. Therapeutic efficacy of pyronaridine-artesunate (Pyramax) in treating Plasmodium vivax malaria in the central highlands of Vietnam. Antimicrobial agents and chemotherapy. 2024;68(9):1-15.
346. Djimde M, Tshiongo JK, Muhindo HM, Tinto H, Sevene E, Traore M, et al. Efficacy and safety of pyronaridine-artesunate (PYRAMAX) for the treatment of P. falciparum uncomplicated malaria in African pregnant women (PYRAPREG): study protocol for a phase 3, non-inferiority, randomised open-label clinical trial. BMJ Open. 2023;13(e065295):1-8.
347. Chang C, Lin-Hua T, Jantanavivat C. Studies on a new antimalarial compound: Pyronaridine. Transactions of the Royal Society of Tropical Medicine and Hygiene. 1992;86(1):7-10.
348. Bailly C. Pyronaridine: An update of its pharmacological activities and mechanisms of action. Biopolymers. 2021;112(4):1-12.
349. Gupta S, Thapar MM, Mariga ST, Wernsdorfer WH, Björkman A. Plasmodium falciparum: in Vitro Interactions of Artemisinin with Amodiaquine, Pyronaridine, and Chloroquine. Experimental Parasitology. 2002;100(1):28-35.
350. Vivas L, Rattray L, Stewart L, Bongard E, Robinson BL, Peters W, et al. Anti-malarial efficacy of pyronaridine and artesunate in combination in vitro and in vivo. Acta Tropica. 2008;105(3):222-228.
351. Croft SL, Duparc S, Arbe-Barnes SJ, Craft JC, Shin C-S, Fleckenstein L, et al. Review of pyronaridine anti-malarial properties and product characteristics. Malaria Journal. 2012;11(270):1-28.

University of Ghana http://ugspace.ug.edu.gh

352. Khan J, Rudrapal M. “Old” and current antimalarial drugs, mechanism of action, significance of fever and therapeutic hyperthermia. Reviews on Clinical Pharmacology and Drug Therapy. 2025;23(1):29-40.
353. Chu WY, Dorlo TPC. Pyronaridine: a review of its clinical pharmacology in the treatment of malaria. The Journal of Antimicrobial Chemotherapy. 2023;78(10):2406-2418.
354. Auparakkitanon S. Pyronaridine–the Current Antimalarial Standing Up to Parasite Resistance. Ramathibodi Medical Journal. 2024;47(4):34-45.
355. Sauthier S, Lazrek Y, Volney B, Mathieu L, Florimond C, Carod JF, et al. Absence of Plasmodium falciparum resistance to pyronaridine in vitro over 2009-2023 in French Guiana. Médecine et Maladies Infectieuses Formation. 2024;3(4):22-35.
356. Madamet M, Briolant S, Amalvict R, Benoit N, Bouchiba H, Cren J, et al. The Plasmodium falciparum chloroquine resistance transporter is associated with the ex vivo P. falciparum African parasite response to pyronaridine. Parasites & Vectors. 2016;9(77):1-5.
357. Pradines B, Briolant S, Henry M, Oeuvray C, Baret E, Amalvict R, et al. Absence of association between pyronaridine in vitro responses and polymorphisms in genes involved in quinoline resistance in Plasmodium falciparum. Malaria Journal. 2010;9(339):1-7.
358. Adam I, Ibrahim Y, Gasim GI. Efficacy and safety of artemisinin-based combination therapy for uncomplicated Plasmodium falciparum malaria in Sudan: a systematic review and meta-analysis. Malaria Journal. 2018;17(110):1-8.
359. Sinclair D, Zani B, Donegan S, Olliaro P, Garner P. Artemisinin-based combination therapy for treating uncomplicated malaria. Cochrane Database of Systematic Reviews. 2009;2009(3):1-220.
360. Shibeshi W, Baye AM, Alemkere G, Engidawork E. Efficacy and Safety of Artemisinin-Based Combination Therapy for the Treatment of Uncomplicated Malaria in Pregnant Women: A Systematic Review and Meta-Analysis. Therapeutics and clinical risk management. 2021;17(1):1353-1370.
361. Karunajeewa HA. Parasite clearance after malaria therapy: staying a step ahead of drug resistance. BMC Medicine. 2015;13(251):1-4.
362. Zheng S, Liang Y, Wang Z, Liu M, Chen Y, Ai Y, et al. Polymorphisms in the K13-propeller gene in Artemisinin-resistant plasmodium in mice. Infection and Drug Resistance. 2022;15(1):6533-6544.
363. Xie SC, Ralph SA, Tilley L. K13, the Cytostome, and Artemisinin Resistance. Trends in Parasitology. 2020;36(6):533-544.
364. Rosenthal MR, Vijayrajratnam S, Firestone TM, Ng CL. Enhanced cell stress response and protein degradation capacity underlie artemisinin resistance in Plasmodium falciparum. Msphere. 2024;9(11):1-17.
365. Behrens HM, Schmidt S, Henshall IG, López-Barona P, Peigney D, Sabitzki R, et al. Impact of different mutations on Kelch13 protein levels, ART resistance, and fitness cost in Plasmodium falciparum parasites. American Society for Microbiology. 2024;15(6):1-19.
366. Thriemer K, Hong NV, Rosanas-Urgell A, Phuc BQ, Ha DM, Pockele E, et al. Delayed parasite clearance after treatment with dihydroartemisinin-piperaquine in Plasmodium falciparum malaria patients in central Vietnam. Antimicrobial agents and chemotherapy. 2014;58(12):7049-7055.
367. Hassett MR, Roepe PD. Origin and Spread of Evolving Artemisinin-Resistant Plasmodium falciparum Malarial Parasites in Southeast Asia. American Journal of Tropical Medicine and Hygiene. 2019;101(6):1204-1211.
368. Dondorp AM, Nosten F, Yi P, Das D, Phyo AP, Tarning J, et al. Artemisinin Resistance in Plasmodium falciparum Malaria. New England Journal of Medicine. 2009;361(5):455-467.

University of Ghana http://ugspace.ug.edu.gh

369. Ashley EA, Dhorda M, Fairhurst RM, Amaratunga C, Lim P, Suon S, et al. Spread of artemisinin resistance in Plasmodium falciparum malaria. New England Journal of Medicine. 2014;371(5):411-423.
370. Ménard D, Khim N, Beghain J, Adegnika AA, Shafiul-Alam M, Amodu O, et al. A Worldwide Map of Plasmodium falciparum K13-Propeller Polymorphisms. New England Journal of Medicine. 2016;374(25):2453-2464.
371. WHO. Artemisinin resistance and artemisinin-based combination therapy efficacy: status report. World Health Organization.; 2018.
372. Uwimana A, Legrand E, Stokes BH, Ndikumana J-LM, Warsame M, Umulisa N, et al. Emergence and clonal expansion of in vitro artemisinin-resistant Plasmodium falciparum kelch13 R561H mutant parasites in Rwanda. Nature Medicine. 2020;26(10):1602-1608.
373. Ishengoma DS, Mandara CI, Bakari C, Fola AA, Madebe RA, Seth MD, et al. Evidence of artemisinin partial resistance in northwestern Tanzania: clinical and molecular markers of resistance. The Lancet Infectious Diseases. 2024;24(11):1225-1233.
374. Meier-Scherling CPG, Watson OJ, Asua V, Ghinai I, Katairo T, Garg S, et al. Selection of Plasmodium falciparum kelch13 mutations in Uganda in comparison with southeast Asia: a modelling study. The Lancet Microbe: Elsevier; 2024. p. 1-26.
375. Balikagala B, Fukuda N, Ikeda M, Katuro OT, Tachibana S-I, Yamauchi M, et al. Evidence of Artemisinin-Resistant Malaria in Africa. New England Journal of Medicine. 2021;385(13):1163-1171.
376. Rosenthal PJ, Asua V, Conrad MD. Emergence, transmission dynamics and mechanisms of artemisinin partial resistance in malaria parasites in Africa. Nature Reviews Microbiology. 2024;22(6):373-384.
377. Jeang B, Zhong D, Lee M-C, Atieli H, Yewhalaw D, Yan G. Molecular surveillance of Kelch 13 polymorphisms in Plasmodium falciparum isolates from Kenya and Ethiopia. Malaria Journal. 2024;23(36):1-11.
378. Derbie A, Mekonnen D, Adugna M, Yeshitela B, Woldeamanuel Y, Abebe T. Therapeutic Efficacy of Artemether-Lumefantrine (Coartem®) for the Treatment of Uncomplicated Falciparum Malaria in Africa: A Systematic Review. Journal of Parasitology Research. 2020;2020(7371681):1-14.
379. Aminu B, Mukhtar M, Deeni Y. Assessment of Therapeutic Efficacy of Artemisinins Based Combination Therapy (ACT) against Plasmodium falciparum Malaria in Kano and Katsina States, Nigeria. UMYU Journal of Microbiology Research. 2017;2(2):56-64.
380. Abuaku B, Duah-Quashie NO, Quaye L, Matrevi SA, Quashie N, Gyasi A, et al. Therapeutic efficacy of artesunate–amodiaquine and artemether–lumefantrine combinations for uncomplicated malaria in 10 sentinel sites across Ghana: 2015–2017. Malaria Journal. 2019;18(206):1-12.
381. Scott N, Ataide R, Wilson DP, Hellard M, Price RN, Simpson JA, et al. Implications of population-level immunity for the emergence of artemisinin-resistant malaria: a mathematical model. Malaria Journal. 2018;17(279):1-11.
382. Masserey T, Lee T, Golumbeanu M, Shattock AJ, Kelly SL, Hastings IM, et al. The influence of biological, epidemiological, and treatment factors on the establishment and spread of drug-resistant Plasmodium falciparum. eLife. 2022;11(e77634):1-39.
383. Chhibber-Goel J, Sharma A. Profiles of Kelch mutations in Plasmodium falciparum across South Asia and their implications for tracking drug resistance. International Journal for Parasitology: Drugs and Drug Resistance. 2019;11(2019):49-58.
384. Balmer AJ, White NFD, Ü nlü ES, Lee C, Pearson RD, Almagro-Garcia J, et al. Understanding the Global Spread of Artemisinin Resistance: Insights from over 100K Plasmodium falciparum Samples. bioRxiv2024. p. 1-64.

University of Ghana http://ugspace.ug.edu.gh

385. Kokori E, Olatunji G, Akinboade A, Akinoso A, Egbunu E, Aremu SA, et al. Triple artemisinin-based combination therapy (TACT): advancing malaria control and eradication efforts. Malaria Journal. 2024;23(25):1-7.
386. Ansbro MR, Itkin Z, Chen L, Zahoranszky-Kohalmi G, Amaratunga C, Miotto O, et al. Modulation of Triple Artemisinin-Based Combination Therapy Pharmacodynamics by Plasmodium falciparum Genotype. ACS Pharmacology & Translational Science. 2020;3(6):1144-1157.
387. van der Pluijm RW, Tripura R, Hoglund RM, Pyae Phyo A, Lek D, ul Islam A, et al. Triple artemisinin-based combination therapies versus artemisinin-based combination therapies for uncomplicated Plasmodium falciparum malaria: a multicentre, open-label, randomised clinical trial. The Lancet. 2020;395(10233):1345-1360.
388. Nguyen TD, Gao B, Amaratunga C, Dhorda M, Tran TN, White NJ, et al. Preventing antimalarial drug resistance with triple artemisinin-based combination therapies. Nature Communications. 2023;14(4568):1-10.
389. Dini S, Zaloumis S, Cao P, Price RN, Fowkes FJI, Pluijm RWvd, et al. Investigating the Efficacy of Triple Artemisinin-Based Combination Therapies for Treating Plasmodium falciparum Malaria Patients Using Mathematical Modeling. Antimicrobial agents and chemotherapy. 2018;62(11):1-11.
390. de Haan F, Amaratunga C, Thi VAC, Orng LH, Vonglokham M, Quang TN, et al. Strategies for deploying triple artemisinin-based combination therapy in the Greater Mekong Subregion. Malaria Journal. 2023;22(261):1-11.
391. Keating C. Artesunate versus quinine: the controlled trials watershed. The Lancet. 2023;401(10385):1329-1331.
392. Ngoumboute I, editor Efficacy and safety of Triple ACTs compared to conventional ACTs for the treatment of uncomplicated malaria: preliminary results of the DeTACT trial in Niger. Epicentre Scientific Day Paris 2023; 2023.
393. Investigators DP, editor DeTACT Development of Triple Artemisinin-based Combination Therapies

SMC Alliance Meeting; 2023; Conakry.
394. Oxford Uo. A Trial to Compare the Efficacy, Safety and Tolerability of Combinations of 3 Anti-malarial Drugs Against Combina-tions of 2 Anti-malarial Drugs. (DeTACT-Africa): ICH GCP; US clinical trials registry; 2024 [Available from: https://ichgcp.net/clinical-trials-registry/NCT03923725.
395. Tindana P, de Haan F, Amaratunga C, Dhorda M, van der Pluijm RW, Dondorp AM, et al. Deploying triple artemisinin-based combination therapy (TACT) for malaria treatment in Africa: ethical and practical considerations. Malaria Journal. 2021;20(119):1-7.
396. van der Pluijm RW, Phyo AP, Lek D, White NJ, Dondorp AM. Triple artemisinin-based combination therapies for malaria: proceed with caution; Authors' reply. The Lancet. 2020;396(10267):1976-1977.
397. Xu C, Wong YK, Liao FL, Jiang T, Wang J, Tu Y. Is triple artemisinin-based combination therapy necessary for uncomplicated malaria? The Lancet Infectious Diseases. 2022;22(5):585-586.
398. Bassat Q, Maïga-Ascofaré O, May J, Clain J, Mombo-Ngoma G, Groger M, et al. Challenges in the clinical development pathway for triple and multiple drug combinations in the treatment of uncomplicated falciparum malaria. Malaria Journal. 2022;21(61):1-8.
399. de Haan F, Amaratunga C, Thi VAC, Orng LH, Vonglokham M, Quang TN, et al. Strategies for deploying triple artemisinin-based combination therapy in the Greater Mekong Subregion. Malaria Journal. 2023;22(261):1-11.

University of Ghana http://ugspace.ug.edu.gh

400. Witkowski B, Camille R, Cosson A, Mairet-Khedim M, Khim N, Kloeung N, et al. Tolerance of Plasmodium falciparum mefloquine-resistant clinical isolates to mefloquine-piperaquine: implications for triple artemisinin-based combination therapy strategies. In: Square R, editor. 2025. p. 1-8.
401. Bangkok M. New MORU-led study to test a single pill to fight drug-resistant malaria in Africa and Asia: Mahidol Oxford Tropical Medicine Research Unit (MORU), Faculty of Tropical Medicine, Mahidol University; 2023 [Available from: https://www.tropmedres.ac/news/new-moru-led-study-to-test-a-single-pill-to-fight-drug-resistant-malaria-in-africa-and-asia.
402. Oxford Uo. MORU leads study testing a single pill for drug-resistant malaria in Africa and Asia: Offices of the Nuffield Professor of Medicine, Nuffield Department of Medicine, University of Oxford; 2023 [Available from: https://www.ndm.ox.ac.uk/news/moru-leads-study-testing-a-single-pill-for-drug-resistant-malaria-in-africa-and-asia.
403. Svennas KL, Macdonald SJ, Willis PA. Small molecule anti-malarial patents: a review (January 2010–June 2011). Expert Opinion on Therapeutic Patents. 2012;22(6):607-643.
404. Siqueira-Neto JL, Wicht KJ, Chibale K, Burrows JN, Fidock DA, Winzeler EA. Antimalarial drug discovery: progress and approaches. Nature reviews Drug discovery. 2023;22(10):807-826.
405. Fong KY, Wright DW. Hemozoin and antimalarial drug discovery. Future Medicinal Chemistry. 2013;5(12):1437-1450.
406. Rasool F, Dar NJ. Medicinal Chemistry and the Design of Small Molecules. Small Molecules in Neurodegeneration: CRC Press.Page; 91-110.
407. Sun Y. Advances in the clinical application of small molecule chemical drugs. Theoretical and Natural Science. 2024;74(1):136-143.
408. Southey MW, Brunavs M. Introduction to small molecule drug discovery and preclinical development. Frontiers in Drug Discovery. 2023;3(1314077):1-8.
409. Huszar M, Varga A, Horvath A, Lorand T, Agocs A, Idei M, et al. Comparative characterization of experimental and calculated lipophilicity and anti-tumour activity of isochromanone derivatives. Current Medicinal Chemistry. 2010;17(4):321-333.
410. Arkin MR, Wells JA. Small-molecule inhibitors of protein–protein interactions: progressing towards the dream. Nature reviews Drug discovery. 2004;3(4):301-317.
411. Hoelder S, Clarke PA, Workman P. Discovery of small molecule cancer drugs: successes, challenges and opportunities. Molecular oncology. 2012;6(2):155-176.
412. Robert A, Benoit-Vical F, Liu Y, Meunier B. Small molecules: the past or the future in drug innovation. Metal Ions in Life Sciences Series. 192019.Page; 17-48.
413. Mader MM, Rudolph J, Hartung IV, Uehling D, Workman P, Zuercher W. Which small molecule? selecting chemical probes for use in cancer research and target validation. Cancer Discovery. 2023;13(10):2150-2165.
414. Clegg MA, Tomkinson NC, Prinjha RK, Humphreys PG. Small molecules and their role in effective preclinical target validation. Future Medicinal Chemistry. 2017;9(14):1579-1582.
415. Azam NNSFNM, Othman S, Choo Y-M. Antimalarial Drug Discovery from Natural and Synthetic Sources. Current Medicinal Chemistry. 2025;32(1):87-110.
416. H. Gilbert I, Leroy D, A. Frearson J. Finding new hits in neglected disease projects: target or phenotypic based screening? Current topics in medicinal chemistry. 2011;11(10):1284-1291.

University of Ghana http://ugspace.ug.edu.gh

417. Guerra F, Winzeler EA. New targets for antimalarial drug discovery. Current Opinion in Microbiology. 2022;70(102220):1-9.
418. Werbovetz KA. Target-based drug discovery for malaria, leishmaniasis, and trypanosomiasis. Current Medicinal Chemistry. 2000;7(8):835-860.
419. Fernandes JF, Lell B, Agnandji ST, Obiang RM, Bassat Q, Kremsner PG, et al. Fosmidomycin as an antimalarial drug: a meta-analysis of clinical trials. Future Microbiology. 2015;10(8):1375-1390.
420. Sulyok M, Rückle T, Roth A, Mürbeth RE, Chalon S, Kerr N, et al. DSM265 for Plasmodium falciparum chemoprophylaxis: a randomised, double blinded, phase 1 trial with controlled human malaria infection. The Lancet Infectious Diseases. 2017;17(6):636-644.
421. Olotu F, Tali MBT, Chepsiror C, Sheik Amamuddy O, Boyom FF, Tastan Bishop Ö. Repurposing DrugBank compounds as potential Plasmodium falciparum class 1a aminoacyl tRNA synthetase multi-stage pan-inhibitors with a specific focus on mitomycin. International Journal for Parasitology: Drugs and Drug Resistance. 2024;25(100548):1-23.
422. Miley GP, Pou S, Winter R, Nilsen A, Li Y, Kelly JX, et al. ELQ-300 prodrugs for enhanced delivery and single-dose cure of malaria. Antimicrobial agents and chemotherapy. 2015;59(9):5555-5560.
423. Wagner BK, Schreiber SL. The power of sophisticated phenotypic screening and modern mechanism-of-action methods. Cell chemical biology. 2016;23(1):3-9.
424. Rasul A, Riaz A, Sarfraz I, Khan SG, Hussain G, Zara R, et al. Target Identification Approaches in Drug Discovery. In: Scotti MT, Bellera CL, editors. Drug Target Selection and Validation. Cham: Springer International Publishing; 2022.Page; 41-59.
425. Sharma V, Gupta S, Singh S. Contemporary Approaches for Malaria Drug Discovery. Drug Design: Principles and Applications: Springer; 2017.Page; 45-56.
426. Cheuka PM, Mayoka G, Okombo J, Chibale K. Medicinal chemistry progression of antimalarial hits from phenotypic whole cell screening of SoftFocus libraries. Annual reports in medicinal chemistry. 53: Elsevier; 2019.Page; 25-71.
427. Palmer M. Phenotypic screening. Small Molecule Medicinal Chemistry: Strategies and Technologies2015.Page; 281-304.
428. Cully M. Next-generation antimalarial from phenotypic screen shows clinical promise. Nature reviews Drug discovery. 2014;13(717):1-22.
429. Terstappen GC, Schlüpen C, Raggiaschi R, Gaviraghi G. Target deconvolution strategies in drug discovery. Nature reviews Drug discovery. 2007;6(11):891-903.
430. Berg EL, Denker SP, O'Mahony A. Development and Validation of Disease Assays for Phenotypic Screening. Phenotypic Drug Discovery2020.Page; 20-36.
431. Shabajee P, Gaudeau A, Legros C, Dorval T, Stéphan J-P. From high content screening to target deconvolution: New insights for phenotypic approaches. Medecine Sciences: M/S. 2021;37(3):249-257.
432. Patra AT, Hingamire T, Belekar MA, Xiong A, Subramanian G, Bozdech Z, et al. Whole-Cell Phenotypic Screening of Medicines for Malaria Venture Pathogen Box Identifies Specific Inhibitors of Plasmodium falciparum Late-Stage Development and Egress. Antimicrobial agents and chemotherapy. 2020;64(5):1-15.
433. Kato N, March S, Bhatia SN, Marti M. Phenotypic Screening of Small Molecules with Antimalarial Activity for Three Different Parasitic Life Stages. Methods in Molecular Biology. 2018;1787(1):41-52.
434. Luo A-P, Giannangelo C, Siddiqui G, Creek DJ. Promising antimalarial hits from phenotypic screens: a review of recently-described multi-stage actives and their modes of action. Frontiers in Cellular and Infection Microbiology. 2023;13(1308193):1-12.

University of Ghana http://ugspace.ug.edu.gh

435. Patel OPS, Beteck RM, Legoabe LJ. Exploration of artemisinin derivatives and synthetic peroxides in antimalarial drug discovery research. European Journal of Medicinal Chemistry. 2021;213(113193):1-45.
436. Shukla M, Rathi K, Hassam M, Yadav DK, Karnatak M, Rawat V, et al. An overview on the antimalarial activity of 1, 2, 4-trioxanes, 1, 2, 4-trioxolanes and 1, 2, 4, 5-tetraoxanes. Medicinal Research Reviews. 2024;44(1):66-137.
437. Nagle A, Wu T, Kuhen K, Gagaring K, Borboa R, Francek C, et al. Imidazolopiperazines: lead optimization of the second-generation antimalarial agents. Journal of medicinal chemistry. 2012;55(9):4244-4273.
438. Turner H. Spiroindolone NITD609 is a novel antimalarial drug that targets the P-type ATPase PfATP4. Future Medicinal Chemistry. 2016;8(2):227-238.
439. Nilsen A, LaCrue AN, White KL, Forquer IP, Cross RM, Marfurt J, et al. Quinolone-3-diarylethers: a new class of antimalarial drug. Science translational medicine. 2013;5(177):1-36.
440. Kumari G, Jain R, Kumar Sah R, Kalia I, Vashistha M, Singh P, et al. Multistage and transmission-blocking tubulin targeting potent antimalarial discovered from the open access MMV pathogen box. Biochemical Pharmacology. 2022;203(115154):1-21.
441. Malebo HM, Sarah DA, A. EY, Harouna S, R. TGA, J. KS, et al. In vitro Multistage Malaria Transmission Blocking Activity of Selected Malaria Box Compounds. Drug Design, Development and Therapy. 2020;14(1):1593-1607.
442. Reader J, van der Watt ME, Taylor D, Le Manach C, Mittal N, Ottilie S, et al. Multistage and transmission-blocking targeted antimalarials discovered from the open-source MMV Pandemic Response Box. Nature Communications. 2021;12(269):1-15.
443. Priest BT, Erdemli G. Phenotypic screening in the 21st century. Frontiers Media SA; 2014. p. 1-2.
444. Warchal SJ, Asier U-B, and Carragher NO. Next-Generation Phenotypic Screening. Future Medicinal Chemistry. 2016;8(11):1331-1347.
445. Linciano P, Quotadamo A, Luciani R, Santucci M, Zorn KM, Foil DH, et al. High-Throughput Phenotypic Screening and Machine Learning Methods Enabled the Selection of Broad-Spectrum Low-Toxicity Antitrypanosomatidic Agents. Journal of medicinal chemistry. 2023;66(22):15230-15255.
446. Butera JA. Phenotypic screening as a strategic component of drug discovery programs targeting novel antiparasitic and antimycobacterial agents: an editorial. Journal of medicinal chemistry. 2013;56(20):7715-7718.
447. Roy K. Multi-target drug design using chem-bioinformatic approaches: Springer; 2019. 1-563 pages.
448. Kern S, Agarwal S, Huber K, Gehring AP, Ströddke B, Wirth CC, et al. Inhibition of the SR protein-phosphorylating CLK kinases of Plasmodium falciparum impairs blood stage replication and malaria transmission. Plos one. 2014;9(9):1-15.
449. McNamara CW, Lee MC, Lim CS, Lim SH, Roland J, Nagle A, et al. Targeting Plasmodium PI (4) K to eliminate malaria. Nature. 2013;504(7479):248-253.
450. Spillman Natalie J, Allen Richard JW, McNamara Case W, Yeung Bryan KS, Winzeler Elizabeth A, Diagana Thierry T, et al. Na+ Regulation in the Malaria Parasite Plasmodium falciparum Involves the Cation ATPase PfATP4 and Is a Target of the Spiroindolone Antimalarials. Cell Host & Microbe. 2013;13(2):227-237.
451. Wright MH, Clough B, Rackham MD, Rangachari K, Brannigan JA, Grainger M, et al. Validation of N-myristoyltransferase as an antimalarial drug target using an integrated chemical biology approach. Nature Chemistry. 2014;6(2):112-121.

University of Ghana http://ugspace.ug.edu.gh

452. Phillips MA, Lotharius J, Marsh K, White J, Dayan A, White KL, et al. A long-duration dihydroorotate dehydrogenase inhibitor (DSM265) for prevention and treatment of malaria. Science translational medicine. 2015;7(296):1-14.
453. Biagini GA, Viriyavejakul P, O'neill PM, Bray PG, Ward SA. Functional characterization and target validation of alternative complex I of Plasmodium falciparum mitochondria. Antimicrobial agents and chemotherapy. 2006;50(5):1841-1851.
454. Patel V, Shah M. Artificial intelligence and machine learning in drug discovery and development. Intelligent Medicine. 2022;2(3):134-140.
455. Zhang L, Tan J, Han D, Zhu H. From machine learning to deep learning: progress in machine intelligence for rational drug discovery. Drug Discovery Today. 2017;22(11):1680-1685.
456. Gupta R, Srivastava D, Sahu M, Tiwari S, Ambasta RK, Kumar P. Artificial intelligence to deep learning: machine intelligence approach for drug discovery. Molecular diversity. 2021;25(3):1315-1360.
457. Barber BE, Fernandez M, Patel HB, Barcelo C, Woolley SD, Patel H, et al. Safety, pharmacokinetics, and antimalarial activity of the novel triaminopyrimidine ZY-19489: a first-in-human, randomised, placebo-controlled, double-blind, single ascending dose study, pilot food-effect study, and volunteer infection study. The Lancet Infectious Diseases. 2022;22(6):879-890.
458. Nangia AK. Importance of Structural Databases, Molecular Pharmacophores, Supramolecular Heterosynthons, and Artificial Intelligence–Machine Learning–Neural Network Tools in Drug Discovery. Crystal Growth & Design. 2024;24(16):6888-6910.
459. Ncube NB, Tukulula M, Govender KG. Leveraging computational tools to combat malaria: assessment and development of new therapeutics. Journal of Cheminformatics. 2024;16(1):1-14.
460. Lagunin A, Stepanchikova A, Filimonov D, Poroikov V. PASS: prediction of activity spectra for biologically active substances. Bioinformatics. 2000;16(8):747-748.
461. Ramsundar B, Eastman P, Walters P, Pande V. Deep learning for the life sciences: applying deep learning to genomics, microscopy, drug discovery, and more. 1st ed. Loukides M, editor: O'Reilly Media; 2019. 209 pages.
462. Heid E, Greenman KP, Chung Y, Li S-C, Graff DE, Vermeire FH, et al. Chemprop: a machine learning package for chemical property prediction. Journal of Chemical Information and Modeling. 2023;64(1):9-17.
463. Vangala SR, Bung N, Krishnan SR, Roy A. An interpretable machine learning model for selectivity of small-molecules against homologous protein family. Future Medicinal Chemistry. 2022;14(20):1441-1453.
464. Bosc N, Felix E, Gardner JMF, Mills J, Timmerman M, Asveld D, et al. MAIP: An Open-Source Tool to Enrich High-Throughput Screening Output and Identify Novel, Druglike Molecules with Antimalarial Activity. ACS Medicinal Chemistry Letters. 2023;14(12):1733-1741.
465. Borba JV, Salazar-Alvarez LC, Ferreira LT, Silva-Mendonça S, Silva MFBd, Sanches IH, et al. Innovative multistage ML-QSAR models for malaria: from data to discovery. ACS Medicinal Chemistry Letters. 2024;15(8):1386-1395.
466. Keshavarzi Arshadi A, Salem M, Collins J, Yuan JS, Chakrabarti D. DeepMalaria: Artificial Intelligence Driven Discovery of Potent Antiplasmodials. Frontiers in Pharmacology. 2019;10(1526):1-13.
467. Lamptey E, Oparebea J, Anyaele G, Ofosu B, Hanson G, Sakyi PO, et al. PLASMOpred: A Machine Learning-Based Web Application for Predicting Antimalarial

University of Ghana http://ugspace.ug.edu.gh

Small Molecules Targeting the Apical Membrane Antigen 1–Rhoptry Neck Protein 2 Invasion Complex. Pharmaceuticals. 2025;18(6):1-18.
468. Koul S. Divergent Approaches Toward Drug Discovery and Development. The Quintessence of Basic and Clinical Research and Scientific Publishing: Springer; 2023.Page; 557-578.
469. Umumararungu T, Nkuranga JB, Habarurema G, Nyandwi JB, Mukazayire MJ, Mukiza J, et al. Recent developments in antimalarial drug discovery. Bioorganic & Medicinal Chemistry. 2023;88(89):1-21.
470. Rawe SL. Artemisinin and artemisinin-related agents. Antimalarial Agents: Elsevier; 2020.Page; 99-132.
471. Badeliya SN, Kapupara PP, Chauhan NF, Panchal II. A contemporary chemical entities infiltrating in the antimalarial therapy era: a comprehensive review. Folia Medica. 2021;63(5):637-646.
472. Blank BR, Gonciarz RL, Talukder P, Gut J, Legac J, Rosenthal PJ, et al. Antimalarial trioxolanes with superior drug-like properties and in vivo efficacy. ACS Infectious Diseases. 2020;6(7):1827-1835.
473. Valecha N, Looareesuwan S, Martensson A, Mohammed Abdulla S, Krudsood S, Tangpukdee N, et al. Arterolane, a new synthetic trioxolane for treatment of uncomplicated Plasmodium falciparum malaria: a phase II, multicenter, randomized, dose-finding clinical trial. Clinical infectious diseases. 2010;51(6):684-691.
474. Terent'ev AO, Borisov DA, Vil' VA, Dembitsky VM. Synthesis of five- and six-membered cyclic organic peroxides: Key transformations into peroxide ring-retaining products. Beilstein Journal of Organic Chemistry. 2014;10(1):34-114.
475. Opsenica D, Šolaja B. Artemisinins and synthetic peroxides as highly efficient antimalarials. Macedonian Journal of Chemistry and Chemical Engineering. 2012;31(2):137-182.
476. Vennerstrom JL, Arbe-Barnes S, Brun R, Charman SA, Chiu FCK, Chollet J, et al. Identification of an antimalarial synthetic trioxolane drug development candidate. Nature. 2004;430(7002):900-904.
477. Valecha N, Looareesuwan S, Martensson A, Mohammed Abdulla S, Krudsood S, Tangpukdee N, et al. Arterolane, a New Synthetic Trioxolane for Treatment of Uncomplicated Plasmodium falciparum Malaria: A Phase II, Multicenter, Randomized, Dose-Finding Clinical Trial. Clinical infectious diseases. 2010;51(6):684-691.
478. Toure OA, Valecha N, Tshefu AK, Thompson R, Krudsood S, Gaye O, et al. A Phase 3, Double-Blind, Randomized Study of Arterolane Maleate–Piperaquine Phosphate vs Artemether–Lumefantrine for Falciparum Malaria in Adolescent and Adult Patients in Asia and Africa. Clinical infectious diseases. 2016;62(8):964-971.
479. Hamaluba M, van der Pluijm RW, Weya J, Njuguna P, Ngama M, Kalume P, et al. Arterolane–piperaquine–mefloquine versus arterolane–piperaquine and artemether–lumefantrine in the treatment of uncomplicated Plasmodium falciparum malaria in Kenyan children: a single-centre, open-label, randomised, non-inferiority trial. The Lancet Infectious Diseases. 2021;21(10):1395-1406.
480. Varo R, Bassat Q. Arterolane-based combinations for the treatment of uncomplicated falciparum malaria in Kenyan children. The Lancet Infectious Diseases. 2021;21(10):1338-1339.
481. Patil C, Katare S, Baig M, Doifode S. Fixed dose combination of arterolane and piperaquine: a newer prospect in antimalarial therapy. Annals of medical and health sciences research. 2014;4(4):466-471.

University of Ghana http://ugspace.ug.edu.gh

482. Charman SA, Arbe-Barnes S, Bathurst IC, Brun R, Campbell M, Charman WN, et al. Synthetic ozonide drug candidate OZ439 offers new hope for a single-dose cure of uncomplicated malaria. Proceedings of the National Academy of Sciences. 2011;108(11):4400-4405.
483. Kim HS, Hammill JT, Guy RK. Seeking the elusive long-acting ozonide: discovery of Artefenomel (OZ439). Journal of medicinal chemistry. 2017;60(7):2651-2653.
484. Vennerstrom JL, Arbe-Barnes S, Brun R, Charman SA, Chiu FC, Chollet J, et al. Identification of an antimalarial synthetic trioxolane drug development candidate. Nature. 2004;430(7002):900-904.
485. Dong Y, Wang X, Kamaraj S, Bulbule VJ, Chiu FCK, Chollet J, et al. Structure–Activity Relationship of the Antimalarial Ozonide Artefenomel (OZ439). Journal of medicinal chemistry. 2017;60(7):2654-2668.
486. Rosenthal PJ. Artefenomel: a promising new antimalarial drug. The Lancet Infectious Diseases. 2016;16(1):6-8.
487. Burrows JN, Duparc S, Gutteridge WE, Hooft van Huijsduijnen R, Kaszubska W, Macintyre F, et al. New developments in anti-malarial target candidate and product profiles. Malaria Journal. 2017;16(26):1-29.
488. Abd-Rahman AN, Kaschek D, Kümmel A, Webster R, Potter AJ, Odedra A, et al. Characterizing the pharmacological interaction of the antimalarial combination artefenomel-piperaquine in healthy volunteers with induced blood-stage Plasmodium falciparum to predict efficacy in patients with malaria. BMC Medicine. 2024;22(563):1-14.
489. Macintyre F, Adoke Y, Tiono AB, Duong TT, Mombo-Ngoma G, Bouyou-Akotet M, et al. A randomised, double-blind clinical phase II trial of the efficacy, safety, tolerability and pharmacokinetics of a single dose combination treatment with artefenomel and piperaquine in adults and children with uncomplicated Plasmodium falciparum malaria. BMC Medicine. 2017;15(181):1-19.
490. Gansane A, Lingani M, Yeka A, Nahum A, Bouyou-Akotet M, Mombo-Ngoma G, et al. Randomized, open-label, phase 2a study to evaluate the contribution of artefenomel to the clinical and parasiticidal activity of artefenomel plus ferroquine in African patients with uncomplicated Plasmodium falciparum malaria. Malaria Journal. 2023;22(2):1-16.
491. Adoke Y, Zoleko-Manego R, Ouoba S, Tiono AB, Kaguthi G, Bonzela JE, et al. A randomized, double-blind, phase 2b study to investigate the efficacy, safety, tolerability and pharmacokinetics of a single-dose regimen of ferroquine with artefenomel in adults and children with uncomplicated Plasmodium falciparum malaria. Malaria Journal. 2021;20(222):1-25.
492. McCarthy JS, Rückle T, Elliott SL, Ballard E, Collins KA, Marquart L, et al. A Single-Dose Combination Study with the Experimental Antimalarials Artefenomel and DSM265 To Determine Safety and Antimalarial Activity against Blood-Stage Plasmodium falciparum in Healthy Volunteers. Antimicrobial agents and chemotherapy. 2019;64(1):1-10.
493. Blank BR, Gut J, Rosenthal PJ, Renslo AR. Artefenomel regioisomer RLA-3107 is a promising lead for the discovery of next-generation endoperoxide antimalarials. ACS Medicinal Chemistry Letters. 2023;14(4):493-498.
494. Klope MT, Tapia Cardona JA, Chen J, Gonciarz RL, Cheng K, Jaishankar P, et al. Synthesis and In Vivo Profiling of Desymmetrized Antimalarial Trioxolanes with Diverse Carbamate Side Chains. ACS Medicinal Chemistry Letters. 2024;15(10):1764-1770.
495. Chibale K. How Africa is helping expand the global antimalarial drug pipeline research. Quest. 2016;12(3):22-23.

University of Ghana http://ugspace.ug.edu.gh

496. Paquet T, Le Manach C, Cabrera DG, Younis Y, Henrich PP, Abraham TS, et al. Antimalarial efficacy of MMV390048, an inhibitor of Plasmodium phosphatidylinositol 4-kinase. Science translational medicine. 2017;9(387):1-15.
497. Ashton TD, Devine SM, Möhrle JJ, Laleu B, Burrows JN, Charman SA, et al. The Development Process for Discovery and Clinical Advancement of Modern Antimalarials. Journal of medicinal chemistry. 2019;62(23):10526-10562.
498. Paymode DJ, Chang L, Chen D, Wang B, Kashinath K, Gopalsamuthiram V, et al. Application of Vinamidinium Salt Chemistry for a Palladium Free Synthesis of Anti-Malarial MMV048: A "Bottom-Up" Approach. Organic Letters. 2021;23(14):5400-5404.
499. Mogwera KSP, Chibale K, Arendse LB. Developing kinase inhibitors for malaria: an opportunity or liability? Trends in Parasitology. 2023;39(9):720-731.
500. Sinxadi P, Donini C, Johnstone H, Langdon G, Wiesner L, Allen E, et al. Safety, tolerability, pharmacokinetics, and antimalarial activity of the novel Plasmodium phosphatidylinositol 4-kinase inhibitor MMV390048 in healthy volunteers. Antimicrobial agents and chemotherapy. 2020;64(4):1-12.
501. Mohammed R, Asres MS, Gudina EK, Adissu W, Johnstone H, Marrast AC, et al. Efficacy, safety, tolerability, and pharmacokinetics of MMV390048 in acute uncomplicated malaria. The American Journal of Tropical Medicine and Hygiene. 2022;108(1):81-84.
502. Singh V, Mambwe D, Korkor CM, Chibale K. Innovation Experiences from Africa-Led Drug Discovery at the Holistic Drug Discovery and Development (H3D) Centre. ACS Medicinal Chemistry Letters. 2022;13(8):1221-1230.
503. Brunschwig C, Lawrence N, Taylor D, Abay E, Njoroge M, Basarab GS, et al. UCT943, a Next-Generation Plasmodium falciparum PI4K Inhibitor Preclinical Candidate for the Treatment of Malaria. Antimicrobial agents and chemotherapy. 2018;62(9):12-18.
504. Gibhard L, Njoroge M, Mulubwa M, Lawrence N, Smith D, Duffy J, et al. Dose-fractionation studies of a Plasmodium phosphatidylinositol 4-kinase inhibitor in a humanized mouse model of malaria. Antimicrobial agents and chemotherapy. 2024;68(10):1-18.
505. Gamo F-J. Antimalarial drug resistance: new treatments options for Plasmodium. Drug Discovery Today: Technologies. 2014;30(20):81-88.
506. Yeung BKS, Zou B, Rottmann M, Lakshminarayana SB, Ang SH, Leong SY, et al. Spirotetrahydro β-Carbolines (Spiroindolones): A New Class of Potent and Orally Efficacious Compounds for the Treatment of Malaria. Journal of medicinal chemistry. 2010;53(14):5155-5164.
507. Ruch T, Siirola E, Snajdrova R. Cipargamin: Biocatalysis in the Discovery and Development of an Antimalarial Drug. Pharmaceutical Biocatalysis: Jenny Stanford Publishing; 2019.Page; 559-577.
508. Rottmann M, McNamara C, Yeung BKS, Lee MCS, Zou B, Russell B, et al. Spiroindolones, a Potent Compound Class for the Treatment of Malaria. Science. 2010;329(5996):1175-1180.
509. Li H, Ji S, Ariefta NR, Galon EMS, El-Sayed SAES, Do T, et al. Efficacy and mechanism of action of cipargamin as an antibabesial drug candidate. eLife. 2025;13(RP101128):1-17.
510. Goldgof GM, Durrant JD, Ottilie S, Vigil E, Allen KE, Gunawan F, et al. Comparative chemical genomics reveal that the spiroindolone antimalarial KAE609 (Cipargamin) is a P-type ATPase inhibitor. Scientific reports. 2016;6(27806):1-13.
511. Bouwman SAM, Zoleko-Manego R, Renner KC, Schmitt EK, Mombo-Ngoma G, Grobusch MP. The early preclinical and clinical development of cipargamin (KAE609), a novel antimalarial compound. Travel Medicine and Infectious Disease. 2020;36(101765):1-8.

University of Ghana http://ugspace.ug.edu.gh

512. Huskey S-EW, Zhu C-q, Fredenhagen A, Kühnöl J, Luneau A, Jian Z, et al. KAE609 (Cipargamin), a New Spiroindolone Agent for the Treatment of Malaria: Evaluation of the Absorption, Distribution, Metabolism, and Excretion of a Single Oral 300-mg Dose of [14C]KAE609 in Healthy Male Subjects. Drug Metabolism and Disposition. 2016;44(5):672-682.
513. McCarthy JS, Abd-Rahman AN, Collins KA, Marquart L, Griffin P, Kümmel A, et al. Defining the Antimalarial Activity of Cipargamin in Healthy Volunteers Experimentally Infected with Blood-Stage Plasmodium falciparum. Antimicrobial agents and chemotherapy. 2021;65(2):1-11.
514. Schmitt EK, Ndayisaba G, Yeka A, Asante KP, Grobusch MP, Karita E, et al. Efficacy of Cipargamin (KAE609) in a Randomized, Phase II Dose-Escalation Study in Adults in Sub-Saharan Africa With Uncomplicated Plasmodium falciparum Malaria. Clinical infectious diseases. 2021;74(10):1831-1839.
515. Koller R, Mombo-Ngoma G, Grobusch MP. The early preclinical and clinical development of ganaplacide (KAF156), a novel antimalarial compound. Expert Opinion on Investigational Drugs. 2018;27(10):803-810.
516. White NJ, Duong TT, Uthaisin C, Nosten F, Phyo AP, Hanboonkunupakarn B, et al. Antimalarial activity of KAF156 in falciparum and vivax malaria. New England Journal of Medicine. 2016;375(12):1152-1160.
517. Wu T, Nagle A, Kuhen K, Gagaring K, Borboa R, Francek C, et al. Imidazolopiperazines: Hit to Lead Optimization of New Antimalarial Agents. Journal of medicinal chemistry. 2011;54(14):5116-5130.
518. LaMonte GM, Rocamora F, Marapana DS, Gnädig NF, Ottilie S, Luth MR, et al. Pan-active imidazolopiperazine antimalarials target the Plasmodium falciparum intracellular secretory pathway. Nature Communications. 2020;11(1780):1-15.
519. Abdoulaye D, Martin PG, Rella Zoleko M, Ghyslain M-N, Stephane P, Issaka S, et al. OC 8721 WANECAM II – A clinical trial programme to assess safety, efficacy and transmission-blocking properties of a new antimalarial KAF156 (Ganaplacide) in uncomplicated malaria in West and Central Africa. BMJ global health. 2019;4(Suppl 3):A1–A68.
520. Yipsirimetee A, Chiewpoo P, Tripura R, Lek D, Day Nicholas PJ, Dondorp Arjen M, et al. Assessment In Vitro of the Antimalarial and Transmission-Blocking Activities of Cipargamin and Ganaplacide in Artemisinin-Resistant Plasmodium falciparum. Antimicrobial agents and chemotherapy. 2022;66(3):1-10.
521. Gal IR, Demarta-Gatsi C, Fontinha D, Arez F, Wicha SG, Rottmann M, et al. Drug Interaction Studies of Cabamiquine:Ganaplacide Combination against Hepatic Plasmodium berghei. ACS Infectious Diseases. 2025;11(1):69-79.
522. Ogutu B, Yeka A, Kusemererwa S, Thompson R, Tinto H, Toure AO, et al. Ganaplacide (KAF156) plus lumefantrine solid dispersion formulation combination for uncomplicated Plasmodium falciparum malaria: an open-label, multicentre, parallel-group, randomised, controlled, phase 2 trial. The Lancet Infectious Diseases. 2023;23(9):1051-1061.
523. Manaranche J, Laurent M, Tressieres R, Nguyen M, Salim M, Ouji M, et al. In vitro evaluation of ganaplacide/lumefantrine combination against Plasmodium falciparum in a context of artemisinin resistance. Journal of Antimicrobial Chemotherapy. 2024;79(11):2877-2886.
524. Sangana R, Ogutu B, Yeka A, Kusemererwa S, Tinto H, Toure AO, et al. Pharmacokinetics of Ganaplacide and Lumefantrine in Adults, Adolescents, and Children with Plasmodium falciparum Malaria Treated with Ganaplacide Plus Lumefantrine Solid

University of Ghana http://ugspace.ug.edu.gh

Dispersion Formulation: Analysis of Data from a Multinational Phase 2 Study. The Journal of Clinical Pharmacology. 2025;65(2):179-189.
525. Thakare R, Kapoor E, Dasgupta A, Chopra S. DSM-265. Plasmodium falciparum dihydroorotate dehydrogenase (PfDHODH) inhibitor, Treatment of malaria. Drugs of the Future. 2019;44(2):123-129.
526. Bélard S, Ramharter M. DSM265: a novel drug for single-dose cure of Plasmodium falciparum malaria. The Lancet Infectious Diseases. 2018;18(8):819-820.
527. Tse EG, Korsik M, Todd MH. The past, present and future of anti-malarial medicines. Malaria Journal. 2019;18(93):1-21.
528. Phillips MA, Lotharius J, Marsh K, White J, Dayan A, White KL, et al. A long-duration dihydroorotate dehydrogenase inhibitor (DSM265) for prevention and treatment of malaria. Science translational medicine. 2015;7(296):1-14.
529. White J, Dhingra SK, Deng X, El Mazouni F, Lee MCS, Afanador GA, et al. Identification and Mechanistic Understanding of Dihydroorotate Dehydrogenase Point Mutations in Plasmodium falciparum that Confer in Vitro Resistance to the Clinical Candidate DSM265. ACS Infectious Diseases. 2019;5(1):90-101.
530. Deng X, Kokkonda S, El Mazouni F, White J, Burrows JN, Kaminsky W, et al. Fluorine Modulates Species Selectivity in the Triazolopyrimidine Class of Plasmodium falciparum Dihydroorotate Dehydrogenase Inhibitors. Journal of medicinal chemistry. 2014;57(12):5381-5394.
531. Russo TA, Umland TC, Deng X, El Mazouni F, Kokkonda S, Olson R, et al. Repurposed dihydroorotate dehydrogenase inhibitors with efficacy against drug-resistant Acinetobacter baumannii. Proceedings of the National Academy of Sciences. 2022;119(51):1-10.
532. McCarthy JS, Lotharius J, Rückle T, Chalon S, Phillips MA, Elliott S, et al. Safety, tolerability, pharmacokinetics, and activity of the novel long-acting antimalarial DSM265: a two-part first-in-human phase 1a/1b randomised study. The Lancet Infectious Diseases. 2017;17(6):626-635.
533. Llanos-Cuentas A, Casapia M, Chuquiyauri R, Hinojosa J-C, Kerr N, Rosario M, et al. Antimalarial activity of single-dose DSM265, a novel plasmodium dihydroorotate dehydrogenase inhibitor, in patients with uncomplicated Plasmodium falciparum or Plasmodium vivax malaria infection: a proof-of-concept, open-label, phase 2a study. The Lancet Infectious Diseases. 2018;18(8):874-883.
534. Dini S, Zaloumis SG, Price DJ, Gobeau N, Kümmel A, Cherkaoui M, et al. Seeking an optimal dosing regimen for OZ439/DSM265 combination therapy for treating uncomplicated falciparum malaria. Journal of Antimicrobial Chemotherapy. 2021;76(9):2325-2334.
535. Nandal R, Kumar D, Aggarwal N, Kumar V, Narasimhan B, Marwaha RK, et al. Recent advances, challenges and updates on the development of therapeutics for malaria. Experimental and clinical sciences journal. 2024;23(1):672-713.
536. Jiménez-Díaz MB, Ebert D, Salinas Y, Pradhan A, Lehane AM, Myrand-Lapierre M-E, et al. (+)-SJ733, a clinical candidate for malaria that acts through ATP4 to induce rapid host-mediated clearance of Plasmodium. Proceedings of the National Academy of Sciences. 2014;111(50):E5455-E5462.
537. Gaur AH, McCarthy JS, Panetta JC, Dallas RH, Woodford J, Tang L, et al. Safety, tolerability, pharmacokinetics, and antimalarial efficacy of a novel Plasmodium falciparum ATP4 inhibitor SJ733: a first-in-human and induced blood-stage malaria phase 1a/b trial. The Lancet Infectious Diseases. 2020;20(8):964-975.

University of Ghana http://ugspace.ug.edu.gh

538. Chen Y, Zhu F, Hammill J, Holbrook G, Yang L, Freeman B, et al. Selecting an anti-malarial clinical candidate from two potent dihydroisoquinolones. Malaria Journal. 2021;20(107):1-15.
539. Floyd DM, Stein P, Wang Z, Liu J, Castro S, Clark JA, et al. Hit-to-Lead Studies for the Antimalarial Tetrahydroisoquinolone Carboxanilides. Journal of medicinal chemistry. 2016;59(17):7950-7962.
540. Nureye D, Salahaddin M, Zewudie A. Current Medicines for Malaria Including Resistance Issues. Journal of Pharmacology and Pharmacotherapeutics. 2020;11(3):90-99.
541. Gaur AH, Panetta JC, Smith AM, Dallas RH, Freeman BB, III, Stewart TB, et al. Combining SJ733, an oral ATP4 inhibitor of Plasmodium falciparum, with the pharmacokinetic enhancer cobicistat: An innovative approach in antimalarial drug development. eBioMedicine. 2022;80(104065):1-11.
542. Biot C, Nosten F, Fraisse L, Ter-Minassian D, Khalife J, Dive D. The antimalarial ferroquine: from bench to clinic. Parasite. 2011;18(3):207-214.
543. Wani WA, Jameel E, Baig U, Mumtazuddin S, Hun LT. Ferroquine and its derivatives: new generation of antimalarial agents. European Journal of Medicinal Chemistry. 2015;101(2015):534-551.
544. Biot C, Glorian G, Maciejewski LA, Brocard JS, Domarle O, Blampain G, et al. Synthesis and Antimalarial Activity in Vitro and in Vivo of a New Ferrocene−Chloroquine Analogue. Journal of medicinal chemistry. 1997;40(23):3715-3718.
545. Delhaes L, Biot C, Berry L, Delcourt P, Maciejewski LA, Camus D, et al. Synthesis of ferroquine enantiomers: first investigation of effects of metallocenic chirality upon antimalarial activity and cytotoxicity. ChemBioChem. 2002;3(5):418-423.
546. Fraisse L, Struxiano A, inventors; Google Patents, assignee. Use of ferroquine in the treatment or prevention of malaria. USA2012.
547. Amewu RK, Ade CF, Otchere ID, Morgan P, Yeboah-Manu D. Synthesis and initial testing of novel antimalarial and antitubercular isonicotinohydrazides. Results in Chemistry. 2022;4(100287):1-8.
548. Bérubé G. An overview of molecular hybrids in drug discovery. Expert Opinion on Drug Discovery. 2016;11(3):281-305.
549. Muregi FW, Ishih A. Next-generation antimalarial drugs: hybrid molecules as a new strategy in drug design. Drug development research. 2010;71(1):20-32.
550. Larik FA, Saeed A, Fattah TA, Muqadar U, Channar PA. Recent advances in the synthesis, biological activities and various applications of ferrocene derivatives. Applied Organometallic Chemistry. 2017;31(8):1-22.
551. Jagdale D, Battellu K, Bhosale S, Sawant Y, Nadar G. Exploring the Versatility of Ferrocene and Its Derivatives: A Comprehensive Review. Biomedical and Pharmacology Journal. 2024;17(3):1433-1444.
552. Kondratskyi A, Kondratska K, Vanden Abeele F, Gordienko D, Dubois C, Toillon R-A, et al. Ferroquine, the next generation antimalarial drug, has antitumor activity. Scientific reports. 2017;7(15896):1-15.
553. Chavain N, Vezin H, Dive D, Touati N, Paul J-F, Buisine E, et al. Investigation of the Redox Behavior of Ferroquine, a New Antimalarial. Molecular Pharmaceutics. 2008;5(5):710-716.
554. Dubar F, Khalife J, Brocard J, Dive D, Biot C. Ferroquine, an Ingenious Antimalarial Drug –Thoughts on the Mechanism of Action. Molecules. 2008;13(11):2900-2907.
555. Henry M, Briolant S, Fontaine A, Mosnier J, Baret E, Amalvict R, et al. In vitro activity of ferroquine is independent of polymorphisms in transport protein genes implicated

University of Ghana http://ugspace.ug.edu.gh

in quinoline resistance in Plasmodium falciparum. Antimicrobial agents and chemotherapy. 2008;52(8):2755-2759.
556. Barends M, Jaidee A, Khaohirun N, Singhasivanon P, Nosten F. In vitro activity of ferroquine (SSR 97193) against Plasmodium falciparum isolates from the Thai-Burmese border. Malaria Journal. 2007;6(81):1-5.
557. Baragaña B, Hallyburton I, Lee MC, Norcross NR, Grimaldi R, Otto TD, et al. A novel multiple-stage antimalarial agent that inhibits protein synthesis. Nature. 2015;522(7556):315-320.
558. Murithi JM, Pascal C, Bath J, Boulenc X, Gnädig NF, Pasaje CFA, et al. The antimalarial MMV688533 provides potential for single-dose cures with a high barrier to Plasmodium falciparum parasite resistance. Science translational medicine. 2021;13(603):1-14.
559. Boss C, Aissaoui H, Amaral N, Bauer A, Bazire S, Binkert C, et al. Discovery and characterization of ACT-451840: an antimalarial drug with a novel mechanism of action. ChemMedChem. 2016;11(18):1995-2014.
560. Chughlay MF, El Gaaloul M, Donini C, Campo B, Berghmans P-J, Lucardie A, et al. Chemoprotective antimalarial activity of P218 against Plasmodium falciparum: a randomized, placebo-controlled volunteer infection study. The American Journal of Tropical Medicine and Hygiene. 2021;104(4):1348–1358.
561. Sindhe KM, Wu W, Legac J, Zhang Y-K, Easom EE, Cooper RA, et al. Plasmodium falciparum resistance to a lead benzoxaborole due to blocked compound activation and altered ubiquitination or sumoylation. MBio. 2020;11(1):1-15.
562. Ashley EA, Phyo AP. Drugs in Development for Malaria. Drugs. 2018;78(9):861-879.
563. Duffey M, Blasco B, Burrows JN, Wells TNC, Fidock DA, Leroy D. Assessing risks of Plasmodium falciparum resistance to select next-generation antimalarials. Trends in Parasitology. 2021;37(8):709-721.
564. Chalapareddy SK, Sajid A, Saxena M, Arora K, Guha R, Arora G. Chapter 10 - Emerging therapeutic modalities against malaria. In: Hasija Y, editor. Translational Biotechnology: Academic Press; 2021.Page; 267-286.
565. Hooft van Huijsduijnen R, Wells TNC. The antimalarial pipeline. Current Opinion in Pharmacology. 2018;42(1):1-6.
566. Wunberg T, Hendrix M, Hillisch A, Lobell M, Meier H, Schmeck C, et al. Improving the hit-to-lead process: data-driven assessment of drug-like and lead-like screening hits. Drug Discovery Today. 2006;11(3):175-180.
567. Teague SJ, Davis AM, Leeson PD, Oprea T. The Design of Leadlike Combinatorial Libraries. Angew Chem Int Ed Engl. 1999;38(24):3743-3748.
568. Słoczyńska K, Gunia-Krzyżak A, Koczurkiewicz P, Wójcik-Pszczoła K, Żelaszczyk D, Popiół J, et al. Metabolic stability and its role in the discovery of new chemical entities. Acta Pharmaceutica. 2019;69(3):345-361.
569. Masimirembwa CM, Bredberg U, Andersson TB. Metabolic Stability for Drug Discovery and Development. Clinical pharmacokinetics. 2003;42(6):515-528.
570. Gajula SNR, Nadimpalli N, Sonti R. Drug metabolic stability in early drug discovery to develop potential lead compounds. Drug Metabolism Reviews. 2021;53(3):459-477.
571. Sodhi JK, Benet LZ. Successful and Unsuccessful Prediction of Human Hepatic Clearance for Lead Optimization. Journal of medicinal chemistry. 2021;64(7):3546-3559.
572. Kumar V, Wahlstrom JL, Rock DA, Warren CJ, Gorman LA, Tracy TS. CYP2C9 Inhibition: Impact of Probe Selection and Pharmacogenetics on in Vitro Inhibition Profiles. Drug Metabolism and Disposition. 2006;34(12):1966-1975.

University of Ghana http://ugspace.ug.edu.gh

573. Hefti FF. Requirements for a lead compound to become a clinical candidate. BMC Neuroscience. 2008;9 (S7):1-7.
574. Lipinski CA. Drug-like properties and the causes of poor solubility and poor permeability. Journal of Pharmacological and Toxicological Methods. 2000;44(1):235-249.
575. Trager W, Jensen JB. Human malaria parasites in continuous culture. Science. 1976;193(4254):673-675.
576. Makler MT, Hinrichs DJ. Measurement of the lactate dehydrogenase activity of Plasmodium falciparum as an assessment of parasitemia. The American Journal of Tropical Medicine and Hygiene. 1993;48(2):205-210.
577. Zhou L, Yang L, Tilton S, Wang J. Development of a high throughput equilibrium solubility assay using miniaturized shake-flask method in early drug discovery. Journal of Pharmaceutical Sciences. 2007;96(11):3052-3071.
578. Kerns EH, Di L, Carter GT. In vitro solubility assays in drug discovery. Current drug metabolism. 2008;9(9):879-885.
579. Siqueira-Neto JL, Song O-R, Oh H, Sohn J-H, Yang G, Nam J, et al. Antileishmanial high-throughput drug screening reveals drug candidates with new scaffolds. PLoS neglected tropical diseases. 2010;4(5):1-8.
580. Usia T, Watabe T, Kadota S, Tezuka Y. Metabolite-cytochrome P450 complex formation by methylenedioxyphenyl lignans of Piper cubeba: mechanism-based inhibition. Life Sciences. 2005;76(20):2381-2391.
581. Dinger J, Meyer MR, Maurer HH. In vitro cytochrome P450 inhibition potential of methylenedioxy-derived designer drugs studied with a two-cocktail approach. Archives of Toxicology. 2016;90(2):305-318.
582. Díaz Chávez ML, Rolf M, Gesell A, Kutchan TM. Characterization of two methylenedioxy bridge-forming cytochrome P450-dependent enzymes of alkaloid formation in the Mexican prickly poppy Argemone mexicana. Arch Biochem Biophys. 2011;507(1):186-193.
583. Baker JW, Davies MM, Gaunt J. The mechanism of the reaction of aryl iso cyanates with alcohols and amines. Part IV. The evidence of infra-red absorption spectra regarding alcohol–amine association in the base-catalysed reaction of phenyl iso cyanate with alcohols. Journal of the Chemical Society (Resumed). 1949;1(1):24-27.
584. Bengtström L, Salden M, Stec AA. The role of isocyanates in fire toxicity. Fire Science Reviews. 2016;5(4):1-23.
585. Nudelman A, Bechor Y, Falb E, Fischer B, Wexler BA, Nudelman A. Acetyl Chloride-Methanol as a Convenient Reagent for: A) Quantitative Formation of Amine Hydrochlorides B) Carboxylate Ester Formation C) Mild Removal of Nt-Boc-Protective Group. Synthetic communications. 1998;28(3):471-474.
586. George N, Ofori S, Parkin S, Awuah SG. Correction: Mild deprotection of the N-tert-butyloxycarbonyl (N-Boc) group using oxalyl chloride. RSC advances. 2021;11(2):780-780.
587. Abdel-Magid AF, Carson KG, Harris BD, Maryanoff CA, Shah RD. Reductive Amination of Aldehydes and Ketones with Sodium Triacetoxyborohydride. Studies on Direct and Indirect Reductive Amination Procedures(1). The Journal of Organic Chemistry. 1996;61(11):3849-3862.
588. Pediconi N, Ghirga F, Del Plato C, Peruzzi G, Athanassopoulos CM, Mori M, et al. Design and Synthesis of Piperazine-Based Compounds Conjugated to Humanized Ferritin as Delivery System of siRNA in Cancer Cells. Bioconjugate Chemistry. 2021;32(6):1105-1116.
589. Oliphant SJ, Morris RH. Density Functional Theory Study on the Selective Reductive Amination of Aldehydes and Ketones over Their Reductions to Alcohols Using Sodium Triacetoxyborohydride. ACS Omega. 2022;7(34):30554-30564.

University of Ghana http://ugspace.ug.edu.gh

590. Ortiz A, Farfán N, Höpfl H, Santillan R, Ochoa MaE, Gutiérrez A. A new method for the preparation of unsymmetrical 1,4-substituted piperazine derivatives. Tetrahedron: Asymmetry. 1999;10(4):799-811.
591. Wodtke R, Steinberg J, Köckerling M, Löser R, Mamat C. NMR-based investigations of acyl-functionalized piperazines concerning their conformational behavior in solution. RSC advances. 2018;8(71):40921-40933.
592. Rohl CA, Baldwin RL. Exchange kinetics of individual amide protons in 15N-labeled helical peptides measured by isotope-edited NMR. Biochemistry. 1994;33(25):7760-7767.
593. Green AR, Li K, Lockard B, Young RP, Mueller LJ, Larive CK. Investigation of the Amide Proton Solvent Exchange Properties of Glycosaminoglycan Oligosaccharides. The Journal of Physical Chemistry B. 2019;123(22):4653-4662.
594. Fulmer GR, Miller AJ, Sherden NH, Gottlieb HE, Nudelman A, Stoltz BM, et al. NMR chemical shifts of trace impurities: common laboratory solvents, organics, and gases in deuterated solvents relevant to the organometallic chemist. Organometallics. 2010;29(9):2176-2179.
595. Tang Q, Wang S, Zhai X, Kim SB, Achanta P, Malca-Garcia GR, et al. Applications of quantitative 13C NMR in pharmaceutical analysis: From small molecule drugs to biopolymers. Journal of Pharmaceutical Analysis. 2025;101346(1):1-56.
596. Balci M. Basic 1H-and 13C-NMR spectroscopy: Elsevier; 2005. 427 pages.
597. Kricheldorf HR, Rieth KH. 13C-NMR sequence analysis 8. Investigation on piperazine-containing copolyamides. Journal of Polymer Science: Polymer Letters Edition. 1978;16(8):379-391.
598. Nakanishi W, Hayashi S, Matsuzaki K. Origin of (13)C NMR chemical shifts elucidated based on molecular orbital theory: paramagnetic contributions from orbital-to-orbital transitions for the pre-α, α, β, α-X, β-X and ipso-X effects, along with effects from characteristic bonds and groups. RSC advances. 2025;15(3):1924-1940.
599. Xiao Z, Yuan M, Zhang S, Wu J, Qi S, Li Q. Complete assignments of 1H and 13C NMR data for ten phenylpiperazine derivatives. Magnetic resonance in chemistry. 2005;43(10):869-872.
600. Sari S, Yilmaz M. Synthesis and characterization of piperazine-substituted dihydrofuran derivatives viaMn(OAc) (3) mediated radical cyclizations. Turkish Journal of Chemistry. 2020;44(5):1303-1313.
601. Stewart CD, White NG, Barrow RA, Reekie TA. Synthesis and spectroscopic investigation of substituted piperazine-2,5-dione derivatives. Tetrahedron. 2024;153(133838):1-16.
602. He X, Liu X, Nie B, Song D. FTIR and Raman spectroscopy characterization of functional groups in various rank coals. Fuel. 2017;206(2017):555-563.
603. Abidi N. Sample Preparation, Data Acquisition, Spectral Data Processing and Analysis. In: Abidi N, editor. FTIR Microspectroscopy : Selected Emerging Applications. Cham: Springer International Publishing; 2021.Page; 125-128.
604. Nandiyanto ABD, Oktiani R, Ragadhita R. How to read and interpret FTIR spectroscope of organic material. Indonesian Journal of Science and Technology. 2019;4(1):97-118.
605. Möbitz H. Design principles for balancing lipophilicity and permeability in beyond rule of 5 space. ChemMedChem. 2024;19(5):1-11.
606. Walters WP. Going further than Lipinski's rule in drug design. Expert Opinion on Drug Discovery. 2012;7(2):99-107.

University of Ghana http://ugspace.ug.edu.gh

607. Tice CM. Selecting the right compounds for screening: does Lipinski's Rule of 5 for pharmaceuticals apply to agrochemicals? Pest Management Science: formerly Pesticide Science. 2001;57(1):3-16.
608. Clark DE. What has polar surface area ever done for drug discovery? Future Medicinal Chemistry. 2011;3(4):469-484.
609. Karami TK, Hailu S, Feng S, Graham R, Gukasyan HJ. Eyes on lipinski's rule of five: a new “rule of thumb” for physicochemical design space of ophthalmic drugs. Journal of ocular pharmacology and therapeutics. 2022;38(1):43-55.
610. Aldrich C, Bertozzi C, Georg GI, Kiessling L, Lindsley C, Liotta D, et al. The Ecstasy and Agony of Assay Interference Compounds. ACS Chemical Biology. 2017;12(3):575-578.
611. Hermann JC, Chen Y, Wartchow C, Menke J, Gao L, Gleason SK, et al. Metal impurities cause false positives in high-throughput screening campaigns. ACS Medicinal Chemistry Letters. 2013;4(2):197-200.
612. Sepehri S, Khedmati M, Yousef-Nejad F, Mahdavi M. Medicinal chemistry perspective on the structure–activity relationship of stilbene derivatives. RSC advances. 2024;14(28):19823-19879.
613. Shah A, Desai K, Bhanusali A, Agrawal S, Patel K, Naik N, et al. In vitro and in silico evaluation of fluorinated diphenylamine chalcone derivatives as potential antimalarial and anticancer agents. Scientific reports. 2025;15(18928):1-19.
614. Elhemely MA, Belgath AA, El-Sayed S, Burusco KK, Kadirvel M, Tirella A, et al. SAR of novel 3-arylisoquinolinones: meta-substitution on the aryl ring dramatically enhances antiproliferative activity through binding to microtubules. Journal of medicinal chemistry. 2022;65(6):4783-4797.
615. Papadatos G, Alkarouri M, Gillet VJ, Willett P, Kadirkamanathan V, Luscombe CN, et al. Lead optimization using matched molecular pairs: inclusion of contextual information for enhanced prediction of HERG inhibition, solubility, and lipophilicity. J Chem Inf Model. 2010;50(10):1872-1886.
616. Shao J, Kuiper BP, Thunnissen AWH, Cool RH, Zhou L, Huang C, et al. The Role of Tryptophan in π Interactions in Proteins: An Experimental Approach. Journal of the American Chemical Society. 2022;144(30):13815-13822.
617. Yajima T, Takamido R, Shimazaki Y, Odani A, Nakabayashi Y, Yamauchi O. π–π Stacking assisted binding of aromatic amino acids by copper (II)–aromatic diimine complexes. Effects of ring substituents on ternary complex stability. Dalton Transactions. 2007(3):299-307.
618. Jing P, Rodgers PJ, Amemiya S. High lipophilicity of perfluoroalkyl carboxylate and sulfonate: implications for their membrane permeability. Journal of the American Chemical Society. 2009;131(6):2290-2296.
619. Lipinski CA, Lombardo F, Dominy BW, Feeney PJ. Experimental and computational approaches to estimate solubility and permeability in drug discovery and development settings. Advanced drug delivery reviews. 1997;23(1-3):3-25.
620. Ippolito MM, Moser KA, Kabuya JB, Cunningham C, Juliano JJ. Antimalarial Drug Resistance and Implications for the WHO Global Technical Strategy. Current Epidemiology Reports. 2021;8(2):46-62.
621. Iwanaga S, Kubota R, Nishi T, Kamchonwongpaisan S, Srichairatanakool S, Shinzawa N, et al. Genome-wide functional screening of drug-resistance genes in Plasmodium falciparum. Nature Communications. 2022;13(1):1-12.
622. Dechering KJ, Timmerman M, Rensen K, Koolen KMJ, Honarnejad S, Vos MW, et al. Replenishing the malaria drug discovery pipeline: Screening and hit evaluation of the MMV

University of Ghana http://ugspace.ug.edu.gh

Hit Generation Library 1 (HGL1) against asexual blood stage Plasmodium falciparum, using a nano luciferase reporter read-out. SLAS Discovery. 2022;27(6):337-348.
623. Hill AP, Young RJ. Getting physical in drug discovery: a contemporary perspective on solubility and hydrophobicity. Drug Discovery Today. 2010;15(15-16):648-655.
624. Lopes MS, de Souza Pietra RCC, Borgati TF, Romeiro CFD, Júnior PAS, Romanha AJ, et al. Synthesis and evaluation of the anti parasitic activity of aromatic nitro compounds. European Journal of Medicinal Chemistry. 2011;46(11):5443-5447.
625. Manzano JI, Cochet F, Boucherle B, Gómez-Pérez V, Boumendjel A, Gamarro F, et al. Arylthiosemicarbazones as antileishmanial agents. European Journal of Medicinal Chemistry. 2016;123(2016):161-170.
626. Krauth-Siegel RL, Meiering SK, Schmidt H. The parasite-specific trypanothione metabolism of trypanosoma and leishmania. Biological chemistry. 2003;384(4):1-4.
627. Santi AMM, Murta SMF. Antioxidant defence system as a rational target for Chagas disease and Leishmaniasis chemotherapy. Memórias do Instituto Oswaldo Cruz. 2022;117(e210401):1-7.
628. Waring MJ. Lipophilicity in drug discovery. Expert Opinion on Drug Discovery. 2010;5(3):235-248.
629. Arnott JA, Planey SL. The influence of lipophilicity in drug discovery and design. Expert Opinion on Drug Discovery. 2012;7(10):863-875.
630. Ritchie TJ, Macdonald SJF. The impact of aromatic ring count on compound developability – are too many aromatic rings a liability in drug design? Drug Discovery Today. 2009;14(21):1011-1020.
631. Leeson PD, Young RJ. Molecular Property Design: Does Everyone Get It? ACS Medicinal Chemistry Letters. 2015;6(7):722-725.
632. Prabhath MRR, Williams L, Bhat SV, Sharma P. Recent Advances in Cyanamide Chemistry: Synthesis and Applications. Molecules. 2017;22(4):1-28.
633. Carey FA, Sundberg RJ. Part B: Reactions and Synthesis: Springer; 2013. 947 pages.
634. Pawar GP, Barve IJ, Shen LC, Sun CM. Base-Mediated Four-Component Intramolecular Cyclization Reaction: One-Pot Access to Imidazole-4-(2H)-Ones. Advanced Synthesis & Catalysis. 2025;367(8):1-7.
635. Deng X, Han Y, Lin L-C, Ho WW. A new measurement of amine steric hindrance–N exposure. Separation and Purification Technology2022.Page. 1-6.
636. Bender ML. Mechanisms of catalysis of nucleophilic reactions of carboxylic acid derivatives. Chemical Reviews. 1960;60(1):53-113.
637. Sivaraj C, Gandhi T. Solvent-controlled amidation of acid chlorides at room temperature: new route to access aromatic primary amides and imides amenable for late-stage functionalization. RSC advances. 2023;13(14):9231-9236.
638. Davidson D, Skovronek H. The Acylation of Amides. Journal of the American Chemical Society. 1958;80(2):376-379.
639. Báscuas J, García-Río L, Leis JR. Cyclodextrin effect on solvolysis of substituted benzoyl chlorides. Organic and Biomolecular Chemistry. 2004;2(8):1186-1193.
640. Bentley TW, Harris HC. Solvolyses of Benzoyl Chlorides in Weakly Nucleophilic Media. International Journal of Molecular Sciences. 2011;12(8):4805-4818.
641. Tebes-Stevens C, Patel JM, Jones WJ, Weber EJ. Prediction of Hydrolysis Products of Organic Chemicals under Environmental pH Conditions. Environmental Science and Technology. 2017;51(9):5008-5016.
642. Tasic L, Abraham RJ, Rittner R. Substituent effects on 1H and 13C NMR chemical shifts in α-monosubstituted ethyl acetates: principal component analysis and 1H chemical shift calculations. Magnetic resonance in chemistry. 2002;40(7):449-454.

University of Ghana http://ugspace.ug.edu.gh

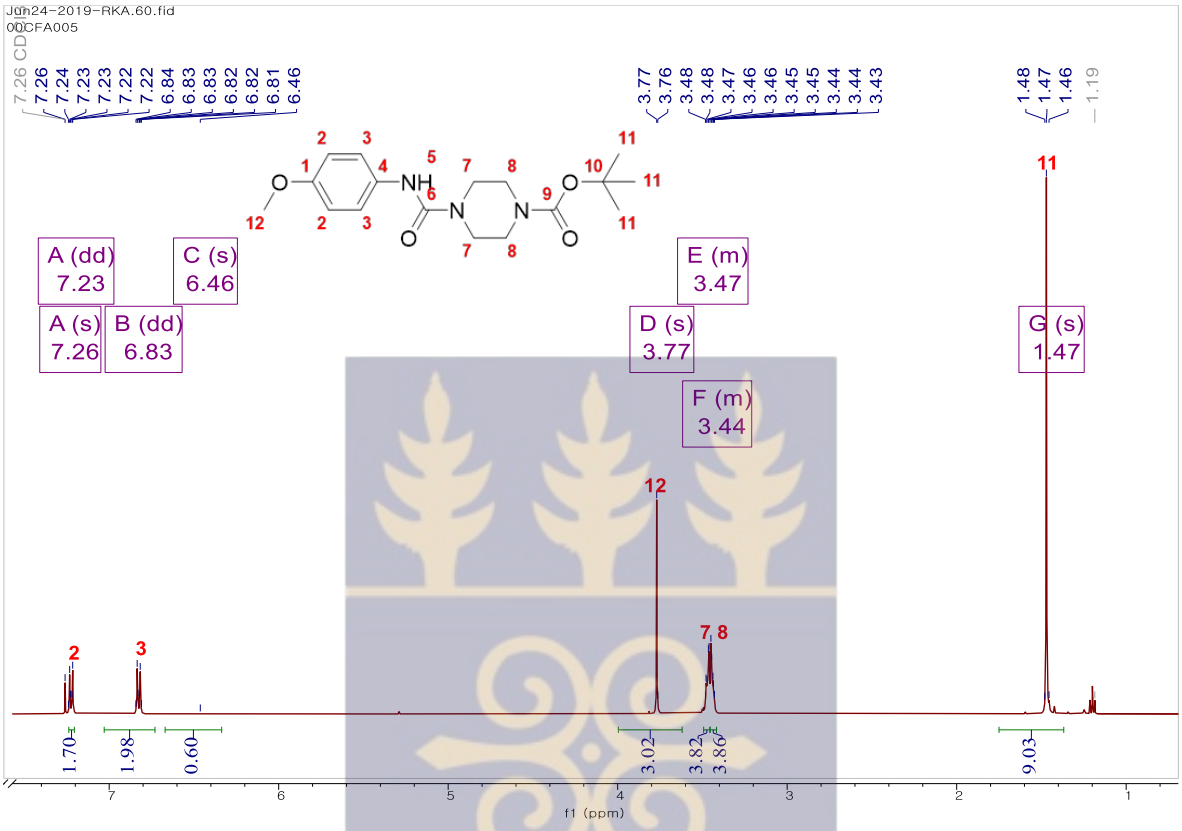
643. Abraham RJ, Griffiths L, Perez M. 1H NMR spectra. Part 30: 1H chemical shifts in amides and the magnetic anisotropy, electric field and steric effects of the amide group. Magnetic resonance in chemistry. 2013;51(3):143-155.
644. Mandhapati AR, Kato T, Matsushita T, Ksebati B, Vasella A, Böttger EC, et al. Fluorine-Decoupled Carbon Spectroscopy for the Determination of Configuration at Fully Substituted, Trifluoromethyl- and Perfluoroalkyl-Bearing Carbons: Comparison with 19F–1H Heteronuclear Overhauser Effect Spectroscopy. The Journal of Organic Chemistry. 2015;80(3):1754-1763.
645. Agar S, Durmaz H, Gunay US, Hizal G, Tunca U. Polymer grafting onto polyurethane backbone via D iels–A lder reaction. Journal of Polymer Science Part A: Polymer Chemistry. 2015;53(4):521-527.
646. Fujita Y, Yonehara M, Kitahara K, Shimokawa J, Hashimoto Y, Ishikawa M. Confirmation of molecular planarity disruption effect on aqueous solubility improvement of β-naphthoflavone analogs. Heterocycles. 2011;83(11):2563-2575.



University of Ghana http://ugspace.ug.edu.gh

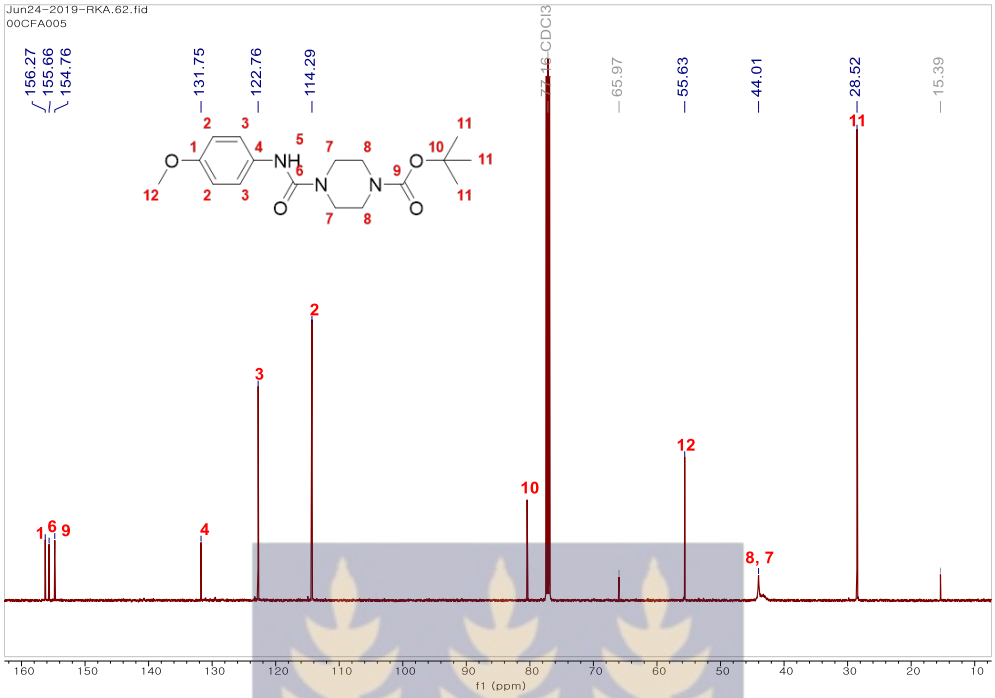
APPENDICES

Appendix 1: ^{1}H and ^{13}C NMR Spectra.

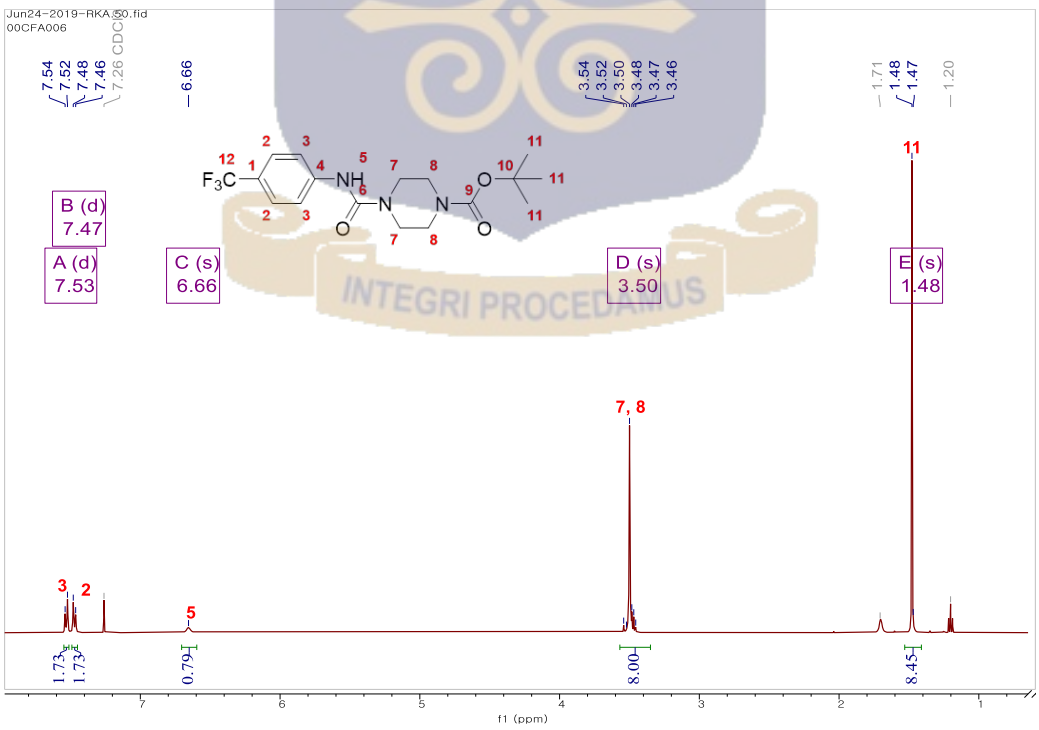


Appendix 1.1: ^{1}H NMR (500 MHz, $CDCl_3$) of *tert*-butyl 4-((4-methoxyphenyl)carbamoyl)piperazine-1-carboxylate (CFA005), **3.2**.

University of Ghana http://ugspace.ug.edu.gh

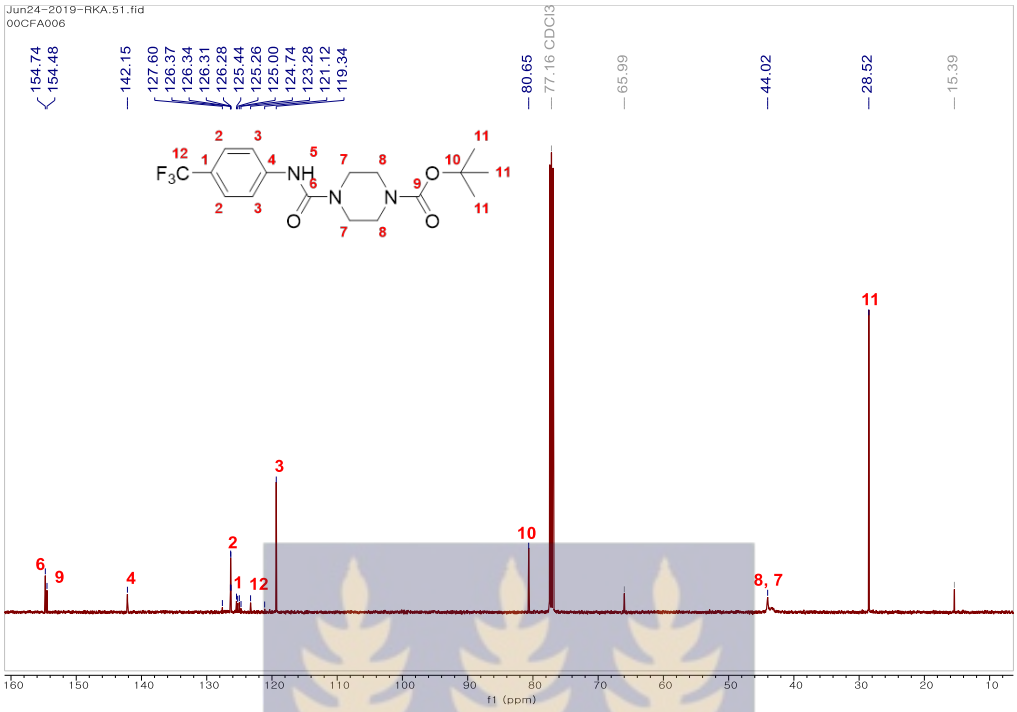


Appendix 1.2: ^{13}C NMR (126 MHz, $CDCl_3$) of *tert*-butyl 4-((4-methoxyphenyl)carbamoyl)piperazine-1-carboxylate (CFA005), **3.2**.

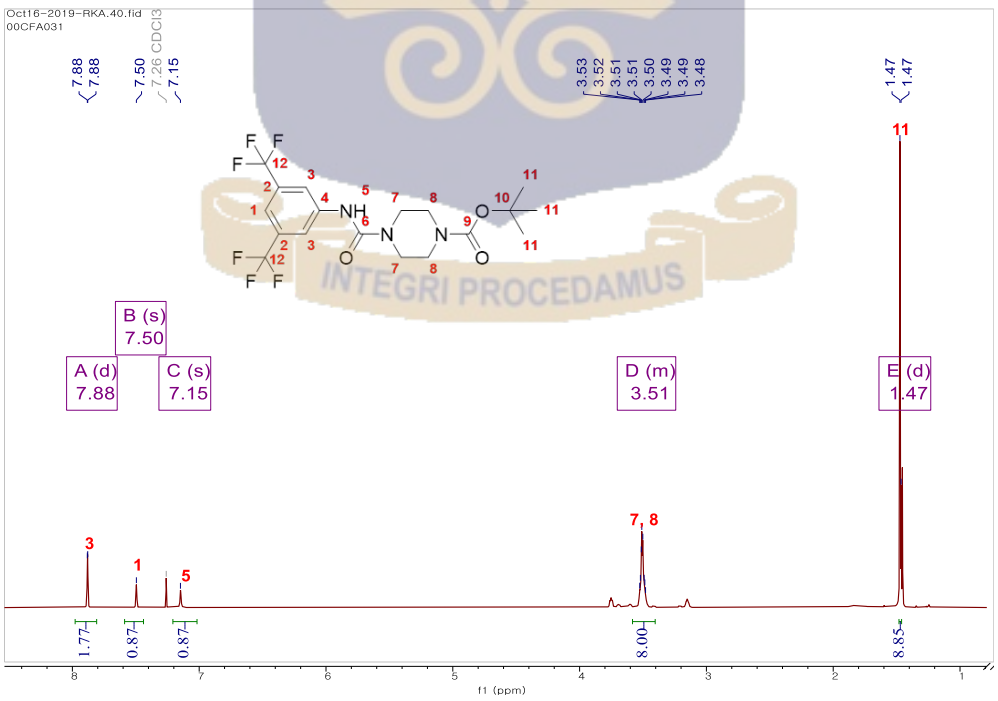


Appendix 1.3: ^{1}H NMR (500 MHz, $CDCl_3$) of *tert*-butyl 4-((4-(trifluoromethyl)phenyl)carbamoyl)piperazine-1-carboxylate (CFA006), **3.3**.

University of Ghana http://ugspace.ug.edu.gh

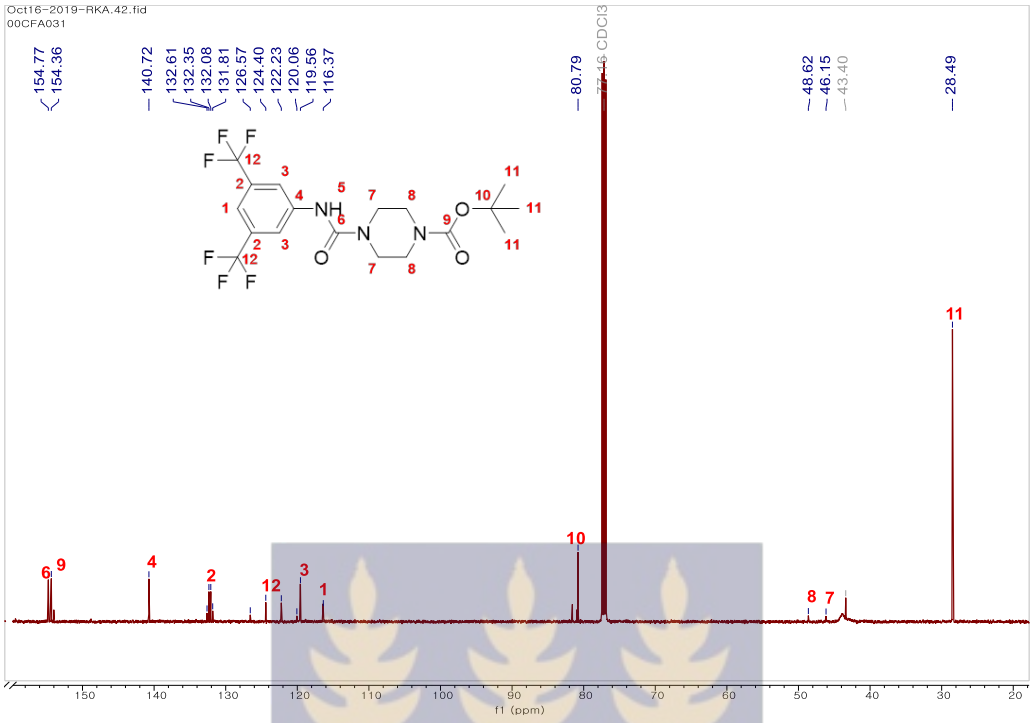


Appendix 1.4: ^{13}C NMR (126 MHz, $CDCl_3$) of *tert*-butyl 4-((4-(trifluoromethyl)phenyl)carbamoyl)piperazine-1-carboxylate (CFA006), **3.3**.

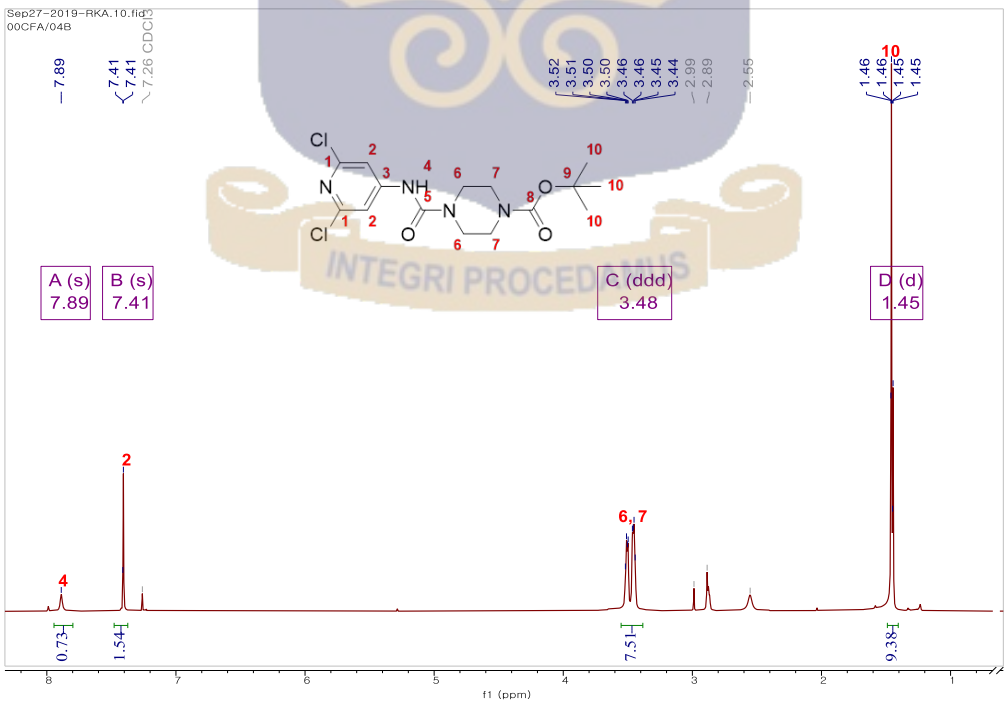


Appendix 1.5: ^{1}H NMR (500 MHz, $CDCl_3$) of *tert*-butyl 4-((3,5-bis(trifluoromethyl)phenyl)carbamoyl)piperazine-1-carboxylate (CFA031), **3.4**.

University of Ghana http://ugspace.ug.edu.gh

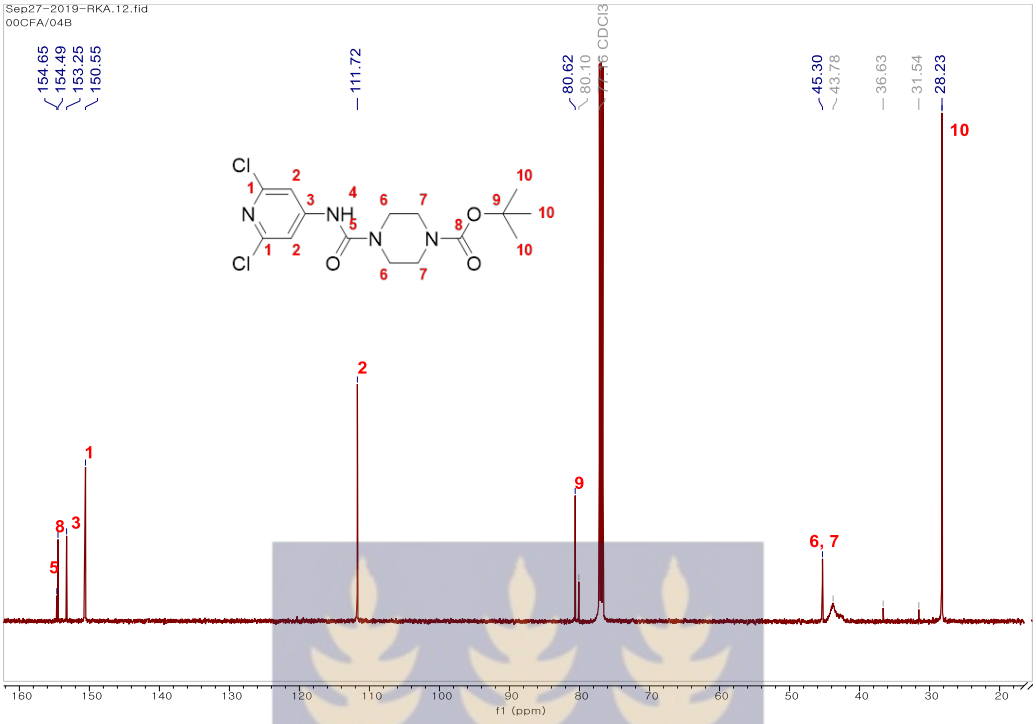


Appendix 1.6: ^{13}C NMR (126 MHz, $CDCl_3$) of *tert*-butyl 4-((3,5-bis(trifluoromethyl)phenyl)carbamoyl)piperazine-1-carboxylate (CFA031), **3.4**.

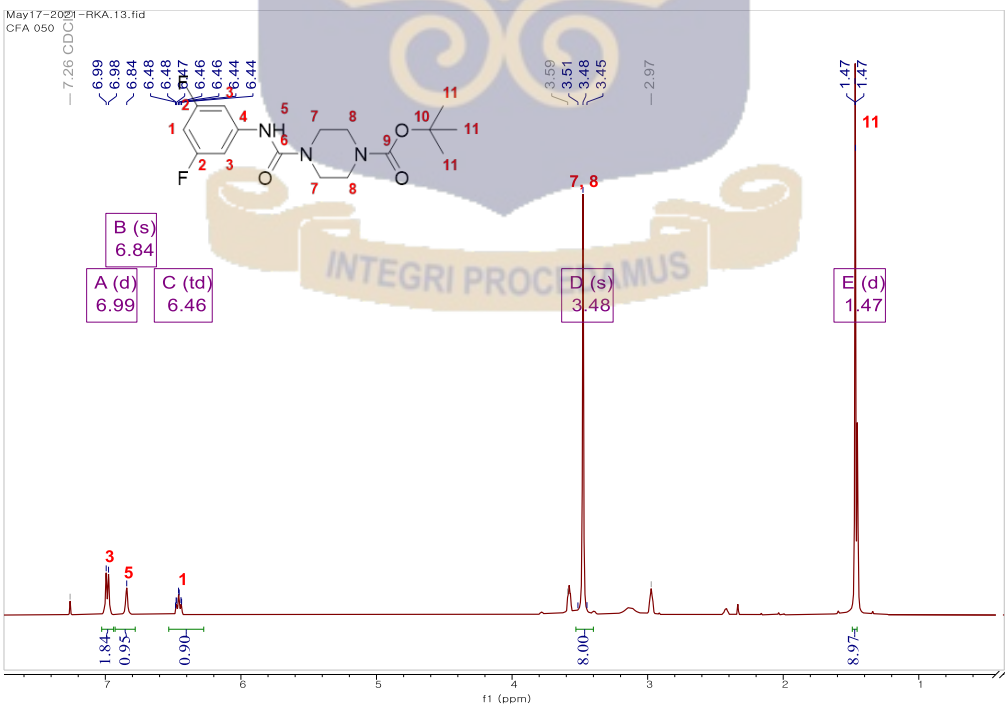


Appendix 1.7: ^{1}H NMR (500 MHz, $CDCl_3$) of *tert*-butyl 4-((2,6-dichloropyridin-4-yl)carbamoyl)piperazine-1-carboxylate (CFA040), **3.5**.

University of Ghana http://ugspace.ug.edu.gh

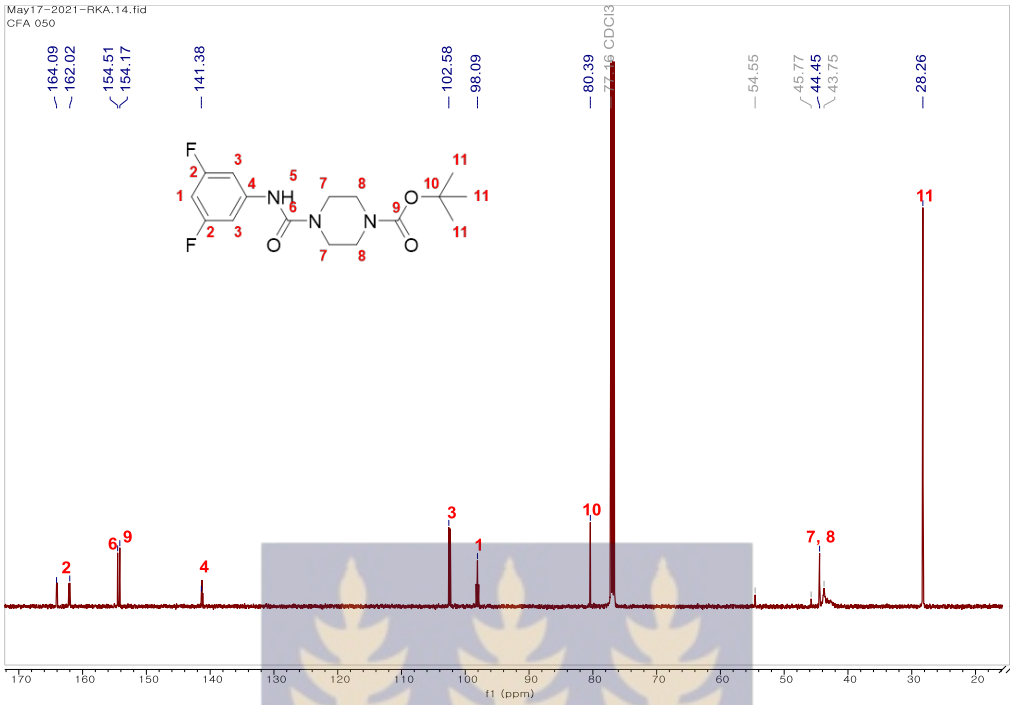


Appendix 1.8: ^{13}C NMR (126 MHz, $CDCl_3$) of *tert*-butyl 4-((2,6-dichloropyridin-4-yl)carbamoyl)piperazine-1-carboxylate (CFA040), **3.5**.

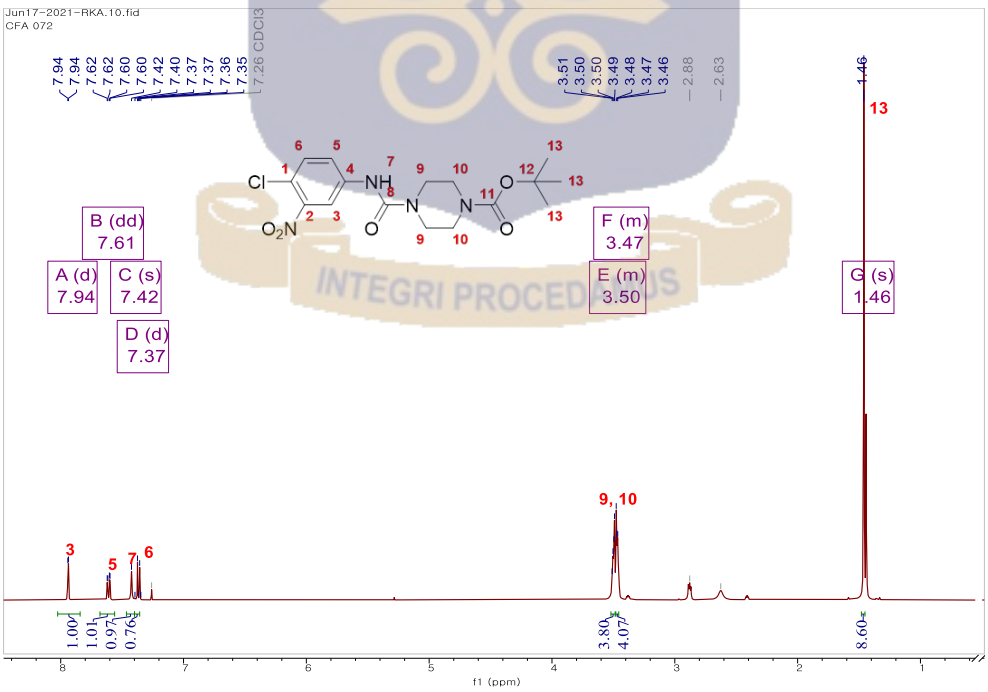


Appendix 1.9: ^{1}H NMR (500 MHz, $CDCl_3$) of *tert*-butyl 4-((3,5-difluorophenyl)carbamoyl)piperazine-1-carboxylate (CFA050), **3.6**.

University of Ghana http://ugspace.ug.edu.gh

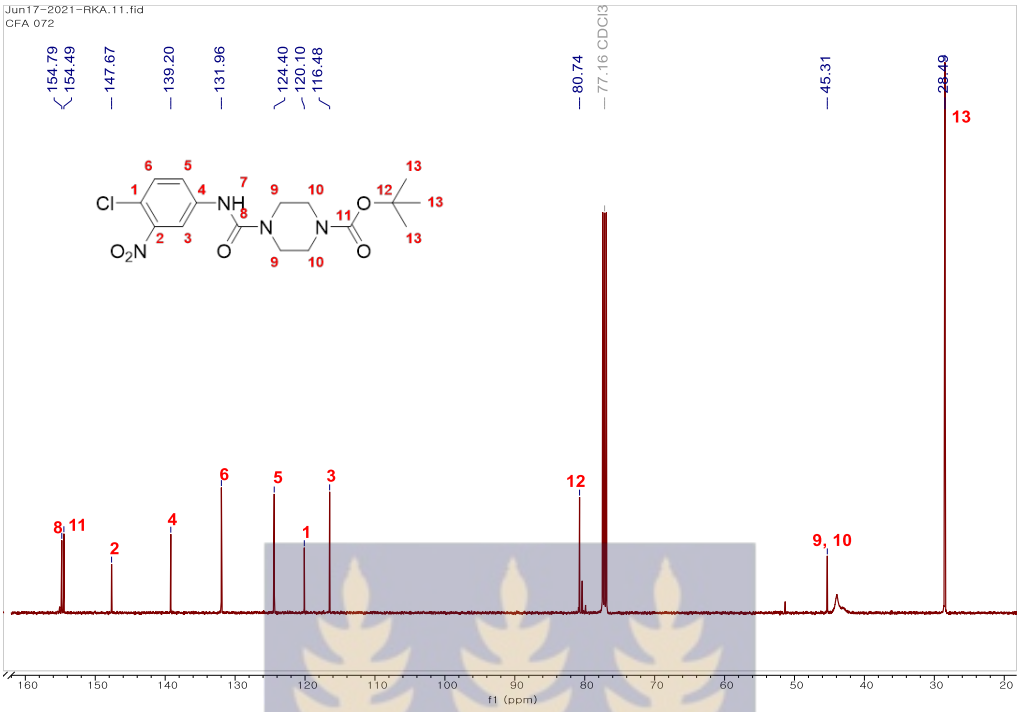


Appendix 1.10: ^{13}C NMR (126 MHz, $CDCl_3$) of *tert*-butyl 4-((3,5-difluorophenyl)carbamoyl)piperazine-1-carboxylate (CFA050), **3.6**.

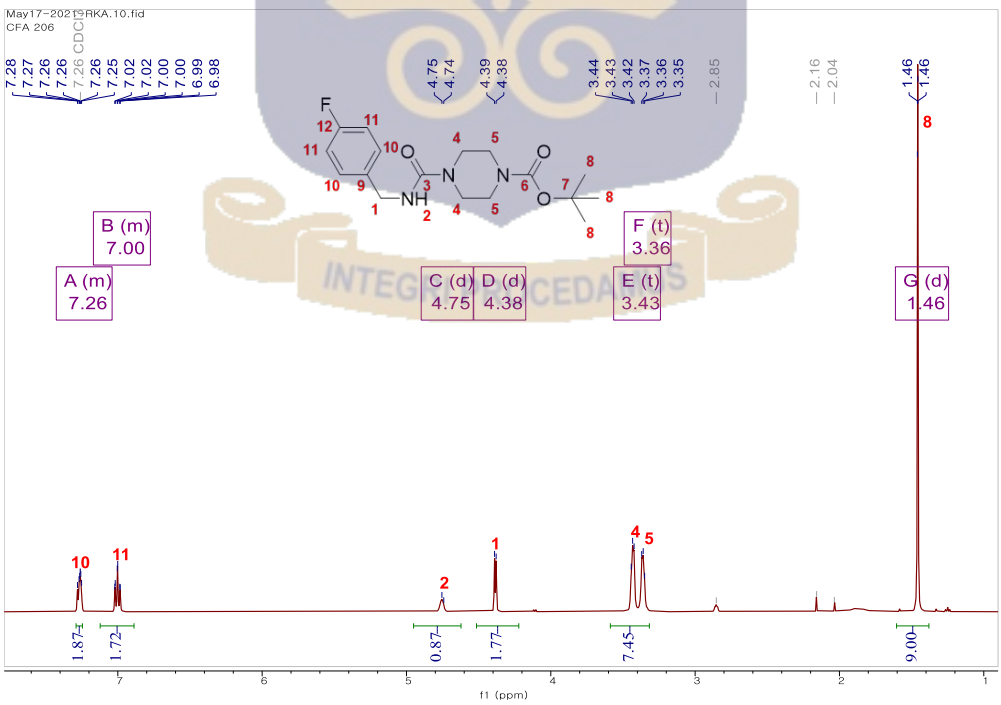


Appendix 1.11: ^{1}H NMR (500 MHz, $CDCl_3$) of *tert*-butyl 4-((4-chloro-3-nitrophenyl)carbamoyl)piperazine-1-carboxylate (CFA072), **3.8**.

University of Ghana http://ugspace.ug.edu.gh

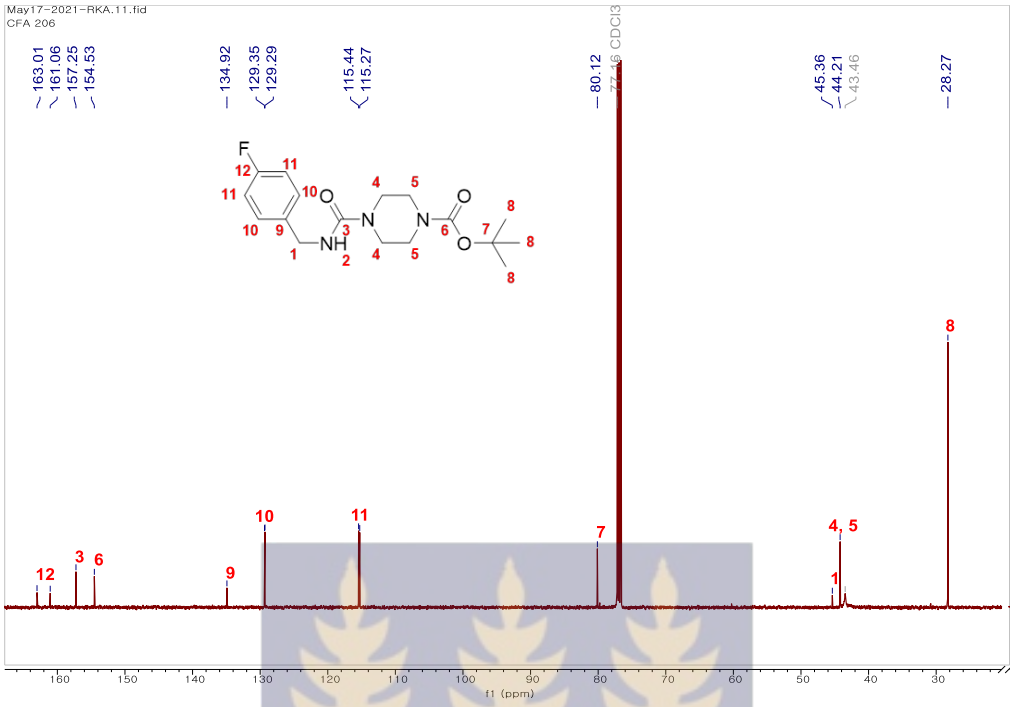


Appendix 1.12: ^{13}C NMR (126 MHz, $CDCl_3$) *tert*-butyl 4-((4-chloro-3-nitrophenyl)carbamoyl)piperazine-1-carboxylate (CFA072), **3.8**.

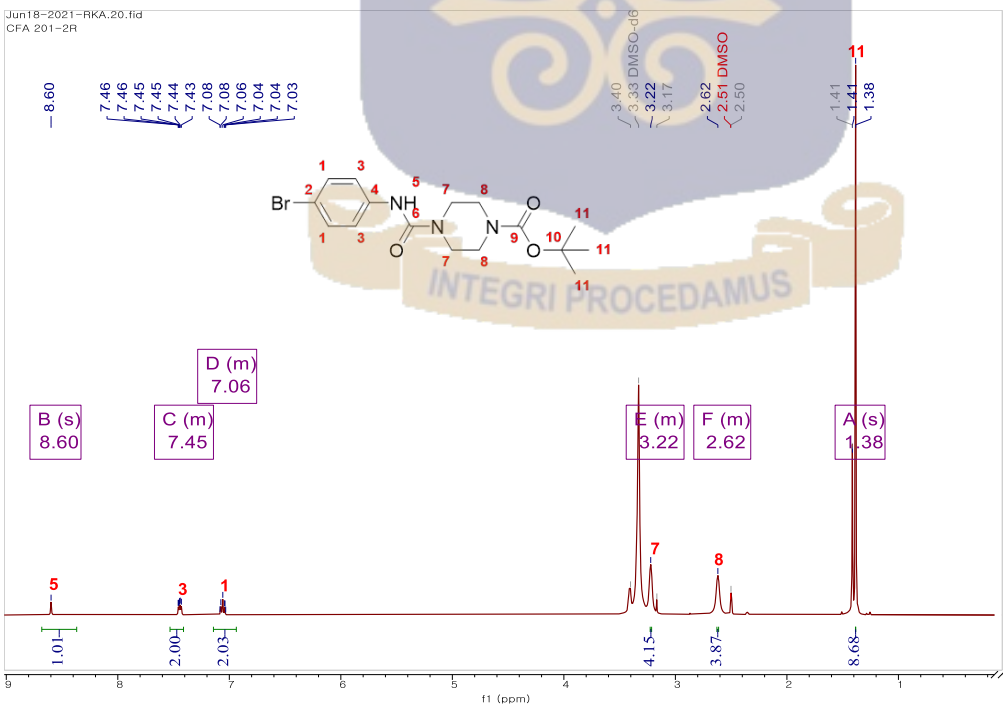


Appendix 1.13: ^{1}H NMR (500 MHz, $CDCl_3$) of *tert*-butyl 4-((4-fluorobenzyl)carbamoyl)piperazine-1-carboxylate (CFA206), **3.20**.

University of Ghana http://ugspace.ug.edu.gh

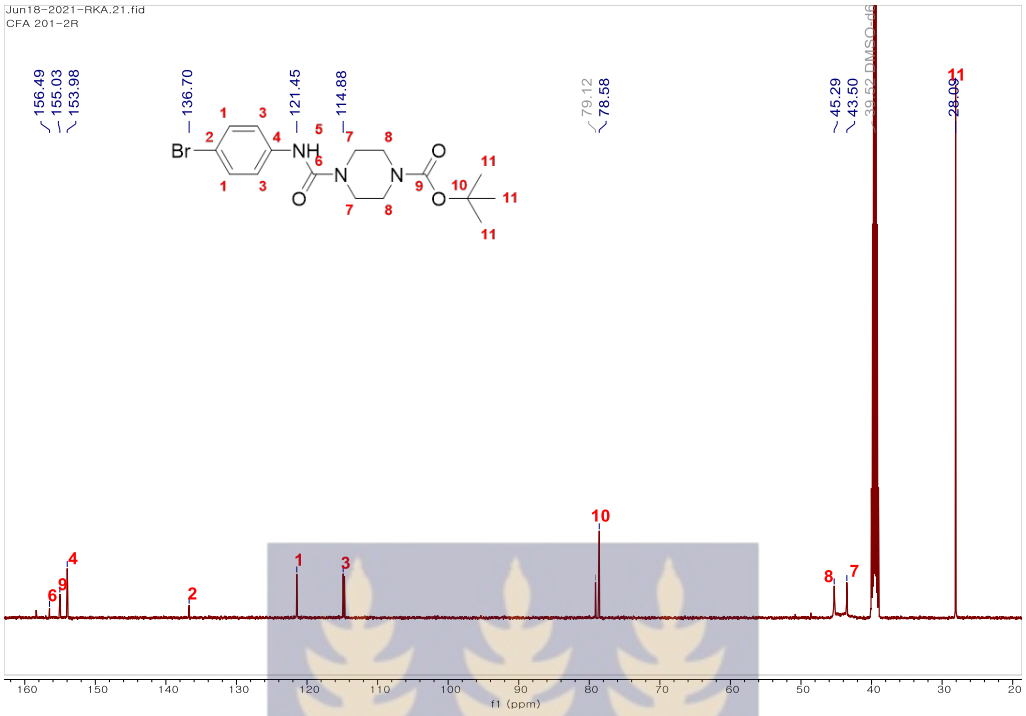


Appendix 1.14: ^{13}C NMR (126 MHz, $CDCl_3$) *tert*-butyl 4-((4-fluorobenzyl)carbamoyl)piperazine-1-carboxylate (CFA206), **3.20**.

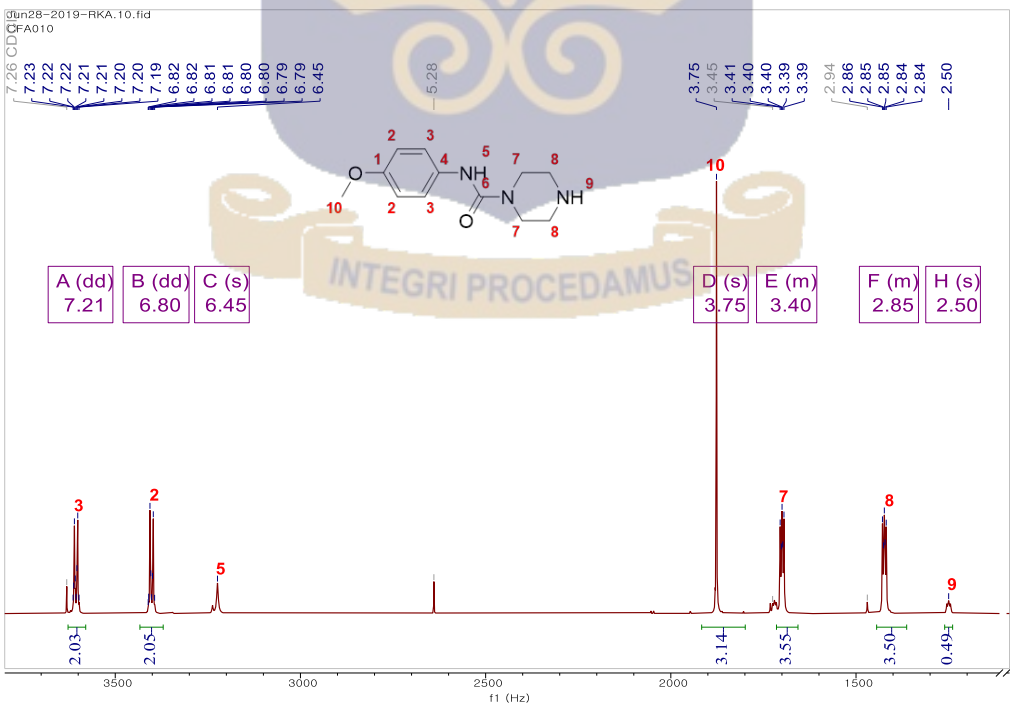


Appendix 1.15: ^{1}H NMR (500 MHz, DMSO) of *tert*-butyl 4-((4-bromophenyl)carbamoyl)piperazine-1-carboxylate (CFA201), **3.18**.

University of Ghana http://ugspace.ug.edu.gh

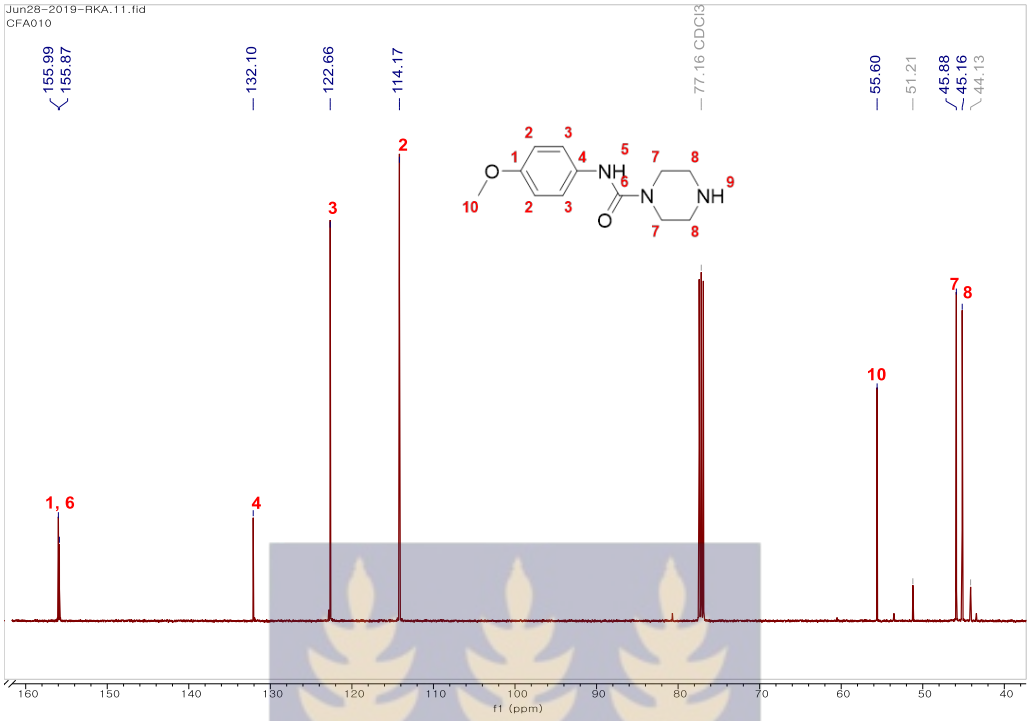


Appendix 1.16: ^{13}C NMR (126 MHz, DMSO) *tert*-butyl 4-((4-bromophenyl)carbamoyl)piperazine-1-carboxylate (CFA201), **3.18**.

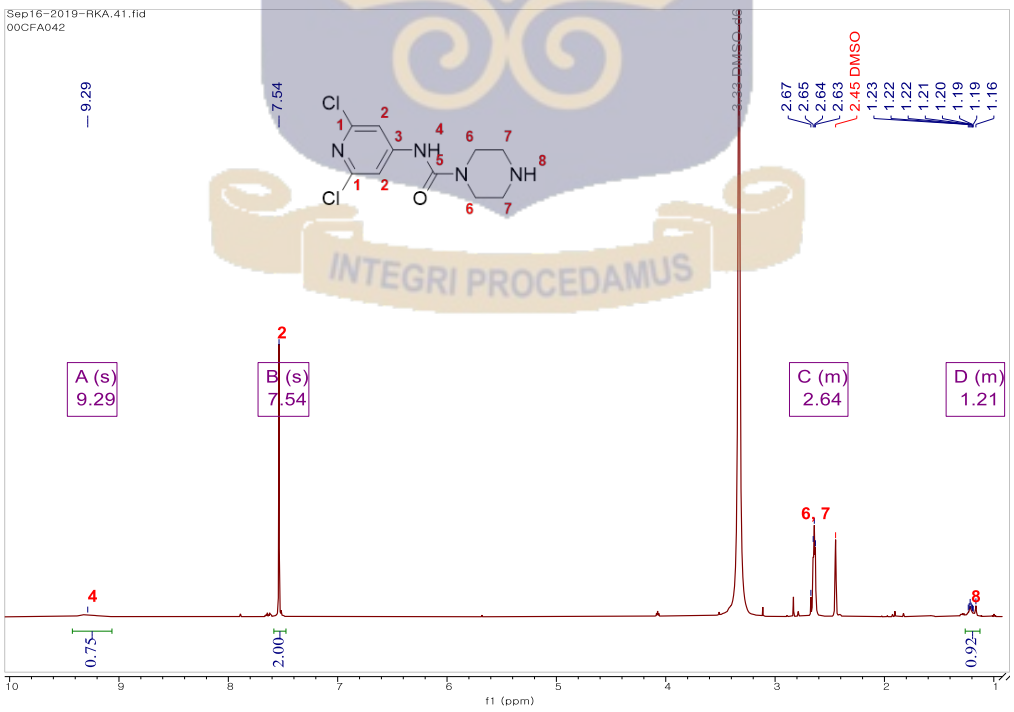


Appendix 1.17: ^{1}H NMR (500 MHz, $CDCl_3$) of *N*-(4-methoxyphenyl)piperazine-1-carboxamide (CFA008), **3.19**.

University of Ghana http://ugspace.ug.edu.gh

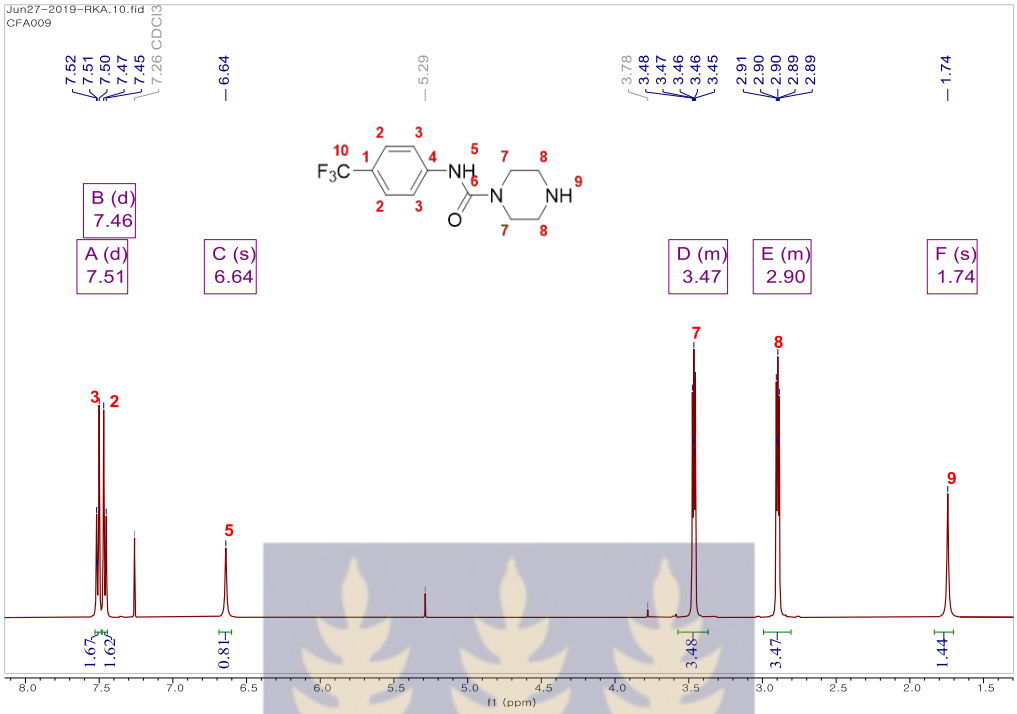


Appendix 1.18: ^{13}C NMR (126 MHz, $CDCl_3$) *N*-(4-methoxyphenyl)piperazine-1-carboxamide (CFA008), **3.19**.

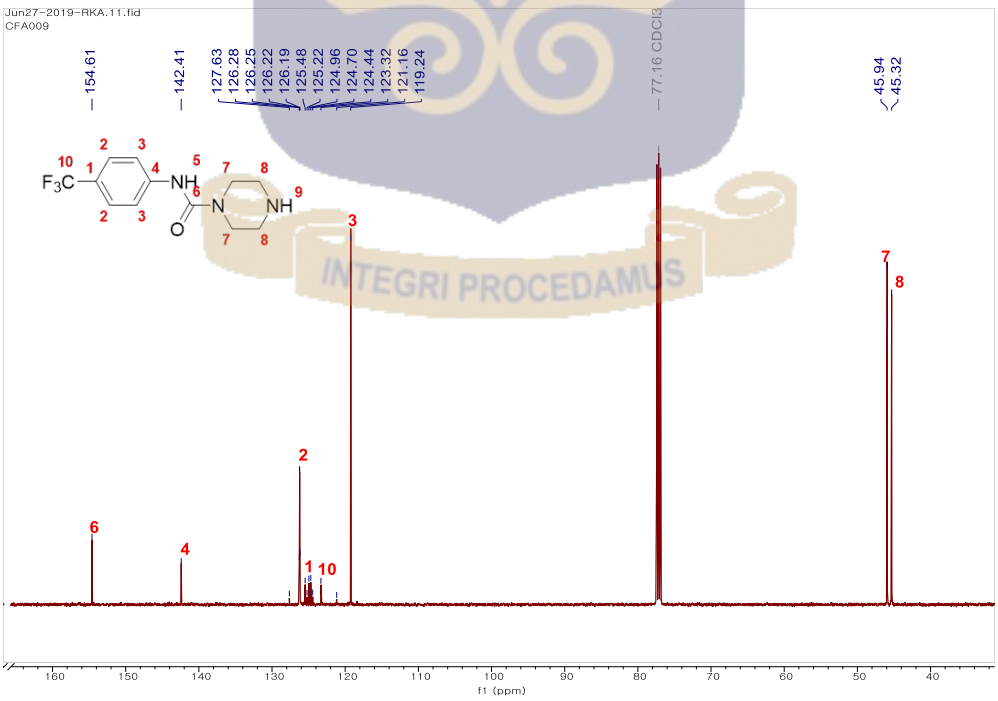


Appendix 1.19: ^{1}H NMR (500 MHz, DMSO) of *N*-(2,6-dichloropyridin-4-yl)piperazine-1-carboxamide (CFA042), **3.20**.

University of Ghana http://ugspace.ug.edu.gh

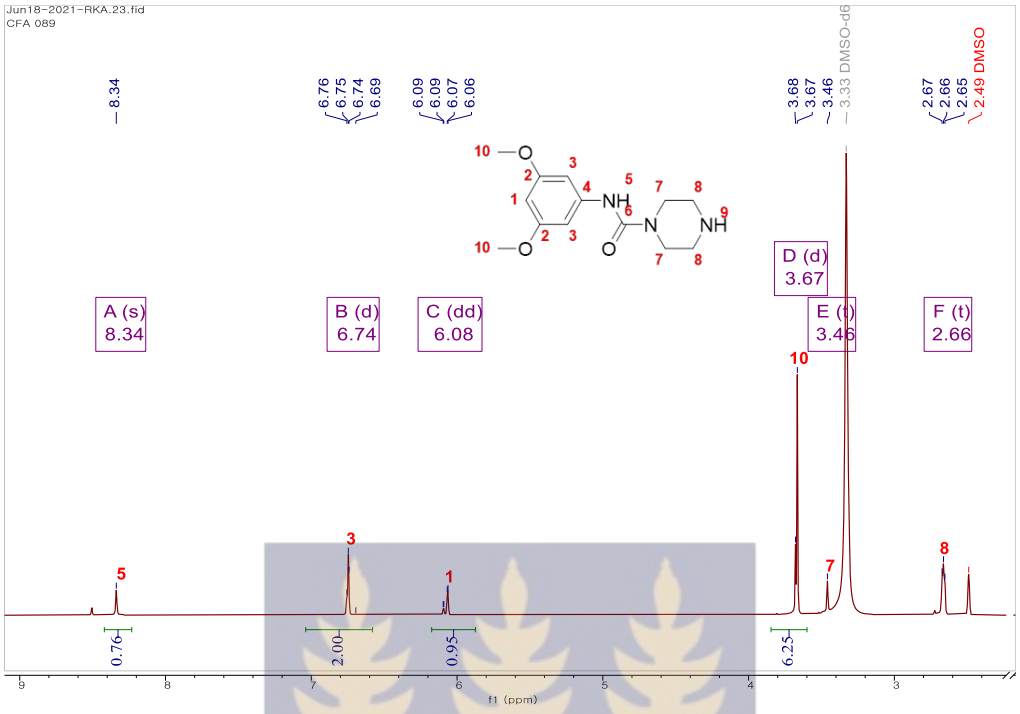


Appendix 1.20: ^{1}H NMR (500 MHz, DMSO) of *N*-(4-(trifluoromethyl)phenyl)piperazine-1-carboxamide (CFA009), **3.22**.

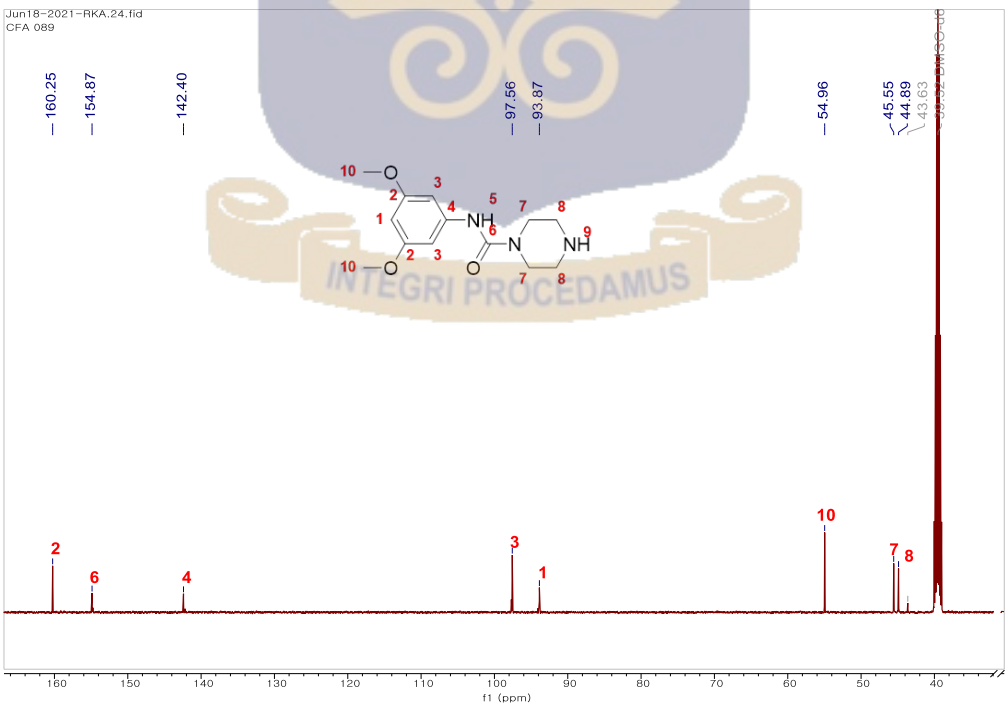


Appendix 1.21: ^{13}C NMR (126 MHz, $CDCl_3$) *N*-(4-(trifluoromethyl)phenyl)piperazine-1-carboxamide (CFA009), **3.22**.

University of Ghana http://ugspace.ug.edu.gh

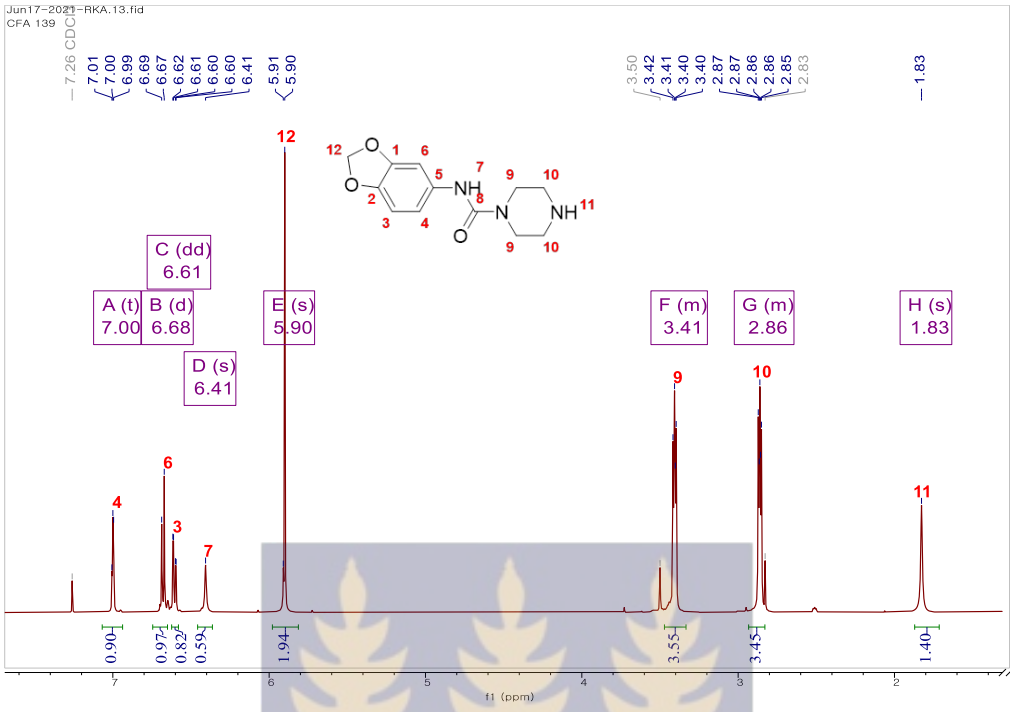


Appendix 1.22: ^{1}H NMR (500 MHz, DMSO) of *N*-(3,5-dimethoxyphenyl)piperazine-1-carboxamide (CFA089/168), **3.27**.

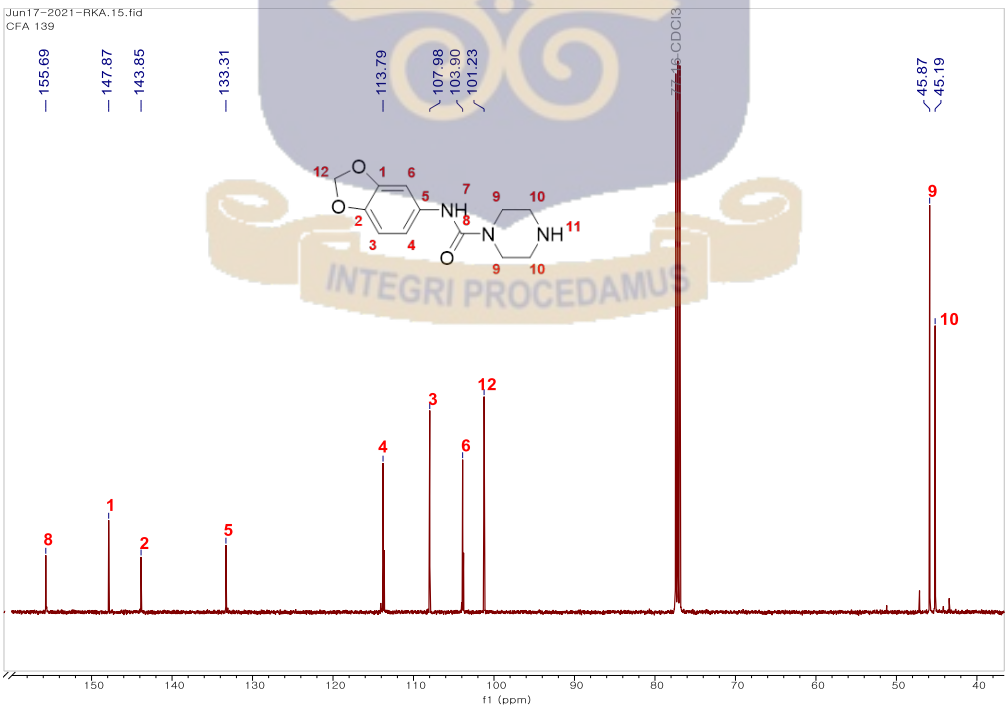


Appendix 1.23: ^{13}C NMR (126 MHz, DMSO) *N*-(3,5-dimethoxyphenyl)piperazine-1-carboxamide (CFA089/168), **3.27**.

University of Ghana http://ugspace.ug.edu.gh

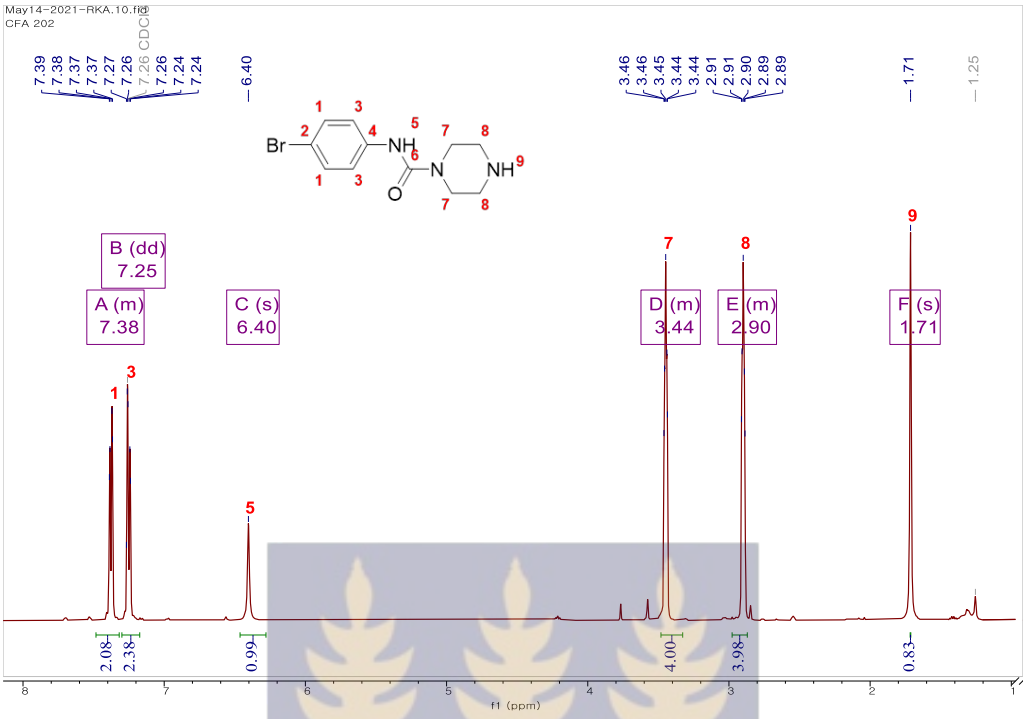


Appendix 1.24: ^{1}H NMR (500 MHz, $CDCl_3$) of *N*-(benzo[d][1,3]dioxol-5-yl)piperazine-1-carboxamide (CFA139), **3.33**.

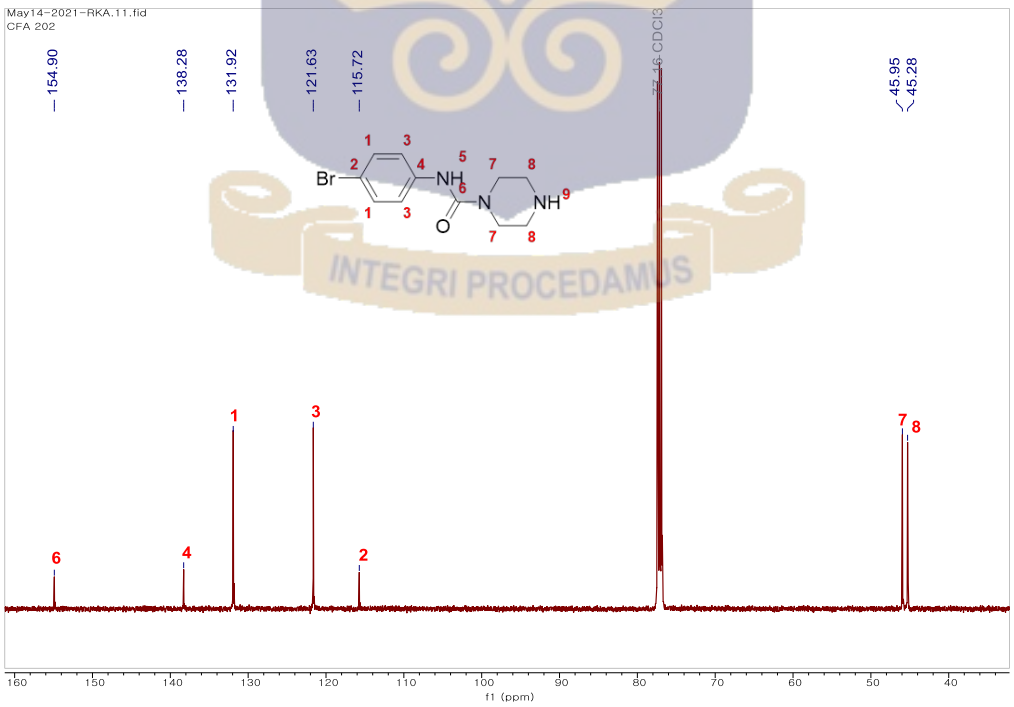


Appendix 1.25: ^{13}C NMR (126 MHz, $CDCl_3$) *N*-(benzo[d][1,3]dioxol-5-yl)piperazine-1-carboxamide (CFA139), **3.33**.

University of Ghana http://ugspace.ug.edu.gh

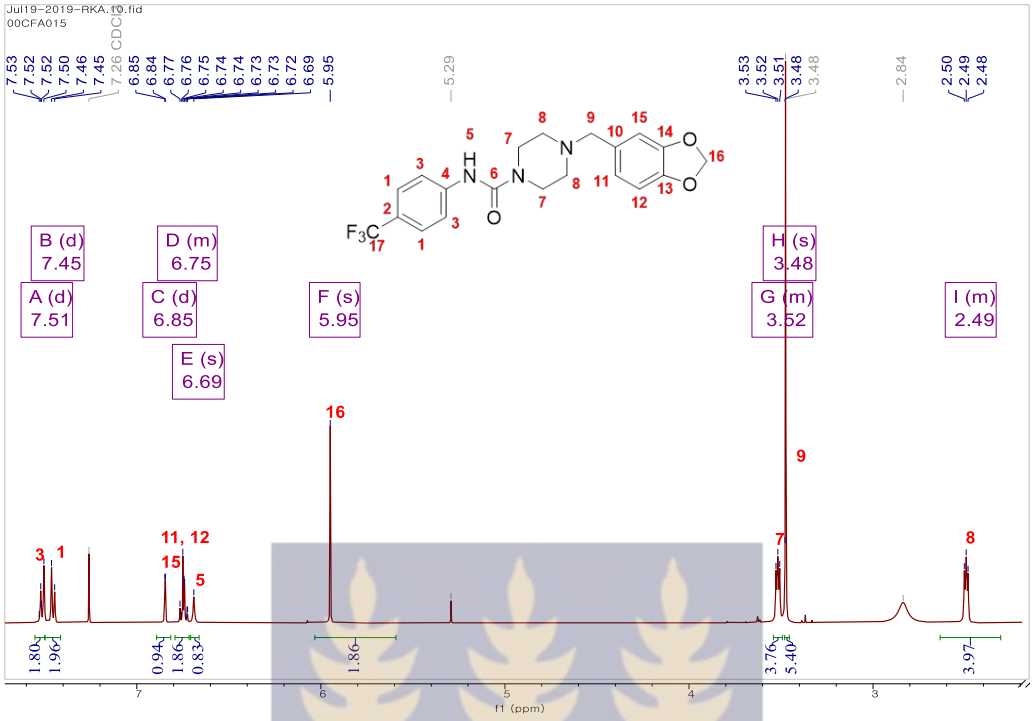


Appendix 1.26: ^{1}H NMR (500 MHz, $CDCl_3$) of *N*-(4-bromophenyl)piperazine-1-carboxamide (CFA202), **3.35**.

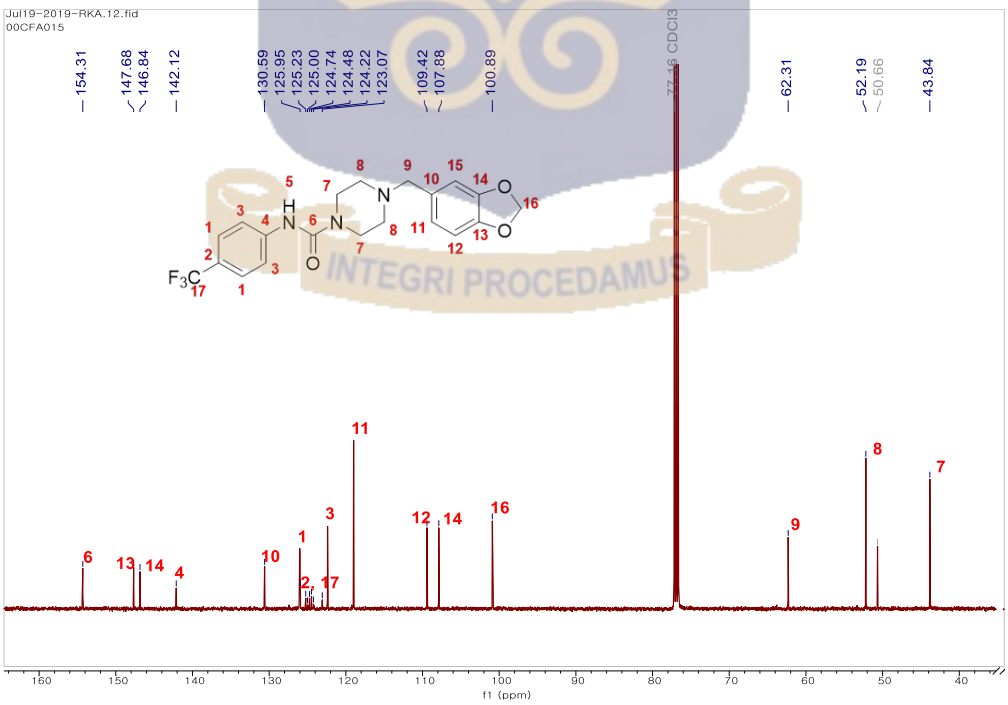


Appendix 1.27: ^{13}C NMR (126 MHz, $CDCl_3$) *N*-(4-bromophenyl)piperazine-1-carboxamide (CFA202), **3.35**.

University of Ghana http://ugspace.ug.edu.gh

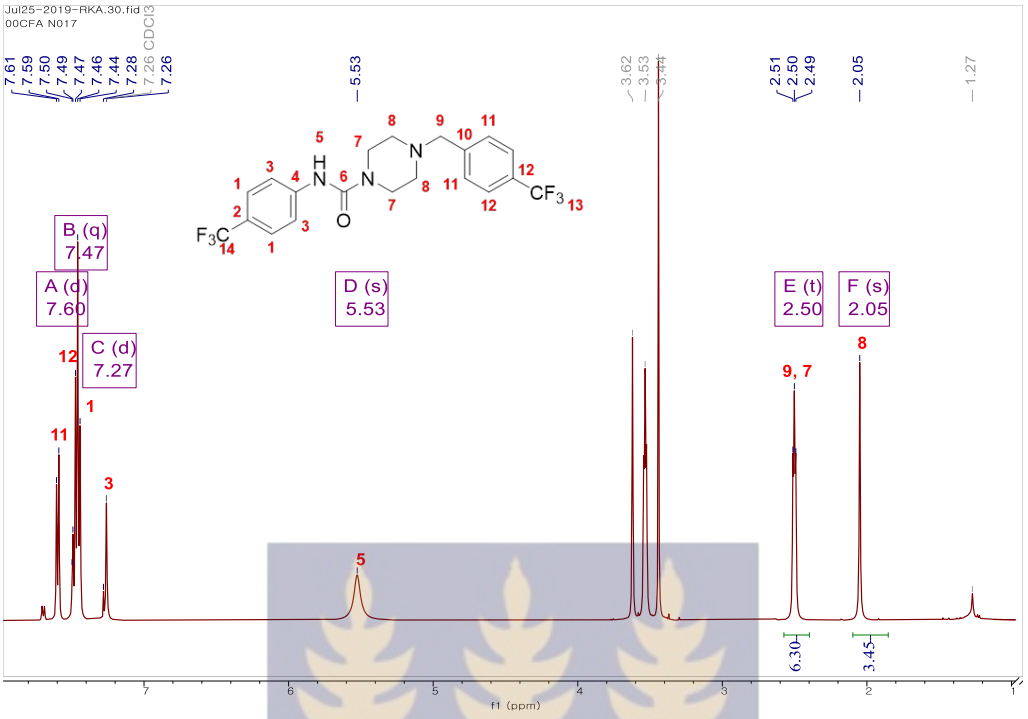


Appendix 1.28: ^{1}H NMR (500 MHz, $CDCl_3$) of 4-(benzo[*d*][1,3]dioxol-5-ylmethyl)-*N*-(4-(trifluoromethyl)phenyl)piperazine-1-carboxamide (CFA015), **3.36**.

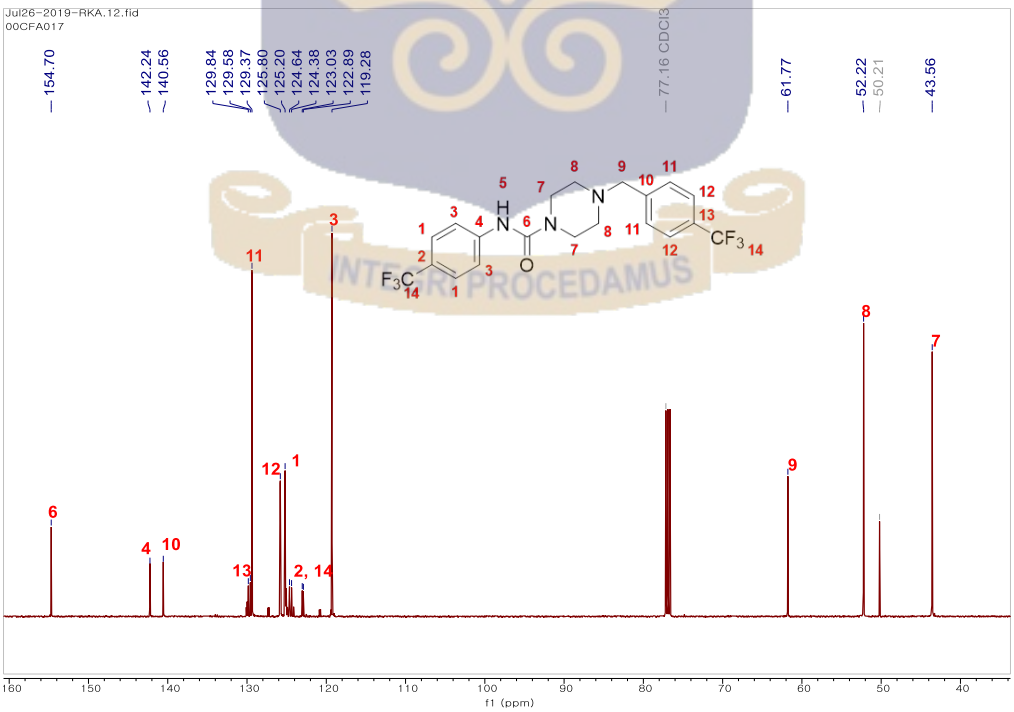


Appendix 1.29: ^{13}C NMR (126 MHz, $CDCl_3$) of 4-(benzo[*d*][1,3]dioxol-5-ylmethyl)-*N*-(4-(trifluoromethyl)phenyl)piperazine-1-carboxamide (CFA015), **3.36**.

University of Ghana http://ugspace.ug.edu.gh

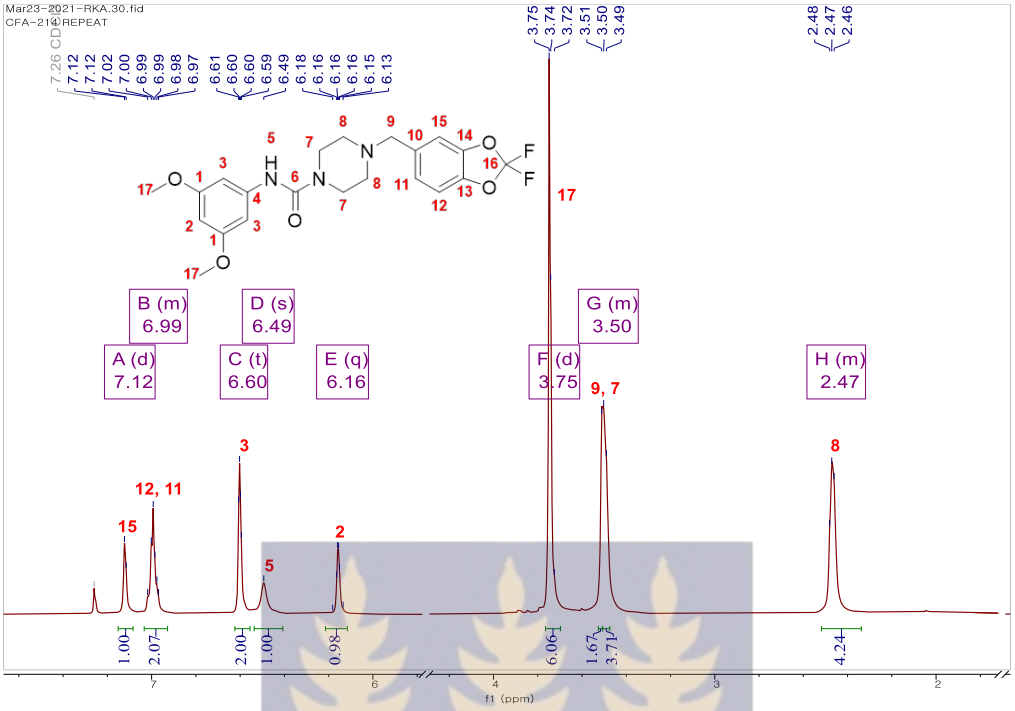


Appendix 1.30: ^{1}H NMR (500 MHz, $CDCl_3$) of 4-(benzo[*d*][1,3]dioxol-5-ylmethyl)-*N*-(3,5-dimethoxyphenyl)piperazine-1-carboxamide (CFA017), **3.37**.

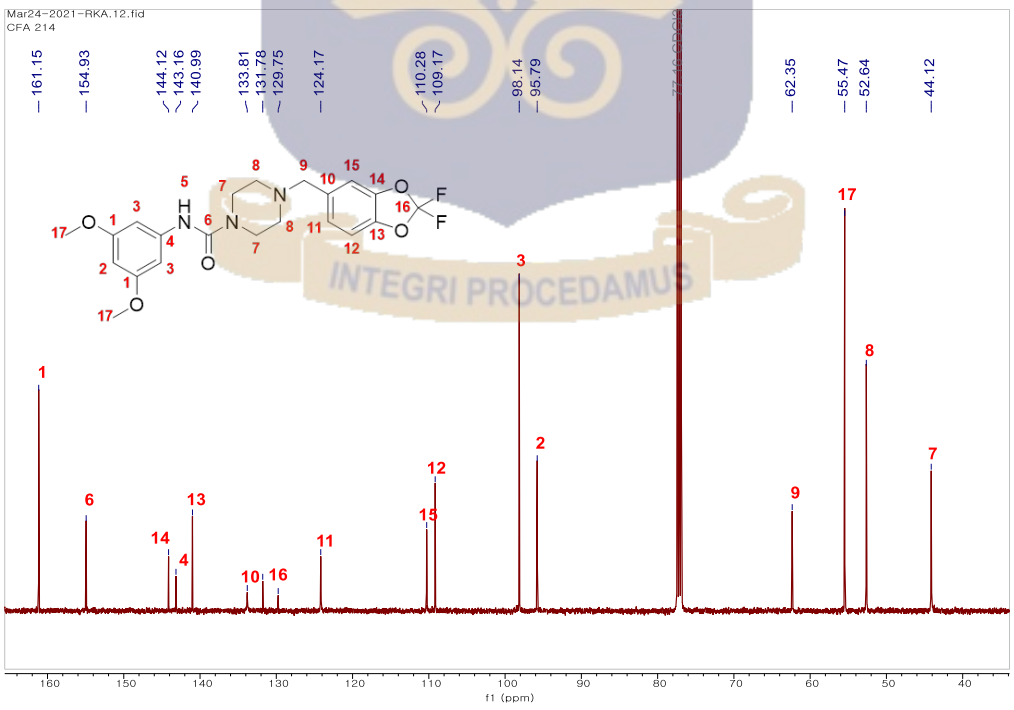


Appendix 1.31: ^{13}C NMR (126 MHz, $CDCl_3$) of 4-(benzo[*d*][1,3]dioxol-5-ylmethyl)-*N*-(3,5-dimethoxyphenyl)piperazine-1-carboxamide (CFA017), **3.37.**

University of Ghana http://ugspace.ug.edu.gh

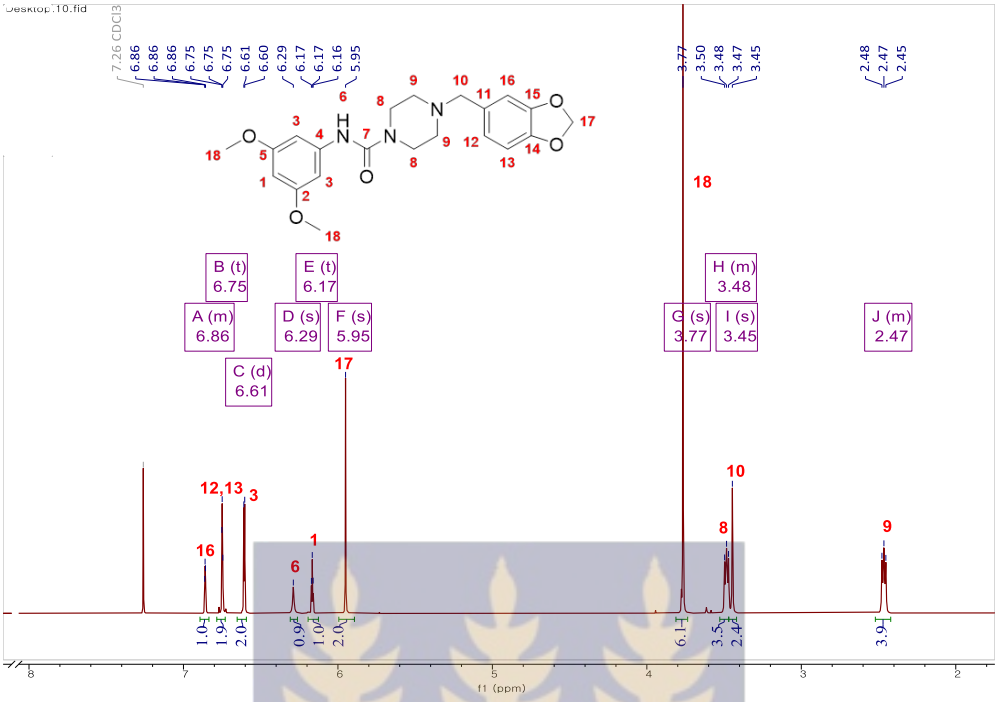


Appendix 1.32: ^{1}H NMR (500 MHz, $CDCl_3$) of 4-((2,2-difluorobenzo[*d*][1,3]dioxol-5-yl)methyl)-*N*-(3,5-dimethoxyphenyl)piperazine-1-carboxamide (CFA214), **3.39**.

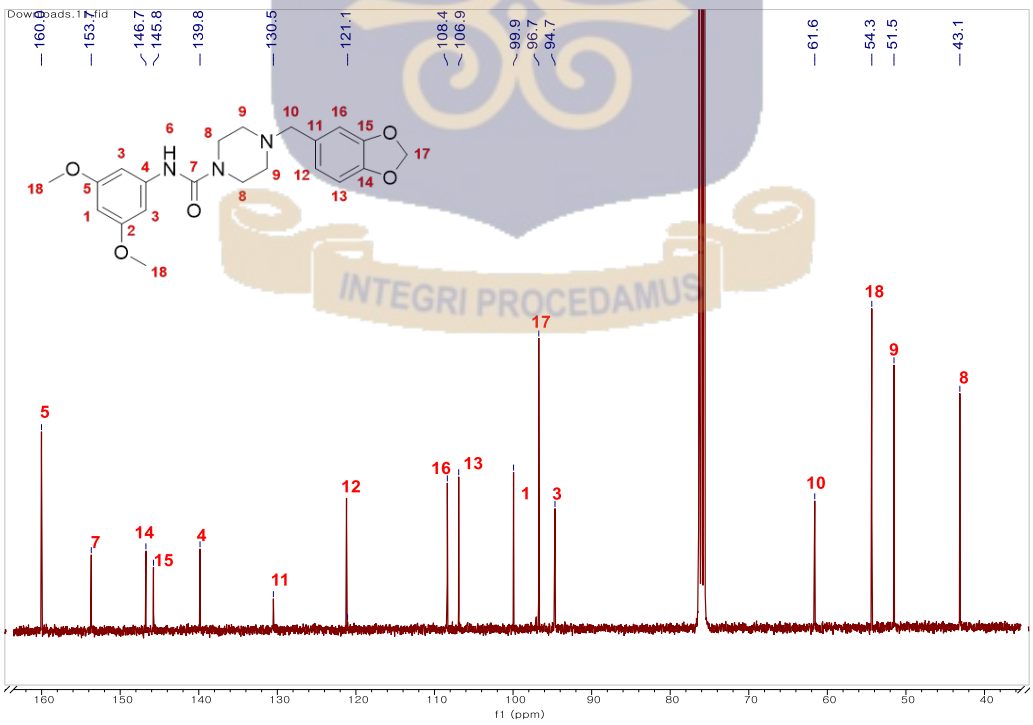


Appendix 1.33: ^{13}C NMR (126 MHz, $CDCl_3$) of 4-((2,2-difluorobenzo[*d*][1,3]dioxol-5-yl)methyl)-*N*-(3,5-dimethoxyphenyl)piperazine-1-carboxamide (CFA214), **3.39**.

University of Ghana http://ugspace.ug.edu.gh

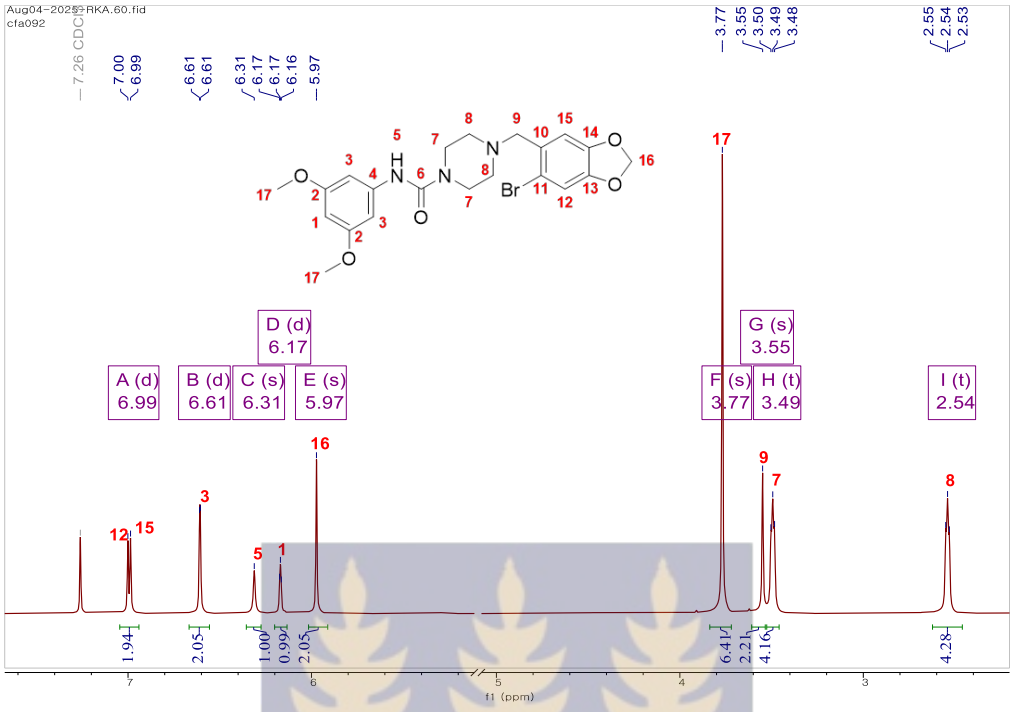


Appendix 1.34: ^{1}H NMR (400 MHz, $CDCl_3$) of 4-(benzo[*d*][1,3]dioxol-5-ylmethyl)-*N*-(3,5-dimethoxyphenyl)piperazine-1-carboxamide (CFA099), **3.40**.

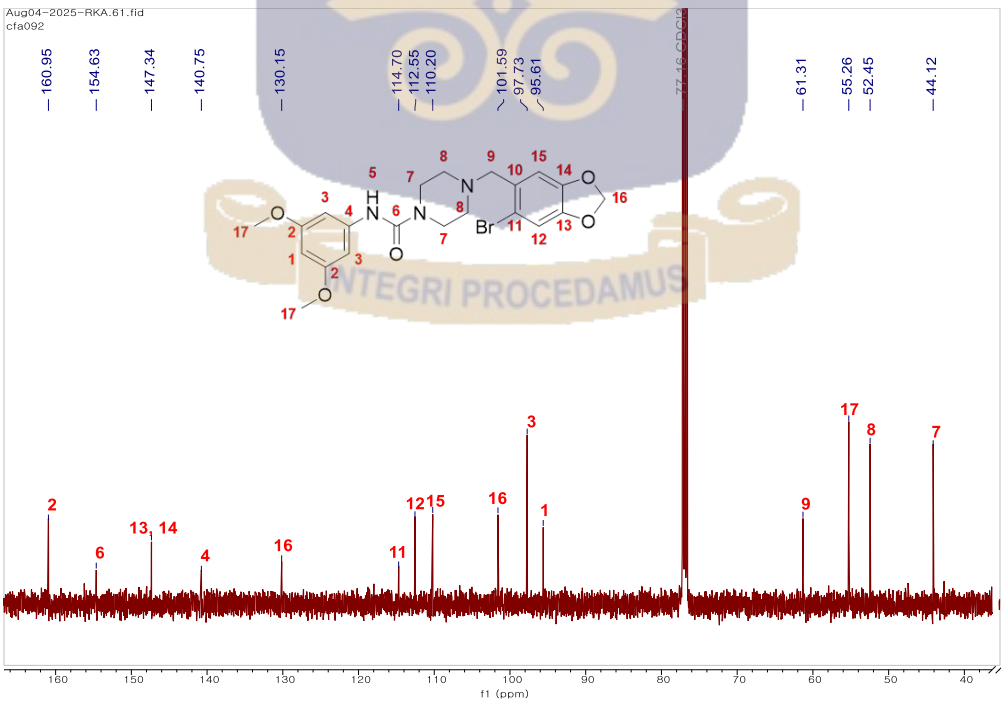


Appendix 1.35: ^{13}C NMR (101 MHz, $CDCl_3$) of 4-(benzo[*d*][1,3]dioxol-5-ylmethyl)-*N*-(3,5-dimethoxyphenyl)piperazine-1-carboxamide (CFA099), **3.40**.

University of Ghana http://ugspace.ug.edu.gh

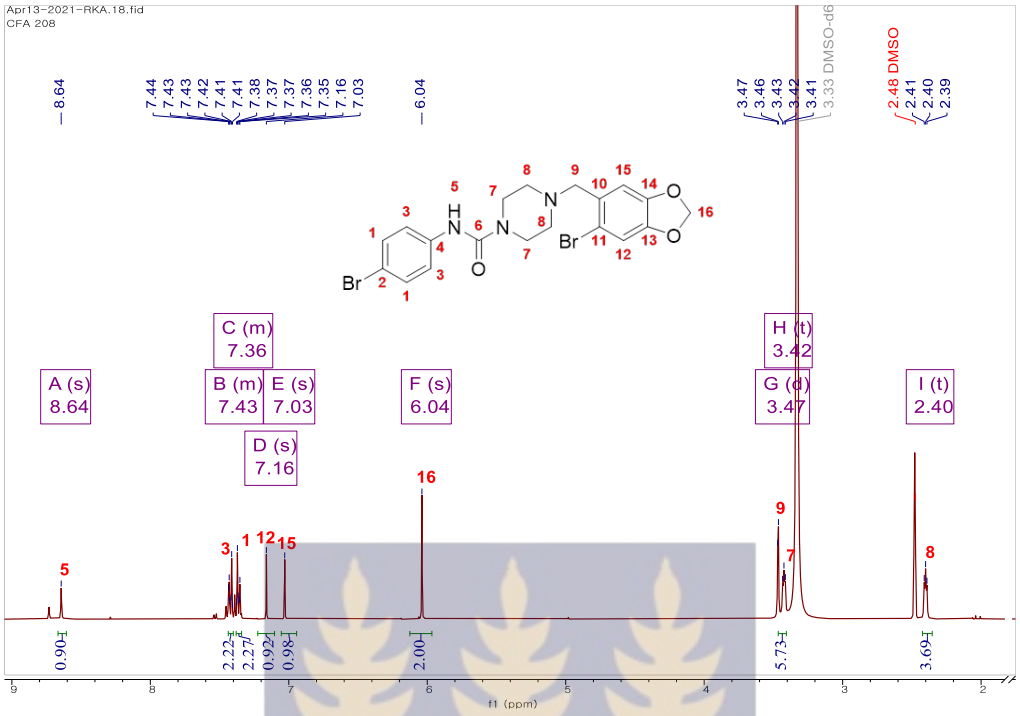


Appendix 1.36: ^{1}H NMR (500 MHz, $CDCl_3$) of 4-((6-bromobenzo[*d*][1,3]dioxol-5-yl)methyl)-*N*-(3,5-dimethoxyphenyl)piperazine-1-carboxamide (CFA092), **3.41**.

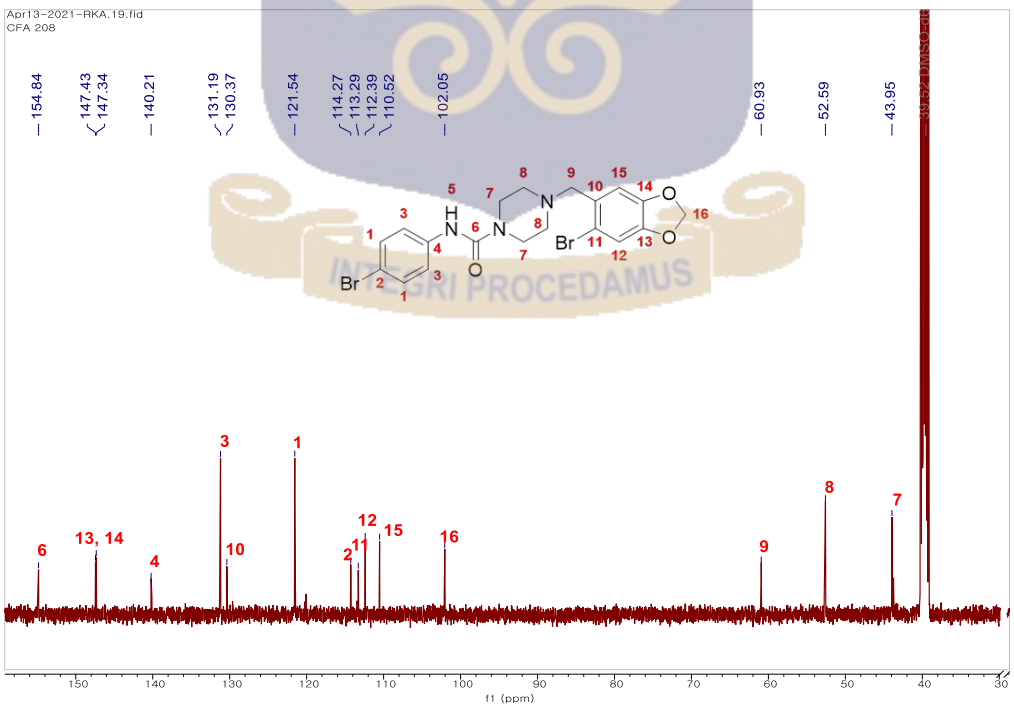


Appendix 1.37: ^{13}C NMR (126 MHz, $CDCl_3$) of 4-((6-bromobenzo[*d*][1,3]dioxol-5-yl)methyl)-*N*-(3,5-dimethoxyphenyl)piperazine-1-carboxamide (CFA092), **3.41**.

University of Ghana http://ugspace.ug.edu.gh

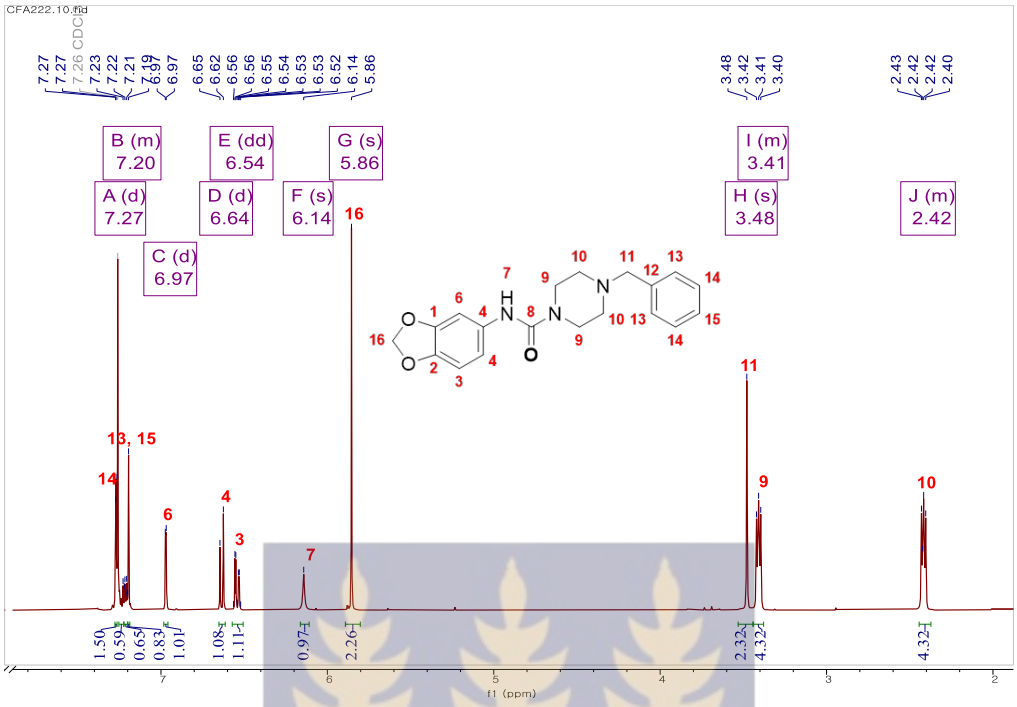


Appendix 1.38: ^{1}H NMR (500 MHz, DMSO) of 4-((6-bromobenzo[d][1,3]dioxol-5-yl)methyl)-N-(4-bromophenyl)piperazine-1-carboxamide (CFA208), **3.38**.

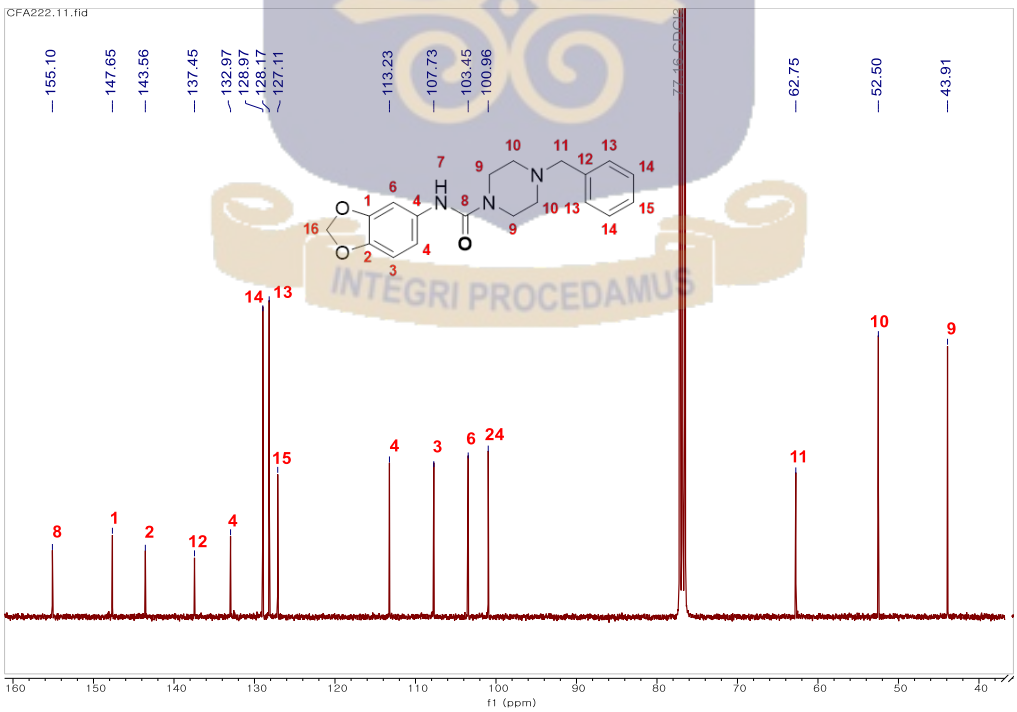


Appendix 1.39: ^{13}C NMR (126 MHz, DMSO) of 4-((6-bromobenzo[d][1,3]dioxol-5-yl)methyl)-N-(4-bromophenyl)piperazine-1-carboxamide (CFA208), **3.38**.

University of Ghana http://ugspace.ug.edu.gh

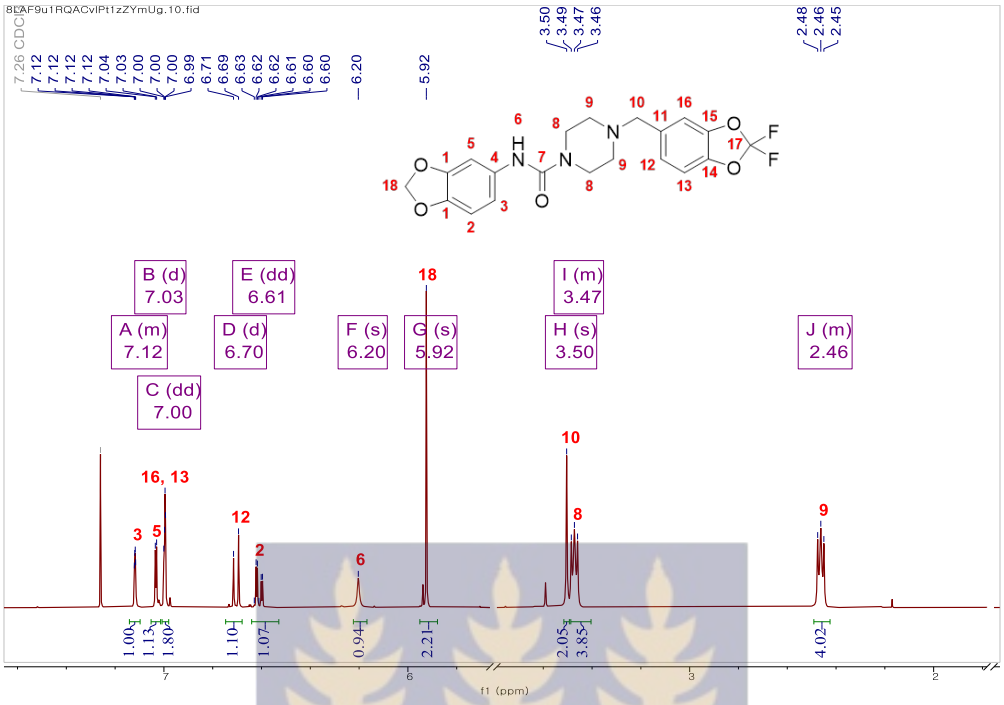


Appendix 1.40: ^{1}H NMR (400 MHz, $CDCl_3$) of *N*-(benzo[*d*][1,3]dioxol-5-yl)-4-((2,2-difluorobenzo[d][1,3]dioxol-5-yl)methyl)piperazine-1-carboxamide (CFA222), **3.42**.

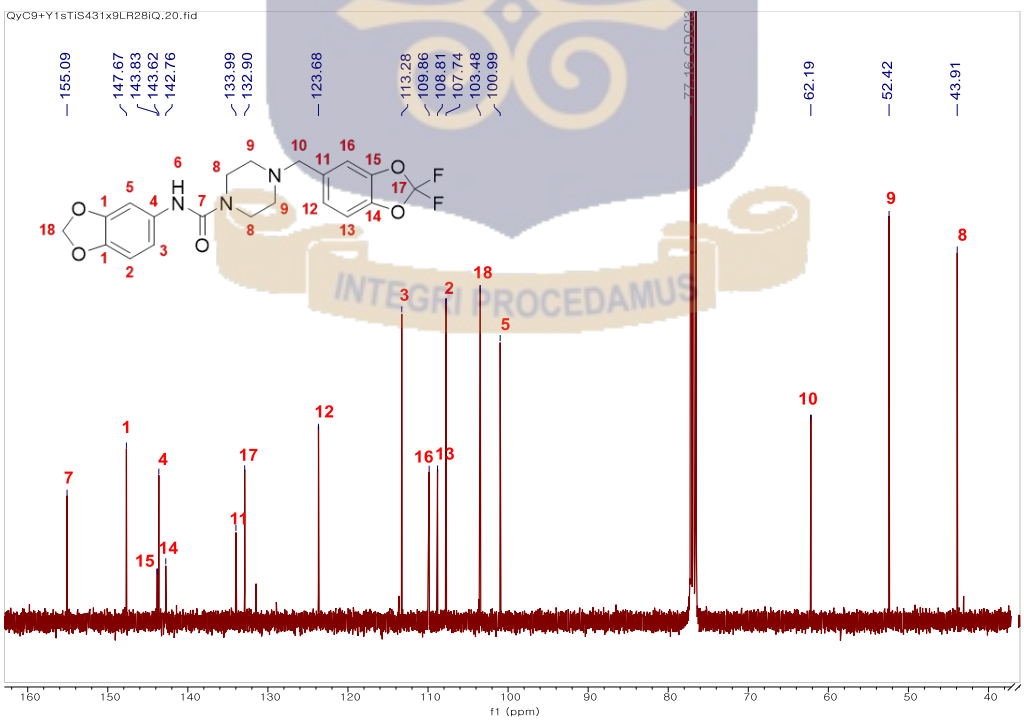


Appendix 1.41: ^{13}C NMR (101 MHz, $CDCl_3$) of *N*-(benzo[*d*][1,3]dioxol-5-yl)-4-((2,2-difluorobenzo[d][1,3]dioxol-5-yl)methyl)piperazine-1-carboxamide (CFA222), **3.42**.

University of Ghana http://ugspace.ug.edu.gh

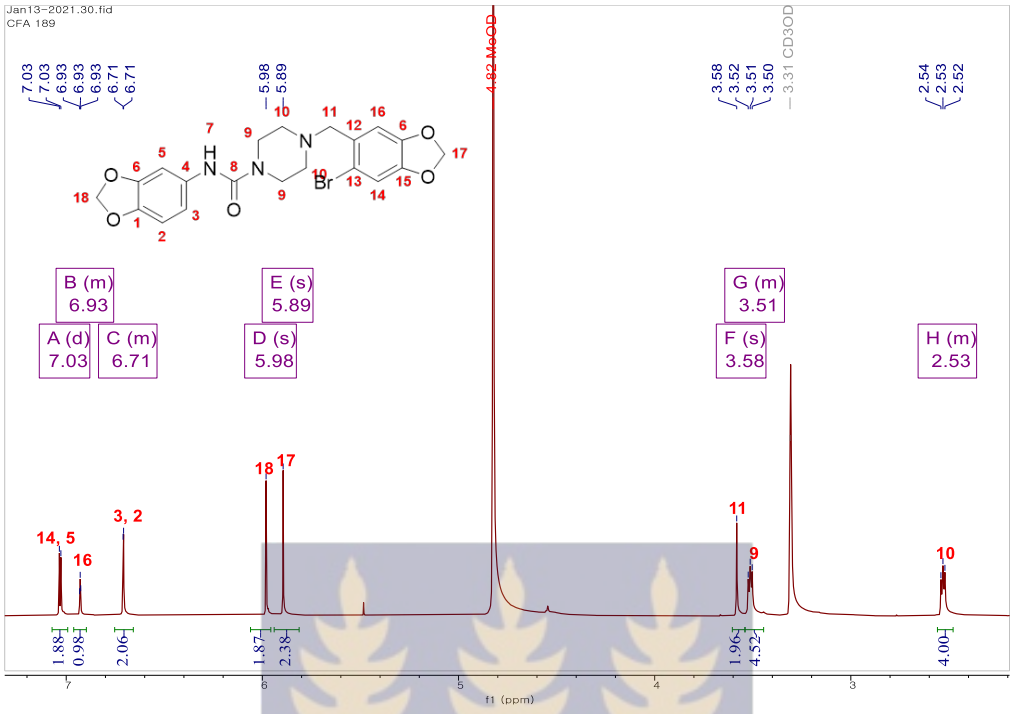


Appendix 1.42: ^{1}H NMR (400 MHz, $CDCl_3$) of *N*-(benzo[*d*][1,3]dioxol-5-yl)-4-((6-bromobenzo[d][1,3]dioxol-5-yl)methyl)piperazine-1-carboxamide (CFA147), **3.43**.

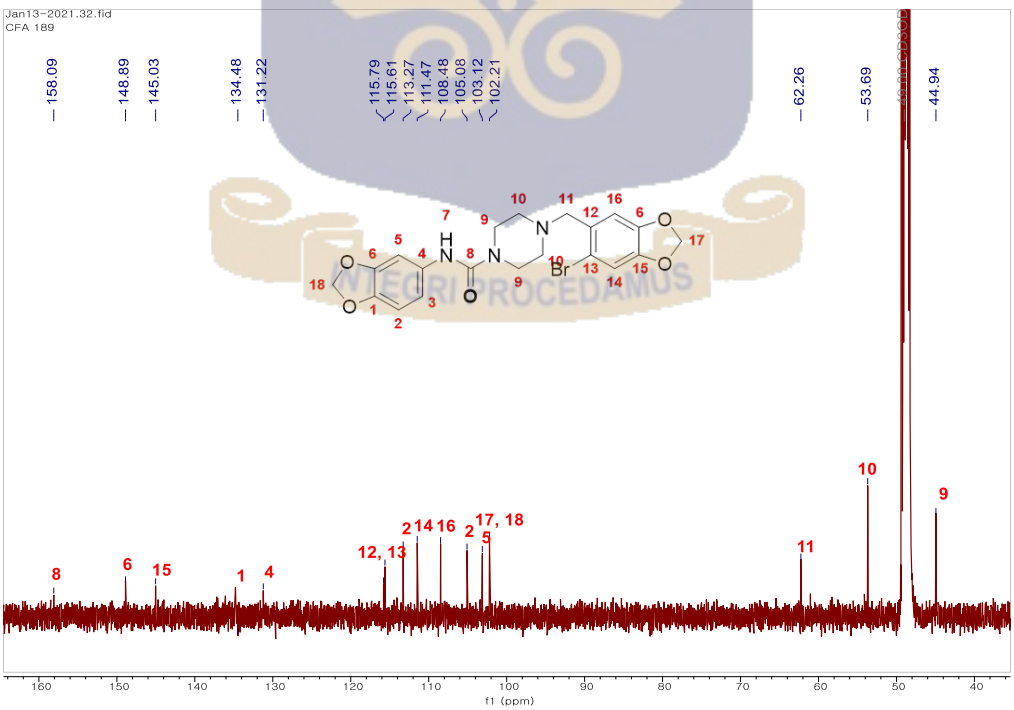


Appendix 1.43: ^{13}C NMR (101 MHz, $CDCl_3$) of *N*-(benzo[*d*][1,3]dioxol-5-yl)-4-((6-bromobenzo[d][1,3]dioxol-5-yl)methyl)piperazine-1-carboxamide (CFA147), **3.43**.

University of Ghana http://ugspace.ug.edu.gh

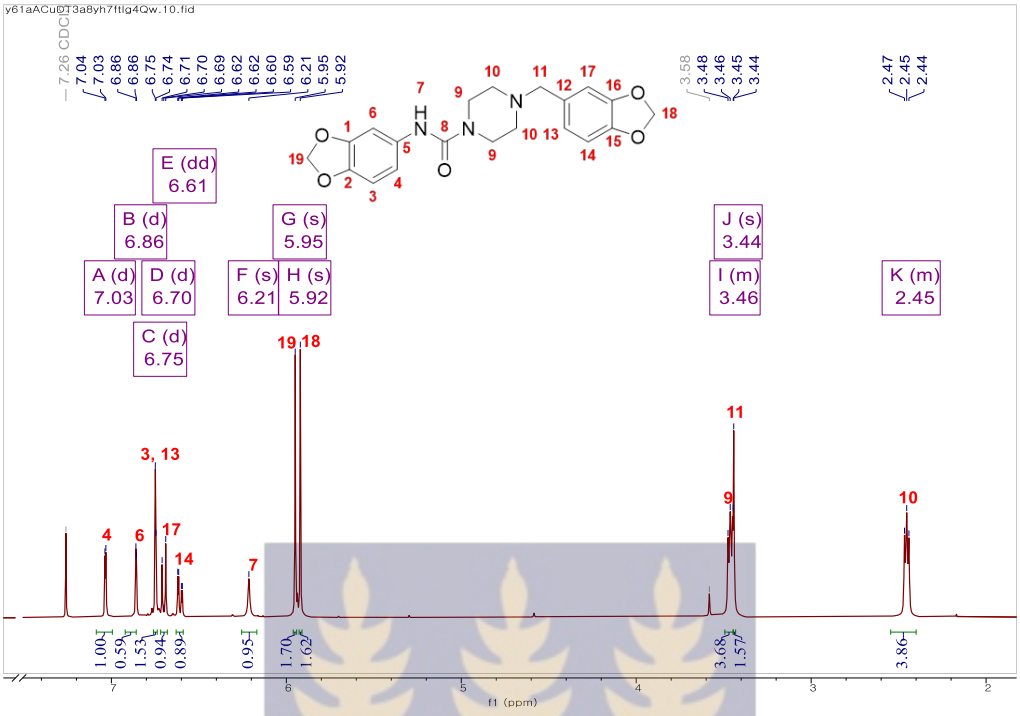


Appendix 1.44: ^{1}H NMR (500 MHz, MeOD) of *N*-(benzo[*d*][1,3]dioxol-5-yl)-4-((6-bromobenzo[d][1,3]dioxol-5-yl)methyl)piperazine-1-carboxamide (CFA189), **3.44**.

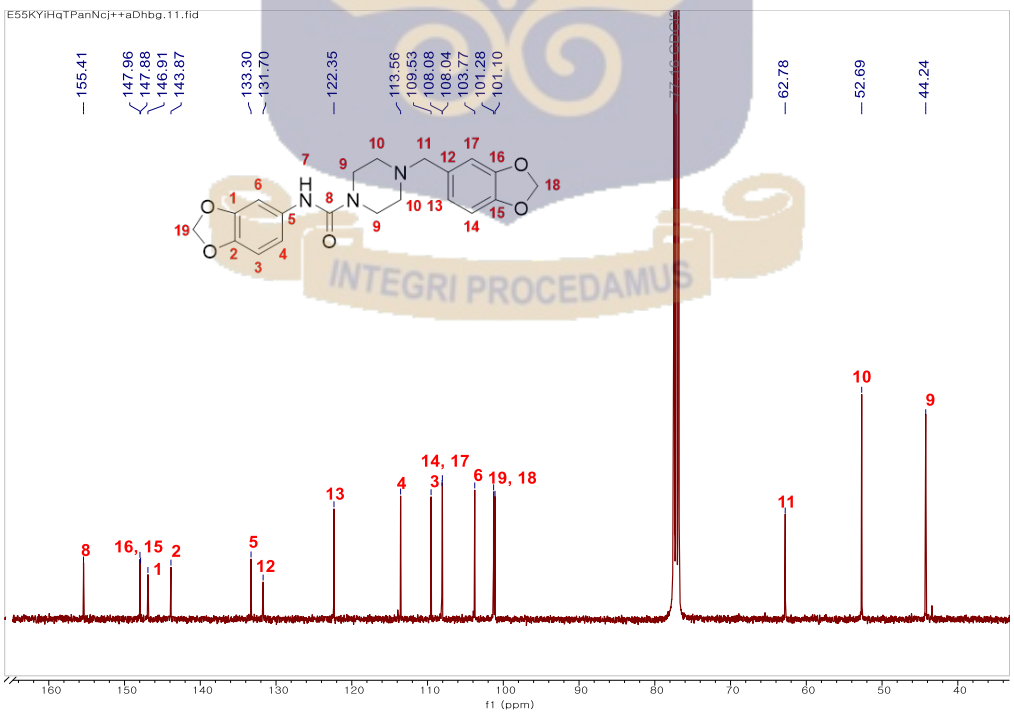


Appendix 1.45: ^{13}C NMR (126 MHz, MeOD) of *N*-(benzo[*d*][1,3]dioxol-5-yl)-4-((6-bromobenzo[d][1,3]dioxol-5-yl)methyl)piperazine-1-carboxamide (CFA189), **3.44**.

University of Ghana http://ugspace.ug.edu.gh

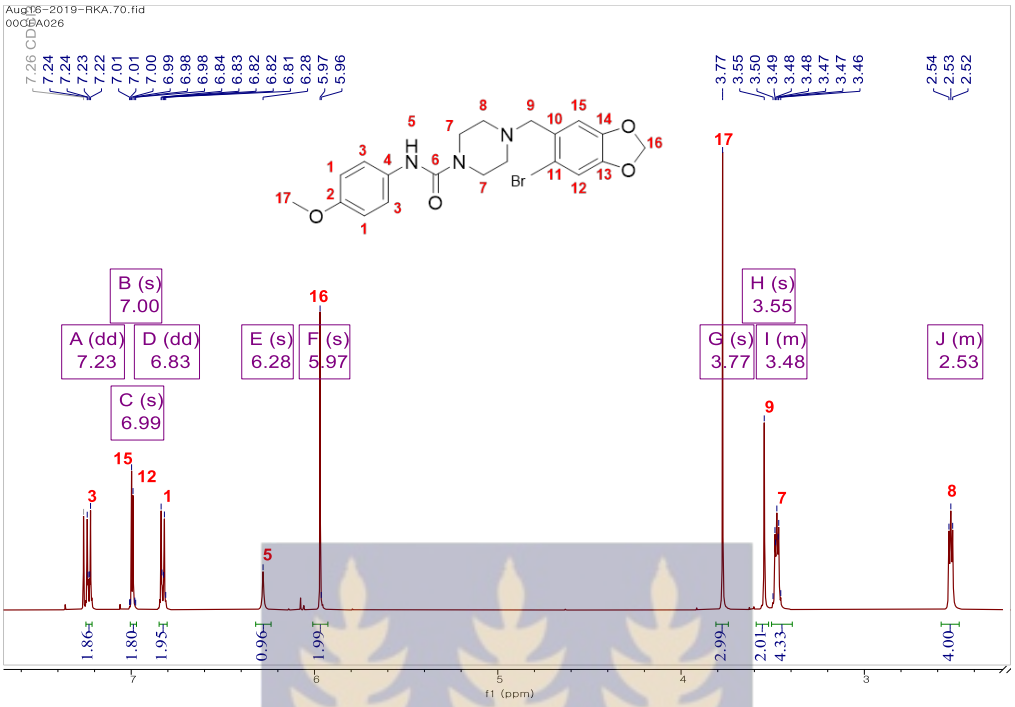


Appendix 1.46: ^{1}H NMR (400 MHz, $CDCl_3$) of *N*-(benzo[*d*][1,3]dioxol-5-yl)-4-(benzo[*d*][1,3]dioxol-5-ylmethyl)piperazine-1-carboxamide (CFA140), **3.45**.

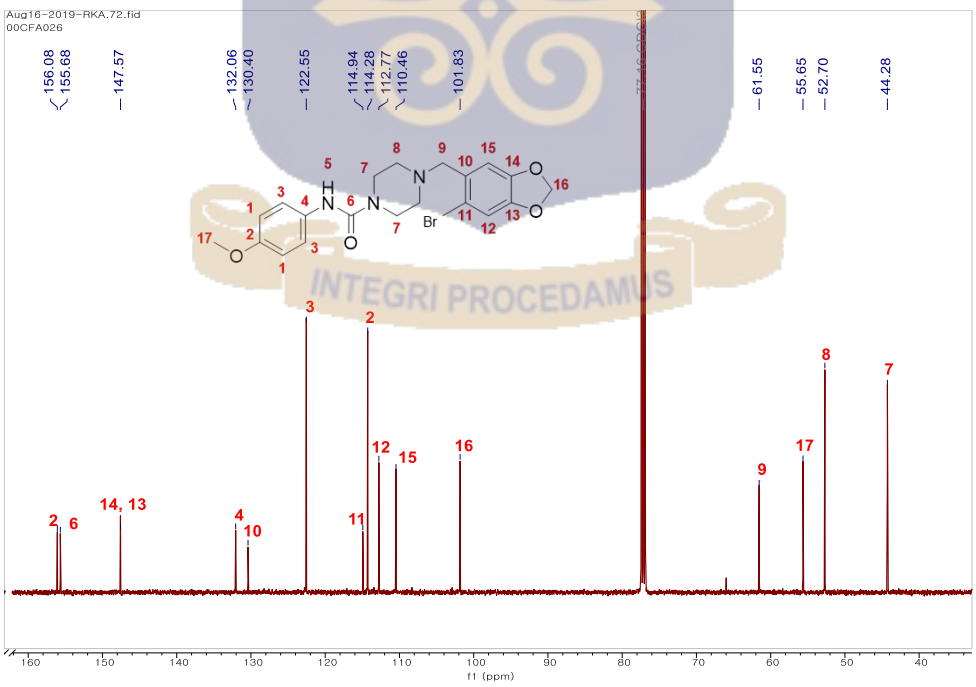


Appendix 1.47: ^{13}C NMR (101 MHz, $CDCl_3$) of *N*-(benzo[*d*][1,3]dioxol-5-yl)-4-(benzo[*d*][1,3]dioxol-5-ylmethyl)piperazine-1-carboxamide (CFA140), **3.45.**

University of Ghana http://ugspace.ug.edu.gh

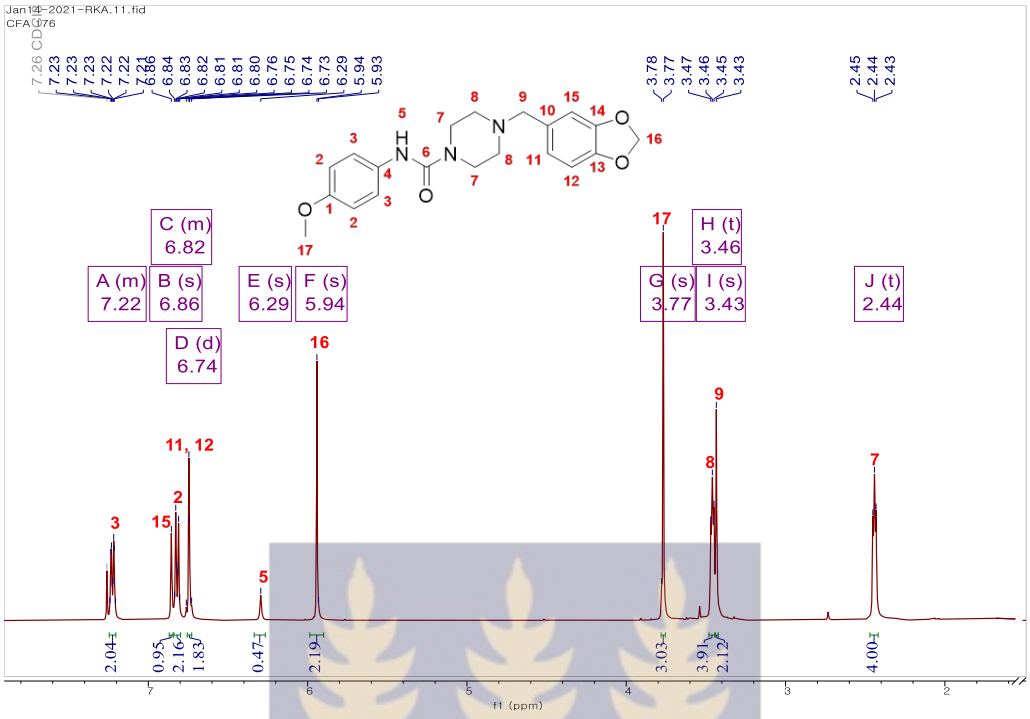


Appendix 1.48: ^{1}H NMR (500 MHz, $CDCl_3$) of 4-((6-bromobenzo[*d*][1,3]dioxol-5-yl)methyl)-*N*-(4-methoxyphenyl)piperazine-1-carboxamide (CFA026), **3.46**.

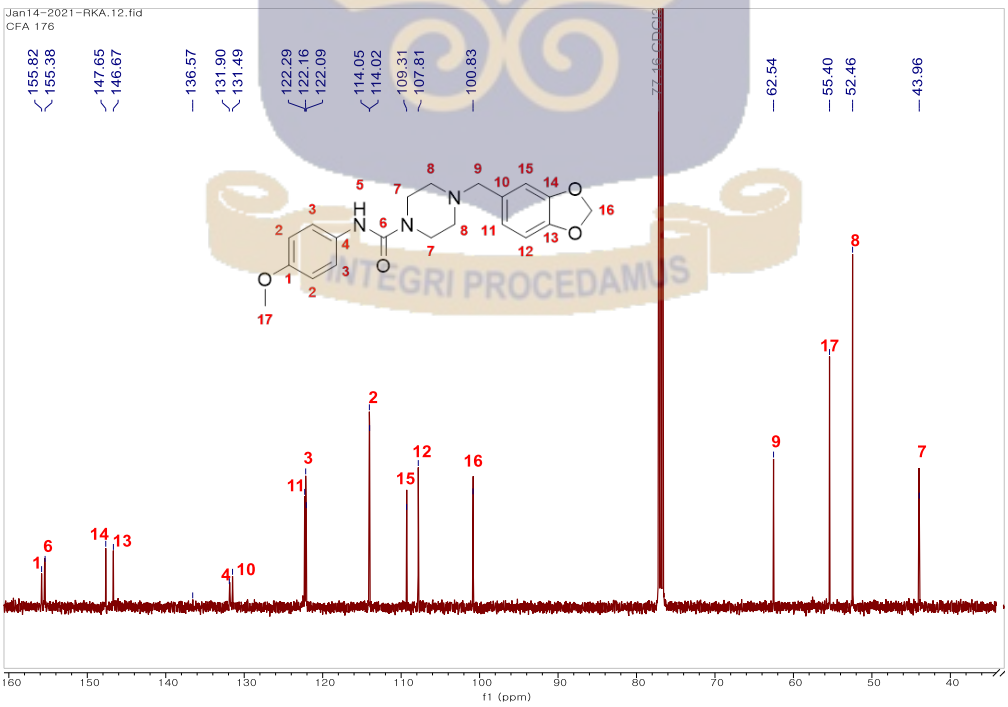


Appendix 1.49: ^{13}C NMR (126 MHz, $CDCl_3$) of 4-((6-bromobenzo[*d*][1,3]dioxol-5-yl)methyl)-*N*-(4-methoxyphenyl)piperazine-1-carboxamide (CFA026), **3.46.**

University of Ghana http://ugspace.ug.edu.gh

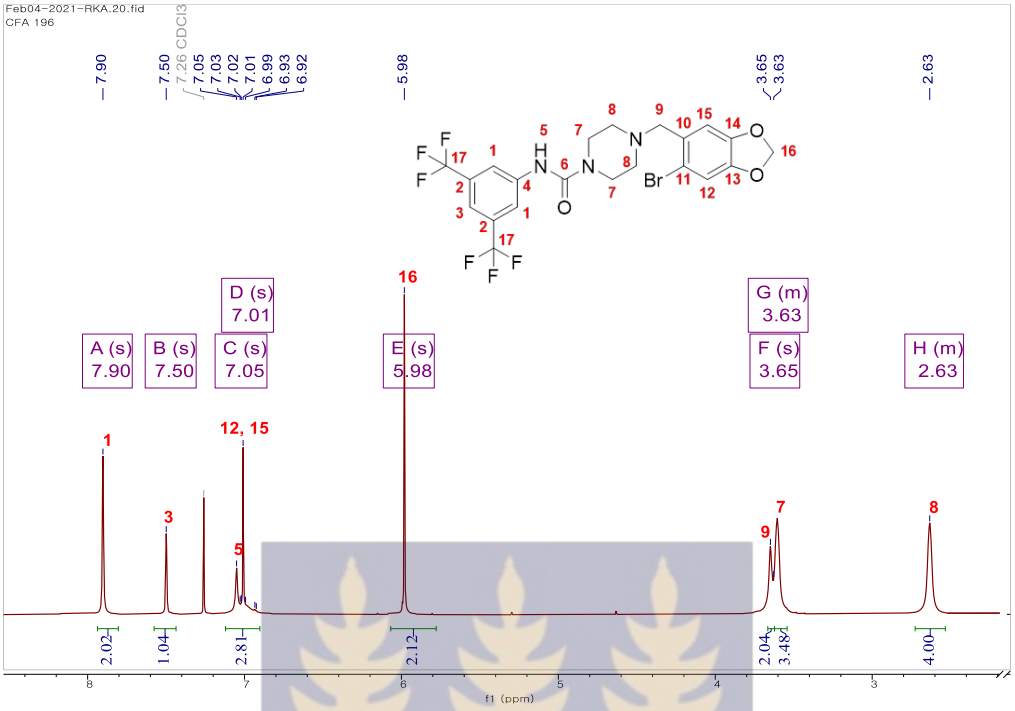


Appendix 1.50: ^{1}H NMR (500 MHz, $CDCl_3$) of 4-(benzo[d][1,3]dioxol-5-ylmethyl)-N-(4-methoxyphenyl)piperazine-1-carboxamide (CFA170), **3.47**.

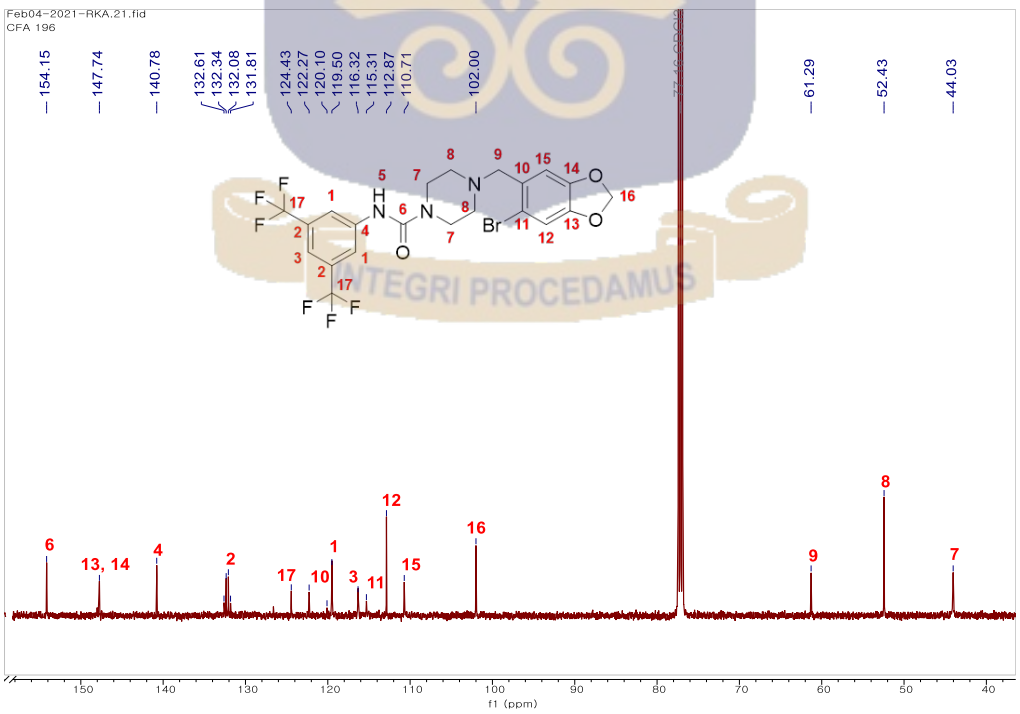


Appendix 1.51: ^{13}C NMR (126 MHz, $CDCl_3$) of 4-(benzo[d][1,3]dioxol-5-ylmethyl)-N-(4-methoxyphenyl)piperazine-1-carboxamide (CFA170), **3.47.**

University of Ghana http://ugspace.ug.edu.gh

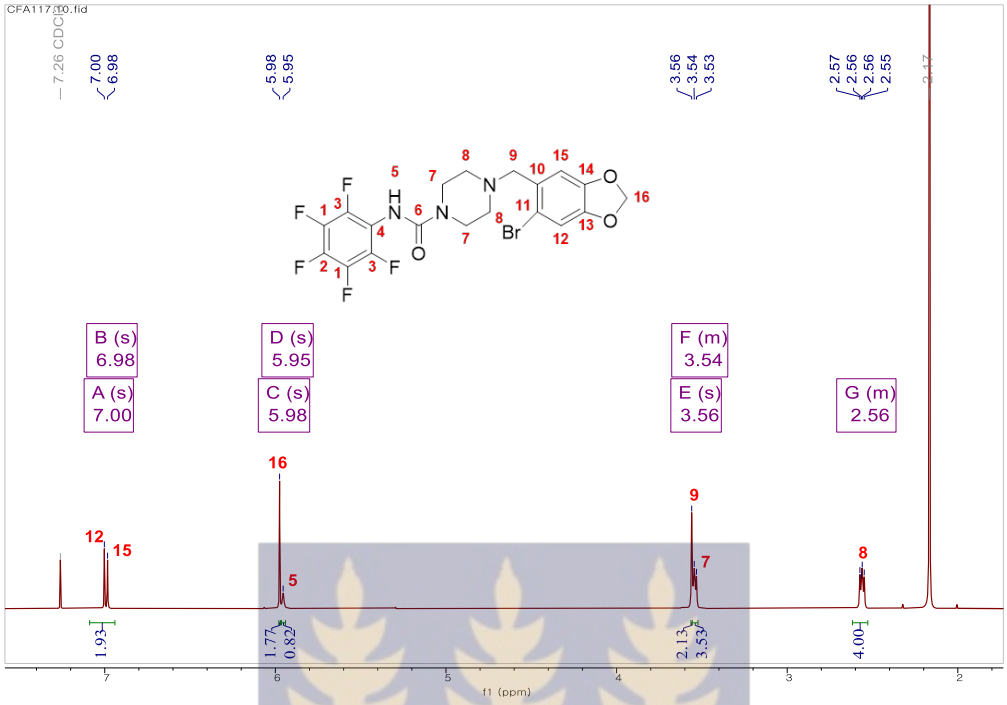


Appendix 1.52: ^{13}H NMR (500 MHz, $CDCl_3$) of *N*-(3,5-bis(trifluoromethyl)phenyl)-4-((6-bromobenzo[*d*][1,3]dioxol-5-yl)methyl)piperazine-1-carboxamide (CFA196), **3.48**.

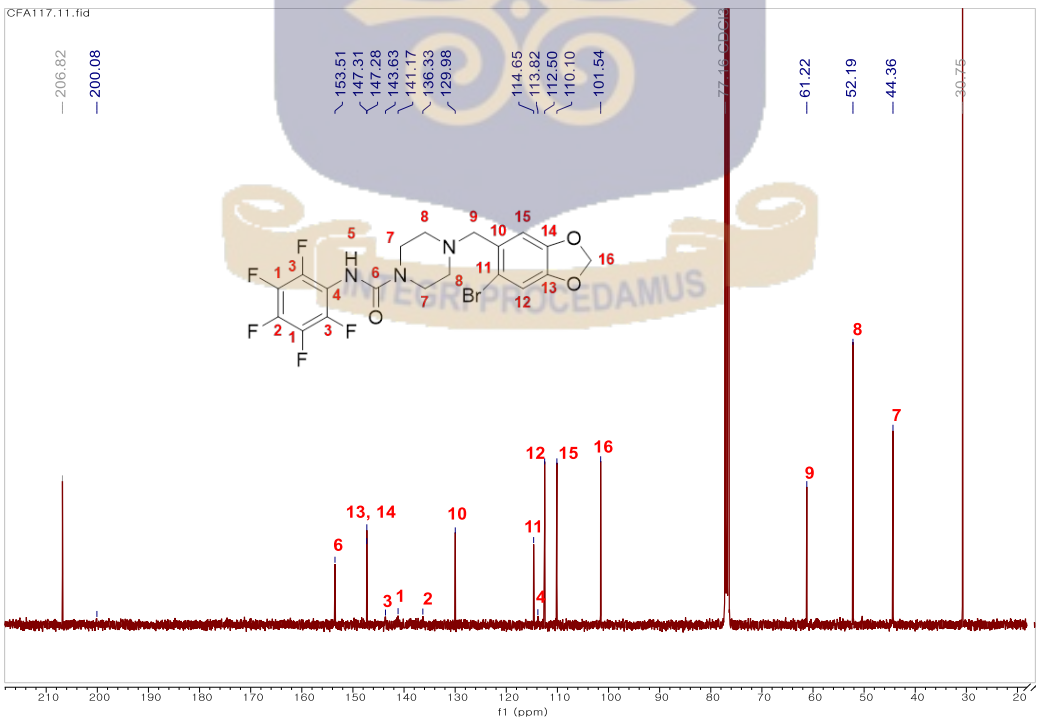


Appendix 1.53: ^{13}C NMR (126 MHz, $CDCl_3$) of *N*-(3,5-bis(trifluoromethyl)phenyl)-4-((6-bromobenzo[*d*][1,3]dioxol-5-yl)methyl)piperazine-1-carboxamide (CFA196), **3.47**.

University of Ghana http://ugspace.ug.edu.gh

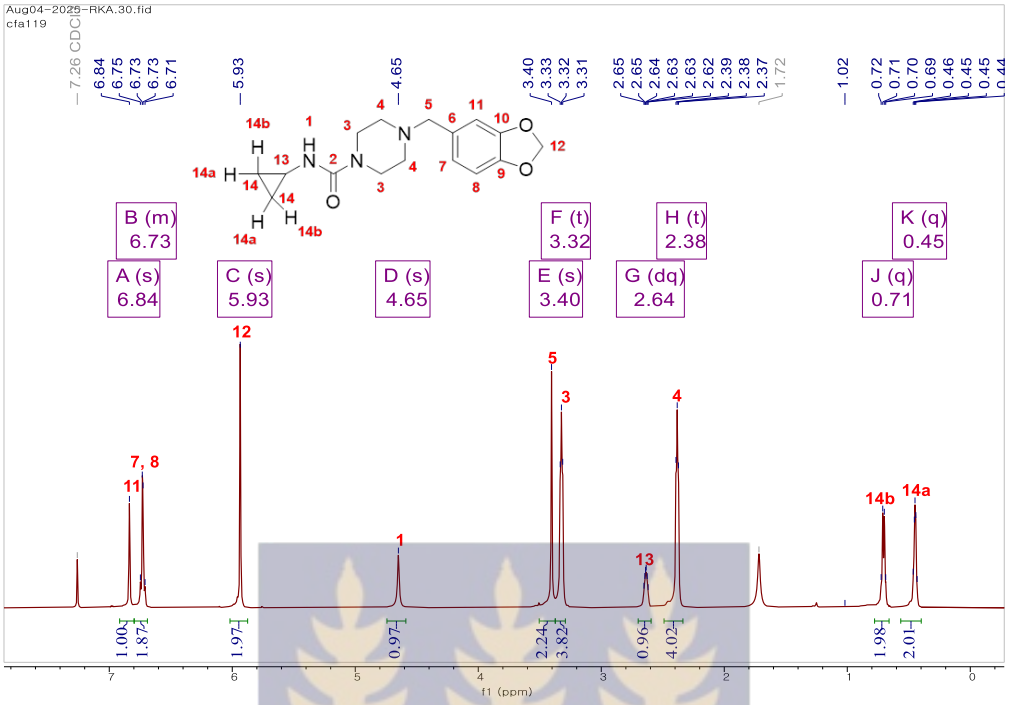


Appendix 1.54: ^{1}H NMR (500 MHz, $CDCl_3$) of 4-((6-bromobenzo[*d*][1,3]dioxol-5-yl)methyl)-*N*-(perfluorophenyl)piperazine-1-carboxamide (CFA117), **3.49**.

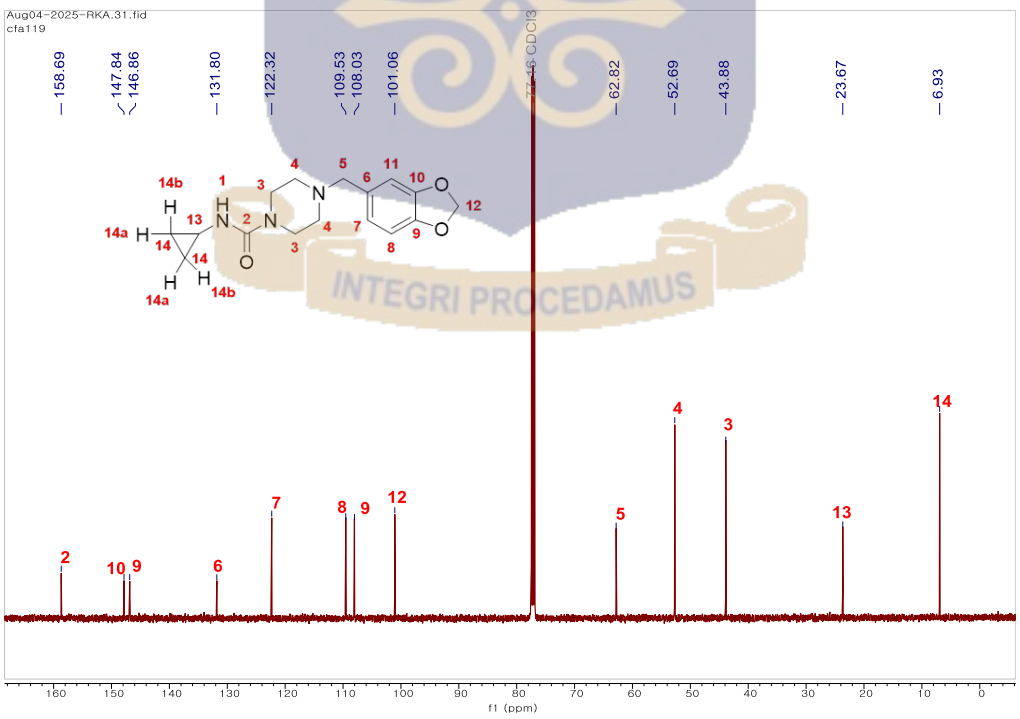


Appendix 1.55: ^{13}C NMR (126 MHz, $CDCl_3$) of 4-((6-bromobenzo[*d*][1,3]dioxol-5-yl)methyl)-*N*-(perfluorophenyl)piperazine-1-carboxamide (CFA117), **3.49**.

University of Ghana http://ugspace.ug.edu.gh

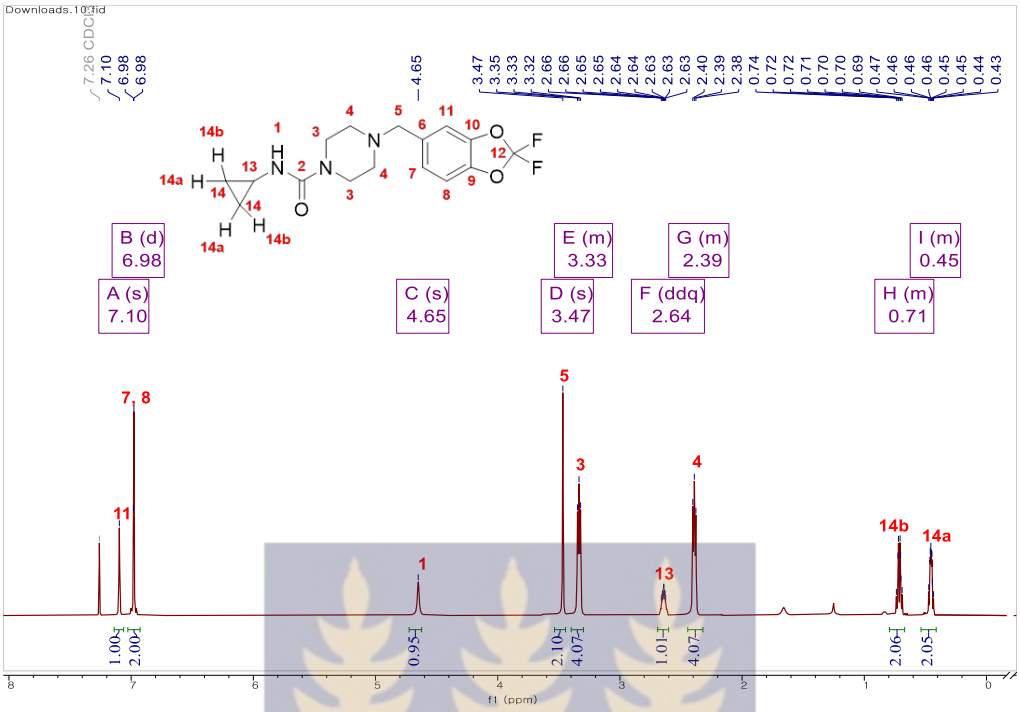


Appendix 1.56: ^{1}H NMR (500 MHz, $CDCl_3$) of 4-(benzo[*d*][1,3]dioxol-5-ylmethyl)-*N*-cyclopropylpiperazine-1-carboxamide (CFA119), **3.50**.

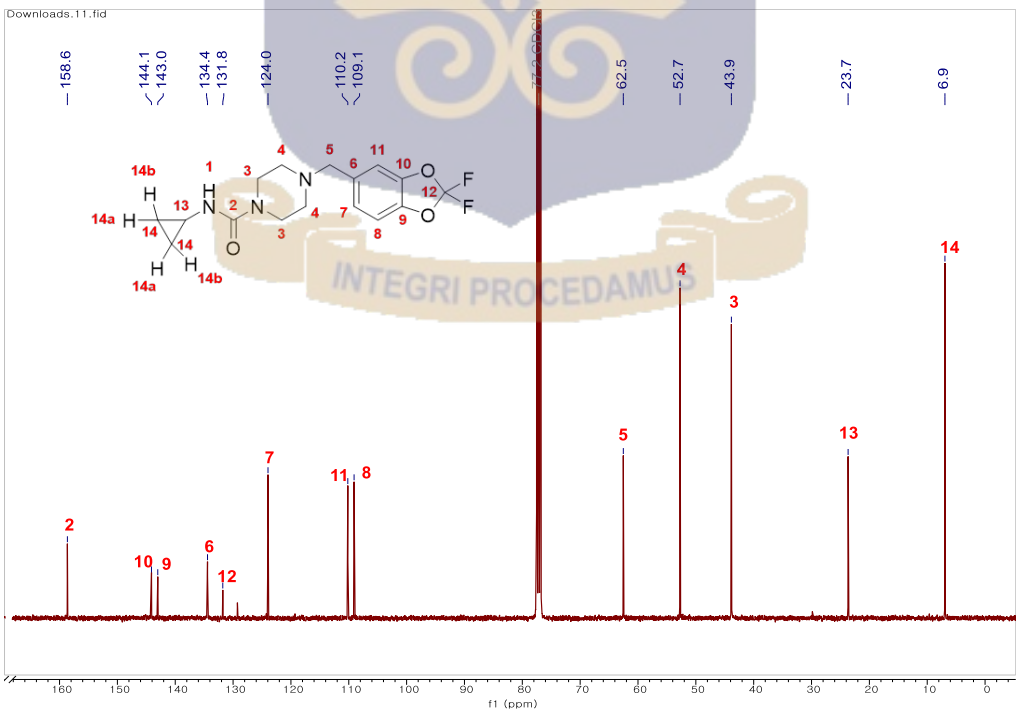


Appendix 1.57: ^{13}C NMR (126 MHz, $CDCl_3$) of 4-(benzo[*d*][1,3]dioxol-5-ylmethyl)-*N*-cyclopropylpiperazine-1-carboxamide (CFA119), **3.50**.

University of Ghana http://ugspace.ug.edu.gh

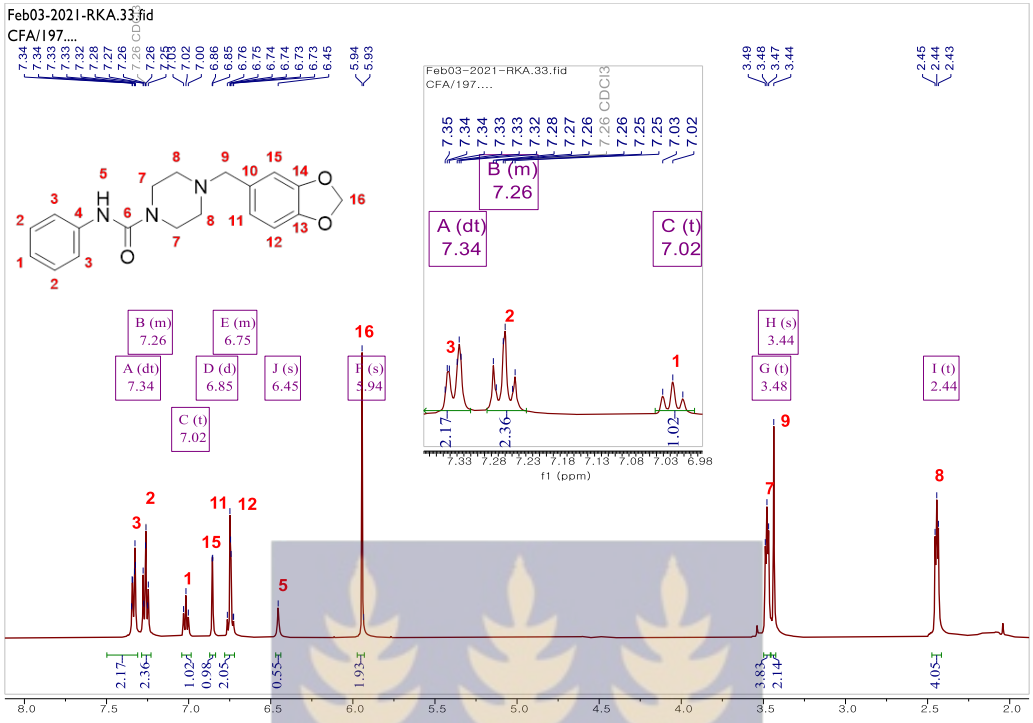


Appendix 1.58: ^{1}H NMR (400 MHz, $CDCl_3$) of N-cyclopropyl-4-((2,2-difluorobenzo[d][1,3]dioxol-5-yl)methyl)piperazine-1-carboxamide (CFA121), **3.51**.

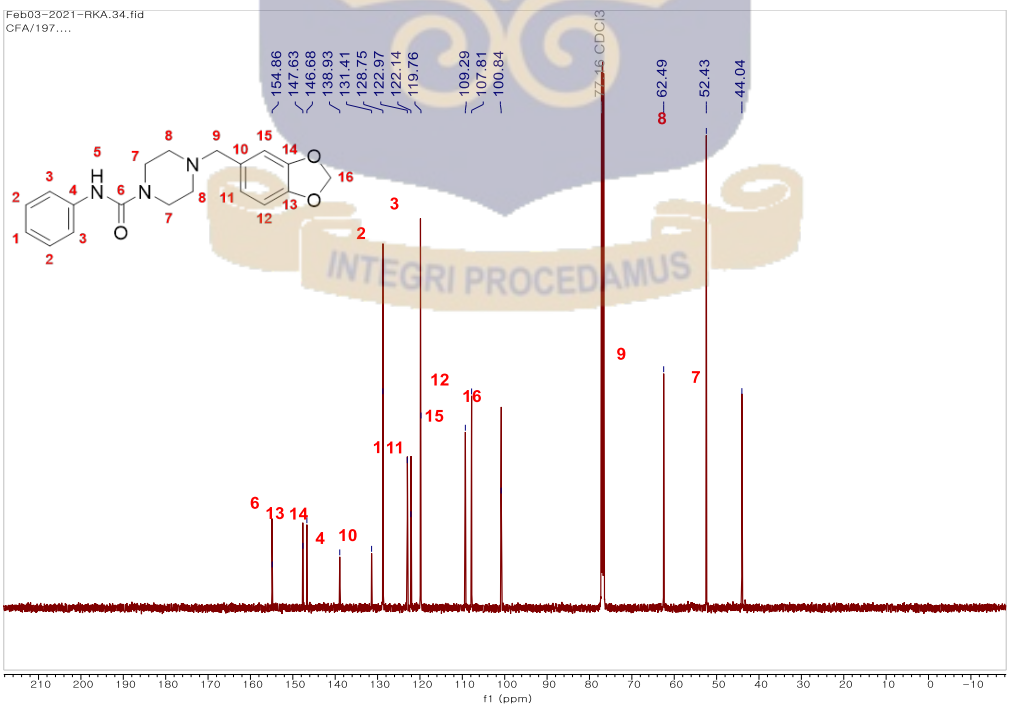


Appendix 1.59: ^{13}C NMR (101 MHz, $CDCl_3$) of N-cyclopropyl-4-((2,2-difluorobenzo[d][1,3]dioxol-5-yl)methyl)piperazine-1-carboxamide (CFA121), **3.51**.

University of Ghana http://ugspace.ug.edu.gh

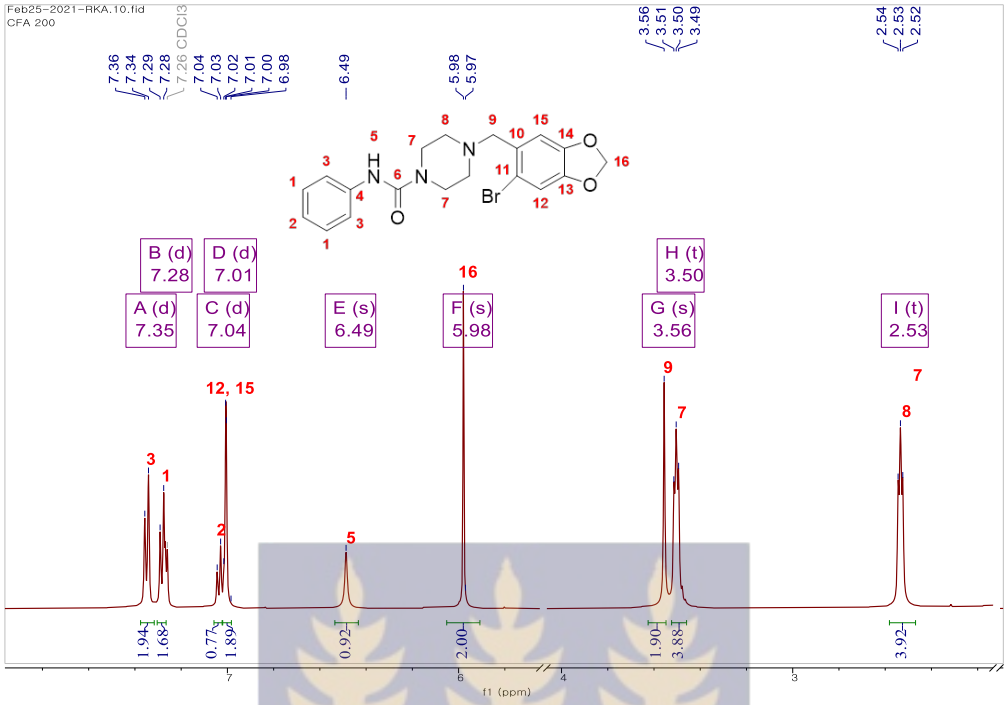


Appendix 1.60: ^{1}H NMR (500 MHz, $CDCl_3$) of 4-(benzo[*d*][1,3]dioxol-5-ylmethyl)-*N*-phenylpiperazine-1-carboxamide (CFA066/197), **3.52**.

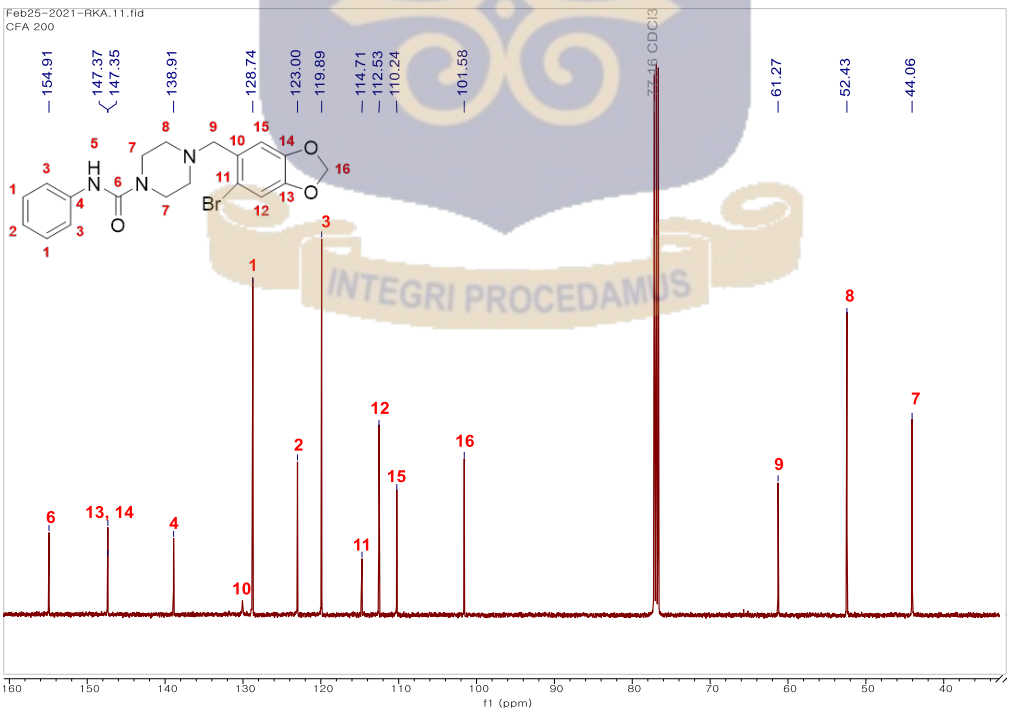


Appendix 1.61: ^{13}C NMR (126 MHz, $CDCl_3$) of 4-(benzo[*d*][1,3]dioxol-5-ylmethyl)-*N*-phenylpiperazine-1-carboxamide (CFA066/197), **3.52**.

University of Ghana http://ugspace.ug.edu.gh

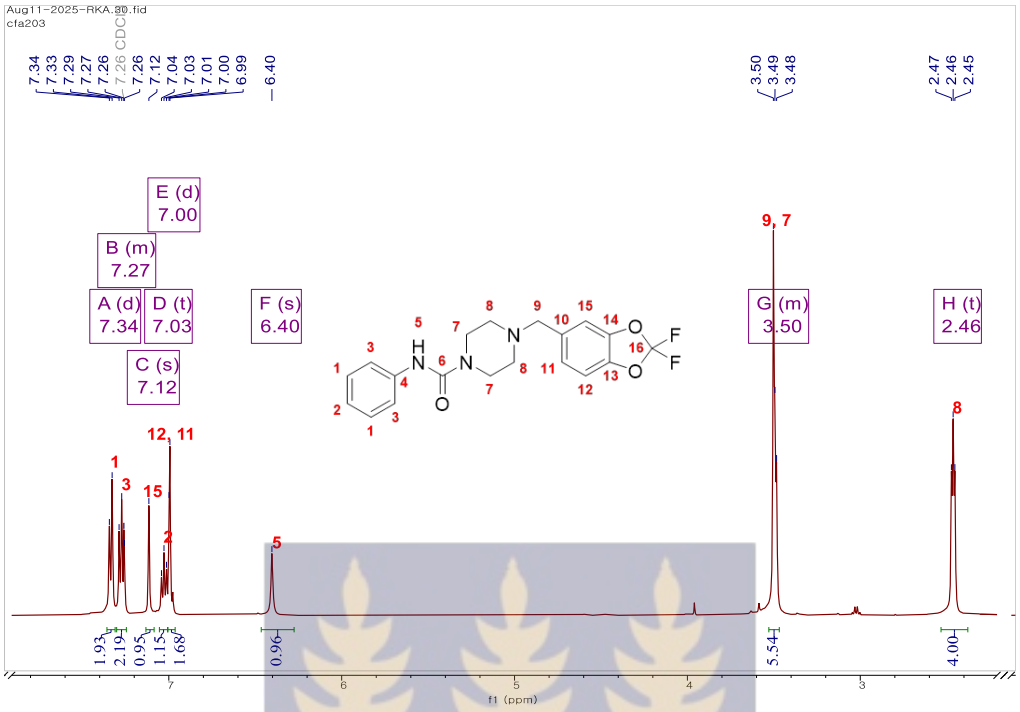


Appendix 1.62: ^{1}H NMR (500 MHz, $CDCl_3$) of 4-((6-bromobenzo[*d*][1,3]dioxol-5-yl)methyl)-*N*-phenylpiperazine-1-carboxamide (CFA067/200), **3.53**.

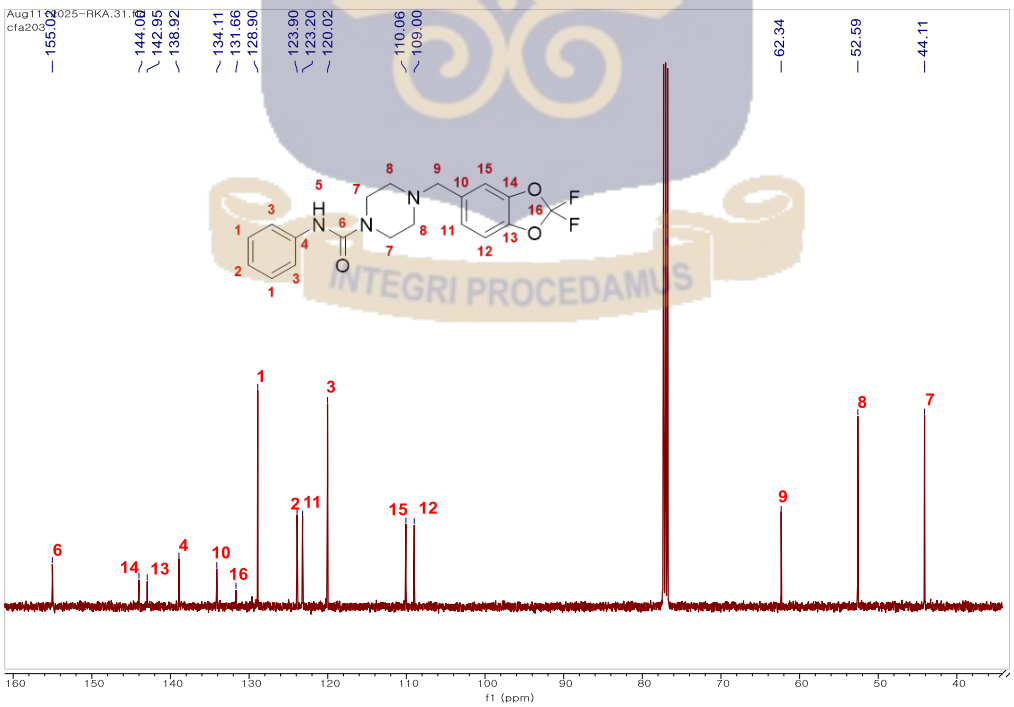


Appendix 1.63: ^{13}C NMR (126 MHz, $CDCl_3$) of 4-((6-bromobenzo[*d*][1,3]dioxol-5-yl)methyl)-*N*-phenylpiperazine-1-carboxamide (CFA067/200), **3.53**.

University of Ghana http://ugspace.ug.edu.gh

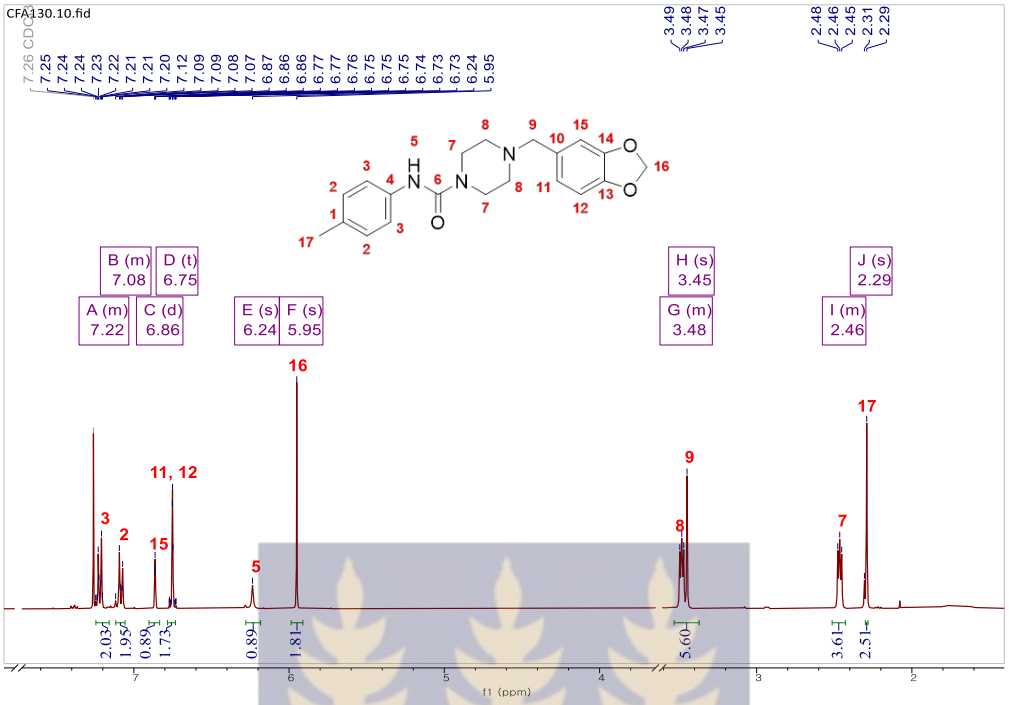


Appendix 1.64: ^{1}H NMR (500 MHz, $CDCl_3$) of 4-((2,2-difluorobenzo[*d*][1,3]dioxol-5-yl)methyl)-*N*-phenylpiperazine-1-carboxamide (CFA068/203), **3.54**.

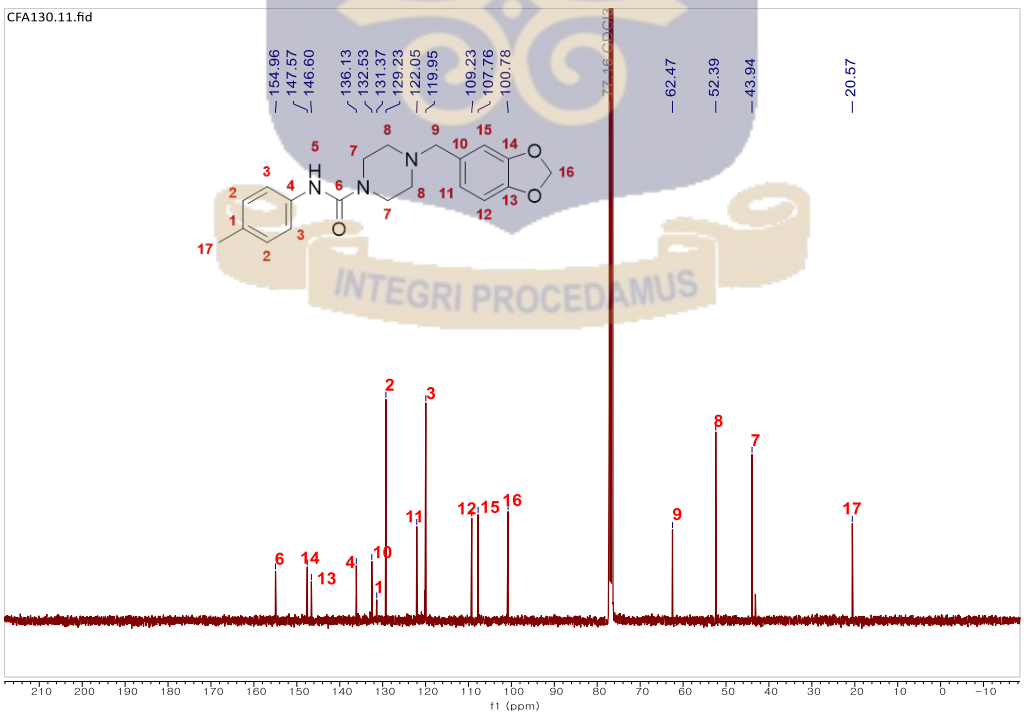


Appendix 1.65: ^{13}C NMR (126 MHz, $CDCl_3$) of 4-((2,2-difluorobenzo[*d*][1,3]dioxol-5-yl)methyl)-*N*-phenylpiperazine-1-carboxamide (CFA068/203), **3.54**.

University of Ghana http://ugspace.ug.edu.gh

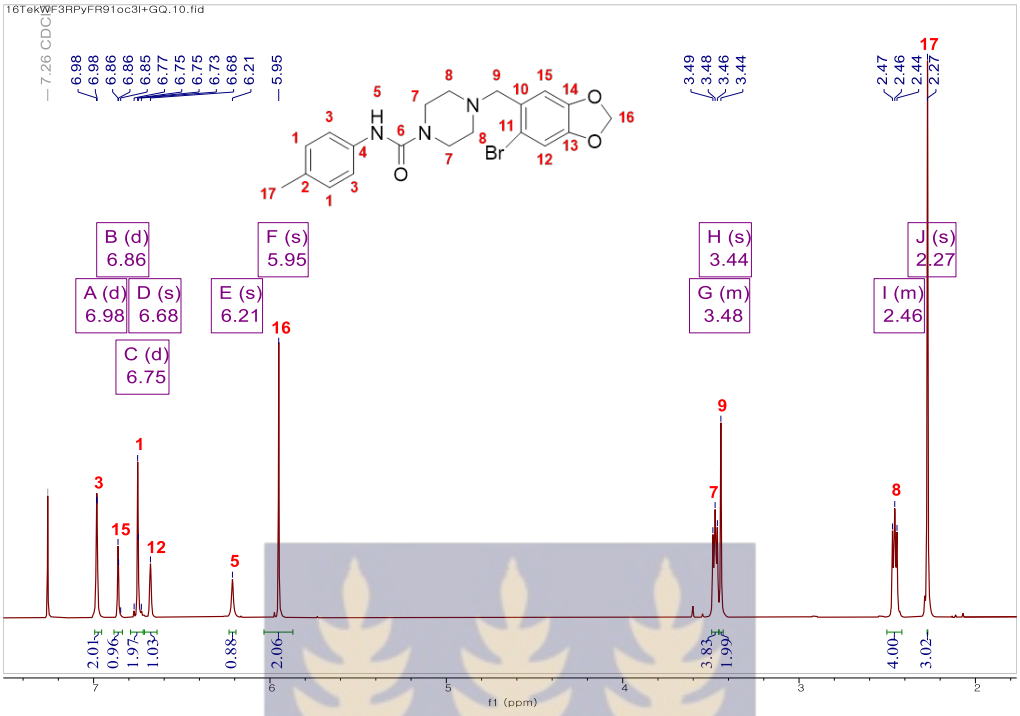


Appendix 1.66: ^{1}H NMR (500 MHz, $CDCl_3$) of 4-(benzo[*d*][1,3]dioxol-5-ylmethyl)-*N*-(p-tolyl)piperazine-1-carboxamide (CFA130), **3.55**.

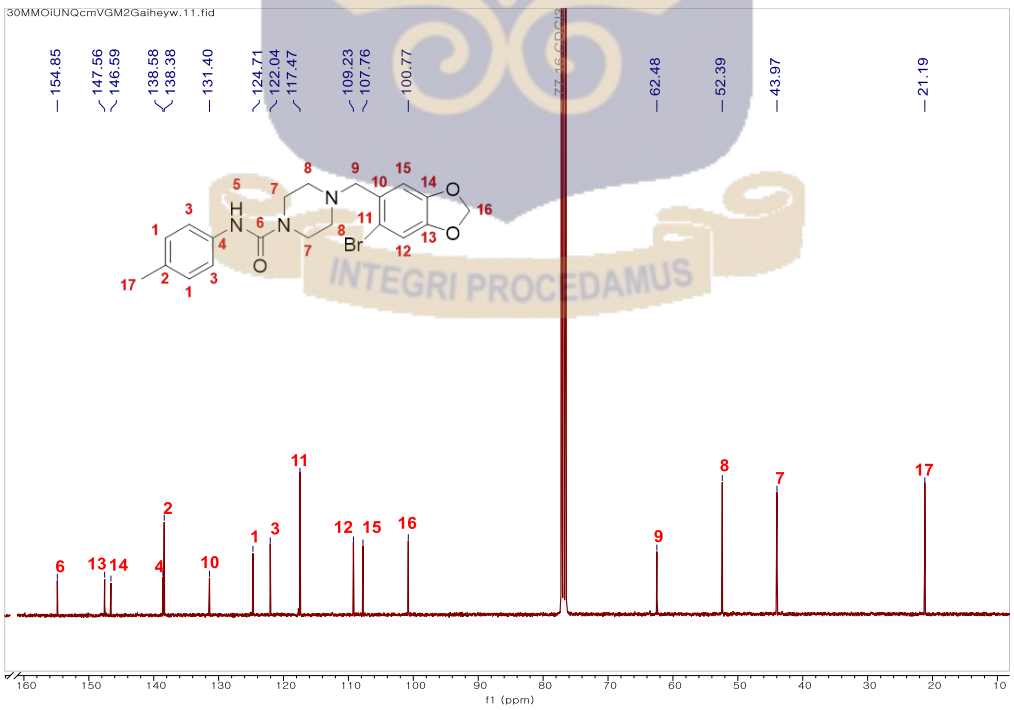


Appendix 1.67: ^{13}C NMR (126 MHz, $CDCl_3$) of 4-(benzo[*d*][1,3]dioxol-5-ylmethyl)-*N*-(p-tolyl)piperazine-1-carboxamide (CFA130), **3.55.**

University of Ghana http://ugspace.ug.edu.gh

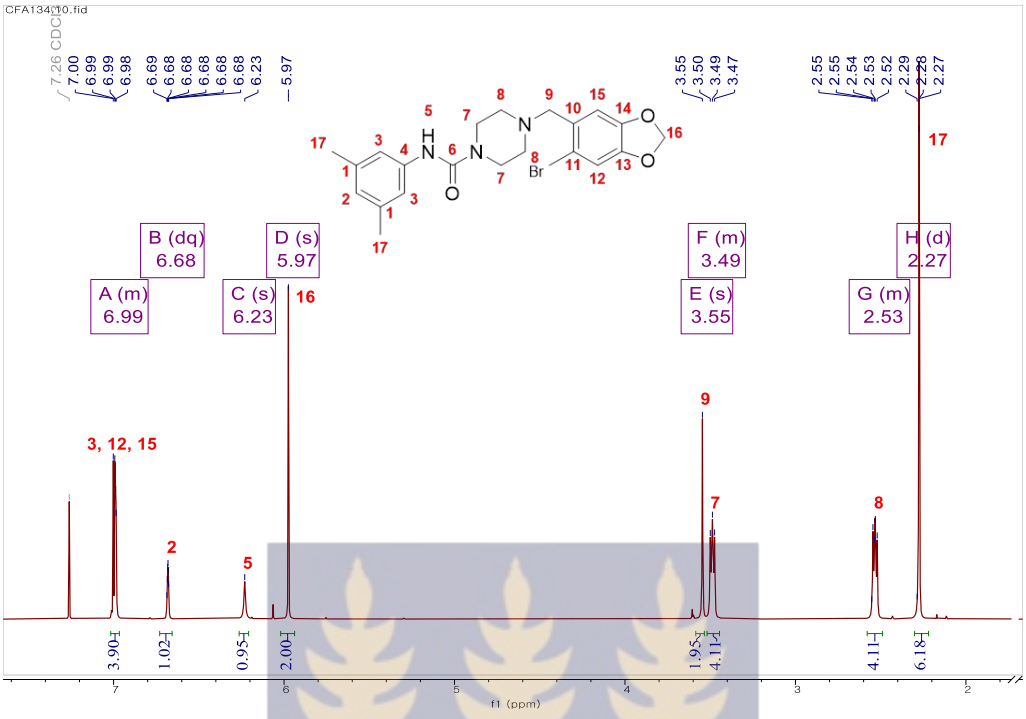


Appendix 1.68: ^{1}H NMR (500 MHz, $CDCl_3$) of 4-((6-bromobenzo[*d*][1,3]dioxol-5-yl)methyl)-*N*-(p-tolyl)piperazine-1-carboxamide (CFA131), **3.56**.

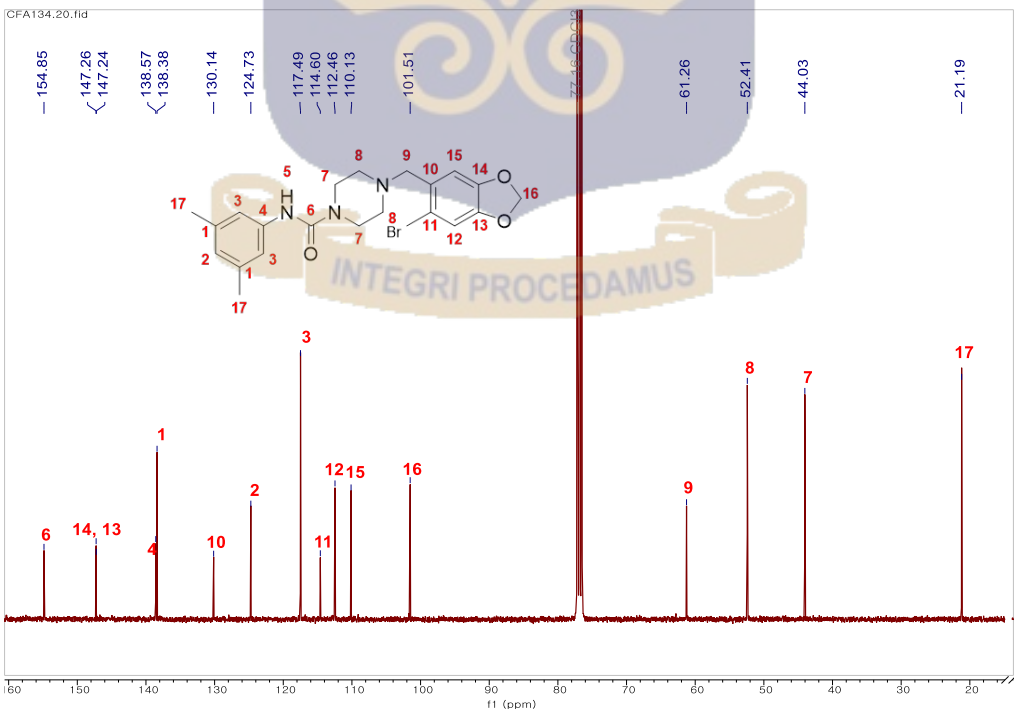


Appendix 1.69: ^{13}C NMR (126 MHz, $CDCl_3$) of 4-((6-bromobenzo[*d*][1,3]dioxol-5-yl)methyl)-*N*-(p-tolyl)piperazine-1-carboxamide (CFA131), **3.56.**

University of Ghana http://ugspace.ug.edu.gh

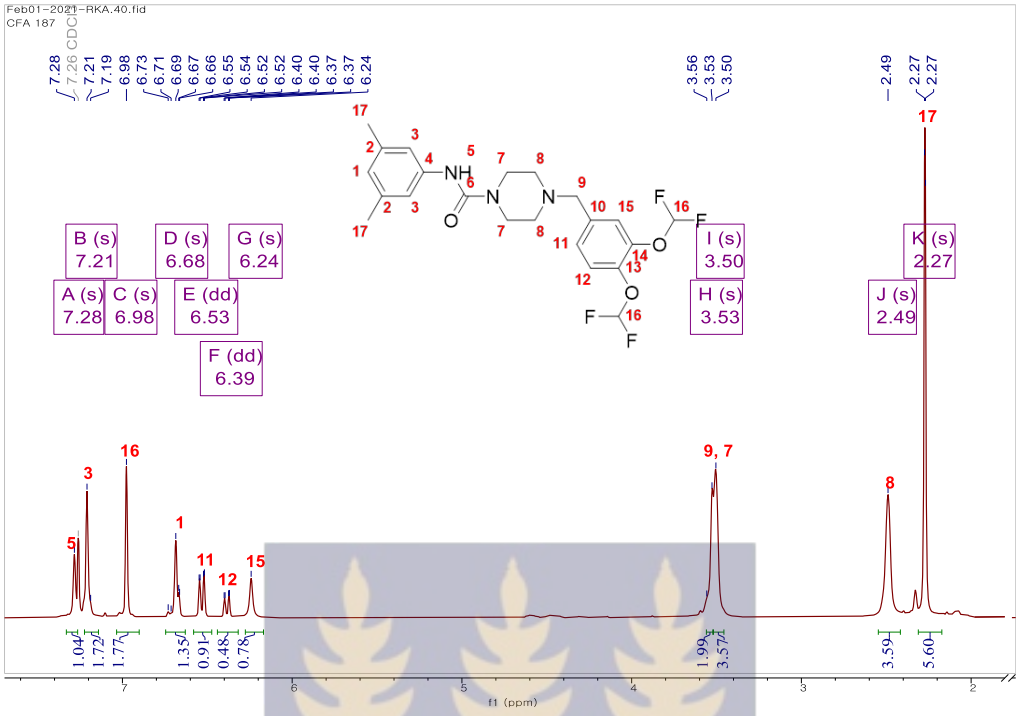


Appendix 1.70: ^{1}H NMR (400 MHz, $CDCl_3$) of 4-((6-bromobenzo[*d*][1,3]dioxol-5-yl)methyl)-*N*-(3,5-dimethylphenyl)piperazine-1-carboxamide (CFA134), **3.57**.

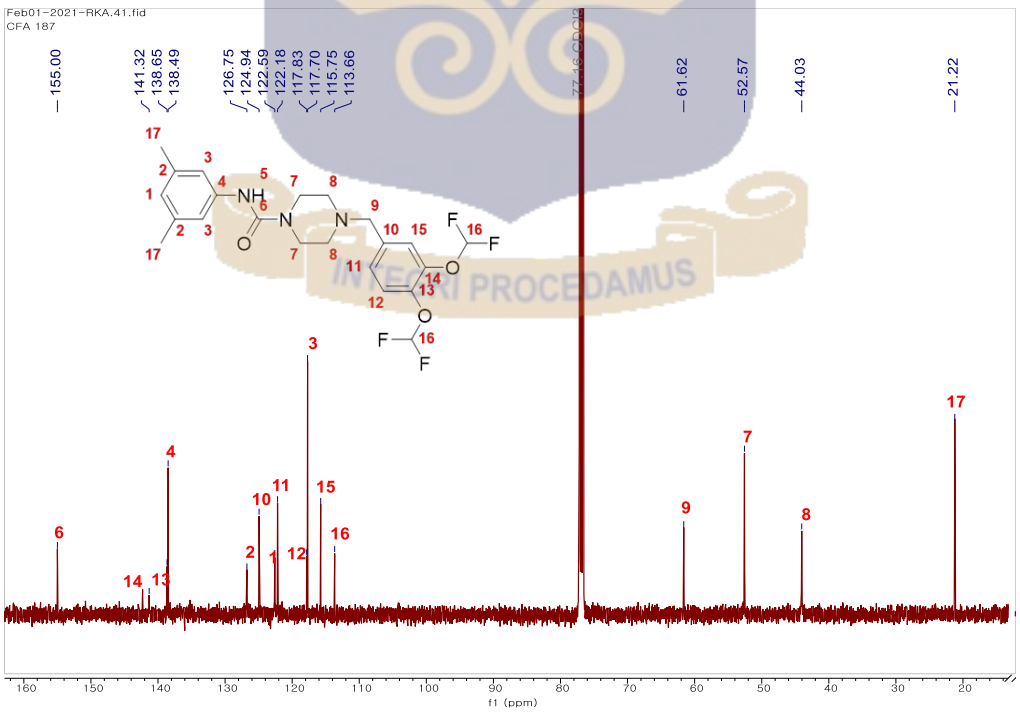


Appendix 1.71: ^{13}C NMR (101 MHz, $CDCl_3$) of 4-((6-bromobenzo[*d*][1,3]dioxol-5-yl)methyl)-*N*-(3,5-dimethylphenyl)piperazine-1-carboxamide (CFA134), **3.57**.

University of Ghana http://ugspace.ug.edu.gh

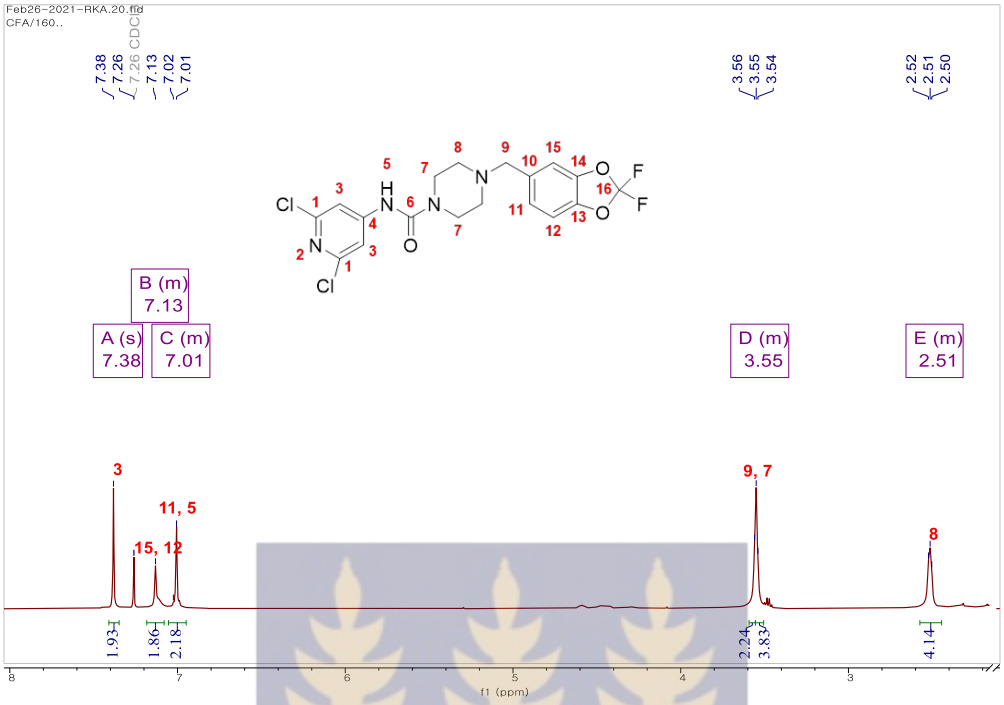


Appendix 1.72: ^{1}H NMR (400 MHz, $CDCl_3$) of 4-(3,4-bis(difluoromethoxy)benzyl)-N-(3,5-dimethylphenyl)piperazine-1-carboxamide (CFA187), **3.58**.

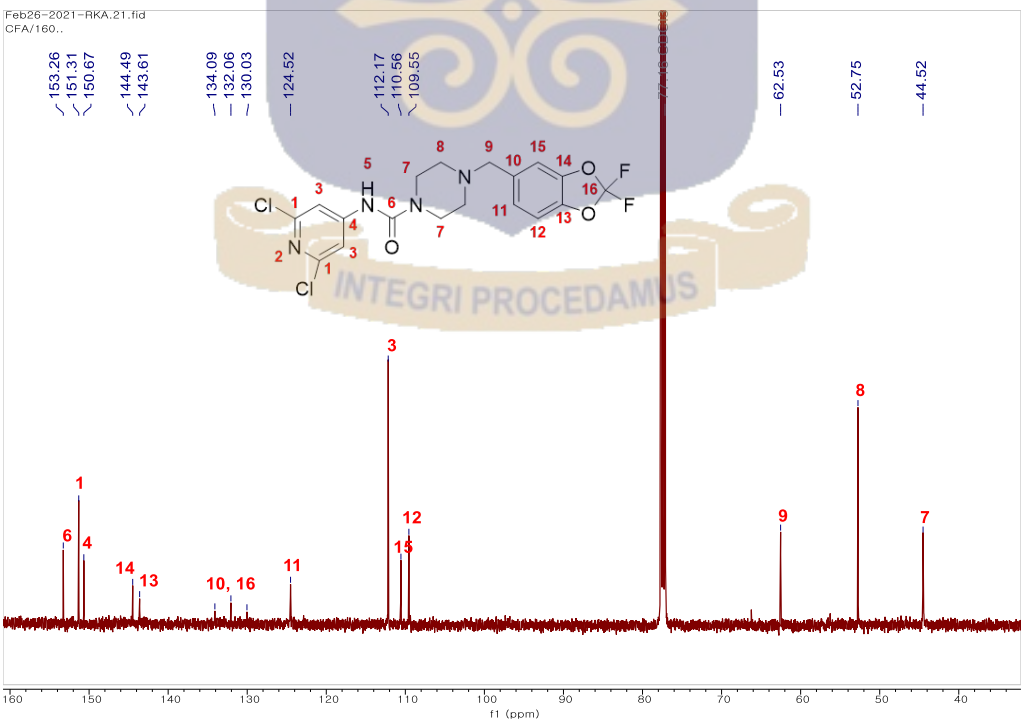


Appendix 1.73: ^{13}C NMR (101 MHz, $CDCl_3$) of 4-(3,4-bis(difluoromethoxy)benzyl)-N-(3,5-dimethylphenyl)piperazine-1-carboxamide (CFA187), **3.58**.

University of Ghana http://ugspace.ug.edu.gh

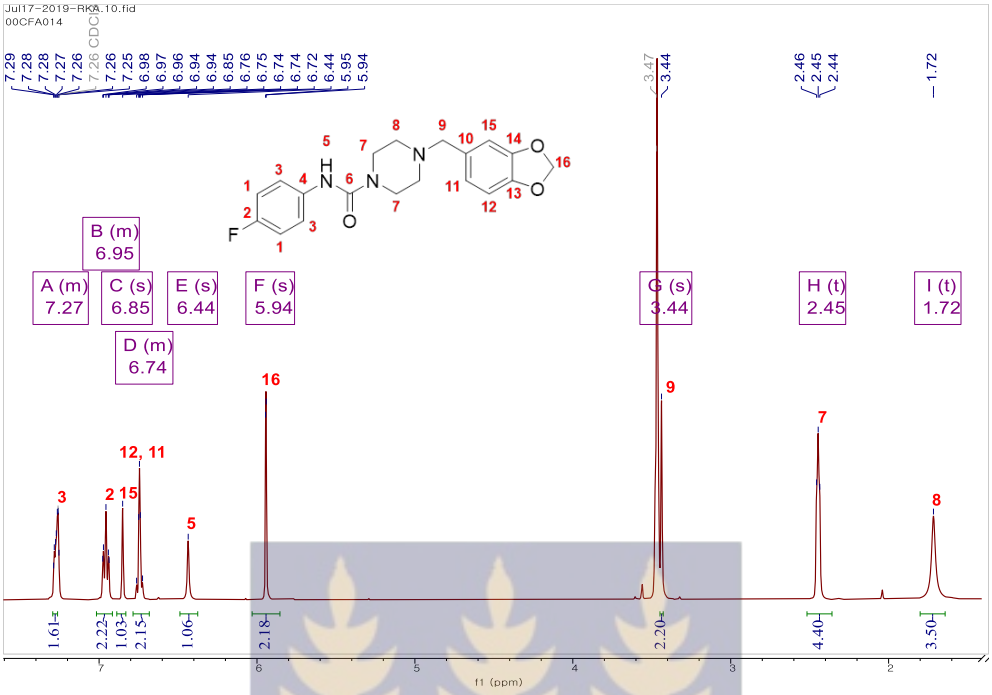


Appendix 1.74: ^{1}H NMR (500 MHz, $CDCl_3$) of *N*-(2,6-dichloropyridin-4-yl)-4-((2,2-difluorobenzo[*d*][1,3]dioxol-5-yl)methyl)piperazine-1-carboxamide (CFA160), **3.59**.

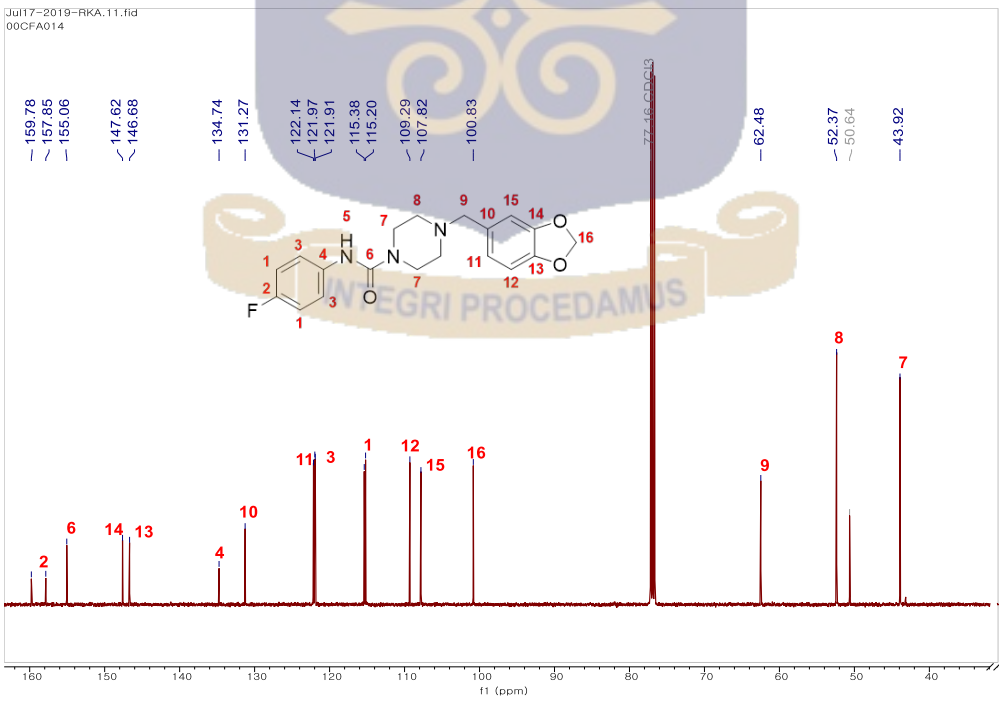


Appendix 1.75: ^{13}C NMR (126 MHz, $CDCl_3$) of *N*-(2,6-dichloropyridin-4-yl)-4-((2,2-difluorobenzo[*d*][1,3]dioxol-5-yl)methyl)piperazine-1-carboxamide (CFA160), **3.59**.

University of Ghana http://ugspace.ug.edu.gh

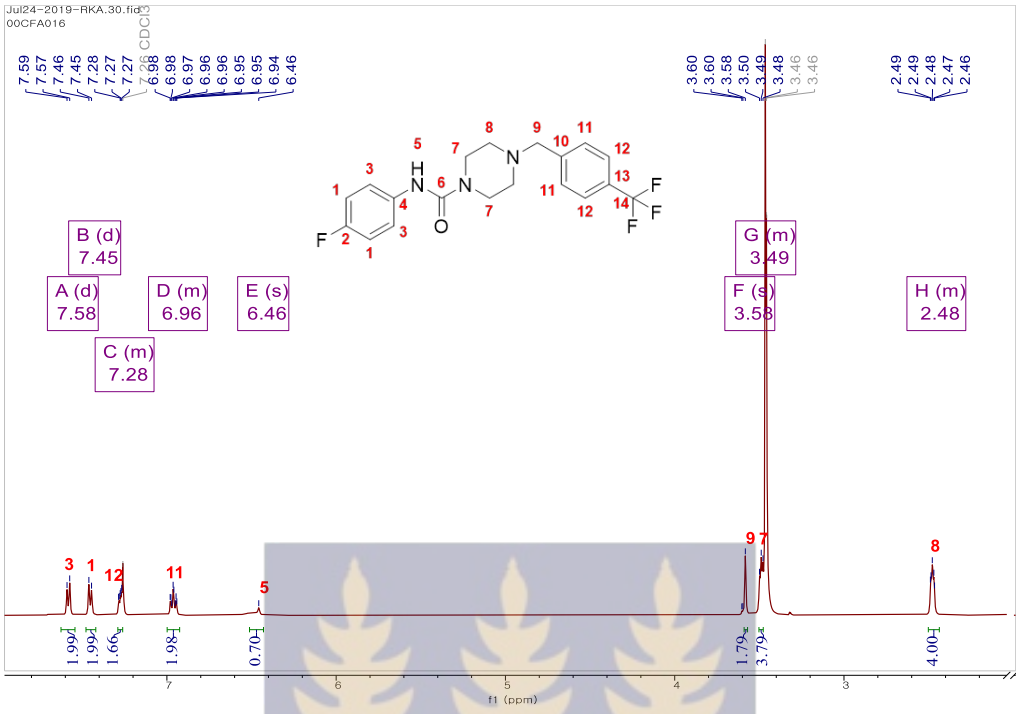


Appendix 1.76: ^{1}H NMR (500 MHz, $CDCl_3$) of 4-(benzo[*d*][1,3]dioxol-5-ylmethyl)-*N*-(4-fluorophenyl)piperazine-1-carboxamide (CFA014), **3.61**.

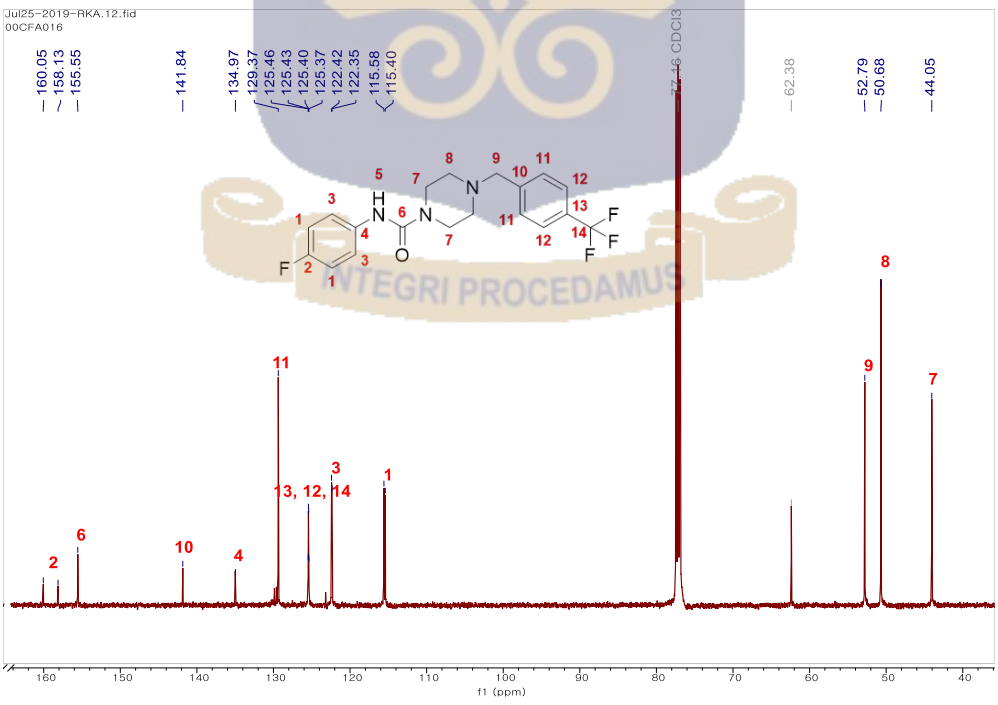


Appendix 1.77: ^{13}C NMR (126 MHz, $CDCl_3$) of 4-(benzo[*d*][1,3]dioxol-5-ylmethyl)-*N*-(4-fluorophenyl)piperazine-1-carboxamide (CFA014), **3.61**.

University of Ghana http://ugspace.ug.edu.gh

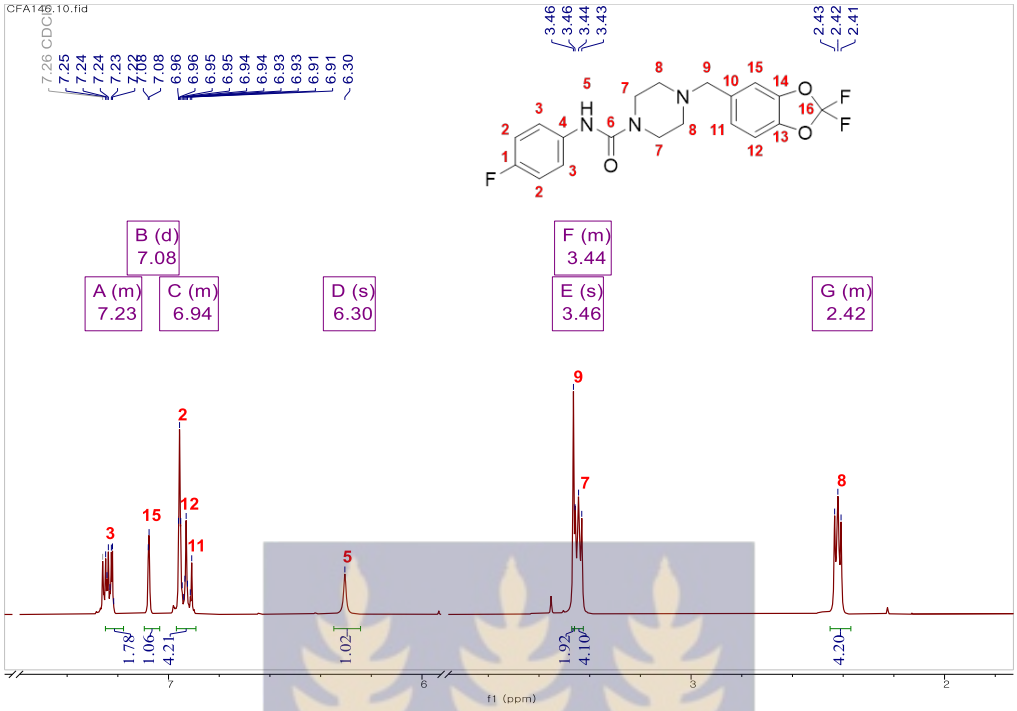


Appendix 1.78: ^{1}H NMR (500 MHz, $CDCl_3$) of *N*-(4-fluorophenyl)-4-(4-(trifluoromethyl)benzyl)piperazine-1-carboxamide (CFA016), **3.62**.

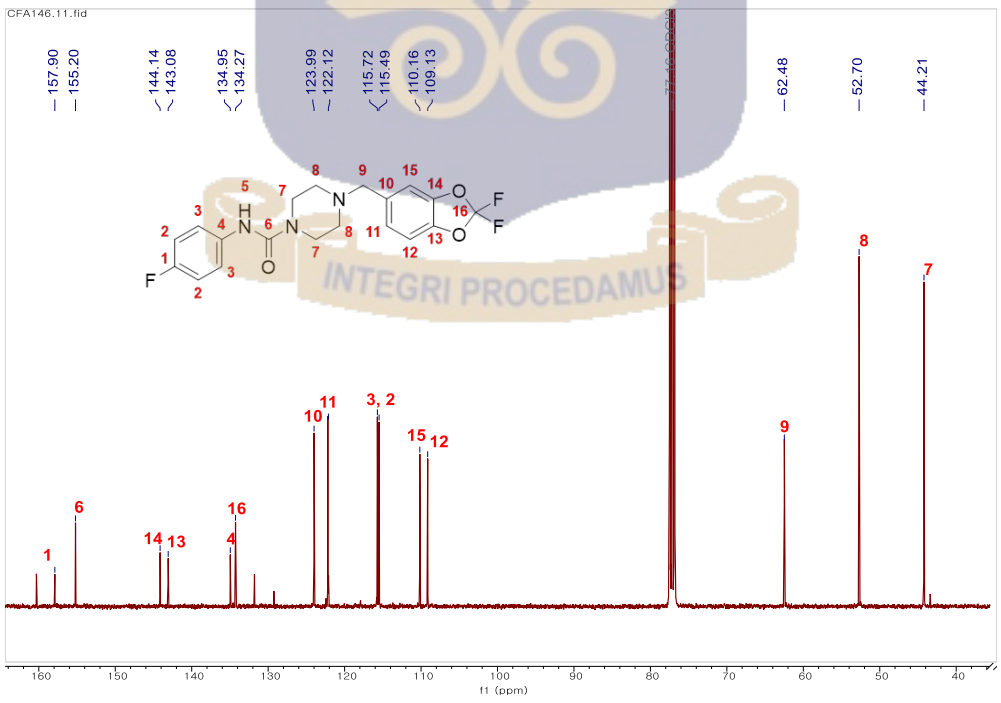


Appendix 1.79: ^{13}C NMR (126 MHz, $CDCl_3$) of *N*-(4-fluorophenyl)-4-(4-(trifluoromethyl)benzyl)piperazine-1-carboxamide (CFA016), **3.62**.

University of Ghana http://ugspace.ug.edu.gh

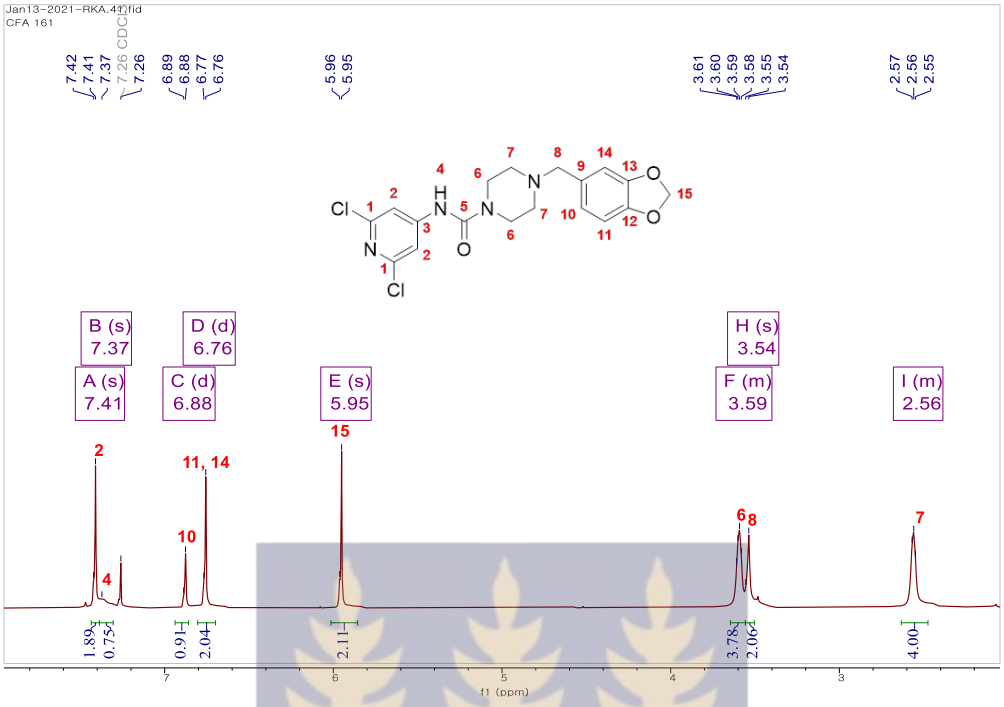


Appendix 1.80: ^{1}H NMR (400 MHz, $CDCl_3$) of 4-((2,2-difluorobenzo[d][1,3]dioxol-5-yl)methyl)-N-(4-fluorophenyl)piperazine-1-carboxamide (CFA146), **3.57**.

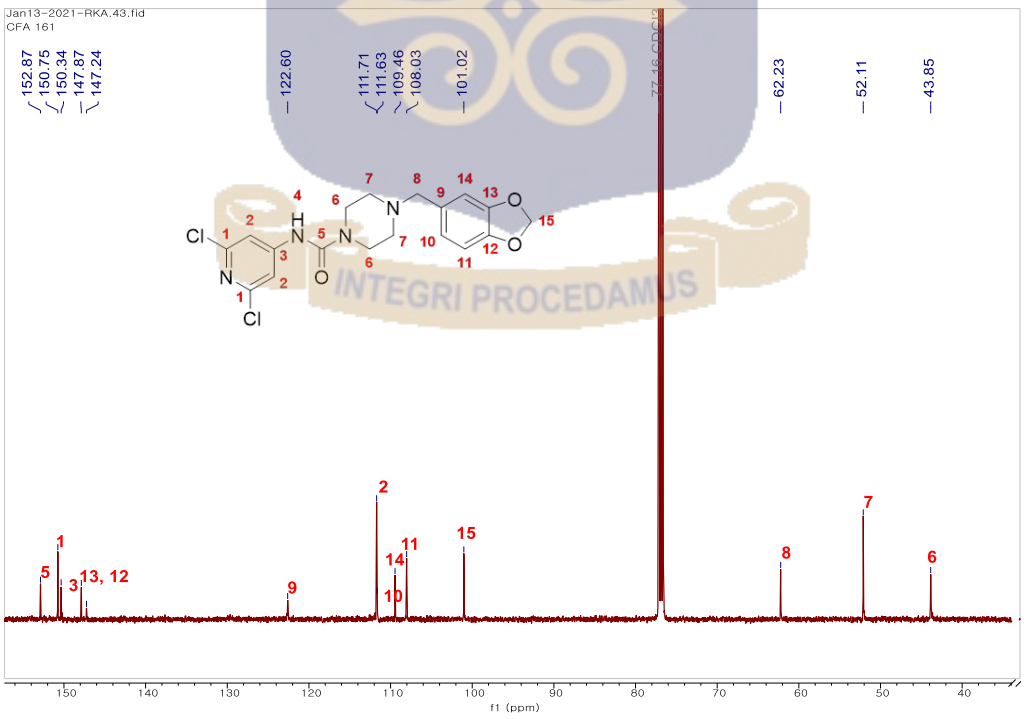


Appendix 1.81: ^{13}C NMR (101 MHz, $CDCl_3$) of 4-((2,2-difluorobenzo[d][1,3]dioxol-5-yl)methyl)-N-(4-fluorophenyl)piperazine-1-carboxamide (CFA146), **3.57**.

University of Ghana http://ugspace.ug.edu.gh

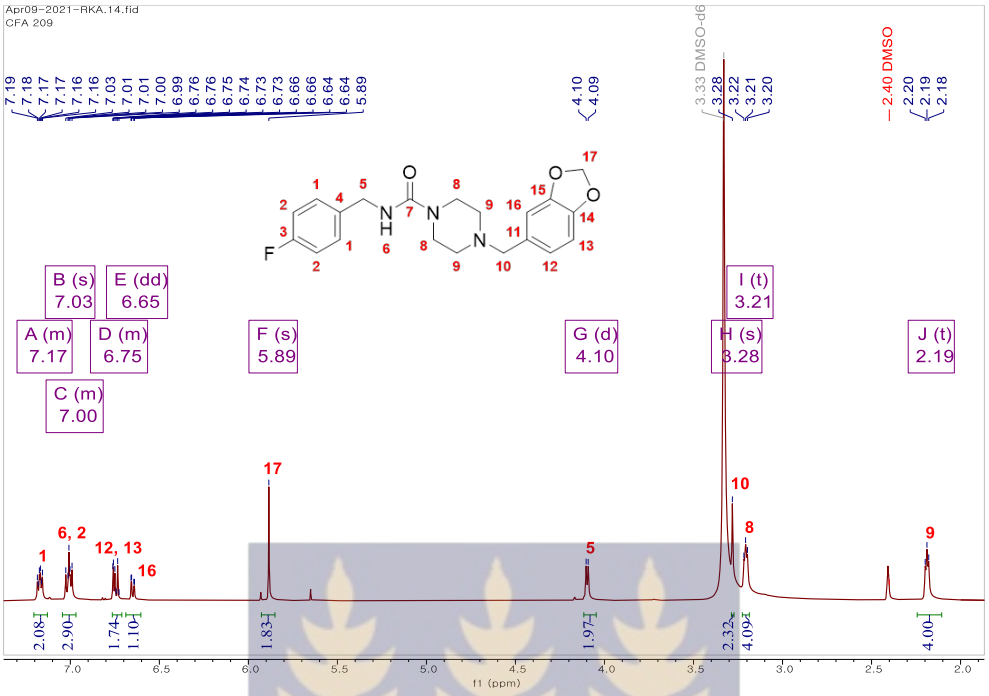


Appendix 1.82: ^{1}H NMR (500 MHz, $CDCl_3$) of 4-(benzo[*d*][1,3]dioxol-5-ylmethyl)-*N*-(2,6-dichloropyridin-4-yl)piperazine-1-carboxamide (CFA161), **3.60**.

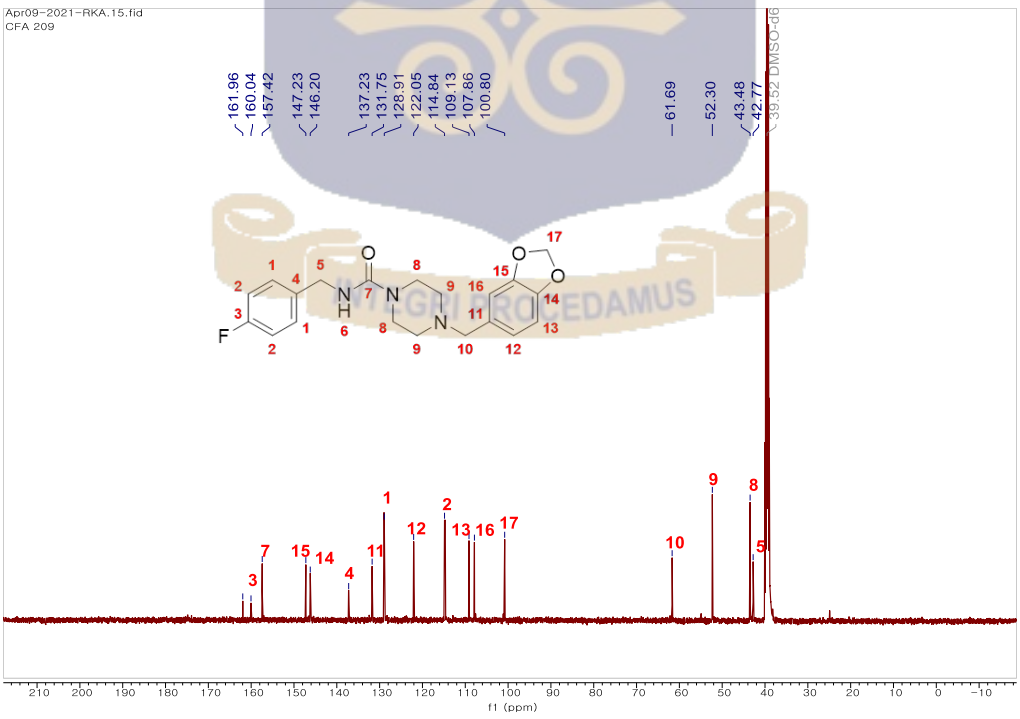


Appendix 1.83: ^{13}C NMR (126 MHz, $CDCl_3$) of 4-(benzo[*d*][1,3]dioxol-5-ylmethyl)-*N*-(2,6-dichloropyridin-4-yl)piperazine-1-carboxamide (CFA161), **3.60**.

University of Ghana http://ugspace.ug.edu.gh

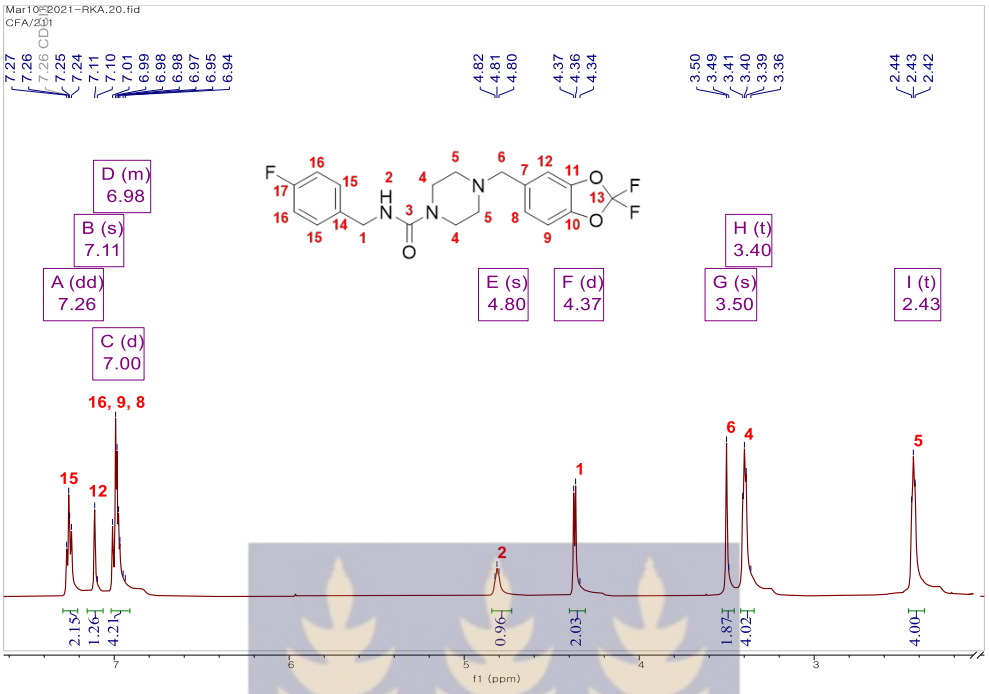


Appendix 1.84: ^{1}H NMR (500 MHz, DMSO) of 4-(benzo[d][1,3]dioxol-5-ylmethyl)-N-(4-fluorobenzyl)piperazine-1-carboxamide (CFA209), **3.64**.

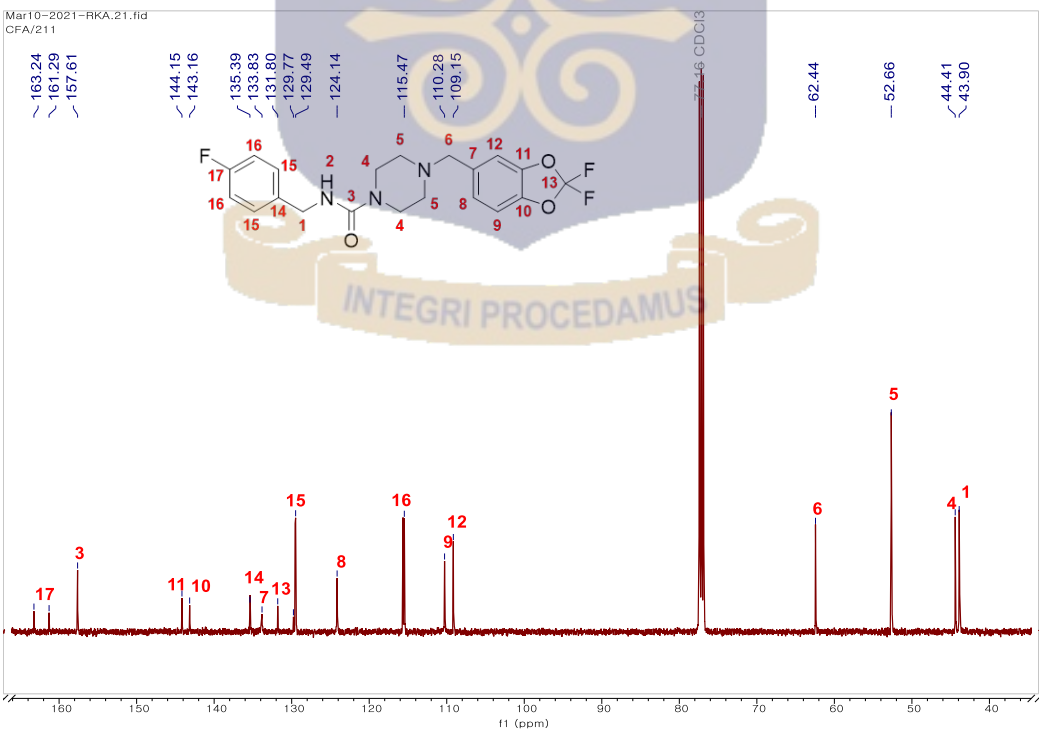


Appendix 1.85: ^{13}C NMR (126 MHz, DMSO) of 4-(benzo[d][1,3]dioxol-5-ylmethyl)-N-(4-fluorobenzyl)piperazine-1-carboxamide (CFA209), **3.64**.

University of Ghana http://ugspace.ug.edu.gh

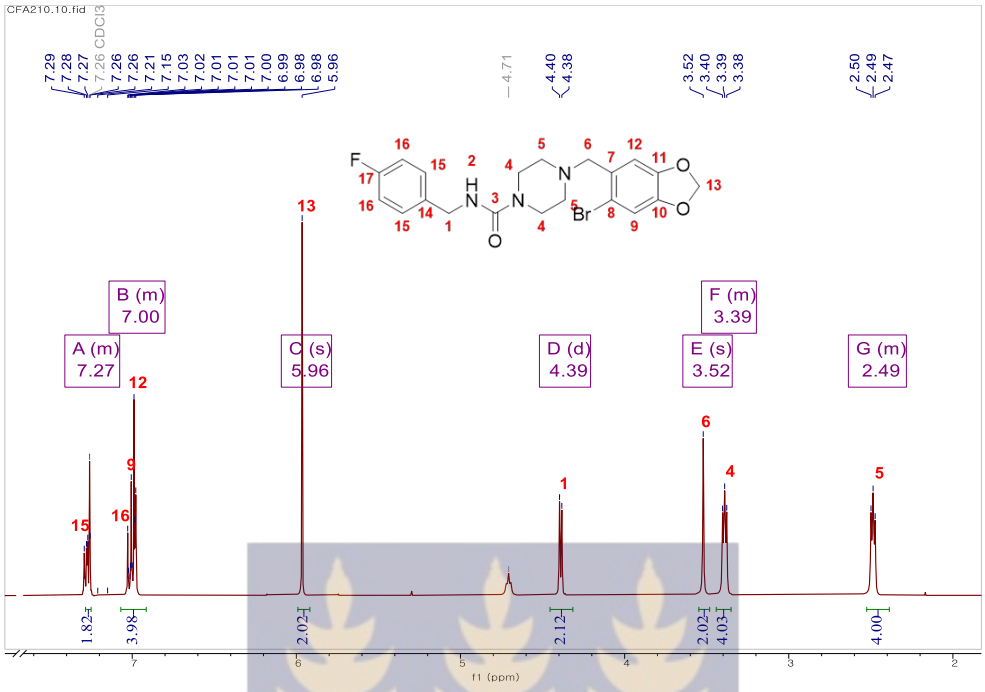


Appendix 1.86: ^{1}H NMR (500 MHz, $CDCl_3$) of 4-((2,2-difluorobenzo[*d*][1,3]dioxol-5-yl)methyl)-*N*-(4-fluorobenzyl)piperazine-1-carboxamide (CFA211), **3.65**.

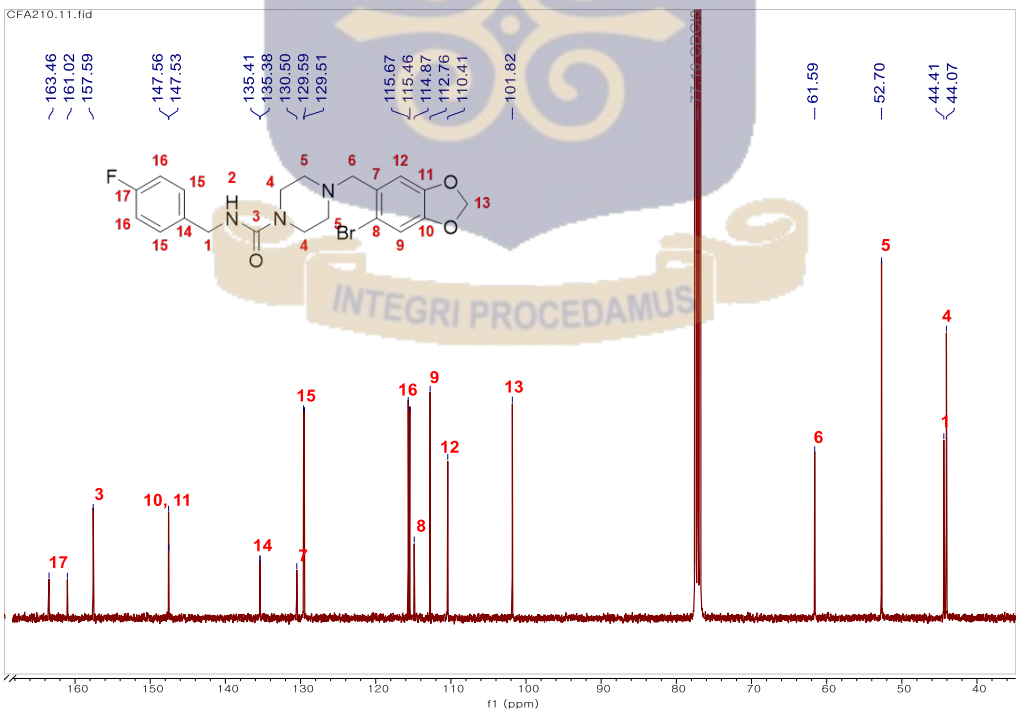


Appendix 1.87: ^{13}C NMR (126 MHz, $CDCl_3$) of 4-((2,2-difluorobenzo[*d*][1,3]dioxol-5-yl)methyl)-*N*-(4-fluorobenzyl)piperazine-1-carboxamide (CFA211), **3.65**.

University of Ghana http://ugspace.ug.edu.gh

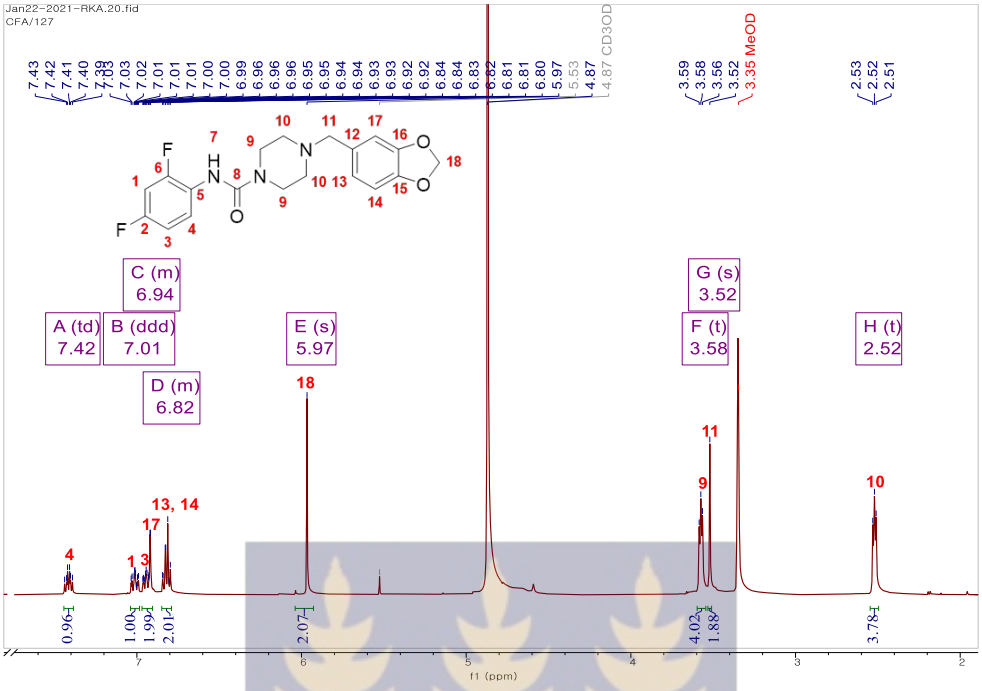


Appendix 1.88: ^{1}H NMR (400 MHz, $CDCl_3$) of 4-((6-bromobenzo[d][1,3]dioxol-5-yl)methyl)-N-(4-fluorobenzyl)piperazine-1-carboxamide (CFA210), **3.66**.

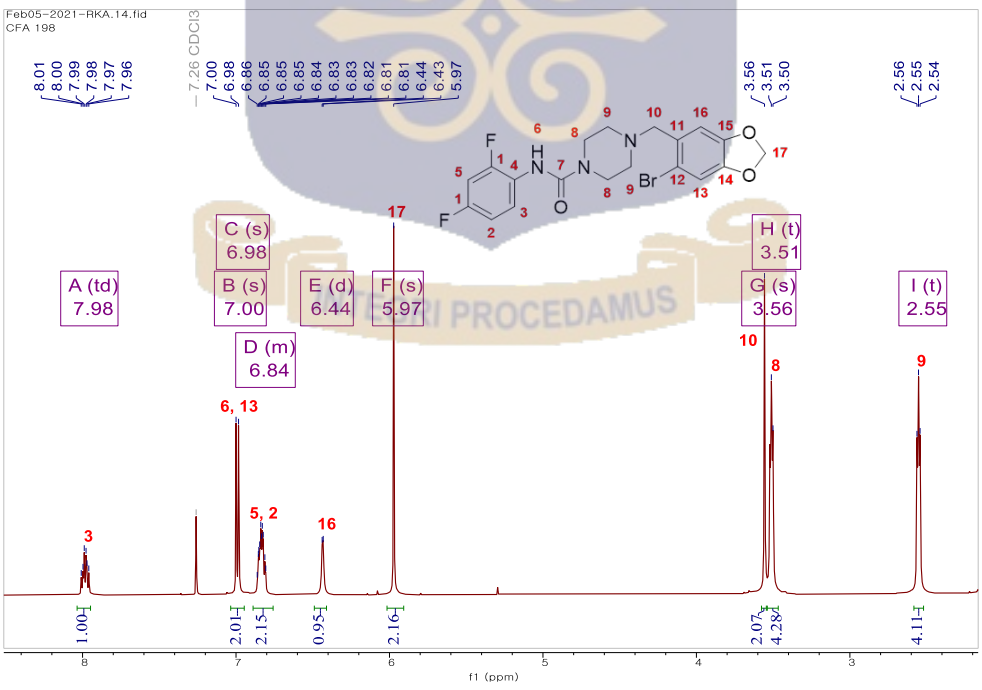


Appendix 1.89: ^{13}C NMR (101 MHz, $CDCl_3$) of 4-((6-bromobenzo[d][1,3]dioxol-5-yl)methyl)-N-(4-fluorobenzyl)piperazine-1-carboxamide (CFA210), **3.66**.

University of Ghana http://ugspace.ug.edu.gh

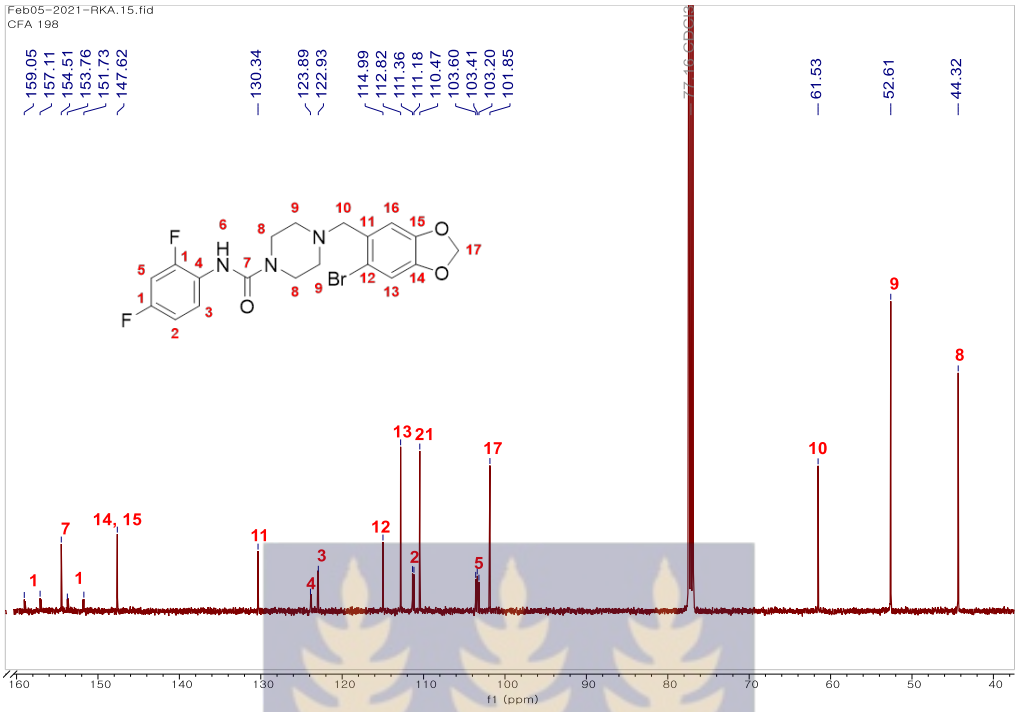


Appendix 1.90: ^{1}H NMR (500 MHz, MeOD) of 4-((6-bromobenzo[*d*][1,3]dioxol-5-yl)methyl)-*N*-(2,4-difluorophenyl)piperazine-1-carboxamide (CFA127/162), **3.67**.

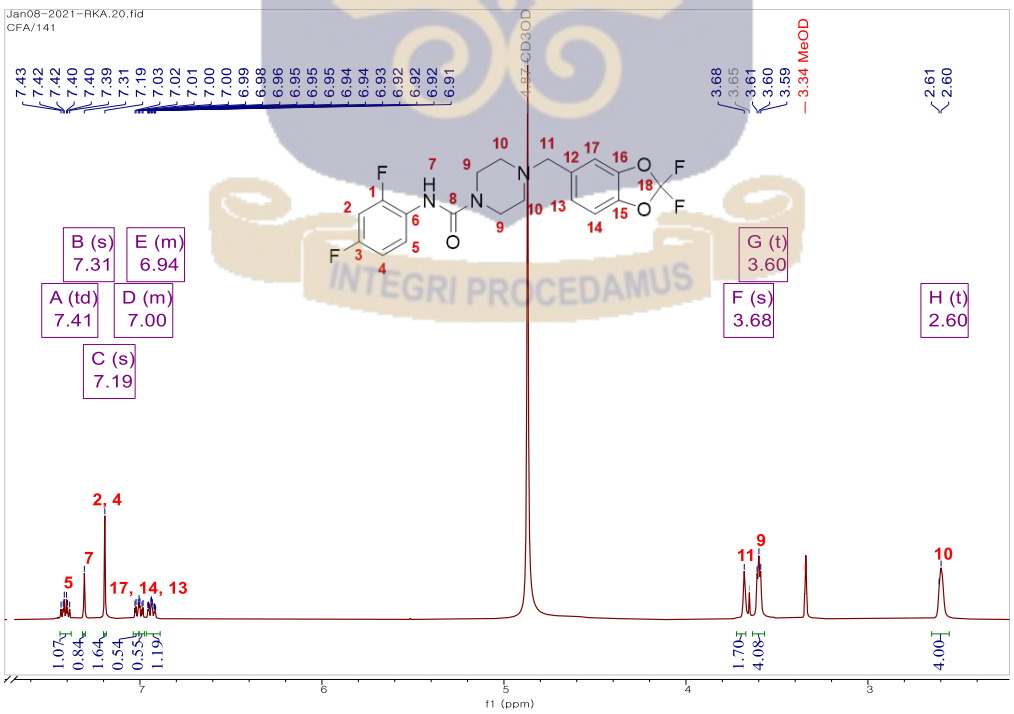


Appendix 1.91: ^{1}H NMR (400 MHz, $CDCl_3$) of 4-((6-bromobenzo[*d*][1,3]dioxol-5-yl)methyl)-*N*-(2,4-difluorophenyl)piperazine-1-carboxamide (CFA198), **3.67**.

University of Ghana http://ugspace.ug.edu.gh

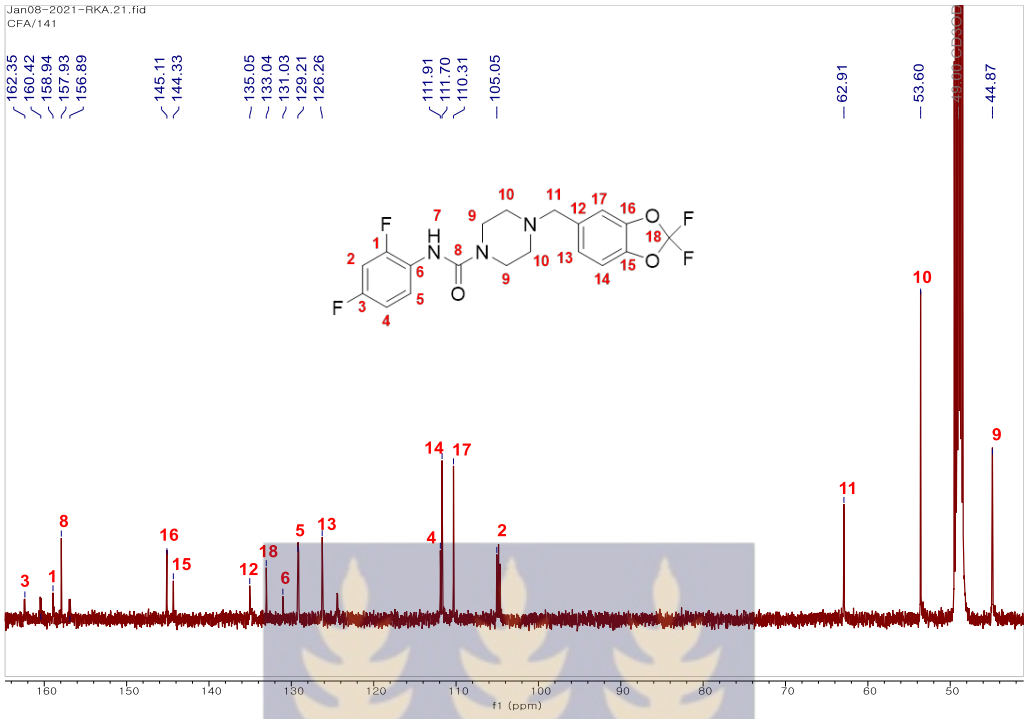


Appendix 1.92: ^{13}C NMR (101 MHz, $CDCl_3$) of 4-((6-bromobenzo[*d*][1,3]dioxol-5-yl)methyl)-*N*-(2,4-difluorophenyl)piperazine-1-carboxamide (CFA198), **3.68**.

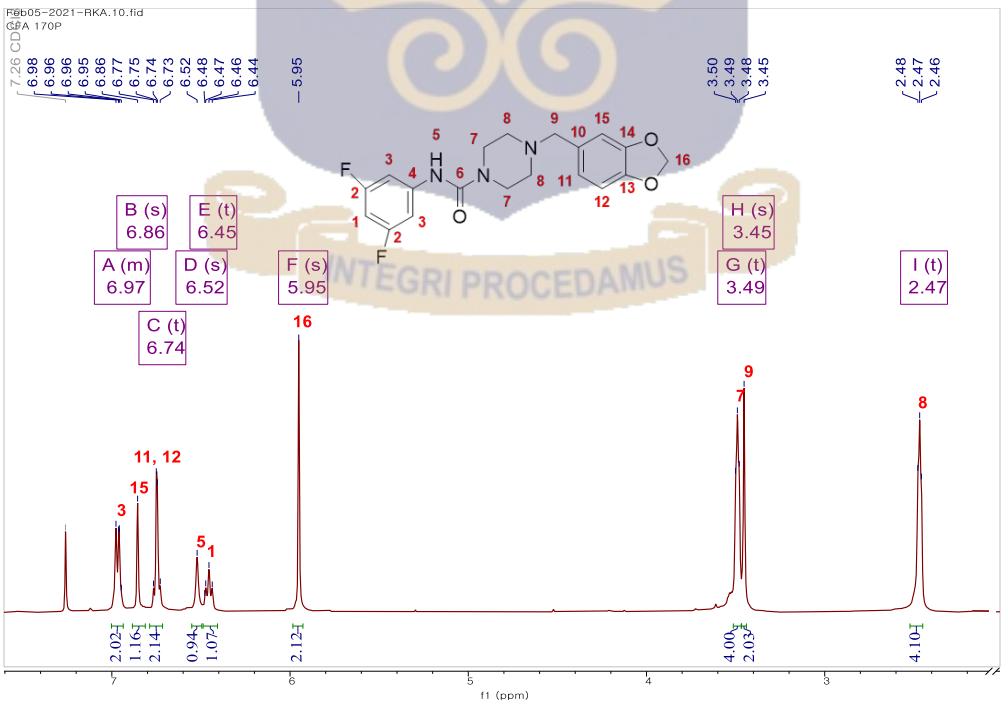


Appendix 1.93: ^{1}H NMR (500 MHz, MeOD) of 4-((2,2-difluorobenzo[d][1,3]dioxol-5-yl)methyl)-N-(2,4-difluorophenyl)piperazine-1-carboxamide (CFA163), **3.69**.

University of Ghana http://ugspace.ug.edu.gh

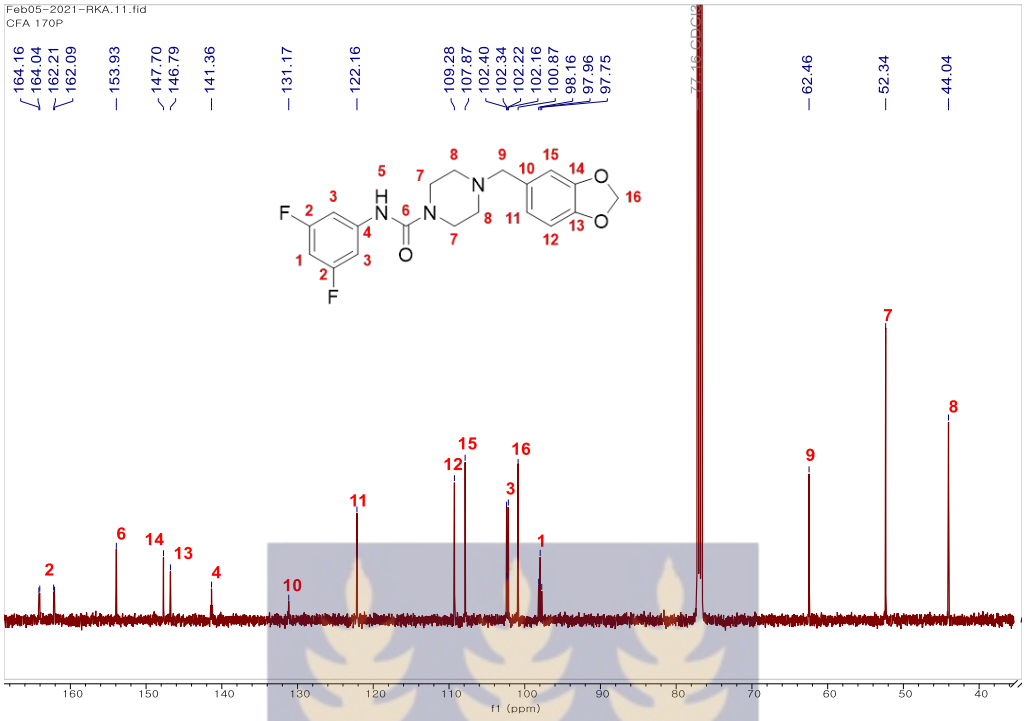


Appendix 1.94: ^{13}C NMR (126 MHz, MeOD) of 4-((2,2-difluorobenzo[d][1,3]dioxol-5-yl)methyl)-N-(2,4-difluorophenyl)piperazine-1-carboxamide (CFA163), **3.69**.

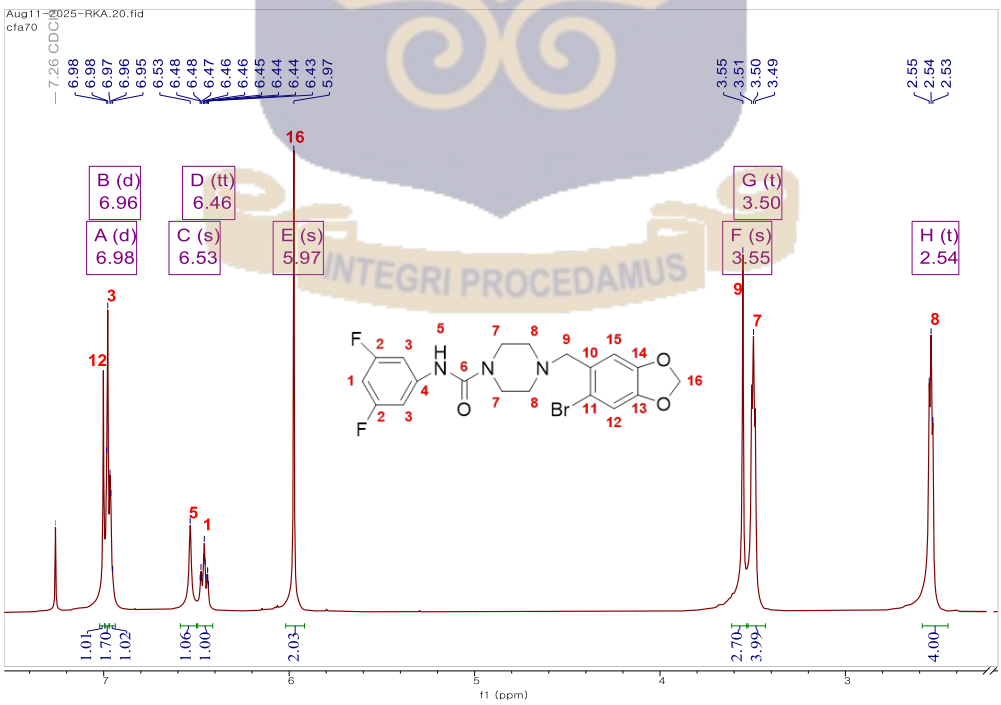


Appendix 1.95: ^{1}H NMR (500 MHz, $CDCl_3$) of 4-(benzo[d][1,3]dioxol-5-ylmethyl)-N-(3,5-difluorophenyl)piperazine-1-carboxamide (CFA176), **3.70**.

University of Ghana http://ugspace.ug.edu.gh

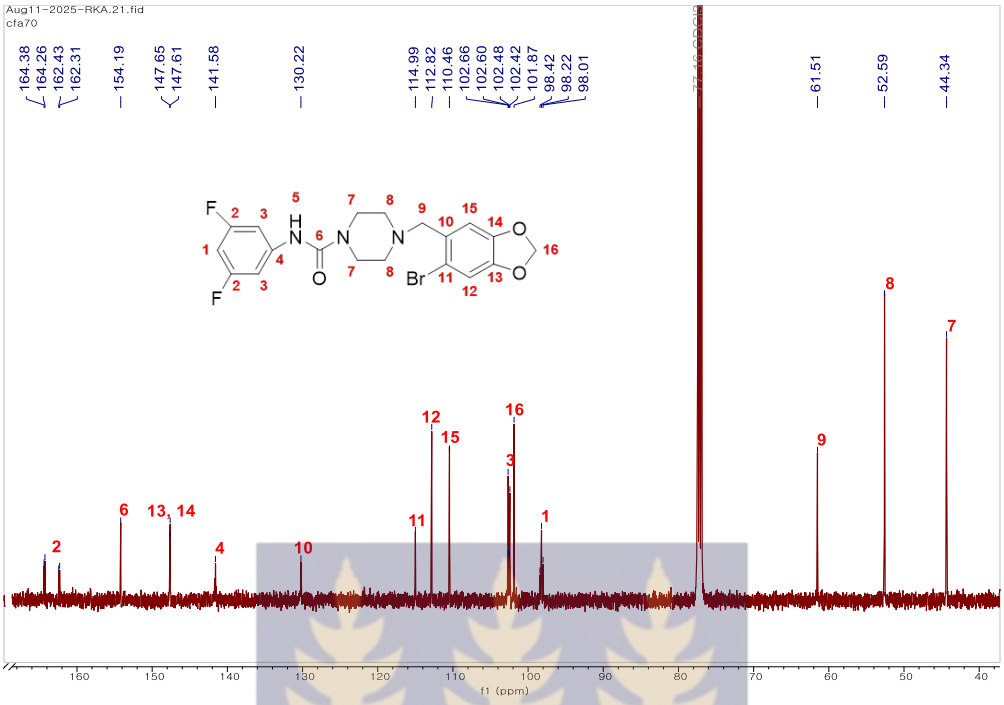


Appendix 1.96: ^{13}C NMR (126 MHz, $CDCl_3$) of 4-(benzo[d][1,3]dioxol-5-ylmethyl)-N-(3,5-difluorophenyl)piperazine-1-carboxamide (CFA176), **3.70**.

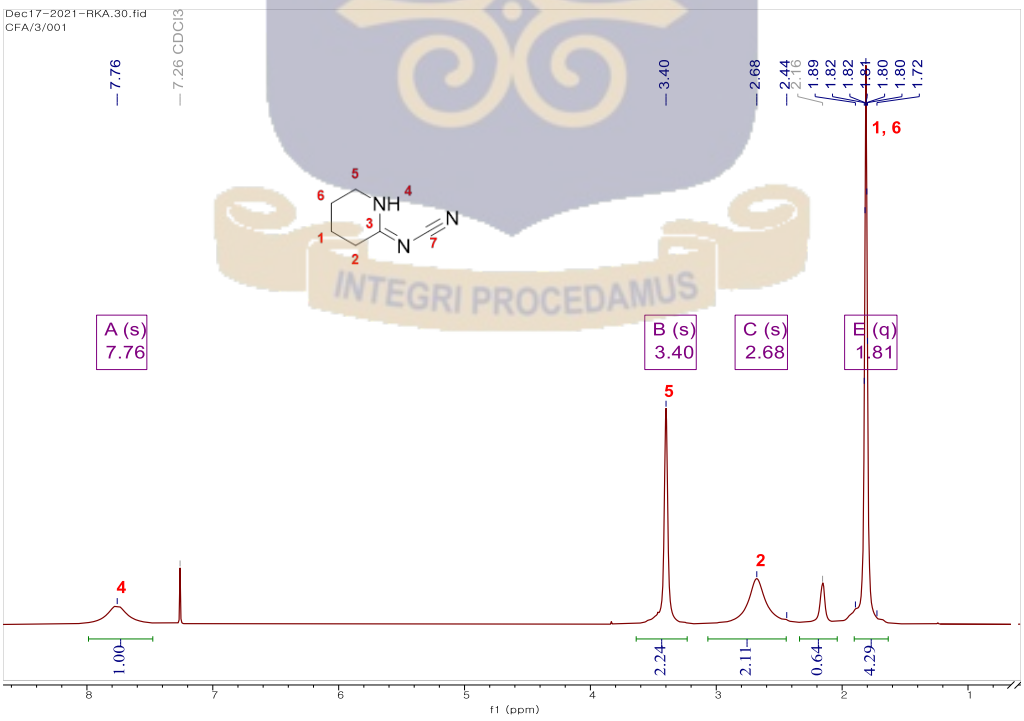


Appendix 1.97: ^{13}H NMR (500 MHz, $CDCl_3$) of 4-((2,2-difluorobenzo[*d*][1,3]dioxol-5-yl)methyl)-*N*-(3,5-difluorophenyl)piperazine-1-carboxamide (CFA070), **3.71**.

University of Ghana http://ugspace.ug.edu.gh

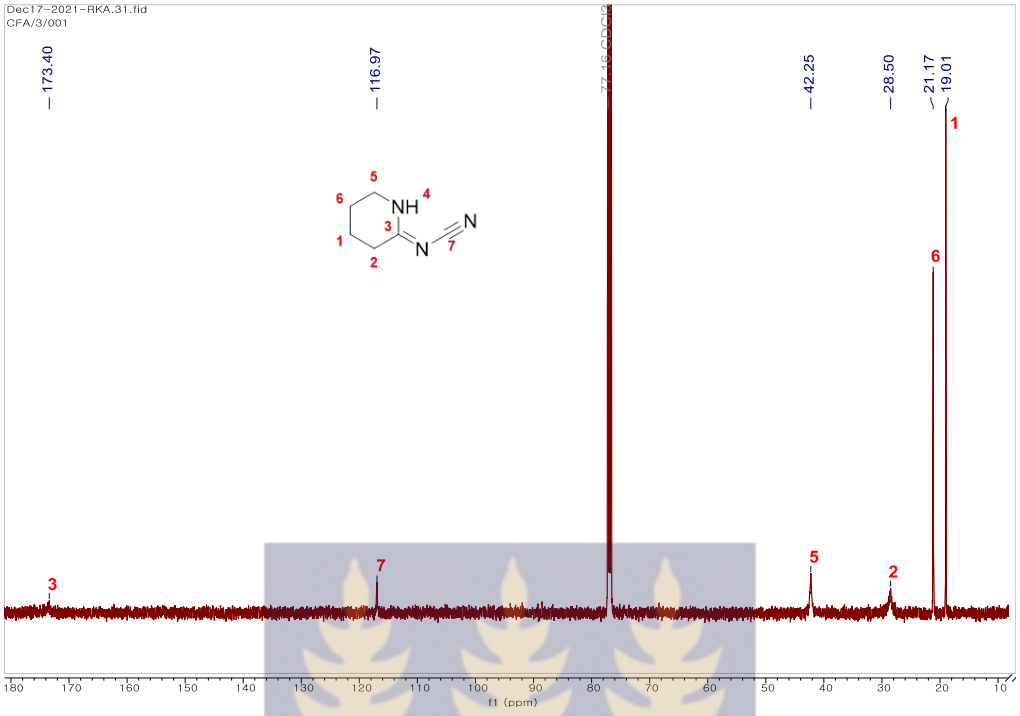


Appendix 1.98: ^{13}C NMR (126 MHz, $CDCl_3$) of 4-((2,2-difluorobenzo[*d*][1,3]dioxol-5-yl)methyl)-*N*-(3,5-difluorophenyl)piperazine-1-carboxamide (CFA070), **3.71**.

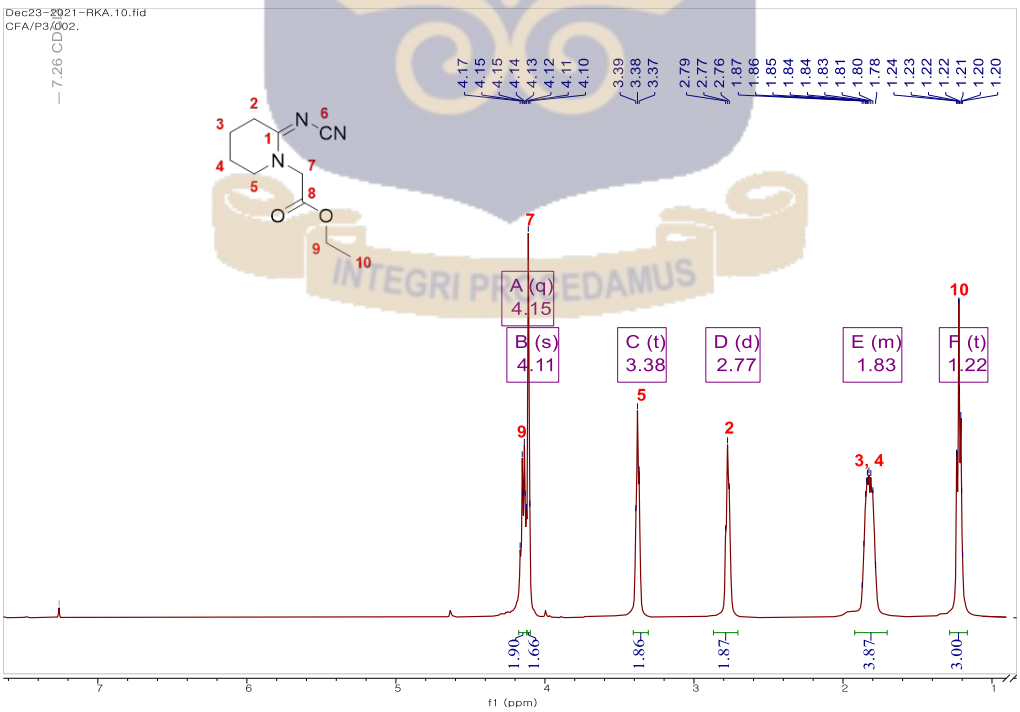


Appendix 1.99: ^{1}H NMR (500 MHz, $CDCl_3$) of (*Z*)-*N*-(piperidin-2-ylidene) cyanamide (CFA/P3/001), **3.73.**

University of Ghana http://ugspace.ug.edu.gh

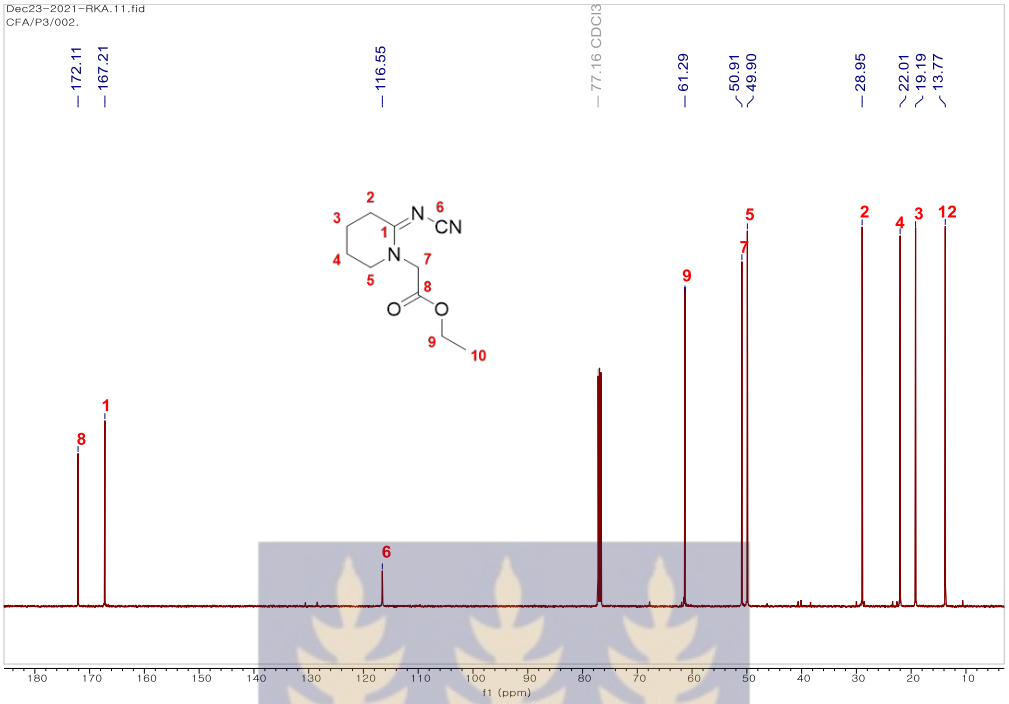


Appendix 1.100: ^{13}C NMR (126 MHz, $CDCl_3$) of (*Z*)-*N*-(piperidin-2-ylidene)cyanamide, (CFA/P3/001), **3.73**.

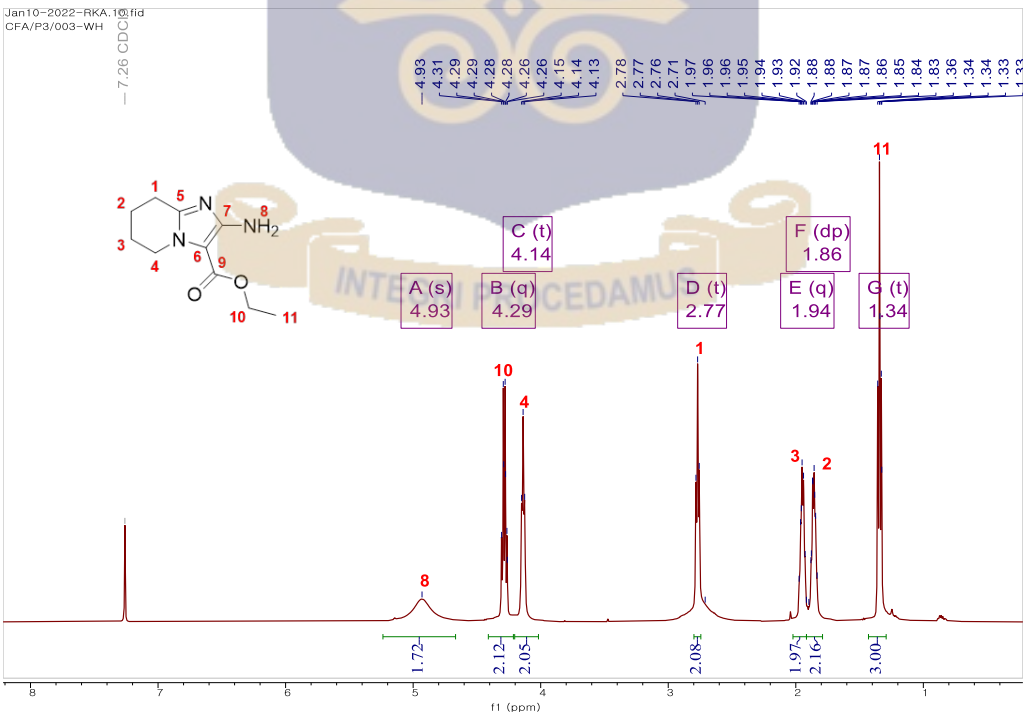


Appendix 1.101: ^{1}H NMR (500 MHz, $CDCl_3$) of ethyl (*Z*)-2-(2-(cyanoimino)piperidin-1-yl)acetate (CFA/P3/002), **3.74**.

University of Ghana http://ugspace.ug.edu.gh

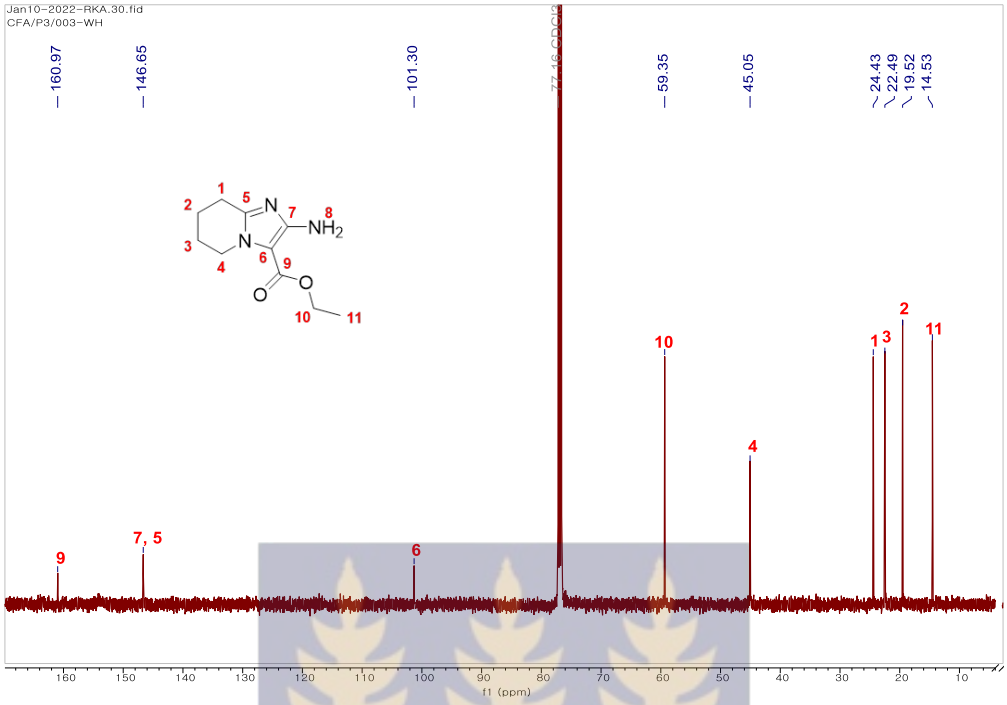


Appendix 1.102: ^{13}C NMR (126 MHz, $CDCl_3$) of ethyl (*Z*)-2-(2-(cyanoimino)piperidin-1-yl)acetate (CFA/P3/002), **3.74.**

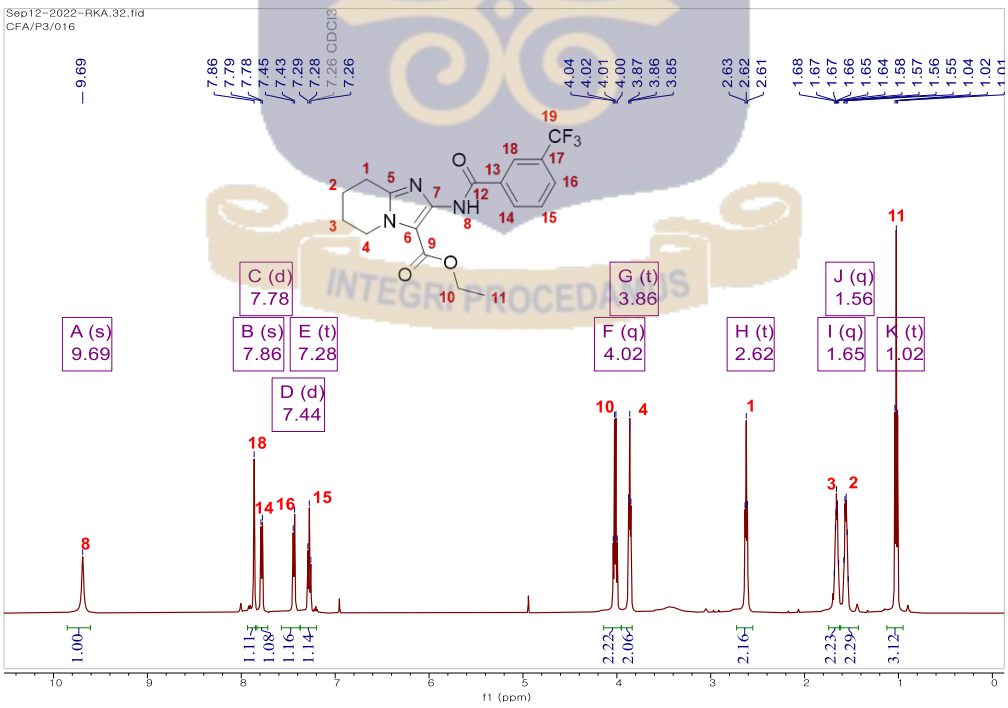


Appendix 1.103: ^{1}H NMR (500 MHz, $CDCl_3$) of ethyl 2-amino-5,6,7,8-tetrahydroimidazo[1,2-a]pyridine-5-carboxylate (CFA/P3/003), **3.75**.

University of Ghana http://ugspace.ug.edu.gh

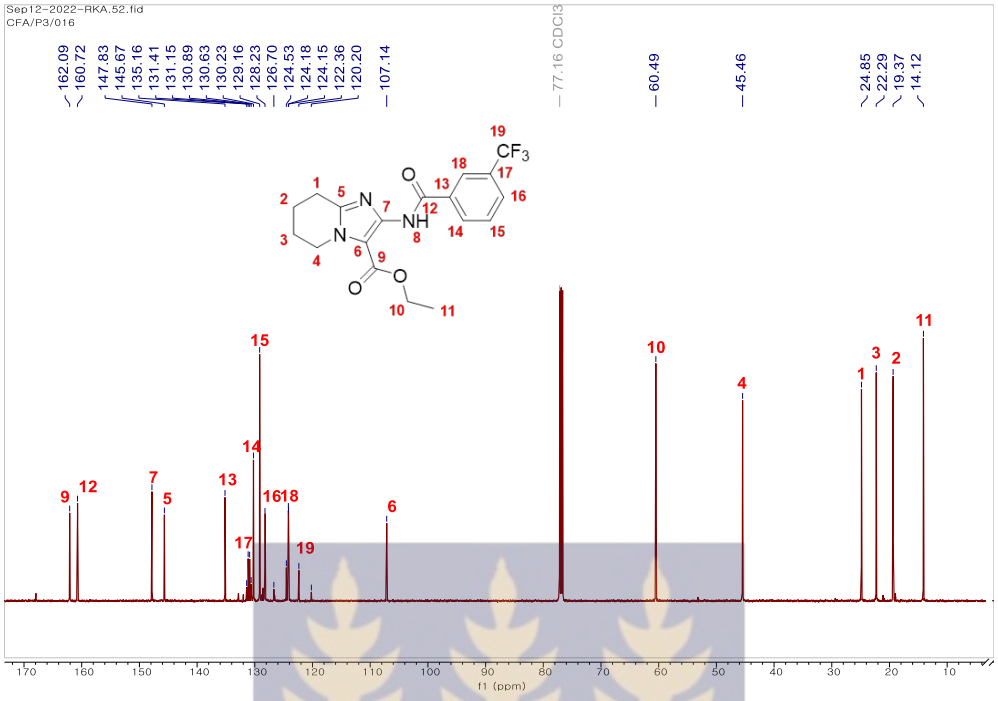


Appendix 1.104: ^{13}C NMR (126 MHz, $CDCl_3$) of ethyl 2-amino-5,6,7,8-tetrahydroimidazo[1,2-a]pyridine-5-carboxylate CFA/P3/003), **3.75**.

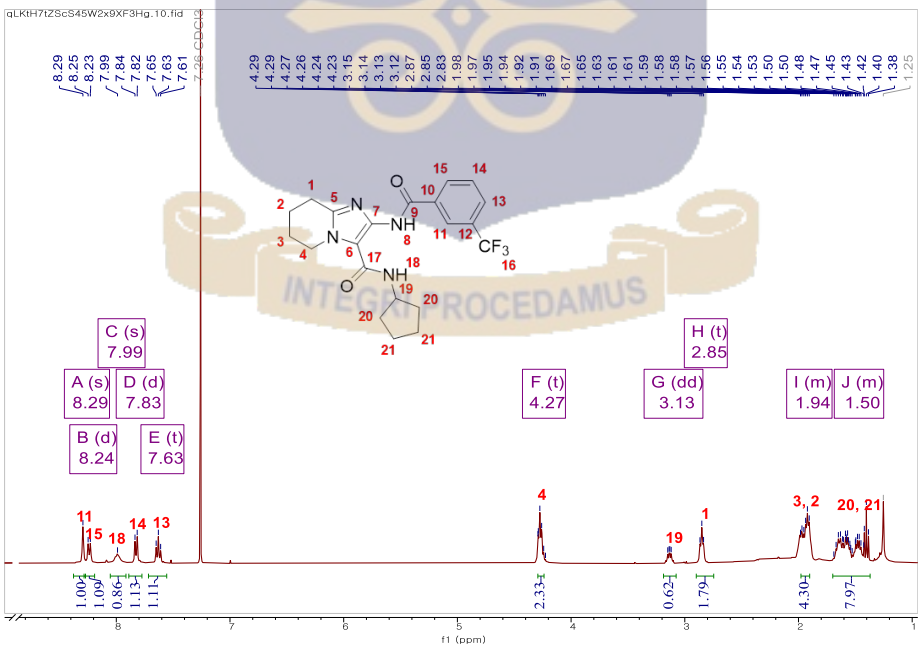


Appendix 1.105: ^{1}H NMR (500 MHz, $CDCl_3$) of ethyl 2-amino-5,6,7,8-tetrahydroimidazo[1,2-a]pyridine-5-carboxylate (CFA/P3/016), **3.76**.

University of Ghana http://ugspace.ug.edu.gh

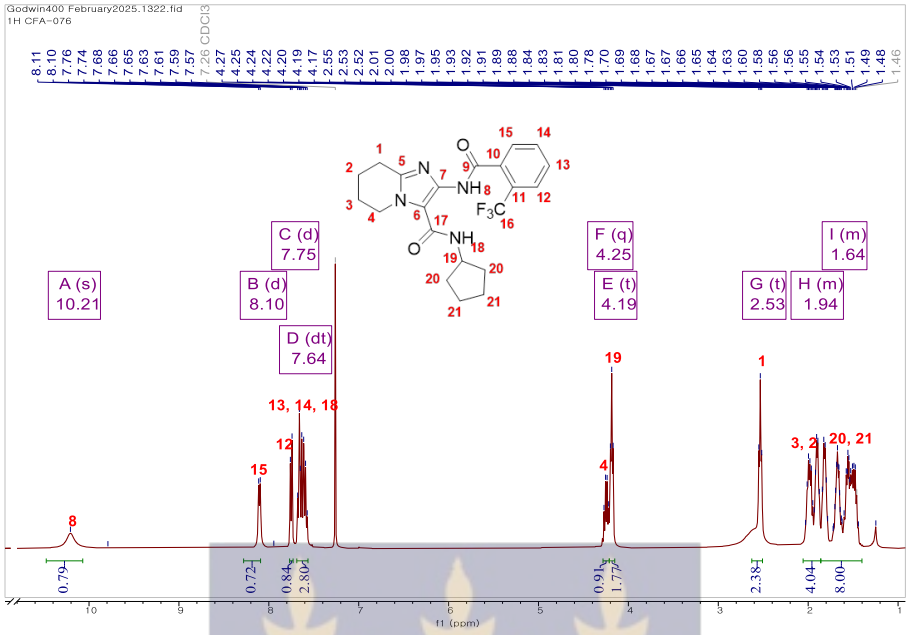


Appendix 1.106: ^{13}C NMR (126 MHz, $CDCl_3$) of ethyl 2-amino-5,6,7,8-tetrahydroimidazo[1,2-a]pyridine-5-carboxylate (CFA/P3/016), **3.76**.

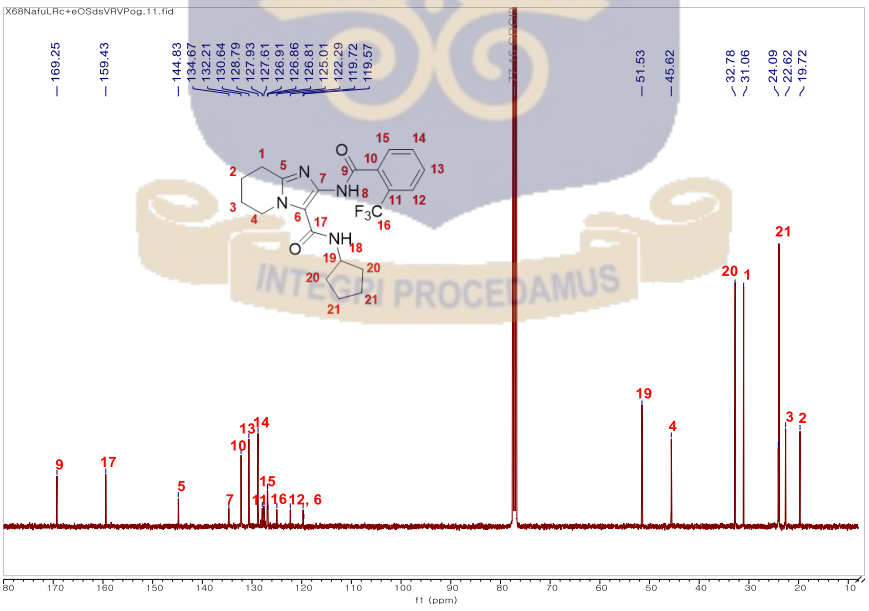


Appendix 1.107: ^{1}H NMR (400 MHz, $CDCl_3$) of *N*-cyclopentyl-2-(3-(trifluoromethyl)benzamido)-5,6,7,8-tetrahydroimidazo[1,2-*a*]pyridine-5-carboxamide (CFA/P3/021), **3.80.**

University of Ghana http://ugspace.ug.edu.gh



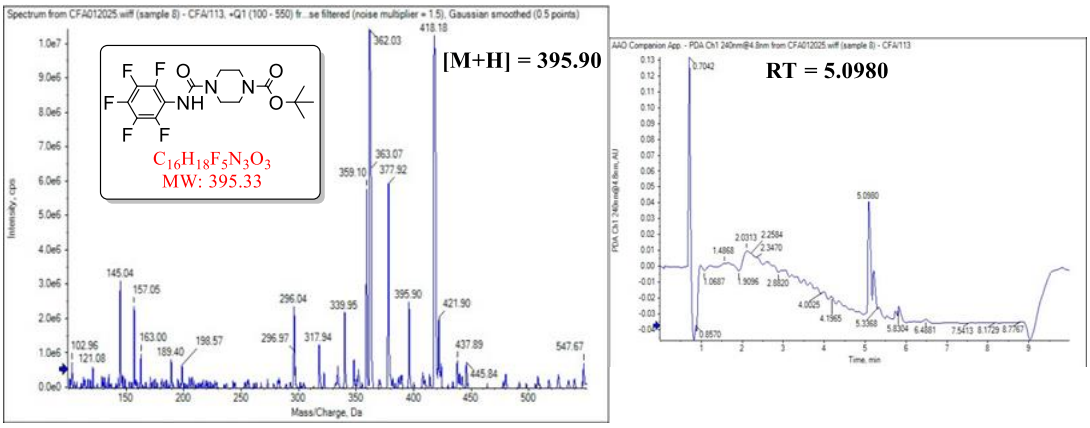
Appendix 1.108: ^{1}H NMR (400 MHz, $CDCl_3$) of *N*-cyclopentyl-2-(2-(trifluoromethyl)benzamido)-5,6,7,8-tetrahydroimidazo[1,2-*a*]pyridine-3-carboxamide (CFA/P3/076), **3.81.**



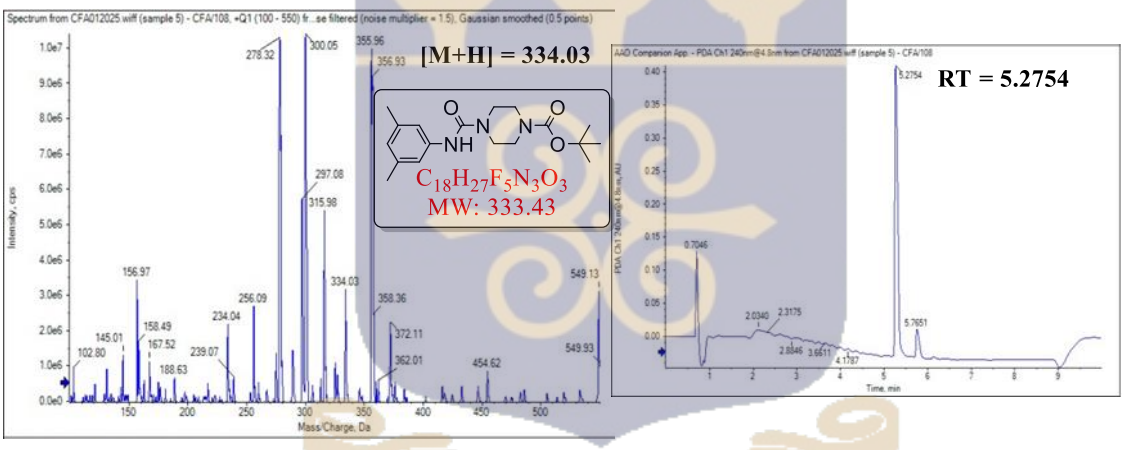
Appendix 1.109: ^{13}C NMR (101 MHz, $CDCl_3$) of *N*-cyclopentyl-2-(2-(trifluoromethyl)benzamido)-5,6,7,8-tetrahydroimidazo[1,2-*a*]pyridine-3-carboxamide (CFA/P3/076), **3.81.**

University of Ghana http://ugspace.ug.edu.gh

Appendix 2: LC-MS Data

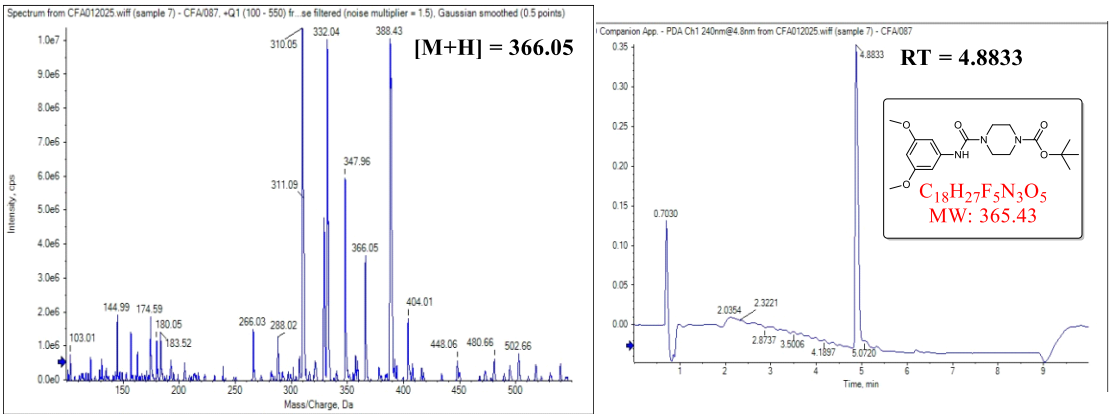


Appendix 2.1: **WAU-ESI** spectrum of tert-butyl 4-((perfluorophenyl)carbamoyl)piperazine-1-carboxylate (CFA113), **3.9**.

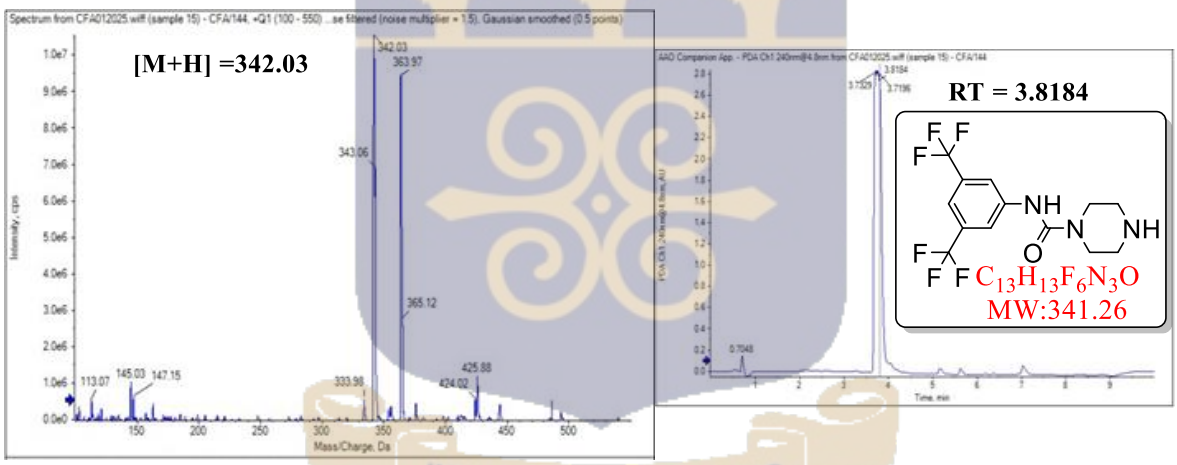


Appendix 2.2: **WAU-ESI** spectrum of 4-((3,5-dimethylphenyl)carbamoyl)piperazine-1-carboxylate (CFA108), **3.12**.

University of Ghana http://ugspace.ug.edu.gh

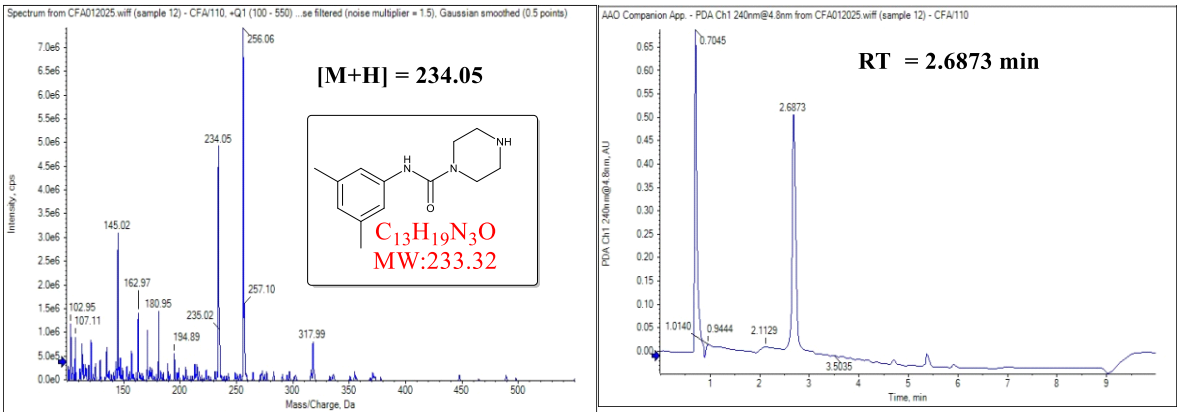


Appendix 2.3: **WAU-ESI** spectrum of *tert*-butyl 4-((3,5-dimethoxyphenyl)carbamoyl)piperazine-1-carboxylate (CFA087/166), **3.11**.



Appendix 2.4: **WAU-ESI** spectrum of *N*-(3,5-bis(trifluoromethyl)phenyl)piperazine-1-carboxamide (CFA144), **3.23**.

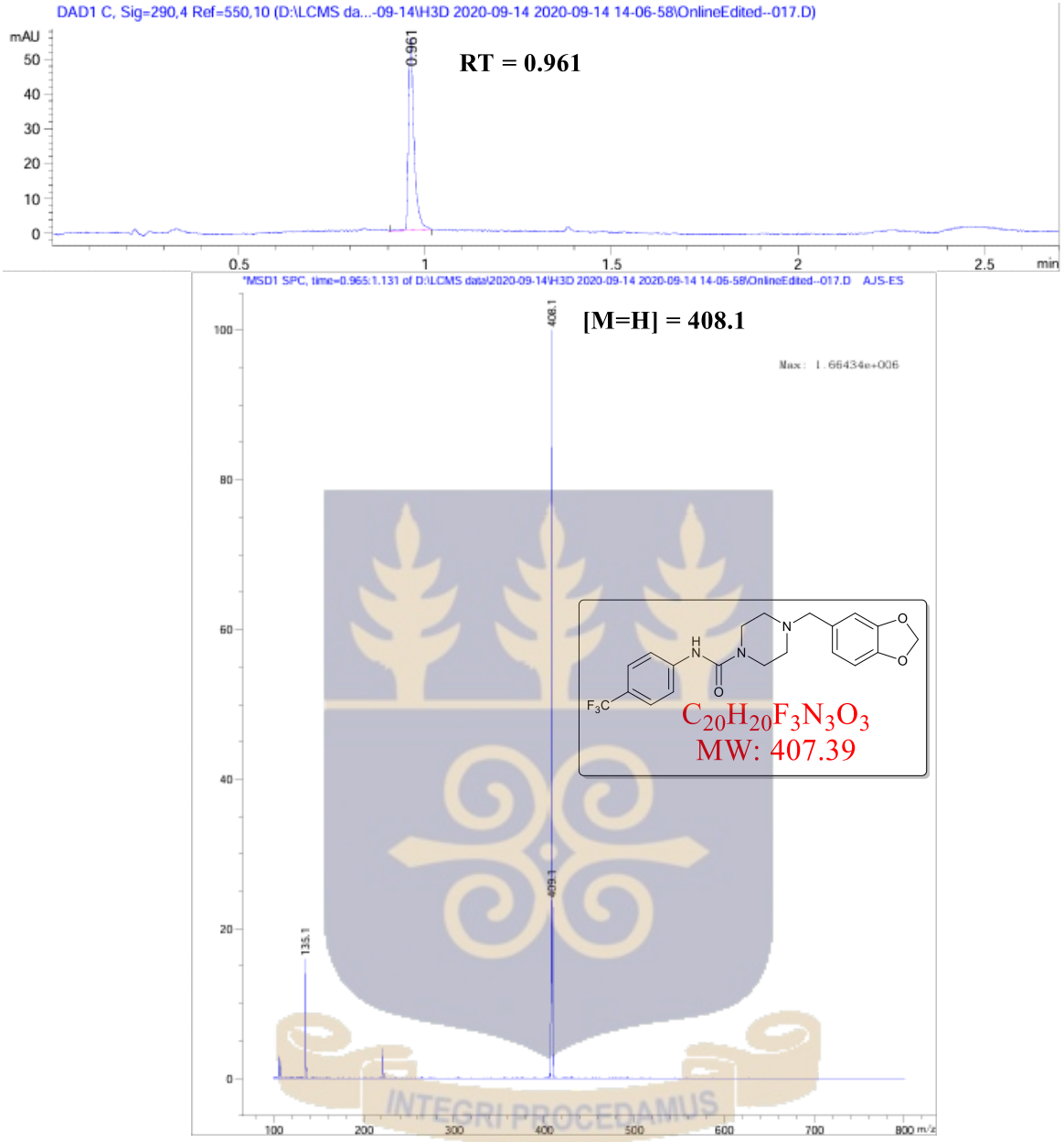
University of Ghana http://ugspace.ug.edu.gh



Appendix 2.5: **WAU-ESI** spectrum of *N*-(3,5-dimethylphenyl)piperazine-1-carboxamide (CFA98/110), **3.28**.

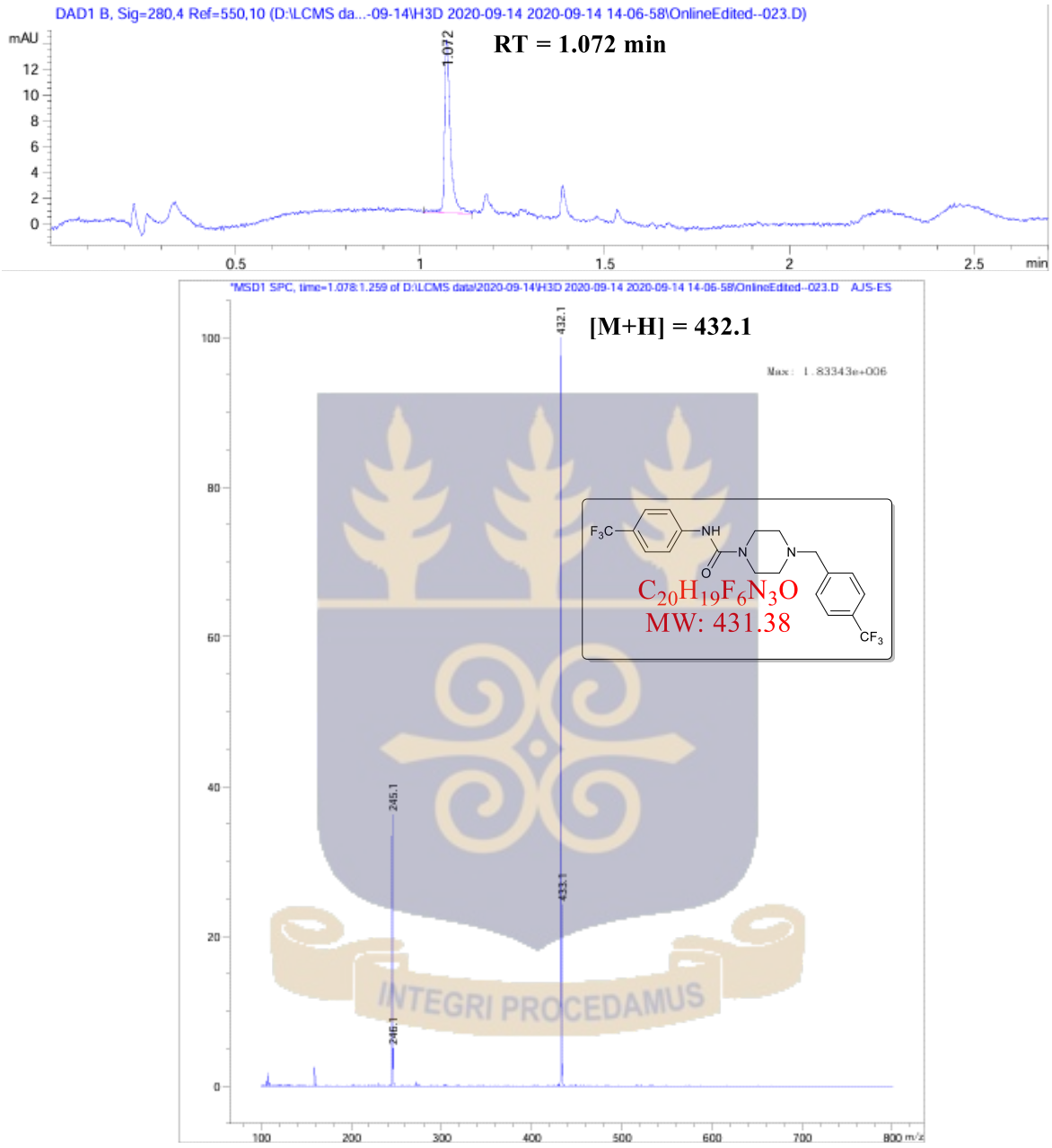
INTEGRI PROCEDAMUS

University of Ghana http://ugspace.ug.edu.gh



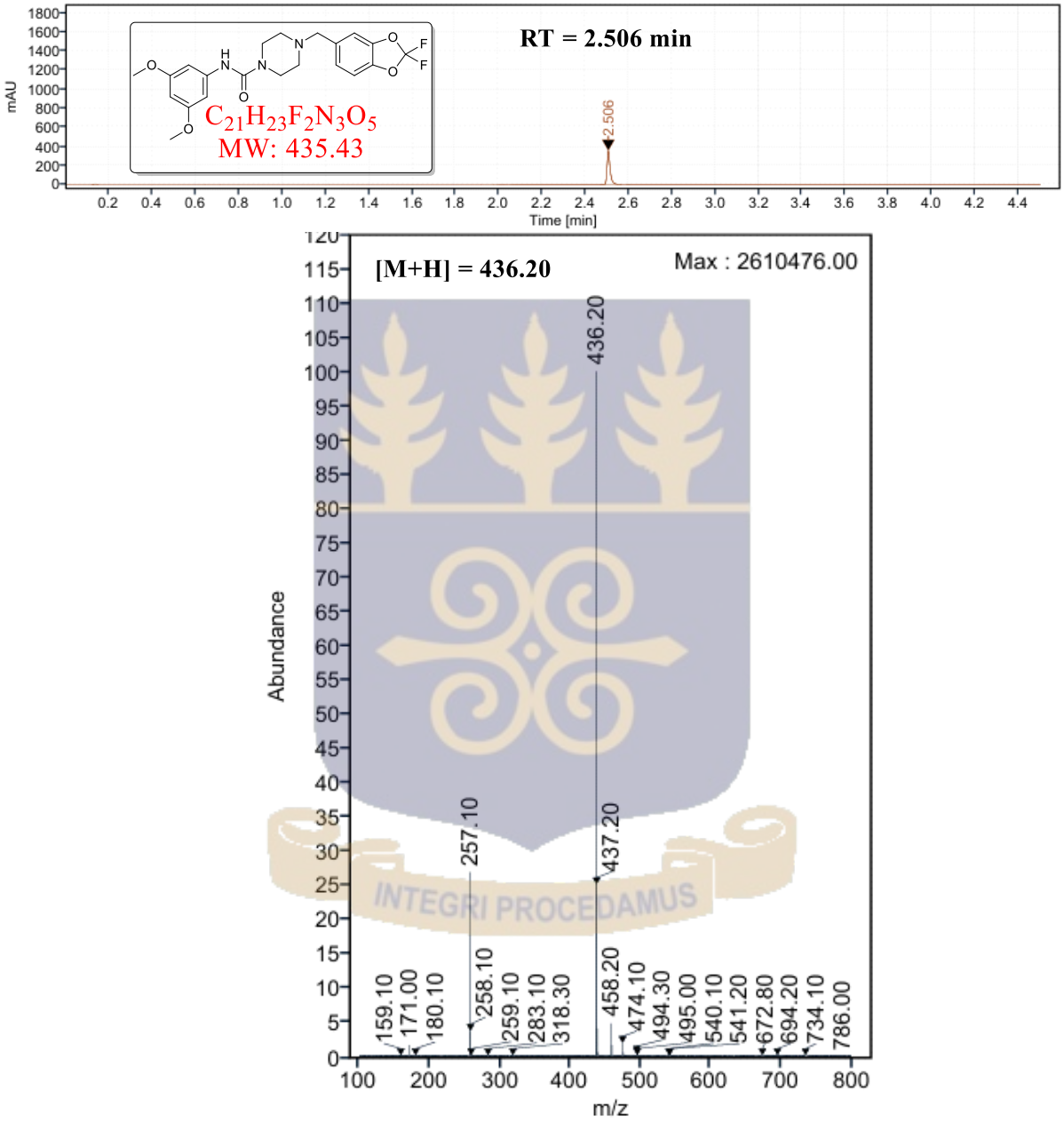
Appendix 2.6: **AJS-ESI** spectrum of 4-(benzo[*d*][1,3]dioxol-5-ylmethyl)-*N*-(4-(trifluoromethyl)phenyl)piperazine-1-carboxamide (CFA015), **3.36**.

University of Ghana http://ugspace.ug.edu.gh



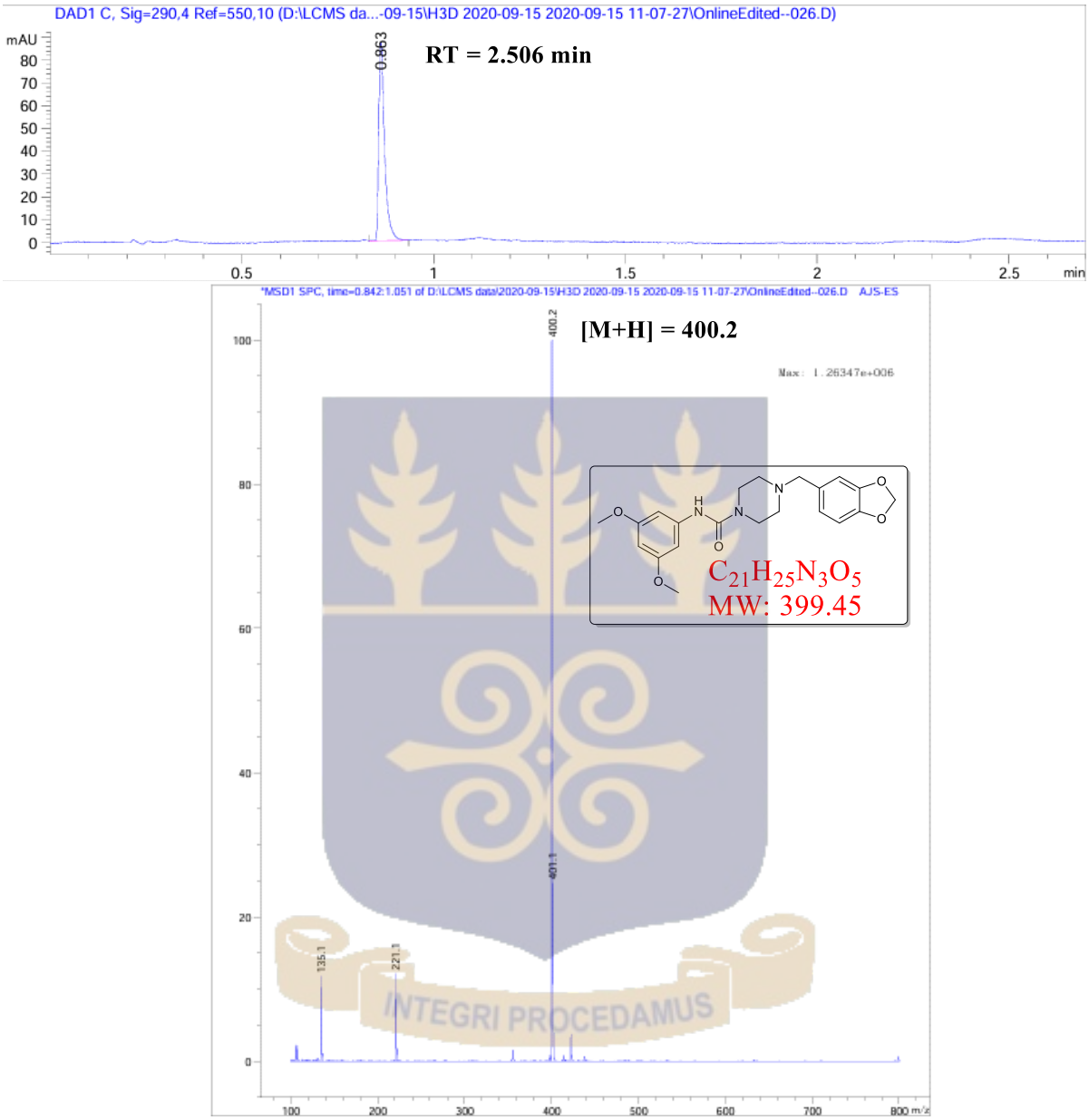
Appendix 2.7: **AJS-ESI** spectrum of 4-(4-(trifluoromethyl)benzyl)-*N*-(4-(trifluoromethyl)phenyl)piperazine-1-carboxamide (CFA017), **3.35**.

University of Ghana http://ugspace.ug.edu.gh



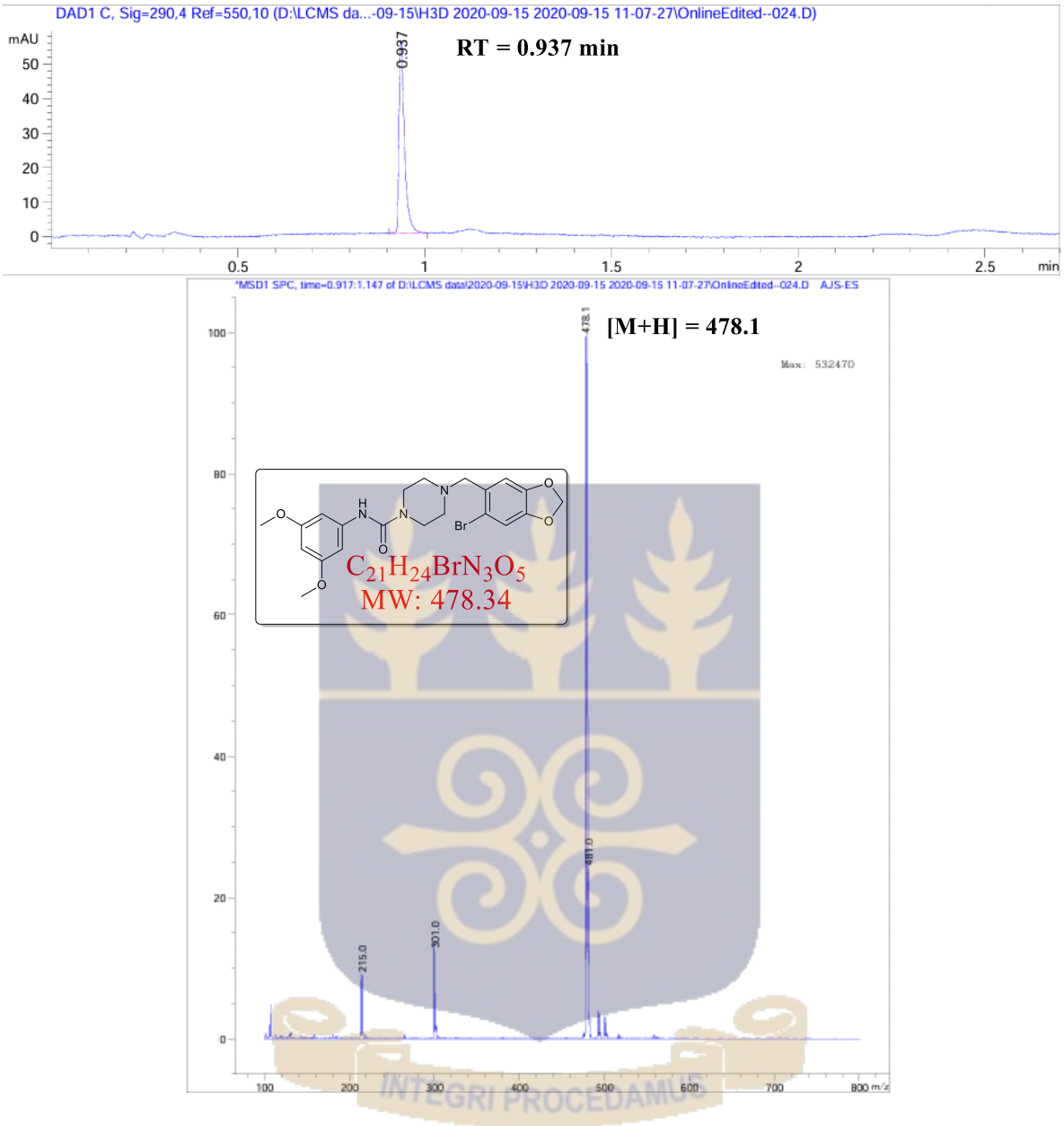
Appendix 2.8: **AJS-ESI** spectrum of *N*-(benzo[*d*][1,3]dioxol-5-yl)-4-((2,2-difluorobenzo[d][1,3]dioxol-5-yl)methyl)piperazine-1-carboxamide (CFA214), **3.39**.

University of Ghana http://ugspace.ug.edu.gh



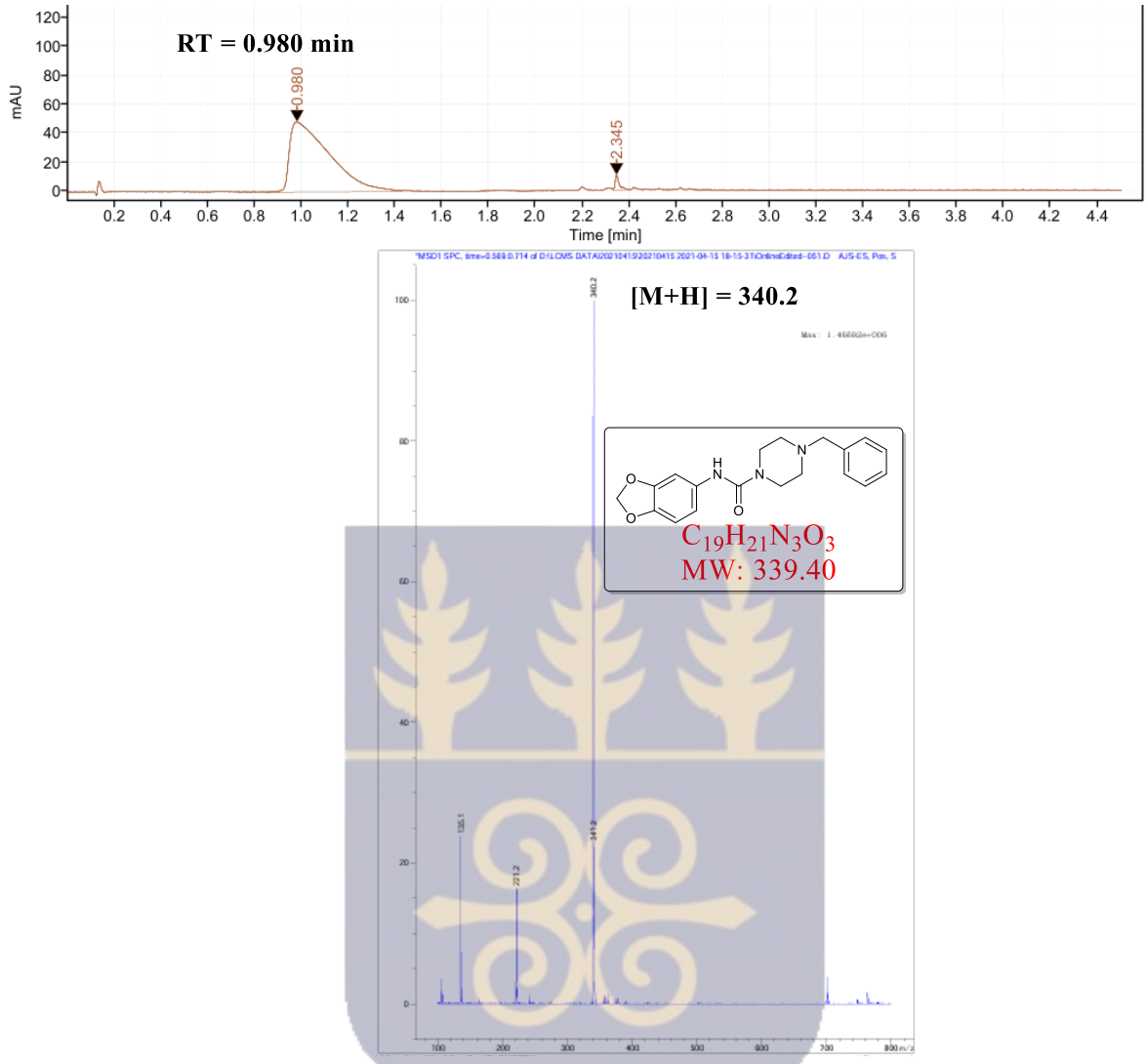
Appendix 2.9: **AJS-ESI** spectrum of 4-(benzo[*d*][1,3]dioxol-5-ylmethyl)-*N*-(3,5-dimethoxyphenyl)piperazine-1-carboxamide (CFA099), **3.40**.

University of Ghana http://ugspace.ug.edu.gh



Appendix 2.10: **AJS-ESI** spectrum of 4-((6-bromobenzo[*d*][1,3]dioxol-5-yl)methyl)-*N*-(3,5-dimethoxyphenyl)piperazine-1-carboxamide (CFA092), **3.41**.

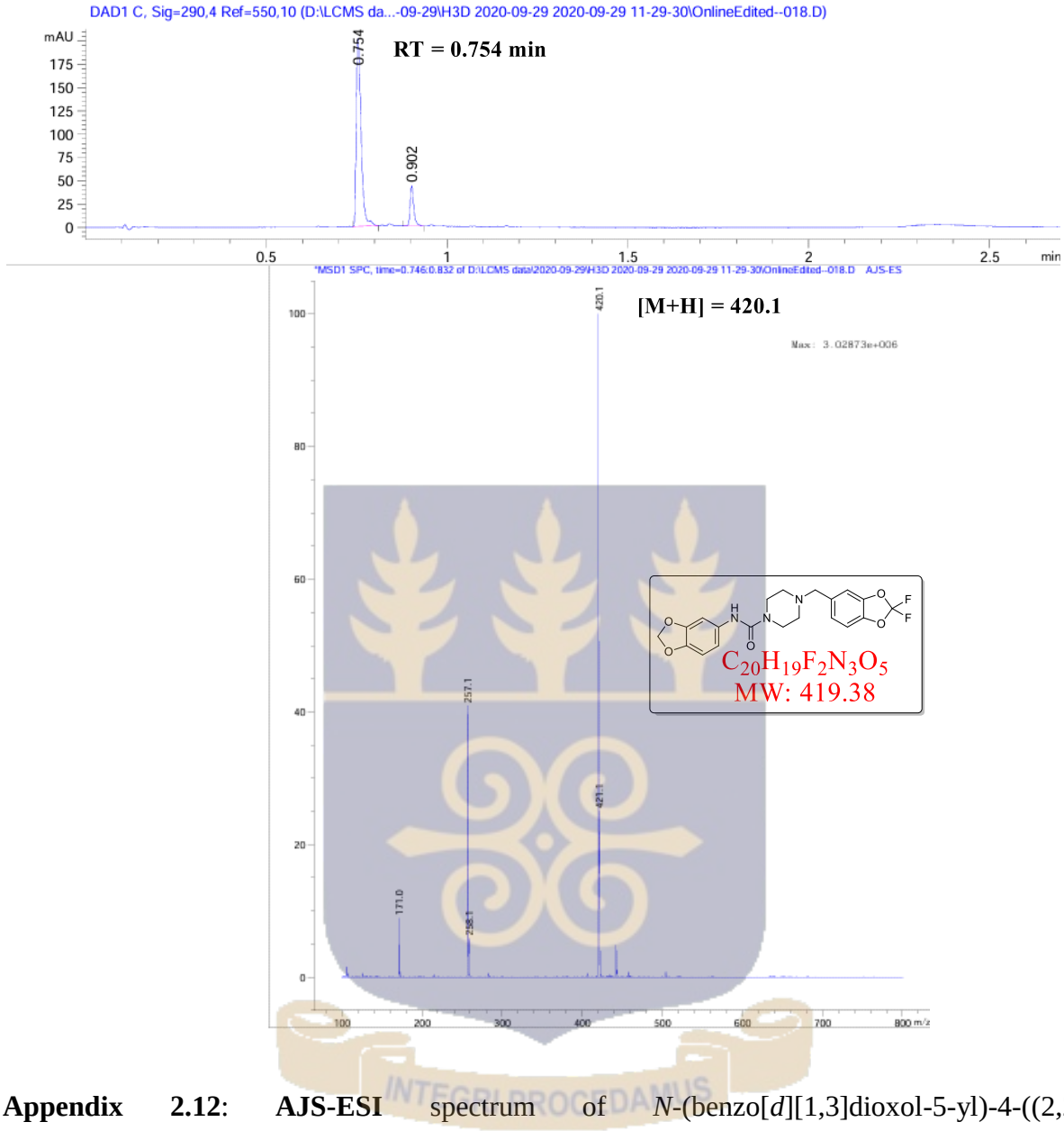
University of Ghana http://ugspace.ug.edu.gh



Appendix 2.11: AJS-ESI spectrum of *N*-(benzo[*d*][1,3]dioxol-5-yl)-4-benzylpiperazine-1-carboxamide (CFA222), **3.42**.

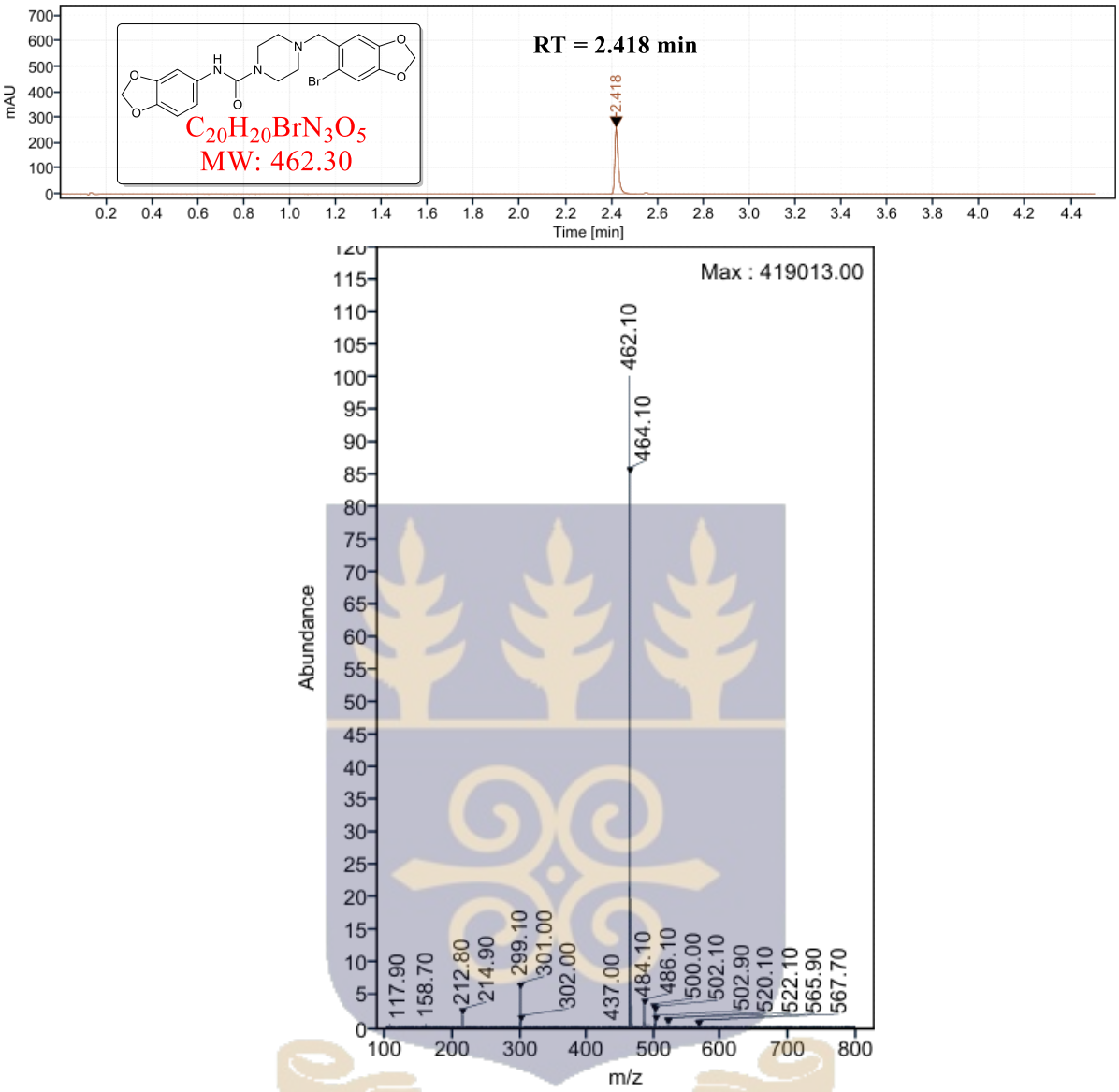
INTEGRI PROCEDAMUS

University of Ghana http://ugspace.ug.edu.gh



Appendix 2.12: **AJS-ESI** spectrum of *N*-(benzo[*d*][1,3]dioxol-5-yl)-4-((2,2-difluorobenzo[d][1,3]dioxol-5-yl)methyl)piperazine-1-carboxamide (CFA147), **3.43**.

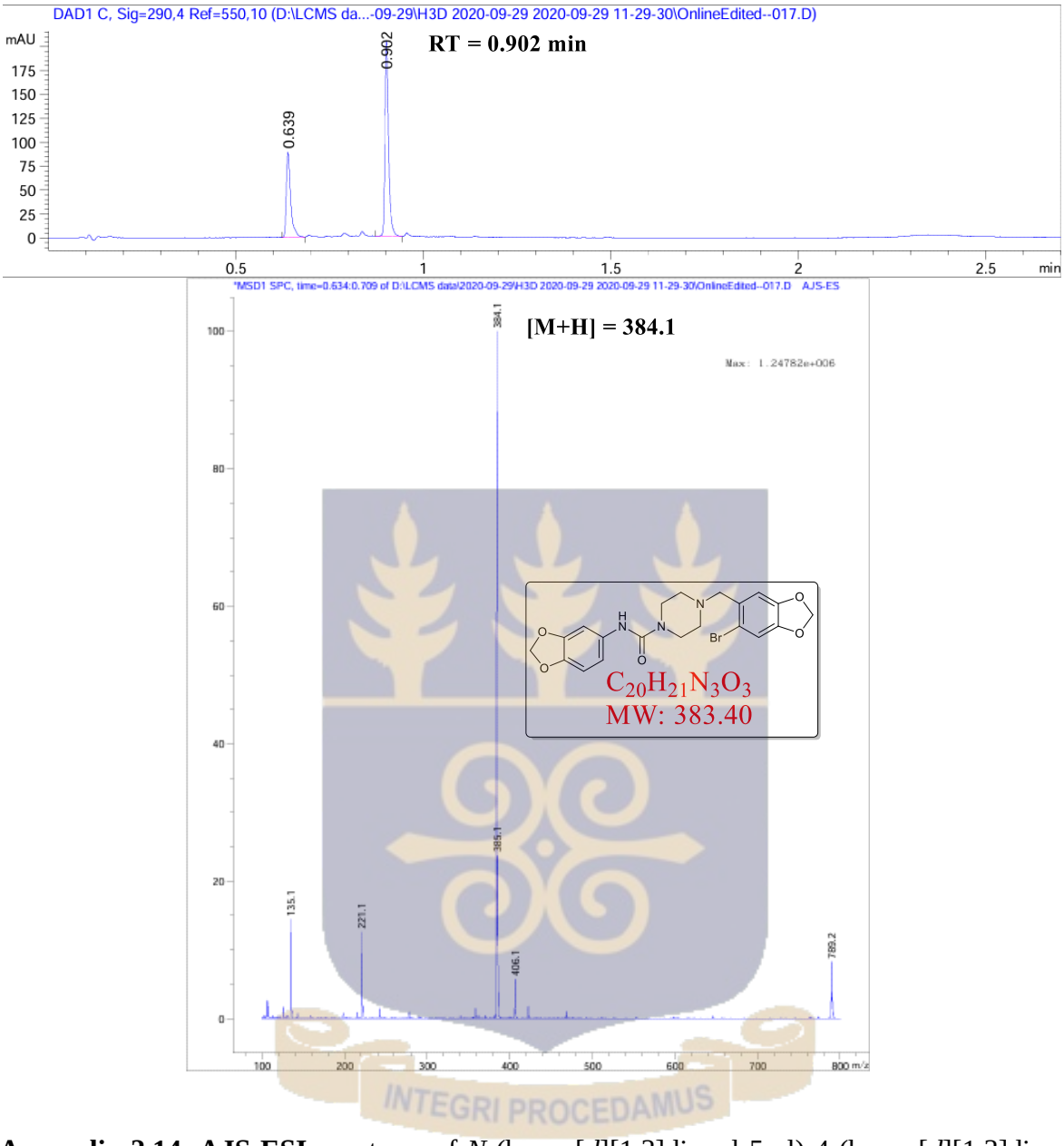
University of Ghana http://ugspace.ug.edu.gh



Appendix 2.13: **AJS-ESI** spectrum of *N*-(benzo[*d*][1,3]dioxol-5-yl)-4-((6-bromobenzo[d][1,3]dioxol-5-yl)methyl)piperazine-1-carboxamide (CFA189), **3.44**.

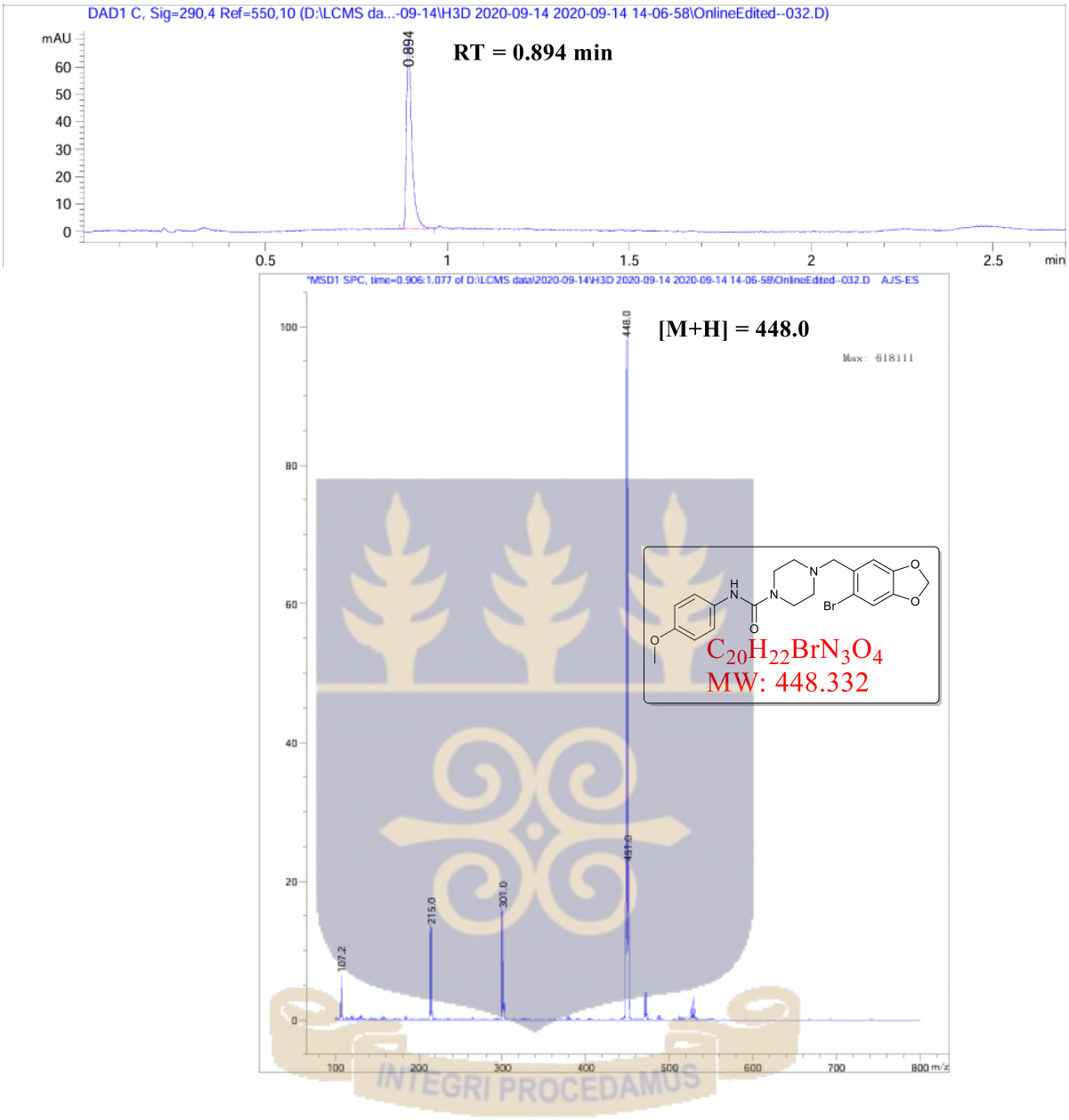
INTEGRI PROCEDAMUS

University of Ghana http://ugspace.ug.edu.gh



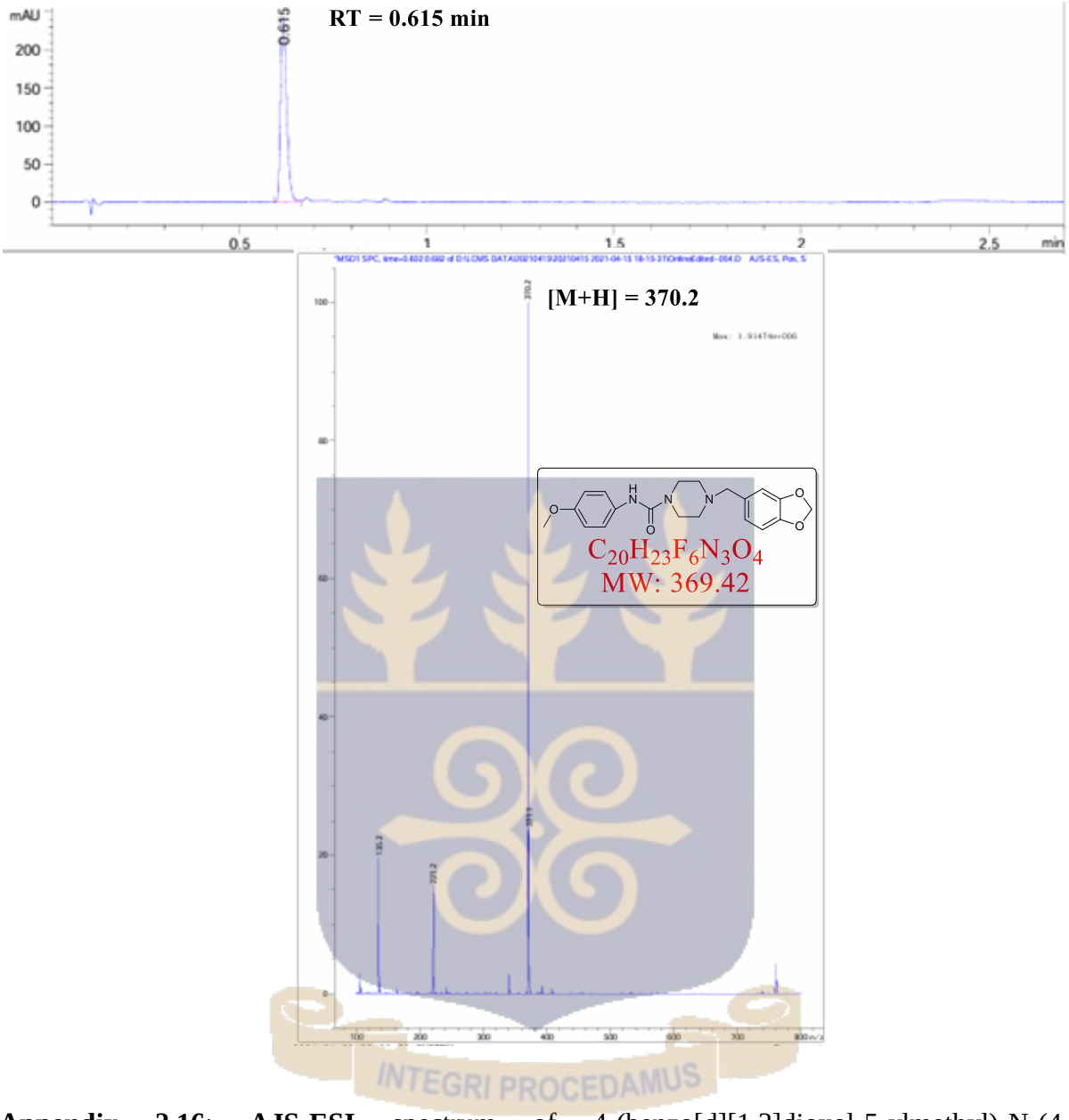
Appendix 2.14: **AJS-ESI** spectrum of *N*-(benzo[*d*][1,3]dioxol-5-yl)-4-(benzo[*d*][1,3]dioxol-5-ylmethyl)piperazine-1-carboxamide (CFA140), **3.45.**

University of Ghana http://ugspace.ug.edu.gh



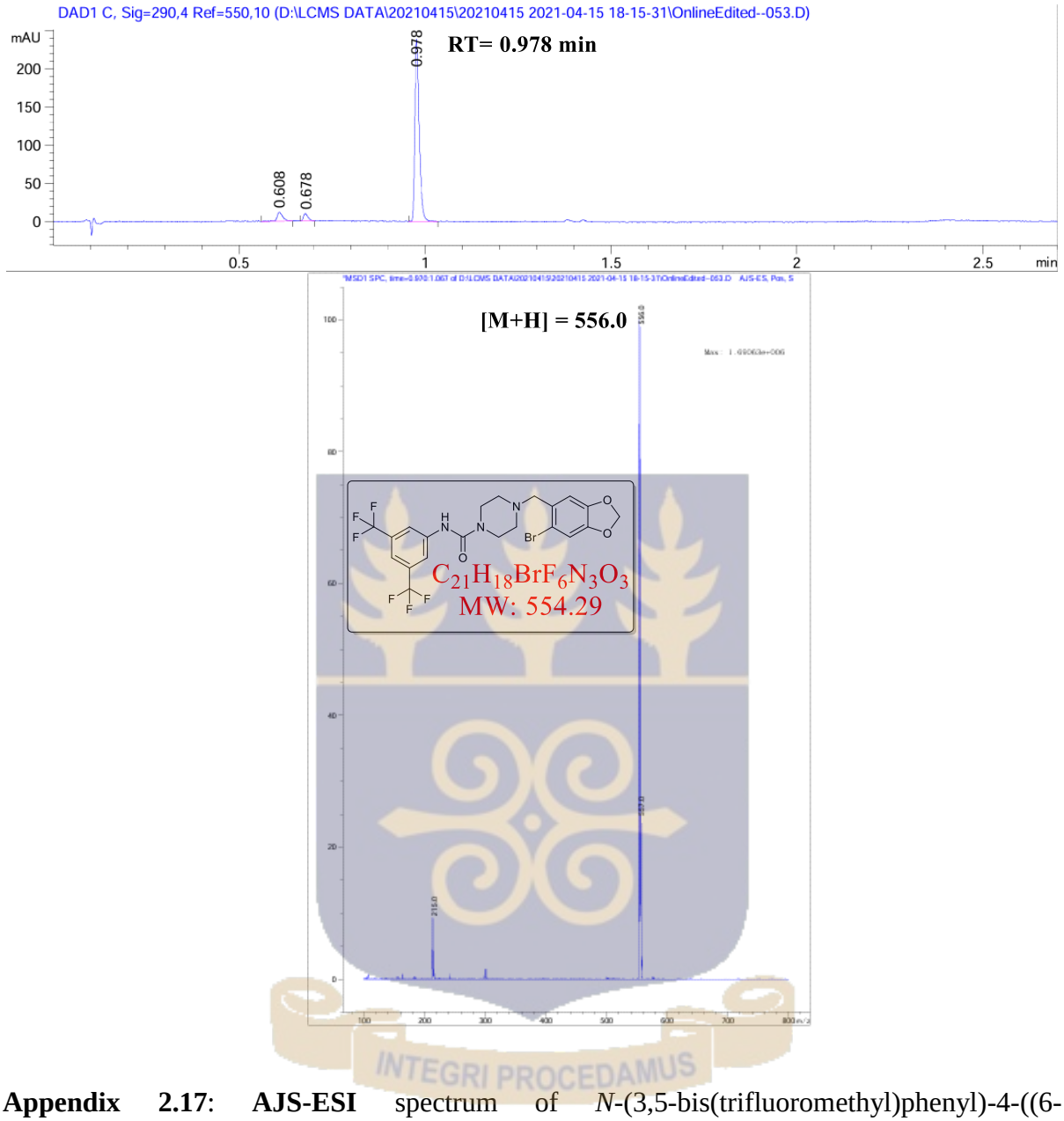
Appendix 2.15: **AJS-ESI** spectrum of 4-((6-bromobenzo[*d*][1,3]dioxol-5-yl)methyl)-*N*-(4-methoxyphenyl)piperazine-1-carboxamide (CFA026), **3.46**.

University of Ghana http://ugspace.ug.edu.gh



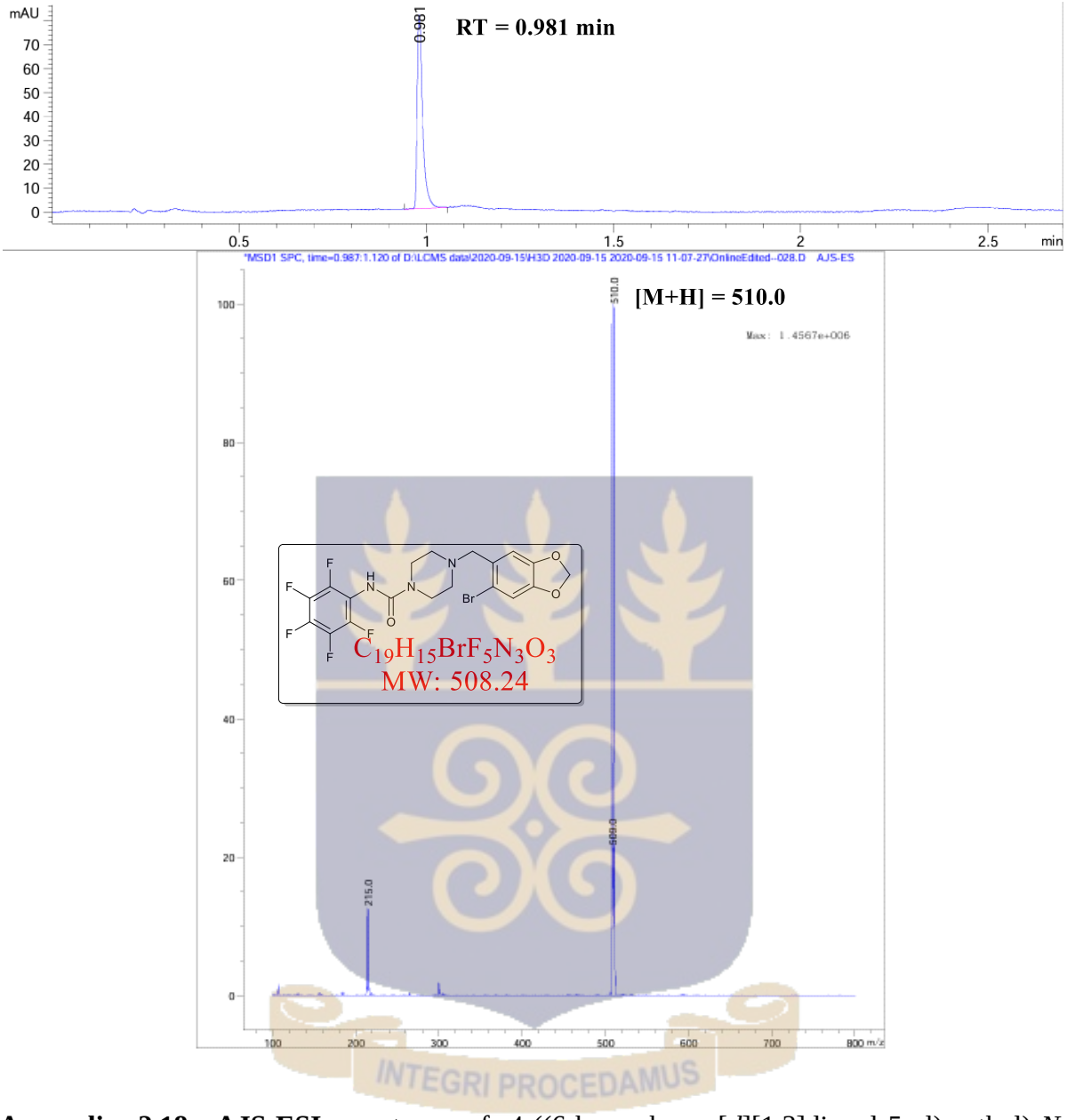
Appendix 2.16: **AJS-ESI** spectrum of 4-(benzo[d][1,3]dioxol-5-ylmethyl)-N-(4-methoxyphenyl)piperazine-1-carboxamide (CFA170), **3.47**.

University of Ghana http://ugspace.ug.edu.gh



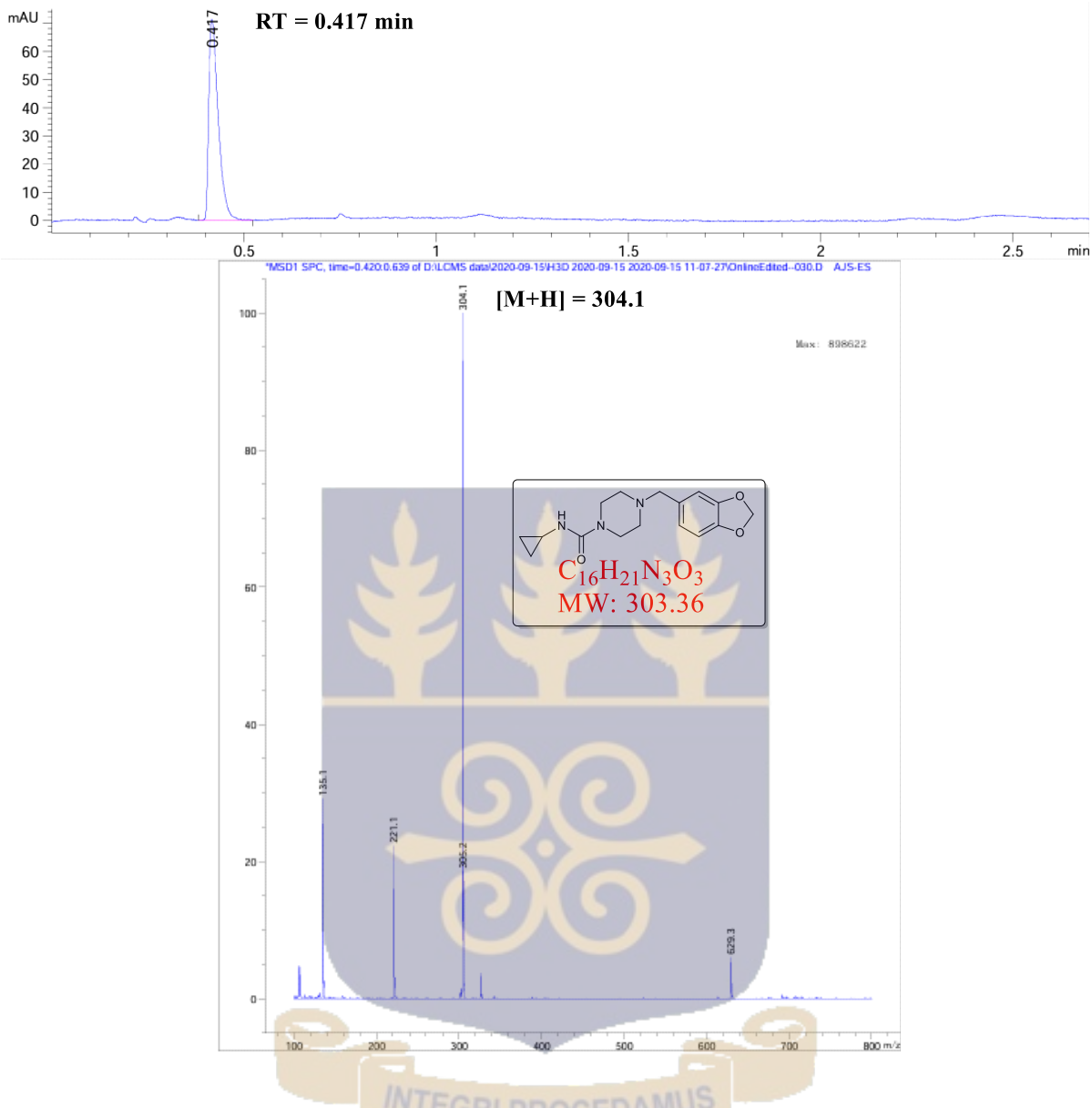
Appendix 2.17: **AJS-ESI** spectrum of *N*-(3,5-bis(trifluoromethyl)phenyl)-4-((6-bromobenzo[*d*][1,3]dioxol-5-yl)methyl)piperazine-1-carboxamide (CFA196), **3.48**.

University of Ghana http://ugspace.ug.edu.gh



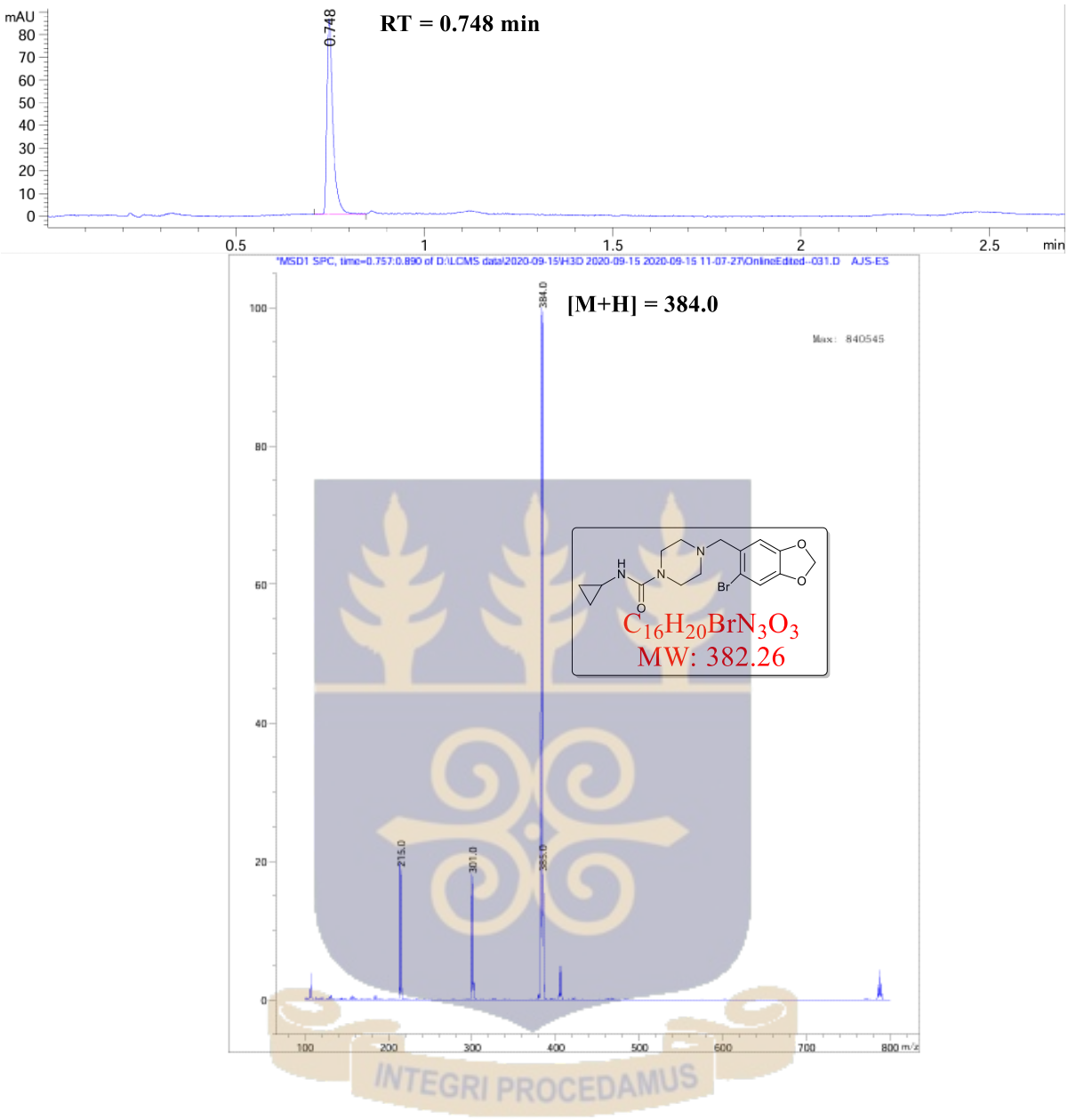
Appendix 2.18: **AJS-ESI** spectrum of 4-((6-bromobenzo[*d*][1,3]dioxol-5-yl)methyl)-*N*-(perfluorophenyl)piperazine-1-carboxamide (CFA117), **3.49**.

University of Ghana http://ugspace.ug.edu.gh



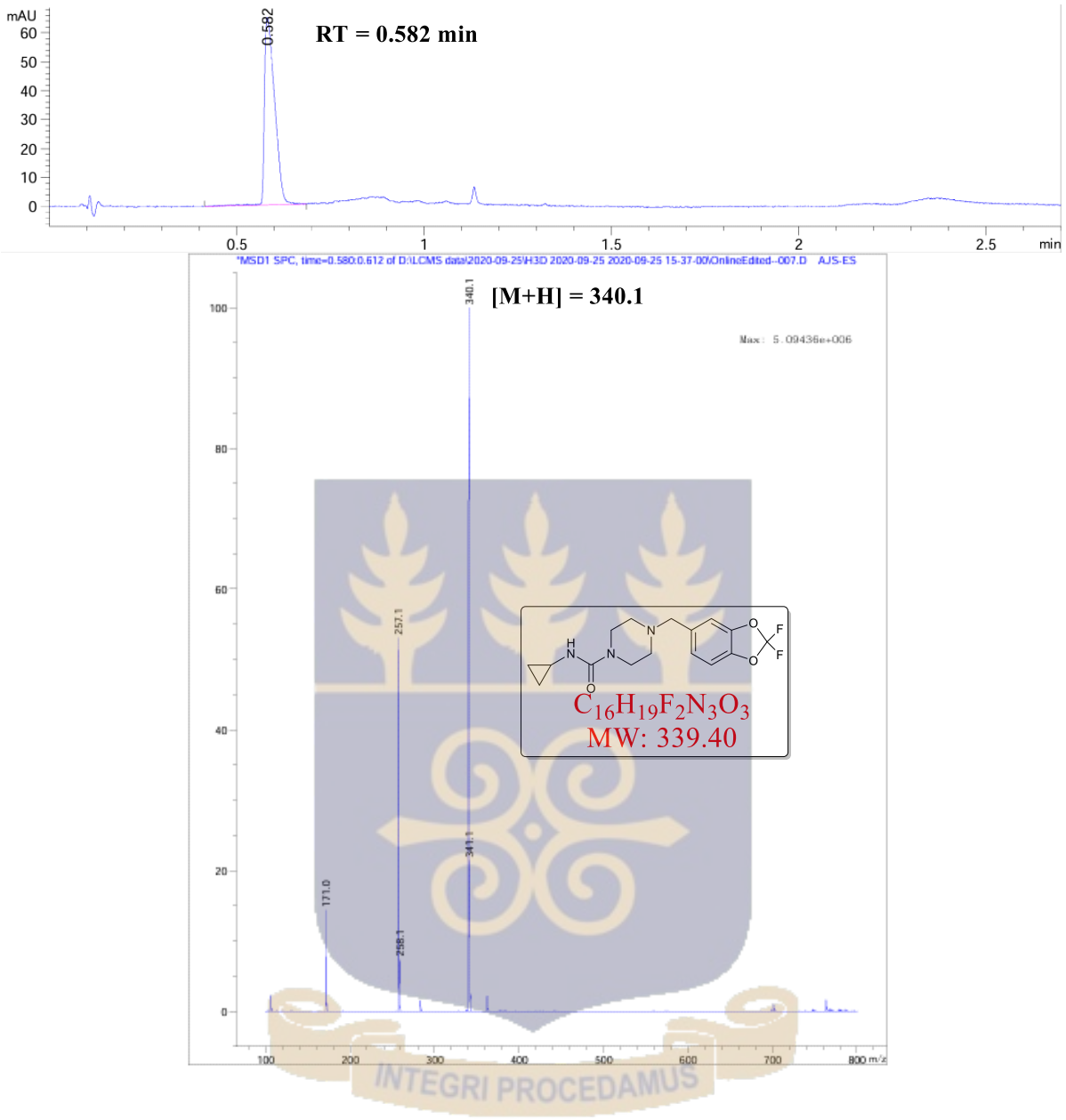
Appendix 2.19: **AJS-ESI** spectrum of 4-(benzo[*d*][1,3]dioxol-5-ylmethyl)-*N*-cyclopropylpiperazine-1-carboxamide (CFA119), **3.50**.

University of Ghana http://ugspace.ug.edu.gh



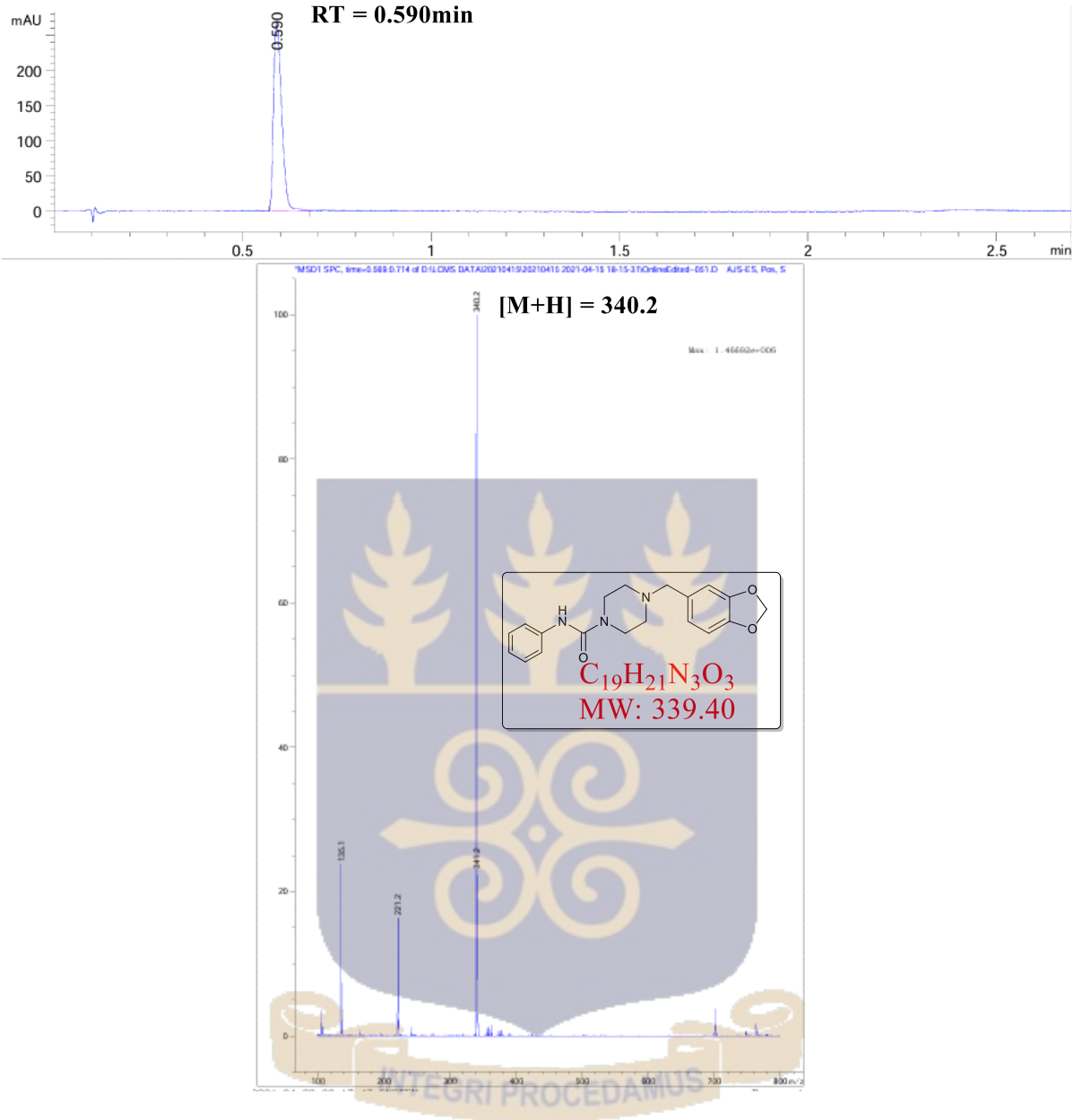
Appendix 2.20: **AJS-ESI** spectrum of 4-((6-bromobenzo[*d*][1,3]dioxol-5-yl)methyl)-*N*-cyclopropylpiperazine-1-carboxamide (CFA120), **3.51**.

University of Ghana http://ugspace.ug.edu.gh



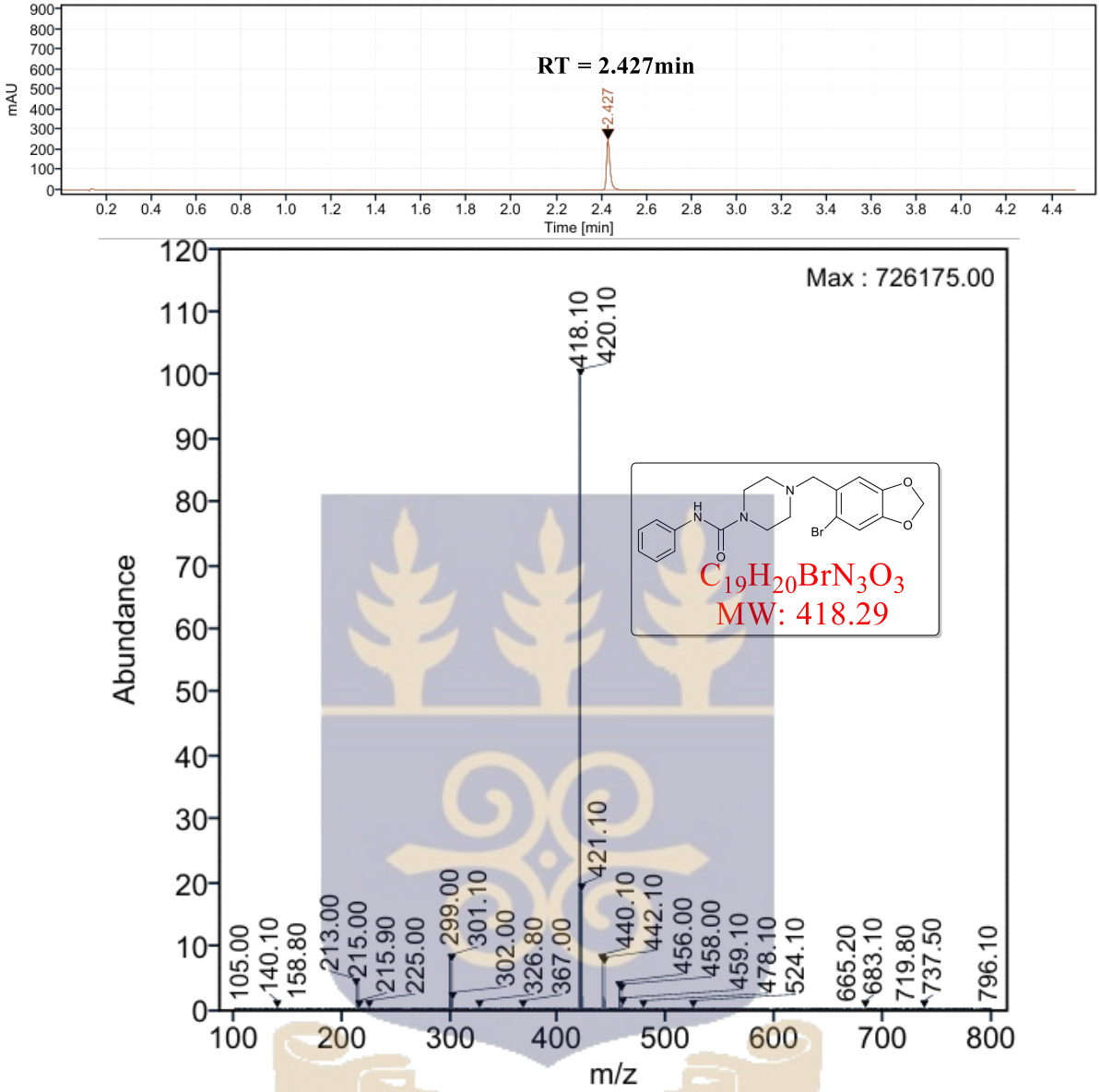
Appendix 2.21: **AJS-ESI** spectrum of N-cyclopropyl-4-((2,2-difluorobenzo[d][1,3]dioxol-5-yl)methyl)piperazine-1-carboxamide (CFA121), **3.51**.

University of Ghana http://ugspace.ug.edu.gh



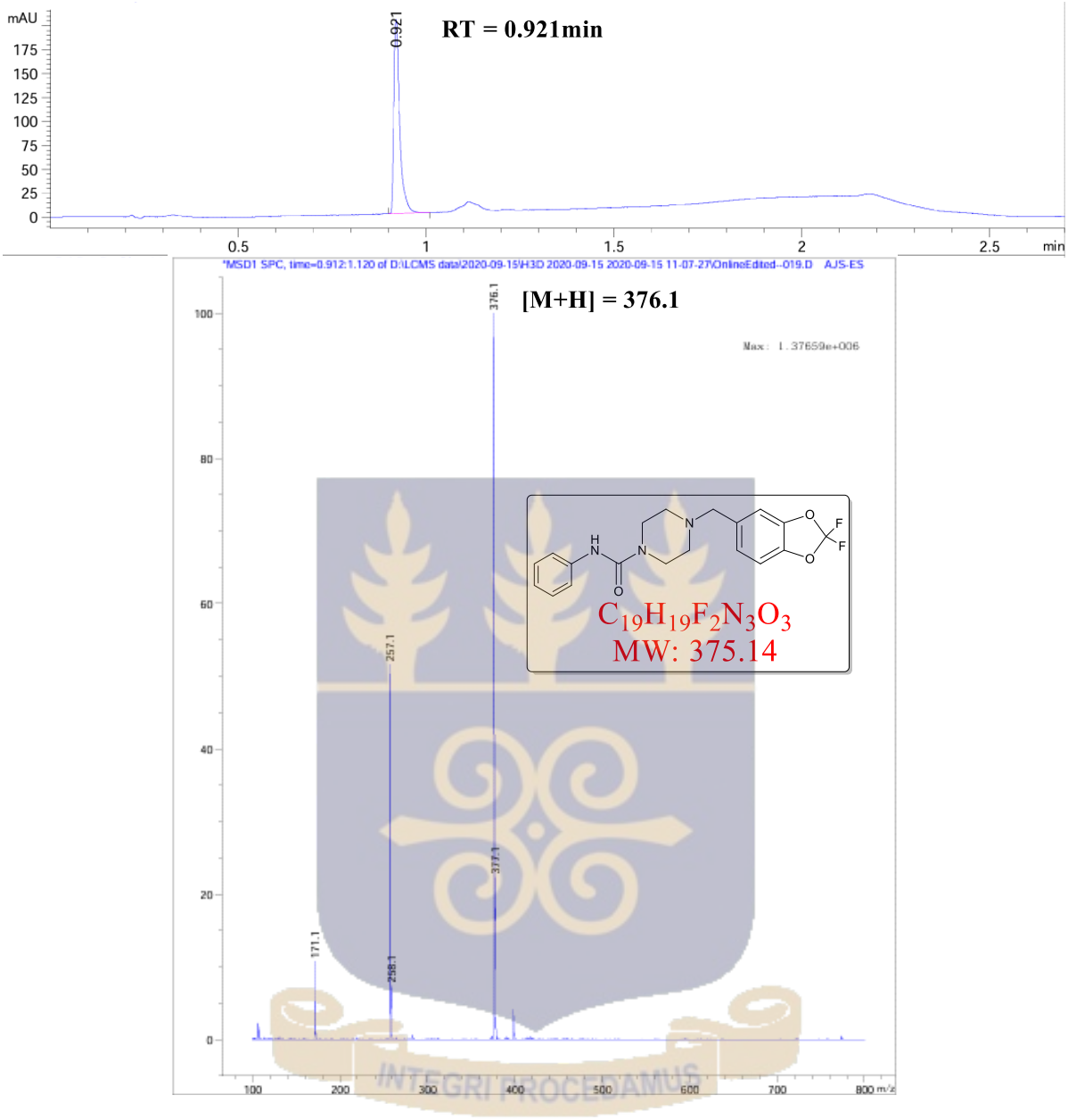
Appendix 2.22: AJS-ESI spectrum of 4-(benzo[*d*][1,3]dioxol-5-ylmethyl)-*N*-phenylpiperazine-1-carboxamide (CFA066/197), **3.52**.

University of Ghana http://ugspace.ug.edu.gh



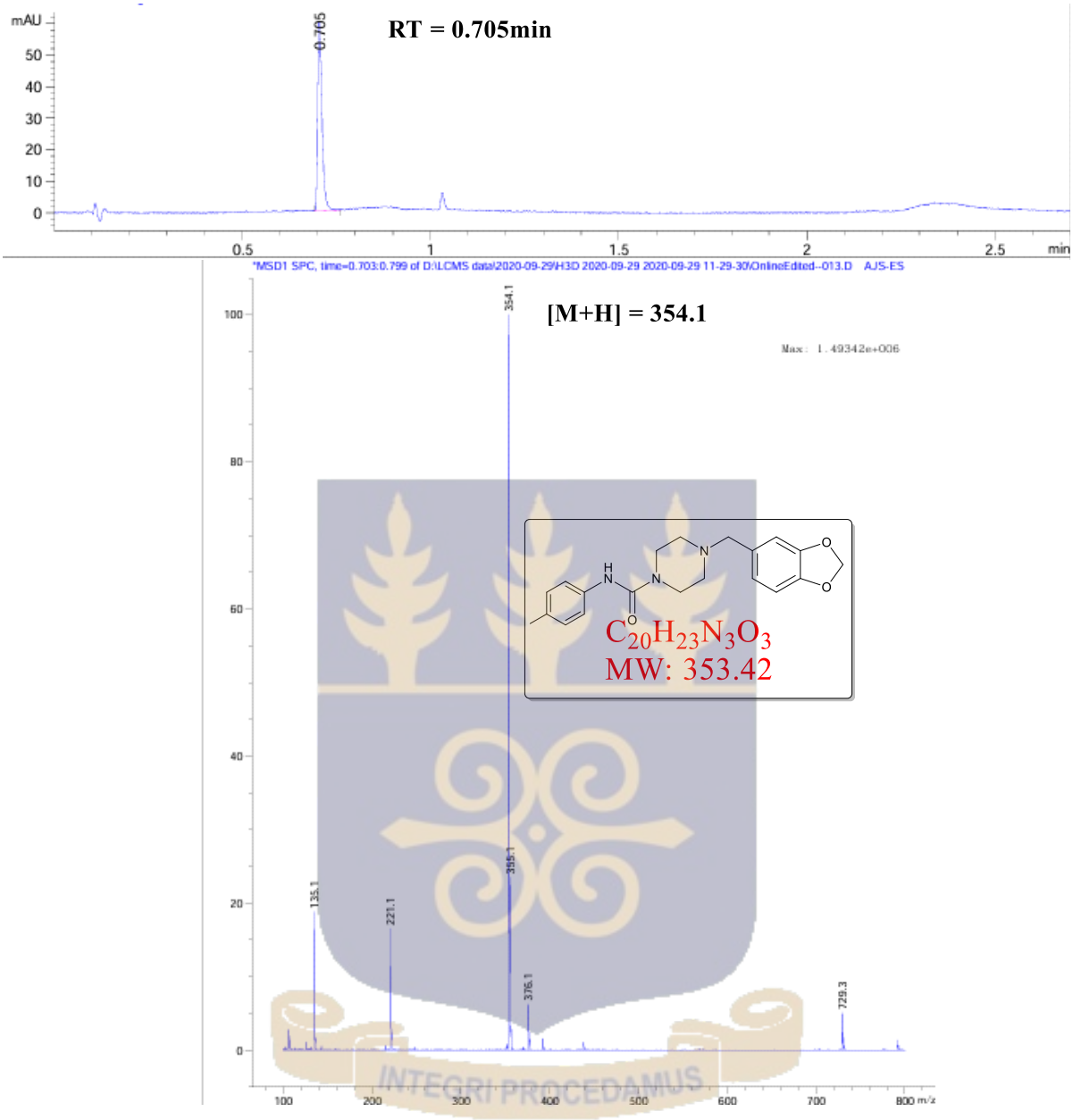
Appendix 2.23: **AJS-ESI** spectrum of 4-((6-bromobenzo[*d*][1,3]dioxol-5-yl)methyl)-*N*-phenylpiperazine-1-carboxamide (CFA067/200), **3.53**.

University of Ghana http://ugspace.ug.edu.gh



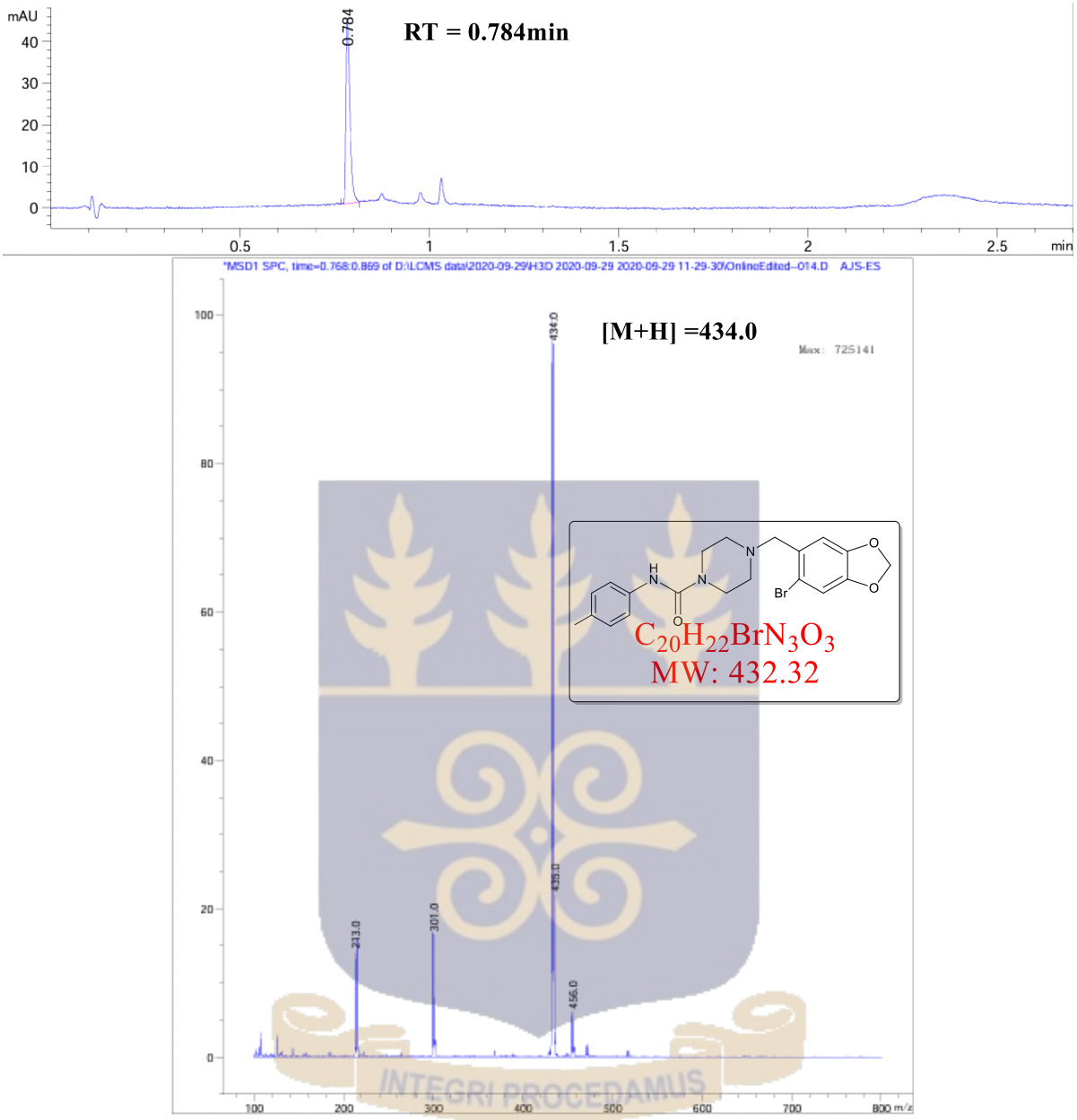
Appendix 2.24: **AJS-ESI** spectrum of 4-((2,2-difluorobenzo[*d*][1,3]dioxol-5-yl)methyl)-*N*-phenylpiperazine-1-carboxamide (CFA068/203), **3.54**.

University of Ghana http://ugspace.ug.edu.gh



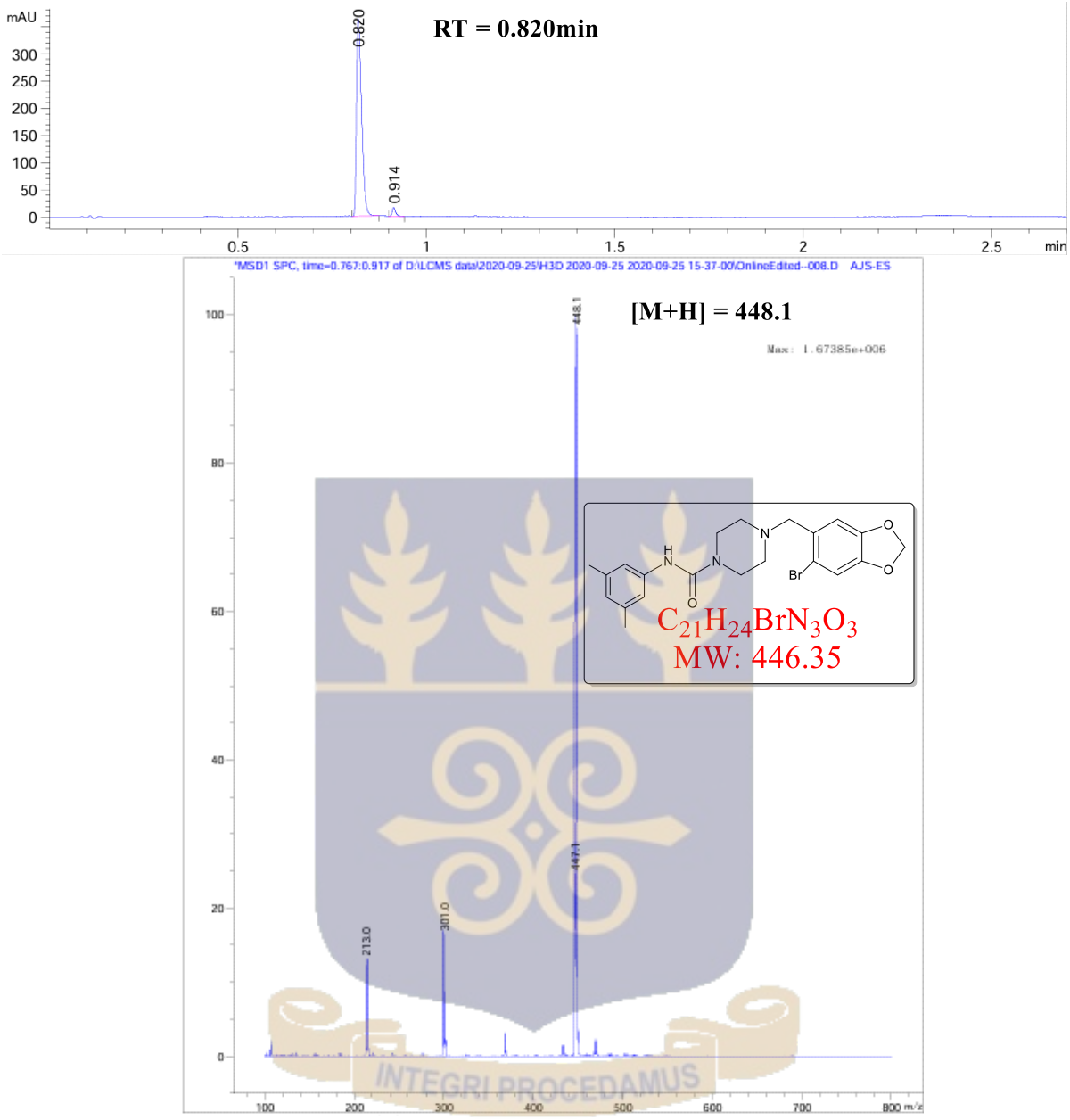
Appendix 2.25: **AJS-ESI** spectrum of 4-(benzo[*d*][1,3]dioxol-5-ylmethyl)-*N*-(p-tolyl)piperazine-1-carboxamide (CFA130), **3.55**.

University of Ghana http://ugspace.ug.edu.gh



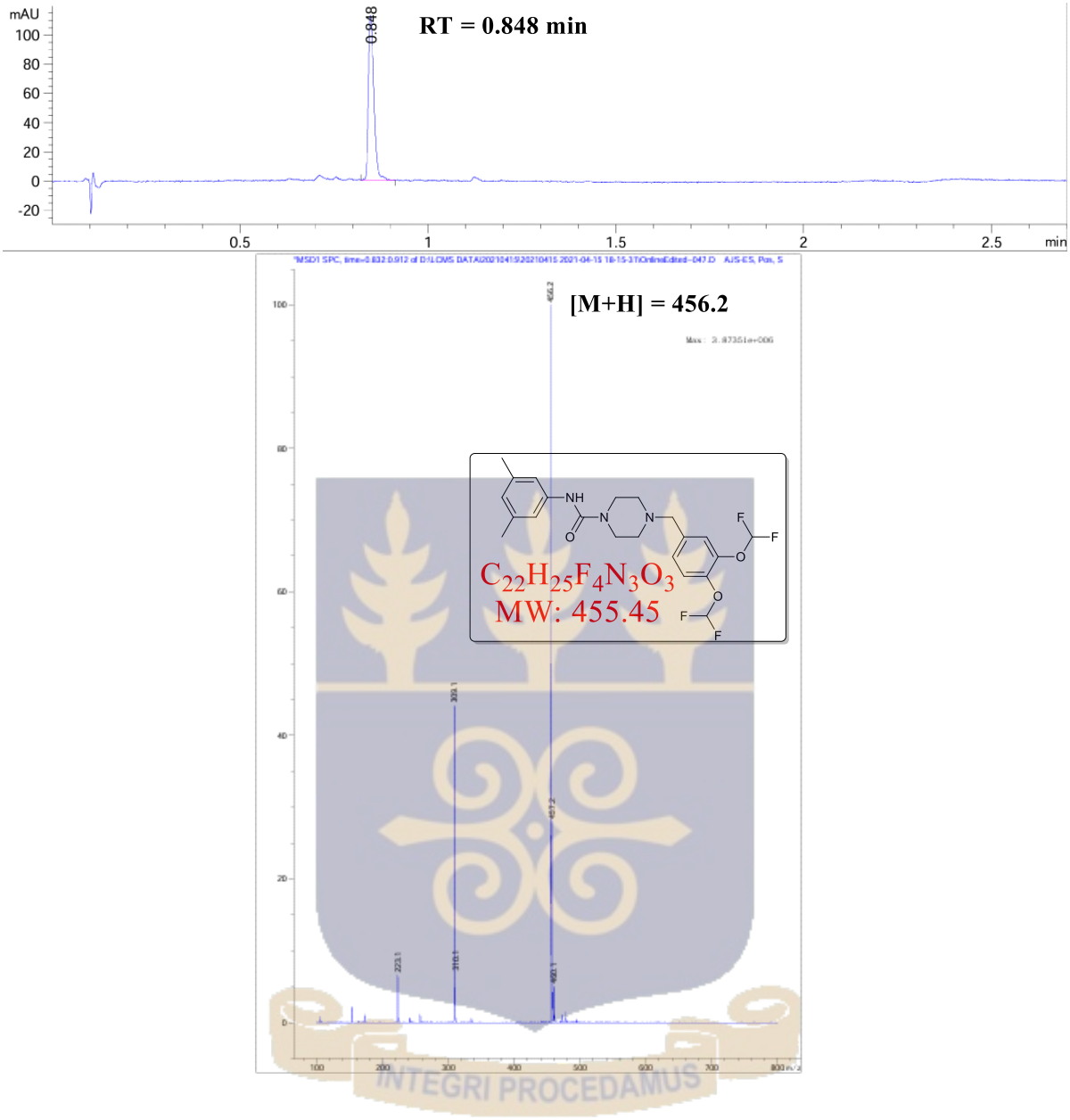
Appendix 2.26: **AJS-ESI** spectrum of 4-((6-bromobenzo[*d*][1,3]dioxol-5-yl)methyl)-*N*-(p-tolyl)piperazine-1-carboxamide (CFA131), **3.56**.

University of Ghana http://ugspace.ug.edu.gh



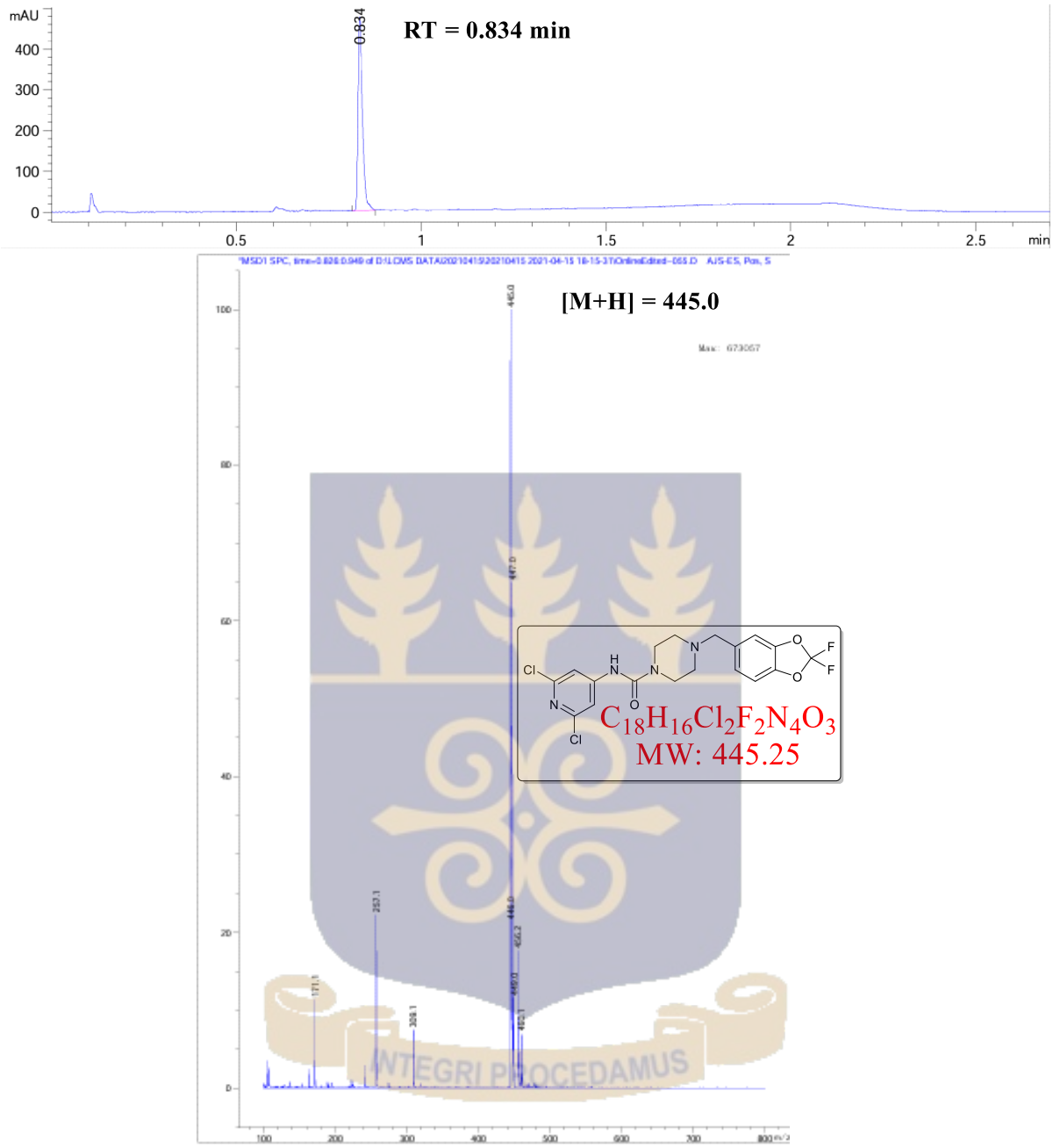
Appendix 2.27: **AJS-ESI** spectrum of 4-((6-bromobenzo[*d*][1,3]dioxol-5-yl)methyl)-*N*-(3,5-dimethylphenyl)piperazine-1-carboxamide (CFA134), **3.57**.

University of Ghana http://ugspace.ug.edu.gh



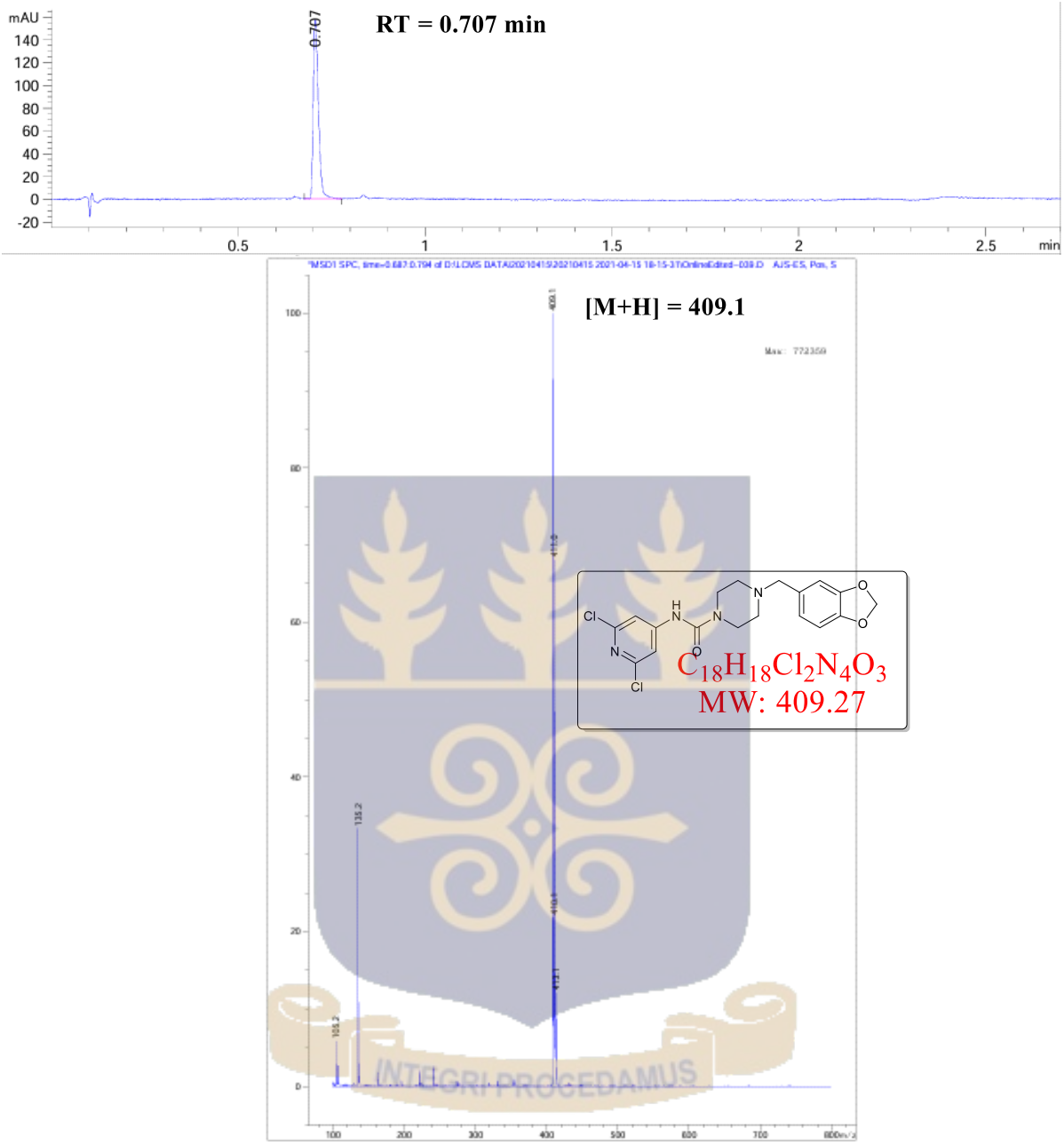
Appendix 2.28: **AJS-ESI** spectrum of 4-(3,4-bis(difluoromethoxy)benzyl)-N-(3,5-dimethylphenyl)piperazine-1-carboxamide (CFA187), **3.58**.

University of Ghana http://ugspace.ug.edu.gh



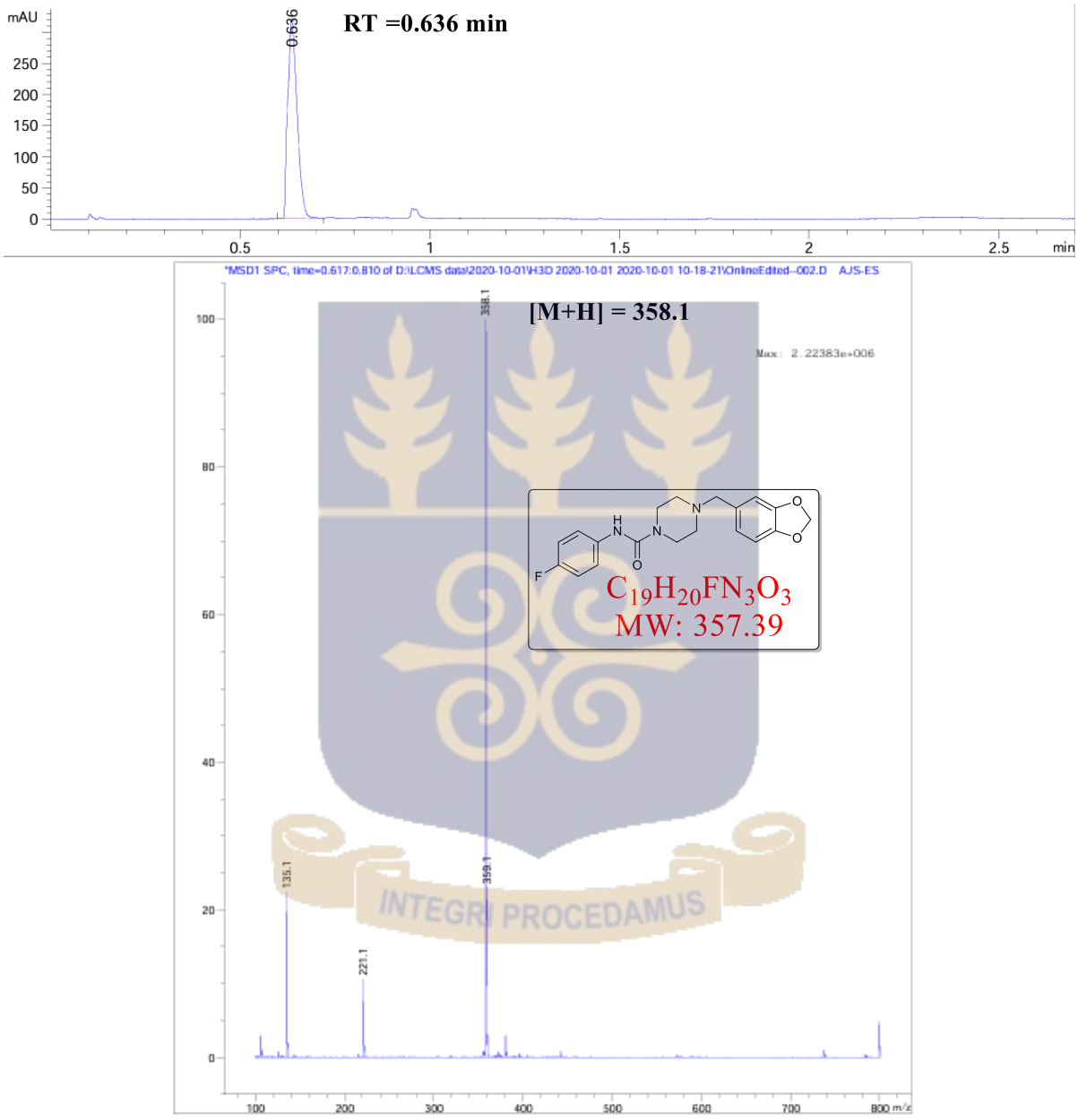
Appendix 2.29: **AJS-ESI** spectrum of *N*-(2,6-dichloropyridin-4-yl)-4-((2,2-difluorobenzo[*d*][1,3]dioxol-5-yl)methyl)piperazine-1-carboxamide (CFA160), **3.59**.

University of Ghana http://ugspace.ug.edu.gh



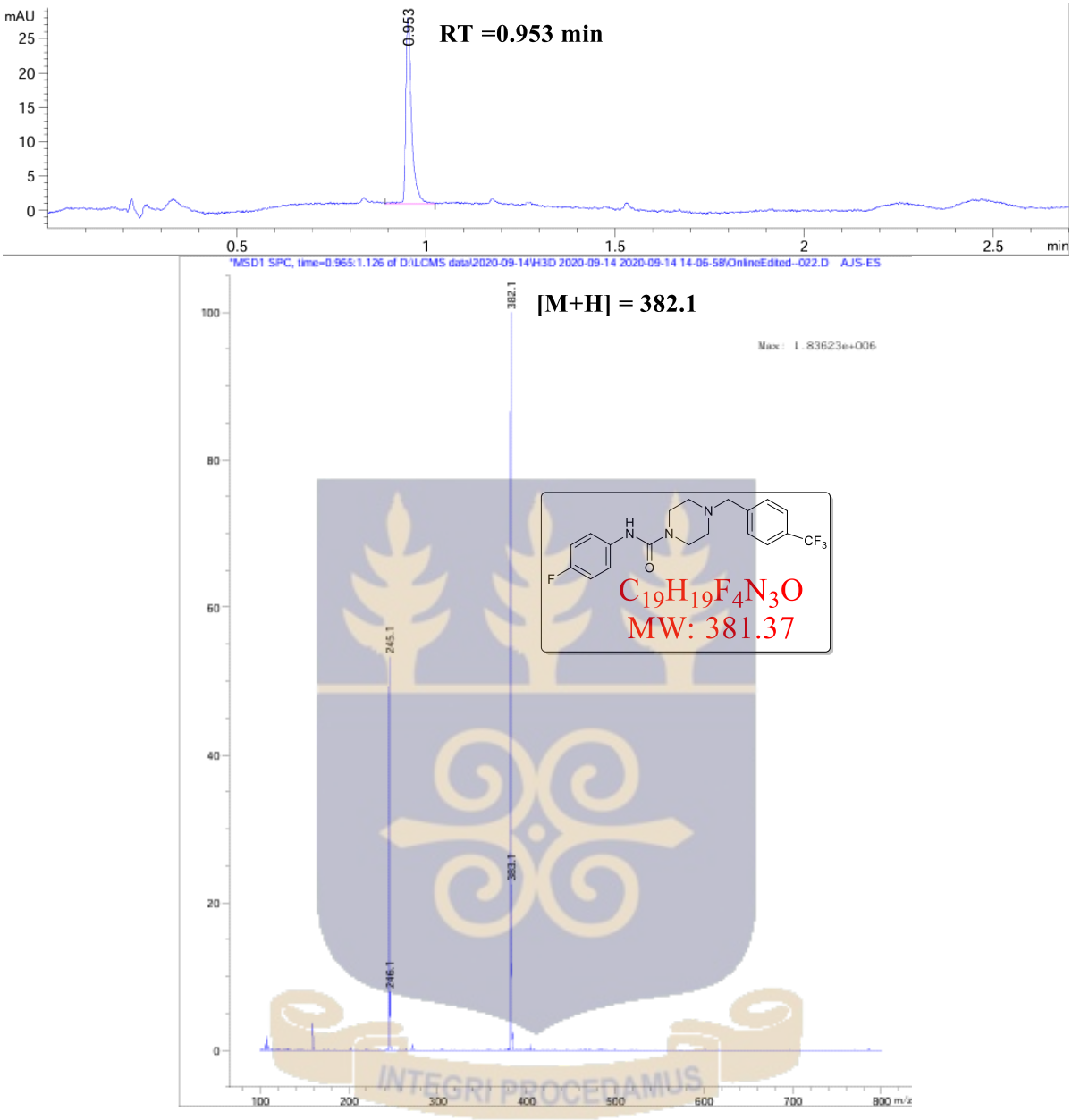
Appendix 2.30: **AJS-ESI** spectrum of 4-(benzo[*d*][1,3]dioxol-5-ylmethyl)-*N*-(2,6-dichloropyridin-4-yl)piperazine-1-carboxamid**e** (CFA161), **3.60**.

University of Ghana http://ugspace.ug.edu.gh



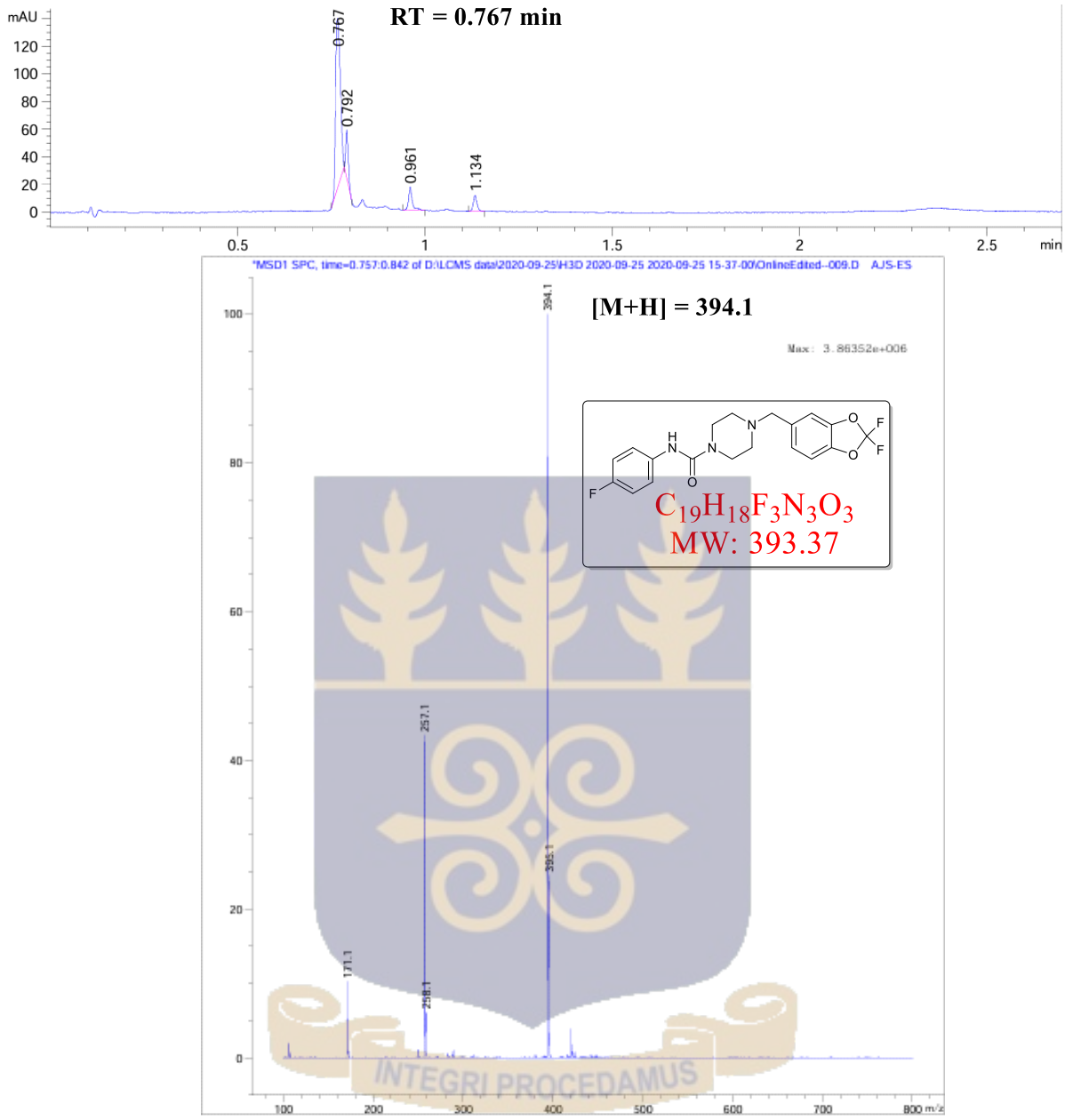
Appendix 2.31: **AJS-ESI** spectrum of 4-(benzo[*d*][1,3]dioxol-5-ylmethyl)-*N*-(4-fluorophenyl)piperazine-1-carboxamide (CFA014), **3.61.**

University of Ghana http://ugspace.ug.edu.gh



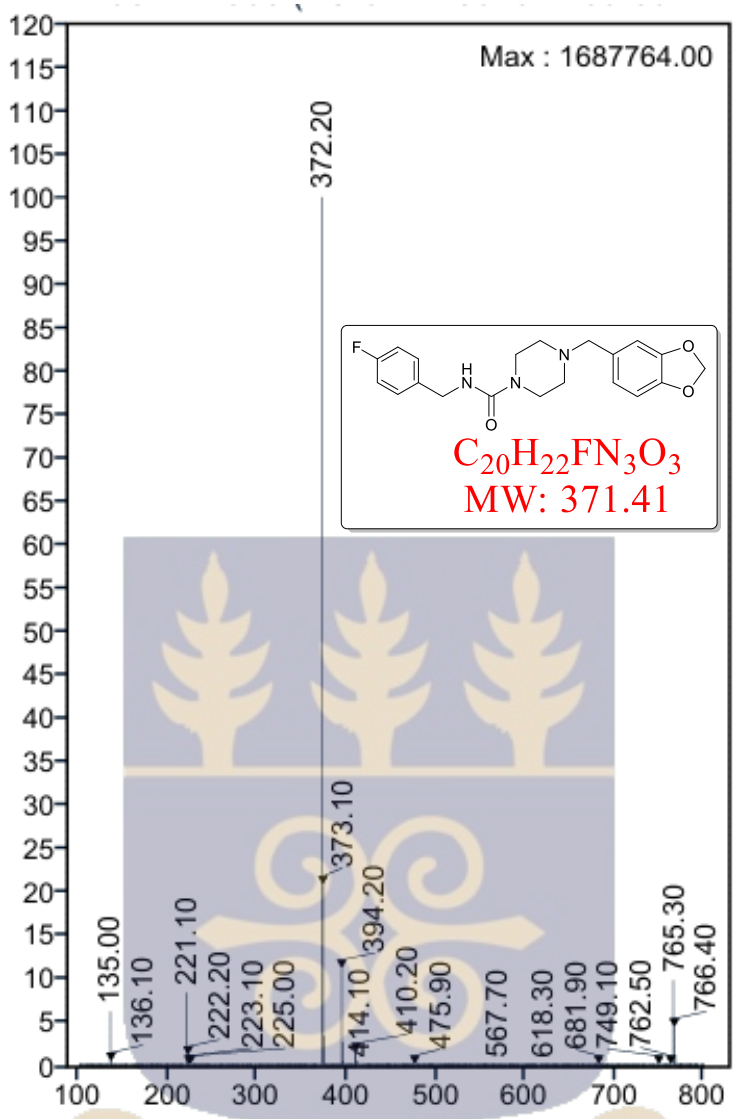
Appendix 2.32: **AJS-ESI** spectrum of *N*-(4-fluorophenyl)-4-(4-(trifluoromethyl)benzyl)piperazine-1-carboxamide (CFA016), **3.62**.

University of Ghana http://ugspace.ug.edu.gh



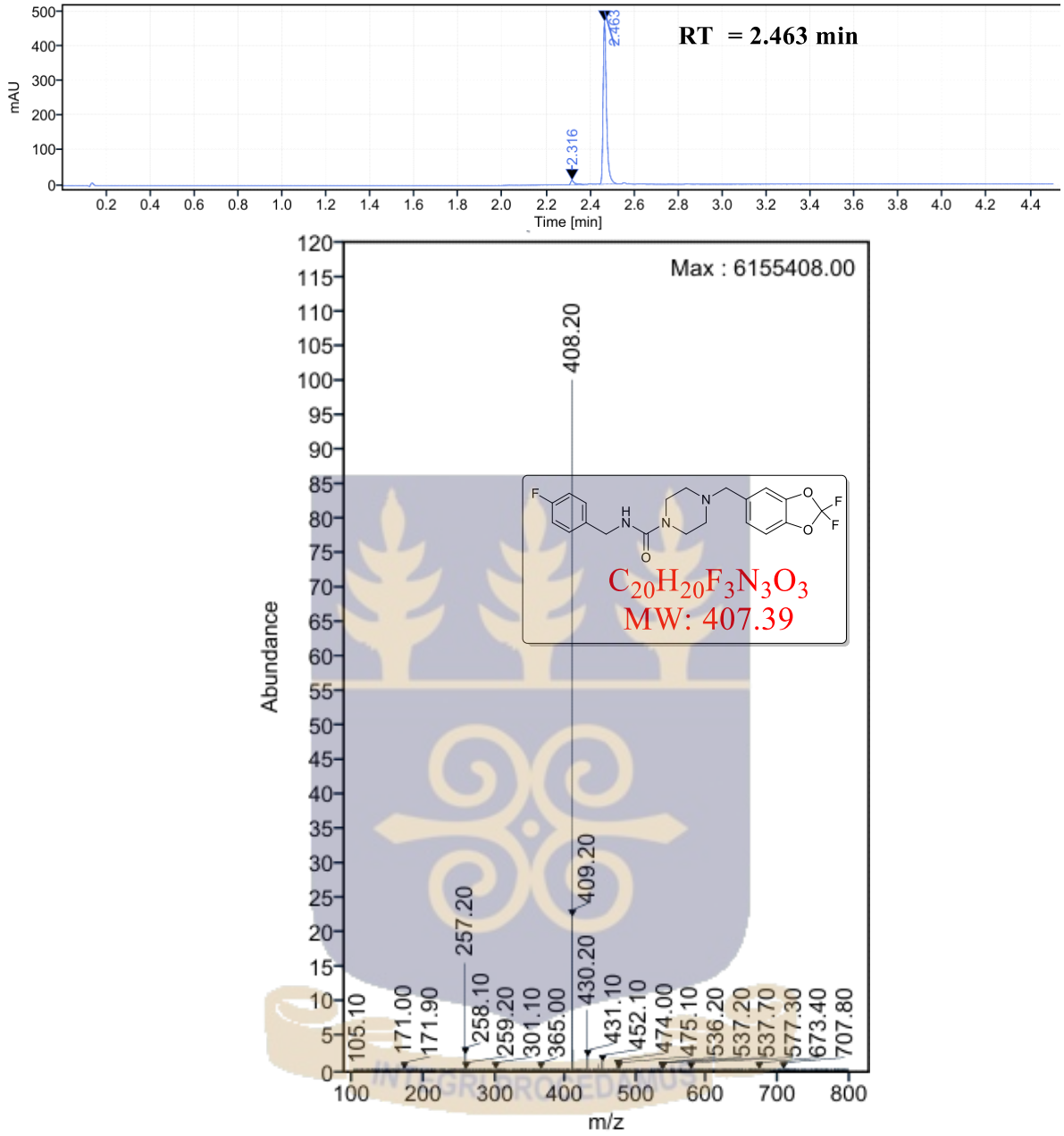
Appendix 2.33: **AJS-ESI** spectrum of 4-((2,2-difluorobenzo[*d*][1,3]dioxol-5-yl)methyl)-*N*-(4-fluorophenyl)piperazine-1-carboxamide (CFA146), **3.63**.

University of Ghana http://ugspace.ug.edu.gh



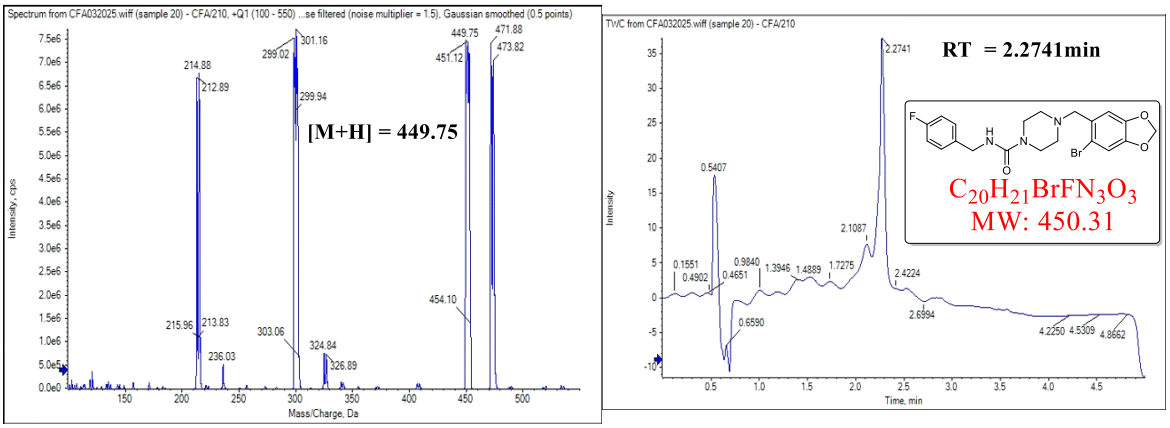
Appendix 2.34: AJS-ESI spectrum of 4-(benzo[d][1,3]dioxol-5-ylmethyl)-N-(4-fluorobenzyl)piperazine-1-carboxamide (CFA209), **3.64**.

University of Ghana http://ugspace.ug.edu.gh

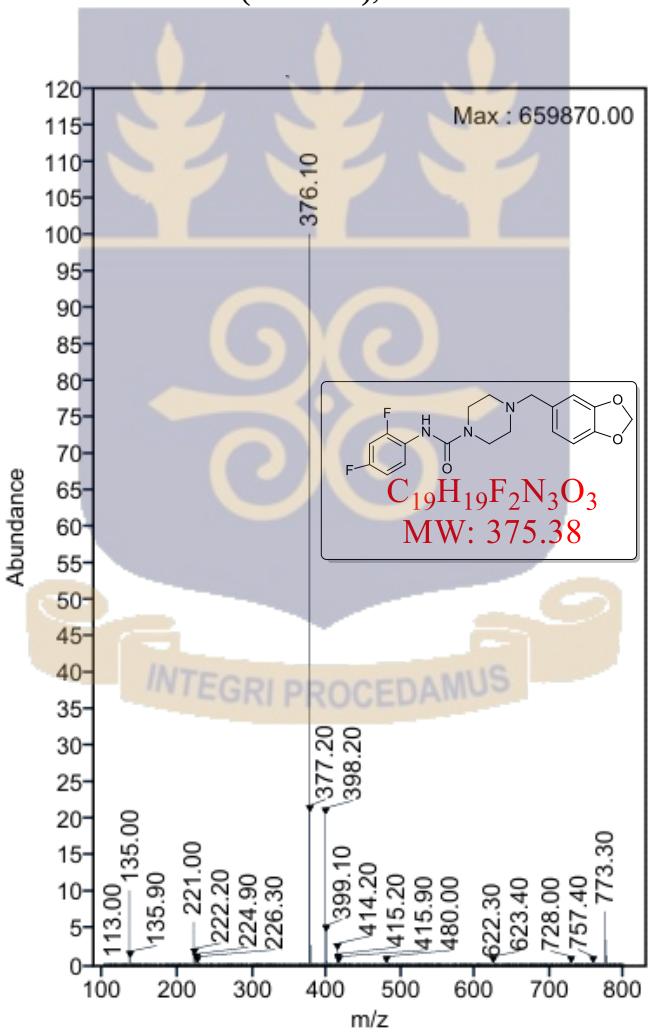


Appendix 2.35: **AJS-ESI** spectrum of 4-((2,2-difluorobenzo[*d*][1,3]dioxol-5-yl)methyl)-*N*-(4-fluorobenzyl)piperazine-1-carboxamide (CFA211), **3.65**.

University of Ghana http://ugspace.ug.edu.gh

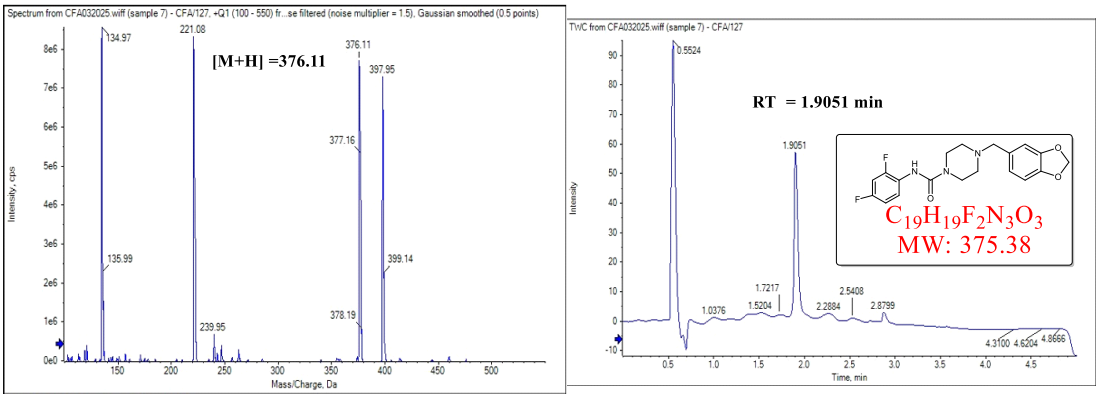


Appendix 2.36: **WAU-ESI** spectrum of 4-((6-bromobenzo[d][1,3]dioxol-5-yl)methyl)-N-(4-fluorobenzyl)piperazine-1-carboxamide (CFA210), **3.66**.

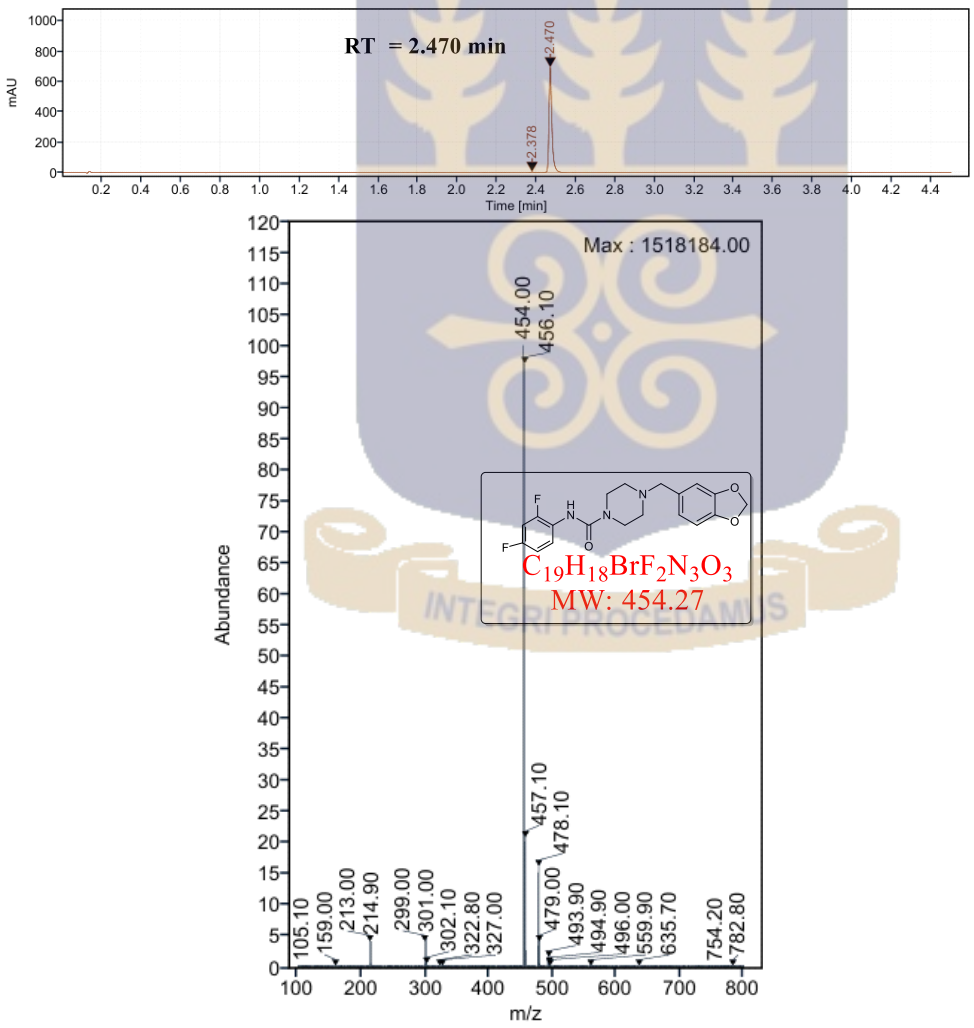


Appendix 2.37: **AJS-ESI** spectrum of 4-(benzo[d][1,3]dioxol-5-ylmethyl)-N-(2,4-difluorophenyl)piperazine-1-carboxamide (CFA127/162), **3.67**.

University of Ghana http://ugspace.ug.edu.gh

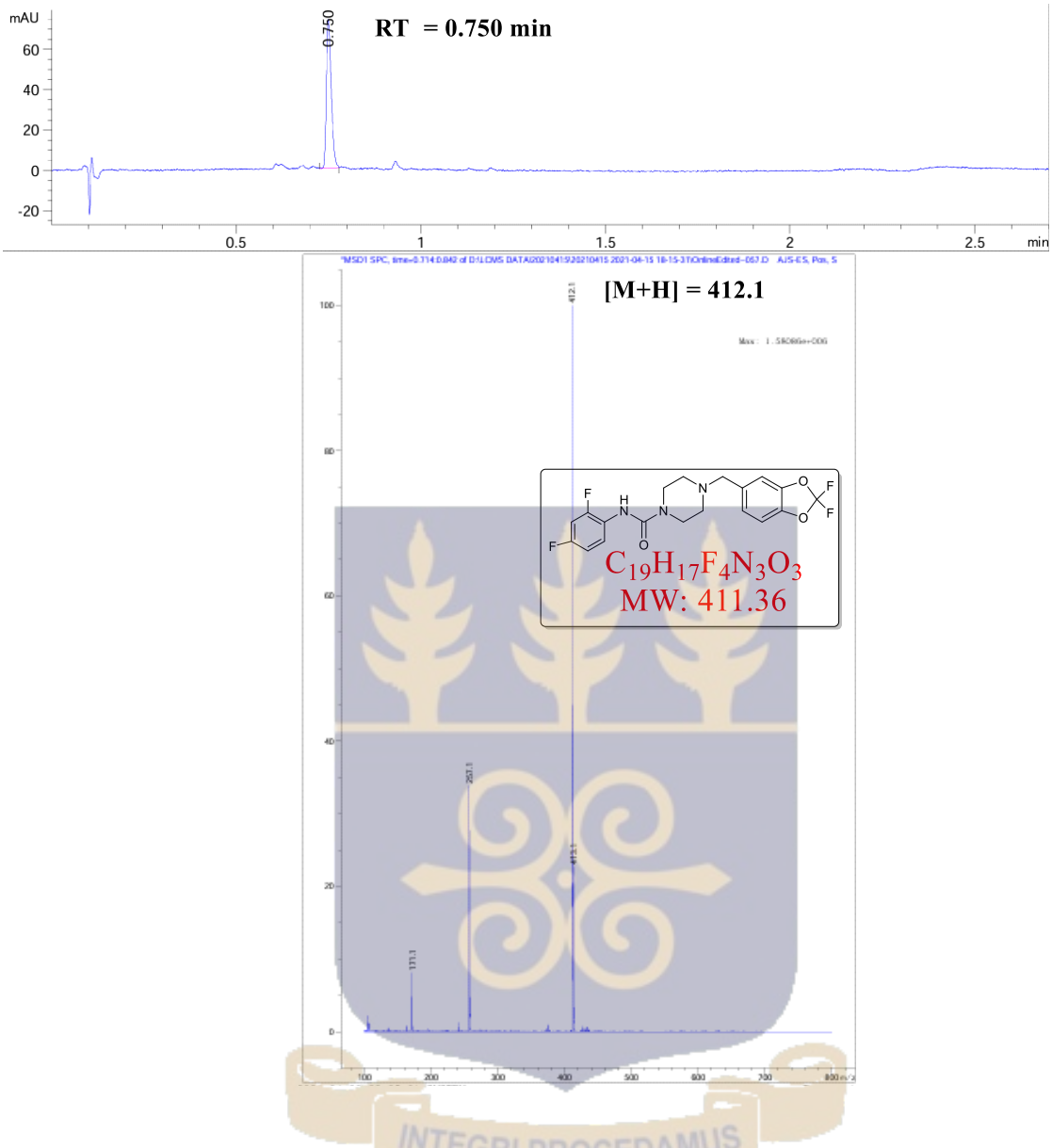


Appendix 2.38: **WAU-ESI** spectrum of 4-(benzo[d][1,3]dioxol-5-ylmethyl)-N-(2,4-difluorophenyl)piperazine-1-carboxamide**, no** (CFA127/162), **3. 67**.



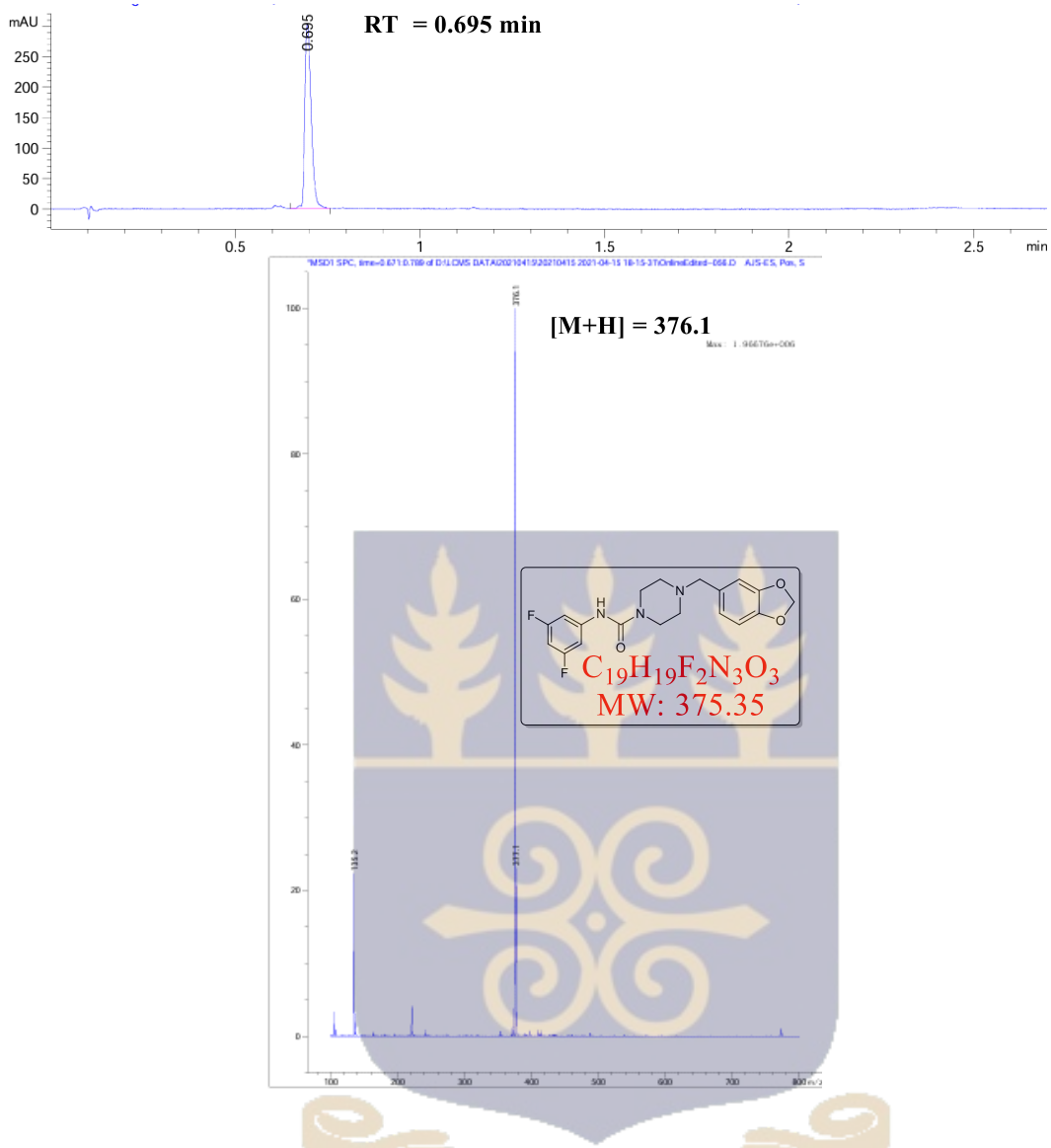
Appendix 2.39: AJS-ESI spectrum of 4-((6-bromobenzo[*d*][1,3]dioxol-5-yl)methyl)-*N*-(2,4-difluorophenyl)piperazine-1-carboxamide (CFA198), **3.68**.

University of Ghana http://ugspace.ug.edu.gh



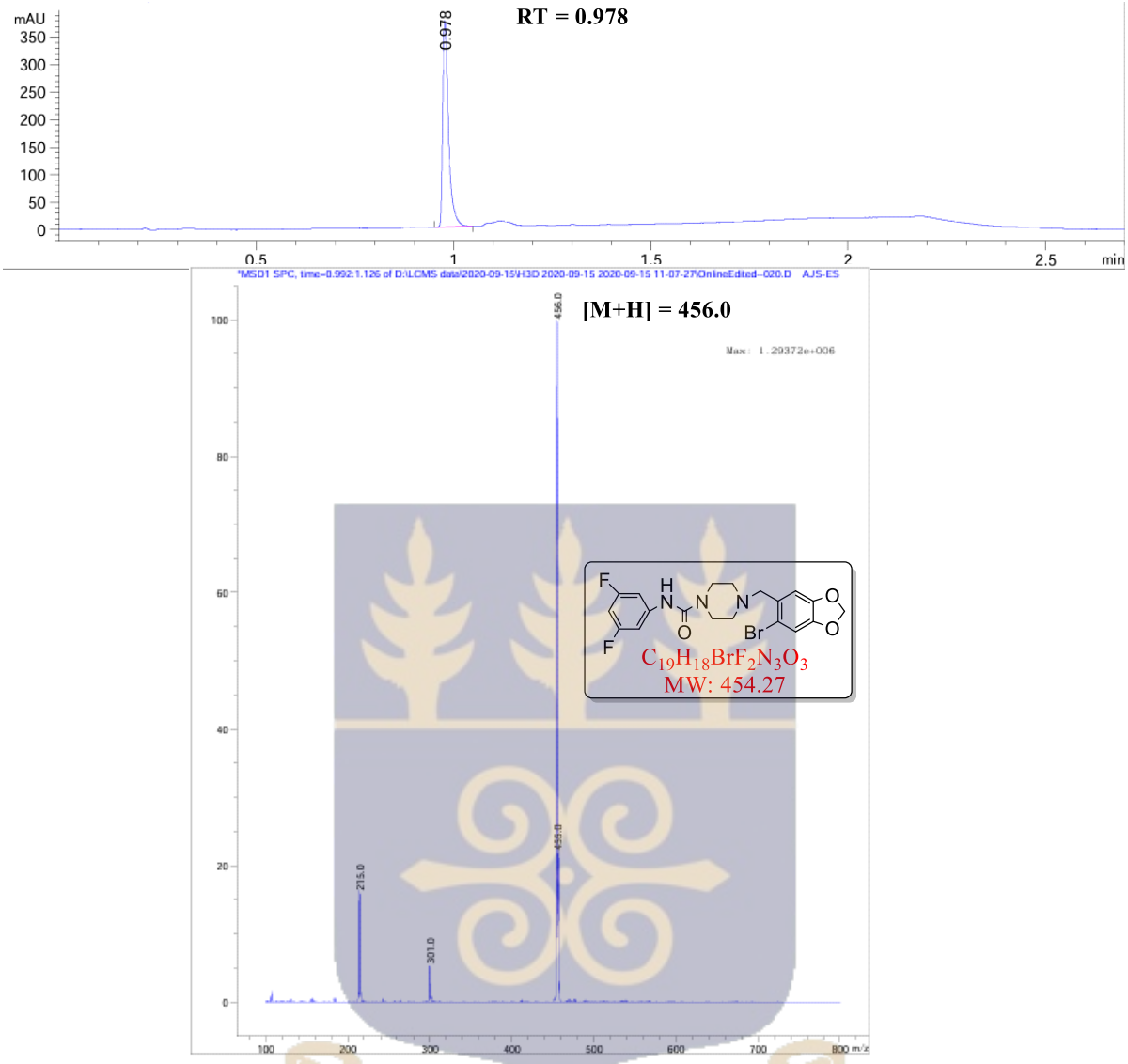
Appendix 2.40: AJS-ESI spectrum of 4-((2,2-difluorobenzo[d][1,3]dioxol-5-yl)methyl)-N-(2,4-difluorophenyl)piperazine-1-carboxamide (CFA163), **3.69**.

University of Ghana http://ugspace.ug.edu.gh



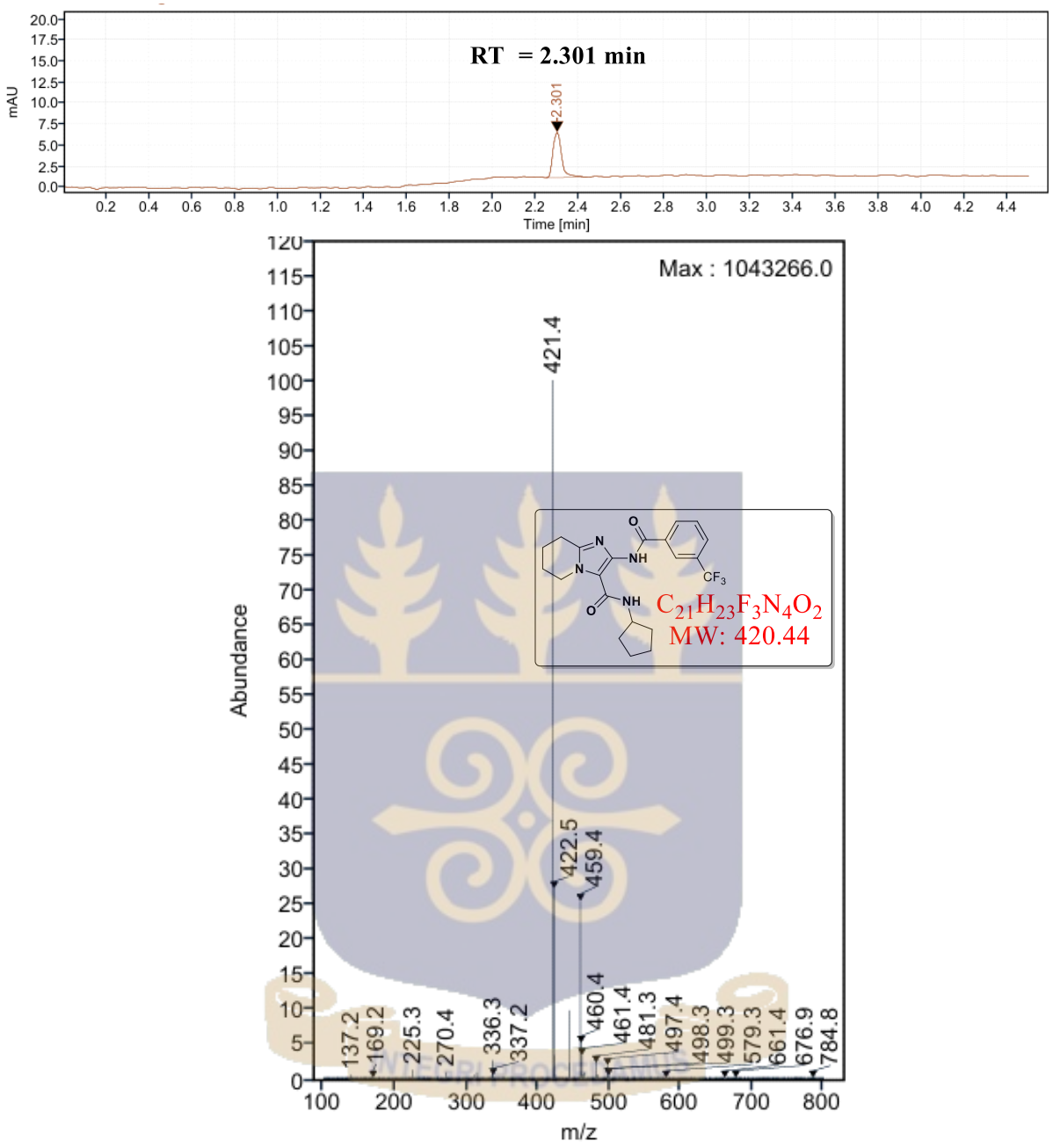
Appendix 2.41: AJS-ESI spectrum of 4-(benzo[d][1,3]dioxol-5-ylmethyl)-N-(3,5-difluorophenyl)piperazine-1-carboxamide (CFA176), **3.70**.

University of Ghana http://ugspace.ug.edu.gh



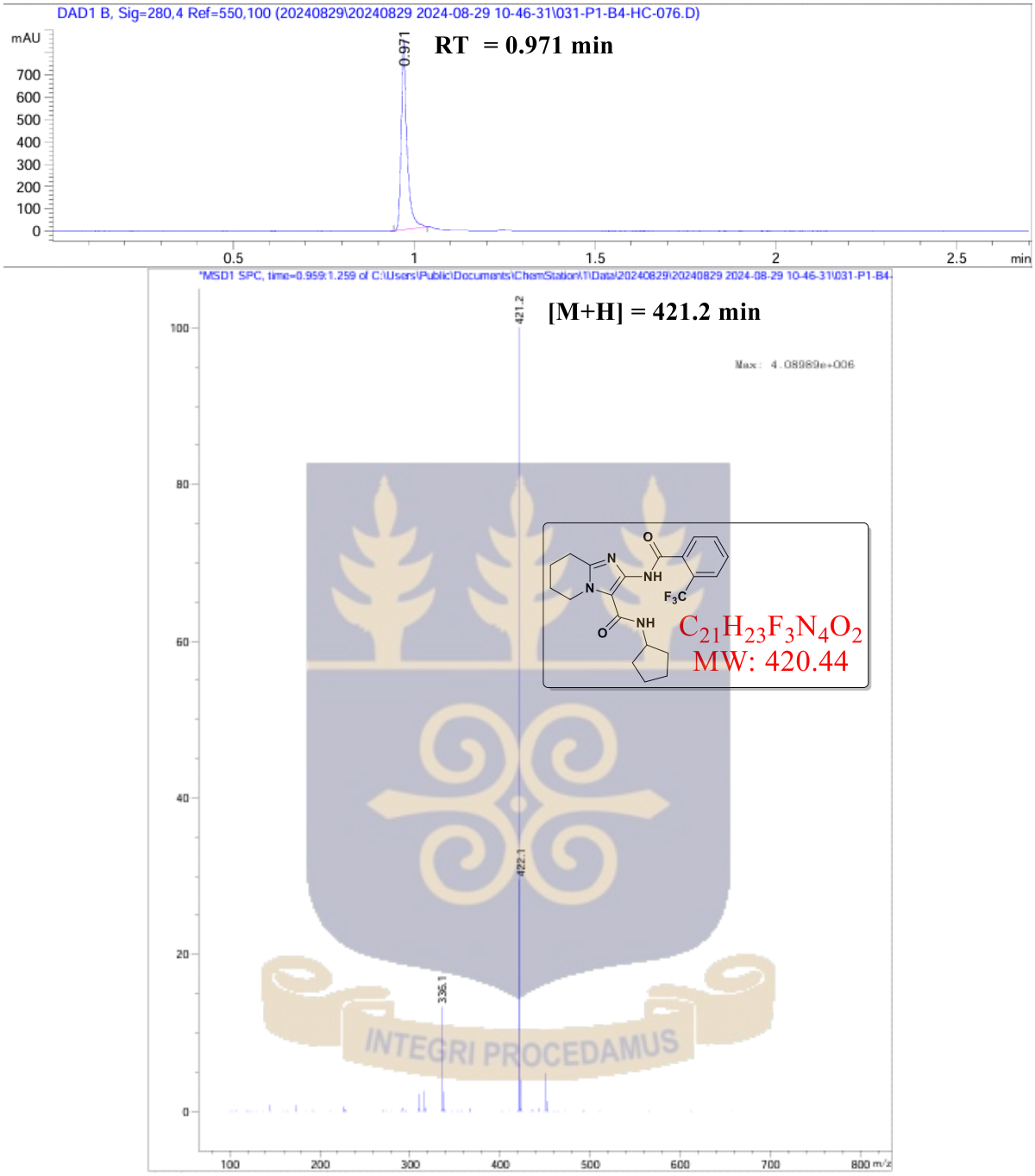
Appendix 2.42: **AJS-ESI** spectrum of 4-((2,2-difluorobenzo[*d*][1,3]dioxol-5-yl)methyl)-*N*-(3,5-difluorophenyl)piperazine-1-carboxamide (CFA070), **3.71**.

University of Ghana http://ugspace.ug.edu.gh



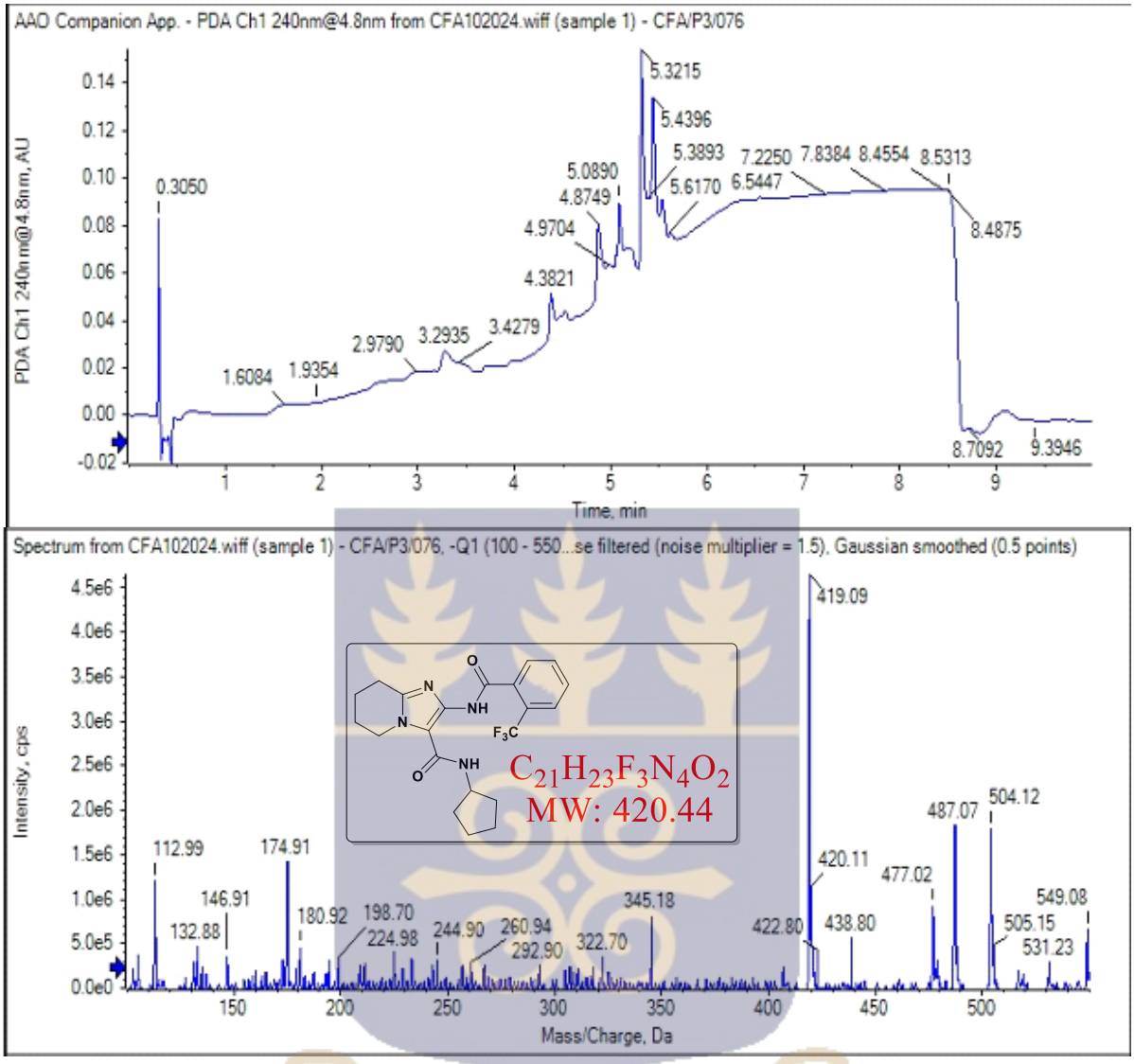
Appendix 2.43: **AJS-ESI** spectrum of *N*-cyclopentyl-2-(3-(trifluoromethyl)benzamido)-5,6,7,8-tetrahydroimidazo[1,2-*a*]pyridine-5-carboxamide (CFA/P3021), **3.80**.

University of Ghana http://ugspace.ug.edu.gh



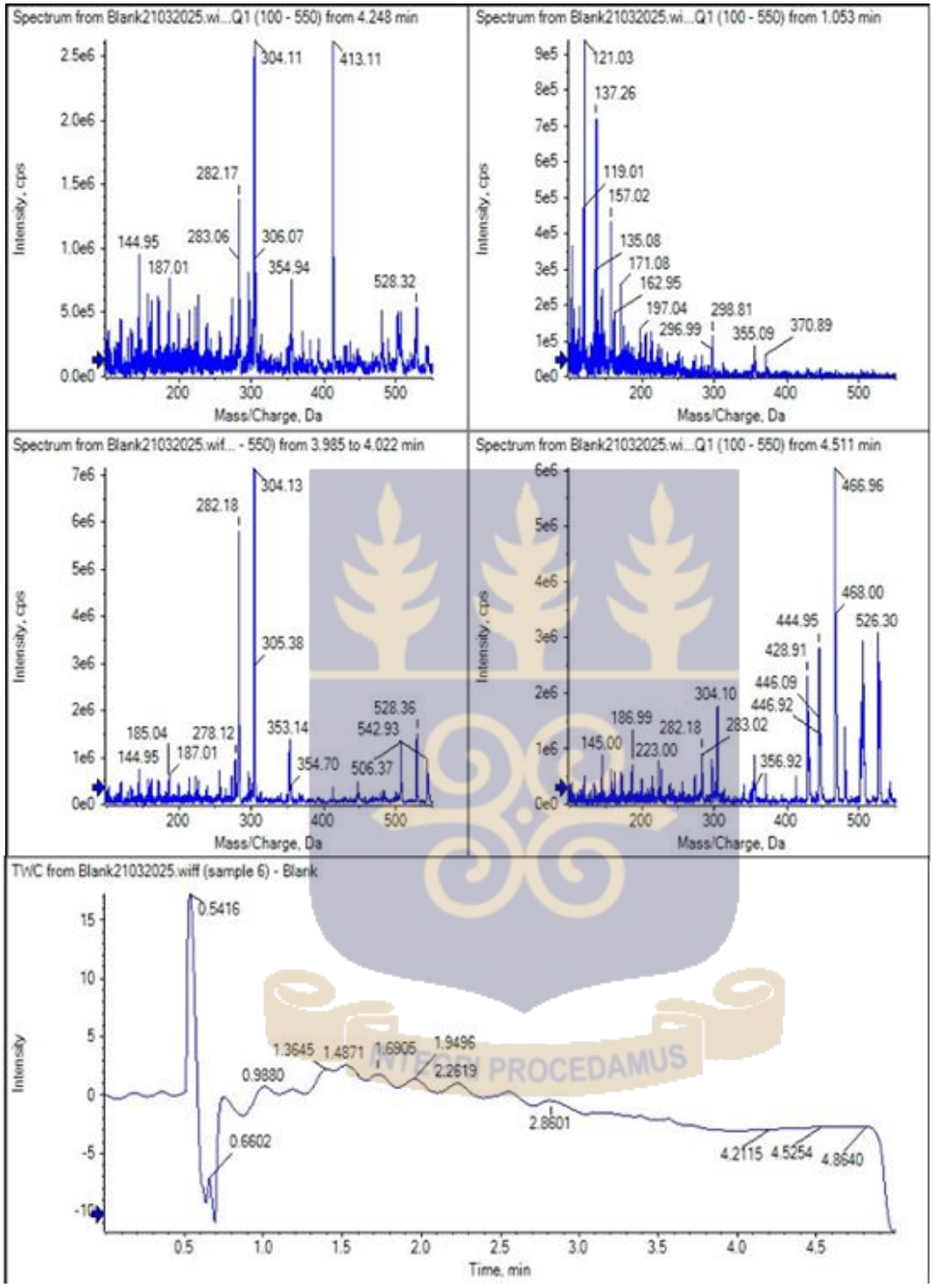
Appendix 2.44: AJS-ESI spectrum of *N*-cyclopentyl-2-(2-(trifluoromethyl)benzamido)-5,6,7,8-tetrahydroimidazo[1,2-*a*]pyridine-3-carboxamide (CFA/P3076), **3.81**.

University of Ghana http://ugspace.ug.edu.gh



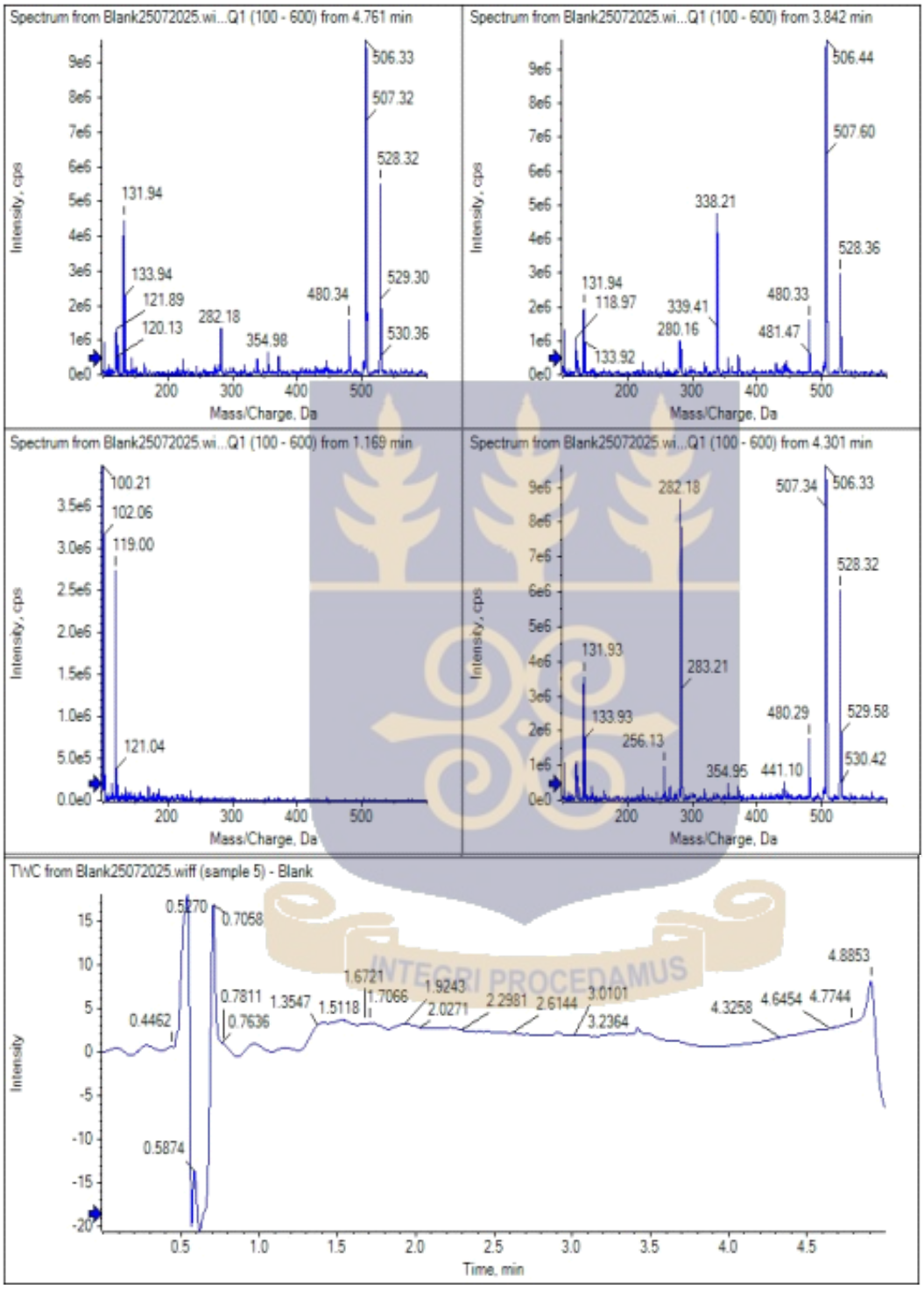
Appendix 2.45: **WAU-ESI** spectrum of *N*-cyclopentyl-2-(2-(trifluoromethyl)benzamido)-5,6,7,8-tetrahydroimidazo[1,2-*a*]pyridine-3-carboxamide (CFA/P3076), **3.81**.

University of Ghana http://ugspace.ug.edu.gh



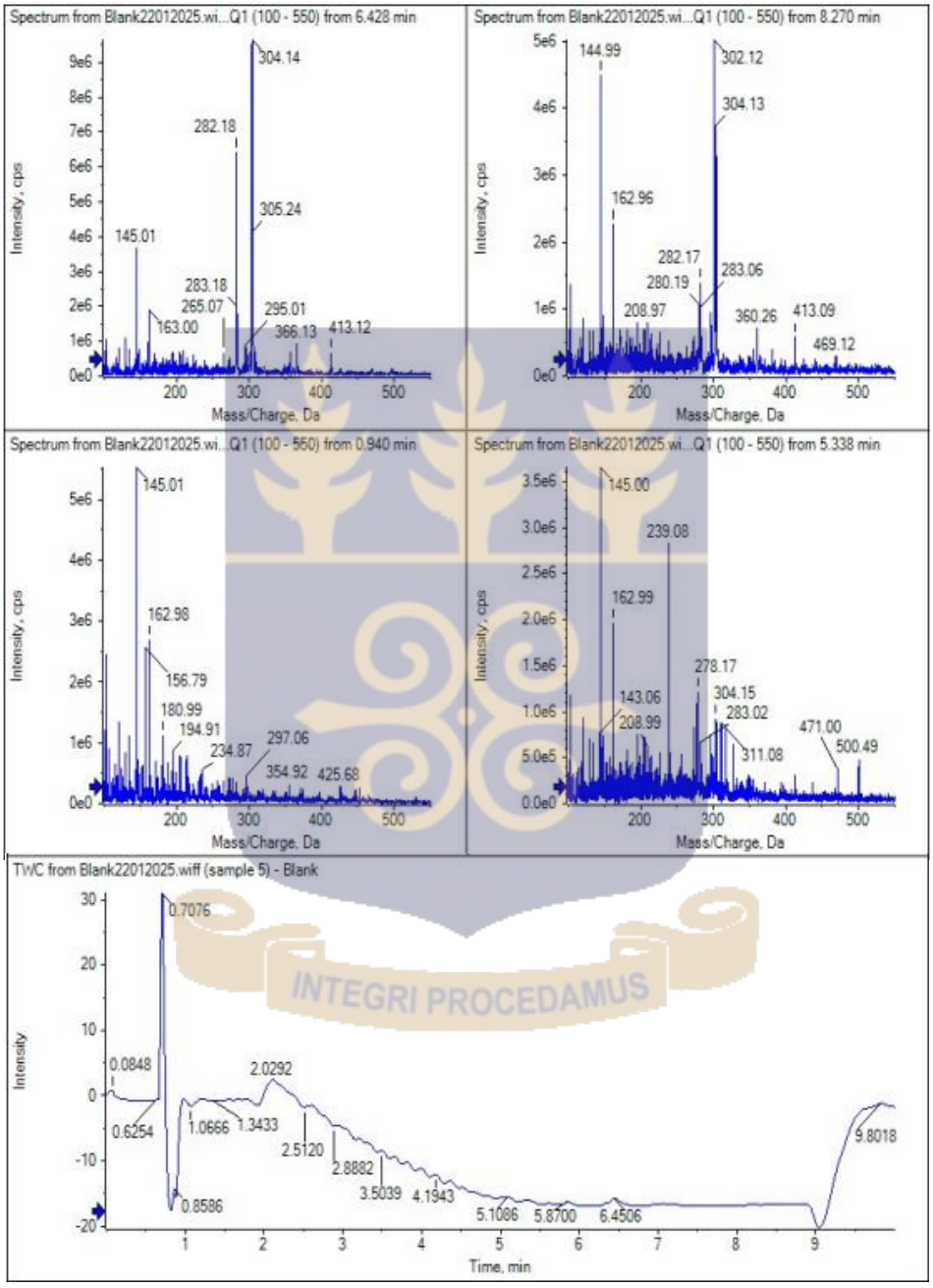
Appendix 2.46: Blank LC-MS spectrum (**WAU-ESI)** serving as baseline reference for compounds **3.66** and **3.38**.

University of Ghana http://ugspace.ug.edu.gh



Appendix 2.46: Blank LC-MS spectrum (**WAU-ESI)** serving as baseline reference for compounds **3.67**.

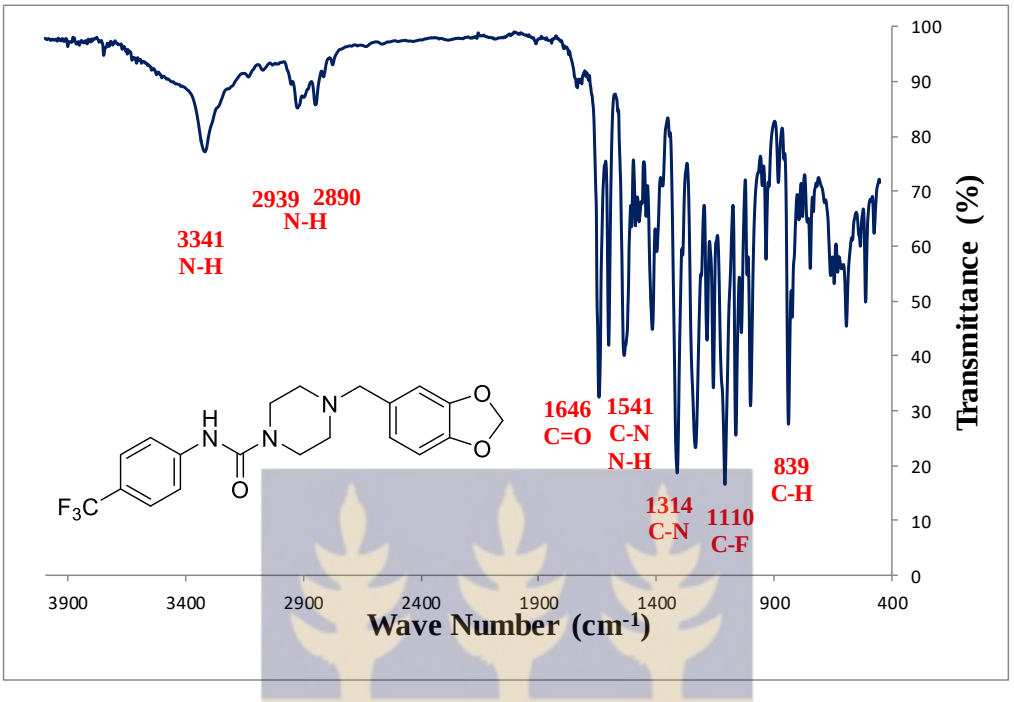
University of Ghana http://ugspace.ug.edu.gh



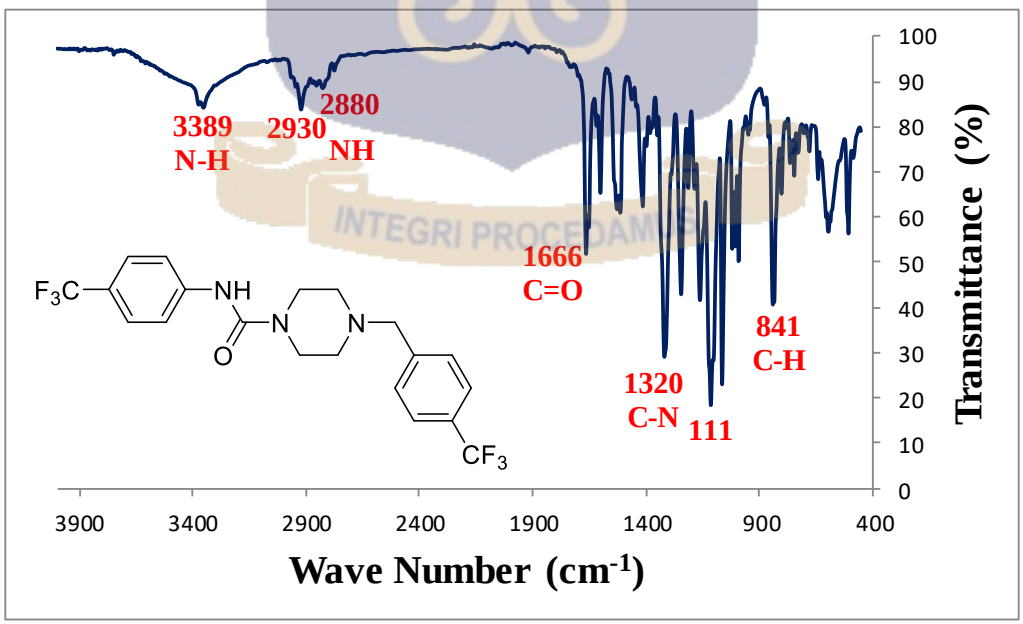
Appendix 2.48: Blank LC-MS spectrum (**WAU-ESI)** serving as baseline reference for compounds **3.9**, **3.11**, **3.12** and **3.23**.

University of Ghana http://ugspace.ug.edu.gh

Appendix 3: FTIR Spectra

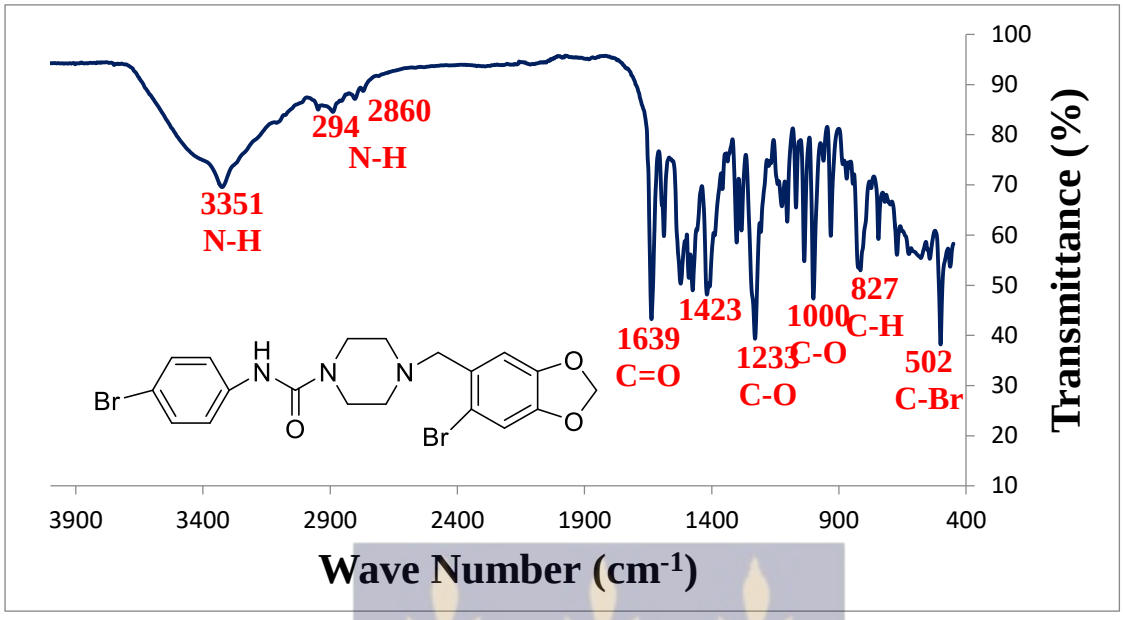


Appendix 3.1: FTIR Spectrum of 4-(benzo[*d*][1,3]dioxol-5-ylmethyl)-*N*-(4-(trifluoromethyl)phenyl)piperazine-1-carboxamide (CFA015), **3.36.**

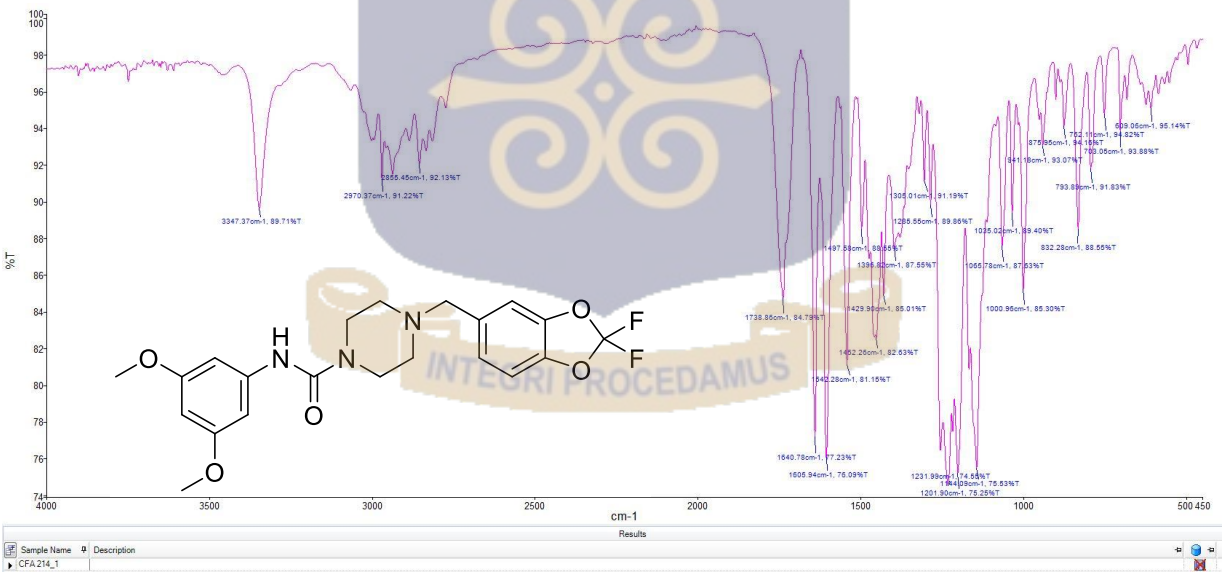


Appendix 3.2: FTIR Spectrum of 4-(4-(trifluoromethyl)benzyl)-*N*-(4-(trifluoromethyl)phenyl)piperazine-1-carboxamide (CFA017), **3.37**

University of Ghana http://ugspace.ug.edu.gh

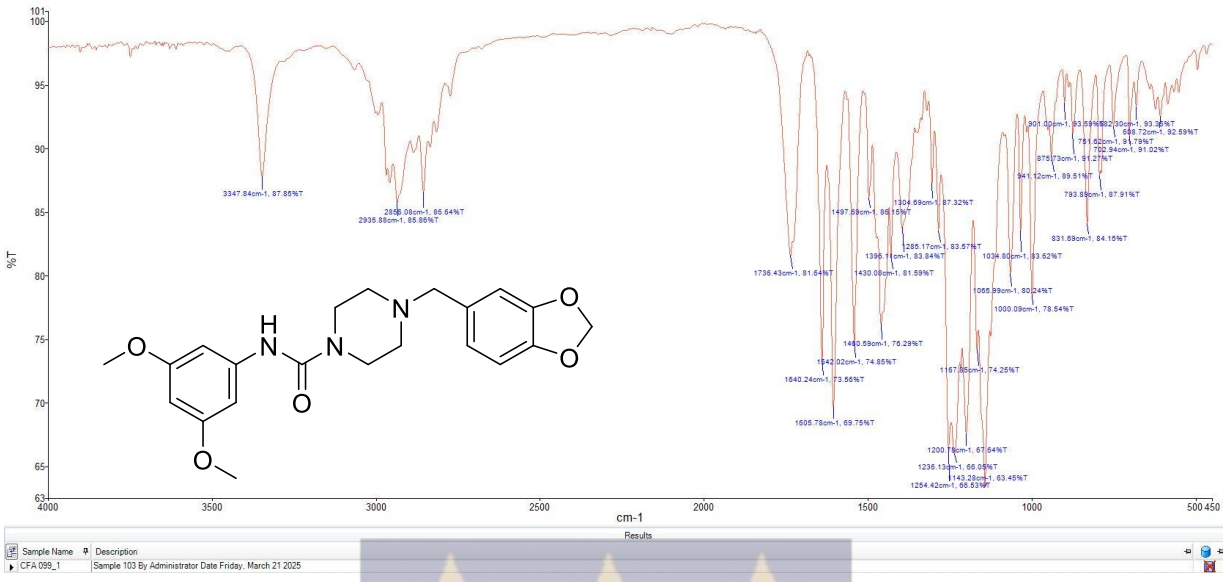


Appendix 3.3: FTIR Spectrum of 4-((6-bromobenzo[d][1,3]dioxol-5-yl)methyl)-N-(4-bromophenyl)piperazine-1-carboxamide (CFA208), **3.38.**

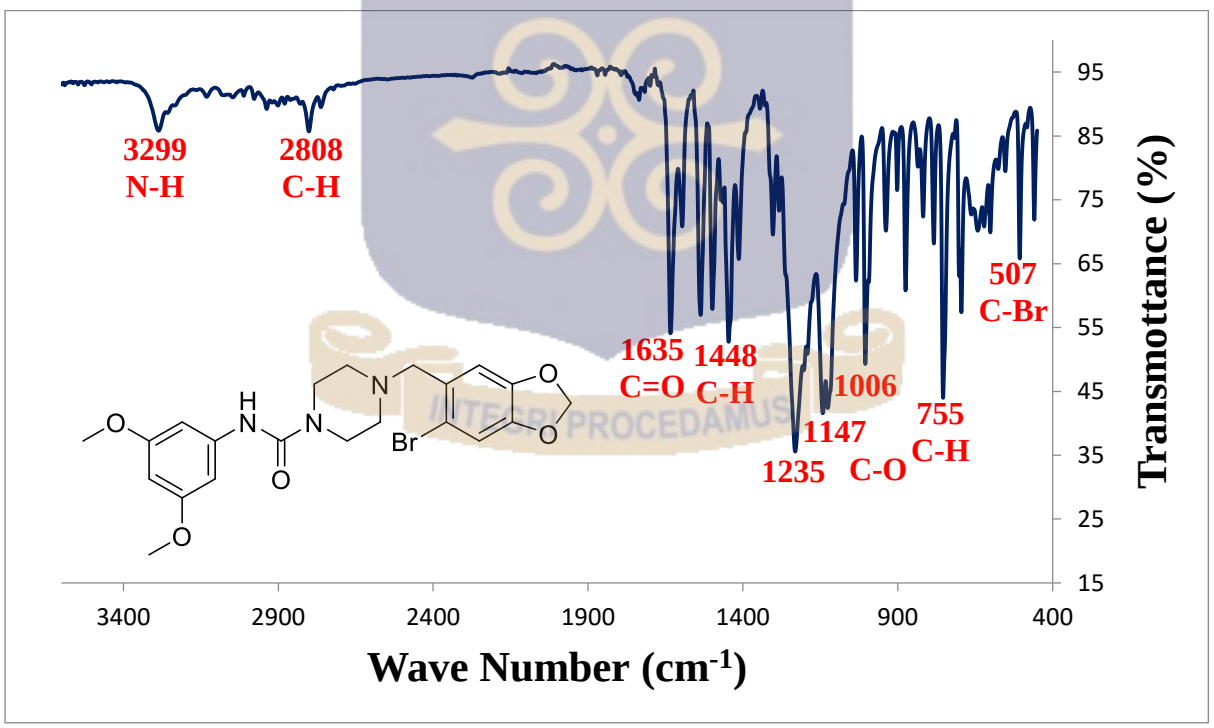


Appendix 3.4: FTIR Spectrum of 4-((2,2-difluorobenzo[*d*][1,3]dioxol-5-yl)methyl)-*N*-(3,5-dimethoxyphenyl)piperazine-1-carboxamide (CFA214), **3.39**.

University of Ghana http://ugspace.ug.edu.gh

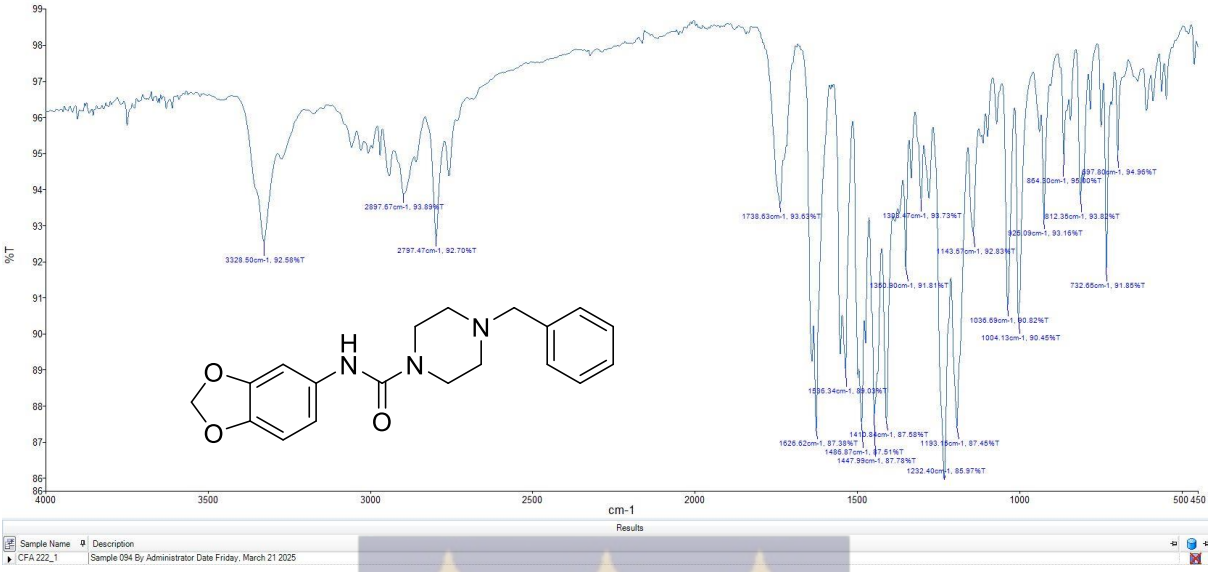


Appendix 3.5: FTIR Spectrum of 4-(benzo[*d*][1,3]dioxol-5-ylmethyl)-*N*-(3,5-dimethoxyphenyl)piperazine-1-carboxamide (CFA099), **3.40.**

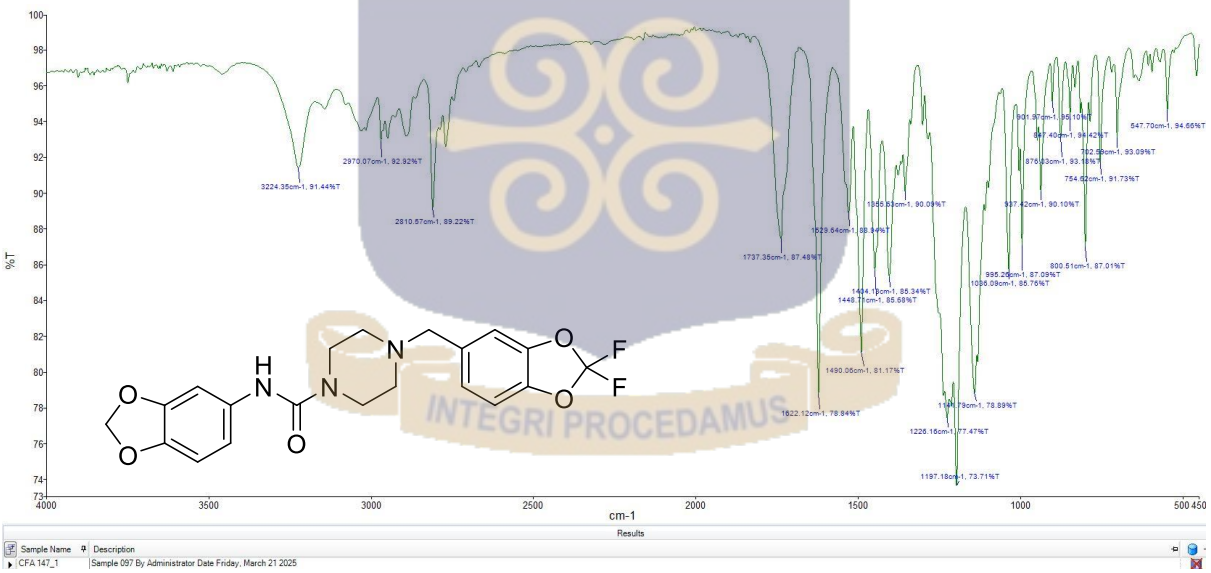


Appendix 3.6: FTIR Spectrum of 4-((6-bromobenzo[*d*][1,3]dioxol-5-yl)methyl)-*N*-(3,5-dimethoxyphenyl)piperazine-1-carboxamide (CFA092), **3.41.**

University of Ghana http://ugspace.ug.edu.gh

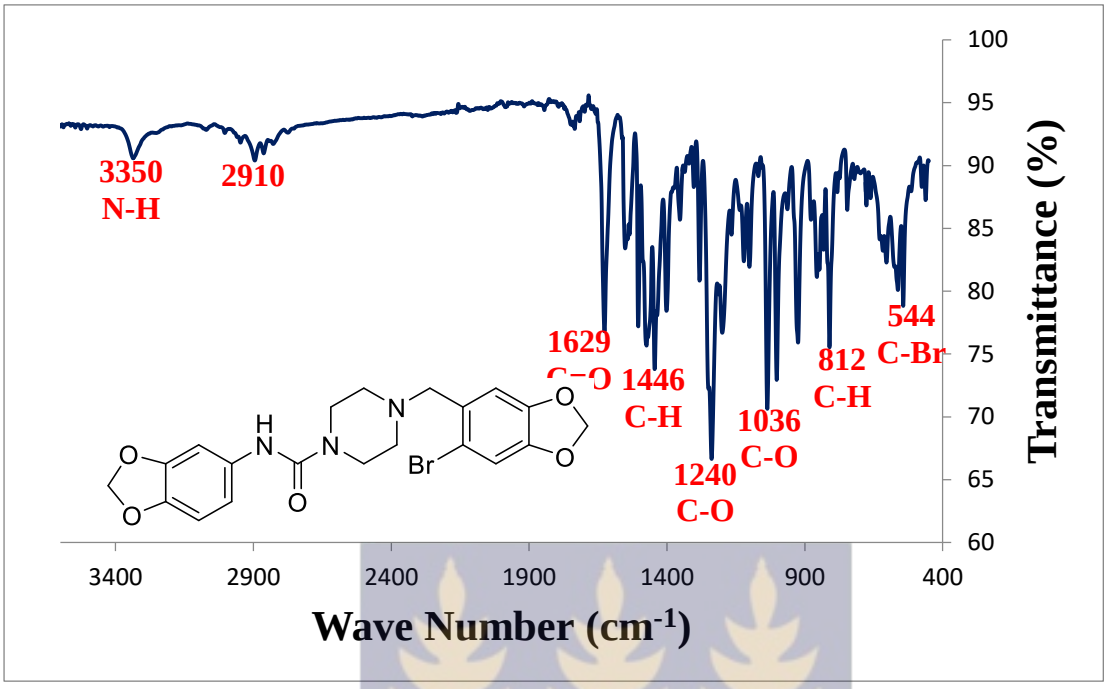


Appendix 3.7: FTIR Spectrum of *N*-(benzo[*d*][1,3]dioxol-5-yl)-4-benzylpiperazine-1-carboxamide (CFA222), **3.42.**

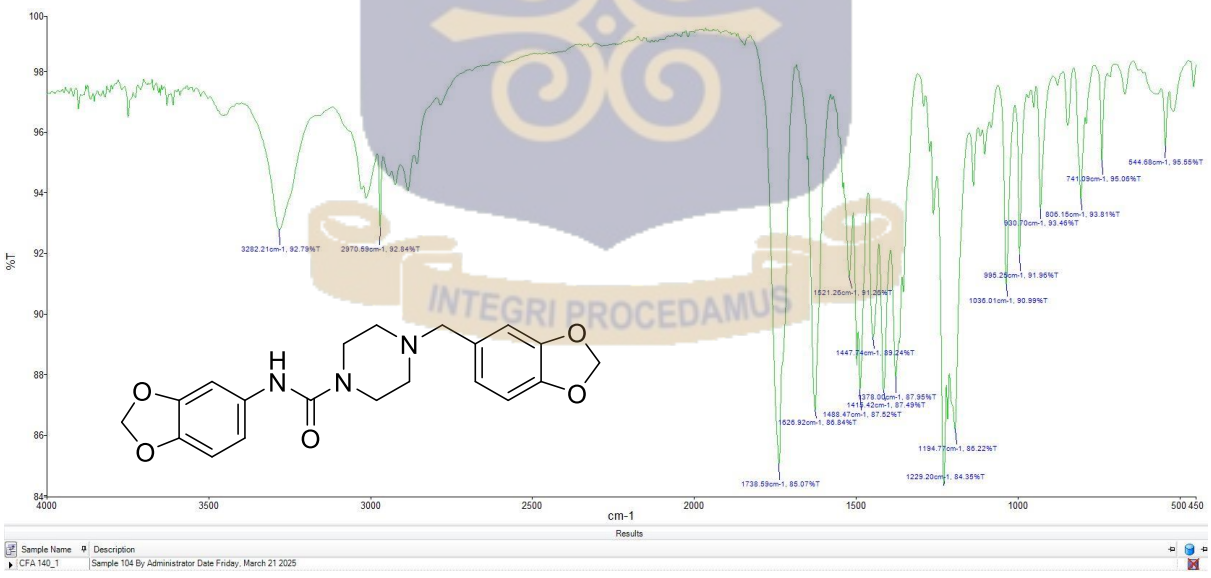


Appendix 3.8: FTIR Spectrum of *N*-(benzo[*d*][1,3]dioxol-5-yl)-4-((2,2-difluorobenzo[d][1,3]dioxol-5-yl)methyl)piperazine-1-carboxamide (CFA147), **3.43.**

University of Ghana http://ugspace.ug.edu.gh

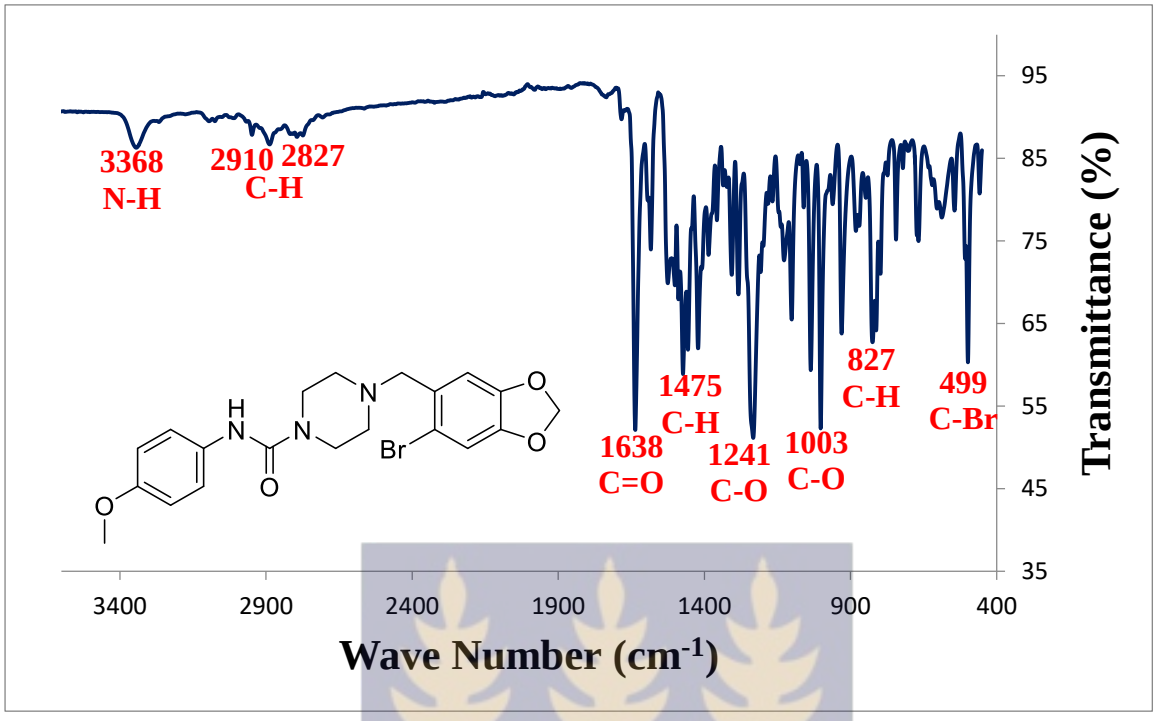


Appendix 3.9: FTIR Spectrum of *N*-(benzo[*d*][1,3]dioxol-5-yl)-4-((6-bromobenzo[d][1,3]dioxol-5-yl)methyl)piperazine-1-carboxamide (CFA189), **3.44.**



Appendix 3.10: FTIR Spectrum of *N*-(benzo[*d*][1,3]dioxol-5-yl)-4-(benzo[*d*][1,3]dioxol-5-ylmethyl)piperazine-1-carboxamide (CFA140), **3.45.**

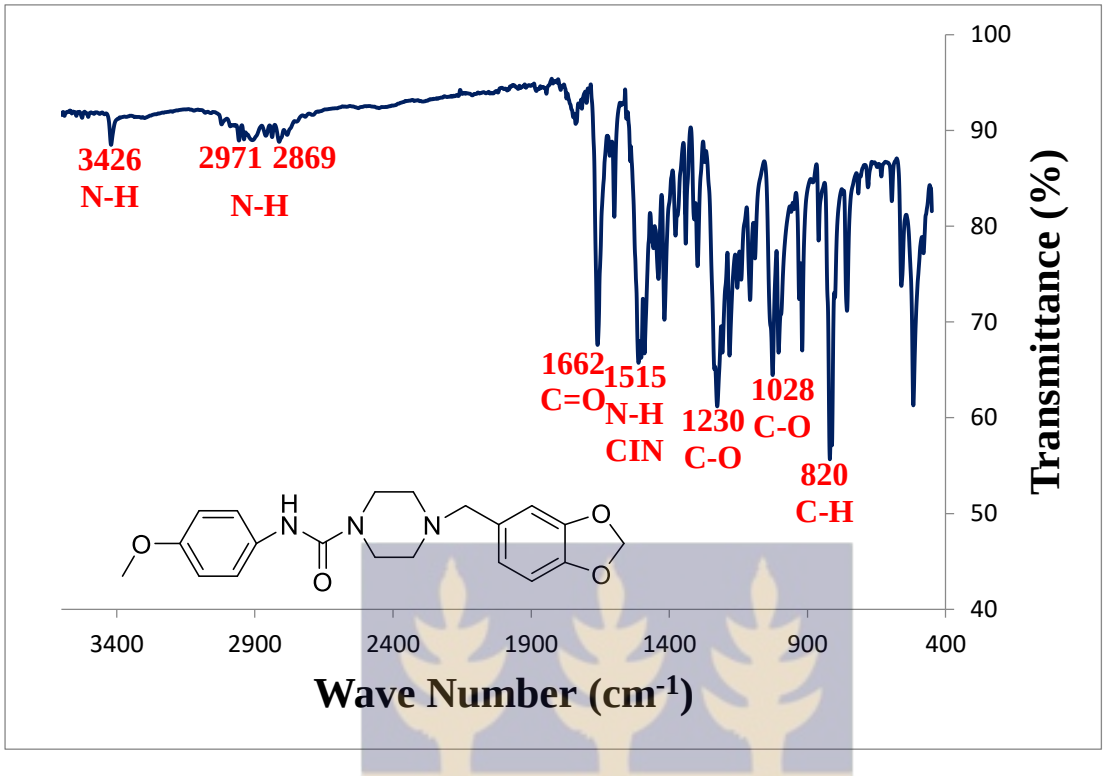
University of Ghana http://ugspace.ug.edu.gh



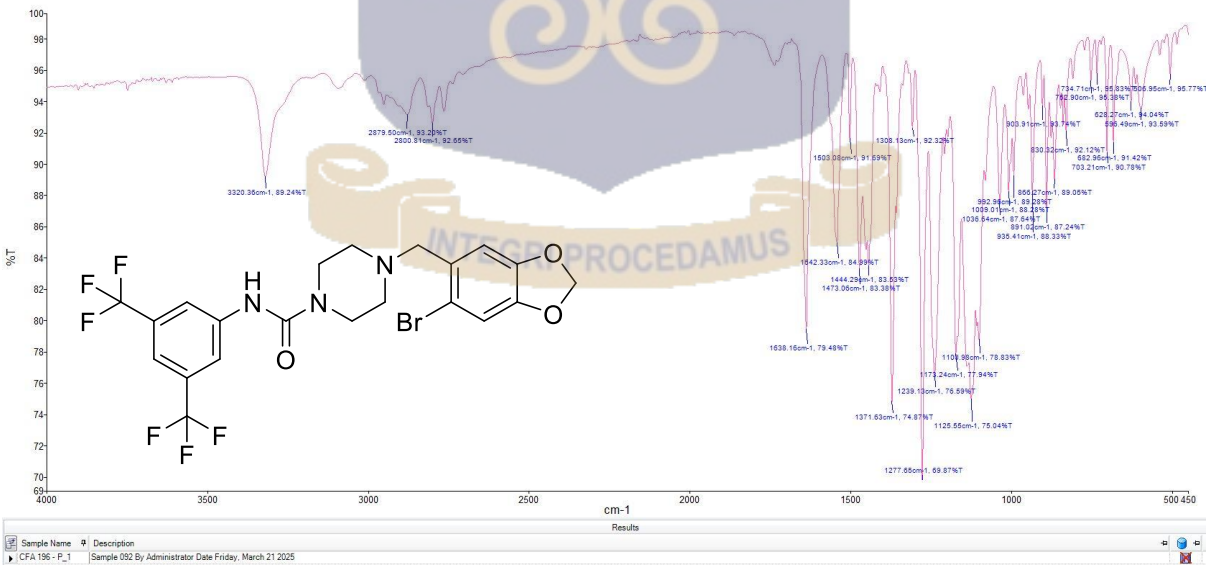
Appendix 3.11: FTIR Spectrum of 4-((6-bromobenzo[*d*][1,3]dioxol-5-yl)methyl)-*N*-(4-methoxyphenyl)piperazine-1-carboxamide (CFA026), **3.46.**

INTEGRI PROCEDAMUS

University of Ghana http://ugspace.ug.edu.gh

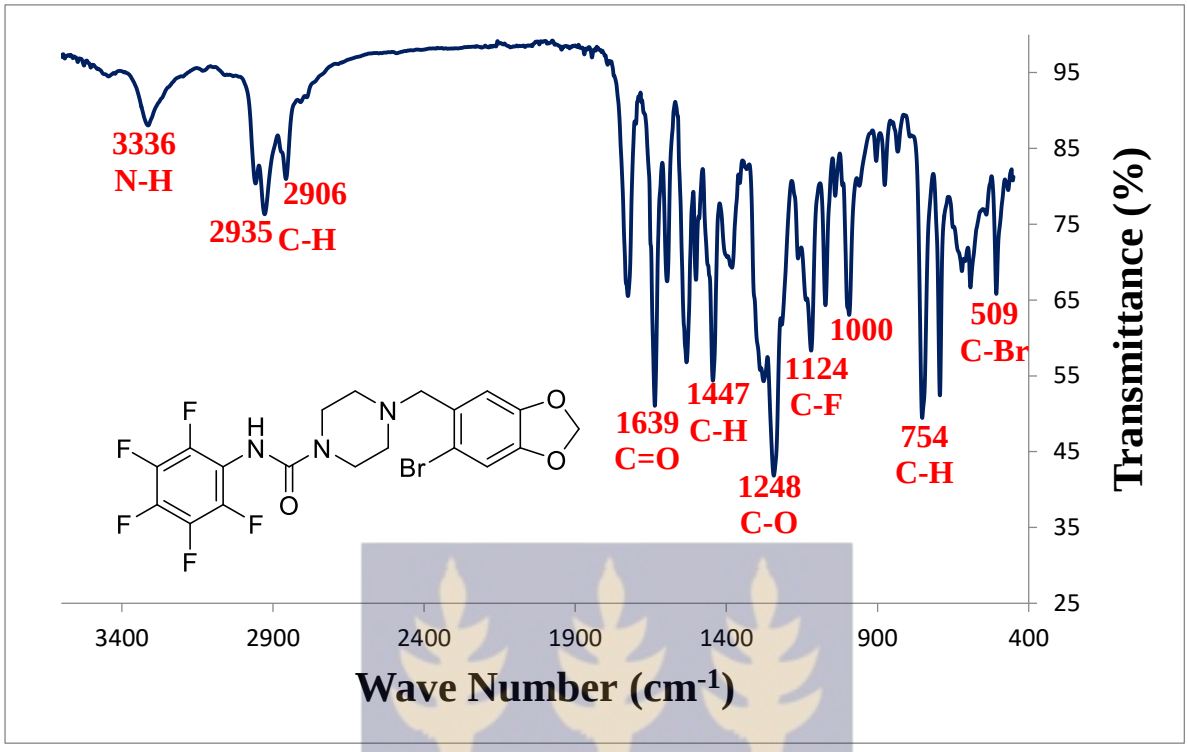


Appendix 3.12: FTIR Spectrum of 4-(benzo[d][1,3]dioxol-5-ylmethyl)-N-(4-methoxyphenyl)piperazine-1-carboxamide (CFA170), **3.47.**

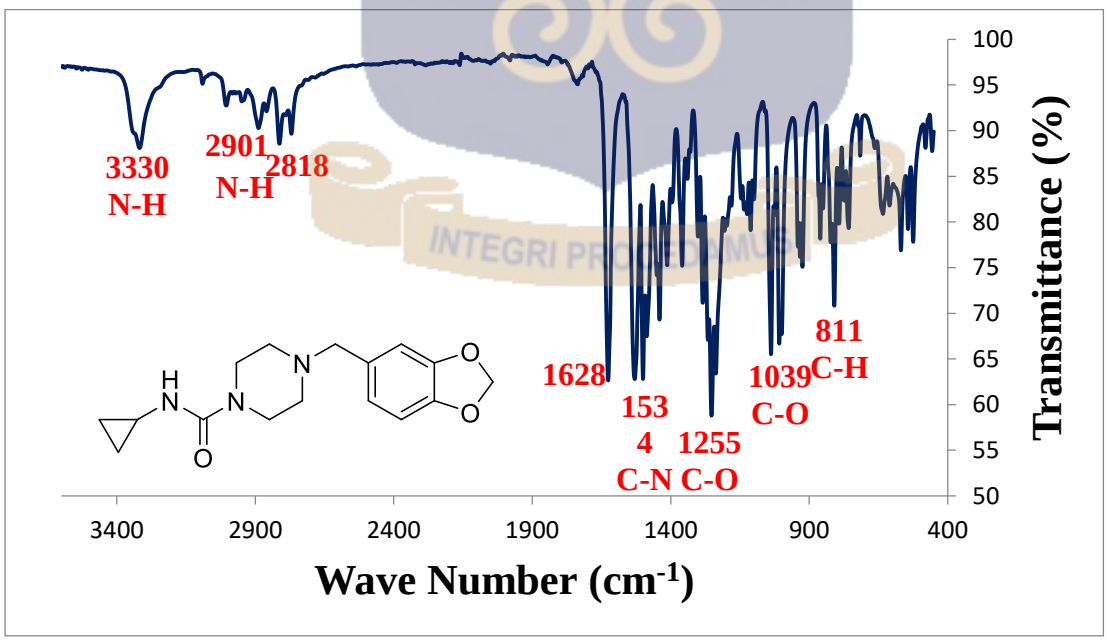


Appendix 3.13: FTIR Spectrum of *N*-(3,5-bis(trifluoromethyl)phenyl)-4-((6-bromobenzo[*d*][1,3]dioxol-5-yl)methyl)piperazine-1-carboxamide (CFA196), **3.48.**

University of Ghana http://ugspace.ug.edu.gh

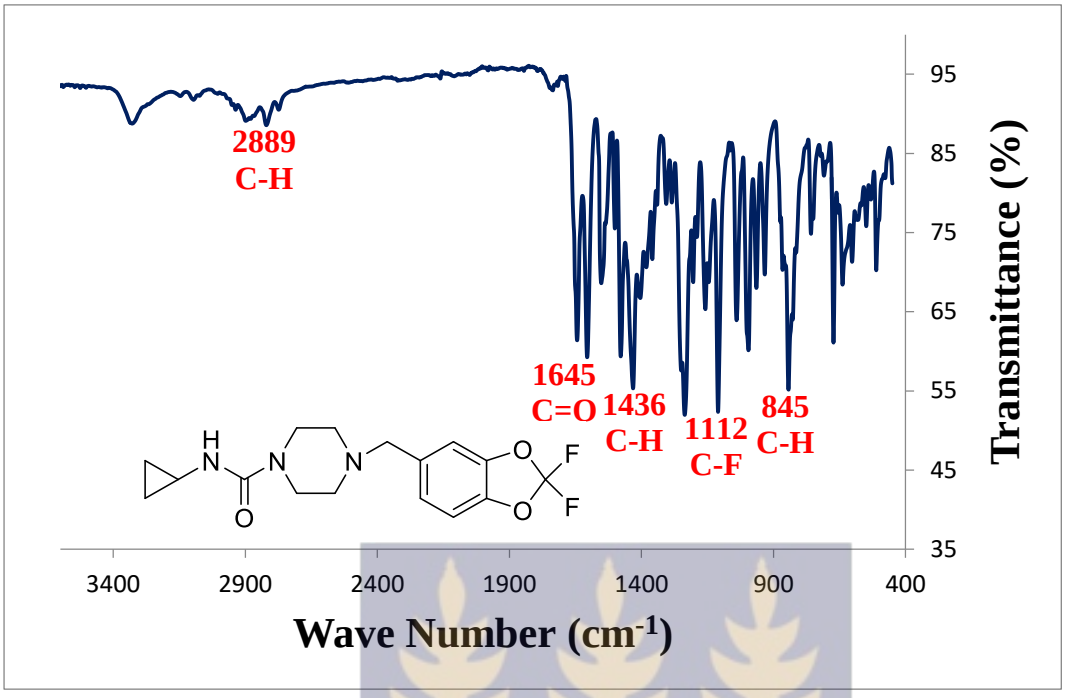


Appendix 3.14: FTIR Spectrum of 4-((6-bromobenzo[*d*][1,3]dioxol-5-yl)methyl)-*N*-(perfluorophenyl)piperazine-1-carboxamide (CFA117), **3.49.**

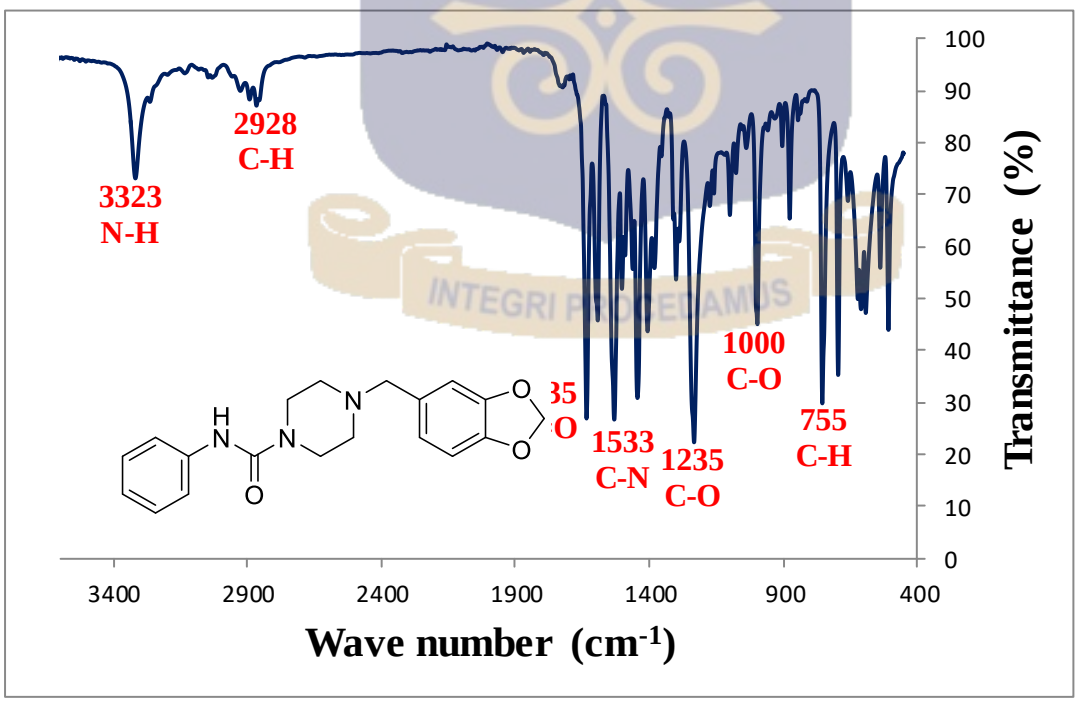


Appendix 3.15: FTIR Spectrum of 4-(benzo[*d*][1,3]dioxol-5-ylmethyl)-*N*-cyclopropylpiperazine-1-carboxamide (CFA119), **3.50.**

University of Ghana http://ugspace.ug.edu.gh

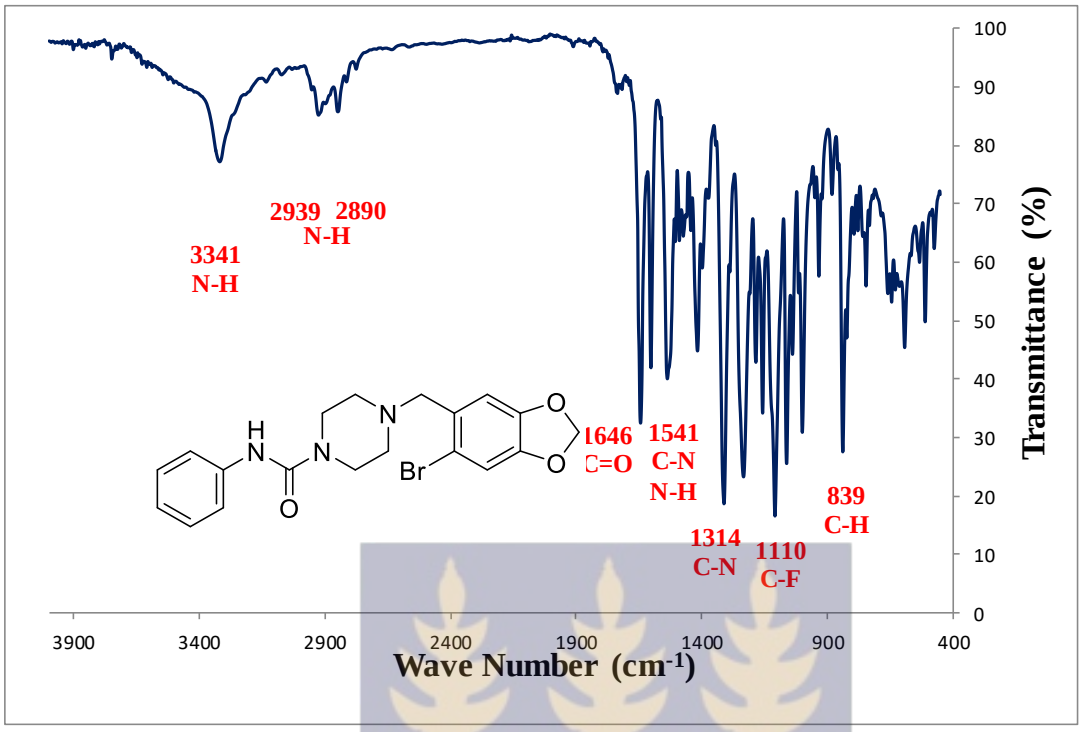


Appendix 3.16: FTIR Spectrum of N-cyclopropyl-4-((2,2-difluorobenzo[d][1,3]dioxol-5-yl)methyl)piperazine-1-carboxamide (CFA121), **3.51.**

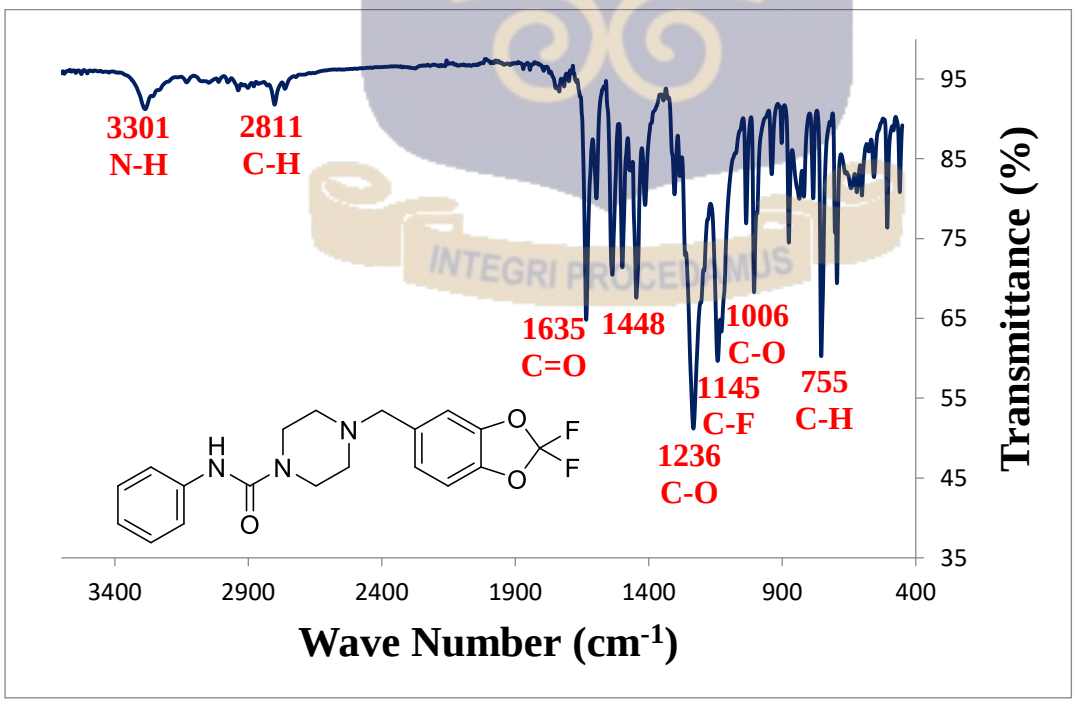


Appendix 3.17: FTIR Spectrum of 4-(benzo[*d*][1,3]dioxol-5-ylmethyl)-*N*-phenylpiperazine-1-carboxamide (CFA066/197), **3.52.**

University of Ghana http://ugspace.ug.edu.gh

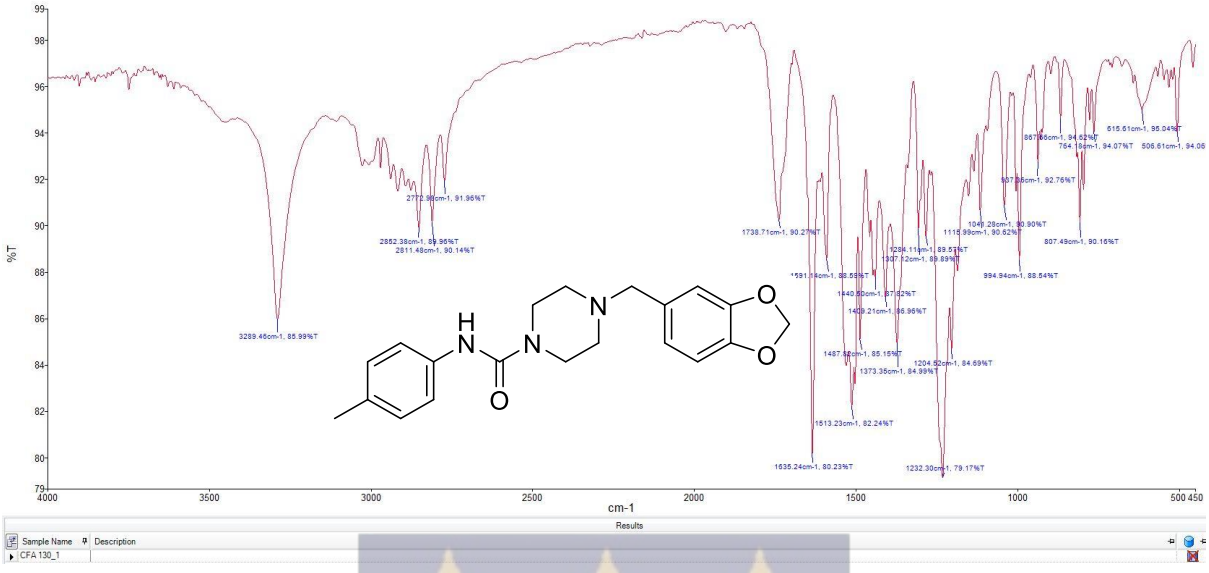


Appendix 3.18: FTIR Spectrum of 4-((6-bromobenzo[*d*][1,3]dioxol-5-yl)methyl)-*N*-phenylpiperazine-1-carboxamide (CFA067/200), **3.53.**

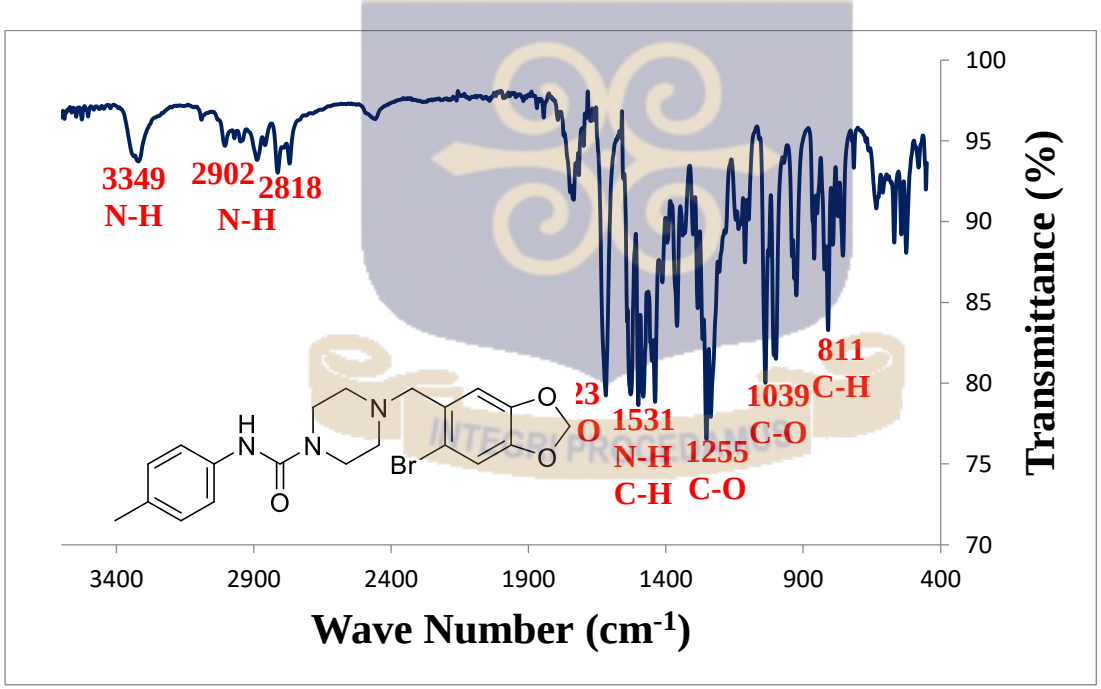


Appendix 3.19: FTIR Spectrum of 4-((2,2-difluorobenzo[*d*][1,3]dioxol-5-yl)methyl)-*N*-phenylpiperazine-1-carboxamide (CFA168/203), **3.54.**

University of Ghana http://ugspace.ug.edu.gh

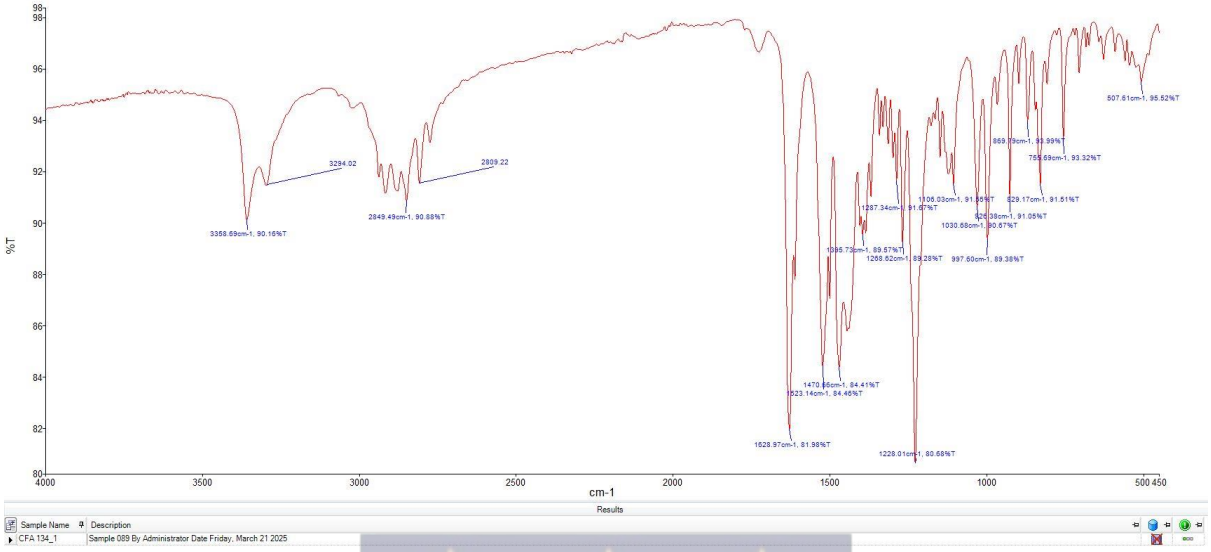


Appendix 3.20: FTIR Spectrum of 4-((2,2-difluorobenzo[*d*][1,3]dioxol-5-yl)methyl)-*N*-phenylpiperazine-1-carboxamide (CFA130), **3.55.**

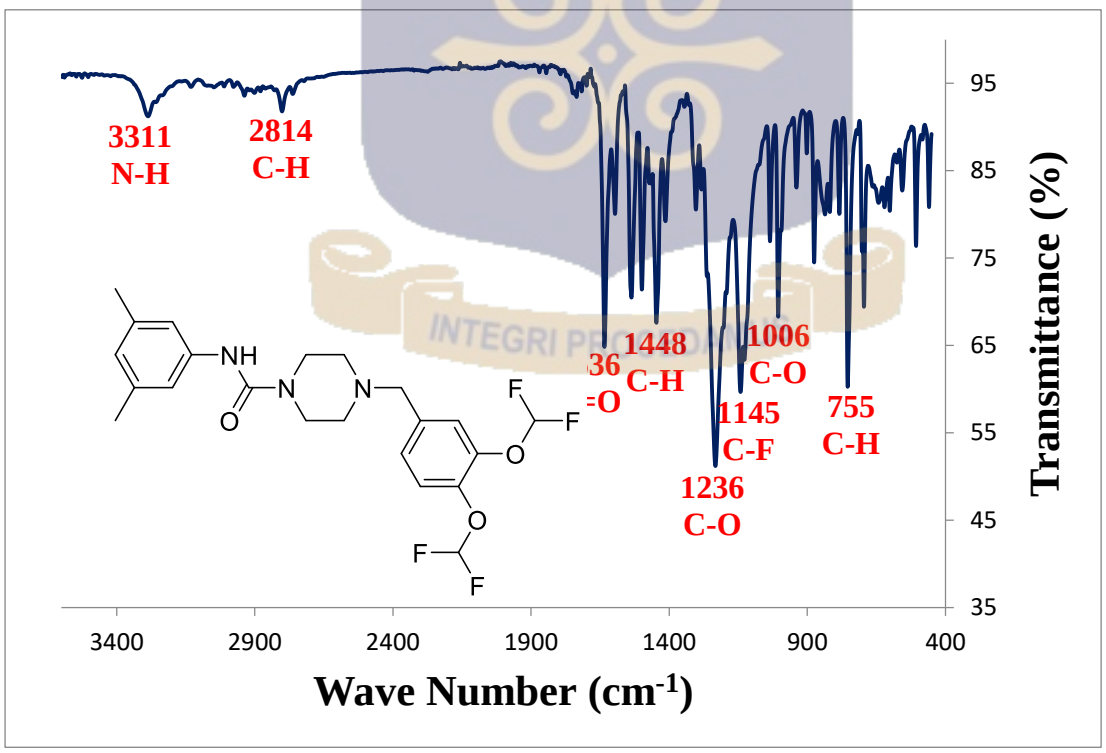


Appendix 3.21: FTIR Spectrum of 4-((6-bromobenzo[*d*][1,3]dioxol-5-yl)methyl)-*N*-(p-tolyl)piperazine-1-carboxamide (CFA131), **3.56.**

University of Ghana http://ugspace.ug.edu.gh

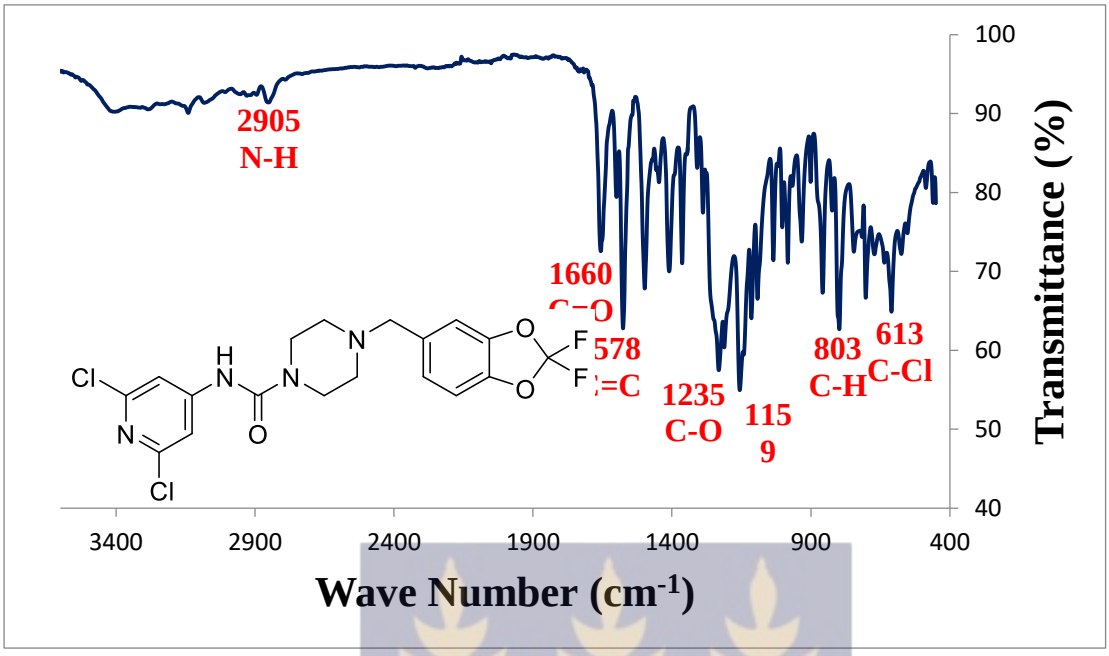


Appendix 3.22: FTIR Spectrum of 4-((6-bromobenzo[*d*][1,3]dioxol-5-yl)methyl)-*N*-(3,5-dimethylphenyl)piperazine-1-carboxamide (CFA134), **3.57.**

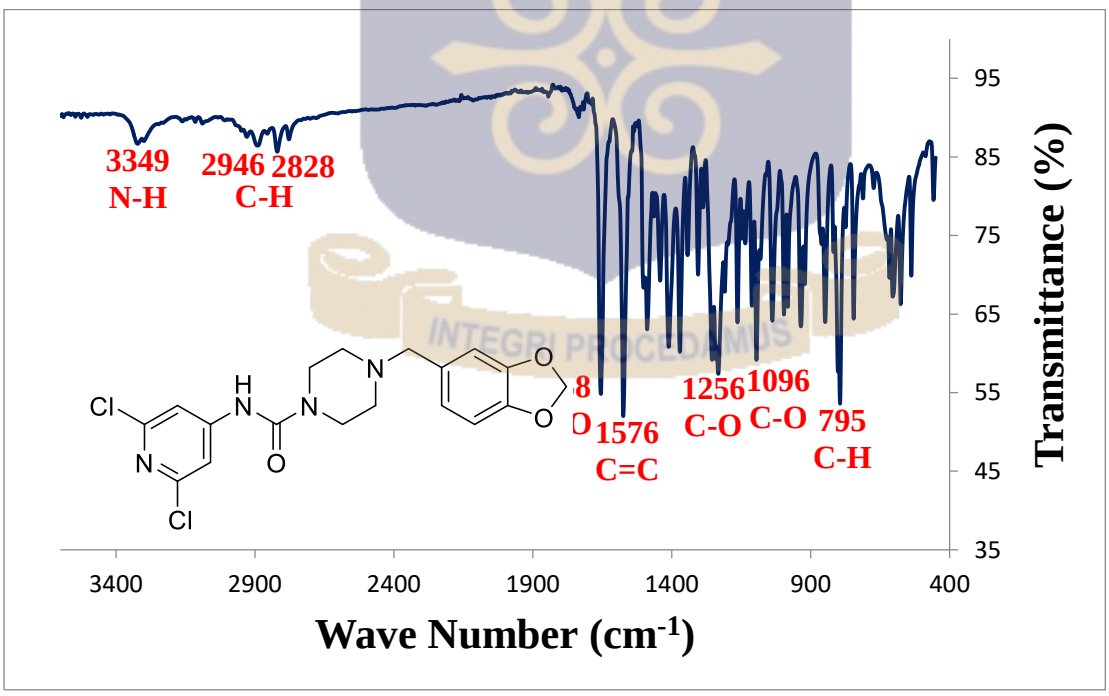


Appendix 3.23: FTIR Spectrum of 4-(3,4-bis(difluoromethoxy)benzyl)-N-(3,5-dimethylphenyl)piperazine-1-carboxamide (CFA187), **3.58.**

University of Ghana http://ugspace.ug.edu.gh

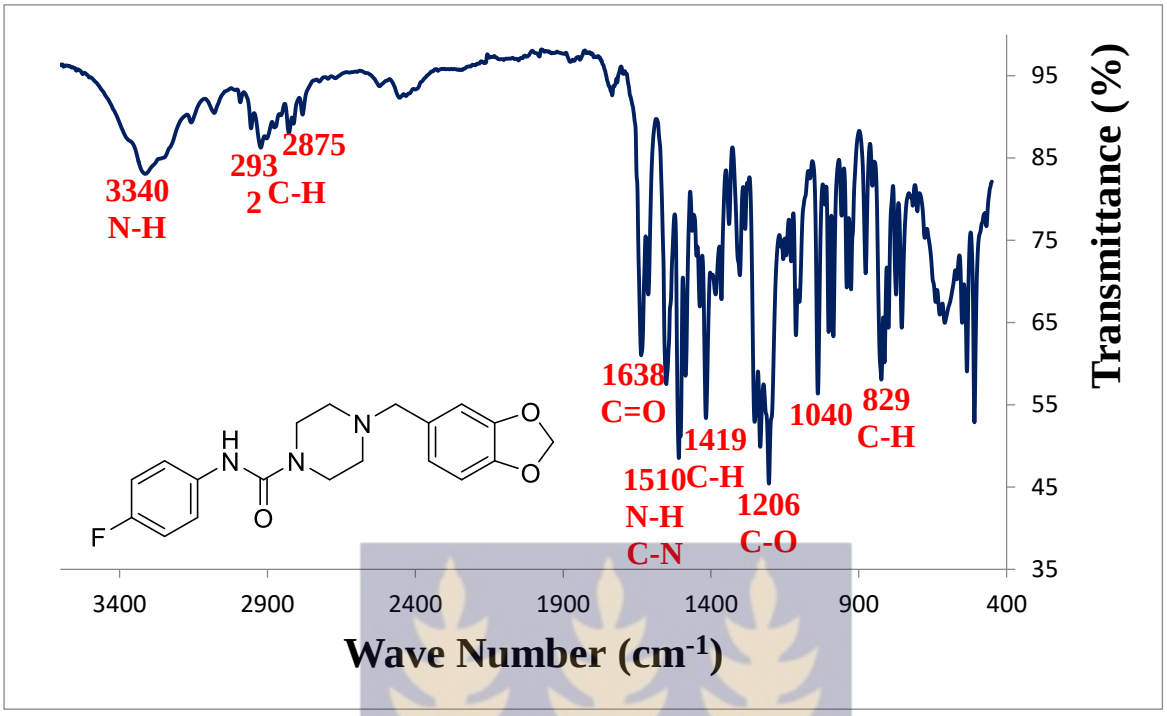


Appendix 3.24: FTIR Spectrum of *N*-(2,6-dichloropyridin-4-yl)-4-((2,2-difluorobenzo[*d*][1,3]dioxol-5-yl)methyl)piperazine-1-carboxamide (CFA160), **3.59.**

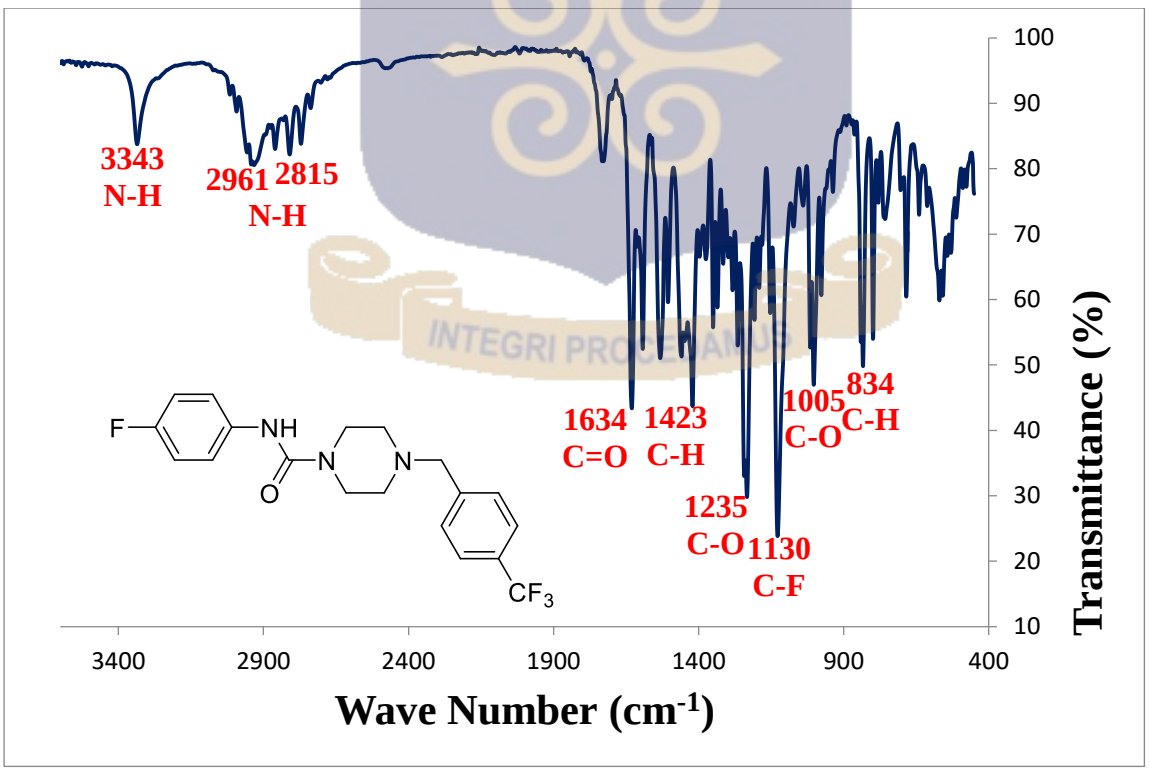


Appendix 3.25: FTIR Spectrum of 4-(benzo[*d*][1,3]dioxol-5-ylmethyl)-*N*-(2,6-dichloropyridin-4-yl)piperazine-1-carboxamide (CFA161), **3.60.**

University of Ghana http://ugspace.ug.edu.gh

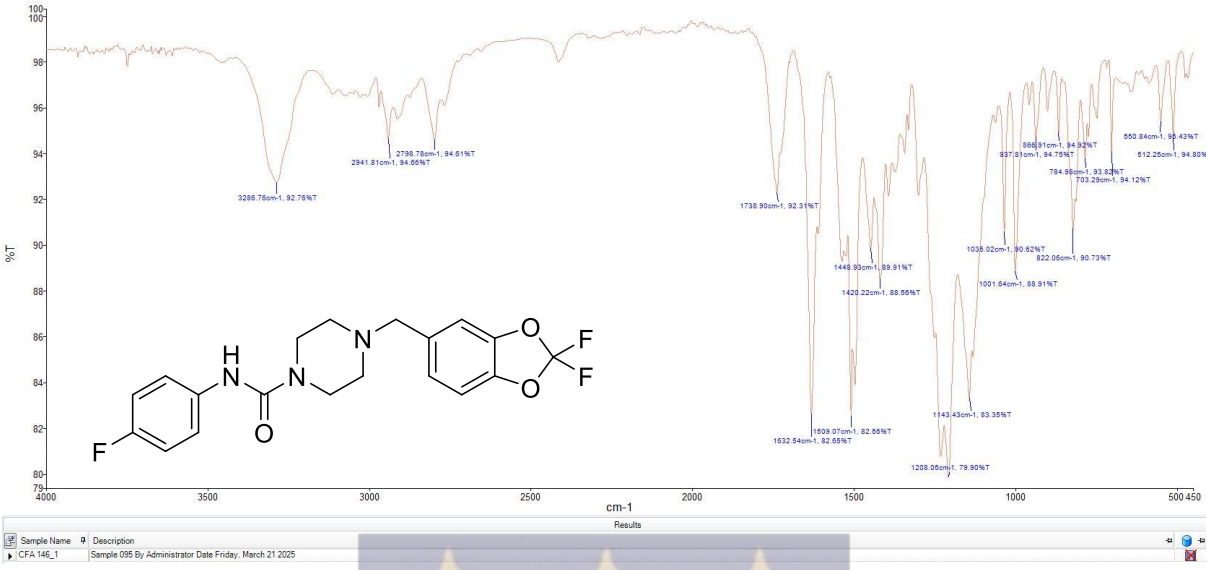


Appendix 3.26: FTIR Spectrum of 4-(benzo[*d*][1,3]dioxol-5-ylmethyl)-*N*-(4-fluorophenyl)piperazine-1-carboxamide (CFA014), **3.61.**

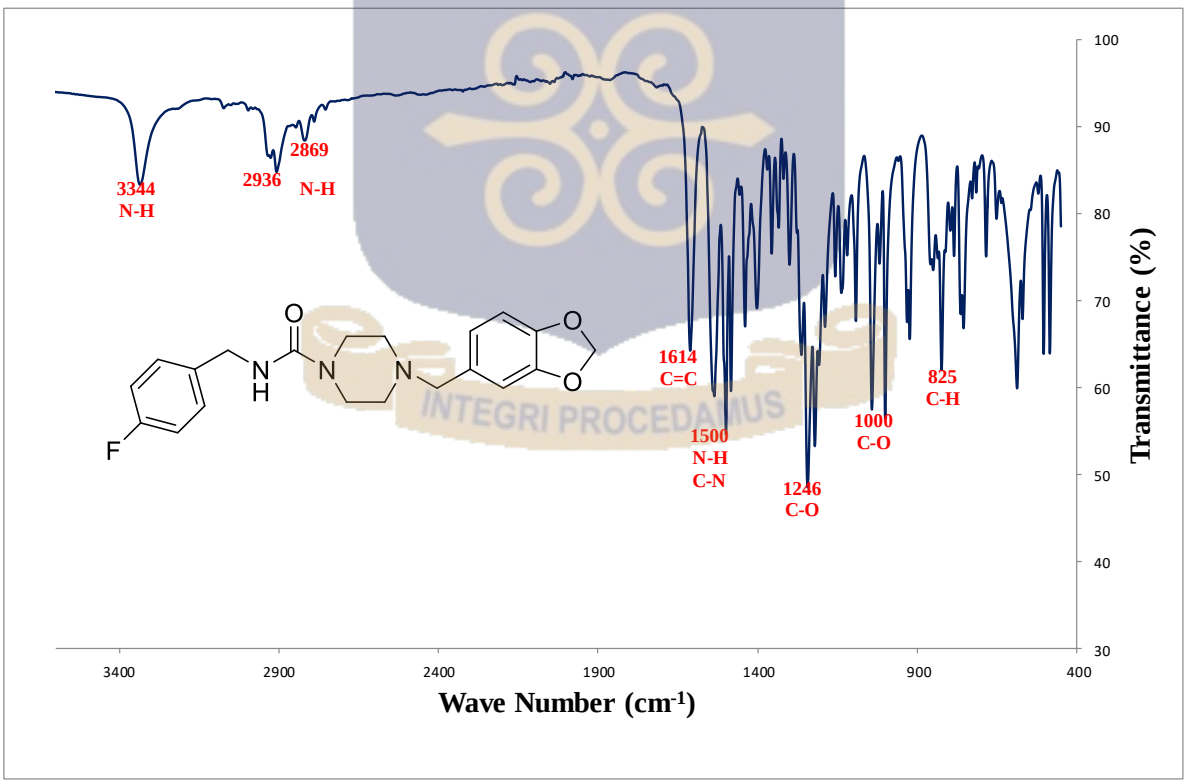


Appendix 3.27: FTIR Spectrum of *N*-(4-fluorophenyl)-4-(4-(trifluoromethyl)benzyl)piperazine-1-carboxamide (CFA016), **3.62.**

University of Ghana http://ugspace.ug.edu.gh

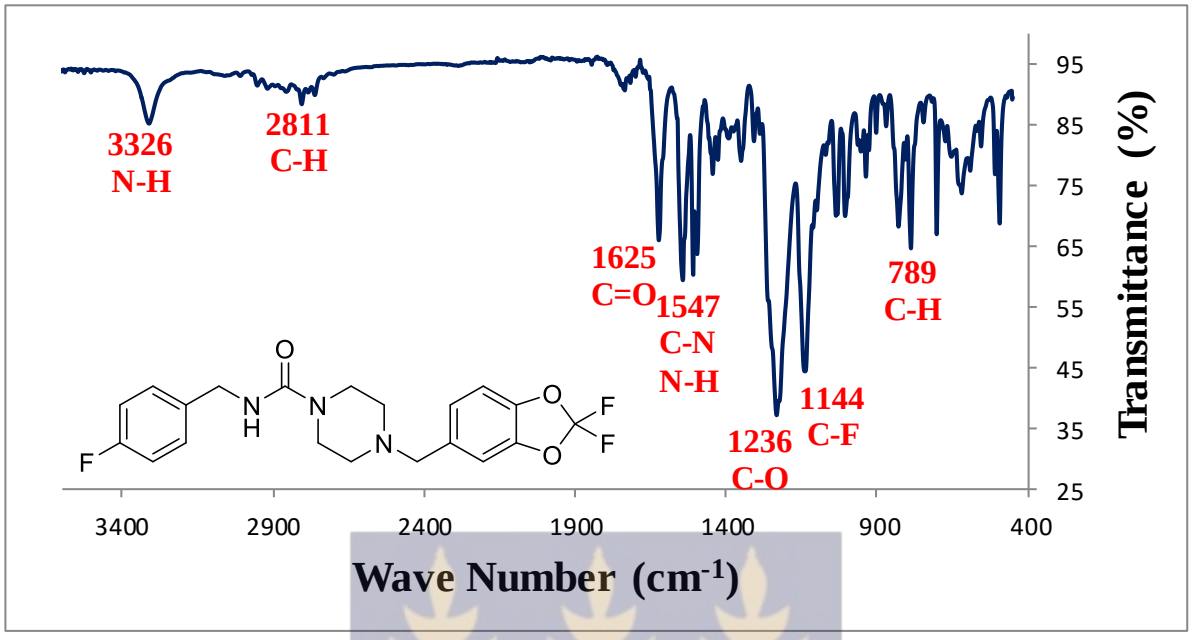


Appendix 3.28: FTIR Spectrum of 4-((2,2-difluorobenzo[*d*][1,3]dioxol-5-yl)methyl)-*N*-(4-fluorophenyl)piperazine-1-carboxamide (CFA146), **3.63**

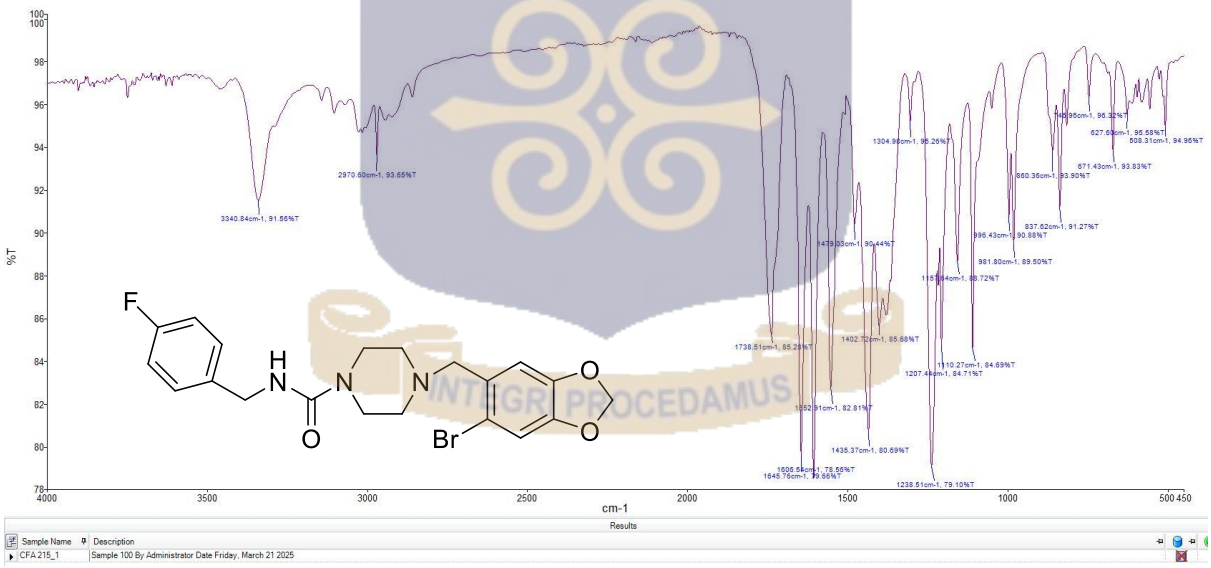


Appendix 3.29: FTIR Spectrum of 4-(benzo[d][1,3]dioxol-5-ylmethyl)-N-(4-fluorobenzyl)piperazine-1-carboxamide (CFA209), **3.64.**

University of Ghana http://ugspace.ug.edu.gh

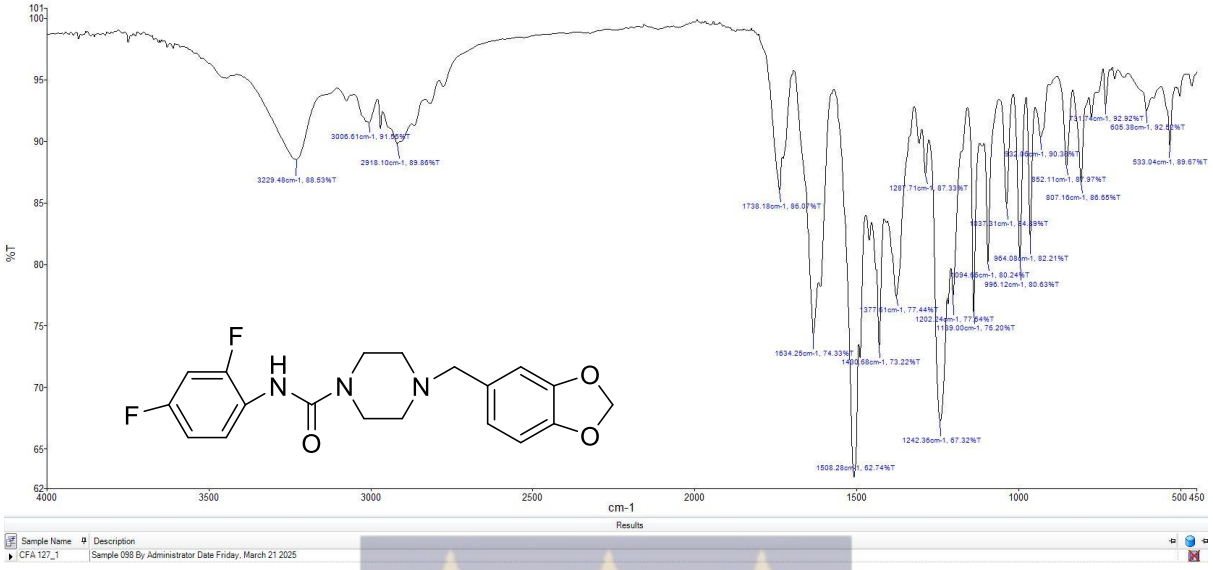


Appendix 3.30: FTIR Spectrum of 4-((2,2-difluorobenzo[*d*][1,3]dioxol-5-yl)methyl)-*N*-(4-fluorobenzyl)piperazine-1-carboxamide (CFA211), **3.65.**

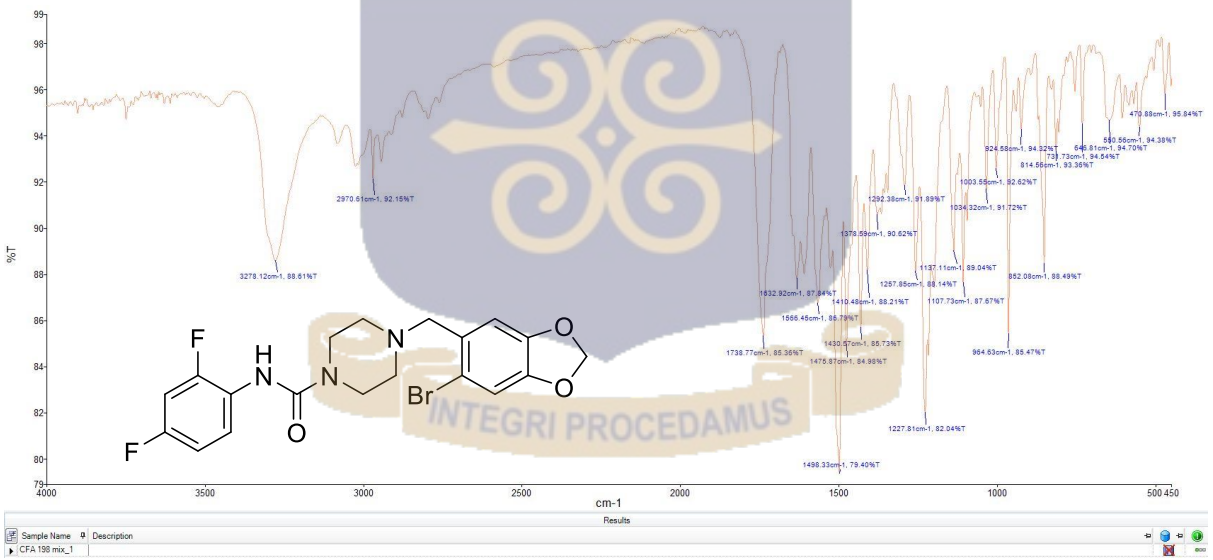


Appendix 3.31: FTIR Spectrum of 4-((6-bromobenzo[d][1,3]dioxol-5-yl)methyl)-N-(4-fluorobenzyl)piperazine-1-carboxamide (CFA210), **3.66.**

University of Ghana http://ugspace.ug.edu.gh

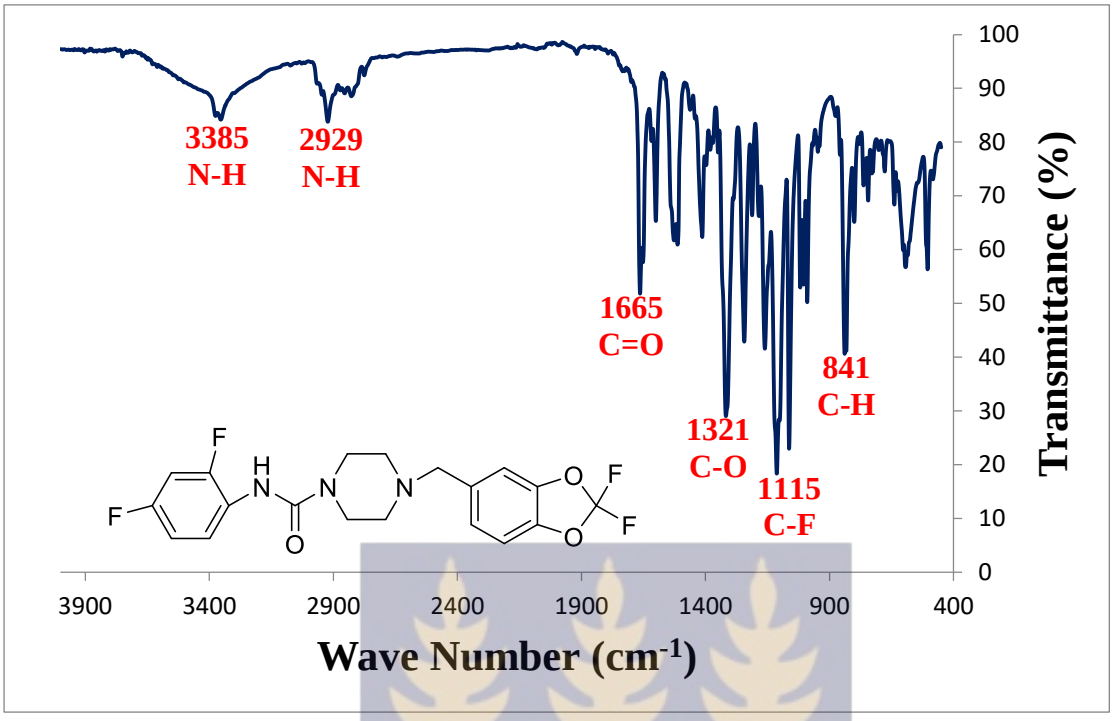


Appendix 3.32: FTIR Spectrum of 4-((6-bromobenzo[*d*][1,3]dioxol-5-yl)methyl)-*N*-(2,4-difluorophenyl)piperazine-1-carboxamide (CFA127/162), **3.67.**

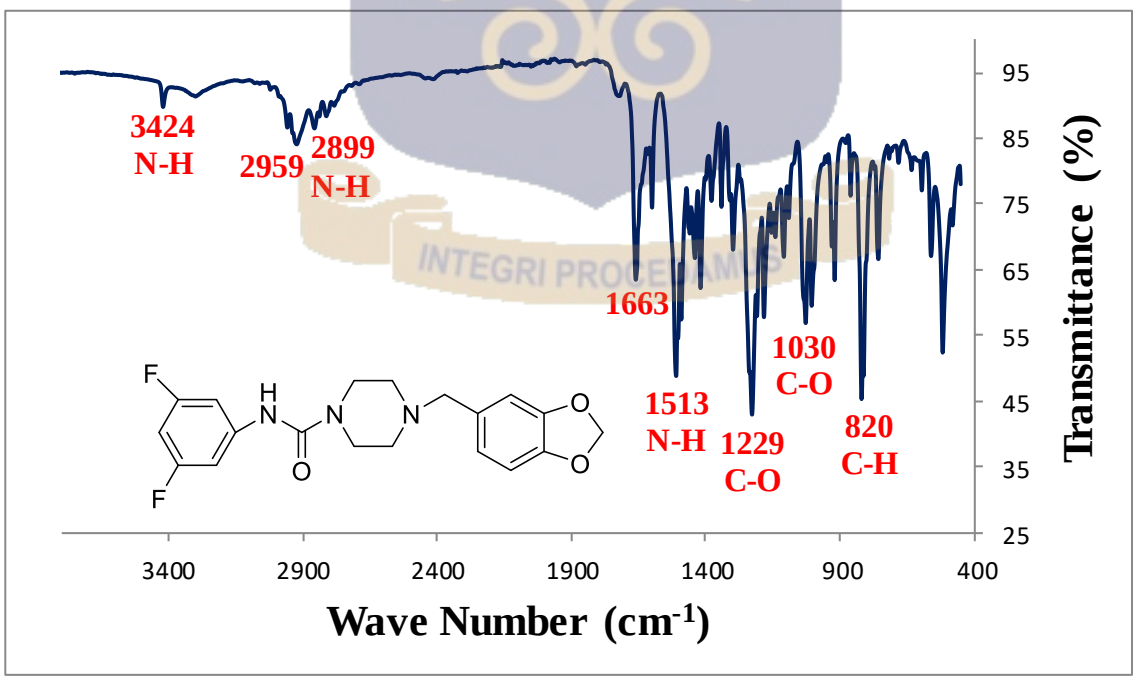


Appendix 3.33: FTIR Spectrum of 4-((6-bromobenzo[*d*][1,3]dioxol-5-yl)methyl)-*N*-(2,4-difluorophenyl)piperazine-1-carboxamide (CFA198), **3.68.**

University of Ghana http://ugspace.ug.edu.gh

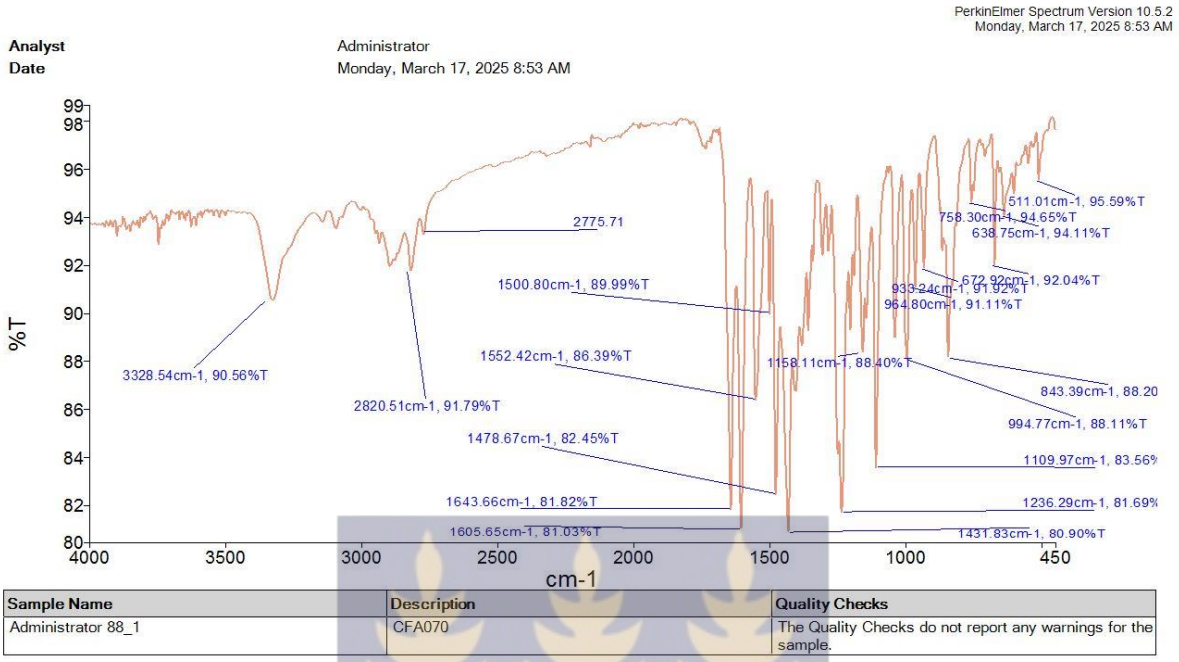


Appendix 3.34: FTIR Spectrum of 4-((2,2-difluorobenzo[d][1,3]dioxol-5-yl)methyl)-N-(2,4-difluorophenyl)piperazine-1-carboxamide (CFA163), **3.69.**



Appendix 3.35: FTIR Spectrum of 4-(benzo[d][1,3]dioxol-5-ylmethyl)-N-(3,5-difluorophenyl)piperazine-1-carboxamide (CFA176), **3.70.**

University of Ghana http://ugspace.ug.edu.gh

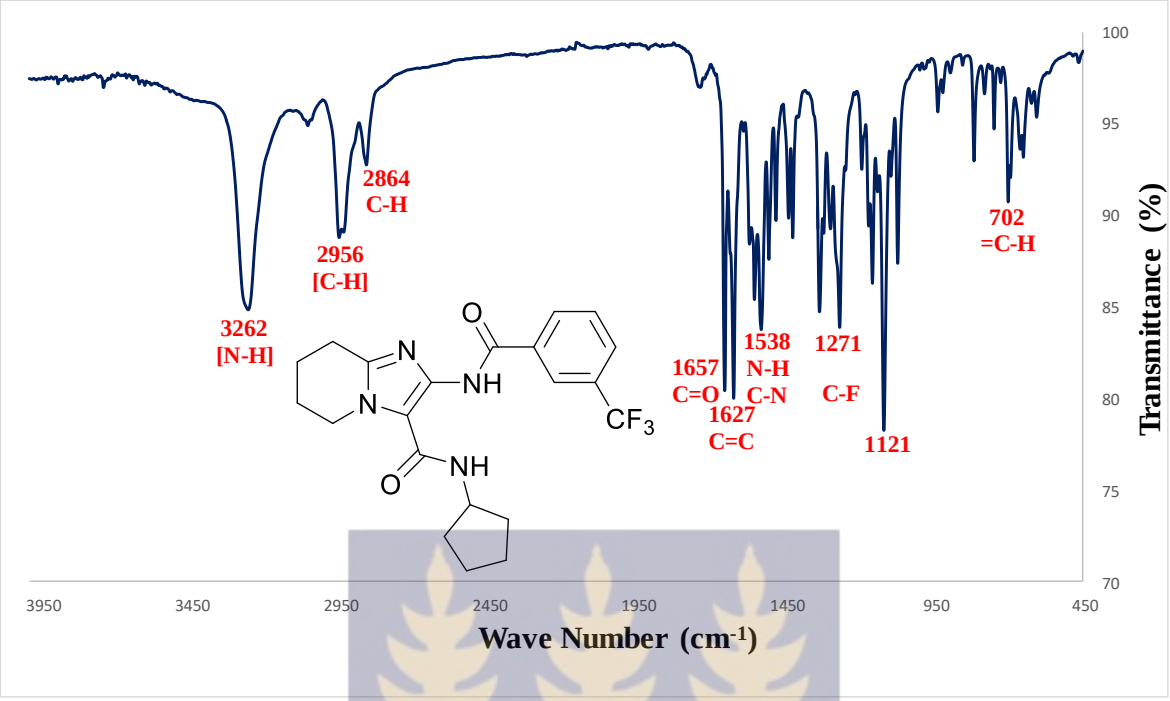


Sample Name	Description	Quality Checks
Administrator 88_1	CFA070	The Quality Checks do not report any warnings for the sample.

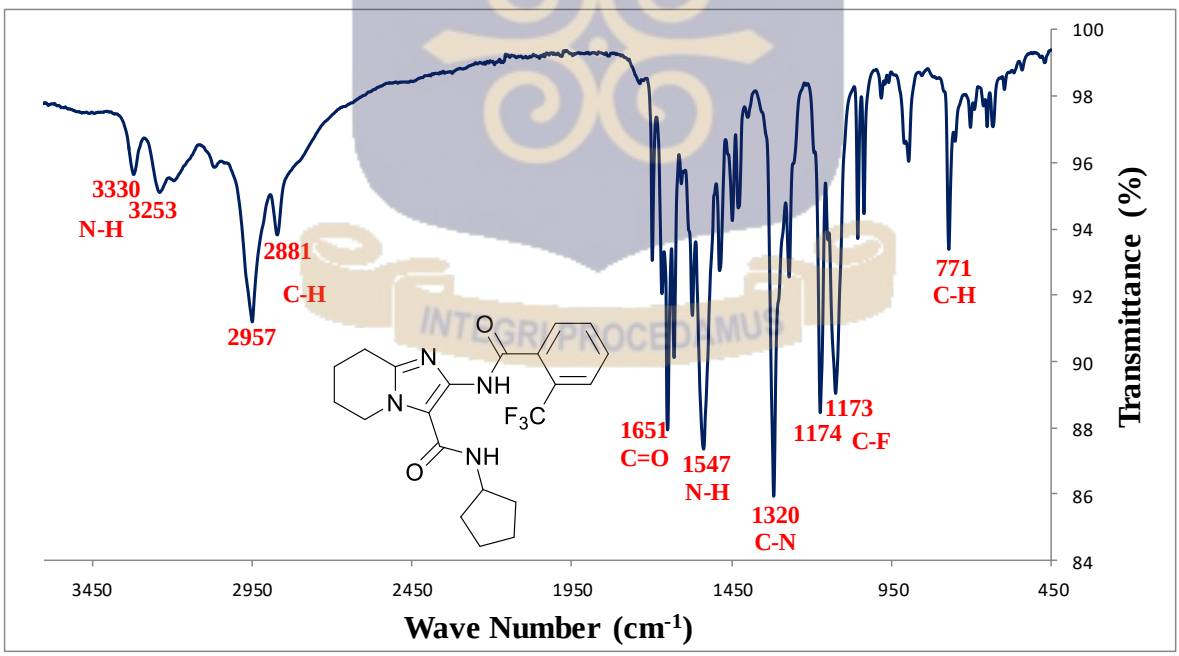
Appendix 3.36: FTIR Spectrum of 4-((2,2-difluorobenzo[*d*][1,3]dioxol-5-yl)methyl)-*N*-(3,5-difluorophenyl)piperazine-1-carboxamide (CFA070), **3.71.**

INTEGRI PROCEDAMUS

University of Ghana http://ugspace.ug.edu.gh



Appendix 3.37: FTIR Spectrum *N*-cyclopentyl-2-(3-(trifluoromethyl)benzamido)-5,6,7,8-tetrahydroimidazo[1,2-*a*]pyridine-5-carboxamide (CFA/P3021), **3.80**.



Appendix 3.38: FTIR Spectrum of *N*-cyclopentyl-2-(2-(trifluoromethyl)benzamido)-5,6,7,8-tetrahydroimidazo[1,2-*a*]pyridine-3-carboxamide (CFA/P3076), **3.81.**

University of Ghana http://ugspace.ug.edu.gh

Appendix 4: Antitubercular activities of screened analogues.

No.	Cmpd ID	Media Composition	Calculated MIC (µM)	Visual MIC (µM)
3.36	CFA015	7H9_ADC_GLU_N_TW	>62.5	-
		7H9_ADC_GLU_TW	>62.5	
		7H9_ADC_GLY_TW	>62.5	
3.40	CFA099	7H9_ADC_GLU_N_TW	>62.5	-
		7H9_ADC_GLU_TW	>62.5	
		7H9_ADC_GLY_TW	>62.5	
3.41	CFA092	7H9_ADC_GLU_N_TW	>62.5	-
		7H9_ADC_GLU_TW	>62.5	
		7H9_ADC_GLY_TW	>62.5	
3.43	CFA147	7H9_ADC_GLU_N_TW	>62.5	-
		7H9_ADC_GLU_TW	>62.5	
		7H9_ADC_GLY_TW	>62.5	
3.45	CFA140	7H9_ADC_GLU_N_TW	>62.5	-
		7H9_ADC_GLU_TW	>62.5	
		7H9_ADC_GLY_TW	>62.5	
3.46	CFA026	7H9_ADC_GLU_N_TW	>62.5	-
		7H9_ADC_GLU_TW	>62.5	
		7H9_ADC_GLY_TW	>62.5	
3.47	CFA117	7H9_ADC_GLU_N_TW	>62.5	-
		7H9_ADC_GLY_TW	>62.5	
		7H9_ADC_GLU_TW	>62.5	
3.53	CFA067	7H9_ADC_GLU_N_TW	>62.5	-
		7H9_ADC_GLU_TW	>62.5	
		7H9_ADC_GLY_TW	>62.5	

University of Ghana http://ugspace.ug.edu.gh

3.54	**CFA068**	**7H9_ADC_GLU_N_TW**	**>62.5**	**-**
		7H9_ADC_GLU_TW	**>62.5**	
		7H9_ADC_GLY_TW	**>62.5**	
3.55	**CFA130**	**7H9_ADC_GLU_N_TW**	**>62.5**	**-**
		7H9_ADC_GLU_TW	**>62.5**	
		7H9_ADC_GLY_TW	**>62.5**	
3.56	**CFA131**	**7H9_ADC_GLU_N_TW**	**>62.5**	**62.5**
		7H9_ADC_GLU_N_TW	**>62.5**	**62.5**
		7H9_ADC_GLU_TW	**>62.5**	**62.5**
		7H9_ADC_GLU_TW	**>62.5**	**62.5**
		7H9_ADC_GLY_TW	**>62.5**	**62.5**
		7H9_ADC_GLY_TW	**>62.5**	**62.5**
3.57	**CFA134**	**7H9_ADC_GLU_N_TW**	**>62.5**	**-**
		7H9_ADC_GLU_TW	**>62.5**	
		7H9_ADC_GLY_TW	**>62.5**	
3.61	**CFA014**	**7H9_ADC_GLU_N_TW**	**>62.5**	**-**
		7H9_ADC_GLU_TW	**>62.5**	
		7H9_ADC_GLY_TW	**>62.5**	
3.63	**CFA146**	**7H9_ADC_GLU_N_TW**	**>62.5**	**-**
		7H9_ADC_GLU_TW	**>62.5**	
		7H9_ADC_GLY_TW	**>62.5**	
3.71	**CFA070**	**7H9_ADC_GLU_N_TW**	**>62.5**	**-**
		7H9_ADC_GLY_TW	**>62.5**	
		7H9_ADC_GLU_TW	**>62.5**	
3.60	**CFA016**	**7H9_ADC_GLU_N_TW**	**>62.5**	**-**
		7H9_ADC_GLU_TW	**>62.5**	

University of Ghana http://ugspace.ug.edu.gh

		7H9_ADC_GLY_TW	>62.5	
3.37	CFA017	7H9_ADC_GLU_N_TW	33.251	-
		7H9_ADC_GLY_TW	>62.5	
		7H9_ADC_GLU_TW	>62.5	
3.50	CFA119	7H9_ADC_GLU_N_TW	>62.5	-
		7H9_ADC_GLU_TW	>62.5	
		7H9_ADC_GLY_TW	>62.5	
3.51	CFA121	7H9_ADC_GLU_N_TW	>62.5	-
		7H9_ADC_GLU_TW	>62.5	
		7H9_ADC_GLY_TW	>62.5	
4.8	CFA077	7H9_ADC_GLU_N_TW	>62.5	-
		7H9_ADC_GLU_TW	>62.5	
		7H9_ADC_GLY_TW	>62.5	
4.10	CFA133	7H9_ADC_GLU_N_TW	>62.5	-
		7H9_ADC_GLU_TW	>62.5	
		7H9_ADC_GLY_TW	>62.5	
4.9	CFA126	7H9_ADC_GLU_N_TW	>62.5	-
		7H9_ADC_GLU_TW	>62.5	
		7H9_ADC_GLY_TW	>62.5	
4.11	CFA093	7H9_ADC_GLU_N_TW	>62.5	-
		7H9_ADC_GLU_TW	>62.5	
		7H9_ADC_GLY_TW	>62.5	

University of Ghana http://ugspace.ug.edu.gh

Isoniazide	**7H9_ADC_GLU_N_TW**	**4.423**	**3.906**
	7H9_ADC_GLU_N_TW	**4.283**	**3.906**
	7H9_ADC_GLU_TW	**3.885**	**3.906**
	7H9_ADC_GLU_TW	**4.312**	**3.906**
	7H9_ADC_GLY_TW	**3.945**	**3.906**
	7H9_ADC_GLY_TW	**4.321**	**3.906**

